สมาคมนวัตกรรมและเทคโนโลยีสร้างสรรค์ ร่วมกับ มหาวิทยาลัยเทคโนโลยีราชมงคล ทั้ง 9 แห่ง
Innovation and Creative Technology Association & Rajamangala University of technology

ICTA

RMUTCON
2025

PROCEEDING BOOK

THE 13TH RAJAMANGALA UNIVERSITY OF TECHNOLOGY INTERNATIONAL CONFERENCE

9 RMUT: DRIVING SOCIAL INNOVATION TOWARDS SUSTAINABLE DEVELOPMENT
JULY 22 – 24, 2025

RMUTCON 2025
14TH RMUTNC & 13TH RMUTIC / 6TH RMUT INNOVATION AWARDS 2025

Proceeding Book

The 13th Rajamangala University of Technology International Conference
9 RMUT: Driving Social Innovation Towards Sustainable Development

July 22 - 24, 2025
Asawin Grand Convention Hotel, Bangkok

Organized by

- Creative Innovation and Technology Association
- Rajamangala University of Technology Phra Nakhon
- Rajamangala University of Technology Krungthep
- Rajamangala University of Technology Rattanakosin
- Rajamangala University of Technology Thanyaburi
- Rajamangala University of Technology Tawan-ok
- Rajamangala University of Technology Isan
- Rajamangala University of Technology Lanna
- Rajamangala University of Technology Suvarnabhumi
- Rajamangala University of Technology Srivijaya

Published by Rajamangala University of Technology Phra Nakhon

Abstract Book:

The 13th Rajamangala University of Technology International Conference
9 RMUT: Driving Social Innovation Towards Sustainable Development

Editorial Boards

1.	Prof.Dr. I Dewa Made Cipta Santosa,	Mechanical Engineering Study Program, Politeknik Negeri Bali, Indonesia
2.	Dr. IM Rajendra	Mechanical Engineering Study Program, Politeknik Negeri Bali, Indonesia
3.	Dr.Ir. I Made Suarta, MT	Mechanical Engineering Study Program, Politeknik Negeri Bali, Indonesia
4.	Prof.Dr. Dewa Ngakan Ketut Putra Negara, S.T., MSc.	Mechanical Engineering Department, Faculty of Engineering, Udayana University, Bali, Indoneaia
5.	Prof.Dr.INS Winaya	Mechanical Engineering Department, Faculty of Engineering, Udayana University, Bali, Indonesia
6.	Dr.Eng. Ni Made Pertiwi Jaya, ST., M.Si., M.Eng.	Environmental Engineering Department, Faculty of Engineering, Udayana University, Bali – Indonesia
7.	Dr. Zhenbo Xu, visiting professor	Massachussett Institute of Technology, Cambridge, United State.
8.	Dr. Junyan Liu (Adjunct Professor)	National Institute of Fundamental Science, Kandy, Sri Lanka.
9.	Dr. Yanrui Ye	South China University of Technology, Guangzhou, China.
10.	Dr. Riz Rupert L. Ortiz	Northwest Samar State University, Philippines
11.	Dr. Catherine B. Rodriguez	Northwest Samar State University, Philippines
12.	Dr. Joseph Emil A. David	Northwest Samar State University, Philippines
13.	Dr. Rolly L. Ortiz	Northwest Samar State University, Philippines
14.	Dr. Nicolas L. Faller	Northwest Samar State University, Philippines
15.	Dr. Ervin L. Rodriguez	Northwest Samar State University, Philippines
16.	Dr. Eugene C. Calumba	Northwest Samar State University, Philippines
17.	Harris C. Tarrayo	Northwest Samar State University, Philippines
18.	Novlloyd E. Celeste	Northwest Samar State University, Philippines
19.	Eduardo Espejon Jr.	Northwest Samar State University, Philippines
20.	Felix John M. Refamonte	Northwest Samar State University, Philippines
21.	Precious Joyce D. Ogdoc	Northwest Samar State University, Philippines
22.	Jessie R. Sabijon	Northwest Samar State University, Philippines
23.	Rhea Jenny A. Ogalesco	Northwest Samar State University, Philippines
24.	Assoc.Prof.Dr. Kiattisak Sangpradit	Rajamangala University of Technology Thanyaburi (RMUTT), Thailand
25.	Dr. Rattanapol Phanomwan Na Ayutthaya	Rajamangala University of Technology Lanna (RMUTL), Thailand
26.	Assoc.Prof.Dr. Sakrsawee Raweekul	Rajamangala University of Technology Isan (RMUTI), Thailand
27.	Asst.Prof. Praphasri Srichai	Rajamangala University of Technology Srivijaya (RMUTSV), Thailand
28.	Asst.Prof.Dr. Sutham Siwawut	Rajamangala University of Technology Krungthep (RMUTK), Thailand
29.	Assoc.Prof. Prapasri Srichai	Rajamangala University of Technology Rattanakosin (RMUTR), Thailand
30.	Asst.Prof.Dr. Warunee Srisongkram	Rajamangala University of Technology Suvarnabhumi (RMUTSB), Thailand
31.	Asst.Prof.Dr. Dhoungsiri Sayompark	Rajamangala University of Technology Tawan-ok (RMUTTO), Thailand
32.	Dr. Chalakorn Udomraksasakul	Rajamangala University of Technology Phra Nakhon (RMUTP), Thailand

Reviewers

1.	Assoc.Prof.Dr. Olarik Surinta	Mahasarakham University
2.	Assoc.Prof.Dr. Itthiphon Worapan	Rajamangala University of Technology Isan
3.	Assoc.Prof.Dr. Chiti Sritontip	Rajamangala University of Technology Lanna
4.	Assoc.Prof.Dr. Suntorn Wittayakun	Rajamangala University of Technology Lanna
5.	Assoc.Prof.Dr. Chaiyarong Kittiyanpanya	Rajamangala University of Technology Rattanakosin
6.	Assoc.Prof.Dr. Paiboolya Gravinlertvatana	Rajamangala University of Technology Rattanakosin
7.	Assoc.Prof. Worapong Boonchouytan	Rajamangala University of Technology Srivijaya
8.	Assoc.Prof.Dr. Suchada Boonlertnirun	Rajamangala University of Technology Suvarnabhumi
9.	Assoc.Prof.Dr. Yingyong Rungfah	Rajamangala University of Technology Tawan-ok
10.	Assoc.Prof.Dr. Pimolpun Phetsombat	Rajamangala University of Technology Thanyaburi
11.	Asst.Prof.Dr. Chaiyot Damrongkijkosol	King Mongkut's University of Technology North Bangkok
12.	Asst.Prof.Dr. Narumol Chumuang	Muban Chombueng Rajabhat University
13.	Asst.Prof.Dr. Sudthidol Piyadeatsoontorn	Rajamangala University of Technology Isan
14.	Asst.Prof.Dr. Krish Sa-nguanpua	Rajamangala University of Technology Krungthep
15.	Asst.Prof.Dr. Tanongsak Sassa-deepeng	Rajamangala University of Technology Lanna
16.	Asst.Prof.Dr. Taweechai Kalasin	Rajamangala University of Technology Lanna
17.	Asst.Prof.Dr. Songwut Mongkonlerdmanee	Rajamangala University of Technology Phra Nakhon
18.	Asst.Prof.Dr. Kodchasorn Hussaro	Rajamangala University of Technology Rattanakosin
19.	Asst.Prof.Dr. Montri Chaisawang	Rajamangala University of Technology Rattanakosin
20.	Asst.Prof.Dr. Pornpimon Sakda	Rajamangala University of Technology Rattanakosin
21.	Asst.Prof.Dr. Natthapong Wongdamnoen	Rajamangala University of Technology Suvarnabhumi
22.	Asst.Prof.Dr. Warun Na Songkhla	Rajamangala University of Technology Suvarnabhumi
23.	Asst.Prof.Dr. Bancha Wiangsamut	Rajamangala University of Technology Tawan-ok
24.	Asst.Prof.Dr. Dhoungsiri Sayompark	Rajamangala University of Technology Tawan-ok
25.	Asst.Prof.Dr. Jetchan Atthaisong	Rajamangala University of Technology Tawan-ok
26.	Asst.Prof.Dr. Sukanya Boonsri	Rajamangala University of Technology Thanyaburi
27.	Dr. Worawut Yimyam	Phetchaburi Rajabhat University
28.	Dr. Teerawat Ajpru	Rajamangala University of Technology Isan
29.	Dr. Panithi Amatayakul	Rajamangala University of Technology Lanna
30.	Dr. Supanya Singhakorn	Rajamangala University of Technology Phra Nakhon
31.	Dr. Piyanut Muangtong	Rajamangala University of Technology Rattanakosin

Manuscript Compilation Committee

Dr. Chalakorn Udomraksasakul	Institute of Research and Development, RMUTP
Asst.Prof.Dr. Chantana Papattha	Institute of Research and Development, RMUTP
Patcharanun Youngworawichian	Institute of Research and Development, RMUTP
Natcha Dubmai	Institute of Research and Development, RMUTP
Kedsuda Chooseng	Institute of Research and Development, RMUTP
Wallapa Fakprapai	Institute of Research and Development, RMUTP
Chavinee Binkasemen	Institute of Research and Development, RMUTP
Sasiporn Khotcharak	Faculty of Business Administration, RMUTP
Kanha Chomsri	Faculty of Business Administration, RMUTP
Phakpoom Na Boonwong	Faculty of Business Administration, RMUTP
Angsana Anucharnan	Faculty of Home Economics Technology, RMUTP
Thipawan kummin	Faculty of Home Economics Technology, RMUTP
Dusita Isarapakdee	Faculty of Home Economics Technology, RMUTP
Kittipong Maya	Faculty of Home Economics Technology, RMUTP
Napaporn Phuphet	Faculty of Mass Communication Technology, RMUTP
Thanita Thawinwisan	Faculty of Mass Communication Technology, RMUTP

Preface

The Association of Innovation and Creative Technology, together with Rajamangala University of Technology Phra Nakhon, is honored to host the 14th Rajamangala University of Technology National Conference (14th RMUTNC), the 13th Rajamangala University of Technology International Conference (13th RMUTIC), and the 6th RMUT Innovation Awards 2025. These events will take place from July 22–24, 2025, at Asawin Grand Convention Hotel, Laksi District, Bangkok.

This conference provides a platform to share research, inventions, and innovations from faculty, researchers, students, and staff across all nine Rajamangala Universities of Technology. It also welcomes participants from other institutions and organizations in Thailand and abroad. The goal is to promote the exchange of knowledge, experiences, and academic ideas among researchers, scholars, and stakeholders, leading to the development of practical innovations for the country's sustainable economic and social growth.

Rajamangala University of Technology Phra Nakhon, as the host, would like to sincerely thank all administrators, organizing committees, distinguished experts, and participants for their valuable support and contributions to this event.

We hope this conference will inspire new ideas, expand knowledge, and encourage meaningful collaborations that will benefit the nation in the future.

Rajamangala University of Technology Phra Nakhon
July 2025

Message from Ms. Sudawan Wangsuphakijkosol
Minister of Higher Education Science Research and Innovation

The Ministry of Higher Education, Science, Research and Innovation (MHESI) is dedicated to advancing higher education to meet the demands of a rapidly changing world. By fostering research and innovation within universities and promoting collaboration across all sectors—both nationally and internationally—the Ministry underscores its commitment to driving sustainable development that aligns with the nation's strategic goals.

Recognizing the crucial role of research and innovation in responding to the needs of communities and society, MHESI has placed these elements at the heart of its mission. The 14th National RMUT Conference, the 13th International RMUT Conference, and the 6th RMUT Invention and Innovation Contest, held under the theme "Innovation for Society: 9 RMUTs Driving Development towards Sustainability", stand as significant milestones. These events showcase the outcomes of rigorous academic inquiry and creative innovation from researchers, academics, and students, while fostering knowledge exchange and collaboration at national and international levels.

On behalf of the Ministry, I extend my heartfelt congratulations to the Association of Innovation and Technology, the nine Rajamangala Universities of Technology, and all supporting organizations for their collective efforts in organizing these important events. This collaboration reflects the pivotal role of higher education institutions in developing innovations that are deeply connected to and beneficial for communities and society.

I am confident that RMUTCON 2025 will achieve outstanding success and lead to meaningful outcomes—transforming academic research into valuable innovations that contribute to the well-being of communities, strengthen society, and advance national development.

Ms. Sudawan Wangsuphakijkosol
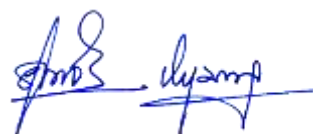Minister of Higher Education Science Research and Innovation

Message from Professor.Dr. Supachai Pathumnakul
Permanent Secretary, Ministry of Higher Education, Science, Research and Innovation

The Ministry of Higher Education, Science, Research and Innovation (MHESI) is steadfast in its commitment to advancing the development of the nation's human capital. Our goal is to equip individuals with the knowledge, skills, and competencies necessary to thrive in the 21st century, enabling them to contribute effectively to national progress. Central to this endeavor is the application of science, research, and innovation as catalysts for sustainable development, ensuring that progress aligns with both societal needs and environmental stewardship.

In alignment with this vision, the Ministry emphasizes the importance of data-driven decision-making and the strategic utilization of knowledge within universities of technology. These institutions are expected to take a leading role in driving technological advancement and fostering innovation, which are critical components for improving quality of life, safeguarding the environment, and achieving the United Nations Sustainable Development Goals (SDGs). Of particular relevance is SDG 9—"Build resilient infrastructure, promote inclusive and sustainable industrialization, and foster innovation"—which underscores the essential role of higher education in supporting resilient and sustainable national development.

The Ministry is pleased to acknowledge the collaborative efforts of the nine Rajamangala Universities of Technology and their dedicated partners in organizing three significant events: the 14th International Conference on Technology and Innovation for Sustainable Development, the 13th National Conference on Technology and Innovation, and the 6th Rajamangala University of Technology National Conference (RMUTCON 2025). These gatherings provide a vital platform for scholars, researchers, and practitioners to share knowledge, exchange ideas, and present groundbreaking research findings that offer tangible benefits to society.

It is my sincere hope that RMUTCON 2025 will serve as a catalyst for fostering innovation and academic excellence, inspiring participants to create impactful knowledge and solutions that address the pressing challenges of our time. May these collective efforts continue to drive forward innovation-led development and promote sustainable progress for the nation and beyond.

Prof. Dr. Supachai Pathumnakul
Permanent Secretary Ministry of Higher Education,
Science, Research and Innovation

Message from the Chairman of the Rajamangala University of Technology Presidents Council
By Assoc.Prof.Dr. Udomvit Chaisakulkiet
President of Rajamangala University of Technology Rattanakosin
Chairman of the Rajamangala University of Technology Presidents Council

On behalf of the Rajamangala University of Technology Presidents Council, I would like to express my heartfelt appreciation for the organization of the 14th Rajamangala University of Technology National Conference, the 13th International Conference, and the 6th RMUT Innovation and Invention Contest under the theme "Innovation for Society: 9 Rajamangala Universities Driving Sustainable Development." This reflects the significant role of the nine Rajamangala University of Technology institutions in collaboratively advancing research, technology, and innovation to strengthen the nation's capacity based on knowledge and sustainability.

Rajamangala University of Technology Phra Nakhon has been honored as the main host, in collaboration with the eight other Rajamangala University of Technology institutions and the Association of Creative Innovation and Technology. The event features a variety of key activities, including special lectures by invited speakers, national and international academic conferences, innovation and invention contests, RMUT Startup presentations, the RMUT IP Fair exhibition, business matching sessions, and academic showcases from educational institutions and organizations both within and outside the network. This conference serves as an important mechanism to foster academic collaboration and provides a platform for the exchange of knowledge among researchers, scholars, students, as well as representatives from government, private, and civil society sectors, both domestically and internationally. Such integration of knowledge will further the development of technologies, innovations, and research that can be applied practically and sustainably.

I extend my sincere thanks to all parties involved in organizing this event. I reaffirm the Rajamangala University of Technology network's commitment to continuously driving knowledge and innovation for the benefit of society. It is my earnest hope that this conference will serve as a vital force in enhancing the quality of the nation's research and innovation, contributing sustainably to society, the nation, and the global community.

Assoc.Prof.Dr. Udomvit Chaisakulkiet
Chairman of the Rajamangala University of Technology Presidents Council

Message from the Chairperson of the Rajamangala University of Technology Research and Development Institute Network
By Asst. Prof.Dr. Bowonkitti NekomanurakDirector
Research and Development Institute, Rajamangala University of Technology Rattanakosin Chairperson,
Research and Development Institute Network, Rajamangala University of Technology

The Research and Development Institute Network of the nine Rajamangala Universities of Technology has continuously collaborated to promote, support, and develop the management of research to enhance the quality of research outputs, inventions, and innovations. These efforts aim to produce tangible benefits for communities and the nation, both in the fields of social sciences and industry. This is achieved through multi-sectoral cooperation, integrating knowledge to deliver concrete outcomes.

This conference serves as a vital platform for exchanging academic knowledge and showcasing the research and innovation potential of all nine Rajamangala Universities of Technology. It also creates an opportunity for networking and brainstorming among faculty members, researchers, and students at both national and international levels. Such interactions will inspire the development of new research, inventions, and innovations that can truly address the country's sustainable development goals.

On behalf of the Chairperson of the Rajamangala University of Technology Research and Development Institute Network, I extend my heartfelt thanks to Rajamangala University of Technology Phra Nakhon for hosting this event, as well as to all stakeholders involved in its strong organization. I firmly believe that this conference will be another powerful driver in advancing research, inventions, and innovations toward wider recognition and contributing positively and sustainably to society and the nation.

Asst. Prof. Dr. Bowonkitti Nekomanurak
Chairperson, Research and Development Institute Network,
Rajamangala University of Technology

Message from Dr. Natworapol Rachsiriwatcharabul
President of Rajamangala University of Technology Phra Nakhon (RMUTP)

The network of nine Rajamangala Universities of Technology has continuously collaborated in organizing academic conferences. This year, Rajamangala University of Technology Phra Nakhon is honored to serve as the main host, in partnership with the Association of Creative Innovation and Technology, for the 14th National Rajamangala University of Technology Academic Conference, the 13th International Rajamangala University of Technology Academic Conference, and the 6 th Rajamangala Innovation and Invention Contest (RMUTCON 2025). The theme of the event, "Innovation for Society: 9 Rajamangala Universities Driving Development Towards Sustainability," reflects the role of higher education institutions in the contemporary era, not limited to teaching and learning but extending to applying knowledge for research and innovation to solve societal problems, meet community needs, and serve as a crucial force in driving the nation toward stable and sustainable development.

This academic conference not only serves as a platform for faculty members, researchers, and students to present their research but also provides an excellent opportunity to exchange knowledge and experiences with academics from both domestic and international institutions, thereby fostering global academic collaboration networks.

On behalf of Rajamangala University of Technology Phra Nakhon, I would like to express my sincere gratitude to all sectors involved in making this conference a success. May this event be a significant step forward in academic cooperation and serve as an inspiration for all participants to continue creating meaningful and impactful work for society.

Dr. Natworapol Rachsiriwatcharabul
President, Rajamangala University of Technology Phra Nakhon

The 13th Rajamangala University of Technology International Conference 9 RMUT: Driving Social Innovation Towards Sustainable Development

July 22 - 24, 2025
Asawin Grand Convention Hotel, Bangkok

Rationale

Rajamangala University of Technology Phra Nakhon is an institution of higher learning committed to cultivating practice-oriented graduates equipped with advanced knowledge and expertise in science and technology. The University has established a comprehensive vision, mission, strategic priorities, and clearly defined objectives that align with Group 2 of the strategic higher education institutions, which focus on technological advancement and the promotion of innovation. Emphasis is placed on enhancing teaching and learning, research, and innovation development as mechanisms to propel the nation's targeted industries. These endeavors are further reinforced by efficient organizational management, research capacity-building, and the fostering of innovation ecosystems.

The academic conference is organized to serve as a platform for the dissemination of research findings, inventions, and innovations produced by university personnel, as well as a medium for showcasing the institution's scholarly contributions to the broader public. Additionally, the event provides opportunities for faculty members and researchers to engage in academic exchange, strengthen collaborative networks in research and academic services, and cultivate a dynamic research environment. These efforts are aimed at generating impactful research, fostering technological advancement, and producing knowledge that contributes to societal and national development. As part of its core mission, the University's Office of Research and Development is tasked with organizing the Rajamangala University of Technology National Conference in collaboration with the network of nine RMUT institutions. Past conferences have been hosted as follows:

1. **10th RMUT National Conference**
   Theme: "Rajamangala Driving Innovation Forward Towards Thailand 4.0"
   Date: 1–3 August 2018
   Venue: Rua Rasada Hotel, Trang Province
   Host: Rajamangala University of Technology Srivijaya
2. **11th RMUT National Conference**
   Theme: "Rajamangala Innovation Pathways for Economic and Social Advancement"
   Date: 24–26 July 2019
   Venue: Chiang Mai International Exhibition and Convention Centre
   Host: Rajamangala University of Technology Lanna
3. **12th RMUT National Conference**
   Theme: "Nine RMUTs Driving Innovation, Leading Economic Development, and Fostering Green Technology for Sustainable Growth"
   Date: 18–20 May 2022
   Venue: Royal Cliff Grand Hotel, Chonburi Province
   Host: Rajamangala University of Technology Thanyaburi
4. **13th RMUT National Conference**
   Theme: "Nine RMUTs Empowering Sustainable Innovation and Shaping Future Lifestyles through the BCG Model"
   Date: 30 August – 1 September 2023
   Venue: Nongnooch Tradition Center Hall, Nongnooch Tropical Garden, Chonburi Province
   Host: Rajamangala University of Technology Tawan-ok

In 2025, Rajamangala University of Technology Phra Nakhon, in collaboration with eight other RMUTs and the Association of Innovation and Creative Technology, will assume the role of host for the following events:

- The 14th Rajamangala University of Technology National Conference
- The 13th Rajamangala University of Technology International Conference
- The 6th RMUT Innovation Awards

These will be held under the overarching theme:

"Innovation for Society: 9 RMUTs Driving Development Towards Sustainability"

Key Activities
- Special lectures by distinguished guest and keynote speakers
- National and international academic paper presentations
- Invention and innovation competitions
- RMUT Startup project showcases and competitions
- RMUT IP Fair and business matching activities
- Academic exhibitions featuring research and innovation outputs from all nine RMUTs and partner institutions

This academic gathering will serve as a significant venue for the exchange of scholarly knowledge and research experiences among academics, researchers, and professionals from the public and private sectors. Furthermore, it aims to promote the dissemination and application of research-based knowledge and innovation in practical settings, thereby fostering the development of high-impact, quality research.

Objectives
1. To provide a platform for the presentation and dissemination of research, inventions, and creative innovations in the fields of science, technology, humanities, and social sciences at both national and international levels by faculty members, researchers, students, and academic personnel from within and beyond the RMUT network.
2. To strengthen academic cooperation and promote the exchange of knowledge and experiences among researchers from the nine RMUTs and external academic institutions.

Conference Activities
1. National and international academic presentations
   - Oral presentation sessions
   - Poster presentation sessions
2. Invention and innovation competitions
3. RMUT Startup competitions
4. RMUT IP Fair and business matching sessions
5. Academic exhibitions by RMUTs and partnering organizations
   Session 1 Humanities and Social Sciences
   Session 2 Agricultural and Food Innovation
   Session 3 Science and Engineering Technology
   Session 4 Architecture and Creative Works
   Session 5 Business and Economics

Fields Open for Submission Topics for Oral Presentation and Poster Presentation
National Level — Divided into 7 sessions as follows:
- Session 1: Humanities and Social Sciences
- Session 2: Agricultural Technology and Food Innovation
- Session 3: Engineering
- Session 4: Science and Information Technology
- Session 5: Architecture, Arts, and Creative Works
- Session 6: Business Administration and Economics
- Session 7: Routine to research

International Level — Divided into 6 sessions as follows:
- Session 1: Humanities and Social Sciences
- Session 2: Agricultural and Food Innovation
- Session 3: Science and Engineering Technology
- Session 4: Architecture and Creative Works
- Session 5: Business and Economics
- Session 6: Resource Management

Topics for the Invention, Innovation, and RMUT Startup Competition
Eligible participants: faculty members, students, and the general public.
- Group A: Food Technology and Food Innovation
- Group B: Engineering and Technology
- Group C: Science and Information Technology
- Group D: Architecture, Arts, and Design
- Group E: Quality of Life Development and Creative Economy

Awards for Poster and Oral Presentation Competitions

The following distinctions were conferred in recognition of outstanding performance in the Poster and Oral Presentation categories:
1. **Gold Award**: Recipients were awarded a gold medal and a certificate of achievement.
   - National Level: 7 awards
   - International Level: 5 awards
2. **Silver Award**: Recipients were awarded a silver medal and a certificate of achievement.
   - National Level: 7 awards
   - International Level: 5 awards
3. **Bronze Award**: Recipients were awarded a bronze medal and a certificate of achievement.
   - National Level: 7 awards
   - International Level: 5 awards

Awards for the Invention and Innovation Competition

Category: Faculty Members and the General Public
1. **Gold Award**: Recipients received a commemorative plaque, a gold medal, and a monetary prize of 8,000 THB (5 awards).
2. **Silver Award**: Recipients received a silver medal and a monetary prize of 4,000 THB (5 awards).
3. **Bronze Award**: Recipients received a bronze medal and a monetary prize of 2,000 THB (5 awards).

Category: Students
1. **Gold Award**: Recipients received a commemorative plaque, a gold medal, and a monetary prize of 5,000 THB (5 awards).
2. **Silver Award**: Recipients received a silver medal and a monetary prize of 2,500 THB (5 awards).
3. **Bronze Award**: Recipients received a bronze medal and a monetary prize of 1,500 THB (5 awards).

RMUTP Startup Competition Awards

Category: Students
1. **Gold Award**: The recipient was awarded a commemorative plaque, a gold medal, and a monetary prize of 5,000 THB (1 award).
2. **Silver Award**: The recipient was awarded a silver medal and a monetary prize of 2,500 THB (1 award).
3. **Bronze Award**: The recipient was awarded a bronze medal and a monetary prize of 1,500 THB (1 award).

Note: All awardees will receive a certificate of achievement.

Tentative Schedule for the National and International Academic Conference (14ᵗʰ Rajamangala University of Technology National Conference – RMUTNC, and 13ᵗʰ Rajamangala University of Technology International Conference – RMUTIC)

Period	Activity
15 June 2025	Notification of review results
25 June 2025	Deadline for submission of final revised papers
25 June - 20 July 2025	Early bird registration for paper presenters
10 - 20 July 2025	Regular registration for paper presenters
1–15 July 2025	Submission of oral presentation files
22–24 July 2025	RMUTCON 2025 Academic Conference

Tentative Schedule for the 6ᵗʰ Rajamangala Innovation Awards and RMUT Startup Award

Period	Activity
15 June 2025	Announcement of shortlisted entries (preliminary selection results)
25 June - 10 July 2025	Early bird registration fee payment
10 - 20 July 2025	Regular registration fee payment
21 July 2025	Installation of exhibition booths for innovations, inventions, and startups
22–24 July 2025	RMUTCON 2025 Academic Conference and Innovation Exhibition

Venue
Asawin Grand Convention Hotel
88 Vibhavadi Rangsit Road (Kamphaeng Phet 6), Talat Bang Khen Subdistrict, Lak Si District, Bangkok, Thailand.

Conference Website: https://rmutcon2025.rmutp.ac.th/

Schedule
The 14th Rajamangala University of Technology National Conference
The 13th Rajamangala University of Technology International Conference
The 6th Innovation and Invention Contest (RMUTCON 2025)
22 – 24 July 2025
At Asawin Grand Convention Hotel, Grand Conference Room, 4th Floor, Bangkok

Tuesday, 22 July 2025		
Opening Ceremony		
Time	**Details**	**Venue**
08.30 – 09.00 a.m.	Registration for invited guests/media/speakers	Grand Conference Room A B C, 4th Fl.
09.00 – 09.10 a.m.	Opening Performance	
09.10 – 09.30 a.m.	**Opening Ceremony** - Dr. Natworapol Rachsiriwatcharabul, President of Rajamangala University of Technology Phra Nakhon, delivers the report. - Lt. Gen. Chainaronk Kijrungrojjarean, Acting President of the University Council, presides over and officially opens the conference.	
09.30 – 10.15 a.m.	**Special Lecture: "Developing Technological Human Resources through Teaching, Research, and Social Needs"** by Prof. Dr. Yuttana Kumsuwan, Faculty of Engineering, Chiang Mai University	
10.15 – 11.00 a.m.	**Special Lecture: "The Language of Change: How Communication Powers Sustainable Social Innovation"** by Assoc. Prof. Dr. Jinlong Zhang, Director of Media Practice Teaching Center, Yangtze Normal University, People's Republic of China (PRC).	
11.00 – 12.00 a.m.	**Exhibition and Poster Presentations of Research, Innovation, and RMUT Startups** by the Chairperson and Executive Teams	
12.00 – 01.30 p.m.	Lunch	3rd Fl.
Project and Contest Presentations		
Time	**Details**	**Venue**
09.00 a.m. – 05.00 p.m.	RMUT Startup Contest Presentations	Meeting Room, 2nd Fl.
01.00 – 05.00 p.m.	Oral Presentations: Technology and Innovation (national and international levels)	Meeting Room, 2nd Fl.
01.00 – 05.00 p.m.	- Poster Presentations: Technology and Innovation (national and international levels) - Innovation and Invention Contest Presentations - Academic Exhibition	Grand Conference Room A, 4th Fl.

Wednesday, 23 July 2025		
Project and Contest Presentations		
Time	**Details**	**Venue**
08.30 – 12.00 a.m.	Oral Presentations: Technology and Innovation (national and international levels)	Meeting Room, 2nd Fl.
09.00 – 12.00 a.m.	- Poster Presentations: Technology and Innovation (national and international levels) - Innovation and Invention Contest Presentations - RMUT Startup Presentations - Academic Exhibition	Conference Room A, 4th Fl.
09.00 – 12.00 a.m.	E-Sports Competition: Arena of Valor (ROV)	Grand Hall B C, 4th Fl.
12.00 – 01.30 p.m.	Lunch	3rd Floor
01.00 – 05.00 p.m.	Oral Presentations: Technology and Innovation (national and international levels)	Meeting Room, 2nd Fl.
	- Poster Presentations: Technology and Innovation (national and international levels) - Innovation and Invention Contest Presentations - RMUT Startup Presentations - Academic Exhibition	Conference Room A, 4th Fl.
06.00 – 10.00 p.m.	Welcome Party	Grand Conference Room B C, 4th Fl.
Thursday, 24 July 2025		
Closing Ceremony		
Time	**Details**	**Venue**
08.30 – 09.00 a.m.	Registration for invited guests/award recipients	Grand Conference Room B C, 4th Fl.
09.00 a.m. – 04.00 p.m.	**Closing Ceremony** - Launching Ceremony: "Innovation Partnership" by Association and related organizations - Award Presentations for Oral and Poster Presentations - Award Presentations for Innovation and Invention Contest - RMUT Startup Awards - Closing Remarks by Dr. Natworapol Rachsiriwatcharabul, President of Rajamangala University of Technology Phra Nakhon - Handover of the RMUTCON 2026 host flag	Grand Conference Room B C, 4th Fl.

Note : Coffee breaks   :   10.30 – 10.45 a.m. and 02.30 – 02.45 p.m.
        Lunch   :   12.00 – 01.30 p.m.

List of International Articles – Full paper

Code Paper No.	Topics	Aothors	Page
Session 1: Humanities and Social Sciences			**21**
OIH-01	The Analysis on Writing Errors of 2nd Undergraduate Students at English Department, Faculty of Linguistics and Humanities, Savannakhet University, Lao People's Democratic Republic	- Pakaysit Keomanyvanha - Wichai Pornmalairungruaengb - Lanta Ketoukhama - hounkham Nanthavongsaa - Souvantha Keovongsaa - Dalavone Vonghibouth	22
OIH-02	Learning with PRIDE: A Decade of English Camp Innovation and Student Empowerment	- Dhunyawat Treenatea - Thanya Pakpoom	38
OIH-03	Moral Lessons in Children's Literature: A Content Analysis of Ethical Themes in Charlotte's Web for Higher Education	- Thanya Pakpooma - Dhunyawat Treenate	44
OIH-04	The Study of Problems found in the workplace during Co-operative Education of students from Rajamangala University of Technology Rattanakosin Bophit Phimuk Chakkrawat Campus	- Maswika Chaiyapooa - Rungrudee Na-on	51
PIH-01	Applying the Theory of Planned Behavior to Understand Electric Vehicle Purchase Intentions in Phra Nakhon Si Ayutthaya	- Adisai Watanaputia - Chitsanu Pakdeewanich - Nitinop Tongwassanasongc - Chadaporn Prasatkul	60
Session 2: Agricultural and Food Innovation			**66**
OIA-01	Influence of Fertigation on Growth, Yield, and Ratooning Ability of Sugarcane (Saccharum Officinarum L.) var. Khon Kaen 3	- Yuphadet Tesmee - Sodchol Woonprasaid - Nirut Khamchumphol - Thitiporn Machikowa	67
OIA-02	Utilization of Pectin from Pomelo Peel as the Stabilizer in Synbiotic Yyogurt	- Warakorn Seesuk - Chompoonuch Khonglaa - Sumalee Musikaa - Araya Ranoka - Chanida Kupradita - Kungnang Bunsroema - Seksan Mangkalanan	76
OIA-03	Enhancing Cassava Yield and Water Use Efficiency Through Drip Irrigation Controlled by Wireless Sensors and a Water Balance Model in Clay Loam Soil	- Watcharaporn Saiphoo - Sodchol Wonprasaid - Thitiporn Machikowa	85
OIA-04	Biogenic Amine Formation and Microbiological Profile in Asian Seabass and Short-Bodied Mackerel During Refrigerated Storage	- Watcharacha Krongkeha	91
OIA-05	Effect of Dictyophora Indusiata Powder and Purple Rice Flour on The Baking Quality Characteristics and Volatile Flavor of Cookies	- Yuyue Qin et al.	96
PIA-01	Natural Colorant from Chara corallina and Application in Ma Muang Bao Gummy Jelly	- Nopparat Mahaea - Donrudee Pichairata - Uraiwan Wattanakula - Wanninee Chankaew	110
PIA-02	Postharvest Preservation of Trimmed Coconuts: Evaluating Citric Acid, Sodium Chloride, and Peroxyacetic Acid Treatments	- Jeeranan Wongwatanyua - Sansanee Thimthongb - Nomjit Suteebutc - Sansanee Tempiamc - Supuksorn Masavang	115
PIA-03	Effects of Protein- and Carbohydrate-Based Foaming Agents on Foam Stability and Microstructure in Freeze-Dried Coffee	- Janyawat T Vuthijumnonk - Sureewan Rajchasom - Penwarat Panpatarachai - Maneerat Muangjai4	123

Code Paper No.	Topics	Aothors	Page
PIA-04	Comparative Evaluation of Antioxidant Potential and Basic Chemical Properties of Thai Honeys from Four Floral Sources	- Warawaran Shimbhanao - Sureewan Rajchasom1 - Janyawat ancharoenrat Vuttijamnong - Veerin Peerathamrongrat - Maneerat Mueangjai - Phowpinyo Shimbhanao	131
PIA-06	Enhancing Protein and Functional Properties of Gluten-Free Black Rice Flour and Tapioca Starch Pasta Fortified with Chicken Meat	- Supuksorn Masavanga - Duangkamol Tungsatitporna - Kasarin Pedcharata - Chompoonuch Phuenpipoba - Tinnapop Sompong	137
PIA-05	Characterization of a Commercial β-Mannanase: Activity and Molecular Weight Determination	- Chompoonuch Phuenpipoba - Chaleeda Borompichaichartkulb - Kittipong Rattanaporn	148
PIA-08	Role of Calcium Silicate for Growth Enhancement and Possibility to Alternaria Leaf Spot Control in Chinese Cabbage	- Santiti Bincadera - Nutthawoot Premjita - Tanawan Promkhlibnila - Arunee Kongsorna - Sirorat Khienmana - Chonlada Songnirundron - Thipwara Tiansawanga - Pisut Keawmaneec	155
PIA-10	Efficacy of Probiotic Yeasts in Controlling Vibrio parahaemolyticus and Vibrio harveyi in Whiteleg Shrimp (Litopenaeus Vannamei)	- Chakhriya Chalada - Wikit Phinrub	165
Session 3: Science and Engineering Technology			**170**
OIS-01	The Cytotoxicity and Alkaline Phosphatase Activity of Water-Soluble Extract from the Abalone Nacre on the Preosteoblast	- Nijjareeya Sirisriroa - Ruethairat Boonsombat	171
OIS-02	Sitting Posture Detection and Prevention of Office Syndrome Using MediaPipe Technology	- Panadda Solod - Napaphat Kongrit - Thapanic Teerapan - Wasu Suksuwan - Wannadear Nawae	175
OIS-03	Real-Time pH Monitoring and Automated Control System for Sustainable Aquaculture	- Wannadear Nawae - Wasu Suksuwan - Panadda Solod	181
OIS-04	IoT-Based Remote Monitoring and Alert System for Bedridden Patient Care in Thailand	- Teerayut Luengsrisakula - Natthawich Nilsakooa - Wutthikrai Buakaewa - Vorakamol Bookyayothinb - Nattasit Dancholvichit	186
OIS-05	Herbal Sheet-Free Peel-off Facial Mask Development from Cissampelos spp. Leaf Powder	- Wiphada Temrama - Araya Ranoka - Chanida Kupradita - Chompoonuch Khonglaa - Sumalee Musikaa - Seksan Mangkalanan	192
OIS-07	Analysis of the Advancement Technologies and Development Trends of Photovoltaic Module	- Pasist Suwanapingkarla - Surachet Dechphunga - Manat Boonthienthongaa - Nati Sukyama - Thanaporn Buakarna - Aphichat Saisuda - Kwanchanok Srivallop	200

SESSION 1
Humanities and Social Sciences

The Analysis on Writing Errors of 2nd Undergraduate Students at English Department, Faculty of Linguistics and Humanities, Savannakhet University, Lao People's Democratic Republic

Pakaysit Keomanyvanh[a], Wichai Pornmalairungruaeng[b*],
Lanta Ketoukham[a], Khounkham Nanthavongsa[a], Souvantha Keovongsa[a],
Dalavone Vonghibouth[a]

[a] English Department, Faculty of Linguistics and Humanities, Savannakhet University, Savannakhet Province, Lao PDR
[b] Faculty of Science and Technology, Rajamangala University of Technology, Thailand
*Corresponding author. Tel. (066)08-4991-5268; E-mail address: wichai.p@mail.rmutk.ac.th

Abstract

Writing is one of the most important skills in learning a new language. It can open up a world of possibilities for any student. Writing is one of the two productive skills in learning English that comes after speaking. As a productive skill, many college and university students struggle to master English writing. Researchers found that differences in English cause some problems that happen in students' English writing, and they do not know well how to make a good writing, lack vocabulary and errors made by students because grammatical errors especially sentence structure, words order, punctuation, spelling, subject-verb agreement. The purpose of this study was 1) to find out cause of errors students' writing at Department of English, Faculty of Linguistics and Humanities, Savannakhet University, 2) to explore the types of errors those are typical in their writing paragraph and 3) to identify the frequency of writing errors performed by English students as well. This study focused on writing paragraphs because the researchers found that errors in English students' paragraphs. The research used the mixed-method research design. The instruments used writing paragraphs for the students' writing assignment to identify the frequency of writing errors and questionnaires to find the error analysis of writing errors on the English written paragraphs. The result indicated that the most frequently committed errors were punctuation, while the least frequent performed errors were third person singular. Punctuations were the most frequently made error type (11.50%). Other error types were verb tenses (9.90%), word choices (9.58%), preposition (8.62%), capitalization (8.62%), spelling (8.30%), subject verb agreement (7.02%), fragment (6.38%), article (6.38%), using singular and plural forms (6.38%), words order (5.43%), run on sentences (4.79%), and third person singulars (1.59%). Several recommendations are put in the highlight to reduce further problems regarding writing English paragraphs.

Keywords: Analysis, Writing, Errors, Undergraduate Students

1. Introduction

Writing skills will help students to express their ideas in answering the paragraph and accomplishing their assignment from their teacher. The ability to write in any form will give many advantages in students' life as gaining success in their studies at school. Ms. Satya Sri Durga and Dr. C. S. Rao (2018). Good writing skills are needed for all students to accomplish their educational and employment requirements.

Savannakhet University is located in Savannakhet province in the central part of Laos. Savanakhet University is one of four universities in Lao PDR under higher education by the Ministry of Education and Sports. At Savanakhet University, there are eight faculties, 1 academic affair such Faculty of Agriculture and Environment, the Faculty of Business Administration, the Faculty of Linguistics and Humanities, the Faculty of Education, the Faculty of Natural Science, the Faculty of Food Science, the Faculty of Engineering, and and Faculty of Information Technical (IT). The international course is under the academic affairs office. There is also the Faculty of Linguistics and Humanities among the eight faculties. Savannakhet University was established in 2009. There were departments: Department of English, Department of French, and Department of Mass Media. In 2016 there was a Department of Vietnamese and a Department of Japanese in 2017. The Department of English is the first department in the faculty.

From the interviews with students and asking advisors as well as researchers monitoring writing skills in researchers' learning subject, researchers found that differences in English cause some problem that happens in students' English writing and they do not know how to make good writing, lack vocabulary and errors made by students because grammatical errors especially sentence structure, words order, punctuation, spelling, subject-verb agreement. So that Adrian Roscoe, Rahma Al-Mahrooqi, Vijay Singh Thakur (2014), mentioned that 4 major problems that they face in their writing are finding an apt word suitable for the topic, using appropriate tense base on the situation, using correct spelling and punctuation, organizing idea nearly and coherently paragraphs. Mohammedamin Hussen, (2015), found that problems of organization, unity, adequacy, grammar, punctuation, capitalization and spelling, lack of knowledge of strategic use, students' writing apprehension, shortage of vocabulary and lack of regular practice, and teachers' related factors such as teachers' ways of giving feedback. According to the scores of second-year students, the researcher found that writing subjects in the second year is difficult for students to understand and has low student potential.

From above students' writing problems are always a primary concern in writing classrooms, and knowing the common errors that frequently occur on students' writing papers is usually what the writing was conducted in the classrooms. This study seeks to study error analysis by focusing on the grammatical structure in writing due to it is

one of the important skills for students of English at Savannakhet University. The researchers conducted this error analysis by focusing on grammar due to error analysis plays an important role in language learning.

1.1 Objectives

1) To find out the cause of errors in students' writing skills.
2) To explore the types of errors those are typical in their writing paragraph
3) To identify the frequency of writing errors performed by English students.

1.2 Literature Review

1) Definition of errors

This definition is adequate to very the errors showing up in the same written text. An error is different from a mistake, so we have to be careful to differentiate them. Linguists have devised different definitions for the term "errors. According to Pham Vu Phi Ho (2015), the most internal and external problems faced by students in writing class and the impacts of students' understanding of their writing problems in implementing writing as self-assessment to promote students' writing skills. Taiseer Mohammed Y (2008) said that errors were classified and tabulated according to their number of frequencies in the student's essays. Jabeen (2015) stated that errors are made by second and foreign language (L2) learners to understand the strategies and techniques used in the process of second and foreign language learning.

2) Errors Analysis

s

Error analysis, as explored by various researchers, is a crucial approach in language learning, particularly in EFL contexts. It highlights that learners' errors are not solely due to interference from their native language but also reflect universal learning strategies. Studies suggest that analyzing these errors can help improve teaching methods, materials, and communication, thereby enhancing the overall language acquisition process.

3) Grammatical errors

Grammar is the most important aspect of writing. To make a well-structured writing, one should be matered in grammar. It consists of rules to change the meaning (morphology), arrangement of words (syntax), clause and phrase structure and the classification of part of speech (noun, verb, etc), and issues regarding cohesion and coherence of the whole text. Yasir Bdaiwi Jasim Al-Shujairi and Helen Tan (2017) found that several studies have been conducted to investigate the grammatical errors of Iraqi postgraduates and undergraduates in their academic writing. However, few studies have focused on the writing challenges that Iraqi pre-university students face.

The types of grammatical errors made in writing paragraph. Hourani (2008), mentioned that the most common and salient grammatical errors found in the students' essays included passivation, verb tense and form, subject-verb agreement, word order, prepositions, articles, plurality, and auxiliaries. Kanyakorn Sermsook1, Jiraporn Liamnimitr 1 & Rattaneekorn Pochakorn1 (2017), showed that the most frequently committed errors were punctuation, articles, subject-verb agreement, spelling, capitalization, and fragments, respectively. According to Kaladevi Subramaniam (2009), the six most common errors committed by the participants were singular/plural form, verb tense, word choice, preposition, subject-verb agreement, and word order. Charles Owu-Ewie and Miss Rebecca Williams (2017) identified that the lexical errors in the students' writing were due to homophone problems and semantic lexical errors. The grammatical errors identified were agreement errors, tense errors, singular-plural (number) errors, prepositional errors, and article errors and they found that the most frequently committed grammatical error was tense errors followed by agreement errors. (Murad Hassan Mohammed Sawalmeh, 2013) showed that in written essay errors; (1) verb tense, (2) word order, (3) singular/plural form, (4) subject-verb agreement, (5) double negatives, (6) spellings, (7) capitalization, (8) articles (9) sentence fragments and (10) prepositions. Dr. Ibrahim Mohamed Alfaki (2015) stated that the students make the errors and mistakes.

Dr. Amina Gogo Tafida and Dr Shittu Kelani Okunade, (2016), anyone who speaks or writes the English language without errors in subject/verb agreement, among others, is considered a good and an experienced speaker. One of the most difficult structural elements for EFL learners is the English article system (definite & indefinite). Saara Sirkka Mungungu , November (2010) found that the most frequently committed grammatical error was tense errors followed by agreement errors. Charanjit Kaur Swaran Singh (2017), revealed that subject-verb agreement and tenses were the most common types of errors.

4) Type of errors

There are two major differences in writing errors from analyzing learners' oral and written performance. According to Afifuddin (2016), the error types were identified and described, and then the grammatical error type made the most by those students. (Hsiao-ping Wu, 2014), showed that participants made more mistakes on interlingual/transfer errors than on intralingual/developmental errors. Rizky Edo Pratama (2015) stated that the type of this research is descriptive qualitative research. In collecting the data, the writer uses elicitation. there are three steps to collect data, namely (1) The researcher enter the class and asks students to make a descriptive text, (2) The researcher collects the data of students' writing then reads and marks the types of errors that occur in students' writing, (3) The researcher document the erroneous then classifies the type of errors based on linguistic category and surface strategy category. Siti Himmatul Auliya (2016-2017) showed the research was conducted to (1) describe the types of errors made by the second health analysis students of SMK Semesta Bumiayu in the academic year 2015/2016 in writing descriptive text and (2) describe the causes of the errors. Found in English learners' pieces of writing are analyzed and categorized into various categories. Errors are categorized according to their features by Dulay, Burt,

and Krashen (1982) into six different categories: omission of grammatical morphemes, double marking of semantic features, use of irregular rules, use of wrong word forms, alternating use of two or more forms, and misordering. (Lulu Meilina Alfiyani, 2013) based on the analysis of the grammatical errors, four types of errors were found. These four errors are as follows. Omission error was found 281 times, misformation error was committed 119 times, addition error occurred 189 times, and misordering errors 6 times in the analysis.

Moh Hussain Akbary (2017) revealed that most common and frequent error made by the students were79 places of word choice errors, 48 places of subject-verb agreement errors, 46 places of preposition errors, 35 places of verb tense and form errors, 31 plurality errors, 28 sentencesprawl errors, 23 run-on errors, 15 article errors, 14 to be verb errors, and 13 word order errors. Based on these findings, teachers are suggested to raise students' awareness of these errors and provide sufficient remedies to prevent students from internalizing such errors. Faiza Hawa, Rahma Sukmningum, and Oscar Yustino (2016) revealed that second-semester students commit several errors in their paragraphs. Those are verbs tense, subject-verb agreement, fragment and capitalization, spelling, word order, use of pronoun, preposition, and article. The types of errors and the linguistics levels present the most errors in their writing. Pimpisa Rattanadilok Na Phuket, Associate Professor Dr. Normah Binti Othman (2015) showed that the most frequent types of errors were translated words from Thai, word choice, verb tense, preposition, and comma. The errors derived from two sources: interlinguas and intralinguas.

Studies on learners' writing errors highlight that common mistakes stem from both interlinguas and intralinguas sources. Frequent errors include issues with word choice, verb tense, subject-verb agreement, and word order. Researchers emphasize the importance of raising students' awareness of these errors and providing effective strategies to prevent them in future writing.

5) The cause of errors

The causes of errors can be explained by referring to language theories and learning theories. According to Ibrahim Mohamed Alfaki (2015: pp.40), university students have various writing problems: language problems at the levels of morphology and syntax; usage errors and mechanical mistakes, that is, spelling, punctuation, and capitalization; lack of several writing development skills; cognitive problems; and graphomotor problems. Huwari & Al-Khasawneh (2013: pp.35) revealed that grammatical weakness, knowledge and understanding, less practice, and educational background were the main themes discovered by the students. Huwari & Al-Khasawneh (2013: pp.35) concluded that the fear of teacher's negative comments, linguistic difficulties, pressure of time and perfect work, insufficient writing practice, and problems with topic affect a lot while writing in English. Sermsook et al. (2017: pp.101) found that errors in Thai EFL students' sentence construction may lead to miscommunication. Souriyavongsa, Rany, Jafre Zainol Abidin, & Lai Mei (2013: pp.179) found that the main causes have been included namely: first, the majority of students stated that the English teachers are not well-trained; for instance, they use Lao language when teaching, so they cannot perform well to attract the interest of the students. Secondly, students lack an English foundation background. Third, students lack the confidence to use English because they are afraid of making mistakes and feeling shy. Fourth, the curriculum is inappropriate for helping students improve their English proficiency. Last, the English language is difficult to learn due to students not being well-motivated, encouraged, and having gained learning strategy. Adetuyi (2019) contends that these errors provide useful starting points for a person who teaches scholarly writing. Tashi (2018: pp.7) showed that Bhutanese foreign language learners committed errors both intralingually and interlingually.

The causes of writing errors can be attributed to various factors, including linguistic difficulties, lack of practice, cognitive challenges, and inadequate educational backgrounds. Research highlights issues such as grammatical weaknesses, fear of negative feedback, time pressure, and insufficient writing practice. Additionally, factors like low confidence, untrained teachers, and inappropriate curricula contribute to learners' struggles with English writing. These findings suggest that addressing these underlying causes is crucial for improving students' writing skills.

5.1) Limited Knowledge of Vocabulary

Vocabulary is one of most important factors that support students for mastering language skills and it is the basic element of language that will make language meaningful. Vocabulary, as one of the elements of language, is important to study because, without adequate vocabulary mastery, the ability to communicate and to convey cannot be established. The learning of vocabulary is an important part of foreign language learning. Susanto (2017: pp.182) said that vocabulary is considered as central in language teaching and is of paramount importance to a language learner. Vocabulary was to find out kinds of difficulties faced by students and factors of students' difficulties in vocabulary learning. Rohmatillah (2014: pp.69) said that kinds of difficulties faced by the students were (1) most almost all of the students have difficulties in pronouncing the words, (2) how to write and spell, (3) the different grammatical form of a word known as inflections was one of causes of students difficulties in learning vocabulary. Farjami (2013: pp.1) presented that practical vocabulary learning strategies can help learners and offer influential teaching techniques and activities, which are of help to the teachers. Alqahtani (2015: pp.21) stated that vocabulary learning is an essential part in foreign language learning as the meanings of new words are very often emphasized, whether in books or classrooms. Alfaki (2015: pp.1) stated that the characteristic features of the lexical items included in book five: their total number, frequencies, recycling, and usefulness for learners, and suitability to learners' level, grading and presentation. Hosni (2016: pp.5) mentioned that the significance of academic vocabulary in L2 writing has widely been recognized in some of the studies with little research on it.

Vocabulary plays a crucial role in mastering language skills, as it is the foundation of communication and meaning. Adequate vocabulary knowledge is essential for effective language use, and difficulties in vocabulary

learning, such as pronunciation, spelling, and understanding word inflections, are common challenges faced by students. Effective vocabulary learning strategies, as well as teaching techniques, can support students in overcoming these challenges. Additionally, the significance of academic vocabulary in second language writing is increasingly recognized, emphasizing the importance of well-designed vocabulary instruction tailored to students' levels and needs.

5.2) Learners' Lack of Motivation

Dislen (2013: pp.35) mentioned that motivation has been the centre of attention among teachers throughout the years because it constitutes the backbone of the learning process. Win (2018: pp.224) found that the students lack motivation and interest. Wagiyo (2018: pp.1) found that most students have little motivation to learn English. Hamidun, Hashim, & Othman (2013: pp.591) found that the feedback provided to the students' writing gave a signification increase in the students' level of motivation in writing. Wimolmas (2012: pp.904) showed that the students are relatively "highly" motivated and found to be slightly more "instrumentally" motivated to learn English. Asmali (2017: pp.360) indicated that parents, teachers, and favorable learning conditions and activities were important factors in determining young learners' attitudes and motivation to learn English. Wimolmas (2012: pp.904) showed that some potential and incorporates reading skills with writing, grammar, peer crique and discussion. Rahman et al. (2017: pp.63) showed that teachers ' personal attitudes and parental influence do have an influence on students' motivation to learn a second language. Man (2010: pp.85) found that English journal writing can be promoted as an extensive activity to improve students' writing skills, build up the rapport between the teacher and the students, as well as enhance their writing motivation, enjoyment, and attitude towards English writing.

Motivation is a key factor in the learning process, particularly in language acquisition. Several studies have shown that lack of motivation is a common issue among students, affecting their interest and engagement in learning English. However, factors such as teacher feedback, parental influence, and favorable learning conditions can significantly boost students' motivation. Additionally, activities like journal writing have been found to improve writing skills, foster positive attitudes toward English, and enhance motivation. Understanding and addressing these motivational factors can play a critical role in improving students' language learning outcomes.

5.3) Students' Lack of English Foundation Background.

Sa'ad & Usman (2014: pp.41) found that the dominance of mother tongue, inadequate qualified teacher of English language, negative attitudes of students toward English language, improper use of method in teaching English language, inadequate instructional media and facilities, lack of language laboratory of teaching English language are cause of poor performance in English language among secondary school students of Dutse metropolis of Jiawa state. Ismagulova, Polevaya, Balgabayeva, Kulakhmetova, & Kapanova (2016: pp.4194) showed the need to introduce a special discipline in the educational process for the development of academic skills. Alsanie, Alrezqi, Al-Sayeud, & Shukri (2018: pp.306) indicated that extensive writing classes must be given to students to improve their writing skills and that the writing topics must be contextualised and taken from the students' daily life to keep them interested. Matthew Kraft (2017: pp.139) found that empirical evidence for the well-established theory on the multidimensional nature of teaching and the need to identify strategies for improving the full range of teachers' skills.

Various factors contribute to poor performance in English among students, including the dominance of the mother tongue, inadequate teacher qualifications, negative attitudes towards English, and insufficient teaching resources. Studies emphasize the importance of introducing specialized courses to develop academic skills and promoting extensive writing practices that are relevant to students' daily lives. Additionally, enhancing teacher training and identifying strategies to improve teaching skills are crucial for improving student outcomes in English language learning. Addressing these challenges can help create a more effective and engaging learning environment for students.

5.4) Students' Lack of Confidence

Lack of confidence is a headache for both the teachers and the learners, especially at the University level. Arango (2015: pp.1) mentioned that self-confidence is one of the most influential variables that affect foreign language learning. Nurhayati, Rosmaiyadi, & Buyung (2017: pp.13) showed that the collaborative learning model can improve students' self-confidence. Jamila (2014: pp.10) found that students overcome their lack of confidence for ensuring better oral communication being the members of the global community. Telbis, Helgeson, & Kingsbury (2014: pp.330) revealed that students who scored in confidence for completing their programs of study also scored low on their confidence of these four aforementioned issues.

Lack of confidence significantly affects foreign language learning, particularly at the university level. Studies highlight that self-confidence plays a crucial role in students' success. Collaborative learning models have been shown to improve students' self-confidence, while overcoming this barrier is essential for better oral communication and integration into the global community. Additionally, students with higher confidence in their abilities tend to perform better academically, underscoring the importance of fostering a positive, supportive learning environment to boost students' self-assurance.

5.5) Grammatical Weakness

The traditional grammar classes can often follow a teacher-led, sequential pattern, which may arguably be of benefit to early learners of a similar level in their second language course. Al-Khasawneh (2013: pp.14) revealed that grammatical weakness, knowledge and understanding, less practice, and educational background were the main themes discovered by the students. Jairos Gonye (2012: pp.71) revealed that the first year undergraduate university students' written papers are riddled with a multiplicity of weaknesses, and suggests that students should view writing as different from speech and that they should treat writing as a process rather than a product. Dyan (2010:

1) showed that there was an improvement in the students' writing skills. Jim Christzer I. Pablo (2018: pp.46) showed that the students have difficulties in writing academic essays such as lack of varity of ideas in terms of content and ideas, lack of connectives in terms organization, incorrect word or idiom and usage in terms vocabulary and word choice, poor sentence structures in terms of language use, use of first person pronoun in terms of formality and objectivity, and lack of citations in terms of referencing.

Grammar can be beneficial for early learners, especially when taught in a structured, teacher-led approach. However, many students face challenges in their writing, including grammatical weaknesses, limited practice, and lack of understanding. Issues such as poor sentence structure, vocabulary misuse, and improper organization are common, particularly in academic writing. It is crucial for students to view writing as a process rather than just a product and to be mindful of the differences between spoken and written language. Addressing these weaknesses through targeted practice and feedback can significantly improve students' writing skills.

The literature review shows the extent to which scholars explore errors in students' writing, especially within the context of Savannakhet University. A detailed analysis of the literature on error analysis showed that there is no significant difference between the errors detected in writing paragraphs in EFL contexts. This highlights the complex nature of the writing process in the English language especially by non-native speakers of English. However, with all these numerous studies, especially at various Savannakhet University, the researchers are yet to find a study that has to explore errors within students' writing in the context of the Savannakhet University. It is based on the gap that this study seeks to explore the type of errors that typify the paragraph of the second-year students of Savanakhet University.

2. Methodology

The research used the mixed-method research design because the analysis is purely descriptive. Though there are some instances whereby the study uses some frequency counts to rate errors identified in the students' writing, it is an undeniable fact that the research skews towards the descriptive approach. The study adopted the qualitative and quantitative research designs because both research designs typically make use of in-depth and verbal description in place of numerical data. The study is aimed to analyze and to explain what dominant type of grammatical errors in English Department's students, Savannakhet University make in writing skills, to find out what the cause of the errors are and to explore the frequency of writing errors performed by English students.

The population of this study was 50 students who have been studying English the 2ⁿᵈ year at the Department of English, Faculty of Linguistics and Humanities, Savannakhet University.

The population of the study consisted of 2ⁿᵈ year English students in the Bachelor of Art program at the Department of English during the second semester of the academic year 2023-2024. They consist of 50 students. Based on using the Krejcie & Morgan formula to randomize, there are 44 people that they had used for the sample group in this research. The sample group is 44 of 50 students at the Department of English, Faculty of Linguistics and Humanities, Savannakhet University.

Participants	Sample groups	Participants	Sample groups	Participants	Sample groups
10	10	120	92	500	217
20	19	140	103	600	234
30	28	160	113	700	254
40	36	180	123	1000	278
50	**44**	200	132	1500	306
60	52	250	152	2000	322
70	59	300	169	5000	357
80	66	360	186	10000	370
90	73	400	196	50000	381
100	80	460	210	100,000	384

Figure 1 The Krejcie & Morgan simulation to calculate the sample size
Source: The Krejcie and Morgan stimulation (1970)

The instrument used was writing paragraphs for the students' writing assignment. It was vital to note that the error analysis used in this study focuses on grammarticle especially on the run on sentences, words orders, punctuations, spellings, subject-verb agreements, capitalizations, word choices, articles, prepositions, fragments, verb tenses, third person singulars, and singular and plural as well as frequency of writing errors performed by English students And also using questionnaire to find the error analysis of writing errors on the English written paragraph produce by the subjects of the study during their class in academic year 2023-2024.

In writing, students' assignment wrote a paragraph during the course as normal curriculum. Apart from the paragraph, to encourage students to practice their writing skills. The topics for writing analyses are time-consuming.

Three errors were addressed in this study: grammar errors. The errors made by students are grammatical errors, especially in sentence structure, word order, punctuations, spelling, subject-verb agreements, capitalizations, word choices, articles, prepositions, fragments, verb tenses, third person singulars, and singular and plural. The researchers gave the students a topic /1 paragraph.

The researcher asked them to use their free time in writing; they could produce any writing on the topic. The purpose of the researcher is to assign students to write 3 times on the old topic to help the 2nd year students get used to writing in a foreign language and to improve their writing fluency. At the end of the course, they submitted their writing to the researcher for data analysis.

After collecting students' writing assignments, their work was retained for use in this study; each writing was analyzed for errors and the errors recorded. First, the researcher will count the words in every writing to explore the types of errors that are typical in their writing paragraph and to identify the frequency of writing errors made by English students. Second, the researcher will analyze the errors in their writing. Errors will see as mostly frequent errors appear in the students' writing by checking from native speaker who come from United State and she is an English volunteer teacher from U.S Embrassy to teach English at English Language. The data analyzed on the writing samples is followed by a detailed discussion on both of them. It included lack of vocabularies, paragraph structure and six grammatical categories: sentence structure, words order, punctuation, spelling, and subject-verb agreement.

The errors in the students' writing were analyzed as following examples of the coding scheme in the table below.

Table 1 Coding scheme for error analysis

Categories	Definitions	Examples of errors	Corrections
Articles	Articles: An article is a word that is used with a noun to indicate the type of reference being made by the noun. English has two articles: **the** and **a/an**. **The** is used to refer to specific or particular nouns; **a/an** is used to modify non-specific or non-particular nouns. We call the the definite article and a/an the indefinite article. • the=definite article • a/an=indefinite article (Artical, https://owl.purdue.edu/owl/general_writing/grammar/using_articles.html)	• My daughter really wants **dog** for Christmas. • Somebody call **policeman.** • When I was at the zoo, I saw **a elephant**. • I am teaching at **the** Savannakhet University. • If I say, Let's read book.	• My daughter really wants **a dog** for Christmas. • Somebody call **a policeman.** • When I was at the zoo, I saw **an elephant.** • I am studying at Savannakhet University. • If I say, "Let's read **the** book.
Fragment	A sentence fragment is a group of words that looks like a sentence, but actually isn't a complete sentence. Sentence fragments are usually missing a subject or verb, or they do not express a complete thought. While it may be punctuated to look like a complete sentence, a fragment cannot stand on its own. (https://writingcenter.ashford.edu/sentence-fragments)	• There are lots of mistakes. If you look closely at her work. • Ashley hasn't arrived yet. The girl who's bringing the cake. • Although the result of the study was inconclusive. • If the result of the study confirmed the writer's hypothesis.	• If you look closely at her work, you'll see there are lots of mistakes. • Ashley, the girl who's bringing the cake, hasn't arrived yet. • Although the result of the study was inconclusive, the committee decided to implement the policy. • If the result of the study confirmed the writer's hypothesis, it would be a major breakthrough in the world of biochemistry.
erb tenses	The verb tense tells you when a person did something or when something exist or happened. In English, there are three main tenses: the present, the past, and the future.	• He **had** fair hair and blue eyes; some birds **ate** worms and insects.	He **has** fair hair and blue eyes; some birds **eat** worms and insects.
Singular and plural forms	The difference between singular and plural nouns is easy to spot. When a **noun** indicates one only, it is a singular noun. When a noun indicates more than one, it is plural. (https://www.gingersoftware.com/content/grammar-rules/nouns/plural-nouns/)	• The **boy** were throwing **baseball** back and forth between **base**. • Our horse are much happier wearing lightweight English saddle. • Those **cat** never seem to tire of chasing one another in and out of those **box**. • You stole my **idea** and didn't give me any credit. • Our **mom** are going to be upset that **we** stayed out all night going to **party**. • I can't believe you allow your **dog** to climb all over the **seat** while you are driving.	• The **boys** were throwing **baseball**s back and forth between **base**s. • Our **horses** are much happier wearing lightweight English **saddles.** • Those **cats** never seem to tire of chasing one another in and out of those **boxes**. • You stole my **ideas** and didn't give me any credit. • Our **moms** are going to be upset that **we** stayed out all night going to **parties**. • I can't believe you allow your **dogs** to climb all over the **seats** while you are driving
Word choice	Using a word that sounds similar to the intended word but has a different meaning is one of the most common	Attained and obtained	8. The sensors **obtained** steady state reading at high temperature.

Categories	Definitions	Examples of errors	Corrections
	errors in word choice. Among native speakers, such an error is often just a slip of the tongue. Among non-native speakers, however, it could be the result of genuine confusion. (https://www.editage.com/insights/6-types-of-word-choice-errors-in-scientific-writing)	2. The sensors **attained** steady state readings at high temperatures. 3. The **principle** components of the thermochemical state were used to derive the transport equations. 4. The **poles** were displaced in the direction of the applied pressure. 5. We have **devised** a method to calculate the exergy efficiency. 6. **Alternate** measures were developed to reliably calculate the losses. 7. Thee structure changes were **determinated** through microscopy studies.	9. The **principal** components of the thermochemical state were used to derive the transport equations. 10. The **pores** were displaced in the direction of the applied pressure. 11. We have developed a new method to calculate the exergy efficiency. 12. **Alternative** measures were developed to reliably calculate the losses. 13. The structural changes were **determined** through microscopy studies.
Word orders	Word order is important: it's what makes your sentences make sense! So, proper word order is an essential part of writing and speaking—when we put words in the wrong order, the result is a confusing, unclear, and an incorrect sentence. (https://englishsentences.com/word-order/)	• 2 brothers and 2 sisters have I at home. • In middle school I am. • You are how today?	• I have 2 brothers and 2 sisters at home. • I am in middle school. • How are you today?
Spelling	A way of pronouncing a word which is based on its spelling and which may differ from the way the word is generally pronounced. (Richards & Schmidt, 2010)	• **Use to, used to** • I **used** to shop at that store. ('Used to' is a habit done in the past.) • This is the car I'll **use to** drive to the shore. ('Use to' is a verb meaning to utilize something in the present.) • **break and brake** • I'll need a **break** before going back to work. ('Break' means to separate or interrupt.). • This car needs a new set of **brakes**. ('Brake' is a mechanism for slowing down or stopping.) • **complement, compliment** • That pink blouse **complements** your gray pants. ('Complement' means to make complete or makes perfect.) • My instructor gave me a **compliment** on my essay. ('Compliment' means to give praise.) • **advice, advise** • Diane gave him great **advice.** ('Advice' means to give recommendation.) • The doctor will **advise** you about which exercises work best. ('Advise' is a verb that means counsel.) (https://study.com/academy/lesson/spelling-mistakes-common-examples-quiz.html)	
Punctuation	Punctuation is the collection of marks that we use to make sentences flow smoothly and express meaning clearly. It tells us when to pause or add a certain feeling to our words; it separates ideas so that sentences are clear, it points out titles, quotes, and other key parts of language punctuation is important	• The fox was **fast sneaky** and quiet in the forest. • Billy likes **pancakes** he ate them every day for breakfast. • The car costs **$10000,** I am going to buy it. • Before going to the **school Joe** stopped at my house. (https://www.copyblogger.com/punctuation-mistakes/)	• The fox was **fast, sneaky,** and quiet in the forest. • Billy likes **pancakes;** he ate them every day for breakfast. • The car costs **$10000.** I am going to buy it. • The car costs **$10000, and** I am going to buy it. • Before going to the **school, Joe** stopped at my house.
Subject-verb agreement	The inflection of the verb to correspond or agree with the subject of the sentence, as in the third person present tense of verbs in English which is marked by adding "s" (Richards & Schmidt, 2010) Example: • Interviews **are** one way to collect data and allow researchers to gain an in-depth understanding of participants.	• Annie and her brothers **is** at school. • Either **my mother or my father** are coming to the meeting. • **The dog** or the **cat are** outside. • Either my shoes or your coats **is** always on the floor. • George and Tamara **doesn't** want to see that movie. • Benito **don't** know the answer. • One of my **sister are** going on a trip to France.	• Annie and her brothers are at school. • Either my mother or my father **is** coming to the meeting. • The dog or the cats are outside. • Either my shoes or your coat is always on the floor. • George and Tamara **don't** want to see that movie. • Benito **doesn't** know the answer • One of my sisters **is** going on a trip to France.

Categories	Definitions	Examples of errors	Corrections
	• An assumption **is** something that is generally accepted as true and is an important consideration when conducting a doctoral study.	• The man with all the birds **live** on my street. • The movies, including all the previews, **takes** about two hours to watch. (https://owl.purdue.edu/owl_exercises/sentence_structure/subject_verb_agreement/subject_verb_agreement_exercise_answers.html)	• The man with all the birds **lives** on my street. • The movie, including all the previews, **takes** about two hours to watch.
Preposition	A preposition is a word that shows the relationship between a noun or pronoun and other words in a sentence. (https://7esl.com/mistakes-with-prepositions/)	• I cannot agree **to** you in this situation. • She is **waiting the** arrival of the postman. • Please wait **inside** the white line. • I have been waiting **from** three hours. • He reached **at** the airport at 3 pm. • We should pay our bills **in** time. • He was prevented **to** come. • I met **with** your friend. • She insisted **to** pay.	• I cannot agree **with** you in this situation. • She is waiting **for** the arrival of the postman. • Please wait **behind** the white line. • I have been waiting **for** three hours. • He reached the airport at 3 pm. • We should pay our bills **on** time. • He was prevented **from** coming. • I met your friend. • She insisted **on** paying.
Gerund	A **gerund** always acts as a noun. A present participle is always part of a verb phrase. The gerund is a common part of speech that most of us use every day, whether we know it or not. Here, we'll take an in-depth look at gerunds and provide you with several examples of gerunds so you'll feel comfortable using them in your writing, and so that you will be able to recognize them when you see them. (https://www.gingersoftware.com/content/grammar-rules/nouns/gerunds/)	• They were counting on me helping them. • They insisted on me resigning the post. • I am thinking to write my autobiography. • The clever girl was confident to win the first medal. • I am hopeful to secure a loan to build my house. (https://www.englishpractice.com/common-mistakes/common-errors-gerunds/)	• They were counting on my helping them. • They insisted on my resigning the post. • I am thinking of writing my autobiography. • The clever girl was confident of winning the first medal. • I am hopeful of securing a loan to build my house.
Capitalization	Writing a word with it is first letter as a capital letter and the remaining letters in small letter. (https://virtualwritingtutor.com/practice/capitalization_correct.htm)	• **what** is your name? • **this** is the first tim **i** have met some with that name. • **my** name is john. I am from **montreal, quebec, canada.** • I study applied linguistics at **concordia university.** • My professor is **canadian**, too. • She speaks English, **french** and **korean.** • My baby brother was born on **september** 7th, 2011. • He was born on a **wednesday.**	• **What** is your name? • **This** is the first time **I** have met some with that name. • **My** name is john. I am from **Montreal**, **Quebec, Canada**. • I study applied linguistics at **Concordia University.** • My professor is **Canadian**, too. • She speaks English, **French** and **Korean.** • My baby brother was born on **September** 7th, 2011. He was born on a **Wednesday**
Conjunction	Conjunction is a word that connects or joins clauses, words, phrases together in a sentence. Conjunctions are used to coordinate words in a sentence. "But", "although", "while" are some common conjunctions. Three types of conjunctions are Coordinating Conjunctions, Subordinating Conjunctions, and Correlative Conjunctions. Let us learn the types and examples of conjunctions and their correct use. (https://www.toppr.com/guides/english/conjunction/introduction-to-conjunctions/)	• The teacher asked that why I was late. • When I reached there then it was raining. • Unless you do not try, you will never succeed. • Not only he abused me but also beat me. • Though he is fat, still he runs fast. • She did not come to school. Because she was ill. (http://www.perfectyourenglish.com/grammar/conjunctions-common-errors.htm)	• The teacher asked **why** I was late. • **When** I reached there, it was raining. • **Unless** you try, you will never succeed. • **Not only did** he abuseme **but** he also beat me. • **Though** he is fat, he runs fast. • She did not come to school because she was ill.

For the questionnaire, researchers coded manually and analyzed statically by using an algorithm. Descriptive statistics of data are computed, and the mode is used as a central tendency measure to find out the cause of errors in students' writing skills.

The data from this study the research bring to analyze as following:

Bring the questionnaire that finished check to analyze by using algorithm to calculate the statistics as frequency, mean ($\bar{x}$) and standard deviation (S.D). The percentage is used to calculate describing in the first section from question interview as general information.

Mean ($\bar{x}$) and standard deviation (S.D.) are used to analyze the second section of the question interview as the benefit of them for measurement the importance.

The research used questionnaires of scale by rating a scale of 1- 5 to measure the level of the importance factors as follows:

Average means score between 5.00 – 4.20=Strongly agree.
Average means score between 4.19 – 3.40=Agree.
Average mean score between 3.39 – 2.60=Moderate.
Average mean score between 2.59 – 1.80=Disagree.
Average mean score between 1.79 – 1.00=strongly disagree.
By: (Likert Scale, 1932)

The percentage analyzed the sample group's answers. The data was inputted into the SPSS Program to estimate the level for the Arithmetic mean of the 4-point Likert format. In the first step of data analysis, a table of frequency is used to present the data in percentages, means regarding scaled data of writing assignments and interviews. The analysis is carried out by identifying the lowest and the highest value of the mean ($\bar{x}$), interpreting it for the results of the study. After that, paired samples t-test run and standard deviation (S.D.) to identify the developmental patterns of the errors across tasks. Then, a correlational analysis was conducted to examine how the errors related to the students' writing performance. Meanwhile, the survey data is analyzed in terms of frequency and percentage to reveal the perceptions on the difficulties and possible causes for making paragraph errors in their English writing.

The research evaluated types of grammar errors they made in students' writing. The techniques of the data analysis were firstly through calculating the frequency of errors in each category and obtaining quantitative data of the errors into each of category. The percentages of the dominant errors were calculated by using the following formula:

$$P = \frac{F \, X \, 100}{N}$$

P= percentage.
F= frequency of errors.
N= total errors.
Next, the errors were explained in a detailed discussion based on the category of error

Average

Average is the middle or typical number of a list of numbers; different concepts of average are different contexts. Often "average" refers to the sum of the number divided by how many numbers are being averaged, in mathematics and statistics, this will be called the arithmetic mean. In statistics, mean, median, and mode are all known as measures of central tendency and in colloquial usage, sometimes any of may be called an average value.

$$\bar{X} = \frac{\sum X}{N}$$

x: Represents the average
∑X: Represents the summation
N: Represents the number of scores

Standard deviation (S.D.)

In statistics, the standard deviation (S.D.) is a measure that is used to qualify the amount of variation or dispersion of a set of data values. A low standard deviation indicates that data points tend to be close to the mean of the set, while a high standard deviation indicates that the data points are spread out over a wider range of values.

$$S.D. = \sqrt{\frac{\sum(X - \bar{X})^2}{N - 1}}$$

S.D.: Represents the average
$\sum X$:Represents the summation
X: Represents each value of the population
$(\bar{X})$:It is the mean value of the sample
N: It's the number of the sample

30

3. Results

This chapter presents the results and discusses what has been mentioned in the research questions. First; the overall results of the study have been presented, followed by the Analysis of Errors Writing Skills of 2nd Undergraduate Students at English Department, Faculty of Linguistics and Humanities, Savannakhet University.

3.1   Gender

Table 1: Gender

No	Gender	Frequency	Percent
1	Male	19	43.20
2	Female	25	56.80
	Total	44	100.00

Table 1: shows the proportion of male and female English students. There were 25 females, equal to 56.80%, and 19 males, equal to 43.20 %. The difference in gender did not affect the overall result of the study, as gender was not the main variable to measure and compare.

3.2   Cause of students' errors in writing paragraph.

This section presents the results, which aim to give answers to the first research questions: What are the causes of errors in their writing skills?

The results obtained from this study revealed that the cause of errors in students' writing skills.

Table 2: the causes of errors in their writing skills

No.	The causes of errors in their writing skills	Mean	S.D.	Interpreter
1	I have various writing problems: language problems at the levels of morphology and syntax; usage errors and mechanical mistakes, that is, spelling, punctuation, and capitalization; lack of several writing development skills; cognitive problems; and graph motor problems	3.37	0.76	Moderate
2	I have difficulties in pronouncing the words	3.58	0.69	Agree
3	The different grammatical form of a word known as inflections was one of causes of student's difficulties in learning vocabulary.	3.21	0.85	Moderate
4	I have little motivation in learning English	3.32	0.88	Moderate
5	Parents, teachers, and favorable learning conditions and activities were important factors in determining young learners' attitudes and motivation to learn English.	3.11	0.73	Moderate
6	The collaborative learning model can improve student's self-confidence	3.32	1.05	Moderate
7	The scored in confidence for completing their programs of study also scored low on their confidence of these four aforementioned issues.	3.42	1.12	Agree
8	I have difficulties in writing such as a lack of verity of ideas in terms of content and ideas, lack of connectives in terms of organization, incorrect word or idiom and usage in terms of vocabulary and word choice, poor sentence structures in terms of language use, use of first-person pronoun in terms of formality and objectivity, and lack of citations in terms of referencing	3.95	0.91	Agree
	Total	3.32	0.08	Moderate

As shown in Table 3 the results present that I have difficulties in writing academic essays such as lack of variety of ideas in terms of content and ideas, lack of connectives in terms of organizations, incorrect word or idiom and usage in terms of vocabulary and word choice, poor sentence structures in terms of language use, use of the first-person pronouns in terms of formality and objectivity, and lack of citations in terms of referencing shown in this table were at the highly level of frequency (mean=3.95 and S.D.=0.91). This might imply that I have difficulties in pronouncing the words (Mean=3.58 and S.D.=0.69), followed by "The scored in confidence for completing their programs of study also scored low on their confidence of these four aforementioned issues" (Mean=3.42 and S.D.=91).

3.3   The types of errors are typical in students' writing paragraphs.

This section intends to show the results, which aim to give answers to the second research questions: What are the types of errors that are typical in their writing paragraph? The results obtained from this study revealed that the students committed many writing errors when writing English paragraphs.

Table 4: Writing Errors Committed by Students when Writing English Paragraphs.

No	Types of writing Errors
1	Prepositions
2	Articles
3	Words orders
4	Using singular and plural forms
5	Verb tenses
6	Word choices
7	Spellings
8	Subject verb agreements
9	Punctuations
10	Conjunctions
11	Gerunds
12	Capitalizations
14	Fragments

As shown in Table 4, the results revealed that Savanakhet University students have committed several types of errors when they were writing English paragraphs. These errors include prepositions, articles, using singular and plural forms, verb tenses, spellings, subject-verb agreements, punctuations, conjunctions, gerunds, capitalizations, word orders, and fragments.

3.4　Frequency of Writing Errors Committed by the Students

This section presents the results, which aim to give answers to the third research question: How frequently do writing errors occur in the students' written paragraphs? The results obtained from this study revealed that the students committed writing errors in frequently way.

Table 5: Frequency of Writing Errors Committed by the Students.

No	Types of writing Errors	Frequency	Percentage
1	Prepositions	27	8.62%
2	Articles	22	7.02%
3	Words orders	17	5.43%
4	Using singular and plural forms	20	6.38%
5	Verb tenses	31	9.90%
6	Word choices	30	9.58%
7	Spellings	26	8.30%
8	Subject verb agreements	22	7.02%
9	Punctuations	36	11.50%
10	Conjunctions	15	4.79%
11	Fragments	20	6.38%
12	Capitalizations	27	8.62%
13	Gerunds	15	4.79%
	Total	**313**	

As shown in Table 5, the students committed several errors when writing English paragraphs. The most frequent error was the wrong use of punctuation, while the least frequent performed errors were third person singular. Punctuations were the most frequently made error type (11.50%). Other error types were verb tenses (9.90%), word choices (9.58%), prepositions (8.62%), capitalizations (8.62%), spellings (8.30%), subject-verb agreements (7.02%), fragments (6.38%), articles (6.38%), singular and plural forms (6.38%), word orders (5.43%), conjunctions (4.79%) and gerunds (4.79%).

A deeper analysis of the errors revealed that the fourteen types of errors found to be the greatest difficulties of the participants were punctuation, verb tenses, word choices, prepositions, capitalizations, spelling, subject-verb agreements, fragments, articles, using singular and plural forms, words orders, and gerunds respectively.

Table 6: Most Frequent Errors, Examples of Errors and Corrections

Categories	Definitions	Examples of errors	Corrections
Words order	Word order is important: it is what makes your sentences make sense! Therefore, proper word order is an essential part of writing and speaking- when we put words in the wrong order, the result is a confusing, unclear, and an incorrect sentence.	• I study in class **in the morning at 8:30** every day. • I am studying **English a foreign language. Department of English faculty of Linguistics**. • I have lunch **at 12:00 at the lunch time in the University.**	• I study **in the class at 8:30 in the morning** every day. • I am studying **English as a foreign language, at Department of English, Faculty of Linguistics and Humanities.** • I have lunch in university at 12:00.
Spelling	A way of pronouncing a word which is based on its spelling and which may differ from the way the word is generally pronounced.	• I have lunch at the **resturant** in **the shcool** with my friends. • I **stream** rice. • My first class **beging** at 8: 00.	• I have lunch at the **restaurant in school with my friends.** • I **steam rice** • My first class begins at 8: 00.
Punctuation	Punctuation is the collection of marks that we use to make sentences flow smoothly and express meaning clearly. It tells us when to pause or add a certain feeling to our words; it separates ideas so that sentences are clear, it points out titles, quotes, and other key parts of language punctuation is important.	• **Every morning** I get up at 6:30 **AM I** make my **bed after that** I go to bathroom. • I do some **exercise I** put my clothes **on then** I prepare my school **bag and** go to **school**. • I go the scond class. **Afterthat** I go to have lunch **break** and lunch with my friends.	• Every morning, I get up at 6:30 **AM. I** make my bed. **After that,** I go to bathroom. • I do some exercise, I put my clothes on**. Then I** prepare my school bag, and go to school. • I go to the second class. **After that,** I go to have a lunch **break.** Then I have lunch with my friends.
Subject-verb agreement	The inflection of the verb to correspond or agree with the subject of the sentence, as in the third person present tense of verbs in English which is marked by adding "s"	• **I always wakes** up at 7 O'clock. • **I studying** English in Savannakhet University. • I and my sister **goes** to school by bus.	• **I always wake** up at 7 O'clock. • **I am studying** English in Savannakhet University. • **I and my sister go** to school by bus.
Fragments	A sentence fragment is a group of words that looks like a sentence, but actually isn't a complete sentence. Sentence fragments are usually missing a subject or verb, or they do	• I wear uniform of scool and **go to school at 7:30 in the morning I reach school and drive riding to school.**	• I wear uniform of school, **and ride to school at 7:30 in the morning**

Categories	Definitions	Examples of errors	Corrections
	not express a complete thought. While it may be punctuated to look like a complete sentence, a fragment cannot stand on its own. (https://writingcenter.ashford.edu/sentence-fragments)	• I go to lunch at 12:00, **take a nap and chat with my friends and go to school at 12:00**.	• I have lunch at 12:00. **Then I chat with my friends, take a nap and go to school at 13:00**.
Articles:	Articles: An article is a word that is used with a noun to indicate the type of reference being made by the noun. English has two articles: **the** and **a/an**. **The** is used to refer to specific or particular nouns; **a/an** is used to modify non-specific or non-particular nouns. We call the the definite article and a/an the indefinite article. • the=definite article • a/an=indefinite article (Artical, https://owl.purdue.edu/owl/general_writing/grammar/using_articles.html)	• I get up **in morning** around 6:00 AM**.** • I steam rice then I go **to bathroom** to brush my teeth, clean my face, **take bath…** • I do my **homework then I** go to bed at the midnight	• I get up **in the morning** around 6:00 AM • I steam rice. Then I go to **the bathroom** to brush my teeth, clean my **face and take a bath….** • I do my **homework and then I** go to bed at the midnight
Conjunction	The action or an instance of two or more events or things occurring at the same point in time or space	• I go to bathroom for brushing my teeth, wash my **face, I** take a bath at 7:15 in the morning. • I read a **book chat** with my mother **and go** to bed at 10:00 PM. • I do my **homework, video** call with friends **and go** to bed at 9:30 PM.	• I go to bathroom for brushing my teeth, washing **my face, and I** take a bath at 7:15 in the morning. • I read a **book, and chat** with my mother. Finally, I go to bed at 10:00 PM. • …After I do my homework, I do video call with my friends. Finally I go to bed at 9:30 PM.
Capitalization	Writing a word with it is first letter as a capital letter and the remaining letters in small letter.	• I always get up at four in the morning. **then i** make my bed….. • I help my **Mom** to do **HouseWork** before go to bathroom. • I am studying in Savannakhet University.	• I always get up at four in the morning. **Then I** make my bed….. • I help my **mom to do housework** before I go to bathroom. • I am studying in Savannakhet University
Preposition	A preposition is a word that shows the relationship between a noun or pronoun and other words in a sentence.	• I usually chat with my sister **in** the weekend. • I always get up **in 6:30** AM everyday. • I usually read English newspaper **on** living room.	• I usually chat with my sister **at** the weekend. • I always get up **at** 6:30 AM every day. • I usually read English newspaper **in** living room.
Word choice	Word Choice is the use of rich, colorful, precise language that communicates not just in a functional way, but also in a way that moves and enlightens the reader. In good descriptive writing, strong word choice paints pictures in the reader's mind. In informational writing, strong word choice clarifies, explains, and expands ideas.	• I **have take** a bath. • I do **homework** at 4 O'clock in the morning as steaming stricky rice, clean house… • I **have** very happy in daily routine	• I **have** a bath/I **take** a bath. • I do **my** housework at 4 O'clock in the morning as steaming sticky rice, clean house… • I **am** very happy in daily routine
Singular and plural	The difference between singular and plural nouns is easy to spot. When a <u>noun</u> indicates one only, it is a singular noun. When a noun indicates more than one, it is plural. (https://www.gingersoftware.com/content/grammar-rules/nouns/plural-nouns/)	• I usually brush my tooth and clean my face. • I play **footballs** with my **friend.** • I study English with **many friend** in the living room.	• I usually brush my **teeth** and clean my face. • I play **football** with my **friends.** • I study English with **many friends** in the living room.
4 Verb tenses	The verb tense tells you when a person did something or when something exist or happened. In English, there are three main tenses: the present, the past, and the future. (https://www.lexico.com/grammar/verb-tenses)	• In my routine, I always **got** up at six o'clock. • I **had** breakfast. Then I go to school everyday. • I **am studying** English in the livingroom and finally, I **am going** to bed at the midnight every Friday.	• In my routine, I always **get** up at six o'clock. • I **have** breakfast. Then I go to school everyday. • I **study** English in the livingroom and finally, I **go** to bed at the midnight every Friday.

Table 6 shows that students committed writing errors such as the use of punctuation, subject-verb agreement, articles, use of prepositions, subject-verb agreements, word order, spellings, verb tenses, singular and plurals form, word choice, capitalizations, gerunds, conjunctions, and fragments.

4. Discussion

The study aimed to find the cause of students' errors committed at the Department of English, Faculty of Linguistics and Humanities, and Savannakhet University when they write English paragraphs. The results revealed that the students committed writing errors such as grammatical, and students showed insufficient vocabulary is a big problem for them. They did not how to learn words, punctuation, spelling, think about new ideas, or which verb should be suitable to go together with other adverbs and adjectives, lastly, they did not know how to write correctly in sentence structure, too panicking about the lack in writing, know how to write and how to spell that word correctly as well.

Table 3: presents I have difficulties in writing academic essays such as lack of variety of ideas in terms of content and ideas, lack of connectives in terms of organization, incorrect word or idiom and usage in terms of vocabulary and word choice, poor sentence structures in terms of language use, use of the first-person pronoun in terms of formality and objectivity, and lack of citations in terms of referencing shown in this table were at the 'highly' level of frequency (mean=3.95 and S.D.=0.91). This might imply that I have difficulties in pronouncing the words (Mean=3.58 and S.D.=0.69), followed by "The scored in confidence for completing their programs of study also scored low on their confidence of these four aforementioned issues" (Mean=3.42 and S.D.=91). As shown in Table 4, the results revealed that Savanakhet University students have committed several types of errors when they were writing English paragraphs. These errors include prepositions, articles, using singular and plural forms, verb tenses, spellings, subject-verb agreements, punctuations, conjunctions, gerunds, capitalizations, word orders, and fragments. As shown in Table 5, the students committed several errors when writing English paragraphs. The most frequent error was the wrong use of punctuation, while the least frequent performed errors were third person singular. Punctuations were the most frequently made error type (11.50%). Other error types were verb tenses (9.90%), word choices (9.58%), prepositions (8.62%), capitalization (8.62%), spelling (8.30%), subject-verb agreement (7.02%), fragment (6.38%), article (6.38%), singular and plural forms (6.38%), words orders (5.43%), conjunctions (4.79%) and gerunds (4.79%).

These results concur with the previous results mentioned in the literature review section. According to Alfaki, (2015), found that the major problems in learners' writing are insufficient linguistic proficiency (including command over grammar, syntax, and vocabulary), writing anxiety, lack of ideas, reliance on L1, and weak structure organization. Dr. Ibrahim Mohamed Alfaki, (2015), found that students have various writing problems: language problems at the levels of morphology and syntax; usage errors, and mechanical mistakes, that is, spelling, punctuation, and capitalization, lack of several writing development skills. And for the types and frequency of writing errors committed at the Department of English, Faculty of Linguistics and Humanities, and also Savannakhet University on writing English paragraphs. The findings of the present study revealed that the students committed several writing errors which were grammatical errors. Regarding their writing performance, the students showed subject-verb agreement, articles, prepositions, subject-verb agreements, word order, spellings, verb tenses, singular and plural forms, word choice, capitalizations, conjunctions, punctuations, and fragments. These results concur with the previous results mentioned in the literature review section by Hourani (2008), which mentioned that the most common and salient grammatical errors which were found in the students' essays included: passivization, verb tense, and form, subject-verb agreement, word order, prepositions, articles, plurality and auxiliaries. Kanyakorn Sermsook, Jiraporn Liamnimitr & Rattaneekorn Pochakorn (2017), showed that the most frequently committed errors were punctuation, articles, subject-verb agreement, spelling, capitalization, and fragment, respectively. Kaladevi Subramaniam (2009) showed that the six most common errors committed by the participants were singular/plural form, verb tense, word choice, preposition, subject-verb agreement, and word order. Charles Owu-Ewie, and Miss Rebecca Williams (2017), identified that the lexical errors in the students' writing were due to homophone problems and semantic lexical errors. The grammatical errors identified were agreement errors, tense errors, singular-plural (number) errors, prepositional errors, and article errors and they also found that the most frequently committed grammatical errors were tense errors followed by agreement errors. Murad Hassan Mohammed Sawalmeh (2013) showed that in written essay errors; (1) verb tense, (2) word order, (3) singular/plural form, (4) subject-verb agreement, (5) double negatives, (6) spellings, (7) capitalization, (8) articles (9) sentence fragments and (10) prepositions. Dr. Ibrahim Mohamed Alfaki (2015), stated that the errors and mistakes made by the students. Dr. Amina Gogo Tafida and Dr. Shittu Kelani Okunade (2016), Anyone who speaks or writes English language without errors in subject/verb agreement among others is considered a good and experienced speaker. One of the most difficult structural elements for EFL learners is the English article system (definite & indefinite). Saara Sirkka Mungungu, November (2010), found that the most frequently committed grammatical errors were tense errors followed by agreement errors. Charanjit Kaur Swaran Singh, (2017), revealed that subject-verb agreement and tenses were the most common type of errors.

These results in errors could cause written miscommunication. Hence, teachers should consider the differences between vocabulary and grammar knowledge of English and those of students' first language. Lastly, but not least, the researchers would like to emphasize that errors found in English students' writing are not wrong, but useful tools to help English students make fewer errors and write better in English.

34

5. Conclusion

English as a foreign language in Laos has influenced many aspects of life. Language has an important role in the intellect, improvement, and society. In Lao schools, English is determined as a compulsory subject in the national curriculum. It is taught at the beginning from elementary school up to the university one of them is Svannakhet University. In English subject, students learn four skills. They are listening, speaking, reading, and writing. Writing skill is one of the most important skills in learning a new language. In addition, an important skill can open up a world of possibilities for any student. Grammar is a set of language rules governing the sounds, words, sentences, and other elements. The purpose of this study was to find out cause of errors students' writing at Department of English, Faculty of Linguistics and Humanities, Savannakhet University, to explore the types of errors those are typical in their writing paragraph and to identify the frequency of writing errors performed by English students as well. This study focused on writing paragraphs because the researchers found that errors in English students' paragraphs. The research used the mixed-method research design. The instruments used writing paragraphs for the students' writing assignment to identify the frequency of writing errors and questionnaires to find the error analysis of writing errors on the English written paragraphs.

6. Acknowledgement

Based on the findings and conclusions drawn, the following recommendations were made. To start with, learners should take care of their training and education and improve their English in general and their writing skills in particular. In addition to this, learners ought to concentrate on the major failures observed, the errors committed, and practice more to improve their writing ability. What is more, students must practice English grammar rules identify the specific rules of the language, and use them in different situations accordingly. Besides, as writers, learners should practice how to plan, generate, organize and put pen to paper relevant ideas. On top of this, instructors should also identify their students' failures so that they can lesson those areas where the chronic loopholes are observed. Once again, instructors should pay attention to the specific areas when marking students' essays so that learners' writing ability might be improved and progressed. Instructors should also use appropriate teaching writing methods and let their students approach various writing strategies. Finally, college curriculum planners should consider their learners' needs and include relevant aspects of English writing when developing teaching materials.

7. References

Abd. Muis Said. (June 2016). Error Analysis Of Word Order Used In Writing Recount Text Made By Students' At Smk Negeri 1 Pinrang. Volume 02, Number 01.

Adrian Roscoe, Rahma Al-Mahrooqi, Vijay Singh Thakur. (2014). Methodologies for Effective Writing Instruction in EFL and ESL Classrooms (Vol. the Advances in Educational Technologies and Instructional Design). British.

Afifuddin. (2016). An Analysis Of Students' Errors In Writing Descriptive Texts. English Education Journal, Vol.7, 131.

Agustina, V. (n.d.). Error analysis in the travel writing made by the students of English study program.

Ahmad Salamin, Mohammed Farrah, Riyad Zahida, Naji Zaru . (2016). An Investigation into Punctuation and Capitalization Errors Made by Hebron University EFL Students.

Ahmed Awad. (2012). The Most Common Punctuation Errors Made by the English and the TEFL Majors at An-Najah National University.

Ahmed Khider Ahmed Othman. (2018). An Investigation of the Most Common Spelling Errors in English committed by English major Male students. Journal of Education and Practice , Vol.9, No.1.

Akbary, M. H. (2017). Analysis of Grammatical Errors Inenglish Writing Made By Efl Students. .

Alfaki, D. I. (2015). UNIVERSITY STUDENTS' ENGLISH WRITING PROBLEMS. International Journal of English Language Teaching, Vol.3, No.3.

Alfiyani, Lulu Meilina. (2013). An analysis of grammatical errors in writing among the second semester students of English department of Yogyakarta state university in the academic year of 2011/2012.

Artical, https://owl.purdue.edu/owl/general_writing/grammar/using_articles.html. (n.d.).

Ayu Triana Resti, Budi Yansah, Citra Indah Syaputri, Lisaf Diningsih, Tri Damayanti and Sherly Aisah. (2015). An Analysis Of Error In Singular-Plural Form In Writingdescriptive Text To The Third Semester of Stkip-Pgrilubuklinggau.

Charanjit Kaur Swaran Singh, A. K. (2017). Grammar Errors Made by ESL Tertiary Students in Writing. English Language Teaching, Vol. 10.

Charles Owu-Ewie, M. R. (2017). Grammatical and Lexical Errors in Students' English Composition Writing. Sino-US English Teaching, Vol. 14.

Charles Owu-Ewie, Miss Rebecca Williams. (2017). Grammatical and Lexical Errors in Students' English. Sino-US English Teaching, Vol.14, 463.

Cook and Richat. (1980). The Scope of Grammar: the Study of Modern Grammar.

Dana R.Ferris. (March 2004). The "Grammar Correction" Debate in L2 Writing. Journal of Second Language Writing, Volume 13(Issue 1), .

Darus, S. (2009). Common Errors in Written English Essays of Form One Chinese Students. European Journal of Social Sciences, Volume 10, 245.

Dayne Sherman, Jayetta Slawson, Natasha Whitton, and Jeff Wiemelt. (2011). Paragraphs. In The Little, Brown Handbook. Southeastern Writing Center.

Dewi Furtina, Ika Apriani and Dohra Fitrisia. (2016). Grammartical Errors in Writtinng Task. 251.

DIAN KUSUMA W and SUPRIANI. (2014). THE CHALLENGES IN TEACHING WRITING SKILL.

Dr. (Mrs) Amina Gogo Tafida and Dr Shittu Kelani Okunade. (2016). Subject-Verb Agreement Problem among English as Second Language learner. International Invention Journal of Education and General Studies, Vol. 2, pp. 20.

Dr. Ahmed Ali Fadul Benyo. (2014). English Spelling Problems among Students at the University of Sudan. Educational Research, Vol. 5(9), pp. 361-367.

Dr. Ibrahim Mohamed Alfaki. (2015). University Students' English Writing Problems: Diagnosis and Remedy. International Journal of English Language Teaching, Vol.3, No.3, pp.40-52.

Erik Söderlind. (2008). The analysis of mistakes in the written production of advanced.

Faiza Hawa, Rahma Sukmningum, OscarYustino. (2016). What Errors are committed by Students in Writing Paragraph? Proceeding of international conference on Language, Literary and culture studies.

Fajariani Emmaryana. (2010). Analysis on the Grammartical Errors in the Students' Writing. Jakarta.

Felicia Lincoln and Anisa Ben Idris. (2015). Teaching The Writing Process as a First and Second Language Revisited. Journal of International Education Research, Volume 11, 119.

Hanna Novariana, Sumardi, Sri Samiati Tarjana. (2018). Senior High School Students' Problems in Writing. English Language and Literature International Conference, Vol. 2, 216.

Heydari, P. (2012). Error Analysis: Sources of L2 Learners' Errors. (M. S. Bagheri, Ed.) Theory and Practice in Language Studies, Vol. 2, No. 8.

Hourani, T. M. (2008). An Analysis of the Common Grammatical errors in English writing. Institute of Education, Dubai.

Hsiao-ping Wu. (2014). Types and Attributes of English Writing Errors in the EFL context. Journal of Language Teaching and Research, Vol. 5, No. 6.

Jabeen, A. (2015). he Role of Error Analysis in Teaching and Learning of Second and Foreign Language. (M. S. Mustafai, Ed.) Education and Linguistics Research, Vol.1.

Jairos Gonye, Rugare Mareva, Washington T. Dudu, Jabulani Sibanda. (2012). Academic writing challenges at Universities. Journal of English and literature, Vol. 3.

Joko Budiarjo. (2018). Students' Errors in Using Conjunctions in Writing English Proceduretext.

Kaladevi Subramaniam. (2009). Error Analysis of the Written English Essays of Secondary School Students in Malaysia: European Journal of Social Sciences, 8.

Kanyakorn Sermsook, Jiraporn Liamnimitr & Rattaneekorn Pochakorn. (2017). An Analysis of Errors in Written English Sentences (Vol. 10). Nakhon Si Thammarat, Thailand: Canadian Center of Science and Education.

Kanyakorn Sermsook1, Jiraporn Liamnimitr 1 & Rattaneekorn Pochakorn1. (2017). An Analysis of Errors in Written English Sentences (Vol. 10). Nakhon Si Thammarat, Thailand: Canadian Center of Science and Education.

Khansir, A. A. (2012). Error Analysis and Second Language Acquisition. Theory and Practice in Language Studies, Vol. 2.

Krismanti, N. (2017). Fragment and Run-On Sentences Analysis on Students' Essays.

Kristin Messuri PhD. (2016). Writing Effective Paragraphs.

Le Thuy Trang. (2014). Errors Analysis of Pre-Intermediate EFL Students' Writings at Leecam LanguageCenter.

Leech, David. (1994). Problematic ESL Content Word Choice in Writing. Vol. 5 No. 1 1.

Lulu Meilina Alfiyani. (2013). An Analysis of Grammatical Errors In Writing Among The Second Semester Students Of The English Department Of Yogyakarta State University In The Academic Year Of 2011/2012.

M.I.M. Safiullah. (2018). A Study of Errors in Using Modal Verbs Made by Grade 11 Students of a Government School in Nintavur Educational Division. International Journal of English, 7.

M.Samanth Reddy. (2016, April). Importance of English Language in today's World. International Journal of Academic Research, 3(4), 179.

Marites Quibol-Catabay. (January 2016). Error Analysis on Students' Writing. International Journal of Advanced Research in Management and Social Sciences, Vol. 5 | No. 1.

Melisa Utari. (2017). An Error Analysis on the use of Preposion in narrative Composition made by the Eleventh Grade Students of SAMAN 1 Babat MUBA.

Miroslava Tsvetkova. (2019). Errors in Using Auxiliary Verbs.

Moh Hussain Akbary. (2017). Analysis of Grammatical Errors Inenglish Writing Made by Efl Students.

Mohammedamin Hussen. (2015). Assessing Students' Paragraph Writing Problems.

Ms. Satya Sri Durga and Dr. C. S. Rao. (2018). Developing Students' Writing Skills in English. Research scholars and professional English language, 2(6), 1.

Muhammad Fareed, Almas Ashraf, and Muhammad Bilal. (2016). ESL Learners' Writing Skills: Problems, Factors and Suggestion. Journal of Education and Social Sciences, Vol. 4(2), 81.

Muhammad Hadi Sucipto. (2018). The Analysis of Common Grammatical Errors in Writing Narrative Essay of English Study Program Students.

Mulianingsih, I. R. (2014). An error analysis of students' English writing at Jambi University.

Murad Hassan Mohammed Sawalmeh. (2013). Error Analysis of Written English Essays. English for Specific Purposes World, Vol. 14(Issue 40).

Nasrudin, H. (2015). An Analysis in Using Punctuation marks in Narrative Writing.

Neil Edward Barrett and Li-mei Chen. (2011). English Article Errors in TaiWanese Collage students EFLWriting. Vol. 16, No. 3-4.

Nelson Mandela. (2016, JUL 1). http://www.klientsolutech.com/importance-of-education-in-life/.

Nokthavivanh SYCHANDONE. (2016). Comparative Error Analysis in English Writing.

Novita, R. (2014). An Analysis of Grammatical Errors in the 1st Year Students' Wring. Vivid Journal V, Vol.3 No.2.

Nurwahyuni. (2017). An Error Analysis of the Punctuations in Students' Writing.

Okoro, Gladys Onyinyechi. (2017). Error Analysis of the Written English Essays of Junior Secondary. International Journal of Education and Evaluation, Vol. 3(No. 5).

Paul. (2003). What is a paragraph?

Pham Vu Phi Ho, P. N. (2015). 2.1.1. Common Errors in Writing Journals of The English-Major Students at Hcmc Open University. Journal of Science Ho Chi Minh City Open University, p52.

Pimpisa Rattanadilok Na Phuket, Associate Professor Dr. Normah Binti Othman. (2015). Understanding EFL Students' Errors in Writing. Journal of Education and Practice, Vol.6, No.32.

Prof. Songi Han and Prof. David Gay. (2012). Technical writing: Its importance & how to do it well. In C. m. Chmelka.

Rentauli Mariah Silalahi. (2014). Error Analysis on Information and Technology Students' Sentence Writing Assignments. Vol. 1, No. 2.

Richards, J. C., & Schmdit, R. (2010). Longman Dictionary of Language Teaching and Applied Linguistics. Pearson Education Ltd.

Rizky Edo Pratama. (2015). An Error Analysis in Writing Descriptive Text Made by Eighth Grade Students of Smp Muhammadiyah 2 Masran In 2014-2015 Academic Year.

Saadiyah Darus. (2009). Common Errors in Written English Essays of Form One Chinese Students. European Journal of Social Sciences, Volume 10(Number 2).

Saara Sirkka Mungungu. (November 2010). ERROR ANALYSIS. 9.

SAARA SIRKKA MUNGUNGU. (November 2010). ERROR ANALYSIS. 9.

Sawalmeh, M. H. (2013). Error Analysis of Written English Essays. English for Specific Purposes World, vol. 14(Issue 40).

Shah Mohammad Sanaul Karim1. (2012-2015). Analysis of Errors in Subject-Verb Agreement among Bangladeshi Tertiary Level Efl Learners. 31. International Journal of social science.

sholihatun. (2017). An Error Analysis on the Use of English Article in Desriptive Text Writing.

Shubhada Deshpande. (2014). Teaching Writing Skills in English: Involvement of Students. European Centre for Research Training and Development UK, Vol.3(No.1), 68-69.

SILVA, T. (1993). Toward an Understanding of the Distinct Nature of L2 Writing: The ESL Research and Its Implications. TESOL Quarterly, Vol. 27, No. 4.

Siti Himmatul Auliya. (2016-2017). An Error Analysis on The Use of Simple Present Tence in Writing Descriptive Text. Vol. 4 No.2, 1.

Sufiyani, Irma Alif. (2016). An Analysis of Students' Error in Applying Punctuation Marks in Writing Paragraph.

Taiseer Mohammed Y. (2008). An Analysis of the Common Grammatical Errors in the.

Ths. Trần Thị Hải Bình. (2014). An Error Analysis on the Use of Conjunctions in the Writing.

Titin Rohayati, Asep Setiawan, Ade Permata Sari, Dian Kusuma W and Supriani. (2014). The Challenges in Teaching Writing Skill.

Touchie, H. Y. (1986). Second language learning errors their types, cause, and treatment. JALT Journal, Volume 8, 77-78.

Widyawati, W. Y. (2 September 2018). An Analysis on the Students' Errors in Using Gerund by the Fourth Semester. TELL-US Journal, Vol. 4 Issue.

Widyawati, Wiwik Yully. (2 September 2018). An Analysis on the Students' Errors in Using Gerund by the Fourth Semester. TELL-US Journal, Vol. 4 Issue.

Y vijay k sharma. (2016, JUL 1). http://www.klientsolutech.com/importance-of-education-in-life/.

Yasir Bdaiwi Jasim Al-Shujairi, Helen Tan. (2017). Grammar Errors in the Writing of Iraqi English Language Learners., 5.

Learning with PRIDE: A Decade of English Camp Innovation and Student Empowerment

Dhunyawat Treenate[a], Thanya Pakpoom2[b]

[a]*Division of English for International Communication, Faculty of Liberal Arts., Institution Rajamangala University of Technology Krungthep, Bangkok, 10120 Thailand*
[b] *Division of English for International Communication, Faculty of Liberal Arts., Institution Rajamangala University of Technology Krungthep, Bangkok, 10120 Thailand*
* *Corresponding author. Tel.:* 6681-939-6469; *Fax:* 662-287-9600; *E-mail address:* dhunyawat.t@mail.rmutk.ac.th

Abstract
Over ten years of managing English camps at Rajamangala University of Technology Krungthep (RMUTK) led to the creation of the PRIDE model, which includes planning, role preparation, idea exchange, doing, and evaluating. The model began as a support system for rural students to learn English, as well as a means for undergraduates to gain practical experience, and has evolved into a recognized method for promoting experiential learning and developing 21st-century competencies. The PRIDE Model combines theoretical classroom instruction with practical application by applying Kolb's experiential learning theory (1984) alongside Dewey's philosophy of experiential learning (1938). This paper defines the theoretical background of the model and details its practical application while demonstrating its usefulness as a structured framework for student development within higher education, especially for language learning and soft skills development.

Keywords: The PRIDE Model, Experiential Learning, 21st-Century Education

1. Introduction

The English Camp organized by RMUTK's English for International Communication Department since 2009 transformed into a powerful experiential learning platform. The camp delivers English language education to students who live in remote and underserved regions throughout multiple Thai provinces, including Tak, Nong Bua Lamphu, Phetchabun, Buriram, Phrae, Prachuap Khiri Khan, Kanchanaburi, and the latest addition being Phetchaburi. For 13 years, the camp operated as a demonstration of RMUTK's dedication to community outreach initiatives alongside student-focused academic advancement.

The RMUTK English Camp started with two main goals. The camp aims to improve English language skills among rural school students who have restricted access to quality English education and genuine communication opportunities. The camp provides undergraduate English majors with real-world experiential learning experiences. Undergraduates majoring in English take charge of planning and organizing camp activities while executing them to develop practical skills in communication and leadership.

Through repeated reflection and refinement over many years, this process eventually led to the development of the PRIDE Model—a structured framework that captures the five key stages of student-led experiential learning: The PRIDE Model identifies five essential stages for student-led experiential learning, which include planning, role preparation, idea exchange, doing, and evaluation. The PRIDE Model functions beyond management capabilities by providing an educational structure that nurtures language acquisition together with 21st-century skills development and follows principles of experiential learning as proposed by Kolb (1984) and Dewey (1938).

The primary goal of this paper is to investigate how the PRIDE Model developed its current form and structure and to discuss its educational benefits for language teaching and student empowerment through community-based experiential learning in higher education settings.

1.1 Objectives

This article explains how the PRIDE Model serves as an impactful framework for student learning through experiential methods while providing transferable skills for real-world situations. The article proposes that university instructors can adapt the PRIDE Model to function as a pedagogical tool which will improve teaching and learning in higher education settings.

The development and implementation of the PRIDE Model is grounded in two major theoretical underpinnings: The PRIDE Model draws from two foundational theories: experiential learning theory and the 21st-century skills framework. The design and results of the English camp project at Rajamangala University of Technology Krungthep (RMUTK) reflect its foundation in these theories, especially in promoting student-driven action-based learning and skill development, which reaches beyond classroom boundaries.

1.2 Theoretical Framework

The development and implementation of the PRIDE Model is grounded in two major theoretical underpinnings: The PRIDE Model draws from two foundational theories: experiential learning theory and the 21st-century skills framework. The design and results of the English camp project at Rajamangala University of Technology Krungthep (RMUTK) reflect its foundation in these theories, especially in promoting student-driven action-based learning and skill development, which reaches beyond classroom boundaries.

1) *Experiential Learning Theory*

According to Kolb (1984), experiential learning involves creating knowledge through transforming experiences. Kolb's model emphasizes a four-stage learning cycle: The four stages of Kolb's learning cycle consist of concrete experience followed by reflective observation, which leads to abstract conceptualization and concludes with active experimentation. Through engagement with real-life tasks, learners build understanding, which develops through reflection and conceptual integration followed by the application of insights in fresh contexts.

The educational philosophy of John Dewey (1938) serves as a basis for this approach by asserting that learning should be experience-based and most effective when students work on real-world problems within authentic settings. Dewey believed that learning becomes continuous and transferable through the practice of reflecting on experiences.

The PRIDE Model represents experiential learning principles through multiple student opportunities to plan their English camp activities and afterwards reflect on their experiences. The phases of the model—planning, role preparation, idea exchange, doing, and evaluation—correspond directly with Kolb's learning cycle. The camp preparation and implementation stage provide students with direct experiences while post-camp evaluations serve as a platform for reflective observation, which leads to the creation of abstract organizational concepts followed by active experimentation in subsequent camps. The method converts students from knowledge receivers into proactive learners who practice their skills.

Multiple research studies demonstrate that experiential learning approaches effectively support profound learning experiences and skill acquisition. Yardley, Teunissen, and Dornan (2012) demonstrated that professional competencies improve substantially when experiential learning takes place in real-world settings, particularly within health and education domains. Healey and Jenkins's 2000 research demonstrated how experiential learning combined with inquiry-based methods increases student engagement and comprehension among undergraduate learners.

2) *21st-Century Skills Framework*

The 21st-century skills framework works in tandem with experiential learning theory to emphasize the essential competencies needed for success in our modern world. The researchers Trilling and Fadel proposed in 2009 that critical thinking together with communication skills, collaboration abilities, and creativity form essential core skills for success in modern personal and professional life. These competencies are frequently grouped into three domains: The three main skill categories include learning and innovation capabilities along with digital literacy abilities and life and career competencies.

Binkley et al. (2012) broadened the original framework to include components of self-regulation, problem-solving abilities, and global awareness. Their educational framework highlights the need for student-focused learning spaces with problem-solving elements that support social interaction and match the educational design and principles of the PRIDE Model.

The RMUTK English Camp requires student organizers to engage in activities that demand simultaneous application of several 21st-century skills. Students develop time management abilities together with task delegation and problem-solving skills during the planning and coordination phases. Students leading activities need to overcome cultural and language differences through effective communication. Through critical thinking and team reflection combined with constructive feedback during evaluation activities, students develop metacognitive abilities and learn to improve continuously.

Contemporary educational research shows that higher education programs need to develop courses that include 21st-century skills. Voogt and Roblin (2012) argued for educational programs that support creative thinking and group work among students. Silva (2009) stated that traditional educational methods need to develop by incorporating soft skills instruction to equip students for work in diverse international settings. The results validate the PRIDE Model's effectiveness as a tool to promote academic advancement while supporting lifelong learning and professional preparedness.

Experiential learning methods connect strongly with contemporary skills, and they play an essential role in teaching languages, which is particularly useful for English as a Foreign Language (EFL) instruction. Language education in our globalized and interconnected world requires teaching beyond vocabulary and grammar to develop learner skills in intercultural communication and adaptability while enhancing their critical thinking and collaboration abilities (Trilling & Fadel, 2009). Experiential learning supports these requirements by combining practical activity with reflective thinking and direct application to real-world situations (Kolb, 1984). Students can achieve meaningful engagement and improved language retention by participating in real-world communication contexts. Integrating experiential approaches into EFL education enables learners to practice English across various practical scenarios while enhancing their language abilities and developing essential modern skills through authentic interactions.

The connection between experiential learning methods and essential 21st-century skills holds significant importance for language education, specifically within English as a Foreign Language settings. Task-based and experiential learning methods place importance on authentic communication practices and collaborative cultural exchanges (Ellis, 2003), while traditional classrooms focus on grammar rules and memorization. Through the PRIDE Model, students gain linguistic proficiency while simultaneously building social and cognitive abilities during genuine communication exercises.

Studies by Beckett & Slater (2005) demonstrate that the inclusion of project-based learning (PBL) within language education frameworks enhances student motivation along with engagement levels and improves their ability

to acquire new skills. The RMUTK English Camp demonstrates how the PRIDE Model creates a PBL learning atmosphere where language serves as both the learning tool and the educational result. Functional English usage enables students to organize activities, deliver instructions, support peers, and reflect on processes that establish practical language contexts while developing leadership abilities and collaboration skills.

In summary, the PRIDE Model stands at the intersection of two powerful educational paradigms: experiential learning and 21st-century skill development. Applying it to language education transforms teaching approaches from passive instruction into active learner-centered participation, which helps students develop English language proficiency alongside leadership and adaptive skills for global success.

2. PRIDE Model Overview

The PRIDE Model originated from more than ten years of accumulated practical experience in directing English camps at Rajamangala University of Technology Krungthep (RMUTK).

2.1 Origin and Development of the PRIDE Model

The PRIDE Model emerged from more than ten years of ongoing learning and practical experience in organizing English camps at Rajamangala University of Technology Krungthep (RMUTK). The English for International Communication Department started annual English camps across Thailand's provinces in 2009 to help under-resourced schools and communities. The community outreach program transformed into a learning ecosystem led by undergraduate English majors who organized and managed the camps with faculty supervision.

Faculty members and student leaders engaged in reflection about the learning process due to ongoing patterns of successful practices and persistent challenges. A structured framework emerged through repeated cycles of preparation followed by implementation and reflection, which led to improvements. The PRIDE model emerged as a result, which stands for Planning, Role Preparation, Idea Exchange, Doing, and Evaluation in an acronym format. The PRIDE Model captures experiential learning cycles within camp management while serving as both a management instrument and educational framework to foster soft skills, practical language use, and learner independence. By studying the chronological development of the RMUTK English Camp, one can better comprehend how the PRIDE Model evolved during twelve years of active educational practice. The following timeline presents important developmental stages such as the expansion of camp activities and the integration of experiential learning theories, which eventually led to the formation of the PRIDE framework.

2009	2011	2013	2015	2017	2019	2021	2023
First camp started	English Camp	Structure roles assignment introduces	Integration of Experiential Learning Principles	Initial Outline of PRIDE Stages Emerges	Student-led Evaluations Shape Camp Design	No English Camp (COVID 19)	Model Refined
Expansion to more provinces of Thailand	English Camp	English Camp	English Camp	English Camp	No English Camp (COVID 19)	PRIDE Acronym Formalized and Piloted	Comprehensive PRIDE Framework Established
2010	2012	2014	2016	2018	2020	2022	2024

Figure 1: Timeline of the Evolution of the RMUTK English Camp Leading to the PRIDE Model

The RMUTK English Camp evolved from 2009 to 2025, which coincided with the development of the PRIDE Model. The RMUTK English Camp reached its first milestone in 2009 when it launched its first camp, followed by important developments such as role structure formalization in 2013, experiential learning theory integration in 2015, PRIDE stage emergence in 2017, and full model establishment in 2023. The English Camps operated on an annual basis but stopped in 2020 due to COVID-19 before restarting in 2022 with the formalized PRIDE acronym introduced and tested. The model evolved to become an all-encompassing experiential learning structure that supported student development.

2.2 Stages of the PRIDE Model

The PRIDE Model's stages perform unique educational and structural functions. The model's structured stages create deep learning experiences by combining active involvement with reflection exercises and repetitive practice.

P—Planning

During the first stage, students team up to establish the camp's main structure. This includes:
Establishing which audience to target and understanding their specific learning requirements
- Defining the learning objectives
- Drafting the activity schedule and lesson plans
- Allocating budget, materials, and logistical responsibilities

Students develop skills in establishing objectives and managing resources while practicing strategic planning during this stage. The stage replicates professional project start-up phases, which helps students learn educational concepts and organizational abilities.

R – Role Preparation

During this stage, team members receive defined roles and necessary training to perform their tasks efficiently. Teams typically include:

• Academic Team: Designs educational content and language games.
• Hospitality Team: Manages meals and participant comfort.
• Recreation Team: Organizes ice-breaking and bonding activities.
• General Affairs: Handles logistics, venues, and equipment.
• Participant Support: Mentors and assists student participants.

Students participate in team-building activities followed by rehearsal simulations and training based on their assigned roles. The stage fosters teamwork along with leadership and accountability clarity throughout the team.

I – Idea Exchange

Students participate in collaborative group discussions to brainstorm and improve ideas before moving forward with their plans. Brainstorming sessions allow for:

Students contributed original ideas for camp activities alongside themes and language content elements.

• Anticipation of potential challenges and solutions
• Cross-functional feedback between teams

This stage encourages students to develop analytical skills while fostering creative expression and transparent communication. The process shows that high-quality programming develops from collective discussions and joint responsibility.

D – Doing (Implementation)

During this execution phase, the English camp gets conducted following the established plan. Students:
• Deliver language games and lessons
• Facilitate group activities and manage transitions.
• Respond to real-time issues and participant needs.
• Monitor engagement and adapt as necessary.

During this stage, students demonstrate their language abilities alongside interpersonal and leadership skills in practical settings. Students face unexpected situations that help them develop resilience and learn to adapt while making decisions under stress.

E – Evaluation

Students critically evaluate their experiences by analyzing both the accomplishments and limitations after camp activities end. Evaluation includes:
• Collecting feedback from participants and team members
• Reviewing individual and team performance
• Documenting lessons learned and best practices
• Proposing improvements for the next iteration

The final phase develops both metacognitive awareness and self-assessment practices while establishing a continuous improvement mindset, which exemplifies experiential learning as described by Kolb in 1984.

The PRIDE Model operates through a repeating cycle instead of a straight line. Every iteration results in enhancements that enhance future results. Evaluation results directly shape the planning phase of the subsequent cycle while promoting continuous learning and development. Below is the PRIDE loop through circular arrows that connect P to R to I to D to E and back to P.
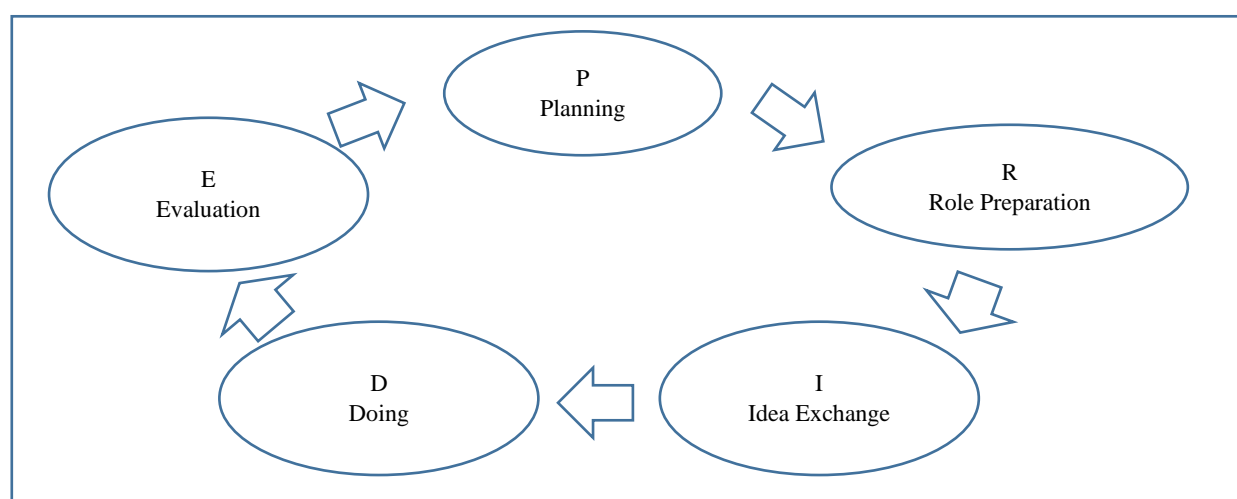

Figure 2: PRIDE Model for Experiential Learning

3. PRIDE in Action: Case from RMUTK English Camp

The RMUTK English Camp exemplifies real-world application of the PRIDE Model within an educational framework. English major students assume full responsibility for organizing the camp each year as faculty advisors

provide guidance. The camp functions as both an outreach initiative for rural educational institutions and a practical setting where students develop soft skills while applying their academic knowledge.

3.1 Team Structure and Roles

Students are grouped into five main teams that mirror professional organizational structures through their functional responsibilities. The Academic Team focuses on creating language games and educational materials, while the Hospitality Team takes care of food provision and participant comfort logistics; additionally, the General Affairs Team is in charge of setting up equipment and preparing venues. The Entertainment Team creates fun and interactive activities that keep participants entertained during the entire training program. The Participant Services Team delivers comprehensive support to trainees so they can effectively participate in all program activities. The variety of organizational roles enables students to develop key abilities in leadership while learning responsibility and teamwork skills.

3.2 Skills Developed Across PRIDE Stages

The PRIDE Model intentionally designs each stage to develop particular soft skills that students need to succeed academically and professionally. Students build their strategic planning capabilities together with organizational skills during the planning phase as they establish objectives and timelines. During role preparation, students strengthen their teamwork abilities and learn to be accountable through designated role assignments and practice sessions. The Idea Exchange stage helps students develop creative solutions and problem-solving skills by working together to improve camp activities. Students must utilize adaptability and communication to execute their plans while adjusting to unforeseen issues during the Doing phase. Evaluation promotes reflective thinking and ongoing development by providing feedback and analyzing activities after camp completion. These stages create an integrated framework for experiential learning, which facilitates ongoing personal and professional development.

3.3 Qualitative Outcomes

Students demonstrate their development in leadership abilities and teamwork skills through their reflective statements, which also show increased personal confidence. Participants commonly state that their experience strengthened their work readiness and expanded their knowledge of teamwork dynamics alongside personal awareness. The camp evolves from a simple academic exercise to a powerful journey of personal transformation.

4. Educational Impact

Through its application, the PRIDE Model has shown a major educational influence by connecting academic learning with practical real-world scenarios. The systematic involvement in the model's stages enables RMUTK students to strengthen their scholastic understanding while developing key 21st-century competencies such as leadership and critical thinking, which are essential for the evolving demands of the global workforce (Binkley et al., 2012; Trilling & Fadel, 2009).

The English Camp setting delivers genuine immersive learning experiences where students practice English in teaching roles and team interactions. The learning approach requires students to modify their language use during real-life interactions, which boosts their fluency and confidence. The approach matches both task-based language teaching and communicative methods because they emphasize contextual use as essential for linguistic development (Ellis, 2003; Richards & Rodgers, 2014).

The camp experience helps young learners develop personal growth by teaching responsibility along with resilience and reflection. Participants consistently observe enhancements in their ability to manage emotions alongside better time organization and cross-cultural understanding. During the final evaluation stage, learners analyze their roles and receive peer feedback, which helps them to pinpoint areas for improvement, thus fostering continuous learning and self-development (Kolb, 1984; Dewey, 1938).

The framework of the PRIDE Model allows teachers to transform their role from traditional instructors to learning facilitators while building educational spaces where students manage their own growth. The PRIDE approach presents a replicable instructional model that promotes student independence alongside profound involvement and practical skills necessary for achievements across educational and career environments (Silva, 2009; Voogt & Roblin, 2012).

5. Implications

The PRIDE Model's creation and application hold essential consequences for educational practice and higher education curriculum design. When students receive structured guidance and reflective opportunities, they can successfully lead meaningful real-world learning experiences. The approach opposes conventional teacher-led models while promoting environments that empower students through project-focused learning.

The PRIDE framework extends beyond language education and camp settings. This scalable framework is adaptable for practicum-based courses and service-learning initiatives as well as community outreach programs and interdisciplinary projects. The model promotes enduring skill development by employing learning cycles that connect active participation with reflective practice according to experiential education theory (Kolb, 1984).

PRIDE provides educators with a structured approach to help students develop outside the classroom environment while transforming instructors into coaching figures instead of lecturers. This model enables institutions to create transformative educational experiences that equip students for challenges they will face in both their local

communities and the wider world. Upcoming studies should investigate how well the model applies to different academic fields and its effects on student success and motivation alongside their preparedness for graduate life.

6. Conclusions

The PRIDE Model, which RMUTK refined during more than ten years of English camp administration, delivers a flexible framework for experiential learning. The model facilitates student development through planning, role preparation, idea exchange, doing, and evaluation stages, which enables learners to transfer academic knowledge to real-world applications while building crucial 21st-century skills like leadership and collaboration.

The model promotes active learning in language education by enabling students to engage in genuine communication while practicing meaningful language activities. The PRIDE framework functions as a scalable project-based learning model within higher education that enables students to become responsible, autonomous learners while transforming educators into growth facilitators. The effective implementation of the framework at English Camp validates the possibility of adopting similar methods throughout various fields to deepen student involvement and foster sustained skill acquisition.

Through the combination of experiential learning methods with structured reflection, the PRIDE Model connects theoretical knowledge and practical application to prepare students for both academic accomplishments and real-world success in ever-changing global settings.

7. Acknowledgements

5. References

Beckett, G. H., & Slater, T. (2005). The project framework: A tool for language, content, and skills integration. *ELT Journal*, 59(2), 108–116. https://doi.org/10.1093/eltj/cci024

Binkley, M., Erstad, O., Herman, J., Raizen, S., Ripley, M., & Rumble, M. (2012). Defining twenty-first century skills. In P. Griffin, B. McGaw, & E. Care (Eds.), Assessment and teaching of 21st century skills (pp. 17–66). Springer.

Dewey, J. (1938). Experience and education. New York, NY: Macmillan.

Ellis, R. (2003). Task-based language learning and teaching. Oxford, UK: Oxford University Press.

Healey, M., & Jenkins, A. (2000). Kolb's experiential learning theory and its application in geography in higher education. *Journal of Geography*, 99(5), 185–195.

Kolb, D. A. (1984). Experiential learning: Experience as the source of learning and development.   Englewood Cliffs, NJ: Prentice Hall.

Richards, J. C., & Rodgers, T. S. (2014). Approaches and methods in language teaching (3rd ed.).   Cambridge, UK: Cambridge University Press.

Silva, E. (2009). Measuring skills for the 21st century. Education Sector Reports, 1(1), 1–16.

Trilling, B., & Fadel, C. (2009). 21st century skills: Learning for life in our times. San Francisco, CA: Jossey-Bass.

Voogt, J., & Roblin, N. P. (2012). A comparative analysis of international frameworks for 21st century   competences: Implications for national curriculum policies. Journal of Curriculum Studies, 44(3), 299–321. https://doi.org/10.1080/00220272.2012.668938

Yardley, S., Teunissen, P. W., & Dornan, T. (2012). Experiential learning: Transforming theory into practice. *Medical Teacher*, 34(2), 161–164. https://doi.org/10.3109/0142159X.2012.643264

Moral Lessons in Children's Literature: A Content Analysis of Ethical Themes in Charlotte's Web for Higher Education

Thanya Pakpoom[a], Dhunyawat Treenate[b]*

[a] *Division of English for International Communication, Faculty of Liberal Arts., Institution Rajamangala University of Technology Krungthep, Bangkok, 10120 Thailand*
[b] *Division of English for International Communication, Faculty of Liberal Arts., Institution Rajamangala University of Technology Krungthep, Bangkok, 10120 Thailand*
* Corresponding author. Tel.: 6681-939-6469; fax: 662-287-9600; *E-mail address:* dhunyawat.t@mail.rmutk.ac.th

Abstract

This research investigates the ethical components present in E. B. White's Charlotte's Web. The study uses qualitative content analysis to explore E. B. White's Charlotte's Web as a potential educational resource for teaching moral values in university settings. The research applies normative ethical theories, including virtue ethics, deontology, and utilitarianism, to reveal key moral themes like self-sacrifice, empathy, loyalty, and moral courage present in the narrative. The research outcomes reveal the transmission of core values via character evolution alongside symbolic visuals and storytelling that evoke emotions. The research examines how children's literature functions as a tool to enhance ethical reflection and moral reasoning while supporting character education at higher education institutions. The report outlines strategies to incorporate literary ethical understanding into diverse academic programs and to develop students' critical thinking using stories as educational tools. According to the study, children's literature likes Charlotte's Web functions as an important tool for developing ethical awareness and comprehensive educational experiences in school settings.

Keywords: Charlotte's Web, Ethical Themes, Children's Literature, Moral Education

1. Introduction

The stories in children's literature serve as strong educational resources for imparting moral principles. Young readers learn about ethical ideas such as empathy and justice by engaging with familiar characters in entertaining stories, according to research by Nikolajeva (2005) and Norton (2010). These narratives drive emotional development and cognitive growth while fostering ethical development through enhanced moral reasoning.

New research highlights the importance of children's books in university settings because they support students in developing critical thinking abilities and moral contemplation. Charlotte's Web serves as an excellent educational tool for teaching university ethics because it presents fundamental ethical themes like loyalty and acceptance of mortality.

Charlotte's Web demonstrates virtue ethics and utilitarian principles through her conduct, while her dedication and sense of responsibility represent deontological ethics according to the theories of Hursthouse (1999), Kant (2002), and Mill (1863). Students gain meaningful opportunities to evaluate moral choices and contemplate ethical principles through the story's rich emotional and symbolic layers. This research investigates the potential of Charlotte's Web to enhance moral instruction and character growth via its narrative educational approach.

Rationale for Selecting Charlotte's Web

The timeless children's book Charlotte's Web (White, 1952) stands as one of literature's most cherished classics because of its emotional resonance and inclusive themes. Wilbur's friendship with Charlotte brings warmth to readers while presenting numerous moral lessons. Charlotte demonstrates exceptional moral principles through her steadfast dedication to saving Wilbur from slaughter at great personal expense by showing selflessness, loyalty, and courage (Norton, 2010). The combination of rich themes and easy readability makes Charlotte's Web an excellent resource for studying ethical stories and their use in teaching morality.

Central Ethical Themes

Altruism, life value assessment, death inevitability, and friendship power form the primary ethical messages in Charlotte's Web. Through her actions, Charlotte demonstrates selfless giving and the employment of her abilities to help others. Wilbur's journey from fear to self-reliance and emotional understanding demonstrates both ethical growth and the importance of profound relationships. Literary themes offer students a valuable framework to investigate their personal values while engaging deeply with moral principles.

1.1 Objectives

This study examines the ethical themes presented in Charlotte's Web through the application of qualitative content analysis techniques. The study conducts a systematic examination and analysis of narrative ethical themes to understand how moral values are represented through character actions and dialogue within the narrative structure. Through their exploration of ethical themes, researchers will develop educational approaches to integrate Charlotte's Web into college ethics courses and character development programs. The research shows the novel functions as a learning tool that fosters critical thinking alongside moral development and ethical reflection among university students.

1.2 Research Questions
1) What ethical themes are presented in Charlotte's Web?
2) How are these ethical themes expressed through the characters and narrative elements?
3) In what ways can Charlotte's Web be effectively used to support moral education in higher education settings?

1.3 Theoretical Framework
The research utilizes an interdisciplinary theoretical framework that integrates ethical philosophy with literary pedagogy and qualitative content analysis. Three distinct domains form the framework that facilitates the analysis of Charlotte's Web as a moral literary artifact and supports its use in ethics education. Through the incorporation of normative ethical theory, there is a structured way to interpret narrative moral themes, while content analysis methodology supplies systematic examination tools. Educational theory about children's literature's impact on moral growth is the pedagogical foundation for the research study.

1) Ethical Theories

This research employs virtue ethics in combination with deontology and utilitarianism to study the ethical dimensions presented in Charlotte's Web. These frameworks serve as essential elements of moral philosophy while providing distinct viewpoints to interpret ethical meanings in literature.

Virtue ethics focuses on building individual character and moral virtues rather than adhering to predetermined rules or evaluating consequences. Aristotle's teachings gave rise to the virtue ethics philosophical school, which modern thinkers like Hursthouse (1999) further developed by explaining that virtuous living through compassion and courage results in a morally beneficial life. Through her character in Charlotte's Web, Charlotte demonstrates the principles of virtue ethics. Her endless selflessness through her tireless efforts to save Wilbur demonstrates her embodiment of virtues like kindness along with loyalty and wisdom. Wilbur develops his character through a journey of moral and ethical growth that transforms him from a dependent individual requiring protection to one who shows emotional strength and understanding that aligns with educational standards for character development.

Immanuel Kant's deontological ethics (1785 & 2002) establish moral value from an action's inherent duty regardless of its outcomes. According to Kantian deontology, every person must adhere to principles they believe should be universally applied while respecting the inherent worth of every human being as well as fictional characters. Charlotte protects Wilbur and maintains her promise because she follows her moral duty instead of pursuing personal gain or practical benefits. By making decisions that ignore external rewards, she demonstrates her loyalty to core principles that match the concepts of deontological ethics.

According to utilitarianism, which Mill developed in 1863, actions are moral if their results lead to the greatest happiness or the least amount of suffering. Charlotte acts on Wilbur's behalf according to utilitarian principles. Through her language abilities, Charlotte turns Wilbur into an exceptional pig, which brings happiness to Wilbur, Fern, and the Zuckermans and brings relaxation to their entire community. Through her deeds that result in her demise, utilitarian ideas are highlighted because they lead to better living conditions for people around her. Students develop comparative moral reasoning skills by applying ethical lenses to understand moral messages in the story.

2) Principles of Content Analysis

The study uses qualitative content analysis to systematically explore the ways ethical messages are integrated into the literary structure of Charlotte's Web. Content analysis functions as a research method that allows all that researchers to organize and understand textual material through the detection of repeated patterns and themes along with conceptual insights (Schreier, 2012). Literary studies benefit from this approach because it supports detailed text examination alongside thematic synthesis across broader contexts.

The analytical process involves three major phases. The initial phase involves identifying analytical units like words, phrases, dialogues, narrative events, events, and character actions that may have ethical significance. The sections where Charlotte weaves her words into her web stand as principal textual elements that demonstrate ethical decision-making. The development of categories and codes depends on criteria derived from both theoretical frameworks and data analysis. There are two types of codes: Codes can originate from ethical frameworks such as "self-sacrifice," "duty," and "consequential outcomes" as well as from inductive analysis performed during textual examination. The researcher examines narrative units to identify their moral meanings through contextual analysis. Charlotte's last letter to Wilbur operates to deliver both a goodbye and to convey ethical responsibility together with her emotional heritage.

This methodology enables her to uphold a systematic examination process while dynamically adjusting to textual variations. When ethical theory is used deductively, it achieves conceptual precision, but induction uncovers hidden ethical insights in literary works. The qualitative content analysis method proves ideal for revealing various moral dimensions in literature and linking literary examination to educational practices.

3) Children's Literature in Educational Contexts

The educational significance of children's literature to teach morality and ethics has been widely recognized by people. This work provides young readers with an understandable medium through which they can examine complex moral issues via familiar storylines beyond its artistic traits. Educational stories for children help develop moral imagination as they allow young learners to explore ethical possibilities and empathize with characters in moral dilemmas, according to Norton (2010) and Tomlinson and Lynch-Brown (2018).

Children's literature features in higher education ethics and character education courses outside traditional teacher training programs. Charlotte's Web seems simple yet leads university students into deep ethical discussions. It raises fundamental questions such as: What constitutes a good life? What does it mean to be loyal? What appropriate actions should we take when faced with death and loss? These questions apply to everyone from children to adults because they address fundamental human concerns.

Ethics education that includes children's literature enables educators to develop students' ethical thinking while enhancing emotional awareness and social understanding. Literature such as Charlotte's Web functions as a mirror and a window: This type of literature acts as a reflective surface for readers to see their core principles while simultaneously opening a view into other people's life experiences and moral perspectives. Literary narratives provide students with a secure imaginative platform to examine moral uncertainties while considering alternative possibilities and sharing their ethical thinking in group interactions. Children's literature serves both aesthetic and ethical educational purposes, according to Nikolajeva (2005), because it produces readers who are both literate and morally aware.

The conceptual model demonstrates how Charlotte's Web functions as an educational tool for ethics through the combination of ethical theory and qualitative content analysis with children's literature teaching methods. The combination of multiple disciplines creates a basis for teaching methods that develop students' moral thought processes as well as critical analysis skills and emotional understanding through literary works.
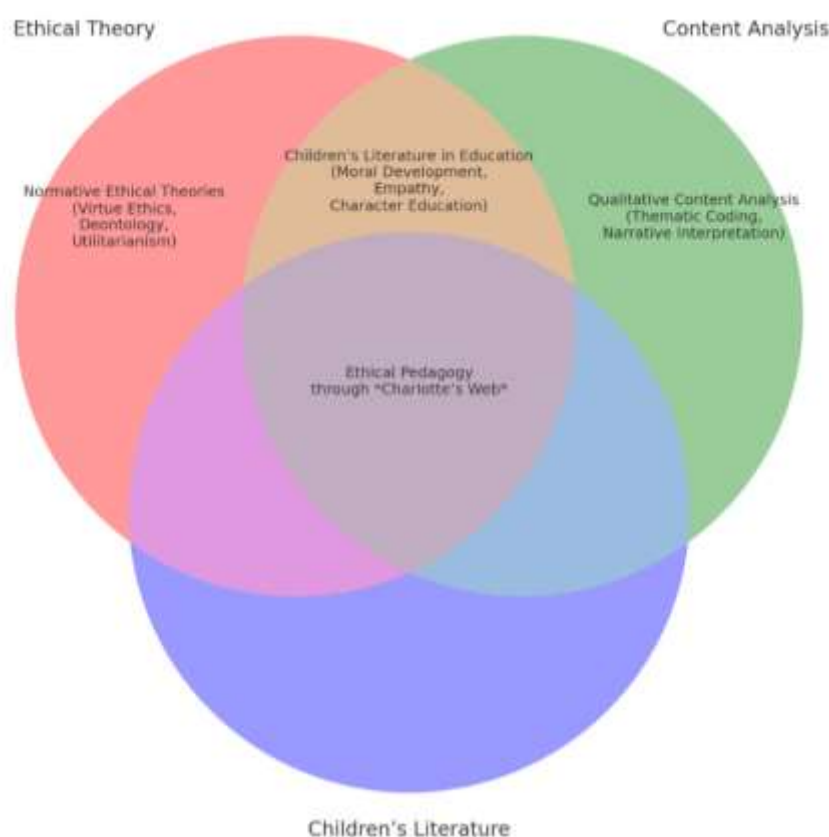

Figure 1. Conceptual Framework: Ethical Pedagogy through Charlotte's Web

The Venn diagram demonstrates where ethical theory meets content analysis methodology and children's literature. These combined elements create a teaching approach that develops ethical thinking skills via narrative examination.

2. Methodology

The investigation adopts qualitative content analysis as its research method to examine ethical themes in Charlotte's Web and explore their application to teaching ethics. The chosen research methodology aligns with interpretive research since it aims to reveal hidden moral values in a literary work and evaluate their usefulness in educational environments.

2.1 Research Design

Researchers employed a textual analysis design using Charlotte's Web (White, 1952) as their primary research source. This book was chosen for its literary depth and its reputation as a moral influence on young readers. The research approach takes an interpretivist paradigm, showing that ethical meaning emerges from the subjective interaction between the text and the reader as well as cultural, educational, and philosophical contexts.

2.2 Data Source and Unit of Analysis

The analysis focuses on key narrative aspects of Charlotte's Web, such as character actions along with their dialogues and pivotal events that contain ethical elements together with descriptive passages. The analysis focuses on scenes that highlight moral challenges as well as displays of selflessness and bravery among friends. Charlotte's choice to protect Wilbur alongside Wilbur's emotional growth and Fern's defense of the pig stand out as key ethical points for analysis.

2.3 Coding and Thematic Development

The analysis of data involved thematic coding through combined deductive and inductive methods. The priori codes developed for analysis were founded on the ethical theories of virtue ethics, deontology, and utilitarianism as outlined in the theoretical framework. The analysis incorporated themes including self-sacrifice, duty, moral courage, and consequential benefit. The close reading of the text resulted in emergent codes that revealed unexpected or context-specific themes such as child advocacy and empathy between species. The research team reviewed the text several times before conducting detailed line-by-line coding on specific excerpts. The research team classified all segments that matched ethical concepts into broader thematic groups. By using this approach, scholars were able to identify recurring moral themes and how they are portrayed in literature.

2.4 Trustworthiness and Rigor

The researcher built credibility using a thorough coding audit trail and reflexive memos to record decision-making during interpretation. The study confirmed its results by comparing them with recognized ethical theory and existing academic work on children's literature and moral education. The study strengthened its rigor by implementing transparent coding procedures alongside theoretical foundations even though literary interpretation requires subjective analysis.

2.5 Ethical Considerations

The study did not require formal ethical approval because it examined publicly available literary texts without involving human participants. The researchers demonstrated intellectual integrity by upholding ethical research standards through the proper citation of sources and honoring authorial intent during their analysis.

3. Findings and Analysis

In Charlotte's Web, the narrative structure alongside its characters presents profound moral complexity and integrates ethical themes through symbolic storytelling. The narrative development of the plot becomes significantly influenced by themes that create opportunities for ethical analysis and educational engagement. Through qualitative content analysis, five major ethical themes were identified: The study finds self-sacrifice together with loyalty and friendship as well as empathy and compassion, moral courage, and acceptance of mortality to be the five central ethical themes. This section shows how each ethical theme relates to narrative content through its specific ethical frameworks. We explore the connections between narrative content and ethical frameworks for each identified theme.

The story's central themes are represented by Wilbur's development from a defenseless piglet into a being with moral awareness. The development of Wilbur's empathy along with his ethical decision-making and personal responsibility forms the moral core of the story. Figure 2 presents the journey visually while serving as a structural framework for the subsequent thematic analysis.

Figure 2: Wilbur's Ethical Development in "Charlotte's Web"

Figure 2 shows Wilbur's moral journey throughout the narrative with structural clarity. The next sections conduct a qualitative content analysis to explore five principal ethical themes extracted from the novel to enhance understanding. The analysis of each ethical theme connects its theoretical basis with its expression during significant events in the story.

3.1 Self-Sacrifice and Altruism (Virtue Ethics / Utilitarianism)

The novel features Charlotte's continuous self-sacrifice as its key ethical theme through her repeated actions to save Wilbur. She uses her immense physical strength to construct her web, ultimately risking her life in the process. The behavior reflects the principles of virtue ethics through its demonstration of altruistic virtue. Charlotte demonstrates moral character through her dedication to helping her friend without seeking personal benefits (Hursthouse, 1999). Her decisions can be analyzed from a utilitarian standpoint because her actions save Wilbur and create happiness for everyone around him, which leads to greater collective happiness (Mill, 1863).

Example from text: "A person who embodies both true friendship and writing talent is a rare find. Charlotte was both."

Students can examine different moral frameworks when they study virtue-based ethics alongside consequence-based reasoning through this dual ethical approach.

3.2 Loyalty and Friendship (Virtue Ethics / Deontology)

The sustained loyalty between Charlotte and Wilbur acts as the second primary ethical theme. As a moral virtue, loyalty requires ongoing support together with honesty and unconditional presence. Charlotte displays Wilbur demonstrating his gratitude for her by taking care of her children and preserving her memory after her passing. her children and keeping her memory alive after she passes away. Charlotte follows her self-imposed responsibility to protect Wilbur according to deontological principles, which can be interpreted as virtue ethics actions (Kant, 2002).

Example from text: Charlotte says, *"You have been my friend. That in itself is a tremendous thing."*

These educational interactions give students the opportunity to evaluate loyalty as either a moral responsibility or an inherent character quality.

3.3 Empathy & compassion (Virtue Ethics / Moral Education)

By saving Wilbur, Fern shows empathy that transcends species boundaries and questions adult reasoning through her emotionally driven ethical behavior.

The story opens with young Fern saving Wilbur and introduces the central theme of cross-species empathy. Fern challenges adult reasoning through her emotion-based moral perspective while revealing the natural compassion of children. Fern's determined efforts to prove Wilbur's life holds value show how emotional responses influence ethical choices and illustrate the importance of conscience in moral learning.

"If you were a tiny creature, would you have killed me?"

The quote presents a perfect chance for students to engage in classroom debates about animal ethics and human moral responsibilities.

3.4 Moral Courage (Virtue Ethics / Deontology)

Throughout the novel, different characters show moral courage when they face tough decisions. Wilbur goes from being a scared piglet to becoming a mature individual who shows compassion and confidence, demonstrating his growing sense of moral responsibility. In the story's ending, Wilbur shows his deep-rooted ethical transformation through his act of bringing Charlotte's egg sac home, which displays his new sense of responsibility and care.

For instance, the text states, "Wilbur stood quietly and proudly." He felt radiant."

The current event allows us to explore courage through its dual nature of bravery and moral integrity in fulfilling ethical obligations.

3.5 Acceptance of mortality (Existential Ethics / Virtue Ethics)

The theme of acceptance of mortality falls under existential ethics and virtue ethics by confronting readers with life's impermanence through Charlotte's death.

The story of Charlotte's death alongside the novel's frank exploration of life and death introduces readers to existential inquiries about life's fleeting nature, one's legacy, and life's purpose. Charlotte's Web shows death as a fundamental aspect of life while encouraging children to understand that meaning comes from the influence we create rather than the duration of our existence. Charlotte's peaceful and stoic acceptance of her destiny represents phronesis, which stands as practical wisdom within virtue ethics.

Example from text: The hundreds who attended the fair remained unaware that the most crucial role belonged to a grey spider. The moment of her death occurred without the presence of any other person. Educational settings that promote existential reflection find this theme particularly impactful.

The following table provides a synthesized overview of five primary ethical themes discovered within Charlotte's Web. The table shows how the five major ethical themes from Charlotte's Web connect to their ethical theories and illustrative characters while highlighting their educational significance. This summary acts as both an analytical overview and a hands-on resource for teachers who want to incorporate moral lessons through literature into classroom instruction.

Ethical Theme	Ethical Theory	Key Characters	Pedagogical Focus
Self-sacrifice	Virtue ethics / Utilitarianism	Charlotte	Altruism, value of others' lives
Loyalty & friendship	Deontology / Virtue ethics	Charlotte, Wilbur	Moral duties in relationships
Empathy & compassion	Virtue ethics	Fern	Moral sensitivity, conscience-based judgment
Moral courage	Deontology / Virtue ethics	Wilbur	Acting rightly despite fear or difficulty
Acceptance of mortality	Existential ethics/ Virtue ethics	Charlotte	Death, impermanence, moral legacy

Figure 3: Summary of Ethical Themes

Analysis of Charlotte's Web shows its potential as a rich source for ethical examination. Moral development in literature emerges from narrative structure and symbolic elements as well as character development rather than just explicit moral lessons. The understanding gained from these studies encourages educators to incorporate children's literature into university moral education programs because these narratives promote deep reflection and critical thinking about ethical dilemmas through their accessible yet meaningful storytelling techniques.

4. Pedagogical Implications

Charlotte's Web becomes a powerful ethical teaching instrument in higher education through its blend of deep ethical ideas and straightforward storytelling, which proves useful in teacher training courses and humanities studies along with interdisciplinary programs that connect literature with moral development. Integrating children's literature into university programs supports both ethical inquiry and boosts students' cognitive and emotional learning outcomes.

Charlotte's Web serves as an effective platform for discussion-based moral inquiry. The combination of structured debate, Socratic questioning, and ethical dilemmas from the story gives university students analytical tools to study the moral decisions of characters like Charlotte, Wilbur, and Fern. Students can assess the ethical principles that Charlotte's sacrifice might represent while examining Fern's dismissal of adult reasoning as a demonstration of children's innate moral sense. Students develop their abstract thinking and ethical comparison skills by applying deontological and utilitarian frameworks to literary analysis during discussions.

Affective and empathic learning promoted by the novel serves as a basic component of moral development. The emotional resonance of the story enables students to establish personal links with moral principles, which amplifies discussions on sacrifice, death, loyalty, and compassion. Students explore their ideas and challenge preconceived notions by using literary narratives as "safe spaces," which provide a distancing effect through fictional elements. When students engage in reflective journals and role-playing that includes ethical storytelling, they deepen their emotional ties to moral concepts.

The story acts as a bridge connecting various academic disciplines. Charrettes in literature and ethics education will gain value from Charlotte's Web when combined with teaching resources from education, philosophy, psychology, and animal studies. The flexible nature of this method makes it ideal for diverse academic programs focused on cultivating moral imagination to help students envision ethical outcomes and future possibilities. Students will examine real-world ethical issues from the novel through projects that address animal welfare and environmental ethics together with educator moral responsibilities.

The text stands as an exemplary model of literature-based character education, which serves as a key element in national educational policies and international global citizenship education frameworks. Future educators can learn essential instructional strategies through Charlotte's Web to develop character education lessons for primary and secondary schools. Students can learn how narrative structure combined with character development through dialogue creates effective educational lessons aimed at developing empathy and moral reasoning together with social responsibility.

The narrative language and symbolism in the novel establish a framework where literary analysis intersects with ethical contemplation. Charlotte's Web operates as both a literal and symbolic tool for moral teaching and communication and creates a lasting educational presence. Through analysis, students develop critical literacy skills to discover complex meanings in texts, which leads to connections with ethical and philosophical discussions.

Charlotte's Web serves as a celebrated literary masterpiece while simultaneously functioning as a teaching tool to enhance moral understanding. The work's enduring themes and emotional stories create an educational approach to ethics that combines mental discipline with emotional awareness and ethical development through literary pleasure.

Contemporary Connections: Applying Themes to Modern Ethics

The moral themes featured in Charlotte's Web remain relevant for analyzing modern ethical challenges even though it stands as a beloved children's book classic. Educators use modern ethical dilemmas to strengthen narrative moral lessons that help students understand abstract ethical theories better and emotionally engage with the material.

Whistleblowing and Moral Courage: Charlotte's all-encompassing courage to protect Wilbur parallels how modern whistleblowers bravely face personal dangers to expose corporate wrongdoing. Frances Haugen displayed ethical responsibility through the disclosure of Meta's (Facebook) internal data while endangering her own personal security. Through this perspective, students can evaluate moral bravery in fictional and actual examples while learning how virtue ethics connects with moral accountability responsibilities.

Animal Rights and Cross-Species Empathy: Fern decides to protect Wilbur because her deep understanding of empathy crosses the boundaries between species. This concept functions as a moral counterpart to current animal rights and veganism movements that challenge human-centered worldviews. Through animal rights dialogue, teachers can guide students to connect Fern's emotions with non-human moral value and compare conscience-based choices with utilitarian principles.

Grief Literacy and the Ethics of Loss: The respectful way Charlotte and Wilbur respond to death triggers essential discussions about mortality and how to honor those we love during worldwide crises when such conversations become especially important. Students explore existential ethical principles when they study how narratives provide guidance through grief and life's brief nature. The ability to understand emotions and bounce back from adversity grows during conversations that connect fictional narratives with real-world emotional and ethical challenges.

Charlotte's Web bridges classic literary principles with modern social issues to function as both a reflective self-assessment tool and a starting point for social discourse. Students at universities discover deeper learning connections when abstract theories relate to real-world moral dilemmas within narratives.

5. Conclusions and Recommendations

5.1 Conclusion

This study conducted a qualitative content analysis of Charlotte's Web to uncover its ethical themes and evaluate their application in university education. The comprehensive analysis of the novel revealed many deep ethical themes, including self-sacrifice and empathy as well as moral courage and acceptance of death. The narrative effectively combines character development and symbolic imagery with deeply emotional events to integrate its moral themes.

The examination of virtue ethics, deontology, and utilitarianism resulted in establishing Charlotte's Web as a useful literary tool for ethical analysis. The ethical lessons embedded in children's literature become evident through the compassionate behavior of Charlotte and Fern's moral consciousness and Wilbur's personal growth into responsible behavior. Through its research findings, literature is shown to extend beyond human values reflection and becomes an educational tool that develops ethical thinking and character while enhancing analytical engagement.

The research demonstrates multiple teaching applications for Charlotte's Web. This work enables classroom discussions about ethics while simultaneously promoting interdisciplinary education along with emotional maturity and philosophical inquiry. The study supports the idea that higher education tends to undervalue children's literature, which possesses great potential for improving ethics education and developing students who are prepared to engage responsibly and empathetically in society.

5.2 Recommendations

Following these research findings, we present recommendations aimed at educators and curriculum developers as well as directions for future research studies.

1) **Integrate children's literature into ethics and education courses.**

University teachers from teacher education and literature departments need to examine the possibility of including ethically meaningful children's books such as Charlotte's Web into their course plans. Literary narratives have the potential to generate thoughtful conversation and build empathy beyond what traditional instructional materials can achieve.

2) Design Literature-Based Moral Education Modules

Create educational modules and lesson plans that integrate ethical theories alongside literary analysis techniques. Students can participate in ethical discussions while writing thematic journals and comparing moral situations from literature to real-world scenarios.

3) **Conduct further research across texts and cultures.**

Researchers must carry out cross-cultural and age-specific analyses on children's literature to determine whether ethical themes maintain their consistency or show variation. Upcoming research should investigate student responses to moral teachings presented through literary works to determine their long-term outcomes.

4) **Encourage Cross-Disciplinary Collaboration**

Collaborate with experts in psychology, education, and philosophy to develop interdisciplinary approaches for ethical literary studies. Literature-based ethical teaching will advance through combined theoretical development and practical implementation enabled by this collaboration.

Through their dual approach as cultural artifacts and moral resources, children's literature enables educators and researchers to shape students' ethical understanding with stories like Charlotte's Web and train them for compassionate, wise actions with integrity in our complex modern world.

6. References

Hursthouse, R. (1999). *On Virtue Ethics*. Oxford University Press.

Kant, I. (2002). *Groundwork for the Metaphysics of Morals (A. Wood, Trans.).* Yale University Press. (Original work published 1785)

Mill, J. S. (1863). Utilitarianism. Parker, Son, and Bourn.

Nikolajeva, M. (2005). *Aesthetic Approaches to Children's Literature: An Introduction.* Scarecrow Press.

Norton, D. E. (2010). *Through the Eyes of a Child: An Introduction to Children's Literature* (8th ed.). Pearson Education.

Schreier, M. (2012). *Qualitative Content Analysis in Practice*. SAGE Publications.

Tomlinson, C. M., & Lynch-Brown, C. (2018). *Essentials of Children's Literature* (9th ed.). Pearson.

White, E. B. (1952). *Charlotte's Web*. Harper & Brothers.

The Study of Problems found in the workplace during Co-operative Education of students from Rajamangala University of Technology Rattanakosin Bophit Phimuk Chakkrawat Campus

Maswika Chaiyapoo[a], Rungrudee Na-on[b]

[a] Division of English for International Communication, Faculty of Liberal Arts, Rajamangala University of Technology Rattanakosin Bophit Phimuk Chakkrawat Campus, Bangkok, 10100.Thailand
[b] Division of English for International Communication, Faculty of Liberal Arts, Rajamangala University of Technology Rattanakosin Bophit Phimuk Chakkrawat Campus, Bangkok, 10100.Thailand
* Corresponding author. Tel.: 0894988954; E-mail address: maswika.cha@rmutr.ac.th

Abstract

The purpose of this research is to study the problems encountered by cooperative education students from the Faculty of Liberal Arts and the Faculty of Business Administration at Rajamangala University of Technology Rattanakosin, Bophit Phimuk Chakkrawat campus, during their work placements, as well as how the students addressed these problems. The research employed survey methods and data collection through cooperative education reports and semi-structured interviews. The results indicated two key findings. First, the problems faced by students could be categorized into four main aspects: (1) problems related to work content and work performance, (2) problems with equipment usage, (3) language-related problems, and (4) personal or life-related problems, including adjustment issues in the workplace. Second, the strategies students used to solve these problems included independent problem-solving, seeking assistance from workplace mentors, and requesting support from supervising teachers. The findings from this research can serve as useful guidelines for preparing students for the workplace. They can also inform teaching and learning management, as well as curriculum development, to better equip students for the demands of professional environments.

Keywords: Co-operative Education, Problems in Cooperative Education Practice, Cooperative Education Problem Solving Guidelines

1. Introduction

1.1 Research Background

Cooperative Education (Co-op) is an education system that combines classroom learning with practical work experience in a business in a systematic and organized manner to provide students with hands-on experience. Students are required to work in a business as full-time temporary employees for one semester. Through this program, students will have the opportunity to understand and become familiar with the real world of work, which supports learning and the development of professional and personal skills. It is an educational approach that integrates learning in academic institutions with full-time work placements in real business environments. The main purpose of the program is to prepare students in all aspects before they begin working in real organizations.

Rajamangala University of Technology Rattanakosin is one of the educational institutions that recognizes the importance of cooperative education. The university actively promotes students in each field of study to have the opportunity to participate in cooperative education. Specifically, Rajamangala University of Technology Rattanakosin, Bophit Phimuk Chakkrawat campus, which comprises two faculties—the Faculty of Liberal Arts and the Faculty of Business Administration—requires students who meet the criteria set by their respective programs within each faculty to undertake cooperative education. This is considered a graduation requirement.

Therefore, in every academic year, fourth-year students are assigned to complete a cooperative education placement for one semester. Upon completion of their program, all students are required to report their cooperative education outcomes to a committee within their department. The report is used to evaluate their performance at their workplace. Prior to the cooperative education period, each faculty provides thorough preparation for students in various aspects to ensure that students are ready to apply the knowledge and skills they have acquired at the university to real-life working situations.

Students from both the Faculty of Liberal Arts and the Faculty of Business Administration have had the opportunity to engage in cooperative education placement at various real workplaces, both within the country and abroad. However, reports from these cooperative educations have shown that most students continue to encounter difficulties in adapting to real work environments, despite the preparation provided by their faculties. This is because each workplace has different expectations and specific requirements. As a result, students often face challenges while working in real-world settings, even though they have undergone pre-cooperative education preparation.

Given the issues mentioned above, the researchers recognize the importance of understanding the problems faced by students from both faculties in the Bophit Phimuk Chakkrawat campus during their cooperative education periods. Therefore, the researcher aims to collect and analyze the problems encountered by students during their cooperative education placements over the past three academic years (2019–2021 academic year). The objective is to explore the causes of these problems and examine possible solutions. The research questions are: What types of problems do students encounter during their cooperative education placement? And how do students solve problems when they encounter problems during their cooperative education placement? The findings from this study will be beneficial for all faculties in improving their preparation processes, helping to ensure that students are more comprehensively equipped for their cooperative education experiences in the workplace.

1.2   Related theories and research studies

1) Rajamangala University of Technology Rattanakosin Bophit Pimuk Chakkrawad

Rajamangala University of Technology Rattanakosin is one of the universities under the nine Rajamangala University of Technology in Thailand. It was established as part of Thailand's efforts to expand educational opportunities for vocational students. The university traces its origins back to the College of Technology and Vocational Education, founded in 1975. In 1988, it was granted the name Rajamangala Institute of Technology to further promote vocational education, research, innovation, and academic services to society. Later, in 2005, Rajamangala University of Technology Rattanakosin was officially established under a specific legislative act. The university offers both undergraduate and graduate programs and is organized into seven faculties and three colleges. These cover diverse fields such as engineering, architecture, business administration, liberal arts, hotel and tourism, science and technology, and management innovation. The university operates across four campuses: Salaya, Bophit Phimuk Chakkrawat, Pohchang College, and Wang Klai Kangwon. (Rajamangala University of Technology Rattanakosin, 2019)

2) Cooperative education

The Cooperative Education Center, Phranakhon Si Ayutthaya Rajabhat University (2019) stated that Cooperative Education is an education system that was initially developed in England and the United States during the years 1903–1909, which, at that time, was referred to as the Cooperative Education system. In the United States, it was found that from 1960 onwards, the system continued to develop and expand further. Phranakhon Si Ayutthaya Rajabhat University (2019) also illustrated that this education system has been supported by government budgets and cooperation from enterprises, making it well-known and advanced. Currently, 33% of educational institutions worldwide use the cooperative education system and have developed it to the aspect of organizing student exchanges for international work placements. In addition, cooperative education has expanded into countries in East and Southeast Asia, where educational institutions have fully integrated cooperative education into their teaching. This is especially evident in institutions within the British educational network, which follow models similar to those in Western countries, such as the Hong Kong Polytechnic University and Nanyang Technological University in Singapore. Later, cooperative education spread to China and Thailand.

Cooperative Education is an educational system that integrates academic learning with practical work experience (Work Integrated Learning) to enhance the quality of graduates through real work experience in organizations, according to academic and professional standards, and aligned with labor market demands. Cooperative education thus plays a crucial role in preparing graduates to enter their careers, enabling them to work immediately after graduation. This educational system benefits students, universities, and employers alike. Graduates of cooperative education are therefore graduates who "know themselves, know others, and know their work" (Ubon Ratchathani University, 2017).

Cooperative Education is an educational system that emphasizes real work experience in organizations by integrating academic instruction with practical work, also known as Work Integrated Learning (WIL). This approach helps students gain an understanding of working life before graduation and develop skills relevant to their profession that meet the needs of employers. It also serves as a key guideline for students to apply theoretical knowledge to practical work in a principled and systematic manner, producing quality graduates who meet labor market demands. Furthermore, it promotes ongoing academic collaboration between organizations and educational institutions. (Supporting Education Division, Faculty of Science, Prince of Songkla University, 2023)

In summary, cooperative education is an education system that combines teaching and learning in an educational institution with real work experience in a workplace (Work-Integrated Learning or WIL). This type of education system allows students to apply the knowledge gained in the classroom to real-world work settings, while also providing opportunities to develop skills and knowledge in areas that may not be accessible in a traditional classroom environment. It enables students to discover their own abilities and interests, which can lead to a clearer and more suitable career path in the future. For some students, if they perform well and work effectively with others during their internship, there may be opportunities to continue working at the organization and eventually become full-time employees. Furthermore, this system fosters collaboration between educational institutions and workplaces in curriculum development and student preparation, ensuring that graduates meet the needs of employers and the labor market.

3) Establishment

Chollada Mongkhonwanich et al. (2021) stated that an "establishment" refers to a government or private organization or agency that shares responsibility for the operation of cooperative education with educational institutions and accepts cooperative education students to work. Similarly, Ubon Ratchathani University (2017) defined an establishment as a government or private organization or agency that collaborates with educational institutions in implementing cooperative education and accepts students for practical training.

Therefore, an establishment is a business organization that supports and contributes to the tangible development of students through cooperative education by accepting them for a one-semester training period. In addition to sharing responsibility with educational institutions by hosting students for cooperative education, establishments also play a significant role in fostering knowledge and understanding of cooperative education operations among their executives and employees. This leads to the organization's development as a source of diverse learning experiences—spanning knowledge, skills, and socialization.

From studies on problems that occur in the workplace or professional environment, including issues faced by students, it was found that experts have conducted research on a number of related topics, as follows:

Natcha Thamrongchot et al. (2012) studied the problems and obstacles in accepting undergraduate students in the Faculty of Business Administration to work in cooperative education, based on the concepts of business establishments in organizing and operating cooperative education, the qualifications of cooperative education students, and professional knowledge and skills. The study was conducted on 180 students who participated in cooperative education. The research results found the following problems and obstacles: the first aspect was the organization and operation of cooperative education—business establishments could not coordinate with educational institutions to set guidelines and prepare students before starting work. In addition, business establishments did not know the purpose of working according to the cooperative education curriculum, and they did not trust students to contact the business establishments themselves. The second aspect was the qualifications of cooperative education students—students could not make decisions to solve problems while working, lacked self-confidence, and showed a lack of meticulousness in their work. The final aspect was professional knowledge and skills—students could not communicate effectively in both Thai and foreign languages, either verbally or in writing; they were unable to analyze and plan their work properly; and they lacked proficiency in using office equipment.

Siriwan Munintrawong (2018) studied the problems related to internships and work skills of Japanese language students at Thammasat University. The research findings revealed that the top five skills students need to develop during their studies, in order of importance, are: 1) Communication skills with others, 2) Japanese language knowledge, 3) Enthusiasm, 4) Teamwork, and 5) Basic knowledge and skills for work. As for the skills that internship students showed little development in, the department should prioritize monitoring the following four skills, in order: 1) Japanese language knowledge, 2) IT skills, 3) Business knowledge, and 4) Management and problem-solving skills.

2. Methodology

The study and collection of problems encountered by students during their internships, as well as the solutions they used to address those problems, employed a mixed-methods research approach, combining both qualitative and quantitative methods. Data were collected from cooperative education reports and semi-structured interviews. The research methodology is detailed as follows:

2.1 Research Sample

The sample population in this study was selected using purposive sampling. The participants were fourth-year students from the Faculty of Liberal Arts and the Faculty of Business Administration who participated in cooperative education programs during the academic years 2019 to 2021, covering a total of three academic years.

2.2 Research Instruments

The research instruments consisted primarily of student internship reports and semi-structured interviews. These tools were used to collect and analyze data. Data were organized and presented separately by department and faculty to clearly illustrate the problems students encountered and the solutions they applied. A coding method was used to analyze open-ended responses from both the reports and the interviews.

3. Results and Discussion

3.1 Results from the analysis of problems encountered during cooperative education placements

In terms of problems found during cooperative education, it was observed that students from the Faculty of Liberal Arts experienced varying problems depending on their majors.

For Chinese language majors, the most common issue was language-related problems, accounting for 30.37%, followed by work content and performance problems at 29.36%. Problems in using various equipment made up 15.19%, while the least common issues were related to living, workplace adjustment, and personal matters, accounting for 6.8%.
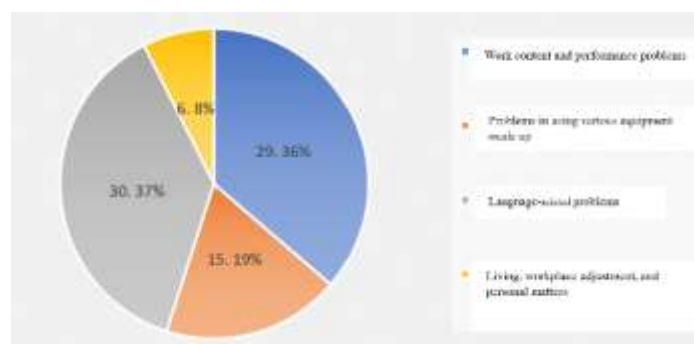

Figure 1 Problems encountered by Chinese language students during cooperative education placements

For Japanese language majors, language problems were also the most frequent, comprising 45.36%, followed by work content and performance issues at 40.32%. Equipment usage problems accounted for 28.22%, and the least common were living and personal adjustment issues, at 12.10%.
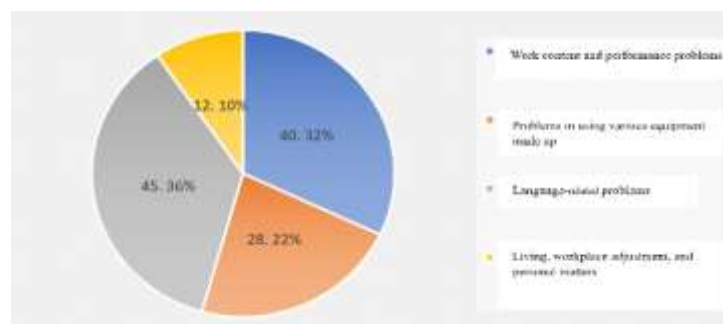
Figure 2 Problems encountered by Japanese language students during cooperative education placements

In contrast, students majoring in English for International Communication experienced the highest number of problems related to work content and performance, at 45%, followed by issues concerning living, adjustment, and personal matters at 25%. Language problems accounted for 23%, and the least common were equipment usage problems, comprising 7%.
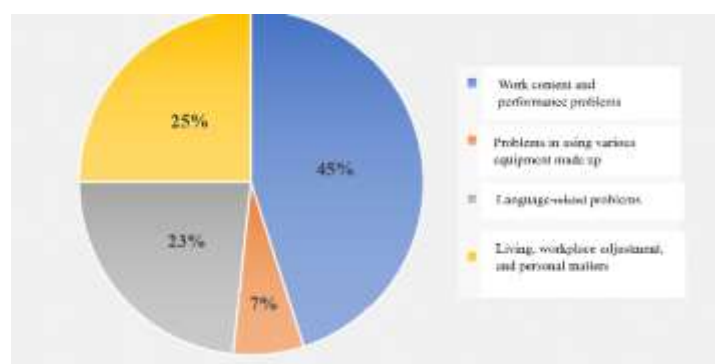

Figure 3 Problems encountered by English for International students during cooperative education placements

For students from the Faculty of Business Administration, it was found that those majoring in Accounting experienced the highest percentage of problems related to the use of various equipment (43%), followed by problems concerning work content and performance (27%). Issues related to living, adjusting to the workplace, and personal matters accounted for 23%, while language problems were the least common, at 7%.
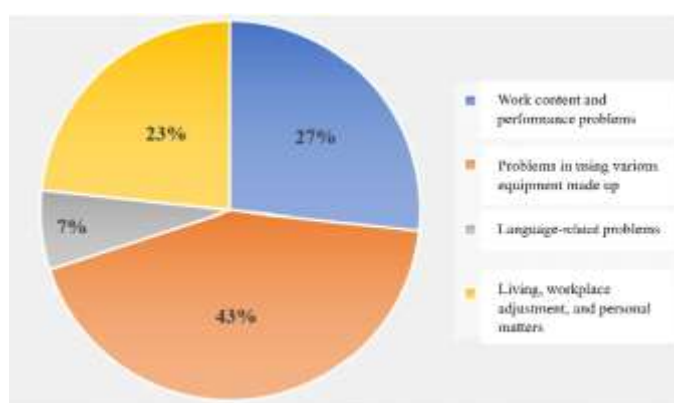

Figure 4 Problems encountered by Accounting students during cooperative education placements

Among students majoring in Management, the most frequently reported issues were related to work content and performance (34%), followed closely by equipment usage problems (33%). Problems related to living, workplace adjustment, and personal matters made up 29%, while language issues were again the least reported, at 4%.
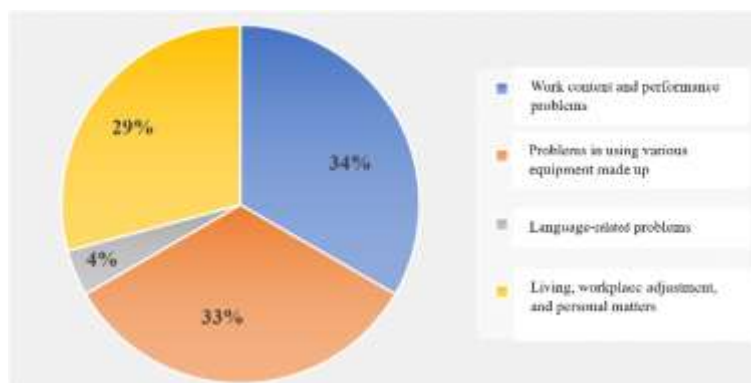
Figure 5 Problems encountered by Management students during cooperative education placements

For Marketing majors, the most prominent problems were associated with work content and performance, accounting for 52%, followed by equipment usage problems at 36%. Issues related to living, adjustment, and personal matters were reported at 7%, and language-related problems were the least common, at 5%.
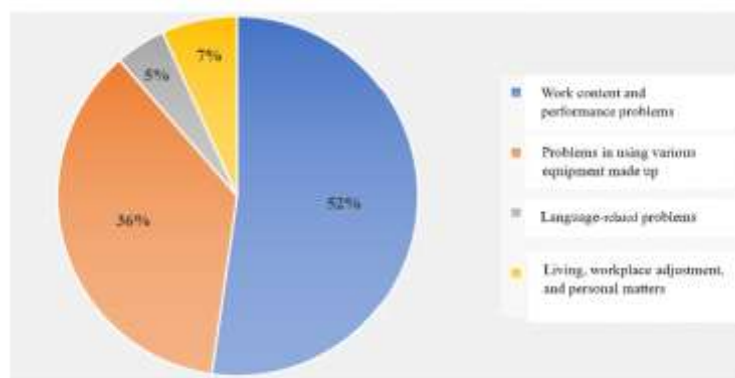

Figure 6 Problems encountered by Marketing students during cooperative education placements

3.2 Results from the Analysis of Problem-Solving Approaches in Cooperative Education placements

In cooperative education practices, after collecting data, students' problem-solving approaches can be classified into three groups based on their characteristics:

1) Independent problem-solving: Students help themselves by finding information independently.
2) Seeking assistance from workplace mentors: Students ask for help from mentors at their workplace.
3) Seeking assistance from supervising teachers: Students ask for help from their academic supervising teachers.

For Chinese language students, based on information obtained from the cooperative education report, students most commonly solved problems by helping themselves and finding information independently, accounting for 56%. The next most common approach was asking for help from a mentor in the workplace, accounting for 44%. Students in the Chinese language program did not seek help from the supervising teacher.
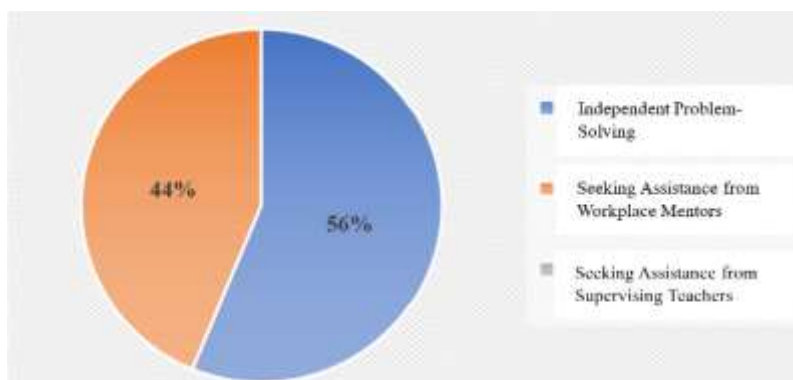

Figure 7 Methods for solving problems encountered in the cooperative education placements of Chinese language students

For Japanese language students, students most commonly solved problems by helping themselves and finding information independently, accounting for 76%. This was followed by solving problems by asking for help from a mentor in the workplace, accounting for 22%, and by asking for help from a supervising teacher, accounting for 2%.
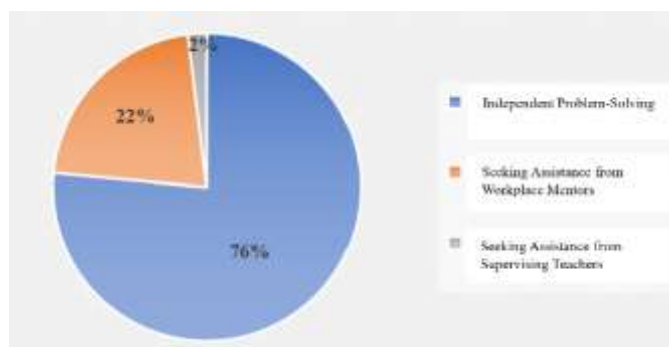

Figure 8 Methods for solving problems encountered in the cooperative education placements of Japanese language students

For students majoring in English for International Communication, students most commonly solved problems by helping themselves and finding information independently, accounting for 58%. This was followed by solving problems by asking for help from a mentor in the workplace, accounting for 42%. Students majoring in English for International Communication did not seek help from the supervising teacher.
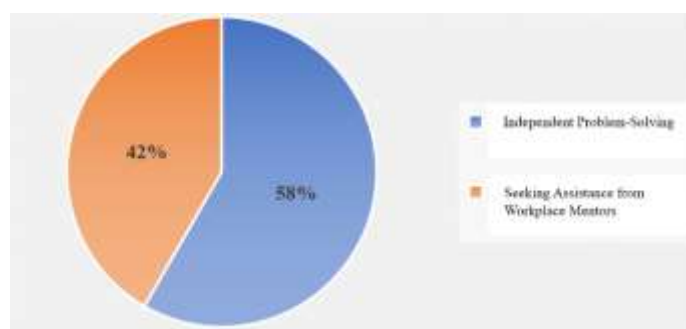

Figure 9 Methods for solving problems encountered in the cooperative education placements of English for International students

For students from the Faculty of Business Administration, it was found that Accounting students most commonly solved problems by helping themselves and finding information independently, accounting for 75%. This was followed by solving problems by asking for help from a mentor in the workplace, accounting for 25%, while Accounting students did not seek help from the supervising teacher.
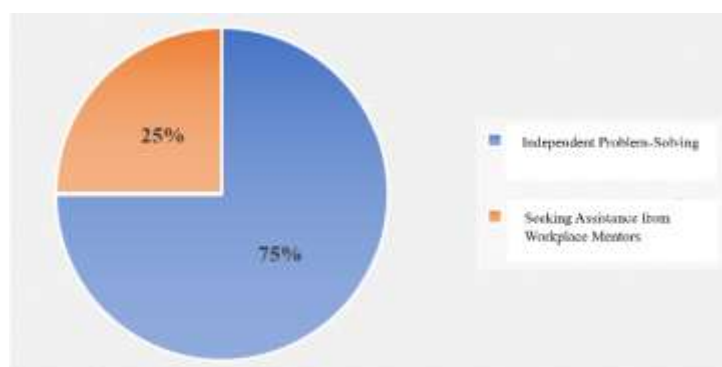

Figure 10 Methods for solving problems encountered in the cooperative education placements of Accounting students

For Management students, students most commonly solved problems by helping themselves and finding information independently, accounting for 50%. This was followed by solving problems by asking for help from a mentor in the workplace, accounting for 46%, and by asking for help from a supervising teacher, accounting for 4%.
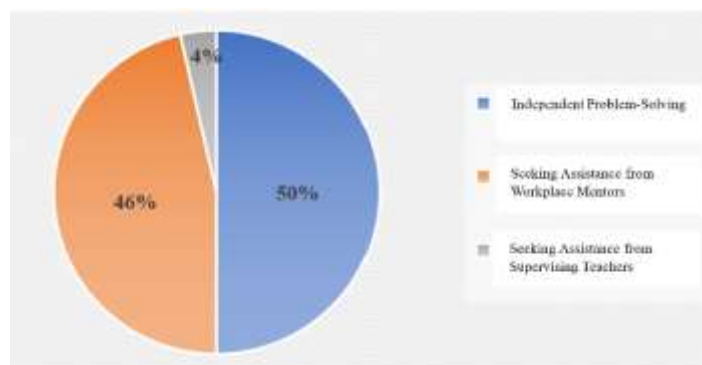
Figure 11 Methods for solving problems encountered in the cooperative education practice of Management students

For Marketing students, students most commonly solved problems by helping themselves and finding information independently, accounting for 72%. This was followed by solving problems by asking for help from a mentor in the workplace, accounting for 28%, while Marketing students did not seek help from the supervising teacher.
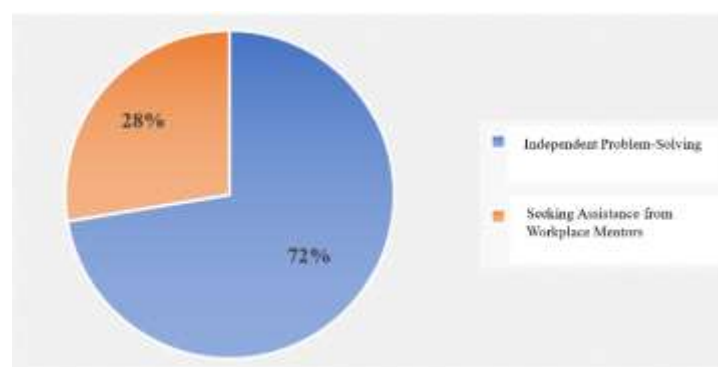

Figure 12 Methods for solving problems encountered in the cooperative education placements of Marketing students

3.3 Results of the interview

In the summary of the interview results, the representative found that the interview answers could be divided into issues similar to those identified in the cooperative education work reports. These issues mainly involved problems with work content and tasks. The interviewees pointed out that the work assigned was often difficult because it involved tasks, they had never done before or tasks not covered in their university studies, making it challenging to perform in real work settings.

Regarding the use of equipment, the interviewees noted difficulties in operating equipment they had never used prior to their work placements. Some also mentioned that the equipment at the workplace was not fully prepared for use, further complicating their tasks.

Language problems were also reported, with interviewees from both faculties facing challenges in communication. When a language problem occurred, the interviewee initially solved it by seeking help from someone with the necessary language skills or by having a mentor assist in resolving the issue. This approach helped them overcome the immediate problem. Additionally, the interviewee made use of technology to reduce communication barriers. This not only helped lessen the obstacles but also improved speaking and communication, allowing the interviewee and their contacts to better understand each other.

Additionally, students encountered issues related to living arrangements, adjusting to the work environment, and interacting with colleagues.

From the interviews, it was also found that most interviewees preferred to try solving problems on their own first, as they did not want to disturb their colleagues or supervisors. Some students also mentioned that they initially attempted to solve problems themselves because they were afraid to ask for help, fearing they might be scolded. However, many interviewees stated that they would first assess the type of problem. If it was something they believed they could handle independently, they would proceed on their own. However, if the problem seemed likely to cause damage or serious issues, they would immediately inform their supervisors.

However, the interviews also provided valuable advice for students preparing for cooperative education. Most interviewees emphasized the importance of carefully selecting a workplace—choosing one where they are likely to fit well—and thoroughly researching the job position before applying. If students are accepted into a position, it is recommended that they gather as much information as possible about the role beforehand.

4. Conclusions

The researcher discussed the results of the study on the problems encountered in the cooperative education of students at Rajamangala University of Technology Rattanakosin, Bophit Phimuk Chakkrawat area, based on the research questions. The first question asked: What types of problems do students encounter while practicing cooperative education? The research findings revealed that students faced problems in four main areas: work-related issues, issues with using various equipment, language difficulties, and challenges related to living, adjusting to work, and personal matters. Upon further analysis by faculty, it was found that work-related problems were the most prevalent across all fields, except for the accounting field, where equipment usage issues were more prominent. Based on the interview results, it appears that accounting work, which is typically office-based, requires the use of various office equipment. However, in the classroom, there is often little emphasis or practice with these tools. As a result, students may not be as comfortable using the equipment, which aligns with the findings of Natcha Thamrongchote et al. (2012), who studied the problems and obstacles in accepting students into cooperative education at the Faculty of Business Administration, Rajamangala University of Technology Phra Nakhon. Their research also found that students lacked proficiency in using office equipment.

Another interesting aspect is the issue of language problems. According to the data presented in the pie chart, students from the Faculty of Business Administration—particularly those in Accounting, Management, and Marketing—experienced only minor language problems, with most reporting issues at less than 10%. This suggests that the nature of their work typically does not require extensive language use. However, language skills are still important for this group of students. In contrast, students from three programs within the Faculty of Liberal Arts reported language problems as the second most common issue after work-related problems. This may be attributed to the nature of their studies, which focus primarily on language, requiring them to apply these skills directly in the workplace. As a result, they may face more difficulties in using language in professional contexts than their peers in the Business Administration faculty. These findings are consistent with the study by Siriwan Munintrawong (2018), who examined internship problems and work skills of students in the Japanese language program at Thammasat University. That study found that students encountered challenges specifically in tasks requiring translation and interpretation, highlighting how work that demands applied language knowledge can be a significant source of difficulty.

Regarding research question 2: How do students solve problems when they encounter issues during their internship? The study found that students across all majors generally attempted to solve problems on their own before seeking help from an advisor or consulting with a faculty supervisor. The interview data provided deeper insight into why students chose to handle problems independently at first. Some reasons included not wanting to disturb colleagues or feeling hesitant to ask for help due to fear of being scolded—especially if the issue caused from a repeated mistake. However, many students also reported that they assessed the nature of the problem before acting. If they believed the issue could be resolved independently, they would do so. Conversely, if the problem seemed likely to cause significant consequences, they would immediately notify their advisor.

Overall, the results of this study revealed the main problems that students faced while participating in cooperative education practice at the workplace. Additionally, the study highlighted the problem-solving methods that students employed when encountering these challenges. It was observed that most students attempted to solve the problems on their own before seeking assistance from their advisor or mentor. For some students who felt that the advisor could not resolve the issue, they would turn to the supervising faculty for help. Furthermore, the study emphasized the importance of selecting a suitable and well-informed workplace, as well as gathering information before starting the actual work, to benefit the students when transitioning into the real-world work environment

5. Acknowledgments

6. References

Chollada Mongkolvanich et al., 2021. *The perception of enterprises towards the quality of cooperative education projects in the tourism and hospitality industry*. Journal of Cultural Stream, pp.19–33. (in Thai)

Natcha Thamrongchote et al., 2012. *Problems and obstacles in accepting students into cooperative education based on the concept of establishments: A case study of the Faculty of Business Administration, Rajamangala University of Technology Phra Nakhon* [online]. Available at: https://shorturl.at/rzFH5 [Accessed 23 Nov. 2022]. (in Thai)

Rajamangala University of Technology Rattanakosin, 2019. *History of Rajamangala University of Technology Rattanakosin campuses* [online]. Available at: http://www.cupt.net/docs/pdfr4/195.pdf [Accessed 20 Nov. 2022]. (in Thai)

Siriwan Munintrawong, 2018. *Internship problems and work skills of Japanese language students at Thammasat University.* Japanese Studies Network Journal, 8(3), pp.206–218. (in Thai)

Supporting Education Division, Faculty of Science, Prince of Songkla University, 2023. What is Co-operative Education? [online]. Available at: https://regis.sci.psu.ac.th/cooperative-education/9-2020-04-03-07-26-05/92-organization-2 [Accessed 1 Dec. 2022]. (in Thai)

Ubon Ratchathani University, 2017. *What is cooperative education?* [online]. Available at: https://www.ubu.ac.th/web/files_up/00046f2020030409131799.pdf [Accessed 28 Nov. 2022]. (in Thai)

Applying the Theory of Planned Behavior to Understand Electric Vehicle Purchase Intentions in Phra Nakhon Si Ayutthaya

Adisai Watanaputi[a], Chitsanu Pakdeewanich[b*], Nitinop Tongwassanasong[c], Chadaporn Prasatkul[d]

[a] Department of Management, Faculty of Business Administration and Information Technology, Rajamangala University of Technology Suvarnabhumi, Pharanakhon Si Ayutthaya, 10300, Thailand.
[b] Department of Manufacturing and Service Industry Management, Faculty of Business and Industrial Development, King Mongkut's University of Technology North Bangkok, Bangkok,10800, Thailand.
[c] Department of Management, Faculty of Business Administration, Rajamangala University of Technology Rattanakosin, Nakhon Pathom, 73170, Thailand.
[d] Faculty of Public Health, Rajapruk University, Nonthaburi, 11130, Thailand.
* Corresponding author. Tel.:096-351-5639; E-mail address: chitsanu.p@bid.kmutnb.ac.th

Abstract

This study aims to examine the influence of three key factors—attitude toward the behavior, subjective norms, and perceived behavioral control on the intention to purchase electric vehicles (EVs) in Phra Nakhon Si Ayutthaya Province. The research framework is based on the Theory of Planned Behavior (TPB). The sample group consisted of 400 individuals aged between 20 and 59 years (Generation X and Y), residing in Phra Nakhon Si Ayutthaya, selected using a convenience sampling method. A questionnaire was used as the data collection tool. The data were analyzed using descriptive statistics, analysis of variance (ANOVA), and multiple regression analysis. The results revealed that most respondents were female, aged between 20–29 years, single, held a bachelor's degree, worked in private companies, and had a monthly income of less than 15,000 baht. The three main factors—attitude, subjective norms, and perceived behavioral control—were rated at a high level of agreement. Furthermore, demographic variables including age, marital status, and monthly income showed statistically significant differences in the intention to purchase EVs at the 0.05 significance level. The three psychological factors together were found to explain 59.3% of the variance in purchase intention, also statistically significant at the .05 level.

Keywords: Electric Vehicles, Theory of Planned Behavior, Purchase Intention, Demographics

1. Introduction

Currently, every country is inevitably facing the phenomenon of global warming — the rise in the average temperature of the Earth's surface air and oceans. This temperature continues to increase annually. According to data from the Climatic Research Unit and the National Oceanic and Atmospheric Administration (NOAA), from 1981 to 2018, the Earth's average temperature has increased by approximately 1°C. Furthermore, the concentration of carbon dioxide (CO_2) in the atmosphere reached 414.3 parts per million (ppm) in 2021, with an annual increase of about 2.4 ppm, as reported by NASA's Goddard Institute for Space Studies (GISS).

The primary causes of global warming stem from human activities such as the burning of coal and fossil fuels for transportation, along with deforestation for human benefit, which rapidly increases CO_2 in the atmosphere. These greenhouse gases accumulate in the Earth's atmosphere, trapping heat. Other contributing natural factors include variations in Earth's orbit and volcanic eruptions, both of which lead to heat retention and global temperature rise. This widespread impact threatens the natural ecosystem (Kritsada Sektakul, 2021). The more fossil fuel-powered vehicles are used, the faster global warming progresses. Although fuel prices may not be the main reason governments promote electric vehicles (EVs), concern about climate change remains a major driver. It is predicted that by 2050, emissions from the transportation sector will account for 30–50% of global greenhouse gas emissions. Hence, many governments are encouraging citizens to reduce private car usage and rely more on public transportation to minimize transportation-related pollution.

One of the most promising solutions many countries are adopting to reduce air pollution is the use of 100% electric vehicles (EVs). These innovative vehicles run solely on electricity, making them more cost-efficient in terms of maintenance and energy usage since electricity is cheaper than fossil fuels. Moreover, electric vehicles emit no exhaust gases, which are typically caused by incomplete fuel combustion, thus being environmentally friendly (Nuengruethai Rattanaporn, 2019).

In Thailand, the electric vehicle policy is one of the top priorities of the Prime Minister and the government. The policy aims to maintain Thailand's automotive production base and position the country as a hub for electric vehicle, motorcycle, and bus production. The national target is to produce 750,000 electric vehicles by 2030 (Ministry of Industry, March 2020). Electric vehicles began playing a more prominent role in Thailand around 2018, with steadily increasing sales. As of December 2019, the number of registered electric vehicles in Thailand totaled 124,085 units (Department of Land Transport), representing only 1% of all new car sales. Consumers are aware that EVs reduce reliance on fossil fuels and help protect the environment. However, many are concerned about the high purchase price, primarily due to the expensive battery component, which is significantly more costly than those in internal combustion engine vehicles. Additionally, most EVs sold in Thailand are imported, contributing to the higher price.

Therefore, the researcher is interested in applying the Theory of Planned Behavior (TPB) to examine consumers' purchase intentions regarding electric vehicles (EVs) in Phra Nakhon Si Ayutthaya Province. The findings of this research are expected to benefit automotive businesses and both government and private sector stakeholders by providing insights and strategies to better educate and inform consumers, ultimately promoting the widespread adoption of electric vehicles in Thailand for environmental sustainability.

The Theory of Planned Behavior (TPB) was chosen as the primary theoretical framework for this study due to its ability to comprehensively capture the interplay between individual attitudes, perceived social pressure (subjective norms), and perceived behavioral control in predicting intentional behavior. Compared to alternative models such as the Technology Acceptance Model (TAM) or the Unified Theory of Acceptance and Use of Technology (UTAUT), TPB is particularly suited for studies involving consumer decision-making where behavioral intention is the focus. TPB's flexibility allows it to be applied across cultural and contextual variations, making it ideal for understanding electric vehicle adoption in a specific Thai province.

2. Methodology

2.1 Population and Sampling

The target population for this study includes 400 individuals aged 20 to 59 years (comprising Generation Y and Generation X) residing in Phra Nakhon Si Ayutthaya Province, as detailed in Table 1.

Table 1 Population Aged 20-59 Years in Phra Nakhon Sri Ayutthaya Province

Generation	Age Range (Years)	Total
Gen Y	20-24	48,420
	25-29	45,008
	30-34	41,669
	35-39	45,973
	40-44	49,522
Gen X	45-49	49,974
	50-54	53,112
	55-59	49,035
Total		**334,293**

Since the exact population size is known, the sample size can be determined using Taro Yamane's formula, with a 95% confidence level and a 5% margin of error. The formula used for sample size calculation in this study is based on Taro Yamane (1967), given a known population size.

$$n = \frac{N}{1 + Ne^2}$$

Where:
n = sample size
N = population size
e = margin of error (.05 for 5%)

$$n = \frac{334,293}{1 + 334,293(.05)^2}$$
$$n = 399.52 \text{ Individuals}$$

Therefore, the sample group consists of individuals aged between 20 and 59 years (Generation Y and Generation X) residing in Phra Nakhon Si Ayutthaya Province. The sampling method used is non-probability sampling, specifically convenience sampling. Questionnaires were distributed to 400 individuals within the specified age group who reside in Phra Nakhon Si Ayutthaya Province.

2.2 Research Instrument

The researcher collected data from the sample group using a **questionnaire** as the primary research instrument. The process of questionnaire construction consisted of the following steps:

1) Studied the development of questionnaires through academic documents, previous research, and theories related to the Theory of Planned Behavior and purchase intention of electric vehicles. This included factors such as **attitude toward behavior, subjective norms**, and **perceived behavioral control**.

2) Designed the questionnaire based on the conceptual framework to collect opinions on the various factors influencing the intention to purchase electric vehicles.

3) Revised and refined the questionnaire before submitting it for approval by the thesis advisor.

4) Conducted a **reliability test** using **Cronbach's Alpha Coefficient** to evaluate the internal consistency of the items. The coefficient ranges from 0 to 1, with values closer to 1 indicating higher reliability.

5) Final review of the questionnaire was conducted after receiving approval from the thesis advisor.

6) Distributed the questionnaire to 400 respondents.

2.3 Instrument Validation

The researcher verified the completeness and content validity of the questionnaire by presenting it to the thesis advisor. The final version of the questionnaire consisted of four parts as follows:

Part 1: Demographic Information

This section includes **closed-ended questions** designed to gather basic demographic data:

Item 1: Gender – Nominal Scale

Item 2: Age – Nominal Scale

Item 3: Marital Status – Nominal Scale

Item 4: Highest Education Level – Ordinal Scale

Item 5: Occupation – Nominal Scale

Item 6: Average Monthly Income – Ordinal Scale

Part 2: Behavioral Factors

This section includes items assessing factors that influence: Attitude toward the behavior Subjective norms (influence of reference groups) Perceived behavioral control Purchase intention for electric vehicles.

Part 3: Suggestions

This section allows respondents to provide additional comments or suggestions related to the study. All items in Parts 2 and 3 were measured using a **5-point Likert Scale,** with the following interpretation:

5 = Strongly Agree

4 = Agree

3 = Neutral

2 = Disagree

1 = Strongly Disagree

To interpret the results, the researcher calculated class intervals using standard formulas to define score ranges and provide meaningful interpretation for each level of response.

2.4 Data Collection

The study was conducted by utilizing two sources of data as follows:

1) Primary Data

Primary data were collected directly from a sample of 400 individuals aged between 20 and 59 years (Generation X and Generation Y) residing in Phra Nakhon Si Ayutthaya Province. Data were gathered using a self-administered questionnaire developed by the researcher and distributed online via Google Forms. The questionnaire link was posted on various social media platforms including Facebook, Instagram, and Line.

2) Secondary Data

Secondary data were obtained from academic documents and related research, including theses, journal articles, academic publications, and other printed materials. Additionally, relevant information from both domestic and international internet sources was reviewed. These data were used to support the conceptual framework and provide background for the study

2.5 Data Processing and Analysis

After collecting the completed questionnaires, the researcher verified the accuracy of the responses and performed data coding. The coded data were then analysed using a statistical software package, specifically the Statistical Package for the Social Sciences (SPSS). This software was used to compute various statistical measures required for data analysis and interpretation.

2.6 Statistical Methods for Data Analysis

In this study, the researcher employed both **descriptive** and **inferential statistics** as follows:

1) Descriptive Statistics

Descriptive statistics were used to summarize and describe demographic characteristics of the sample group, including gender, marital status, age, highest education level, occupation, and average monthly income. These data were presented using: Frequency distributions, Percentage for Part 2 of the questionnaire, the researcher used: Mean (M) Standard Deviation (SD) to describe the level of opinions toward behavioral factors related to the intention to purchase electric vehicles.

2) Inferential Statistics

Inferential statistics were used to test hypotheses and analysed relationships among variables:

Analysis of Variance (ANOVA) at a .05 significance level was used to examine relationships between independent variables such as attitude toward behavior, perceived behavioral control, and subjective norms, and the purchase intention of electric vehicles. Reliability Analysis was conducted using Cronbach's Alpha Coefficient to assess the internal consistency of the questionnaire. Data collected from the 400 respondents were used in this analysis, and an acceptable reliability value was considered to be not less than 0.70. Multiple Regression Analysis was applied to identify the strength and direction of the relationship between independent variables (predictors) and the dependent variable (purchase intention of electric vehicles).

3. Results and Discussion

3.1 Analysis of Demographic Characteristics

The analysis of the demographic characteristics of the sample group revealed the following:

The majority of respondents were female, totalling 241 individuals (60.3%). Most were aged 20–29 years, accounting for 175 individuals (43.8%). The highest proportion of respondents were single, totalling 229 individuals (57.3%). Regarding education, the majority held a bachelor's degree, totaling 220 individuals (55.0%). The most common occupation was company employee, with 149 individuals (37.3%). In terms of average monthly income, the largest group earned less than 15,000 baht, with 120 individuals (30.0%). These details are summarized in Table 2.

Table 2 Demographic Characteristics of the Sample Group (n = 400)

Characteristic	Category	Frequency (n)	Percentage (%)
Gender	Male	159	39.8
	Female	241	60.3
Age Group	20-29 years old (Gen Y)	175	43.8
	30-39 years old (Gen Y)	92	23.0
	40-49 years old (Gen X)	75	18.8
	50-59 years old (Gen X)	58	14.5
Marital Status	Single	229	57.3
	Married	148	37.0
Education Level	Bachelor's degree	220	55.0
	Master's or higher	180	45.0
Occupation	Company employee	149	37.3
	Government officer	100	25.0
	Self-employed	81	20.3
	Student	45	11.3
	Others	25	6.3
Monthly Income (THB)	Less than 15,000	120	30.0
	15,001-30,000	105	26.3
	30,001-45,000	93	23.3
	45,001-60,000	50	12.5
	More than 60,000	32	8.0

3.2 Analysis of Respondents' Opinions on the Application of the Theory of Planned Behavior in Studying the Intention to Purchase Electric Vehicles

The results of the study revealed the following levels of respondents' opinions:

1) Attitude Toward the Behavior

The respondents' overall opinion regarding attitude toward the behavior was at a high level of agreement, with a mean score of 3.78. The highest-rated item was "Electric vehicles will be beneficial to the environment in the long term", which received a mean score of 3.88.

2) Subjective Norm

The overall level of opinion regarding subjective norms was also at a high level of agreement, with a mean score of 3.62. The highest-rated item was "Most people will value you if you use an electric vehicle in the future", with a mean score of 3.66.

3) Perceived Behavioral Control

The respondents' overall opinion on perceived behavioral control was at a high level of agreement, with a mean score of 3.62. The highest-rated item was "The price of an electric vehicle is important to you and you can afford it when you decide to adopt it", which had a mean score of 3.70.

4) Purchasing Intention

The respondents' overall purchasing intention was rated at a high level of agreement, with a mean score of 3.50. The highest-rated item in this category was "I intend to use an electric vehicle in the future", with a mean score of 3.59.

3.3 Differences in Demographic Characteristics and Related Factors

The study found significant differences between demographic characteristics and various behavioral factors, as follows:

1) Age

There were statistically significant differences among age groups in relation to all key behavioral factors: attitude toward the behavior, subjective norm, perceived behavioral control, and purchasing intention.

- Respondents aged 40–49 years showed significantly lower attitudes toward the behavior than those aged 20–29 and 30–39 years.
- For subjective norm and purchasing intention, respondents aged 40–49 and 50–59 years demonstrated significantly lower levels of agreement than those aged 20–29 and 30–39 years.
- For perceived behavioral control, respondents aged 20–29 years showed significantly higher levels of agreement than those in the older age groups (30–39, 40–49, and 50–59 years), while those aged 50–59 years had significantly lower agreement than the 30–39 age group.

2) Marital Status
Marital status showed significant differences across all behavioral factors. Specifically:
- Respondents who were single had significantly higher levels of agreement on attitude toward the behavior, perceived behavioral control, and purchasing intention than those who were married.
- Singles also expressed significantly higher agreement on subjective norm than those who were divorced/widowed/separated.

3) Average Monthly Income
Statistically significant differences were observed in all behavioral factors across income levels:
- Respondents with monthly incomes below 15,000 THB reported significantly higher attitudes toward the behavior than those earning 60,001–75,000 THB and above 75,001 THB.
- Those earning 15,001–30,000 THB and 30,001–45,000 THB also reported significantly higher attitudes than higher-income groups.
- Respondents with incomes below 15,000 THB had significantly higher agreement on subjective norms than those earning 45,001 THB and above.
- Respondents in the lower-income groups (below 45,000 THB) also demonstrated significantly higher perceived behavioral control than those in higher income brackets (45,001 THB and above).
- Even among mid-income earners (45,001–60,000 THB), perceived behavioral control was significantly higher than those earning above 75,001 THB.

It is noteworthy that younger respondents (aged 20–29 years) exhibited higher levels of purchase intention, attitude, and perceived behavioral control than older groups. This may be attributed to greater openness to innovation, environmental consciousness, and influence from peer groups.

Surprisingly, individuals with lower monthly income (less than 15,000 THB) also showed a stronger intention to purchase EVs. This result deviates from the assumption that higher income leads to higher purchasing capacity. A possible explanation is that lower-income groups perceive EVs as a long-term cost-saving option, and the intention may reflect aspiration rather than immediate ability to purchase. This insight could inform strategies targeting aspirational marketing or subsidy programs.

4) Influential Factors on Purchasing Intention
Based on the Theory of Planned Behavior, the key factors influencing purchase intention of electric vehicles among consumers in Phra Nakhon Si Ayutthaya include:
- Attitude Toward the Behavior
- Subjective Norm
- Perceived Behavioral Control

The results revealed that these three variables significantly influenced purchasing intention at the 95% confidence level and together explained 59.3% of the variance in the intention to purchase electric vehicles. Thus, all three factors play a statistically significant role in determining consumers' purchase intentions.

4. Conclusions
The results of this study are discussed according to the research objectives as follows:

4.1 Levels of Attitude, Subjective Norm, Perceived Behavioral Control, and Purchase Intention Toward Electric Vehicles among Consumers in Phra Nakhon Si Ayutthaya

The study found that consumers generally had a high level of attitude toward electric vehicle (EV) adoption. This may be due to the increasing popularity of EVs as a modern innovation and a viable alternative to traditional cars. Many consumers perceive EVs positively and have begun to compare information about EVs, indicating growing interest and expectation that EVs can outperform conventional vehicles. Therefore, if accurate and compelling information about EV features and benefits is effectively communicated, and positive perceptions, experiences, and emotional connections are fostered, consumers' intention to purchase EVs will likely increase.

Subjective norms were also found to influence purchase intention. Although consumers showed a positive intention to purchase EVs, it may stem from general awareness rather than actual usage experience. The decision to buy such a high-value product often depends on confidence in the product. Thus, positive recommendations from reference groups may enhance this confidence and increase consumers' purchase intention.

For perceived behavioral control, the study revealed a high level of consumer confidence and intention. As EVs are still new to many consumers, factors such as innovative technology, operational systems, pricing, and cost-effectiveness play a significant role in shaping trust. When consumers perceive that they have sufficient internal resources (e.g., knowledge, need) and external conditions (e.g., independence, opportunity), their perceived behavioral control increases—thereby strengthening their purchase intention.

4.2 Influence of Attitude, Subjective Norm, and Perceived Behavioral Control on Purchase Intention Toward Electric Vehicles

The findings confirmed that attitude toward behavior significantly influences consumers' purchase intention for EVs in Phra Nakhon Si Ayutthaya. This aligns with the research by Adnan, Nordin, and Rahman (2017), which studied EV acceptance in Malaysia and found that environmental awareness and positive attitudes, subjective norms, and perceived behavioral control significantly influenced intention.

Similarly, Shalender and Sharma (2020), who studied 326 consumers and 57 automotive sales representatives in India, found that attitude positively influenced EV acceptance and purchase intention. Tu and Yang (2019) also found that Taiwanese consumers with positive attitudes toward EVs were more likely to compare technology and cost with traditional cars, leading to higher purchase intention.

Regarding subjective norm, the results support Schmalfuß, Mühl, and Krems (2017), who found that reference groups have a strong influence on EV purchase intention, especially when close individuals introduce the product positively. Likewise, Eneizan (2019) in a study conducted in Jordan, using the Theory of Planned Behavior with 250 respondents, found that subjective norms positively influence EV adoption. Peters and Dütschke (2014) also noted that reference groups significantly influence those who have not yet experienced using EVs, a finding relevant to the current context of EV adoption in Thailand.

As for perceived behavioral control, the study's findings are consistent with Al-Amin, Ambrose, Masud, and Azam (2016), who examined Malaysian consumers and found a significant positive influence of perceived behavioral control on purchase intention. This is also supported by Asadi et al. (2020), whose study of 177 Malaysian respondents revealed that attitude, subjective norm, and perceived behavioral control all positively influenced EV purchase intention. Furthermore, Zhang et al. (2018), studying 124 respondents aged 18–55 in Beijing, found that perceived behavioral control was the most influential factor in car-sharing EV usage intention, followed by subjective norm and attitude.

6. Practical Implications and Limitations

5.1 Practical Implications

The findings provide practical implications for policymakers, manufacturers, and marketers aiming to promote electric vehicle adoption. Strategic communication should emphasize positive environmental outcomes and address perceived behavioral barriers, particularly among older and higher-income segments. Additionally, marketing efforts that leverage social influence and reference group endorsement may effectively strengthen subjective norms and purchasing intention among target consumers.

5.2 Limitations

This study has certain limitations. The use of convenience sampling may limit the generalizability of the findings beyond the province studied. Furthermore, the reliance on self-reported data introduces potential for response bias. Future studies should consider incorporating mixed-method approaches and expanding the geographic scope to validate and enrich the findings.

6. References

Adnan, N., Nordin, S. M., & Rahman, I. (2017). Adoption of electric vehicles in Malaysia: The drivers and barriers. Environmental *Science and Pollution Research*, 24, 21120–21134.

Al-Amin, A., Ambrose, A. F., Masud, M. M., & Azam, M. N. (2016). Environmental concern on adoption of green vehicle. *Environmental Science and Pollution Research,* 23, 11514–11522.

Asadi, S., Nilashi, M., Samad, S., et al. (2020). Drivers of purchase intention for electric vehicles in Malaysia: Does green perceived value matter? *Sustainable Cities and Society,* 61, 102338.

Department of Land Transport. (2019). *Number of vehicles registered in Thailand as of 31 December 2019*. Retrieved from http://www.dlt.go.th/ministe/m_upload/m_download/singburi/file_7cf81db11863f882ac1e6814fbb16c02.pdf.

Eneizan, B. (2019). Acceptance of electric vehicles in Jordan: An application of the theory of planned behavior. International *Journal of Academic Research in Business and Social Sciences*, 9(8), 252–263.

Kim, H., & Kim, H.-M. (2019). Determinants of electric vehicle adoption in South Korea: A test of the technology acceptance model and TPB. *Sustainability*, 11(4), 1103.

Ministry of Industry. (2020, March). *Thailand to be regional EV hub in five years. Bangkok Post.* Retrieved from https://www.bangkokpost.com/business/general/1876469/thailand-to-be-regional-ev-hub-in-five-years.

National Centers for Environmental Information. (2020). *Monthly Climate Reports: Global Climate Report - Annual 2020*. Retrieved from https://www.ncei.noaa.gov/access/monitoring/monthly-report/global/202013.

NASA. (2025). *Carbon Dioxide | Vital Signs – Climate Change*. Retrieved from https://climate.nasa.gov/vital-signs/carbon-dioxide/

Peters, A., & Dütschke, E. (2014). How do consumers perceive electric vehicles? A comparison of German consumer groups. *Journal of Environmental Psychology*, 40, 106–115.

Schmalfuß, F., Mühl, K., & Krems, J. F. (2017). Direct experience with battery electric vehicles (BEVs) matters when evaluating vehicle attributes, attitude and purchase intention. *Transportation Research Part F: Traffic Psychology and Behaviour,* 46, 47–69.

Sektakul, K. (2021, September 10). *Business and Global Warming Solutions (Part 10).* SD Perspectives.

Shalender, K., & Sharma, N. (2020). Using extended theory of planned behaviour (TPB) to predict adoption intention of electric vehicles in India. *Environment, Development and Sustainability*, 23, 665–681.

Simsekoglu, Ö., & Nayum, A. (2019). Predictors of intention to buy a battery electric vehicle in Norway. *Transportation Research Part F: Traffic Psychology and Behaviour*, 65, 208–218.

Tu, J.-C., & Yang, C.-Y. (2019). Key factors influencing consumers' purchase intention toward electric vehicles: An empirical study in Taiwan. *Sustainability,* 11(16), 4333.

Zhang, Y., Guo, L., Yao, Y., Li, Y., Zhang, M., & Wang, Y. (2018). Investigating young consumers' intentions toward electric vehicles using an extended theory of planned behavior. *Transportation Research Part D: Transport and Environment,* 61, 112–125.

SESSION 2

Agricultural and Food Innovation

Influence of fertigation on growth, yield, and ratooning ability of sugarcane (*Saccharum officinarum* L.) var. Khon Kaen 3

Yuphadet Tesmee [a], Sodchol Woonprasaid [a], Nirut Khamchumphol [a]
and Thitiporn Machikowa [a]

[a] *School of Crop Production Technology, Institute of Agricultural Technology, Suranaree University of Technology, Muang District, Nakhon Ratchasima 30000 Thailand*
* Corresponding author, E-mail address: machiko@sut.ac.th

Abstract

This research aimed to compare the effects of drip irrigation and fertilizer application on growth, root length density (RLD), yield, and yield components of sugarcane and to evaluate their impacts on ratooning ability. To achieve this objective, sugarcane cultivation practices were conducted in sandy clay loam soil over two years. The effects of drip irrigation, drip fertigation, and rainfed conditions on growth, yield, irrigation water use efficiency (IWUE), and fertilizer nutrient use efficiency (FNUE) were compared in plant crops. The results showed that the drip fertigation treatment could produce the highest growth and yield. In the first ratoon crop (FRC), the effect of plant crop practices on the adaptation of FRC was evaluated by splitting the treatments of plant crops into two different practices: rainfed condition and drip fertigation. Growth, yield, and RLD were evaluated as indicators of the ratooning ability of the ratoon crop. The results showed that the previous crop practices for the plant crop of sugarcane did not affect the ratoon crop performance. For the FRC practice, drip fertigation exhibited the highest growth, yield, and ratooning ability. However, the RLD in both years of rainfed treatments was higher than in the drip irrigation treatments.

Keywords: Drip Irrigation, Ratooning Potential, Saccharum Officinarum, Root Distribution, First Ratoon Cane

1. Introduction

1.1 Sugarcane practice

Sugarcane (*Saccharum officinarum* L.) is a significant economic crop predominantly grown in tropical and subtropical regions. The world's largest sugarcane producers are Brazil, India, Thailand, China, and Pakistan. Thailand is the fourth-largest producer globally, with annual production reaching 1 trillion metric tons. The Northeastern region of Thailand, the country's largest sugarcane-producing area, covers approximately 0.85 million hectares, yielding 58.7 million tons of fresh produce in 2018/19, representing 43.6% of the country's total production (Office of the Cane and Sugar Board, 2019). However, the region's average yield of 68.13 tons/ha is significantly lower than its potential, highlighting the need for improved production practices. Sugarcane in the Northeast is primarily rainfed, planted towards the end of the rainy season, making it vulnerable to water deficits during the critical early growth stages (3−5 months after planting). Prolonged dry conditions hinder fertilizer uptake due to insufficient soil moisture, reducing stalk and biomass accumulation and, consequently, lowering yield and quality (Jangpromma et al., 2012). This also impacts ratoon crops, where reduced biomass accumulation in the initial crop adversely affects subsequent ratoons (Shrivastava et al., 2018). Farmers generally prefer cultivating two or more ratoon crops due to the lower costs, 25−30% less than planting new crops. However, most farmers struggle to achieve more than two ratoons, often suffering from limited productivity due to suboptimal management and environmental stressors like water scarcity and nutrient deficiencies. Inefficient crop management practices, including shallow soil depth, root stubble accumulation, low nitrogen availability, and inadequate irrigation, further reduce ratoon productivity (Rana et al., 2021).

1.2 Drip irrigation practice

Drip irrigation offers a promising solution by efficiently delivering water directly to the root zone, minimizing losses from deep percolation, runoff, and erosion. This method is particularly beneficial in dryland agriculture, ensuring efficient water and nutrient use and promoting uniform crop growth. Moreover, drip irrigation facilitates fertigation, enhancing nutrient uptake and reducing fertilizer loss, leading to higher yields, improved ratooning ability, and superior crop quality (Jayant et al., 2022; Annappa et al., 2023). Drip irrigation has demonstrated superior water use efficiency, with 74.1% efficiency and 26.3% water savings compared to conventional furrow irrigation (Annappa et al., 2024). Applying 140 kg/ha of N fertilizer via drip irrigation increased stalk and sugar production by 31% in the second ratoon crop compared to non-irrigated plots (Uribe et al., 2013). Optimizing irrigation and fertilization is therefore crucial for maximizing sugarcane yield and ratooning ability, particularly in the Northeastern region of Thailand. This study aimed to compare the effects of drip irrigation and fertilizer application on the growth, yield, root length density (RLD), and ratooning ability of sugarcane in ratoon crops.

2. Methodology

2.1 Experimental description and design

The experiments were conducted under typical field conditions over two planting seasons: 2018/19 for the plant crop (PC) and 2019/20 for the first ratoon crop (FRC) in Muang district, Nakhon Ratchasima, Thailand (14°52'37" N, 102°0'21" E). Khonkaen 3 is a high-yield sugarcane variety known for the strong ratooning ability and excellent disease resistance (Ponragdee et al., 2011) was planted in a double-row configuration with a plant

spacing of 0.3 m and row spacing of 1.6 m. The soil at the experimental site was classified as sandy clay loam, composed of 46.2% sand, 22.5% silt, and 32.3% clay, as shown in Table 1. The bulk density of the soil was 1.25 g/cm³, and the available water holding capacity (AWHC) was 1.65 mm/cm. The soil chemical properties exhibited slightly acidic pH levels (6.68 in 2018/19 and 6.77 in 2019/20), low electrical conductivity (EC=0.031 µS/cm in 2018/19 and 0.072 µS/cm in 2019/20), and organic matter (OM) content that decreased from 1.43% in 2018/19 to 1.08% in 2019/20. The availability of phosphorus was stable around 12.7-12.9 ppm, while exchangeable potassium increased from 63.0 ppm to 74.2 ppm. The amounts of rainfall in 2018/19 and 2019/20 were gauged daily at planting area 748 mm and 1,251 mm, respectively.

The experiments were conducted over two consecutive years with distinct designs. In the first year (2018/19, PC), the experiment was laid out in a randomized complete block design with four replications. Treatments included three irrigation and fertilization practices: T1: Rainfed (no irrigation), T2: Drip irrigation with soil fertilization, and T3: Drip fertigation. In the second year (2019/20, FRC), a split-plot design in RCBD with three replications was employed. Main plots comprised three previous plant crop practices residual: T1: Rainfed, T2: Drip irrigation with soil fertilization, and T3: Drip fertigation. Sub-plots included two FRC treatments: S1: Rainfed and S2: Drip fertigation.

Table 1. Physical and chemical properties of experimental soil

Physical properties		Chemical properties	(2018/19)	(2019/20)
Sand (%)	46.2	pH	6.68	6.77
Silt (%)	22.5	EC (µS/cm)	0.031	0.072
Clay (%)	32.3	OM (%)	1.43	1.08
Bulk density (g/cm³)	1.25	Av. P (ppm)	12.7	12.9
Available water holding capacity AWHC (mm/cm)	1.65	Ex. K (ppm)	63	74.2
		Ca (ppm)	2,030	2,150
		Mg (ppm)	196	212

Note: EC (electrical conductivity), OM (organic matter), AV. P (available phosphorus), EX. K (exchangeable potassium), Ca (calcium), and Mg (Magnesium)

2.2 Water and fertilizer application

Water availability in rainfed conditions depended on the average annual rainfall. Drip irrigation was applied using drip tape with a flow rate of 2 L/h and dropper spacing of 30 cm, with water supplied based on the water balance model. Daily water consumption of sugarcane was calculated using the following equation of Allen et al. (1998)

$$ETc = ETo \times Kc$$

Where   ETc = the crop evapotranspiration (mm/day),
ETo = the amount of water consumed by a standard or reference crop (mm), and an average ETo over 10 years was used in this experiment.
Kc = the crop coefficient.

Fertilizers were applied based on the nutrient balance model, with soil application occurring twice at 1 and 3 MAP. Fertilization was applied every 3 weeks, totalling six applications from 1 st to 5 th MAP. Fertilizer rates according to the nutrient balance model were calculated using the nutrient balance equation as the study of Wonprasaid et al. (2023).

$$NS = \frac{NR - (SAN - SM)}{NUE}$$

Where   NS = the nutrient supply (kg/ha)
NR = the nutrient requirement for a target yield of 187.5 tons/ha
SAN = the amount of soil available nutrients obtained from soil analysis (kg/ha) in sandy clay loam soil with OM=1%, P=10 ppm, and K=60 ppm.

2.3 Data collection

1) Plant growth measurements

Growth parameters were measured at 6 MAP for PC and 6 month after harvest (MAH) for FRC. The number of stalks on a 19.2 m^2 long row section was recorded. Plant height was measured from the soil base to the leaf flag (the highest visible node). Leaf area was measured using a Li-Cor area meter Li-3100e, and leaf area index (LAI) was calculated based on ground area and leaf area.

2) Yield and yield components

Yield and yield component parameters were measured at 12 MAP for PC and 12 MAH for FRC. Yield and number of millable canes (NMC) were measured from millable canes within a 19.2 m^2 area per replication. Cane diameter was measured with a vernier caliper, and Brix (%) was determined using a refractometer.

3) Irrigation water and fertilizer nutrient use efficiency

Irrigation water use efficiency (IWUE) was calculated as the equation of (De Pascale et al., 2011)

$$\text{IWUE (tons/m}^3) = \frac{\text{FY (tons/ha)}}{\text{IW (m}^3/\text{ha)}}$$

Where   FY = the yield of millable cane
IW = the irrigation water.

Fertilizer nutrient use efficiency (FNUE) was calculated by the index of partial factors of productivity of applied nutrient (Doberman, 2007) as:

$$\text{FNUE (tons/kg)} = \frac{\text{FY (tons/ha)}}{\text{NS (kg/ha)}}$$

Where   FY = the yield of millable cane
NS = the amount of nutrient applied.

4) Root length density (RLD)

RLD was measured at 12 MAP for PC and 12 MAH for FRC. Root samples were taken at 0 cm, 40 cm, and 80 cm from the planting row at depths of 0-20 cm, 21-40 cm, and 41-80 cm. RLD was calculated as root length per soil volume using WinRHIZO 2013 software.

5) Germination percentage and ratooning ability

Germination percentage for FRC was assessed by examining underground stubble and estimating shoot germination, as described by Set-Tow et al. (2020).:

$$\text{Germination }_{(\%)} = \frac{\text{Number of shoot germinate in FRC}}{\text{Number of millablecane in PC}} \times 100$$

Ratooning ability (RA) was defined as the yield potential of FRC compared to PC, calculated according to Dlamini et al.(2024a).

$$\text{RA (\%)} = \frac{\text{The productivity (yield and components of FRC)}}{\text{The productivity (yield and components of PC)}} \times 100$$

2.4 Statistical analysis

All parameters were analyzed using ANOVA with SPSS V.16 for Windows. Mean comparisons were performed using Duncan's multiple range test at a significance level of $p<.05$.

3. Results and Discussion

3.1 Growth, yield, and yield components of the planting crop

1) Growth parameters

At 6 MAP, drip fertigation significantly enhanced sugarcane growth, yielding the highest values across all parameters: 82,119 stalks/ha, a plant height of 170 cm, and LAI of 2.70 (Table 2). In contrast, the rainfed treatment produced the lowest growth metrics with 68,150 stalks/ha, a plant height of 102 cm, and an LAI of 1.30. Drip irrigation with soil fertilizer (T2) showed intermediate results, with 72,744 stalks/ha, a plant height of 157 cm, and an LAI of 2.16.

Table 2. Sugarcane growth parameters at 6 MAP under various water and fertilizer applications

Treatments	Number of stalks[1] (stalk/ha)	Plant height (cm)	LAI
T1: Rainfed condition	68,150c	102c	1.30c
T2: Drip irrigation with soil fertilizer	72,744b	157b	2.16b
T3: Drip fertigation	82,119a	170a	2.70a
F-test	**	**	**
CV (%)	12.45	10.91	15.72

[1]Means with different letters within the same column indicate significant differences at p<.05.

2) Yield and yield components

The effects of water and fertilizer treatments on yield and components were significant, as shown in Table 3. Drip fertigation produced the highest yield (140 tons/ha), NMC (80,613 stalks/ha), and Brix (22.3%). In contrast, the rainfed practice resulted in the highest stalk diameter (2.89 cm). Brix levels did not significantly differ among the cultivation practices.

Table 3. Sugarcane yield and yield components under different water and fertilizer applications

Treatments	Yield[1] (tons/ha)	No. of millable cane (stalks/ha)	Stalk diameter (cm)	Brix (%)
T1: Rainfed condition	81.9c	63,963c	2.89a	22.0
T2: Drip irrigation + soil fertilizer	114.4b	69,269b	2.74ab	22.2
T3: Drip fertigation	140.0a	80,613a	2.60c	22.3
F-test (0.05)	**	**	*	ns
CV (%)	14.40	10.45	11.62	9.07

[1]Means with different letters within the same column indicate significant differences at p<.05.

3) Irrigation water and fertilizer nutrient use efficiency

The IWUE results show that drip fertigation achieved the highest IWUE at 14.9 tons/m³, compared to 11.1 tons/m³ for drip irrigation with soil fertilizer (T2). This highlights the effectiveness of combining precise water delivery with nutrient management in enhancing productivity per unit of water applied, particularly in water-scarce regions. T3 also recorded superior FNUE, with efficiencies of 1.243 tons/kg for N, 1.674 tons/kg for P_2O_5, and 0.791 tons/kg for K_2O, significantly outperforming T2 and T1 (Table 4).

Table 4. Irrigation water and fertilizer nutrient use efficiency in sugarcane cultivation.

Treatments	IWUE[1] (tons/m³)	FNUE (tons/kg)		
		N	P_2O_5	K_2O
T1: Rainfed condition	5.0c	0.711c	0.960c	0.452c
T2: Drip irrigation + soil fertilizer	11.1b	1.000b	1.354b	0.639b
T3: Drip fertigation	14.9a	1.243a	1.674a	0.791a
F-test (0.05)	**	**	**	**
CV (%)	8.32	7.32	7.35	7.31

[1]Means with different letters within the same column indicate significant differences at p<.05.

4) Root length density (RLD)

Sugarcane under the rainfed treatment tended to have the highest RLD at 0 cm of planting bed depth, with values of 1.247 cm/cm³ (0-20 cm depth) and 0.080 cm/cm³ (40-80 cm depth). Drip fertigation and drip irrigation with soil fertilizer tended to have the lower RLD values, with T3 showing 0.578 cm/cm³ (0-20 cm) and 0.039 cm/cm³ (40-80 cm), and T2 showing 0.523 cm/cm³ (0-20 cm) and 0.029 cm/cm³ (40-80 cm) (Figure 1).
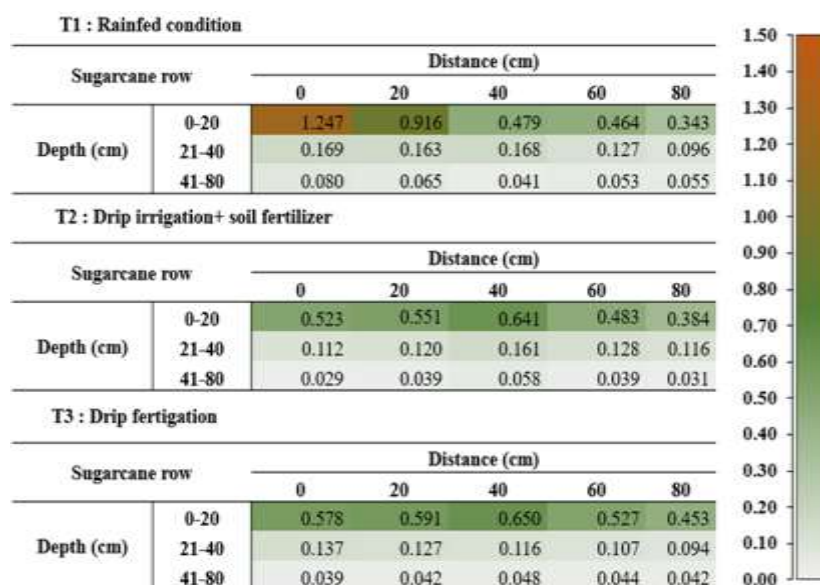

Figure 1. RLD of PC sugarcane: rainfed condition, drip irrigation+soil fertilization, and drip fertigation.

3.2 Growth, ratooning ability, yield, and yield components of the first ratoon crop

1) Germination and growth parameters

Previous crop practices significantly impacted germination rates, with T1 (rainfed) achieving the highest rate (250%), followed by T2 (223%) and T3 (202%). However, these practices did not significantly affect stalk numbers or plant height in the FRC. In contrast, the current crop practice of drip fertigation (S2) significantly increased both stalk numbers (111,213 stalks/ha) and plant height (226 cm) compared to rainfed conditions (S1), which produced 103,188 stalks/ha and a plant height of 189 cm (Table 5). Notably, no significant interaction was found between PC and FRC practices, indicating independent effects on these growth parameters.

70

Table 5. Sugarcane germination at 1 MAH and growth parameters at 6 MAH in FRC practice.

Treatments	Germination[1] (%)	Number of stalks (stalks/ha)	Plant height (cm)
Residual practice from PC (T)	*	ns	ns
T1: Rainfed condition	250a	110,494	212
T2: Drip irrigation + soil fertilizer	223ab	106,944	209
T3: Drip fertigation	202b	104,169	202
Crop practice in FRC (S)	Ns	*	**
S1: Rainfed condition	211	103,188b	189b
S2: Drip fertigation	239	111,213a	226a
T*S	ns	ns	ns
CV (%)	7.51	4.66	4.47

[1]Means with different letters within the same column indicate significant differences at p<.05.

2) Yield and yield components

Table 6 shows that PC practices did not significantly influence yield or yield components such as the NMC, stalk length, stalk diameter, and Brix percentage. Yield ranged from 135.0 to 137.5 tons/ha across PC treatments, with no significant differences. However, current crop practice or drip fertigation (S2) significantly increased yield (153.1 tons/ha) and the NMC (109,275 stalks/ha) compared to rainfed condition (S1) (120.6 tons/ha and 89,000 stalks/ha). Stalk length, diameter, and Brix percentage remained consistent across treatments.

Table 6. Yield and yield components of FRC.

Treatments	Yield[1] (tons/ha)	No. of millable canes (stalk/ha)	Stalk length (cm)	Stalk diameter (cm)	Brix (%)
Residual practice from PC (T)	ns	ns	ns	ns	ns
T1: Rainfed condition	137.5	99,725	290.5	2.59	22.0
T2: Drip irrigation + soil fertilizer	135.0	98,381	293.3	2.58	22.6
T3: Drip fertigation	137.5	99,294	298.1	2.50	22.0
Crop practice in FRC (S)	**	**	ns	ns	ns
S1: Rainfed condition	120.6b	89,000b	291.6	2.54	22.2
S2: Drip fertigation	153.1a	109,275a	296.2	2.58	24.2
T*S	ns	ns	ns	ns	ns
CV (%)	9.63	9.63	4.51	4.94	9.63

[1]Means with different letters within the same column indicate significant differences at p<.05.

3) Ratooning ability based on growth

Table 7 exhibits sugarcane's ratooning ability as measured by the number of stalks and the corresponding yield for the FRC. The data included comparisons across different treatment groups, highlighting the influence of previous crop practices on FRC performance. PC and FRC practices significantly influenced ratooning ability, measured by stalk numbers at 2 and 6 MAH. Rainfed exhibited the highest ratooning ability, with 349% and 154% for stalk numbers, respectively. Drip fertigation (T3) had the lowest ratooning ability, particularly 242% and 116% respectively. Drip fertigation (S2) consistently outperformed S1 across all PC practices, demonstrating its superiority in enhancing ratooning ability. The combination effect of PC and FRC practices was significant for stalk numbers; it suggested that combinations of practices can differentially affect stalk numbers at both periods of FRC.

Table 7. Sugarcane ratooning ability (RA) based on number of stalks of FRC at 2 and 6 MAH.

Treatments	RA based on number of stalks (%)	
	2 MAH	6 MAH
Residual practice from PC (T)	*	**
T1: Rainfed condition	349a	154a
T2: Drip irrigation + soil fertilizer	306ab	135b
T3: Drip fertigation	242b	116c
Crop practice in FRC (S)	**	*
S1: Rainfed condition	246a	131b
S2: Drip fertigation	352b	140a
T*S	**	ns
CV (%)	8.46	4.92

[1]Means with different letters within the same column indicate significant differences at p<.05.

4) Ratooning ability based on yield and number of millable canes.

The results in Table 8 demonstrate the significant effects of previous crop (T) and FRC practices (S) on the ratooning ability of sugarcane, measured by yield and the NMC in the FRC. Influence of previous crop practices, PC practices significantly affected ratooning ability. The rainfed condition residual effect (T1) exhibited the highest ratooning ability, with values of 134% and 144% for yield under S1 (rainfed) and S2 (drip fertigation), respectively. T1 also resulted in the highest ratooning ability for the NMC, achieving 128% under S1 and 135% under S2. Conversely, drip fertigation residual effect (T3) recorded the lowest yield values of 93% under S1 and 105% under S2, and ratooning ability based on NMC at 105% under S1 and 112% under S2. Influence of current crop practices significantly impacted ratooning ability, with drip fertigation (S2) consistently outperforming rainfed conditions (S1) across all PC practices. Under T1, S2 achieved a ratooning ability of 144% for yield and 135% for the NMC, both

higher than those under S1. Interaction effects between PC and FRC practices: T and S practices significantly influenced ratooning ability. Their interaction was significant for both yield and NMC, indicating that combinations of practices can differentially affect the stalk number and plant height of FRC.

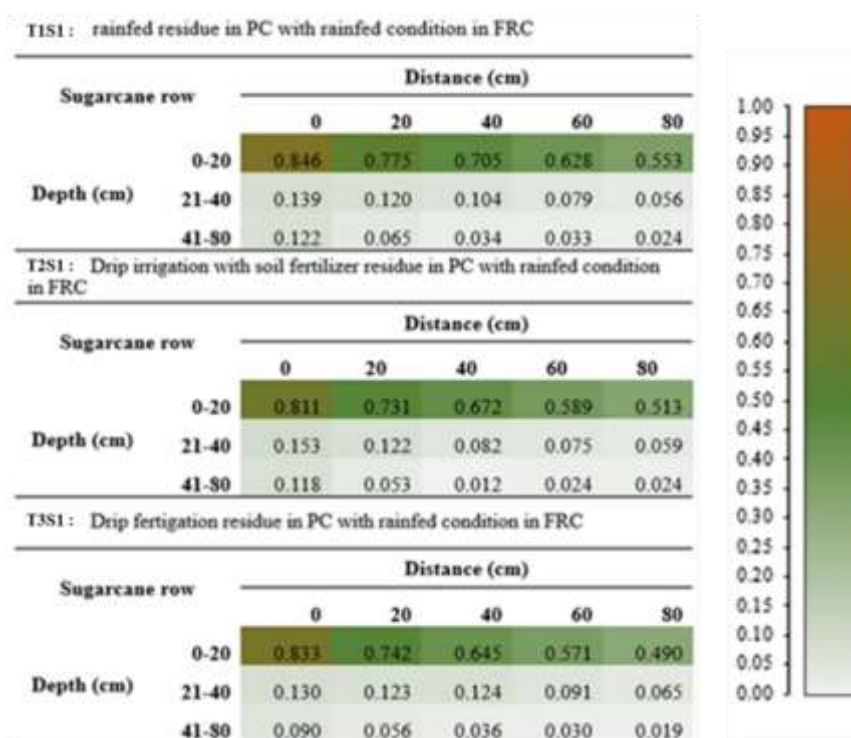Table 8. Sugarcane ratooning ability based on the number of stalks and yield of FRC.

Residual practice from PC	Crop practice in FRC (S)	RA based on yield[1] (%)	RA based on the number of millable cane (%)
Rainfed condition (T1)	Rainfed condition (S1)	134ab	128ab
	Drip fertigation (S2)	144a	135a
Drip irrigation + soil fertilizer (T2)	Rainfed condition (S1)	109cd	121bc
	Drip fertigation (S2)	117bc	128ab
Drip fertigation (T3)	Rainfed condition (S1)	93d	105c
	Drip fertigation (S2)	105cd	112bc
T		**	**
S		*	**
T*S		**	**
CV (%)		15.44	18.36

[1]Means with different letters within the same column indicate significant differences at $p<.05$

  5) Root length density
   Figure 2 illustrates the RLD of the FRC under different irrigation practices. The data indicate that neither the PC nor the current crop practice significantly affected the RLD of the FRC across treatments. Despite the lack of statistical significance, a noticeable trend is observed in RLD distribution across soil depths. Specifically, under rainfed conditions (Figure 2A), RLD tends to be higher at the soil surface (0-20 cm) and at deeper depths (41-80 cm) compared to drip fertigation (Figure 2B). This trend suggests that rainfed conditions may encourage a more extensive root system both at the surface and in deeper soil layers, potentially in response to water availability constraints, driving roots to explore a larger soil volume.
   In contrast, drip fertigation appears to have a more uniform root distribution, with relatively lower RLD at these critical depths, likely due to this practice's more consistent water and nutrient availability. While these observations are not statistically significant, they highlight the potential influence of irrigation practices on root distribution patterns, which could affect water and nutrient uptake efficiency in sugarcane cultivation.
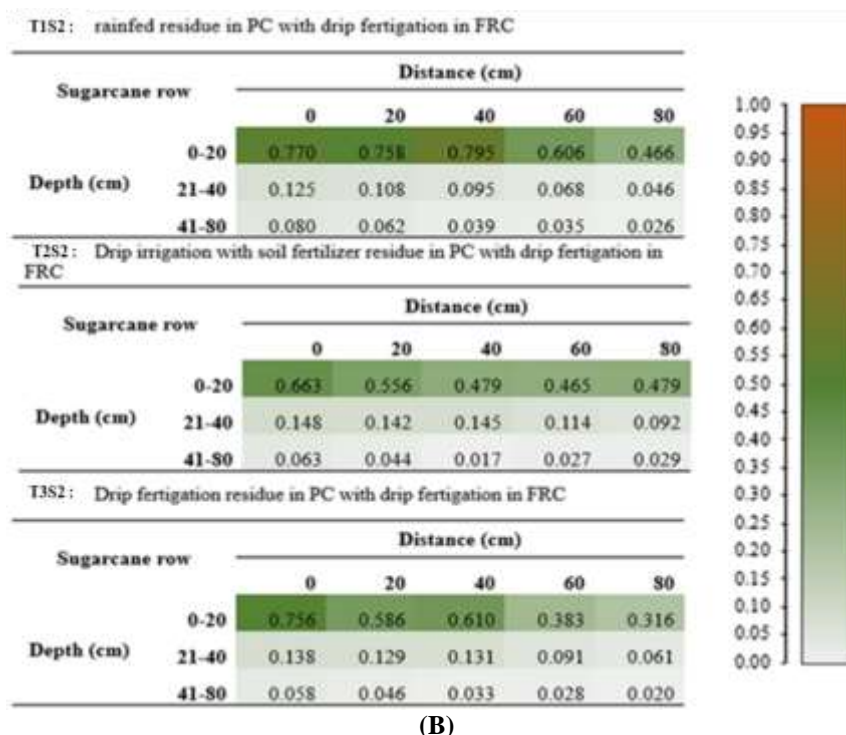

(A)

T1S2 : rainfed residue in PC with drip fertigation in FRC

Sugarcane row		Distance (cm)				
		0	20	40	60	80
Depth (cm)	0-20	0.770	0.758	0.795	0.606	0.466
	21-40	0.125	0.108	0.095	0.068	0.046
	41-80	0.080	0.062	0.039	0.035	0.026

T2S2 : Drip irrigation with soil fertilizer residue in PC with drip fertigation in FRC

Sugarcane row		Distance (cm)				
		0	20	40	60	80
Depth (cm)	0-20	0.663	0.556	0.479	0.465	0.479
	21-40	0.148	0.142	0.145	0.114	0.092
	41-80	0.063	0.044	0.017	0.027	0.029

T3S2 : Drip fertigation residue in PC with drip fertigation in FRC

Sugarcane row		Distance (cm)				
		0	20	40	60	80
Depth (cm)	0-20	0.756	0.586	0.610	0.383	0.316
	21-40	0.138	0.129	0.131	0.091	0.061
	41-80	0.058	0.046	0.033	0.028	0.020

(B)

Figure 2 RLD of the FRC under rainfed condition (A) and drip fertigation (B) practices.

The two-year study revealed that drip-fertigated treatment produced superior growth parameters such as plant height and stalk number and LAI than the rainfed treatment. The consistent water delivery system of drip fertigation led to increased growth rates because of its ability to provide steady water supply. Drip irrigation systems delivered better soil nutrient accessibility while simultaneously improving plant nutrient absorption performance. The research of Wonprasaid and Girdthai (2014) showed that extended irrigation practices in sugarcane farming resulted in better growth and yield production and yield component development than rainfed cultivation methods. The research demonstrated that irrigation extended ratooning capacity beyond five crop cycles whereas rainfed management only reached three cycles. The research by Wiedenfeld and Enciso (2008) showed that adequate water supply led to increased sugarcane biomass, but Rodrigues et al. (2008) discovered that water scarcity negatively impacted plant growth, yield production, and product quality. The research by Khonghintaisong et al. (2018) demonstrated that water stress reduced stomatal conductance and relative leaf water content which resulted in decreased biomass accumulation and reduced crop performance. The research of Yadav and Prasad (1988) showed that sugarcane genotypes under proper irrigation developed higher LAI measurements than those under water-constrained conditions. The growth parameter LAI serves as a crucial indicator of photosynthetic capacity because it measures the plant canopy's effective light-intercepting surface. The lower LAI measurements under rainfed conditions resulted from water stress which limited leaf growth and decreased photosynthetic activities.

The environment, particularly rainfall, plays a crucial role in sugarcane growth and yield due to its unpredictability and the risk of water deficit stress. This study showed that rainfed conditions over two planting seasons resulted in lower growth, yield, and yield components than drip irrigation. Drought stress in rainfed sugarcane significantly reduced internode length, stalk germination, and biomass accumulation (Jangpromma et al., 2012). Early-stage stalk number is vital for supporting dry weight and yield at harvest (Khonghintaisong et al., 2018). The findings emphasize that drip irrigation significantly enhances sugarcane growth and yield compared to rainfed conditions. Water, as a significant component of plant cells, is essential for physiological processes, including nutrient transformation and availability, which are regulated by soil moisture levels.

Drip fertigation, using 1,601 mm of water, achieved a WUE of 74.1% and saved 26.3% more water than furrow irrigation's 2,200 mm with a WUE of 40.9% (Bhuvaneswari et al., 2020). Furthermore, with 140 kg/ha of N, precise drip fertigation increased stalk and sugar production by 31% in the second ratoon crop compared to non-irrigated conditions (Uribe et al., 2013). In rainfed conditions, limited water availability can severely constrain growth or even lead to crop failure if prolonged. Fertilizer application effectiveness was closely tied to the irrigation method. Soil-applied fertilizers resulted in lower growth and yield than fertigation, aligning with findings by Uribe et al. (2013), who noted that fertigation enhances sugarcane yield by synchronizing nutrient supply with crop demand. In this study, drip fertigation treatments showed higher growth and yield than soil fertilizer applications. Solid fertilizers are less effective without adequate soil moisture and are susceptible to being washed away by heavy rain. In contrast, fertigation allows for multiple, smaller applications, ensuring uniform nutrient distribution and reduced nutrient loss, particularly nitrogen. This method is particularly effective in shallow soils with low nitrogen availability, where

mineralized fertilizers can become immobilized in ratoon crops. Fertigation also enhances the immediate uptake of less mobile nutrients like phosphorus, increasing FNUE (Wu et al., 2016; Xie et al., 2020).

The RLD varied between rainfed and irrigated conditions, with rainfed sugarcane roots concentrating more at the plant base and extending deeper than drip-fertigation conditions. Rainfed sugarcane also tended to have taller stalks compared to fertigation treatments. Higher RLD was positively correlated with higher germination rates in second ratoon crops, indicating RLD is important for ratoon crop tillering (Chumphu et al., 2019). Effective tillering, supported by viable roots and lower bud formation on the main stems, is key to achieving higher yields (Khan & Khan, 2022). Root distribution is influenced by soil moisture and nutrient availability; sufficient water typically leads to shallower root systems, while water scarcity prompts deeper root development to access more water and nutrients (Namwongsa et al., 2019; Set-Tow et al., 2020). In addition. The remaining structures including root structures was related in initial stage of ratoon crop growth as they were the source of energy that stimulated the speed of growth and improved the vigor of the next ratoon crop (Pissolato et al., 2021).

Ratooning ability, which reflects sugarcane performance in the current ratoon crop compared to the previous crop, was found to be higher under rainfed conditions in the previous crop but improved with irrigation in the current crop. Although ratooning ability is not a direct indicator of final yield, it is a valuable metric for deciding whether to replant or continue with the ratoon crop. Sugarcane variety, location, and planting density influence ratooning ability (Xu et al., 2021). For instance, Dlamini et al. (2024b) observed that variety N25, despite high plant cane yields, experienced a sharper yield decline in ratoon crops, making it more suitable for short crop cycles. Conversely, variety N36 showed a lower yield decline, suggesting its suitability for longer ratoon cycles. Row spacing also affects ratooning ability, with different genotypes performing best at varying row spacings (Ebid et al., 2022). Dlamini et al. (2024a) identified the ratio of all ratoon crops to the plant cane yield index as the most reliable predictor of long-term ratoon performance, especially for short ratoon cycles. Moreover, the study of Qin et al. (2017) demonstrated that high germination, high tillering rate, and high stalk production were found in the sugarcane cultivar with strong RA.

4. Conclusion

The findings from this study underscore the significant benefits of drip irrigation for sugarcane growth, which demonstrate enhancements in stalk number, plant height, LAI, yield, and yield components compared to rainfed conditions. Fertigation proved more efficient than soil fertilizer application, particularly regarding IWUE and FNUE. Drip irrigation also reduced RLD in the planting bed and deeper soil layers, indicating more effective water and nutrient uptake by the plants. In the FRC, residual effects from previous crop management significantly influenced germination rates, with rainfed conditions during the PC phase resulting in higher germination percentages in the FRC. However, these initial conditions did not affect other growth parameters, yield, or yield components in FRC. Instead, current management practices during the FRC phase (S) were more critical, with drip fertigation yielding the best growth and highest yields, while rainfed conditions produced the lowest. RLD in FRC was not impacted by previous crop residual management but was tended to influence by current year practices, with higher RLD under rainfed conditions.

For RA evaluation, the results showed that both year practices (PC and FRC) influenced the RA of FRC sugarcane. For the previous crop effects the rainfed residual which tended to produce high root structure had the highest initial ratoon germination, RA based on number of stalk, NMC, and RA based on yield. For the current crop practice (S), drip fertigation practice had higher RA based on NMC, and yield than rainfed conditions. However, growth and yield productivity of the FRC did not depend on the RA. RA was only an indicator of the adaptability and high vigor of ratoon crop but the growth and productivity were much more associated with the current crop management (S). Regardless of all residual practices, the current crop fertigation practice produced a higher yield than the rainfed condition practices. Even though drip fertigation was the most effective way to produce growth and yield, but with low RA, it reduced the vigor and adaptability in the next ratoon cane if grown under non suitable condition, including, under rainfed condition. Therefore, drip irrigated sugarcane must be grown under the same practices for all ratoons to maintain growth, yield and RA.

In summary, this study highlights the importance of optimizing irrigation and fertilization management, particularly through drip fertigation, to enhance sugarcane productivity. Drip fertigation improved growth and yield while providing more efficient soil moisture and nutrient management, contributing to sustainable sugarcane production practices.

5. Acknowledgements

6. References

Allen, R. G., Pereira, L. S., Raes, D., & Smith, M. (1998). Crop evapotranspiration: guidelines for computing crop water requirements. In *FAO eBooks* (Issue 1).

Annappa, N.N., Ananthakumar, M.A., Thimmegowda, M.N., & Kadalli, G.G. (2023). Effect of drip fertigation on growth, yield and quality of ratoon sugarcane. *International Journal of Plant & Soil Science*, *35*(15), 14−22.

Annappa, N.N., Ananthakumar, M.A., Thimmegowda, M.N., & Kadalli, G.G. (2024). Studies on nutrient uptake, nutrient use efficiency and water productivity of drip irrigated ratoon sugarcane as influenced by water soluble fertilizers. *Journal of Scientific Research and Reports*, *30*(6), 322−332.

Bhuvaneswari, J., Thiyagarajan, G., Manikandan, M., Natarajan, S.K., Thenmozhi, S., & Prabkandan, M. (2020). Performance evaluation of drip fertigation in sugarcane and banana. *Journal of Pharmacognosy and Phytochemistry*, *9*(6), 53−56.

Chumphu, S., Jongrungklang, N., & Songsri, P. (2019). Association of physiological responses and root distribution patterns to ratooning ability and yield of the second ratoon cane in sugarcane elite clone. *Agronomy*, *9*(4), 200.

De Pascale, S., Costa, L. D., Vallone, S., Barbieri, G., & Maggio, A. (2011). Increasing water use efficiency in vegetable crop production: from plant to irrigation systems efficiency. *HortTechnology*, 21(3), 301–308.

Dlamini, N.E., Franke, A.C., & Zhou, M. (2024a). Indices for measuring ratooning ability of sugarcane varieties. *Crop Science*, *64*(2), 667−677.

Dlamini, N.E., Franke, A.C., & Zhou, M. (2024b). Impact of soil type and harvest season on the ratooning ability of sugarcane varieties. *Experimental Agriculture*, *60*(15), 1−17.

Dobermann, A., (2007). Nutrient use efficiency-measurement and management. In: Krauss, A., Isherwood, K., Heffer, P. (Eds.), *Fertilizer Best Management Practices: General Principles, Strategy for Their Adoption and Voluntary Initiatives Versus Regulations*. International Fertilizer Industry Association, Paris, France, 1–28.

Ebid, M.H.M., El-bakry, A., & Yousif, E.M.M. (2022). Stability and ratooning ability of some sugarcane genotypes under upper-Egypt conditions. *SVU-international Journal of Agricultural Sciences*, *4*(3), 187−202.

Jangpromma, N., Thammasirirak, S., Jaisil, P., & Songsri, P. (2012). Effects of drought and recovery from drought stress on above ground and root growth, and water use efficiency in sugarcane (*Saccharum officinarum* L.). *Australian Journal of Crop Science*, 6(8), 1298-1304.

Jayant, B., Dahiyi, K., Rukhiya, A., Raj, R., & Meena, K. (2022). A review of the drip irrigation system. *Journal of Engineering Research and Application*, 1, 1−8.

Khan, M.E., & Khan, M.I. (2022). Significant difference in technical methods on sugarcane ratooning ability in Pakistan. *Pakistan Sugar Journal*, *37*(4), 17.

Khonghintaisong, J., Songsri. P., Toomsan,, B. & Jongrungklang, N. (2018). Rooting and physiological trait responses to early drought stress of sugarcane cultivars. *Sugar Tech*, *20*. 396-406.

Namwongsa, J., Jongrungklang. N., & Songsri. P. (2019). Genotypic variation in root distribution changes and physiological responses of sugarcane induced by drought stress. *SABRAO Journal of Breeding and Genetics*, *51*, 470−493.

Office of The Cane and Sugar Board. (2019). Sugarcane Production Report, Production Year 2018/2019. Retrieved from https://www.ocsb.go.th/

Pissolato, M. D., Cruz, L. P. D., Silveira, N. M., Machado, E. C., & Ribeiro, R. V. (2021). Sugarcane regrowth is dependent on root system size: an approach using young plants grown in nutrient solution. *Bragantia*, 80.

Ponragdee, W., Sansayawichi, T., Sarawat, P., Moulanon, T., Kapetch, P., & Leabwon, U. (2011). Khon Kaen 3 a sugarcane cultivar for the northeast. *Thai Agricultural Research Journal*, *29*(3), 283–301.

Rana, L., Kumar, M., Kumar, N., Kumar, A., & Sing, A.K. (2021). Multi-ratooning in sugarcane. *Indian Farming*, *71*(5), 28−29.

Rodrigues, F. A., De Laia, M. L., & Zingaretti, S. M. (2008). Analysis of gene expression profiles under water stress in tolerant and sensitive sugarcane plants. *Plant Science*, 176(2), 286–302.

Set-Tow, S., Songsri, P., & Jongrungklang, N. (2020). Variations in root distribution patterns and cane yield of 16 elite sugarcane clones grown under varied soil conditions. *Sugar Tech*, *22*, 1018−1031.

Sheth, K. (2017). Top Sugarcane Producing Countries. Retrieved from https://currentaffairs.adda247.com/top-10-sugarcane-producing-countries-in-the-world/.

Shrivastava, T., Singh, K., Singh, P., Suman, A., Singh, S., Verma, R.R., Singh, V., & Singh, R. (2018). Effect of bio-manures on soil quality, cane productivity, and soil carbon sequestration under long-term sugarcane (*Saccharum officinarum*) plant-ratoon system in Indian sub-tropics. *Indian Journal of Agricultural Sciences, 88*, 1696−1703.

Uribe, R.A.M., Gava, G.J.C., Saad, J.C.C., & Kolln, O.T. (2013). Ratoon sugarcane yield integrated drip irrigation and nitrogen fertigation. *Engenharia Agrícola Journal*, *33*(6), 1124−1133.

Wiedenfeld, B., & Enciso, J. (2008). Sugarcane responses to irrigation and nitrogen in semiarid south Texas. *Agronomy Journal*, 100(3), 665-671.

Wonprasaid, S., & Girdthai, T. (2014). Management for ratoon yield improvement of sugarcane in the northeast. Institute of Agricultural Technology, School of Crop Production Technology, Suranaree University of Technology.

Wonprasaid, S. Xia, X., & Machikowa, T. (2023). Long-term effects of drip irrigation on water use efficiency, yield, and net profit of sugarcane production. *Sugar Tech*, *25*(5): 1014−1024.

Wu, X.H., Zeng, L.H., Li, J.L., Fang, Z.G., Liang, B., & Wei, F.L. (2016). Effects of different fertilizer treatments on yield, quality, and fertilizer utilization ratio of potato under mulching drip irrigation conditions. *Acta Agriculturae Boreali-Sinica*, *31*(5), 193−198.

Xie, X. (2018). Fertigation for cassava production under drip irrigation system. [Doctoral dissertation, Suranaree University of Technology], Nakhon Ratchasima.

Xie, X., Machikowa, T., & Wonprasaid, S. (2020). Fertigation based on a nutrient balance model for cassava production in two different textured soils. *Plant Production Science, 23*(4), 407−416.

Qin, W., CaiWen, W., Jun, Z., PeiFang, Z., Kun, Y., XueKuan, C., Li, Y., & QianChun, Z. (2017). Research on ratoon ability of sugarcane: I. Relationship between ratooning ability and morphological characteristics of ratoon stools. *Southwest China Journal of Agricultural Sciences*, 30(5), 989-993.

Xu, F., Wang, Z., Lu, G., Zhang, R., & Que, Y. (2021). Sugarcane ratooning ability: research status, shortcomings, and prospects. *Biology*, *10*, 1052.

Yadav, R. L., & Prasad, S. R. (1988). Moisture use characteristics of sugarcane genotypes under different available soil moisture regimes in alluvial entisols. *The Journal of Agricultural Science*, 110(1), 5-11.

Utilization of Pectin from Pomelo Peel as the Stabilizer in Synbiotic Yogurt

Warakorn Seesuk[a], Chompoonuch Khongla[a], Sumalee Musika[a],
Araya Ranok[a], Chanida Kupradit[a], Kungnang Bunsroem[a], Seksan Mangkalanan[a*]

[a]*Department of Applied Biology, Faculty of Science and Liberal Arts, Rajamangala University of Technology Isan,
Nakhon Ratchasima, 30000 Thailand*
Corresponding author. Tel.: 044233000 ext. 4340; E-mail address: sek.mangkalanan@gmail.com

Abstract

This study aimed to determine the optimal conditions for pectin extraction from pomelo peel using two types of acid solvents—citric acid and acetic acid—at concentrations of 1% and 5%, a temperature of 60°C, and durations of 30 and 120 minutes. The results indicated that extraction with 5% citric acid yielded a higher quantity of pectin compared to acetic acid. However, galacturonic acid analysis revealed that extraction with 5% acetic acid for 30 minutes resulted in the highest galacturonic acid content ($91.94 \pm 5.40\%$), signifying high purity. This was consistent with methoxyl content values ranging between 13.75% and 15.23%. Consequently, 5% acetic acid extraction for 30 minutes was selected as the optimal method, as it produced a comparable pectin yield and chemical properties to the 120-minute extraction while requiring less time. The extracted pectin was incorporated into yogurt at concentrations ranging from 0.2% to 0.5% (w/w), where a concentration of 0.2% (w/w) proved most effective in reducing yogurt syneresis. Synbiotic yogurt was developed by adding 0.2% (w/w) pectin as a stabilizer, *Bifidobacterium* as a probiotic, and inulin at concentrations of 1%, 1.5%, 2%, and 2.5% (w/w). The synbiotic yogurt formulations (S4, S5, S6, S7) exhibited similar syneresis, acidity, and color to the control yogurt (S1). Among these, formula S5 demonstrated the lowest syneresis and showed no significant difference in color compared to the control during 15 days of cold storage. Lactic acid bacteria (LAB) counts and *Bifidobacterium* probiotic counts remained stable throughout the storage period. The synbiotic yogurt formulation S7, containing 2.5% inulin, received the highest sensory acceptance scores compared to other formulations (S4, S5, S6) on both day 0 and day 15. In conclusion, a novel synbiotic set yogurt with desirable quality was successfully developed using pomelo peel-derived pectin as a stabilizer for delivering the probiotic *Bifidobacterium*. This product not only provides health benefits but also contributes to reducing fruit market waste.

Keywords: Pectin, Pomelo Peel, Inulin, Bifidobacterium, Synbiotic Set Yogurt

1. Introduction

Pectin is a polysaccharide categorized as a heteropolysaccharide, primarily composed of D-galacturonic acid (approximately 65% by weight), methyl galacturonate, and sugars such as rhamnose, galactose, and arabinose. Naturally found in plant cell walls, pectin binds with cellulose, acting as a "cement" to hold cell walls together (Phimphen Phornchaleampong & Nithiya Rattanapanon, 2024). It can be extracted from the thick peels of citrus fruits and apple pomace. Its notable properties include gel forming when combined with sugar and acid in appropriate amounts, making it popular for jams and jellies. Pectin also helps reduce phase separation in acidic products, making it useful in fermented milk and fruit juices (Roy et al. 2018).

Pomelo peels, a by-product of fruit market, contain pectin with high degree of esterification. Therefore, extracting pectin from pomelo peels not only reduces synthetic stabilizer use but also lowers yogurt production costs, promotes natural extracts, and minimizes waste. Pomelo is commercially cultivated, and the white mesocarp of its peel contains a significant amount of fiber and pectin, which can be utilized in the food industry (Chandel et al. 2022).

Yogurt is widely consumed as a popular health food choice. It functions as a synbiotic food, containing probiotics and prebiotics that help stimulate intestinal function, balance gut health, and boost the immune system. Additionally, yogurt is rich in vitamins and minerals such as calcium, phosphorus, and magnesium. It has a soft texture with a slightly tangy flavor. Beneficial microorganisms, mainly lactic acid bacteria (LAB), play a key role in breaking down milk proteins to form thickened, coagulated yogurt (Abdi-Moghadam et al. 2023). However, stabilizers are needed to maintain the viscosity and stability of yogurt over time. The food industry often uses synthetic pectin as a thickener and stabilizer, but it is expensive and less durable (Julmohammad et al. 2024).

This study aims to determine optimal conditions for pectin extraction from pomelo peel for use as a thickener and stabilizer in yogurt development. The goal is to create an inulin-enriched set yogurt or synbiotic yogurt by analyzing probiotic counts in yogurt, testing yogurt's physicochemical characteristics, and conducting sensory evaluations of synbiotic yogurt. The final product is intended to be a functional food promoting health benefits.

2. Methodology

2.1 Pectin extraction from pomelo peel

Pomelo peels were sourced from a pomelo vendor at Terdthai Market, Nakhon Ratchasima Province, Thailand. The green outer peel (exocarp) was removed, and the white pith (mesocarp) was sliced into small pieces and washed several times. The pomelo peel was dried in a hot air oven at 60°C for 24 hours and then ground using an electric grinder. Five grams of ground pomelo peel powder were weighed and placed in a 400 mL beaker. Acidic solvents used for extraction were added, divided into citric acid (1% and 5%, 300 mL) and acetic acid (1% and 5%, 300 mL). Extraction was performed in a temperature-controlled water bath at 60°C with shaking at 50 rpm for 30 and 120 minutes (Roy et al. 2018; Tan Quoc et al. 2014). The mixture was filtered through cheesecloth, and the extract was separated from pomelo peel residue. The clear solution was collected in a 1000 mL bottle, and 95% ethanol was added at a 1:2 ratio to the extract. This was left at room temperature for 24 hours (Chantree Rungsawang, 2018). Pectin was filtered and dried at 60°C. The pectin yield was calculated as follows:

$$Pectin\ yield\ (\%) = \frac{A}{B} \times 100$$

Where:

- A = Weight of extracted pectin
- B = Weight of pomelo peel used

Chemical properties of the extracted pectin, including galacturonic acid content and methoxyl content were analyzed.

2.2 Chemical Property Analysis of Extracted Pectin

1) Galacturonic Acid Content Analysis

A 0.1 g pectin sample was mixed with 0.05 M sodium hydroxide solution in a 100 mL volumetric flask, adjusted to 100 mL volume, and left for 30 minutes. A 10 mL aliquot was diluted to 100 mL with distilled water. The solution was pipetted into 3 test tubes (2 mL each), and 1 mL of 0.1% carbazole solution was added. After mixing, 12 mL of concentrated sulfuric acid was added to each tube, shaken, and left for 25 minutes. Absorbance at 525 nm was measured to calculate galacturonic acid content using a standard curve (Kyriakidis and Psoma 2019).

2) Degree of Esterification and Methoxyl Content Analysis

A 0.1 g pectin sample was placed in a 500 mL conical flask, mixed with 2 mL ethanol, and 100 mL carbon dioxide-free water. Phenolphthalein (3 drops) was added, and the solution was titrated with 0.1 M sodium hydroxide. The titrant volume was recorded (V_1). Ten mL of 0.1 M sodium hydroxide was then added, mixed vigorously, and left for 15 minutes. Hydrochloric acid (0.1 M, 10 mL) was added, mixed until the pink color disappeared, and titrated again with 0.1 M sodium hydroxide (V_2) (adapted from (Suwannarat, Sawasdikarn, and Suwannarat 2019)). The degree of esterification (%DE) was calculated using the equation:

$$Degree\ of\ Esterification\ (\%DE) = \frac{V_1}{(V_1 + V_2)} \times 100$$

2.3 Development of Yogurt Stabilized with Pomelo Peel Pectin

A 500 mL volume of cow's milk was homogenized and pasteurized at 70°C, then cooled to 43±2°C. Yogurt starter culture, and pectin were added according to Table 2. Five experimental groups were prepared, with yogurt without added pectin as the control group (P1). The yogurt was incubated at 43±2°C until pH = 4.6. The yogurts were storage at 4 ℃. Samples at day 0 and day 5 of storage were randomly collected for physicochemical properties evaluation.

2.4 Physicochemical properties evaluation of set yogurt

1) pH Measurement:

Yogurt samples were randomly analyzed for pH using a pH meter. The pH meter probe was submerged into 20 g of yogurt sample (n=6).

2) **Yogurt Acidity Analysis**

Two grams of yogurt were sampled and diluted with 30 mL of distilled water. Three to five drops of phenolphthalein indicator were added, followed by titration with 0.1 N standard sodium hydroxide solution until the endpoint was reached (Sarwar et al. 2019). The volume of sodium hydroxide solution used was recorded, and the percentage of yogurt acidity for each formula was calculated based on lactic acid using the formula:

$$Acidity\ (Lactic\ Acid)(\%) = \frac{NaOH\ concentration \times NaOH\ volume\ (ml) \times 0.09}{Sample\ amount\ (g)} \times 100$$

3) Color

The yogurt samples were analyzed using a Hunter Lab colorimeter. L* represents brightness (0 = black, 100 = white), a* represents green (-a*) to red (+a*), and b* represents blue (-b*) to yellow (+b*).

4) Total Soluble Solids

The yogurt samples were measured using a refractometer or Brix meter. A dropper was used to place the sample on the device, and the reading was taken.

5) Syneresis Analysis

Thirty grams of yogurt were placed in a 50 mL test tube and centrifuged at 4500 rpm for 10 minutes. The clear liquid was discarded, and the remaining weight was recorded to calculate the percentage of whey separation compared to the initial sample weight.

2.5 Development of Synbiotic Set Yogurt

Probiotic 0.001% *Bifidobacterium,* 0.2% pomelo peel pectin and inulin were added as Table 3. Seven experimental groups were prepared, using milk only yogurt as the control formula. The yogurt was incubated at 43±2°C until pH reached 4.6. The samples were randomly collected at day 0, 5, 10 and 15 of storage for physicochemical properties evaluation including pH, acidity, color, total soluble solid and syneresis were conducted as mentioned above.

2.6 Bifidobacterium and Lactic acid bacteria (LAB) viable count

A 1-gram yogurt sample was diluted in a 0.85% sodium chloride solution to a dilution level of 10^{-9}. Samples from dilution levels 10^{-7} to 10^{-9} were used to measure the count of *Bifidobacterium* using the pour plate technique with *Bifidobacterium agar* (HiMedia™). Each dilution level was tested in triplicate. Incubation was carried out at 37 °C for 24 hours under anaerobic conditions, and bacterial counts growing on the medium were recorded in log CFU/g. The count of *Lactic Acid Bacteria* (LAB) was measured using the pour plate technique on *Lactobacillus MRS agar* (HiMedia™) supplemented with 0.004% bromocresol purple. Each dilution level was tested in triplicate. Incubation was carried out at 37 °C for 48 hours. The bacterial count was recorded in log CFU/g by observing growth and the color change of the medium from purple to yellow.

2.7 Sensory Evaluation

The sensory attributes of yogurt samples, including appearance, color, odor, texture, and overall satisfaction, were evaluated after 0 and 15 days of cold storage. Comparisons were made between control yogurt (S1), pectin added yogurt (S2), probiotic yogurt (S3), and synbiotic yogurt samples (S4-7). Twenty untrained panelists conducted evaluations using a 9-point hedonic scale, where the lowest score was 1 and the highest score was 9.

2.8 Statistical Data Analysis

Statistical analysis was conducted with at least three repetitions. Results were presented as mean ± standard deviation. Data analysis included Analysis of Variance (ANOVA) and mean comparisons using Duncan's Multiple Range Test (DMRT) with 95% confidence ($p < 0.05$).

3. Results and Discussion

3.1 Yield, Purity, and Degree of Esterification (DE) of Pomelo Peel Pectin

The evaluation of pomelo peel-derived pectin purity was based on the extraction conditions, focusing on the quantity of galacturonic acid (GalA), the homomeric monomer of pectin. Table 1 presents a summary of pectin yield, GalA content, and methoxyl level obtained through acid extraction. The highest yield of pectin was achieved using 5% citric acid at 60°C for 120 minutes (27.63%) and 30 minutes (25.30%). Citric acid demonstrated greater reactivity with the pomelo mesocarp compared to acetic acid due to its higher complexation capacity (Mazinanian, Odnevall Wallinder, and Hedberg 2015). Additionally, the stronger acidity of citric acid (pKa = 3.13) relative to acetic acid (pKa = 4.756) contributed to this outcome. However, the highest GalA content, indicating superior pectin purity, was observed under condition A3 (1% acetic acid, 30 minutes), yielding 91.94% GalA with a high degree of esterification (DE) of 93.35%. Elevated GalA content signifies enhanced pectin purity, and DE values exceeding 50% categorize pectin as highly esterified, giving it thermo-reversible properties. Methacanon, Krongsin, and Gamonpilas (2014) similarly reported high-methoxyl pectin from pomelo peel (59.4–70.7%), which is lower than DE values reported by Sotanaphun et al. (2012) for pectin extracted from Citrus maxima fruit peel (76.30%). Esterification levels varied significantly between the acidic conditions. Based on these results, the optimal extraction condition for pomelo peel pectin intended for further applications was determined to be 5% acetic acid at 60°C for 30 minutes.

Table 1 Yield, galacturonic acid and methoxyl level of pomelo peel pectin

Condition	Acid	Concentration (%)	Extraction Time (min)	Yield (%)	GalA content (%)	Degree of esterification (%)
A1	Acetic	1	30	11.52^A	73.28^{BCD}	84.28^A
A2	Acetic	1	120	11.17^A	69.67^{CD}	93.35^A
A3	Acetic	5	30	15.00^A	91.94^A	91.62^A
A4	Acetic	5	120	15.37^A	70.44^{CD}	93.31^A
C1	Citric	1	30	13.21^A	65.58^D	61.77^C
C2	Citric	1	120	15.30^A	84.98^{AB}	55.50^C
C3	Citric	5	30	25.30^B	65.92^{CD}	35.93^D
C4	Citric	5	120	27.63^B	79.77^{ABC}	34.06^D

Difference superscript letters indicated statistically significant differences ($p<.05$)

3.2 Physicochemical Characteristics of Set Yogurt

Set yogurt was developed using pasteurized milk supplemented with commercial yogurt starter cultures *Lactobacillus bulgaricus* and *Streptococcus thermophilus* (Meiji Bulgaria Yoghurt, CP-Meiji Co., Ltd.) at a ratio of 4% (w/w). Pectin extracted from pomelo peels was incorporated at concentrations of 0.2%, 0.3%, 0.4%, and 0.5% (w/w), along with commercial pectin at 0.3% (w/w). Yogurt without pectin served as the control formula. The chemical and physical properties of set yogurt were evaluated at low temperatures on storage days 0 and 5, as summarized in Table 2, including measurements of color (L*, a*, b*), pH, acidity, total soluble solids, and syneresis—all of which impact the appearance and taste of yogurt.

The lightness (L*) values, which indicate brightness (0 = black, 100 = white), varied significantly among formulations on day 0 ($p<.05$), ranging from 77.0±2.18 (P5) to 90.6±0.20 (P1), indicating that all yogurt formulations were relatively bright white. However, as pectin concentration increased, the L* values tended to decrease due to the brownish hue of pectin extracted from pomelo peels, affecting yogurt brightness.

Similarly, the a* values, representing green (-a*) and red (+a*) hues, differed significantly among formulations ($p<.05$), ranging from -3.3±0.30 (P5) to -1.5±0.26 (P6). Negative a* values indicate a greenish tint, which became more pronounced with higher pectin concentrations. The b* values, representing blue (-b*) and yellow (+b*) hues, also varied significantly ($p<.05$), ranging from 4.16±0.00 (P4) to -4.47±0.04 (P1). Higher pectin concentrations corresponded to lower b* values, consistent with the brownish hue of pomelo peel-derived pectin.

The total soluble solids content was measured using a hand refractometer, revealing that pectin-added yogurt formulations (P2–P6) exhibited significantly lower total solids than the control formula (P1) on day 0 ($p<.05$). P2–P6 had total solids ranging from 6.80±0.00 to 7.00±0.00, whereas P1 recorded a total solid content of 12.00±0.00, suggesting that yogurt without added pectin had not yet undergone complete transformation. However, after 5 days of refrigerated storage, the total soluble solids content among all formulations did not differ significantly ($p≥0.05$), with values stabilizing between 6.80 and 7.00. These results suggest that added pectin accelerates the solidification process compared to yogurt without pectin.

Pectin also influenced the pH and acidity of yogurt. Across days 0 and 5, pectin-added formulations exhibited a significant decrease in pH values. For P1, the pH declined from 4.66±0.04 (day 0) to 4.47±0.04 (day 5). Pectin-extracted formulations (P2–P5) recorded pH values between 4.38±0.02 and 4.47±0.03 on day 0, further decreasing to 4.24±0.02–4.17±0.02 on day 5. Commercial pectin (P6) resulted in pH values of 4.35±0.01 (day 0) and 4.17±0.01 (day 5). Yogurt containing pectin consistently exhibited lower pH values than the control due to acetic acid used in pectin extraction. Fermentation during storage further lowered pH while increasing acidity, with acidity levels rising proportionally with pectin concentration and storage duration.

Pectin supplementation also affected syneresis rates. On day 0, syneresis varied significantly among formulations ($p<.05$). Yogurt P2 (0.2% w/w pectin) exhibited syneresis at 27.00±5.99%, comparable to the control formula P1 (26.47±1.88%). In contrast, increased pectin concentrations resulted in higher separation rates: P3, P4, and P5 recorded syneresis rates of 50.50±0.70%, 64.70±0.95%, and 58.50±0.70%, respectively. Yogurt with commercial pectin (P6) had a syneresis rate of 30.03±0.51%, differing from the control formula. The observed increase in syneresis with higher pectin concentrations likely stems from elevated acetic acid levels, which accelerate protein denaturation, leading to increased aggregation and whey separation.

After 5 days of refrigerated storage, yogurt P2 maintained stable syneresis rates comparable to day 0, while P1 and P3–P6 exhibited significantly higher syneresis ($p<.05$), likely due to increased microbial activity leading to higher acidity, which further affected protein denaturation and separation. Consequently, yogurt with 0.2% w/w pomelo peel-derived pectin (P2) was found to be optimal for reducing syneresis. As a hydrocolloid, pectin enhances viscosity and facilitates gel formation when heated during pasteurization, contributing to improved yogurt texture.

According to (Luquet 1990), lactic strains have the ability to ferment lactose into lactic acid, with an increase of acidity and a decrease in pH of yohurt. Cais-Sokolińska, Michalski, and Pikul (2004) indicated that, the pH values of milk under processing, from the time it was inoculated with bacterial cultures to the time the yogurt was manufactured, decreased from 6.70 to 4.34. It was demonstrated that during the 21st day period of storage, the pH values decreased to 4.11. *Streptococcus thermophilus* and *Lactobacillus bulgaricus* live in symbiosis and there exists a synergy between the two bacteria which relates to a mutual stimulation. This stimulation relates namely to the growth, acidification, and the production of aromatic compounds. Kumar and Mishra (2004) found that lactic acidity of yogurt increased with the increasing level of addition of pectin to 0.2, 0.4, and 0.6%.

3.3 Physicochemical Characteristics of Synbiotic Set Yogurt

Synbiotic set yogurts were formulated with the addition of 0.2% (w/w) pomelo peel pectin, 0.001% (w/w) *Bifidobacterium*, and 1–2.5% (w/w) inulin. The physicochemical characteristics of the synbiotic set yogurt during cold storage (4°C) for 15 days are summarized in Table 3. Parameters including color, total soluble solids, pH, acidity, and syneresis were monitored throughout the storage period.

The lightness (L*) values of all yogurt samples exhibited no statistically significant differences ($p \geq 0.05$), ranging from 85.83±0.70 to 90.30±0.36, indicating a consistently bright white appearance across formulations. Similarly, the a* values showed no significant variation ($p \geq 0.05$), with values ranging from -2.33±0.15 to -1.57±0.22, suggesting a mild greenish tint in all samples. However, the b* values differed significantly ($p < .05$) and increased over the storage period. Yogurt formulations supplemented with 0.2% pomelo peel pectin (S2–S7) exhibited significantly higher b* values than the control (S1) ($p < .05$), resulting in a more pronounced yellowish tint, likely due to the yellow-brown coloration of pectin extracted from pomelo peels.

Additionally, total soluble solids content increased significantly ($p < .05$) with higher inulin concentrations, ranging from 7.00 to 10.00. The pH values of yogurt samples progressively declined during storage, correlating with an increase in acidity. The pH values ranged from 4.04±0.01 (S5, day 15) to 4.79±0.10 (S1, day 0), while acidity levels varied from 1.33±0.04 (S4, day 0) to 2.21±0.04 (S3, day 15). The viability of probiotics was reported to be affected by many factors such as storage time, oxygen content, fluctuation in temperature, low pH, reduced water activity, and high concentration of salutes (Capela, Hay, and Shah 2006) (Carvalho et al. 2004). The present study employing inulin provided an effective and economic approach in the development of synbiotic yogurt containing the probiotic bacteria with enhanced viability.

Furthermore, appropriate inulin supplementation not only functioned as a prebiotic for probiotic bacteria but also contributed to reducing yogurt separation. Syneresis rates differed significantly ($p < .05$) depending on the inulin concentration in each formulation. Formula S5 (1.5% w/w inulin) exhibited the lowest syneresis rates throughout the storage period, ranging from 21.75±1.73 to 23.12±2.09, significantly lower than other formulations. However, syneresis rates increased across all samples over time, corresponding with declining pH values and rising acidity levels.

3.4 Survivability of Bifidobacterium and Lactic Acid Bacteria in Synbiotic Yogurt

The survival of Bifidobacterium was influenced by varying inulin concentrations in yogurt stored at 4°C, as shown in Figure 1A. Viable bacterial counts were measured in log CFU/g. Over the 15-day storage period, Bifidobacterium levels decreased significantly ($p < .05$). On day 5, formula S5, containing 1.5% (w/w) inulin, exhibited the highest viable bacterial count at 10.08±0.25 log CFU/g, which declined to 9.78±0.07 and 8.97±0.02 log CFU/g on days 10 and 15, respectively.

Table 2 Physicochemical properties of pomelo peel pectin set yogurt during cold storage at 0 and 5 dpi

Sample	Pectin sources	Pectin Concentration	Colour at 0 dpi			Total soluble solid (°Brix)		pH		Acidity (%)		Syneresis (%)	
			L*	0 dpi	5 dpi[ns]	a*	b*	0 dpi	5 dpi	0 dpi	5 dpi	0 dpi	5 dpi
P1	-	-	90.6±0.20^a	12.00±0.00^a	7.00±0.00	-1.9±0.10^{ab}	5.2±0.15^d	4.66±0.04^a	4.47±0.04^a	0.86±0.02^d	2.64±0.85^a	27.00±5.99^d	44.38±2.92^d
P2	Pomelo peel	0.2%	87.7±1.80^b	7.00±0.00^b	6.80±0.00	-2.1±0.21^{bc}	6.2±0.66^c	4.47±0.03^b	4.24±0.02^b	1.39±0.04^c	2.54±0.13^a	26.47±1.88^d	21.68±1.62^f
P3	Pomelo peel	0.3%	83.8±1.53^c	7.00±0.00^b	7.00±0.00	-2.6±0.17^{cd}	7.3±0.64^{ab}	4.38±0.02^c	4.17±0.02^c	2.55±0.68^a	2.53±0.02^a	50.50±0.70^c	50.49±3.02^c
P4	Pomelo peel	0.4%	81.0±1.12^d	6.80±0.00^b	7.00±0.00	-2.6±0.40^d	6.9±0.20^{bc}	4.34±0.01^d	4.16±0.00^c	2.20±0.14^{ab}	2.50±0.13^a	64.70±0.95^a	62.29±0.27^a
P5	Pomelo peel	0.5%	77.0±2.18^e	6.80±0.00^b	7.00±0.00	-3.3±0.30^e	7.1±0.26^b	4.37±0.07^c	4.17±0.01^c	1.90±0.04^b	2.40±0.17^a	58.50±0.70^b	55.95±1.40^b
P6	Commercial	0.3%	87.7±0.67^b	7.00±0.00^b	6.80±0.00	-1.5±0.26^a	8.0±0.10^a	4.35±0.01^{cd}	4.17±0.01^c	2.20±0.12^{ab}	2.39±0.22^a	30.03±0.51^d	34.88±0.69^e

Difference superscript letters indicated statistically significant differences (p<.05). ns = not statistically significant

Table 3 Physicochemical properties of pomelo peel pectin-inulin synbiotic set yogurt during cold storage for 15 days.

Sample	Condition			Day	Colour			Total soluble solid	pH	Acidity	Syneresis
	Pectin	*Bifidobacterium*	Inulin (%)		L*[ns]	a*[ns]	b*	(°Brix)		(%)	(%)
S1	x	x	x	0	89.83±0.49	-1.67±0.06	4.53±0.15^a	7.00±0.00^a	4.79±0.10^l	1.55±0.04^{abcde}	28.48±2.39^{cd}
				5	90.30±0.36	-1.63±0.12	4.80±0.44^{ab}	7.00±0.00^a	4.44±0.04^{jk}	1.76±0.01^{defg}	28.23±3.57^{bcd}
				10	90.20±0.62	-1.60±0.20	4.73±0.32^{ab}	7.00±0.00^a	4.49±0.05^k	1.78±0.05^{efg}	28.28±5.92^{bcd}
				15	90.27±0.06	-1.87±0.25	5.07±0.49^{abc}	7.00±0.00^a	4.37±0.04^{ij}	2.22±0.33^i	34.14±6.52^{efg}
S2	✓	x	x	0	87.17±0.70	-1.90±0.20	6.23±0.40^{efg}	7.00±0.00^a	4.45±0.02^{jk}	1.49±0.10^{abc}	27.98±0.82^{bcd}
				5	87.07±0.68	-2.30±0.36	6.13±0.45^{def}	7.00±0.00^a	4.23±0.01^{efg}	1.78±0.06^{fg}	31.09±0.62^{def}
				10	86.60±0.40	-1.93±0.12	6.40±0.44^{bcd}	7.00±0.00^a	4.14±0.01^{abcde}	2.05±0.02^{hi}	32.61±2.07^{defg}
				15	87.20±0.85	-2.00±0.10	7.30±0.17^k	7.00±0.00^a	4.06±0.01^{ab}	2.18±0.20^{hi}	34.69±0.54^{fg}
S3	✓	✓	x	0	87.73±0.67	-1.93±0.06	6.47±0.42^{fghi}	7.00±0.00^a	4.34±0.05^{hi}	1.53±0.06^{abc}	28.07±1.76^{bcd}
				5	88.07±0.75	-2.03±0.15	6.83±0.32^{fghijk}	7.00±0.00^a	4.26±0.04^{fgh}	1.61±0.10^{bcdef}	30.23±1.74^{def}
				10	87.20±0.87	-1.87±0.15	6.73±0.31^{fghijk}	7.00±0.00^a	4.18±0.01^{def}	1.98±0.17^{gh}	30.65±2.76^{def}
				15	87.80±0.61	-1.87±0.21	7.07±0.12g^{ijk}	7.00±0.00^a	4.13±0.01^{abcd}	2.21±0.04^i	33.97±0.61^{efg}
S4	✓	✓	1	0	86.43±0.59	-2.10±0.10	6.20±0.10^{efg}	8.00±0.00^b	4.43±0.01^{ijk}	1.33±0.04^a	27.79±0.74^{bcd}
				5	88.20±0.26	-1.83±0.21	6.67±0.21^{fghijk}	8.00±0.00^b	4.33±0.05^{ghi}	1.39±0.06^{ab}	31.71±0.45^{defg}
				10	87.07±0.67	-2.03±0.70	6.47±0.51^{fghi}	8.00±0.00^b	4.26±0.01^{fgh}	1.55±0.08^{abcde}	32.30±0.80^{defg}
				15	87.53±0.49	-2.00±0.10	7.17±0.12^{ijk}	8.80±0.00^d	4.18±0.01^{cdef}	2.18±0.27^{hi}	34.52±1.44^{fg}
S5	✓	✓	1.5	0	87.23±0.49	-1.90±0.26	6.03±0.32^{def}	8.60±0.00^e	4.14±0.01^{abcde}	1.54±0.03^{abcd}	21.75±1.73^a
				5	87.33±1.10	-2.07±0.38	6.23±0.38^{efg}	8.80±0.00^e	4.10±0.02^{abcd}	1.53±0.12^{abcd}	22.45±4.21^a
				10	87.53±0.21	-1.73±0.40	6.57±1.01^{cde}	8.80±0.00^e	4.07±0.41^{abc}	1.95±0.02^{gh}	22.80±2.27^a
				15	87.80±0.36	-1.73±0.67	6.70±0.26^{fghijk}	9.00±0.00^f	4.04±0.01^a	2.15±0.09^{hi}	23.12±2.09^{ab}
S6	✓	✓	2	0	85.83±0.70	-1.57±0.22	6.03±0.51^{def}	9.00±0.00^f	4.39±0.01^{ijk}	1.52±0.11^{abc}	21.98±0.76^a
				5	86.93±1.10	-1.83±0.25	6.63±0.06^{fghij}	9.00±0.00^f	4.22±0.01^{ef}	1.69±0.16^{cdef}	24.64±1.12^{abc}
				10	86.17±0.50	-2.33±0.15	6.97±0.23^{fghijk}	9.00±0.00^f	4.19±0.01^{def}	2.22±0.02^i	28.01±1.02^{bcd}
				15	86.43±0.71	-2.27±0.12	7.27±0.15^{jk}	9.40±0.00^g	4.10±0.02^{abcd}	2.49±0.05^j	29.00±4.52^{cde}
S7	✓	✓	2.5	0	85.87±0.12	-2.00±0.10	6.10±0.26^{def}	10.00±0.00^i	4.34±0.01^{hi}	1.51±0.08^{abc}	29.03±2.98^{cde}
				5	85.87±1.40	-2.13±0.32	6.57±0.90^{fghij}	9.80±0.00^h	4.15±0.02^{bcdef}	1.81±0.19^{fg}	30.53±1.39^{def}
				10	86.63±1.16	-1.73±0.25	6.43±0.65^{fgh}	10.00±0.00^i	4.15±0.01^{bcdef}	2.12±0.11^{hi}	31.81±2.31^{defg}
				15	86.03±1.98	-2.07±0.06	7.27±0.06^{jk}	10.00±0.00^i	4.07±0.01^{abc}	2.12±0.12^{hi}	36.57±5.13^g

Difference superscript letters indicated statistically significant differences (p<.05)

Formula S6 maintained relatively stable bacterial counts from days 0 to 10, followed by a reduction on day 15, with values of 9.97±0.39, 9.91±0.11, 9.87±0.06, and 9.26±0.79 log CFU/g, respectively. In contrast, formula S7, which contained the highest inulin concentration (2.5% w/w), exhibited the most rapid decline in Bifidobacterium survival, with counts of 9.98±0.06, 9.76±0.19, 8.96±0.08, and 8.86±0.53 log CFU/g from day 0 to day 15.

These findings suggest that an inulin concentration range of 1.5–2.0% (w/w) supports optimal Bifidobacterium survival in synbiotic set yogurt. Excessive inulin levels accelerated bacterial decline, indicating that maintaining suitable concentrations is essential for efficient and cost-effective synbiotic yogurt formulation with high probiotic viability.

The survival rates of lactic acid bacteria (LAB) also decreased throughout the 15-day storage period. On day 0, the viable LAB counts in samples S1–S7 were 10.67±0.16, 10.94±0.03, 10.75±0.22, 10.75±0.02, 11.02±0.05, 11.03±0.05, and 10.90±0.08 log CFU/g, respectively. By day 15, LAB counts decreased to 10.00±0.15, 9.60±0.27, 9.68±0.06, 9.80±0.12, 9.56±0.05, 9.57±0.07, and 9.59±0.08 log CFU/g, respectively.

These results indicate that LAB survival rates remained relatively high when Bifidobacterium was incorporated into yogurt, reinforcing the importance of balancing inulin concentrations to enhance probiotic stability.
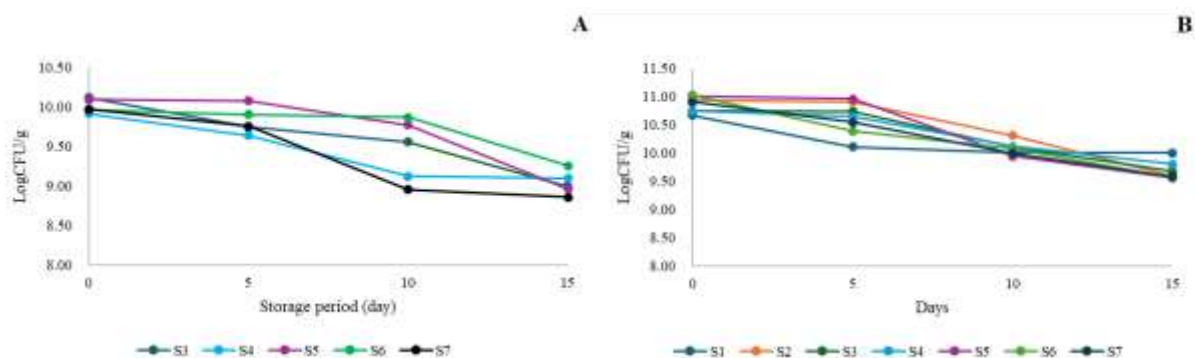
Figure 1 Survival of *Bifidobacterium* (A) and LAB (B) in the synbiotic set yogurt sample during storage at 4°C for 15 days: Control (S1); 0.2% (w/w) pectin (S2); 0.2% (w/w) pectin, 0.001% *Bifidobacterium* (S3); 0.2% (w/w) pectin, 0.001% *Bifidobacterium*, 1% w/w inulin (S4); 0.2% (w/w) pectin, 0.001% *Bifidobacterium*, 1.5% w/w inulin (S5); 0.2% (w/w) pectin, 0.001% *Bifidobacterium*, 2% w/w inulin (S6); 0.2% (w/w) pectin, 0.001% *Bifidobacterium*, 2.5% w/w inulin (S7).

3.5 Sensory Evaluation

The sensory properties of synbiotic set yogurt were assessed based on appearance, color, odor, taste, texture, and overall acceptability by 20 panelists using a 9-point hedonic scale on storage days 0 and 15, as illustrated in Figure 2. A comparison between the control yogurt (S1) and formulations S2–S7 revealed the following findings:

- Appearance: On both days, formula S1 (day 0 = 6.89, day 15 = 7.20) scored comparably to S5 (day 0 = 6.37, day 15 = 6.65) and S7 (day 0 = 6.58, day 15 = 7.00), with significantly higher ratings than the other formulations.

- Color: On day 0, S1 (7.32) received similar scores to S5 (7.00) and S7 (7.37), all significantly outperforming the other formulas (p<.05). By day 15, no significant differences were observed among the formulations (p≥0.05).

- Odor: Formulas S2, S4, and S7 consistently received odor scores comparable to S1 (7.00 on both days), outperforming the remaining formulations (p<.05).

- Taste: On day 0, S1 was significantly preferred over all other formulations (p<.05). Notably, formulations lacking inulin (S2 = 3.11, S3 = 3.84) received the lowest scores. By day 15, taste scores improved significantly across all formulas, although S1 maintained the highest preference.

- Texture: On day 0, all formulas exhibited similar texture acceptability (p≥0.05). By day 15, S1's texture score increased significantly (p<.05).

- Overall Acceptability: On day 0, S7 (6.16) was rated similarly to S1 (6.05), both receiving higher scores than the other formulations (p<.05). S2 (4.68) had the lowest acceptability rating. By day 15, overall acceptability improved across all formulations.

The findings indicate that the inclusion of pomelo pectin in the yogurt formulation notably influenced taste acceptability due to its inherent bitterness from pomelo peel extraction, thereby affecting the yogurt's flavor profile.
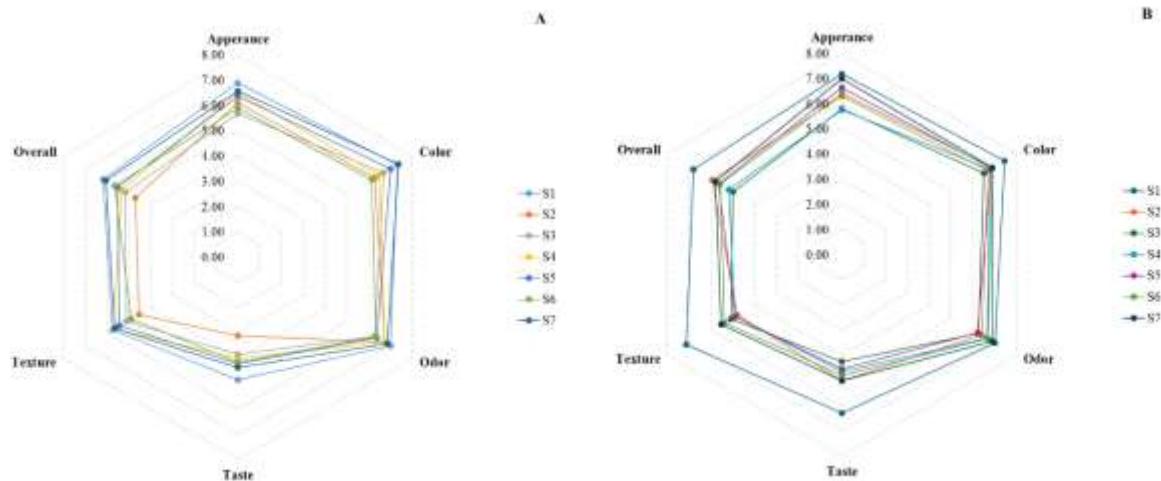
Figure 2 Sensory scores given by panelists (n=20) for each synbiotic yogurt sample on a 9-point hedonic scale: Control (S1); 0.2% (w/w) pectin (S2); 0.2% (w/w) pectin, 0.001% *Bifidobacterium* (S3); 0.2% (w/w) pectin, 0.001% *Bifidobacterium*, 1% w/w inulin (S4); 0.2% (w/w) pectin, 0.001% *Bifidobacterium*, 1.5% w/w inulin (S5); 0.2% (w/w) pectin, 0.001% *Bifidobacterium*, 2% w/w inulin (S6); 0.2% (w/w) pectin, 0.001% *Bifidobacterium*, 2.5% w/w inulin (S7).

4. Conclusions

Pectin is an edible fiber that functions as a gelling agent, stabilizer, emulsifier, and thickener in the food industry. This study investigated the extraction of pectin from pomelo peel using two acid solvents—citric acid and acetic acid—at concentrations of 1% and 5%, under a temperature of 60°C for 30 and 120 minutes.The results demonstrated that extraction with a 5% citric acid solvent for 30 and 120 minutes yielded higher pectin quantities (25.30 ± 9.37, 27.63 ± 8.60) compared to acetic acid. However, further analysis of galacturonic acid, an indicator of pectin purity, and methoxyl content revealed that extraction with 5% acetic acid for 30 minutes resulted in the highest galacturonic acid content ($91.94 \pm 5.40\%$). The methoxyl content, ranging from 13.75% to 15.23%, indicated a high degree of esterification.Based on these findings, 5% acetic acid extraction for 30 minutes was selected as the optimal method for pectin extraction from pomelo peel for synbiotic set yogurt development. When pectin was incorporated into set yogurt at different concentrations (0.2%–0.5% w/w), the optimal concentration was determined to be 0.2% (w/w). Higher concentrations increased syneresis in set yogurt. The acidity analysis aligned with lower pH values, indicating increased acid content across all formulations. The addition of pomelo-derived pectin to synbiotic yogurt reduced syneresis; however, the bitterness of the product requires further evaluation for approval.

5. Acknowledgements

6.References

Abdi-Moghadam, Zohreh, Majid Darroudi, Maryam Mahmoudzadeh, Mahnaz Mohtashami, Amir Mohammad Jamal, Ehsan Shamloo, and Zeinab Rezaei. 2023. 'Functional yogurt, enriched and probiotic: A focus on human health', *Clinical Nutrition ESPEN*, 57: 575-86.

Cais-Sokolińska, D, MM Michalski, and J Pikul. 2004. 'Role of the proportion of yoghurt bacterial strains in milk souring and the formation of curd qualitative characteristics', *Bulletin of the Veterinary Institute in Puławy*, 48: 437–41.

Capela, P., T. K. C. Hay, and N. P. Shah. 2006. 'Effect of cryoprotectants, prebiotics and microencapsulation on survival of probiotic organisms in yoghurt and freeze-dried yoghurt', *Food Research International*, 39: 203-11.

Carvalho, Ana S., Joana Silva, Peter Ho, Paula Teixeira, F. Xavier Malcata, and Paul Gibbs. 2004. 'Relevant factors for the preparation of freeze-dried lactic acid bacteria', *International Dairy Journal*, 14: 835-47.

Chandel, Vinay, Deblina Biswas, Swarup Roy, Devina Vaidya, Anil Verma, and Anil Gupta. 2022. 'Current Advancements in Pectin: Extraction, Properties and Multifunctional Applications', *Foods*, 11: 2683.

Julmohammad, N., D. O. A. Rayang, S. N. Maklin, and E. Tan. 2024. 'Effect of different types of pectin on the physicochemical, rheology, and sensory properties of low-fat yogurt', *IOP Conference Series: Earth and Environmental Science*, 1377: 012066.

Kumar, Pradyuman, and H. N. Mishra. 2004. 'Mango soy fortified set yoghurt: effect of stabilizer addition on physicochemical, sensory and textural properties', *Food Chemistry*, 87: 501-07.

Kyriakidis, Nikolaos B, and Evaggelia Psoma. 2019. 'Hydrocolloid Interferences in the Determination of Pectin by the Carbazole Method', *Journal of AOAC INTERNATIONAL*, 84: 1947-50.

Luquet, FM. 1990. 'Laits et produits laitiers: vache, brebis, chèvre. tome 2: Les produits laitiers, transformation et technologies', *Lavoisier*.

Mazinanian, N., I. Odnevall Wallinder, and Y. Hedberg. 2015. 'Comparison of the influence of citric acid and acetic acid as simulant for acidic food on the release of alloy constituents from stainless steel AISI 201', *Journal of Food Engineering*, 145: 51-63.

Methacanon, Pawadee, Jaruwan Krongsin, and Chaiwut Gamonpilas. 2014. 'Pomelo (Citrus maxima) pectin: Effects of extraction parameters and its properties', *Food Hydrocolloids*, 35: 383-91.

Roy, Manik Chandra, Majbaul Alam, Abu Saeid, Bijoy Chandra Das, Md. Biplob Mia, Md. Atikur Rahman, Jong Bang Eun, and Maruf Ahmed. 2018. 'Extraction and characterization of pectin from pomelo peel and its impact on nutritional properties of carrot jam during storage', *Journal of Food Processing and Preservation*, 42: e13411.

Sarwar, Abid, Tariq Aziz, Sam Al-Dalali, Xiao Zhao, Jian Zhang, Jalal ud Din, Chao Chen, Yongqiang Cao, and Zhennai Yang. 2019. 'Physicochemical and Microbiological Properties of Synbiotic Yogurt Made with Probiotic Yeast Saccharomyces boulardii in Combination with Inulin', *Foods*, 8: 468.

Sotanaphun, Uthai, Amornrut Chaidedgumjorn, Nudchanart Kitcharoen, Malai Satiraphan, Panida Asavapichayont, and Pornsak Sriamornsak. 2012. 'Preparation of pectin from fruit peel of Citrus maxima', *Science, Engineering and Health Studies*: 42-48.

Suwannarat, Yardrung, Jiraporn Sawasdikarn, and Rungtiwa Suwannarat. 2019. 'Extraction and Application of Pectin from Durian Rind', *Rajabhat Rambhai Barni Research Journal*, 13: 25-37.

Tan Quoc, Le Pham, Le–Thi–Lan Anh, M. V. T. K. Tien, and Le–Thi Trang. 2014. 'Optimization Of The Pectin Extraction From Pomelo Peels By Oxalic Acid And Microwave', *Banat's Journal of Biotechnology*, 9: 67-73.

Enhancing Cassava Yield and Water Use Efficiency Through Drip Irrigation Controlled by Wireless Sensors and a Water Balance Model in Clay Loam Soil

Watcharaporn Saiphoo [a], Sodchol Wonprasaid [a], and Thitiporn Machikowa [a]

[a] School of Crop Production Technology, Institute of Agricultural Technology, Suranaree University of Technology, Muang District, Nakhon Ratchasima 30000 Thailand
* Corresponding author Email address: machiko@sut.ac.th

Abstract

This study investigated the effectiveness of drip irrigation systems controlled by wireless sensors and a water balance model on the growth, yield, and water use efficiency (WUE) of cassava cultivated in clay loam soil. Four irrigation treatments were assessed: rainfed (T1), drip irrigation managed by a water balance model (T2), drip irrigation regulated by one sensor set per 1.2 ha (T3), and by three sensor sets per 1.2 ha (T4). Precision drip irrigation significantly enhanced cassava growth, nutrient uptake, biomass accumulation, and tuber yield compared to rainfed conditions. Sensor-based irrigation (T3 and T4) achieved superior WUE by reducing water input without compromising yield. Notably, T3 and T4 used approximately 369 m³/ha less irrigation water than the timer-based treatment (T2). Increasing sensor density beyond one set/plot provided no additional agronomic advantage, highlighting the importance of cost-effective deployment. These findings highlight the potential of precision irrigation technologies to enhance cassava production and resource efficiency in regions characterized by irregular rainfall patterns.

Keywords: Manihot Esculenta, Drip Irrigation, Soil Moisture Sensor, Water Balance Model, Water Use Efficiency

1. Introduction

Cassava (*Manihot esculenta* Crantz) is an economic crop in globally, valued for its adaptability to marginal soils and resilience under drought conditions. Thailand stands among the world's leading producers and exporters of cassava, supplying global markets with products such as tapioca starch, animal feed, and bioethanol. Despite cassava's inherent tolerance to water scarcity, water availability remains a critical factor influencing its growth, yield, and overall productivity. The increasing frequency of erratic and unpredictable rainfall patterns, driven by climate change, presents significant challenges to sustainable cassava production, particularly within Thailand's predominantly rainfed agricultural systems. Conventional irrigation practices, typically based on fixed schedules or empirical judgment, often lack the precision required to address real-time fluctuations in soil moisture, crop water demand, and climatic variability. Such inefficiencies not only result in suboptimal water use but also compromise crop performance and long-term resource sustainability. Enhancing water use efficiency (WUE) through improved irrigation management is therefore essential to ensure stable and sustainable cassava yields under these variable environmental conditions. Recent advancements in precision agriculture offer promising solutions to address these challenges. Among these technologies, soil moisture sensors (SMS) have emerged as effective tools for real-time monitoring and control of irrigation systems. SMS provides continuous data on soil moisture, enabling data-driven irrigation decisions tailored to crop-specific needs (Ojha et al., 2015; Kim et al., 2020). When integrated with drip irrigation, it's highly efficient in delivering water directly to the root zone. SMSs can significantly enhance water distribution uniformity and minimize wastage, supporting sustainable agricultural practices. Precision drip irrigation systems leverage sensor data, automated controllers, and decision-support algorithms to optimize irrigation scheduling and volumes, ensuring crops receive the precise amount of water required at the appropriate time (Pereira et al., 2020). This targeted approach maximizes water productivity while reducing risks associated with over-irrigation, such as nutrient leaching, soil degradation, and root diseases (Bonilla et al., 2021). Empirical studies have demonstrated that precision-controlled drip irrigation can improve crop yields and reduce water consumption by 30–50% compared to conventional irrigation methods (Sadler et al., 2005; Vories et al., 2017). In contrast, traditional irrigation scheduling methods, such as those based on water balance models, offer a theoretical framework for estimating crop water requirements. However, these models often fail to account for dynamic field conditions, potentially leading to inefficient water application through over- or under-irrigation.

Given the critical importance of efficient water management in modern agriculture, particularly for crops like cassava that, while drought-tolerant, remain sensitive to water deficits during key growth stages. There is a clear need to evaluate the performance of precision irrigation technologies relative to conventional approaches. This study addresses this need by assessing the effectiveness of drip irrigation systems controlled by wireless sensors and a water balance model on cassava growth, yield, and water use efficiency in clay loam soil. The findings aim to inform the development of sustainable, resource-efficient irrigation strategies that enhance cassava productivity while conserving water resources in regions affected by climatic variability.

2. Methodology

2.1 Experimental site and design

The field experiment was conducted between 2019 and 2020 in Nakhon Ratchasima Province, Thailand. The experimental site featured clay loam soil, with baseline physicochemical properties assessed before planting. The 'Rayong 13' variety, recognized for its high yield potential and adaptability, was selected. A randomized complete block design was employed, consisting of four irrigation treatments with three replications each. The experimental area covered 4.8 ha, with plot dimensions standardized to ensure uniformity and minimize border effects. Standard agronomic practices for cassava cultivation in the region were consistently applied.

The four irrigation regimes were:

T1: Rainfed condition (control): No supplemental irrigation, reliant solely on natural rainfall.

T2: Drip irrigation scheduled using a conventional water balance model, with intervals calculated based on crop evapotranspiration (ETc) and effective rainfall.

T3: Drip irrigation controlled by a precision system utilizing one sensor set per 1.2 ha.

T4: Drip irrigation controlled by a precision system utilizing three sensors set per 1.2 ha.

All drip systems were equipped with pressure-compensating emitters that delivered water at a rate of 2 L/hr. For T3 and T4, irrigation thresholds were set at 70% depletion of available water holding capacity (AWHC).

2.2 Soil analysis and fertilization

Pre-planting, soil samples (0–40 cm depth) were collected across all plots to determine soil properties. A uniform fertilization was applied across treatments, guided by soil recommendations practices. Fertilizers in T2–T4 were delivered via fertigation through the drip system to enhance nutrient use efficiency. The total N-P-K rates applied were 25-25-25 kg/ha, divided into 8 times split applications over the growing season. The rainfed condition (T1) received fertilizers via conventional broadcasting methods. Field capacity (FC) and permanent wilting point (PWP) were determined using the pressure plate apparatus, and AWHC was calculated to establish irrigation thresholds for precision treatments.

2.3 Principle of soil moisture sensor

Wireless sensor networks (WSNs) serve essential functions in multiple fields. WSNs have become essential tools in precision agriculture because they track essential environmental factors, including temperature, humidity, soil moisture, and soil pH, which leads to better crop yields and quality. The implementation of WSNs helps maximize natural resource utilization through optimized irrigation practices and input application methods. A typical WSN network comprises multiple sensor nodes that collect environmental data in the deployment area and transmit it to end users (Figure 1). The networks operate with limited infrastructure, utilizing 10 to 1,000 nodes that work together to monitor specific areas. WSNs are categorized into two main types: structured and unstructured networks. The deployment of structured WSNs follows a predetermined pattern, which simplifies both setup and maintenance operations when required.

Figure 1 Diagram of irrigation treatment and wireless sensor network installation

2.4 Data collection

Data collection was performed at regular intervals throughout the cassava growth cycle, including:

1) Growth Parameters, including plant height and stem diameter, were measured at 1, 3, and 5 months after planting (MAP).

2) Leaf nutrient analysis, including percentage nitrogen, phosphorus, potassium, calcium, and magnesium in leaf dry weight were measured at 4 MAP.

3) Biomass accumulation yield and starch content

- Biomass accumulation, including dry weight (DW) of leaf, stem DW, and tuber DW (Both root and food storage part) was measured at 3, 6, 9, and 12 MAP (tuber yield).
- Yield and starch content (%) were measured at 12 MAP.

4) Soil moisture dynamic was collected daily for 3 months to show the trends of water content in irrigation treatment, and water use efficiency (WUE) were measured by the equation of De Pascale et al. (2011).

$$WUE = \frac{Yield\ (kg/ha)}{Total\ water\ supply\ (m^3/ha)}$$

2.5 Statistical analysis

All data were subjected to analysis of variance (ANOVA) using SPSS v16.0 to assess treatment effects. Mean separations were conducted using Duncan's Multiple Range Test (DMRT) at a significant level of $p < .05$.

3. Results and Discussion

3.1 Effects of irrigation treatments on growth parameters

At 1 MAP, no significant differences in plant height were observed among treatments. However, by 3 and 5 MAP, all drip irrigation treatments (T2–T4) significantly increased plant height compared to the rainfed condition (T1) (Figure 2). T4 consistently produced the tallest plants and the largest stem diameters by 5 MAP, demonstrating the benefits of enhanced precision irrigation. Drip irrigation effectively mitigated water stress during critical growth stages, supporting superior vegetative development. These findings corroborate previous studies indicating that drought stress limits plant growth through reduced stomatal conductance and photosynthesis (Inman-Bamber & Smith, 2005; Nesreen et al., 2013; Vurayai et al., 2010). No significant differences were detected between T2 and sensor-based treatments (T3 and T4), indicating that both methods adequately satisfied cassava's water demands (~8,531 m³/ha). Increasing sensor density beyond one per 1.2 ha did not enhance growth, aligning with Kizito et al. (2008), who emphasized the need to balance precision with economic feasibility.
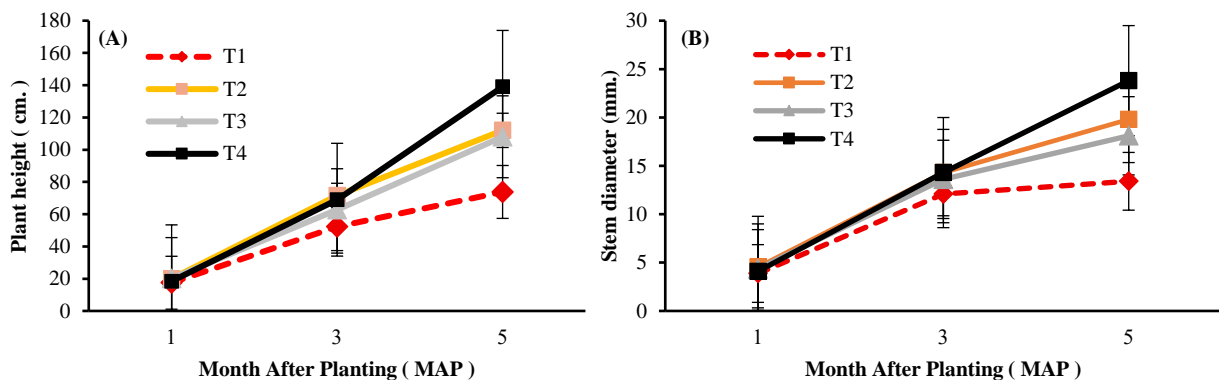
Figure 2 Effect of irrigation treatments on cassava height (A) and stem diameter (B) at 1, 3, and 5 MAP.

3.2 Effects of irrigation treatments on leaf nutrient analysis

Leaf nutrient analysis at 4 MAP revealed significantly higher concentrations of N, P, and K in all drip irrigation treatments compared to T1 (Table 1). Ca and Mg levels showed no significant variation. Improved water availability likely facilitated nutrient uptake, enhancing physiological performance. These results align with those of Rosenthal et al. (2012) and De Souza et al. (2020), who have linked optimal nutrient status with improved photosynthetic efficiency and yield.

Table 1 Effects of irrigation treatments on leaf nutrients analysis at 4 MAP.

Irrigation method	N (%)	P (%)	K (%)	Ca (%)	Mg (%)
T1: Control	4.58b	0.16b	0.90c	0.51	0.24ab
T2: Water balance model	5.18a	0.28a	1.23b	0.58	0.25a
T3: 1 sensor set/1.2 ha	5.14a	0.28a	1.49a	0.54	0.24ab
T4: 3 sensors set/1.2 ha	5.25a	0.30a	1.51a	0.49	0.23b
P-value	*	**	**	ns	ns
CV (%)	4.76	9.50	5.35	8.87	3.09

[1] Means in the same column with different letters are significant differences at P < 0.05.

3.3 Effects of irrigation treatments on biomass accumulation, yield, and starch content

Drip irrigation significantly increased dry biomass accumulation at 3, 6, and 9 MAP, particularly for tubers. By 12 MAP, differences in leaf dry weight diminished, highlighting the importance of early-season water supply (Figure 3). Tuber yield was significantly higher in drip treatments, with T4 achieving the maximum yield (49 tons/ha),

nearly doubling that of T1 (25.8 tons/ha). The starch content remained unaffected across treatments, suggesting water management influences yield quantity rather than quality (Table 2). These outcomes support previous findings on the benefits of drip irrigation in cassava (Phromuthai, 2014). Polthanee and Srisutham (2018) also reported that drip irrigation resulted in higher leaf, stem, tuber, and yield production of cassava than the rainfed cultivation. Samutthong and Sarobol (2006) found that irrigated cassava had a higher yield than non-irrigated cassava.
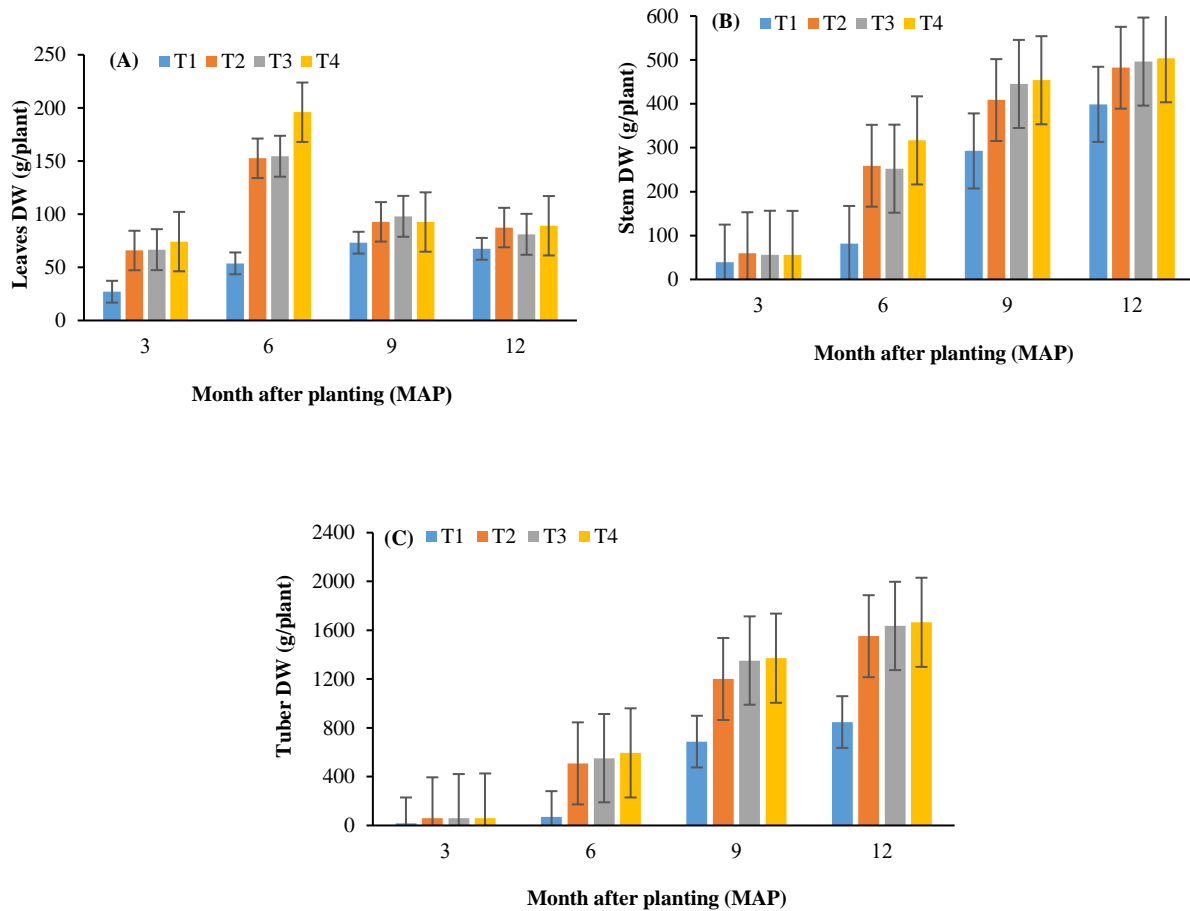
Figure 3 Effects of irrigation treatments on leaves DW (A), stems DW (B), and tubers DW (C) at 3, 6, 9, and 12 MAP.

Table 2 Effects of irrigation treatments on cassava yield and starch content at 12 MAP

Irrigation method	Yield (tons/ha)	Starch (%)
T1: Control	25.8b	26.9
T2: water balance model	47.5a	28.1
T3: 1 sensor set/1.2 ha	47.8a	26.6
T4: 3 sensors set/1.2 ha	49.0a	27.3
P-value	**	ns
CV (%)	13.01	3.91

[1] Means in the same column with different letters are significant differences at P < .05.

3.4 Soil moisture dynamics and water use efficiency

Sensor-controlled treatments (T3 and T4) maintained soil moisture within optimal ranges (30–41% AWHC), while T1 experienced frequent deficits (Figure 4). Although tuber yields were comparable among drip treatments, T3 and T4 used less water than T2, resulting in higher WUE values (13.5–13.8 kg/m³ vs. 12.1 kg/m³) (Table 3). The irrigation water volumes for T3 and T4 were equal, so one sensor per 1.2 ha was sufficient for soil moisture monitoring. The method requires sensor accuracy and uniform field conditions with flat terrain and consistent soil properties. These findings confirm that real-time soil moisture monitoring enhances irrigation efficiency without compromising productivity (Xie et al., 2020). The limitations of water balance models under variable climatic and soil conditions further emphasize the advantages of adaptive, sensor-based irrigation strategies (Fisher & Hanks, 2009; Malik et al., 2021). Zotarelli et al. (2011) investigated grass cultivation and found that moisture sensors resulted in the highest possible yield while reducing water consumption by 7–62%. The research of Tanaka et al. (2011) confirmed that the soil moisture sensor EC-5 successfully measured soil water content after rainfall and detected groundwater presence.
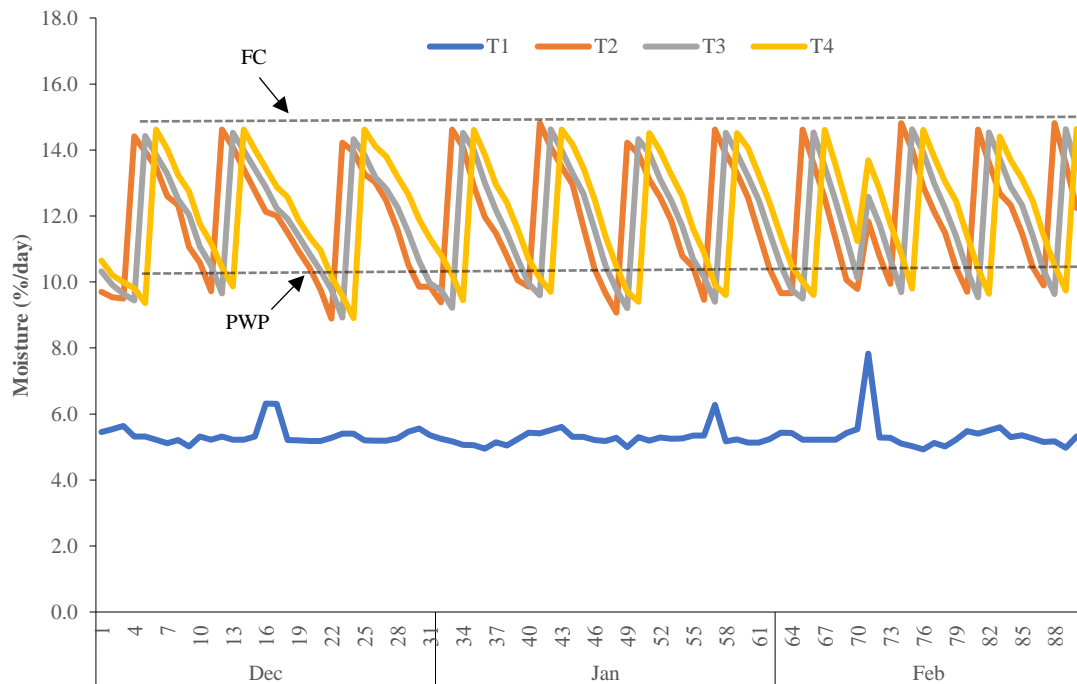
Figure 4 Effects of irrigation treatments on daily soil moisture content.

Table 3 Effects of irrigation treatments on water use efficiency.

Irrigation method	Irrigated water[1] (m³/ha)	WUE (kg/m³)	Rainfall (mm.)
T1: Control	0c	0b	710
T2: water balance model	3,918a	12.1a	710
T3: 1 sensor set/1.2 ha	3,537b	13.5a	710
T4: 3 sensors set/1.2 ha	3,537b	13.8a	710
P-value	**	**	
CV (%)	0.30	17.11	

[1] Means in the same column with different letters are significant differences at $P < 0.05$.

4. Conclusion

This study demonstrated that drip irrigation, particularly when controlled by soil moisture sensors, significantly enhances cassava growth, nutrient uptake, biomass, and yield under clay loam soil conditions. Sensor-based systems improved WUE by reducing water inputs without sacrificing yield, while increasing sensor density beyond one per 1.2 ha offered no additional benefit. Irrigation improved macronutrient uptake but did not affect starch content, indicating that water management primarily boosts yield quantity. Precision drip irrigation with soil moisture sensor integration presents a sustainable solution for improving cassava productivity and resource efficiency, especially in regions prone to irregular rainfall. Future research should focus on economic assessments, sensor deployment in heterogeneous soils, and advanced fertigation integration.

5. Acknowledgements

6. References

Bonilla, C. A., Bonilla, C. A., Tapia, J., Jara, J., Meza, F. J., & Charrier, R., (2021). Precision irrigation for sustainable agriculture: A review. *Agronomy*, 11(4), 675.

De Pascale, S., Costa, L. D., Vallone, S., Barbieri, G., & Maggio, A. (2011). Increasing water use efficiency in vegetable crop production: from plant to irrigation systems efficiency. *HortTechnology*, 21(3), 301–308.

De Souza, R., da Silva, M. A., de Oliveira Ferreira, T. D., & de Souza, L.F. (2020). Nutrient uptake and photosynthetic efficiency in cassava under varying water regimes. *Journal of Plant Nutrition*, 43(7), 1012–1024.

Fisher, J., & Hanks, R.J. (2009). Soil moisture monitoring and irrigation scheduling. *Irrigation Science*, 27(3), 223–237.

Inman-Bamber, N. G., & Smith, D. M. (2005). Water relations of cassava: A review. *Field Crops Research*, 92(2-3), 139–151.

Kim, Y., Evans, R. G., & Iversen, W. M. (2020). Wireless sensor networks for precision agriculture: A review. *Sensors*, 20(3), 715.

Kizito, F., Campbell, C. S., Brenning, A., Lojka, B., de Meyer, K., & Munch, J. C. (2008). Soil moisture sensor deployment strategies for precision irrigation. *Agricultural Water Management*, 95(6), 707–715.

Malik, A., Rustagi, A., Khosla, R., & Amawi, M. (2021). Real-time soil moisture monitoring for efficient irrigation management. *Agricultural Systems*, 189, 103031.

Nesreen, A., El-Hariri, D., & Yakout, G. M. (2013). Effects of drought stress on cassava growth and physiology, *Journal of Agronomy*, 12(1), 45–52.

Ojha, T., Misra, S., & Raghuwanshi, N. S. (2015). Wireless sensor networks for smart irrigation. *Computers and Electronics in Agriculture*, 118, 66–74.

Pereira, L. S., Paredes, P., Jovanovic, N. Z., Pizzigalli, C., Mendes, J., Mainuddin, M., & Xiong, Y. (2020). Advances in precision irrigation technologies. *Irrigation Science*, 38(2), 123–143.

Phromuthai, P. (2014). Effects of drip irrigation on cassava yield in Thailand. *Thai Journal of Agricultural Science*, 47(2), 89–97.

Polthanee, A., & Srisutham, S. (2018). Improving cassava productivity through irrigation management. *Kasetsart Journal: Natural Science*, 52(1), 123–130.

Rosenthal, D. M., Locke, A. M., Fuentes, M., & Ort, D. R. (2012). Nutrient uptake and photosynthesis in cassava. *Plant Physiology*, 160(3), 1234–1245.

Sadler, E. J., Evans, D. E., Stone, K. C., Camp, C. R., & Millen, J. A., (2005). Drip irrigation water savings and yield responses. *Agricultural Water Management*, 77(1-3), 176–196. https://doi.org/10.1016/j.agwat.2004.09.004

Samutthong, N., & Sarobol, E. (2006). Effects of Amount and Rate of Watering on Growth and Yield of Cassava [Doctoral dissertation]. Kasetsart University.

Tanaka, T., Nakano, H., Yano, T., & Toyota, M., (2011). Soil moisture sensor-based irrigation control. *Irrigation Science*, 29(4), 301–310.

Vories, E. D., Evett, S. R., Colaizzi, P. D., & O'Shaughnessy, S.A. (2017). Water use efficiency in drip-irrigated crops. *Agricultural Water Management*, 193, 1–9.

Vurayai, C., Masanganise, J. N., & Manjeru, P. (2010). Drought effects on cassava growth and yield. *Field Crops Research*, 119(3), 280–287.

Xie, Y., Zhang, M., & Chen, Y. (2020). Sensor-based irrigation scheduling for cassava. *Agricultural Water Management*, 231, 106004.

Zotarelli, L., Dukes, M. D., Romero, C. C., Migliaccio, K. W., & Morgan, K. T. (2011). Fertigation and irrigation management for cassava. *Agricultural Water Management*, 98(2), 317–324.

Biogenic Amine Formation and Microbiological Profile in Asian Seabass and Short-Bodied Mackerel During Refrigerated Storage

Watcharacha Krongkeha[1*]

[1]*Department of Food Processing and Culinary Science, Faculty of Science and Technology, Rajamangala University of Technology Rattanakosin, Nakhon Pathom, Thailand.*
* Corresponding author Email address: watcharacha.kro@rmutr.ac.th

Abstract

Biogenic amines (BAs) are key chemical indicators of fish spoilage and potential food safety hazards. This study investigated the formation of four common BAs-histamine, cadaverine, putrescine, and tyramine-and monitored microbial populations in Asian seabass (*Lates calcarifer*) and short-bodied mackerel (*Rastrelliger brachysoma*) stored at 0°C and 4°C for seven days. Total viable counts, staphylococci, and Enterobacteriaceae were assessed using culture-based methods, while BA concentrations were quantified by high-performance liquid chromatography (HPLC). The results revealed that microbial growth and BA accumulation were significantly higher in fish stored at 4°C, with short-bodied mackerel showing a markedly greater susceptibility to spoilage. Histamine levels in short-bodied mackerel at 4°C reached 292.67 ± 1.53 mg/kg by day seven. In contrast, histamine remained undetectable in Asian seabass under the same conditions. These findings provide essential baseline data for spoilage assessment in Thai seafood products and highlight the importance of species-specific storage guidelines and strict temperature control to ensure food safety.

Keywords: Biogenic Amines, Fish Spoilage, Refrigerated Storage, Asian Seabass, Short-bodied Mackerel

1. Introduction

Biogenic amines (BAs) are low molecular weight organic nitrogenous compounds that occur naturally in various foods. They are primarily formed through the microbial decarboxylation of free amino acids, a process facilitated by specific bacterial enzymes. Additionally, BAs can arise via transamination or reductive amination of aldehydes and ketones, especially during food fermentation, spoilage, or under certain physiological conditions (Sivamaruthi et al., 2021). These amines originate from the decarboxylation of specific amino acids: for instance, histidine yields histamine, tyrosine produces tyramine, and tryptophan leads to tryptamine. Among these, certain BAs such as histamine, tyramine, β-phenylethylamine, and tryptamine are biologically active and exert significant physiological effects in humans. Histamine and tyramine are known for their vasoactive properties, influencing vascular tone and blood pressure. Conversely, β-phenylethylamine and tryptamine exhibit psychoactive effects by modulating neurotransmitter systems, thereby affecting mood and cognitive functions (Kalač, 2014; del Rio et al., 2020).

Fish freshness is significantly influenced by storage conditions and the duration before processing. Post-harvest, fish undergo biochemical and microbiological changes as a result of endogenous enzymatic activity and microbial proliferation on the skin, gills, and gastrointestinal tract. The rate of spoilage varies with factors such as fish species, storage time and temperature, and the extent of microbial contamination (Arulkumar et al., 2023). During spoilage, proteins degrade into peptides, free amino acids, and biogenic amines (BAs)-thermally stable compounds whose presence serves as reliable indicators of raw material freshness and spoilage. Elevated levels of BAs such as histamine, cadaverine, and putrescine are closely associated with spoilage and potential health risks (Akkaya et al., 2024).

Biogenic amines are naturally present in a wide range of aquatic food products, reflecting their broad distribution in both marine and freshwater species. Although the global literature has extensively documented BA accumulation in marine fish, much of this research has concentrated on temperate species. In contrast, studies focusing on tropical, market-sourced fish in Southeast Asia-particularly those sold and consumed in countries like Thailand-remain limited. This lack of data is especially concerning given the region's high reliance on fresh fish and the logistical challenges associated with maintaining a reliable cold chain. For example, Tao et al. (2022) investigated BA production in salted mackerel stored under soft frozen conditions, highlighting the complex relationship between microbial diversity and amine formation. Similarly, Biji et al. (2016) reviewed the presence of BAs in seafood, underscoring the critical roles of storage practices and microbial activity. Despite these insights, there is still a noticeable gap in research examining BA content specifically in Asian seabass (*Lates calcarifer*) and short-bodied mackerel (*Rastrelliger brachysoma*) in Thailand. The primary aim of this study, therefore, was to assess the formation of biogenic amines and characterize the associated microbiological profiles in these two commercially important species during refrigerated storage under local handling conditions.

2. Methodology

2.1 Sample preparation

Fishes, Asian seabass (*Lates calcarifer*) and short-bodied mackerel (*Rastrelliger brachysoma*) were purchased from Thonburi market place, Bangkok. The fishes were iced immediately in an ice High Density Poly Ethylene (HDPE) box and brought to the laboratory approximately 2 h later. Upon arrival at the lab, whole ungutted and unfilleted fishes were sectioned, weighted, and subsequently stored at controlled temperatures of 0 and 4°C for 7 days.

2.2 Microbial analysis by the culture-dependent method

The counts of total viable bacteria, staphylococci and Enterobacteriaceae were conducted using a culture-dependent method as described by Ekici et al. (2008) and Pons-Sanchez-Cascado et al. (2005). For each analysis, a 25 g portion of fish sample was aseptically sampled and transferred to a sterile stomacher bag and 225 ml of sterile physiological saline was added. The mixture was homogenised using a stomacher for 2 min at room temperature. To enumerate total viable bacteria and staphylococci, 0.1 ml of the serial dilutions of homogenates was spread on the Plate Count Agar (PCA) and mannitol salt agar (MSA), respectively. These plates were incubated at 37°C for 48 h. For Enterobacteriaceae enumeration, 1 ml of serial dilutions of the homogenates was inoculated to 10 ml of molten violet red bile glucose agar (VRBGA). After solidification, an overlay of 10 ml of the same molten agar was added and the plates were incubated at 30°C for 24 h. The bacterial counts were expressed in the logarithm of colony forming units per gram (Log CFU/g).

2.3 Determination of biogenic amines

Four biogenic amines, namely, histamine, cadaverine, putrescine, and tyramine, were quantified using high-performance liquid chromatography (HPLC) as described by Abré et al. (2023) with slight modifications. Ten milliliters of perchloric acid (0.2 M) and 100 µL of 1-3-diaminopropane (0.8 mg/mL) were added to 5 g of minced fish sample. The resulting homogenate was centrifuged at $7000 \times g$ at 4°C for 5 min. For the derivation of the extracted BAs, 300 µL of saturated sodium carbonate and 400 µL of dansyl chloride solution (7.5 mg/mL in acetone) were added to 100 µL of supernatant. The reaction mixture was vortexed and incubated at 60 °C for 5 min in darkness, then cooled with water. Subsequently, 100 µL of proline (100 mg/mL) was added to quench residual dansyl chloride, followed by a 15-min dark incubation period to ensure complete neutralization. To purify the derivatives, 500 µL of toluene was added, and the samples were incubated at -20°C for a minimum of 30 min. The upper organic phase was then collected and evaporated under a stream of nitrogen. The dry residue was adjusted to 5 ml using acetonitrile and filtered through a 0.45-µm regenerated cellulose membrane filter. Ten microliters of the solution were injected into HPLC (HP 1100, Agilent Technologies Inc., Palo Alto, CS., U.S.A). A Zorbax Eclipse-XDB-C18 column (4.6×150 mm, 5 µm, Agilent Technologies Inc., Palo Alto, CA., U.S.A.) was used. Chromatographic separation was performed using a gradient elution of (A) acetonitrile (100%), (B) acetonitrile (50%) as follows: 0-8 min, A 70% B 30%; 8-12 min, A 80% B 20%; 12-16 min, A 5% B 95%; 16-20 min, A 70% B 30%; at column temperature of 28°C.

2.4 Statistical analysis

Statistical analyses were conducted using one-way analysis of variance (ANOVA), followed by Tukey's post hoc test to determine specific group differences. All analyses were performed using SPSS software, version 17.0 (IBM Corp., Armonk, NY, USA). Differences between group means were considered statistically significant at $p < 0.05$ and highly significant at $p < 0.01$.

3. Results and Discussion

3.1 Microbiological profile during refrigerated storage

The microbiological analysis revealed a progressive increase in bacterial load in both Asian seabass (*Lates calcarifer*) and short-bodied mackerel (*Rastrelliger brachysoma*) over the 7-day storage period. The counts of total viable bacteria, staphylococci, and Enterobacteriaceae exhibited higher growth rates in samples stored at 4°C compared to those stored at 0°C (Figure 1). In both fish species, initial microbial loads were low, reflecting satisfactory freshness at day 0. However, by day 7, substantial microbial proliferation was observed, particularly in short-bodied mackerel stored at 4°C (MF47), which recorded the highest bacterial counts across all tested groups. These results are in accordance with the previous report (Syropoulou et al., 2021), that revealed temperatures facilitated the growth of bacteria in fresh and chill-stored fish.

The increased bacterial activity in short-bodied mackerel may be attributable to species-specific differences in surface microbiota or intrinsic biochemical composition. Additionally, the higher Enterobacteriaceae counts in this species suggest its greater vulnerability to spoilage-related microbial activity. Similar microbial patterns have been reported in scombroid species, which are known for their rapid spoilage and high amine accumulation potential (Biji et al., 2016; Visciano et al., 2012).

These findings reinforce the well-established link between microbial activity and the formation of spoilage indicators such as biogenic amines. In particular, members of the *Enterobacteriaceae* family are well recognized for their amino acid decarboxylase activity, which facilitates the production of biogenic amines during fish spoilage and fermentation (Halász et al., 1994; Zaman et al., 2010)
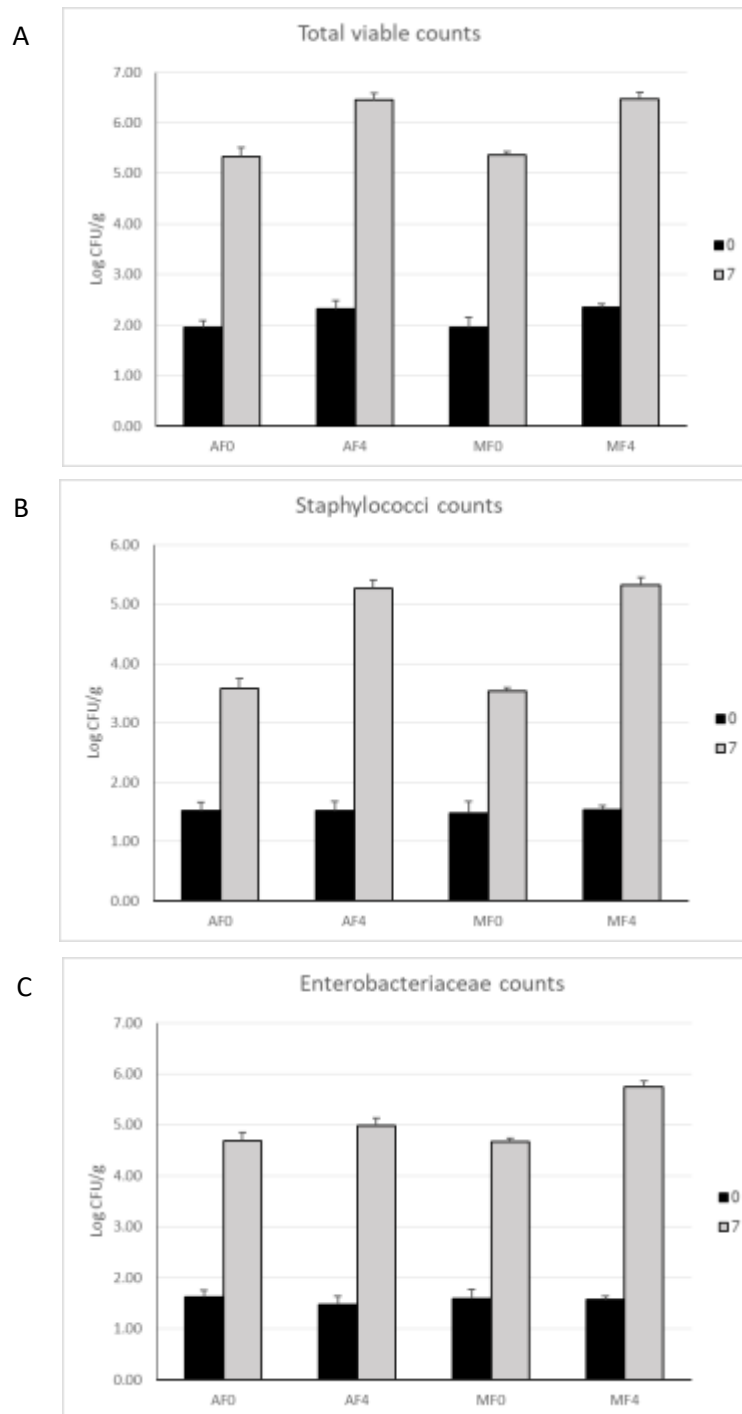
Figure 1 Changes in total viable counts (A), staphylococci counts (B) and Enterobacteriaceae counts (C) in Asian seabass and short-bodied mackerel during storage at 0 and 4°C for 7 days. Error bars represent standard deviation. AF0, Asian seabass at 0°C; AF4, Asian seabass at 4°C; MF0, short-bodied mackerel at 0°C; MF4, short-bodied mackerel at 4°C.

3.2 Biogenic amine accumulation in fish samples

Biogenic amine (BA) content followed a pattern consistent with microbial proliferation (Table 1). At day 0, none of the four targeted amines-histamine, cadaverine, putrescine, and tyramine-were detected in any sample, confirming the initial freshness of the fish. As storage progressed, BA levels remained relatively low in fish kept at 0°C but rose markedly in samples stored at 4°C.

Short-bodied mackerel stored at 4°C for 7 days (MF47) exhibited the highest concentrations of all four amines. Histamine levels reached 292.67 ± 1.53 mg/kg, while cadaverine, putrescine, and tyramine measured 615.00 ± 1.00, 461.67 ± 1.53, and 731.67 ± 1.53 mg/kg, respectively. These concentrations far exceeded acceptable safety thresholds, particularly for histamine, which is regulated at 50 mg/kg by the U.S. Food and Drug Administration (2002) for scombroid fish and/or products. These findings closely align with the previous report of histamine levels exceeding 300 mg/kg in tuna samples collected during a survey in Northern Italy (Morello et al., 2024). Histamine

concentrations have been reported with greater than 50 mg/kg in short-bodied mackerel stored at 8°C over 20 days (Yassoralipour et al., 2016). The faster accumulation observed in the present study may be due to higher initial microbial load or specific conditions within the local supply chain. By contrast, Asian seabass stored at 4°C for the same duration (AF47) showed much lower amine levels, with histamine remaining undetectable. Cadaverine and putrescine were present at 17.67 ± 1.53 and 17.00 ± 2.65 mg/kg, respectively, while tyramine was measured at 8.33 ± 2.08 mg/kg. These values suggest that Asian seabass is less prone to amine accumulation under short-term refrigerated storage, possibly due to lower decarboxylase activity in its associated microbiota or lower free amino acid content. The differences between the two species point to the role of intrinsic and extrinsic factors in BA formation. Similar conclusions were drawn by Barb et al. (2024), who noted that scombroid fish exhibited rapid spoilage and BA accumulation which can increase toxicity by inhibiting intestinal metabolizing enzymes. Cadaverine, putrescine, histamine, and tyramine are among the predominant biogenic amines commonly detected in seafood. Furthermore, the concentrations of these amines tend to rise markedly as storage duration increases (Hu et al., 2012).

In Thailand, there is still a lack of detailed research on the formation of biogenic amines (BAs) in marine species that are commonly consumed locally. This study aims to address that gap by comparing two widely marketed species-Asian seabass (*Lates calcarifer*) and short-bodied mackerel (*Rastrelliger brachysoma*)-under typical refrigerated storage conditions that reflect real-world practices in households and retail settings. Although the accumulation of BAs in marine fish has been well-documented internationally (Kalač, 2014; Kuley, et al., 2017), there is comparatively little data from tropical regions, especially Southeast Asia. This is particularly concerning given the region's challenges in maintaining effective cold chain logistics and Thailand's high consumption of fresh fish.

Thai food safety regulations stipulate that histamine levels in fish should not exceed 200 mg/kg, a limit that is consistent with the standard set by the Codex Alimentarius Commission for scombroid and other histidine-rich fish species (Codex, 2019). In the present study, short-bodied mackerel (*Rastrelliger brachysoma*) stored at 4°C recorded a histamine concentration of 292.67 ± 1.53 mg/kg by the seventh day of storage-well above the established safety threshold. This result highlights a significant risk of histamine poisoning when cold chain practices are not properly implemented. Importantly, these findings provide valuable baseline data to support risk evaluations and inform regulatory oversight. They also underscore the need for improved, species-specific monitoring and more stringent temperature control measures throughout Thailand's seafood distribution system.

Table 1 Biogenic amine content (mg/kg) of Asean seabass and short-bodied mackerel during refrigerated storage.

Sample	Biogenic amine content (mg/kg)			
	Histamine	Cadaverine	Putrescine	Tyramine
AF00	0.00 ± 0.00[b]	0.00 ± 0.00[c]	0.00 ± 0.00[c]	0.00 ± 0.00[d]
AF07	0.00 ± 0.00[b]	10.00 ± 2.00[c]	0.00 ± 0.00[c]	0.00 ± 0.00[d]
AF40	0.00 ± 0.00[b]	0.00 ± 0.00[c]	0.00 ± 0.00[c]	0.00 ± 0.00[d]
AF47	0.00 ± 0.00[b]	17.67 ± 1.53[b]	17.00 ± 2.65[b]	8.33 ± 2.08[c]
MF00	0.00 ± 0.00[b]	0.00 ± 0.00[c]	0.00 ± 0.00[c]	0.00 ± 0.00[d]
MF07	0.00 ± 0.00[b]	19.00 ± 1.00[b]	0.00 ± 0.00[c]	76.30 ± 1.13[b]
MF40	0.00 ± 0.00[b]	0.00 ± 0.00[c]	0.00 ± 0.00[c]	0.00 ± 0.00[d]
MF47	292.67 ± 1.53[a]	615.00 ± 1.00[a]	461.67 ± 1.53a	731.67 ± 1.53[a]

Each value represents the mean ± standard deviation of triplicates followed by different letters in the column are significant different (p < 0.05); AF00, Asian seabass at 0°C and day 0; AF07, Asian seabass at 0°C and day 7; AF40, Asian seabass at 4°C and day 0; AF47, Asian seabass at 4°C and day 7; MF00, Asian seabass at 0°C and day 0; MF07, Asian seabass at 0°C and day 7; MF40, Asian seabass at 4°C and day 0; MF47, Asian seabass at 4°C and day 7.

4. Conclusions

This study highlights the significant impact of storage temperature and fish species on biogenic amine formation and microbial spoilage during refrigeration. Short-bodied mackerel (*Rastrelliger brachysoma*) stored at 4°C showed rapid spoilage, with histamine levels exceeding safety limits by day seven. In contrast, Asian seabass (*Lates calcarifer*) was more resistant under the same conditions, indicating species-specific differences in spoilage rates. To our knowledge, this is the first study to examine biogenic amine accumulation and microbial changes in whole, ungutted specimens of these two species stored at 0°C and 4°C. The results provide important baseline data for assessing spoilage in fish commonly sold in Thai markets and emphasize the need for strict cold storage-especially near 0°C-to minimize microbial growth and histamine formation. Routine monitoring of microbial load and amine content is recommended to ensure seafood safety and quality.

5. Acknowledgement

6. References

Abré, M. G., Kouakou-Kouamé, C. A., N'guessan, F. K., Teyssier, C., & Montet, D. (2023). Occurrence of biogenic amines and their correlation with bacterial communities in the Ivorian traditional fermented fish adjuevan during the storage. *Folia Microbiologica*, *68*(2), 257-275.

Akkaya, E., Colak, H., Hampikyan, H., Engin, A. S., & Bingol, E. B. (2024). Biogenic amine content and shelf-life of salmon fillets packaged in modified atmospheres of low-level carbon monoxide and different carbon dioxide concentrations. *Polish Journal of Food and Nutrition Sciences*, *74*(4), 323-339.

Arulkumar, A., Paramithiotis, S., & Paramasivam, S. (2023). Biogenic amines in fresh fish and fishery products and emerging control. *Aquaculture and Fisheries*, *8*(4), 431-450.

Barp, L., Moret, E., & Moret, S. (2024). Evolution of eight biogenic amines in raw and preserved mackerel (*Scomber scombrus*) fillets monitored by UHPLC-PDA. *Separations*, *11*(8), 235.

Biji, K. B., Ravishankar, C. N., Venkateswarlu, R., Mohan, C. O., & Gopal, T. S. (2016). Biogenic amines in seafood: a review. *Journal of food science and technology*, *53*, 2210-2218.

Codex Alimentarius (Codex). (2019). *Codex General standard for contaminants and toxins in food and feeds (CXS 193-1995)*. Rome: FAO/WHO.

del Rio, B., Redruello, B., Fernandez, M., Martin, M. C., Ladero, V., & Alvarez, M. A. (2020). The biogenic amine tryptamine, unlike β-phenylethylamine, shows *in vitro* cytotoxicity at concentrations that have been found in foods. *Food Chemistry*, *331*, 127303.

Ekici, K., & Alisarli, M. (2008). Histamine formation and microbiological changes in endemic *Chalcalburnus tarichi* Pallas 1811 (Inci Kefali) stored at 4 °C. *Archivos de medicina veterinaria*, *40*(1), 95-98.

Food and Drug Administration. (2002). Scombrotoxin (histamine) formation, fish and fishery products hazards and controls guide. In *Public health service, food and Drug administration, center for food safety and applied nutrition, office of seafood* (pp. 73-93). Department of Health and Human Services Washington, DC.

Halász, A., Baráth, Á., Simon-Sarkadi, L., & Holzapfel, W. (1994). Biogenic amines and their production by microorganisms in food. *Trends in Food Science & Technology*, *5*(2), 42-49.

Hu, Y., Huang, Z., Li, J., & Yang, H. (2012). Concentrations of biogenic amines in fish, squid and octopus and their changes during storage. *Food chemistry*, *135*(4), 2604-2611.

Kalač, P. (2014). Health effects and occurrence of dietary polyamines: A review for the period 2005-mid 2013. *Food Chemistry*, *161*, 27-39.

Kuley, E., Durmus, M., Balikci, E., Ucar, Y., Regenstein, J. M., & Özoğul, F. (2017). Fish spoilage bacterial growth and their biogenic amine accumulation: Inhibitory effects of olive by-products. *International Journal of Food Properties*, *20*(5), 1029-1043.

Morello, S., Lupi, S., Barcucci, E., Fragassi, S., Torres, E., Dosio, D., Marchese, C., Bezzo Llufrio, T., Gili, M., & Bianchi, D. M. (2024). Histamine in fishery: A five-year survey in Northern Italy. *Toxins*, *16*(11), 456.

Pons-Sanchez-Cascado, S., Veciana-Nogués, M. T., Bover-Cid, S., Marine-Font, A., & Vidal-Carou, M. C. (2005). Volatile and biogenic amines, microbiological counts, and bacterial amino acid decarboxylase activity throughout the salt-ripening process of anchovies (Engraulis encrasicholus). *Journal of food protection*, *68*(8), 1683-1689.

Sivamaruthi, B. S., Kesika, P., & Chaiyasut, C. (2021). A narrative review on biogenic amines in fermented fish and meat products. *Journal of Food Science and Technology*, *58*(5), 1623-1639.

Syropoulou, F., Parlapani, F. F., Kakasis, S., Nychas, G. J. E., & Boziaris, I. S. (2021). Primary processing and storage affect the dominant microbiota of fresh and chill-stored sea bass products. *Foods*, *10*(3), 671.

Tao, Z., Liu, W., Hu, Q., Wu, X., Xie, S., Zhang, H., ... & Jiang, Y. (2022). Interaction between bacterial diversity and biogenic amines production in a salted mackerel stored at soft frozen (-7°C-0°C) storage. *Food Science & Nutrition*, *10*(2), 412-421.

Visciano, P., Schirone, M., Tofalo, R., & Suzzi, G. (2012). Biogenic amines in raw and processed seafood. *Frontiers in microbiology*, *3*, 188.

Yassoralipour, A., Hosseini, H., & Rezaei, M. (2016). Histamine formation in Asian seabass (*Lates calcarifer*) fillets stored under modified atmosphere packaging. *Iranian Journal of Fisheries Sciences*, 15(2), 794-804.

ZaMaN, M. Z., Bakar, F. A., SelaMat, J., & Bakar, J. (2010). Occurrence of biogenic amines and amines degrading bacteria in fish sauce. *Czech Journal of Food Sciences*, *28*(5), 440-449.

Effects of *Dictyophora indusiata* powder and purple rice flour on the baking quality characteristics and volatile flavor of cookies

Yuyue Qin[a], Zhouhao Yang[a], Shu Wang[a], Yongliang Zhuang[a], Qiuming Liu[a], Shanshan Xiao[a], Thanapop Soteyome[b]*, Charles Brennan[c]*, Yuanxiang Huang[d]

[a] *Yunnan International Joint Laboratory of Green Food Processing, Faculty of Food Science and Engineering, Kunming University of Science and Technology, Kunming 650550, China*
[b] *Rajamangala University of Technology Phra Nakhon, Bangkok 10300, Thailand*
[c] *School of Science, Royal Melbourne Institute of Technology University, Melbourne 3000, Australia*
[d] *Kunming Gao-Shang-Gao Food Co. LTD, Kunming 650501, China*
** Corresponding authors, E-mail addresses:*thanapop.s@rmutp.ac.th (T. Soteyome),
Charles.brennan@RMIT.edu.au (C. Brennan).

Abstract

This study investigated the effects of incorporating *Dictyophora indusiata* powder and purple rice flour on the baking quality, nutritional composition, antioxidant properties, and flavor profile of cookies. A gradient substitution model was employed, replacing wheat flour with varying proportions of *Dictyophora indusiata* (0–5%) and purple rice flour (0–20%). The results demonstrated that the combination of these ingredients significantly enhanced the dietary fiber content (up to 3.25 g/100 g) and protein levels in the cookies, while also improving antioxidant activity, as evidenced by increased DPPH (2,2-Diphenyl-1-picrylhydrazyl) and ABTS (2,2'-Azino-bis (3-ethylbenzothiazoline-6-sulfonic acid)) radical scavenging rates (up to 75.8% and 72.2%, respectively). Additionally, the *in vitro* digestibility analysis revealed a reduction in starch hydrolysis and GI (glycemic index), attributed to the synergistic effects of resistant starch and fiber. However, sensory evaluation indicated that higher substitution levels led to darker coloration and altered texture, impacting overall acceptability. The study highlights the potential of *Dictyophora indusiata* and purple rice as functional ingredients for developing nutritious, low-glycemic-index baked goods, provided that substitution ratios are optimized to balance health benefits with sensory quality.

Keywords: Dictyophora Indusiata Powder; Purple Tice Flour; Cookies Quality; Antioxidant Activity; Volatile Flavor

1. Introduction

With the deepening of the concept of healthy diet, the baked food industry is facing an urgent need for nutritional and functional transformation. The traditional biscuit formulation system, which relies on refined wheat flour, has structural deficiencies such as a lack of dietary fibre and a high proportion of fast-digesting starch, making it difficult to meet consumers' expectations for low-glycemic and high-fibre foods. Current research focuses on substituting with a single ingredient, such as whole grains or edible mushrooms. While this can improve some nutritional indicators, it generally leads to texture deterioration and flavour clashes. In particular, the interaction between fibre components and the gluten network has not yet been clarified. Purple rice is rich in anthocyanins and resistant starch, and *Dictyophora indusiata* contains unique fungal polysaccharides and chitin. These two ingredients show potential for dietary fibre complementarity and functional synergy, but their combined substitution lacks a systematic study on their multidimensional effects on the baking system.

In this study, we constructed a gradient substitution model using purple rice and *Dictyophora indusiata*, innovatively integrated methods for analysing textural properties, *in vitro* digestion, and flavour, and focused on revealing the synergistic effects between non-cereal raw materials and the gluten matrix. This research breaks through key technological bottlenecks in texture control of high-fibre bakery products, provides theoretical support and practical approaches for developing new types of biscuits that are both nutritionally enhanced and palatable to consumers, and promotes the leap of functional bakery products from proof-of-concept to industrial application.

2. Materials and equipment

2.1 Reagents and materials

Raw materials: purple rice, *Dictyophora indusiata*, low gluten flour, baking powder, water, butter, salt, egg, vanilla extract.

Table 1 Experimental reagents

Name	Specification	Grade	Manufacturer
Sodium hydroxide	50 g	AR	Sinopharm Group
Glucose (GLU) assay kit	96 T	AR	Nanjing Jiancheng Bioengineering Institute
MES-TRIS buffer	500 mL	50mM PH=8.2	Strait Standard Technology Co., Ltd.
Pepsin	5 g	3200U	Sinopharm Group
Acetone	500 mL	AR	Xilong Chemical
Copper sulfate	500 g	AR	Tianjin Fangzheng
Boric acid	500 mL	AR	Xilong Chemical
Methyl red indicator (1g/L)	100 mL	AR	Xilong Chemical
Bromocresol green indicator (1g/L)	100 mL	AR	Xilong Chemical

Name	Specification	Grade	Manufacturer
Methylene blue indicator (1g/L)	100 mL	AR	Xilong Chemical
Methanol	500 mL	AR	Xilong Chemical

2.2 Instruments and equipment

Table 2 Information of experimental equipments

Instrument name	Manufacturer
Freeze concentrator	Alpha 1-2 LD plus, Germany
SB5200D ultrasonic cleaner	Ningbo Xinzhi Biotechnology Co., Ltd.
AL204 electronic balance	Mettler-Toledo Instruments (Shanghai) Co., Ltd.
THZ-100 constant temperature incubator	Beijing Yiheng Scientific Instruments Co., Ltd.
TA.XT Plus texture analyzer	Stable Micro Systems, UK
LXJ-IIB centrifuge	Shanghai Anting Scientific Instrument Factory
HH-4 digital display constant temperature water bath	Jintan Kexi Instrument Co., Ltd.
TU 1901 double-beam UV-visible spectrophotometer	Beijing Puxi General Instrument Co., Ltd.
QP2010 gas chromatography-mass spectrometer	Shimadzu Corporation, Japan
Electronic nose	Shanghai Baosheng Industrial Development Co., Ltd.

2.3 Experimental Methods

1) Cookies preparation

Dictyophora indusiata and purple rice cookies need to be prepared first: dry the *Dictyophora indusiata* and purple rice, then crush them and sieve through a 60-mesh sieve to obtain 250 μm fine powder, which is sealed for later use. Weigh 100 g of low-gluten flour according to the recipe (with *Dictyophora indusiata* substituted at 0% and 5%, and purple rice flour substituted at 0%, 10%, 15%, and 20%), 60 g of butter, 45 g of water, 60 g of sugar, 5 g of salt, 2 g of baking powder, 1 mL of vanilla extract, and 50 g of whole egg. Soften the butter, put all ingredients into a mixer, and mix at medium speed until there is no dry powder left. Then form the mixture into a dough and freeze it for 30-60 minutes to harden. Take out the hardened dough, cut it into pieces, and bake in a preheated oven at 185°C for 15 minutes until the surface turns golden brown. Then cool it down to get the finished product. When mixing the ingredients, avoid over-mixing. Adjust the freezing time according to the softness of the dough to ensure the cutting and shaping effect. The recipe is as follows:

Table 3 Purple rice and *dictyophora indusiata* cookies formula ingredients

Ingredients (g)	CON	P5	P10	P15	P20	D5P5	D5P10	D5P15	D5P20
Dictyophora indusiata	0	0	0	0	0	5	5	5	5
Purple rice	0	5	10	15	20	5	10	15	20
Low Flour	100	95	90	85	80	90	85	80	75
Butter	60	60	60	60	60	60	60	60	60
Water	45	45	45	45	45	45	45	45	45
Sugar	40	40	40	40	40	40	40	40	40
Salt	3	3	3	3	3	3	3	3	3
Baking powder	2	2	2	2	2	2	2	2	2
Vanilla extract	1	1	1	1	1	1	1	1	1
Whole egg	20	20	20	20	20	20	20	20	20

2) Determination of basic ingredients of biscuits

For the determination of dietary fibre in high-fat and high-sugar foods, samples should be extracted and degreased with petroleum ether three times (500 mL each time, shaking for 2 minutes). If the viscosity is too high, 85% ethanol should be used for degreasing three times. After degreasing, the samples should be dried at 40°C, weighed, and then the mass change factor should be calculated. For biscuits, the determination of non-sedimentable soluble dietary fibre (SDFS) is not required, so this step is omitted. cookies do not need to be desugared.

After the samples are dispersed in buffer, heat-stabilised α-amylase (at 95°C) or a combination of enzymes (incubated overnight at 37°C) combined with protease should be used to remove starch and protein. The results should be corrected for protein, ash, and blank values, and expressed as the mean of two determinations. The precision requirement is that the difference between the two determinations should be ≤ 20% of the mean value.

3) Determination of cookies baking losses

Based on the method modified from Wu et al. (2021), the baking loss of cookies biscuits is determined by measuring the weight difference before and after baking. All data are based on the average of three repeated experiments. The formula is as follows:

$$\text{Baking Loss}(\%) = \frac{(m1 - m2)}{m1} * 100\%$$

Where: m1 is the mass before baking; m2 is the mass after baking.

97

Thickness changes were measured using a vernier caliper. The initial thickness of the dough was 8 millimeters. After baking, the actual dimensions were recorded, and the percentage change was calculated. All data are based on the average of three repeated experiments. The formula is:

$$\text{Thickness } (\%) = \frac{(h1 - h2)}{h1} * 100\%$$

Where: h1 is the initial thickness; h2 is the thickness after baking.

4) Texture analysis

The hardness of cookies dough and cookies is measured by the TA-XT Plus texture analyzer (SMS, UK). The settings were: P/6 for the probe, the speed was 1 mm/s pre-test, 2 mm/s during the test, and 5 mm/s post-test. Each sample was tested no less than five times.

5) Total phenolic content

The total phenolic content was determined using the method modified from Liu et al. (2021). A 2.5 g sample was mixed with 50 mL of 95% ethanol solution and sonicated at 37°C for 2 hours at 120 r/min. After centrifugation at 2600 r/min for 15 minutes, the supernatant was collected as the phenolic extract. The total phenolic content was measured using the Folin-Ciocalteu method and expressed as mg/100g.

6) Total flavonoid content

The total flavonoid content was determined using the method modified from Wu et al. (2018). A 120 µL sample was mixed with 380 µL of 60% ethanol, followed by the addition of 30 µL of 50% sodium nitrite solution. After 8 minutes, 30 µL of 10% aluminum nitrate solution was added, and the mixture was allowed to stand for 12 minutes. The absorbance was measured at 510 nm, and the total flavonoid content was calibrated using a catechin standard curve and expressed in terms of catechin equivalents (mg CE/100g DM) or (µg CE/100g DM).

7) DPPH radical scavenging activity

The DPPH radical scavenging activity was assessed according to the national standard GB/T39100-2020, with modifications. A 20 mg sample was dissolved in 5 mL of methanol and extracted for 12 hours at 25°C. Mix 200 µL of the above sample with 2 mL of 0.025 g/L DPPH solution and incubated at 37°C for 30 minutes. The absorbance was measured at 30 nm, and the DPPH radical scavenging activity was calculated using the formula:

$$\text{DPPH Radical Scavenging Activity } (\%) = \frac{A_{DPPH} - A_{Extract}}{A_{DPPH}} \times 100$$

Where A_{DPPH} is the absorbance of the DPPH solution with methanol, and $A_{Extract}$ is the absorbance of the DPPH solution with the sample extract.

8) ABTS radical scavenging activity

The determination of ABTS radical scavenging ability in cookies involves dissolving ABTS and $K_2S_2O_8$ to prepare the ABTS solution. Then, 100 µL of the sample is mixed with 3.9 mL of ABTS solution and reacted for 10 minutes, after which the absorbance at 734 nm is measured (A_1). Meanwhile, 3.9 mL of phosphate buffer solution is mixed with 100 µL of the sample as a control, and the absorbance is measured (A_2). Finally, 3.9 mL of ABTS solution is mixed with 100 µL of ethanol to determine the blank absorbance (A_0). ABTS radical scavenging activity was calculated using the formula:

$$\text{ABTS Radical Scavenging Activity } (\%) = [1 - (A_1 - A_2)A_0] \times 100\%$$

9) In vitro digestibility

The *in vitro* digestion characteristics of cookies were assessed by precisely weighing 100 mg of cookies, followed by the addition of 2 mL of distilled water and 7.5 mL of sodium acetate buffer (0.2 mol/L, pH 6.0). The mixture was incubated in a water bath at 37°C for 180 minutes, with samples collected at 0, 20, 40, 60, 120, and 180 minutes. The reaction was terminated by adding anhydrous ethanol. The glucose concentration in the supernatant was determined using a glucose assay kit (GLU), and the absorbance was measured at 510 nm using a spectrophotometer to calculate the starch hydrolysis rate. Additionally, the contents of rapidly digestible starch (RDS) and slowly digestible starch (SDS), as well as resistant starch (RS), were calculated.

10) Odor analysis

The volatile organic compounds (VOCs) for cookies odor were determined using Headspace Solid Phase Microextraction (HS-SPME) combined with Gas Chromatography-Mass Spectrometry (GC-MS) and Electronic Nose Technique (ENT).

For the HS-SPME/GC-MS method, initially, 0.25 grams of cookies were mixed with a 20% NaCl solution containing an internal standard and stirred in a water bath at 50°C. The headspace adsorption was performed using an SPME fiber, followed by desorption at the GC inlet at 260°C for 5 minutes. GC separation was carried out using a DB Wax (0.25 mm×60 m×0.5µm) column with a programmed temperature increase from 40°C to 220°C at a helium flow rate of 2 mL/min. Linear retention indices were determined using a DB5MS column (0.25 mm×30 m×0.25 µm). Mass spectrometric parameters were set with an ion source at 230°C, a quadrupole at 150°C, and a scan range of m/z

35-350. Qualitative identification was achieved by matching against the NIST library combined with retention indices, and quantification was performed using the internal standard method. The sample mass, pH, and chromatograms were recorded to ensure data reliability.

For the ENT method, 2 g of crushed cookies sample was placed in a 20 mL flask and enriched at 38°C for 20 min (Herráiz-Gil, Arriba, and Escámez, 2023). The system contains 18 metal oxide sensors, each with different sensitivity to the measured gas, as listed in Table 4. The detection conditions of the electronic nose (Shanghai Bohin Industrial Development Co., Ltd., China) were set as follows: detection temperature: 25°C; humidity: 55%; injection time: 60 s; flow rate: 1 L/min; detection time: 60 s; wash time: 120 s.

11) Sensory evaluation

Combined with the 9-point preference scale method, the details of sensory evaluation are shown in the following table:

Table 4 Sensory evaluation standard

Item	Score	Scoring criteria
Colour	7-9	Colour is extremely attractive and fully consistent with desirable characteristics
	4-6	Colour is normal but lacks highlights
	1-3	Slightly dull or slightly discoloured colours
Flavour	7-9	Flavour is perfectly balanced and extremely pleasant
	4-6	Flat or slightly off-flavoured
Flavour	1-3	Flavour has a distinctly undesirable flavour
Crispness	7-9	Extremely crunchy, perfect chewing experience
	4-6	Crispness up to standard, no particular merit
	1-3	Texture too soft or too hard
Appearance	7-9	Perfectly regular and visually pleasing appearance.
	4-6	Form is complete but not refined
	1-3	The morphology is severely irregular.
Overall Acceptability	7-9	Impeccable product, strong desire for repeat consumption
	4-6	Acceptable, but not actively chosen
	1-3	Unacceptable, refuse to continue consumption
Total Score	45	

12) Data processing

Statistical analysis of the data was performed using SPSS 26.0 software. Results are expressed as x ± SD. One-way ANOVA was used to compare the mean values between multiple groups. If $p < .05$, it indicates a significant difference between groups. Origin 2021 software was used for graphing.

3. Experimental results and analyses

3.1 Effects of the addition of Dictyophora indusiata and purple rice on the nutritional composition of biscuits

The data in Table 5 showed that compared to wheat flour, purple rice provides richer minerals, protein, and dietary fibre, while *Dictyophora indusiata* mainly contributes richer ash, protein, and dietary fibre. In particular, its protein and dietary fibre contents are significantly higher than those of ordinary wheat flour. The water content of the biscuits gradually increased as the substitution levels of *Dictyophora indusiata* and purple rice flour increased, which may be attributed to the high water absorption of *Dictyophora indusiata* powder. When the substitution levels of both reached the maximum, the protein content was significantly higher than that of the control group, whereas for biscuit samples with only purple rice flour added, the increase in protein content was not significant. The starch content of *Dictyophora indusiata* was significantly lower than that of gluten flour and purple rice flour; however, due to the small amount of *Dictyophora indusiata* powder added, it did not have a significant effect on the overall starch content of the biscuits.

In Table 5, when only purple rice was added, the increase in dietary fibre content was small. When purple rice was added at 20%, the total fibre content was 2.40%, and the insoluble fibre reached 1.57 g/100 g. Purple rice is rich in cellulose, which accounts for 50-60% of its fibre content; this is mainly insoluble cellulose found in the bran layer. Purple rice also contains resistant starch, which accounts for 5-10% of its starch content, as well as soluble cellulose. Additionally, purple rice contains arabinoxylan, a hemicellulose component that is 20-30% soluble. When dissolved in water, it forms a sticky substance, which can improve the ductility of biscuit dough (Yadav, Hicks, 2015).

The dietary fibre content of the biscuits was significantly enhanced when *Dictyophora indusiata* was substituted at 5%. Although the water content of *Dictyophora indusiata* itself is significantly lower than that of purple rice and low-gluten flour, the water content of the biscuits increased significantly with the addition of purple rice and *Dictyophora indusiata.* The total fibre content of the D5P20 group reached 3.25%, with insoluble fibre accounting for 67%. *Dictyophora indusiata* is rich in chitin and lignin, which significantly increased the insoluble dietary fibre content of the biscuits, while also increasing the soluble fibre content. It is also abundant in β-glucan, a major component of its cell wall, which provides abundant soluble fibre to the biscuits (Jayachandran, Xiao, and Xu. (2017). When the substitution level of purple rice was 20% and that of *Dictyophora indusiata* was 5%, the β-glucan in *Dictyophora indusiata* and arabinoxylan in purple rice synergistically formed a fibre network structure, elevating the

total fibre content to 3.25 g/100 g. Thus, the combined effect of *Dictyophora indusiata* and purple rice endowed the biscuits with rich dietary fibre.

It was shown that the addition of *Dictyophora indusiata* resulted in a positive correlation between the increase in moisture content and fibre content of the biscuits. The network structure formed by the chitin and β-glucan of *Dictyophora indusiata* retained moisture during baking, while its own fibre structure remained relatively intact, suggesting that the cellulose in *Dictyophora indusiata* is heat-resistant.

Table 5 Nutrient composition table of purple rice, *dictyophora indusiata* powder and cookies with different amounts of purple rice and *Dictyophora indusiata*

Group	Moisture	Ash	Crude starch	Crude fat	Crude Protein	Total Fibre	Insoluble Fibre	Soluble fibre
Low gluten flour	12.3±0.35[c]	1.07±0.05[a]	71.4±0.31[c]	2.32±0.04[c]	7.31±0.34[a]	2.89±0.04[a]	1.95±0.04[a]	0.94±0.01[a]
Purple rice	10.9±0.22[b]	1.45±0.03[b]	71.4±0.16[b]	1.98±0.05[b]	8.93±0.29[b]	4.08±0.07[b]	2.79±0.05[b]	1.29±0.05[b]
Dictyophora indusiata	5.94±0.27[a]	5.06±0.05[c]	26.8±0.29[a]	1.63±0.06[a]	20.7±0.34[c]	38.1±0.05[c]	24.3±0.06[c]	13.8±0.04[c]
CON	7.44±0.23[cd]	1.01±0.04[a]	40.5±0.23[bc]	34.2±0.05[a]	6.52±0.19[ab]	1.91±0.06[a]	1.32±0.02[a]	0.59±0.04[a]
P5	7.41±0.18[cd]	1.21±0.04[b]	40.6±0.26[c]	34.2±0.06[a]	6.22±0.36[a]	1.92±0.08[a]	1.34±0.04[a]	0.58±0.04[a]
P10	6.83±0.36[bc]	1.28±0.03[bc]	40.4±0.30[bc]	34.2±0.04[a]	6.58±0.33[ab]	1.96±0.08[a]	1.33±0.05[a]	0.63±0.04[a]
P15	6.46±0.07[ab]	1.31±0.05[bc]	40.5±0.12[bc]	34.2±0.04[a]	6.63±0.27[ab]	2.01±0.08[a]	1.36±0.06[a]	0.64±0.03[a]
P20	6.12±0.27[ab]	1.38±0.04[c]	40.1±0.25[abc]	34.2±0.04[a]	6.76±0.34[ab]	2.40±0.01[b]	1.57±0.04[b]	0.82±0.06[b]
D5P5	7.89±0.24[d]	1.51±0.02[d]	40.1±0.13[abc]	34.2±0.05[a]	7.26±0.09[b]	3.03±0.09[c]	2.04±0.05[c]	0.99±0.05[c]
D5P10	9.17±0.18[e]	1.54±0.05[d]	39.7±0.34[ab]	34.2±0.02[a]	6.73±0.36[ab]	3.11±0.06[c]	2.05±0.05[c]	1.06±0.02[c]
D5P15	9.17±0.20[e]	1.56±0.05[d]	39.9±0.05[abc]	34.1±0.06[a]	7.14±0.25[ab]	3.18±0.06[c]	2.11±0.03[cd]	1.07±0.03[c]
D5P20	9.54±0.18[e]	1.65±0.05[d]	39. 6±0.29[a]	34.1±0.05[a]	7.30±0.27[b]	3.25±0.03[c]	2.18±0.01[d]	1.07±0.03[c]

Note: Different superscript letters for data in the same column represent significant differences in data between groups (P<.05).
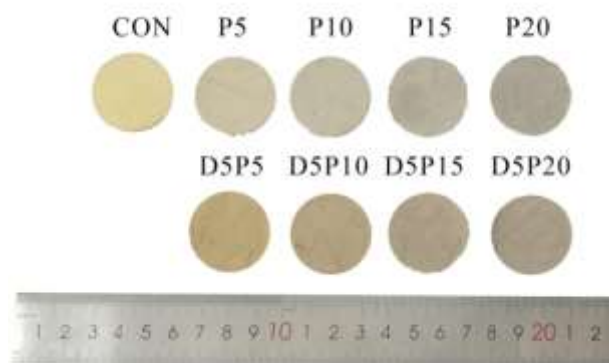
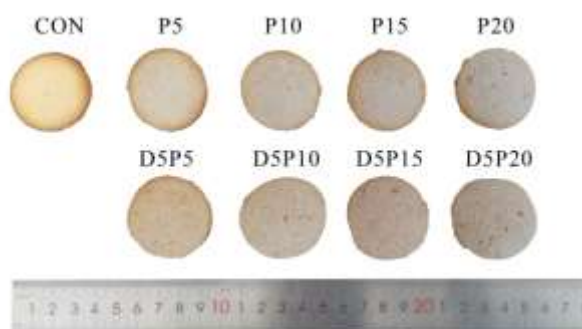### 3.2 Effects of the addition of Dictyophora indusiata and purple rice on the colour difference of biscuits

In Table 6, the L-value of the surface of the control group biscuits was 43.9 with medium brightness, a-value 57.7 with reddish colour and b-value 5.63 with yellowish colour. And with the increase of substitution of purple rice and *Dictyophora indusiata*, the L-value decreased significantly, indicating that the colour of the biscuits became darker. This may be due to the purple colour of purple rice and brown colour of *Dictyophora indusiata*. Meanwhile, the a-value also increased. For example, the a-value of D5P20 was as high as 68, indicating a redder surface, which might be related to the Maillard reaction of certain components in *Dictyophora indusiata* during baking.

The colour L-value of the control biscuit dough was 28.7, whereas with the addition of purple rice, the L-value decreased, and when the substitution amount was 20%, the L-value was significantly reduced taking its colour significantly darker. The addition of purple rice had a great impact on the colour of the dough, while the L-value of the dough increased slightly with the addition of *Dictyophora indusiata*, which was due to the lighter colour of *Dictyophora indusiata*, which neutralised the purple colour of the purple rice.

The biscuits were ground into powder through a grinder and sieved through a 60 mesh sieve, and the colour of the powder in the control group, the L-value was 32.4, whereas D5P20 decreased to 18.4 and became darker in colour. Taken together, the addition of purple rice and *Dictyophora indusiata* significantly affected the colour index of the biscuits, whether it was the dough or the finished biscuits, or the biscuit powder, especially the dark colour of the purple rice dominated the overall hue change.

When only purple rice was added, the dough had the lowest value of L. The black finished surface had an L value equal to 29.1 with a purplish colour, the powder had an L value equal to 14.2, also with a darker colour, whereas the values were both low, showing a greenish colour, and the b values were extremely low, with almost no yellow colour. This is due to the dark purple colour of purple rice bran, such as the anthocyanins and cellulose in purple rice absorb light leading to the colour of the dough is purple, and in the baking process, anthocyanins partially degraded Melad reaction produces black-like essence, and biscuits contain rich butter, caramelization brings reddish-yellow tones, after the biscuit crushed, the colour performance is more uniform, into a light purple.

Combined with Figures 1 and 2, after adding *Dictyophora indusiata*, the light brown colour of *Dictyophora indusiata* neutralised some of the purple colour of the purple rice, but the cellulose still resulted in a very low light-absorbing value and a low brightness of the dough. After baking, the chitin and sugars in the *Dictyophora indusiata* undergo a violent Maillard reaction at high temperatures, producing a large amount of red pigment. When the biscuits are broken into powder, the light absorption of the *Dictyophora indusiata* fibres reduces the brightness, and the products of the Maillard reaction enhance the yellow colour[8]. Figure 2 shows that the effect of purple rice on the colour of the biscuits is extremely significant and dominant, and the several evolutionary systems and sugars in the

Dictyophora indusiata undergo a Melad reaction at high temperatures, which increases the yellow colour and ameliorates the effect of purple colour of the biscuits.

Table 6 Colour of cookies with different amounts of purple rice and *Dictyophora indusiata*

Biscuits surface	L	a	b	ΔL a b
CON	43.9±0.30[d]	57.7±0.35[f]	5.63±0.13[a]	39.8±0.01[a]
P5	22.0±0.46[ab]	54.8±0.39[e]	7.78±0.18[c]	41.7±0.26[b]
P10	19.1±1.15[ab]	51.6±1.28[d]	7.41±0.18[bc]	43.4±0.75[c]
P15	15.0±0.31[a]	44.3±0.36[ab]	6.85±0.25[b]	48.9±0.42[e]
P20	29.1±0.26[c]	54.7±0.56[e]	10.2±0.34[e]	45.8±0.41[d]
D5P5	25.4±0.17[ab]	48.0±0.34[c]	9.31±0.19[d]	49.5±0.40[e]
D5P10	22.0±0.34[ab]	45.6±0.85[b]	9.09±0.05[d]	50.2±0.78[e]
D5P15	18.7±0.37[ab]	42.4±0.18[a]	8.12±0.32[c]	51.9±0.14[f]
D5P20	38.9±1.34[cd]	68.0±0.92[g]	7.45±0.35[bc]	43.0±0.68[bc]
CON	28.7±0.25[h]	69.2±0.17[e]	3.67±0.02[f]	33.6±0.30[a]
P5	16.0±0.03[f]	51.3±0.13[d]	1.42±0.03[d]	41.9±0.13[b]
P10	12.2±0.05[d]	44. 9±0.21[c]	0.35±0.01[b]	47.1±0.21
P15	9.91±0.01[b]	42.5±0.39[b]	1.61±0.04[d]	49.2±0.39[d]
P20	8.01±0.03[a]	42.8±0.47[b]	0.18±0.07[ab]	48.7±0.47[ef]
D5P5	20.2±0.08[g]	51.3±0.31[d]	2.71±0.07[e]	43.3±0.31[c]
D5P10	16.0±0.01[f]	43.0±0.09[b]	0.07±0.02[a]	49.8±0.09[f]
D5P15	13.0±0.02[e]	43.5±0.63[b]	0.67±0.09[c]	48.7±0.61[e]
D5P20	10.8±0.01[c]	35.6±0.07[a]	0.40±0.05[b]	56.1±0.07[g]
Biscuit powder	**L**	**a**	**b**	**ΔE**
CON	32.4±0.29[f]	59.4±0.83[f]	6.84±0.12[c]	43.5±0.44[a]
P5	22.9±0.28[d]	54.8±0.75[e]	2.31±0.23[abc]	41.3±0.64[b]
P10	18.9±0.18[b]	50.7±0.45[d]	1.79±0.17[ab]	43.4±0.39[b]
P15	14.5±0.03[a]	48.9±0.21[c]	1.56±0.16[a]	43.8±0.20[b]
P20	14.2±0.21[a]	44.9±0.54[b]	1.42±0.18[d]	47.6±0.48[d]
D5P5	25.2±0.11[e]	51.5±0.94[d]	3.31±0.11[d]	45.4±0.77[c]
D5P10	22.5±0.35[d]	48.2±0.32[c]	2.97±0.07[bc]	47.2±0.17[d]
D5P15	19.7±0.16[c]	43.9±0.66[ab]	2.02±0.26[abc]	50.0±0.57[e]
D5P20	18.4±0.07[bc]	42.4±0.23[a]	1.96±0.18[e]	51.1±0.21[e]

Note: Different superscript letters for data in the same column represent significant differences in data between groups (P<.05).

Figure 1 cookies pastry picture

Figure 2 Finished cookies picture

3.3 Effects of Dictyophora indusiata and purple rice on physicochemical properties and baking loss of biscuits

According to the data in Table 7, the hardness of the dough increased significantly with the addition of purple rice, and when *Dictyophora indusiata* was added, the hardness of the dough increased again in comparison with the

purple rice group, and the hardness of the dough in the purple rice group was higher than that of the *Dictyophora indusiata* group when the same amount of purple rice was added, and 5% *Dictyophora indusiata* was added to the same amount of purple rice, which indicated that the purple rice was the main factor influencing the hardness of the dough, and the hardness of cookies produced by the dough was higher than that of the *Dictyophora indusiata* group after the addition of 20% *Dictyophora indusiata* and 20% *Dictyophora indusiata* to the same amount of purple rice. Purple rice produced the highest hardness of biscuits, which made the biscuits crispy and hard. It may be because the bran particles of the purple rice disrupt the internal structure of the biscuits, causing them to become brittle (Kowalski, Mikulec, and Mickowska, 2022).

In Table 7, after the addition of *Dictyophora indusiata*, the hardness of the biscuits started to decrease compared to the purple rice group, the rich soluble dietary fibres in *Dictyophora indusiata*, such as β-glucan, formed a gel during baking, which retained the moisture and volatiles, and insoluble dietary fibres, such as lignin, strengthened the internal gluten network of the biscuits, and the increase in the moisture content of the biscuits resulted in the biscuits being hard, but not brittle (Shams, Singh, Dash, 2023).

The purple rice group showed a decreasing trend in baking loss from 23.5% to 21.9% with increasing purple rice substitution. Baking loss is usually due to water evaporation and loss of other volatiles, while high fibre content may affect water holding capacity. Purple rice contains high levels of bran, which is rich in insoluble fibres such as cellulose, and these fibres may absorb water during baking and reduce water loss, thus reducing baking losses. Bran particles may also adsorb fats and oils, reducing losses due to lipid oxidation.

After the addition of *Dictyophora indusiata*, the baking loss showed a decreasing trend with the increase of purple rice substitution and low baking loss comparing to the sample group with the same percentage of purple rice, which suggests that *Dictyophora indusiata* is rich in a large amount of soluble cellulose, such as β-glucan, which is highly absorbent and may reduce water loss. High moisture content usually leads to increased baking loss, but because the soluble fibres in Dicentrarch, such as β-glucan, are extremely absorbent, they may have formed a gel that retained the water and counteracted the negative effect of high moisture content. Therefore, the strong water-holding property of *Dictyophora indusiata* may be the main factor in reducing the baking loss, while the purple rice further reduced the baking loss of the biscuits by adsorbing moisture and oil and inhibiting lipid oxidation, among other effects.

Changes in thickness: decreased with increasing proportion of purple rice, while changes in diameter, gradually increased with increasing proportion of purple rice. This may be due to the fact that cellulose and lignin in purple rice bran increased the hardness of the biscuits and limited the vertical expansion, and bran particles interfered with the gluten structure, leading to an increase in the ductility of the dough, which in turn brought about more lateral changes, resulting in an increase in diameter. With the addition of *Dictyophora indusiata*, the variation in biscuit thickness was gradually minimised, and the insoluble fibres in *Dictyophora indusiata*, such as chitin, further hardened the dough and almost completely inhibited the vertical expansion of biscuits; the variation in biscuit diameter was higher, reaching 45.0% in the D5P20 group, which could be attributed to the fact that fibres from *Dictyophora indusiata* further weakened the formation of the gluten structure, leading to a more pronounced lateral stretching.

The study showed that the addition of purple rice and *Dictyophora indusiata* significantly improved the textural properties of the biscuit dough and biscuits, and reduced the loss of biscuits during baking.

Table 7   The hardness and baking loss of cookies dough and biscuits with different amounts of purple rice and *Dictyophora indusiata*

Sample	Dough hardness (N)	Baking loss (%)	Biscuit hardness (N)	Thickness change (%)	Diameter variation (%)
CON	371±15.8[a]	25.3±0.84[b]	2193±13.5[a]	33.8±3.76[e]	29.2±0.59[b]
P5	429±16.7[a]	25.6±0.11[b]	2994±19.3[c]	30.1±2.51[de]	20.3±0.38[a]
P10	463±18.2[a]	25.5±0.73[b]	3297±28.1[e]	25.3±1.91[cd]	29.1±0.29[b]
P15	482±16.3[ab]	23.1±0.34[ab]	3424±40.2[f]	23.0±1.74[c]	30.9±0.29[c]
P20	485±11.7[ab]	20.9±0.62[a]	3886±13.8[h]	20.2±2.99[bc]	32.4±0.40[d]
D5P5	434±16.7[a]	23.51±0.77[ab]	2891±55.9[b]	16.2±0.93[ab]	32.8±0.59[d]
D5P10	462±15.1[a]	22.9±0.51[ab]	3057±38.4[d]	14.8±0.91[ab]	45.8±0.29[f]
D5P15	483±20.9[ab]	22.5±0.49[ab]	3424±33.2[f]	11.7±0.88[a]	42.1±0.73[e]
D5P20	579±22.1[b]	21.9± 0.73[ab]	3544±66.3[g]	10.3±0.77[a]	45.0±0.69[f]

Note: Different superscript letters for data in the same column represent significant differences in data between groups (P<.05).

3.4   *Effect of Dictyophora indusiata and purple rice addition on antioxidant properties of biscuits*

Based on the data in Table 8, it was concluded that the ABTS free radical scavenging rate of the control group was 26.4%. The free radical scavenging rate gradually increased with the increase of the substitution of purple rice and *Dictyophora indusiata*. 72.2% was reached in the D5P20 group, and the DPPH free radical scavenging rate also gradually increased from 10.1% in the control group to 75.8% in the D5P20 group, and the contents of total phenols and total flavonoids also showed an increasing trend, which indicated that the addition of purple rice and *Dictyophora indusiata* significantly improved the antioxidant properties of the biscuits, and in particular, the *Dictyophora indusiata* which had the most significant effect.

In conjunction with Table 5, the fibres in purple rice and *Dictyophora indusiata* were partially degraded during the digestion process, releasing more classifications and flavonoids. After digestion, D5P20, had the highest values of all antioxidants indicating. There may have been a synergistic effect between the purple rice and *Dictyophora*

indusiata during digestion, and the fibre used in *Dictyophora indusiata* may have helped to release more antioxidants from the purple rice.

In Table 8, the free radical scavenging power was 2.7 and 7.5 times higher than that of the control at 5% addition of *Dictyophora indusiata* and 20% addition of purple rice, respectively, and the polysaccharide compounds (β-glucan) and phenolics in *Dictyophora indusiata* played a dominant role in antioxidant (Lai, Fang, and Guo, 2023). When only purple rice was added to the biscuits, the total phenolic content of the P20 group was elevated by 59% and the flavonoid content by 18% compared to the control group, suggesting that the anthocyanins in the purple rice may have been affected by the fibre and released in smaller amounts prior to *in vitro* digestion.

When the biscuits were digested *in vitro*, the free radical scavenging rate was significantly increased in all groups, and the total phenolic content was doubled in the D5P20 group, suggesting that the fibres of *Dictyophora indusiata* and purple rice were partially degraded in digestion and polyphenolic compounds were released. When *Dictyophora indusiata* was added, the increase in DPPH radical scavenging rate was relatively slower compared to that of the purple rice group, and the lignans in *Dictyophora indusiata* may delay the release of antioxidant components and play a certain role in slowing down the release. The anthocyanins in purple rice may be wrapped in fibre and partially inactivated during high-temperature baking, resulting in a low DPPH radical scavenging rate prior to digestion. After *in vitro* digestion, the fibre structure is destroyed, more free anthocyanins are released, and the phenols in the bound state are converted to free phenols, resulting in a significant enhancement of DPPH radical scavenging rate.

The polysaccharides in *Dictyophora indusiata*, such as β-glucan, may form a viscous gel during the gastric digestion stage, which provides a slow release of antioxidant components. In the intestinal digestion stage, by the action of digestive enzymes, the bound phenols were slowly released. The polyphenols in mushrooms, such as ferulic acid, were stable in digestion and retained for a long time during digestion, and after *in vitro* digestion, the free radical scavenging rate of ABTS in the D5P20 group increased from 72.2% to 90.4%. The addition of *Dictyophora indusiata* and purple rice significantly improved the antioxidant capacity of the biscuits.

Table 8 Antioxidant properties of cookies with different amounts of purple rice and *Dictyophora indusiata*

Before *in vitro* digestion	ABTS (%)	DPPH (%)	Total Phenol (mg GAE/100 g DM)	Total flavonoids (µg CE/100 g DM)
CON	26.4±0.02^a	10.1±0.06^a	0.27±0.01^a	28.7±0.02^a
P5	57.9±0.05^b	18.3±0.06^a	0.30±0.01^a	30.2±0.06^{ab}
P10	64.9±0.02^{cd}	28.0±0.05^{ab}	0.34±0.04^{ab}	31.4±0.02^{bc}
P15	69.9±0.05^{de}	32.5±0.03^{abc}	0.37±0.02^{abc}	32.7±0.08^{bc}
P20	62.0±0.02^{bc}	40.0±0.02^{abc}	0.43±0.03^{bcd}	33.8±0.09^c
D5P5	64.4±0.02^{bcd}	49.8±0.04^{bcd}	0.36±0.03^{abc}	36.3±0.08^d
D5P10	78.4±0.09^f	57.1±0.02^{bcd}	0.41±0.04^{bc}	37.4±0.08^d
D5P15	77.2±0.01^f	63.1±0.06^{cd}	0.46±0.04^{cd}	38.9±0.01^d
D5P20	72.2±0.01^{ef}	75.8±0.04^d	0.53±0.06^d	40.3±0.04^d
CON	43.2±0.01^a	33.2±0.08^a	0.56±0.03^a	59.3±0.01^a
P5	69.8±0.09^b	58.1±0.06^a	0.58±0.01^a	60.3±0.05^a
P10	73.1±0.02^{cd}	60.7±0.05^{ab}	0.67±0.05^b	60.3±0.04^a
P15	78.2±0.03^{de}	62.9±0.03^{abc}	0.69±0.02^b	60.8±0.07^{ab}
P20	83.3±0.01^{bc}	64.5±4.02^{abc}	0.77±0.01^c	61.3±0.01^{ab}
D5P5	76.4±0.04 ^{bcd}	82.4±0.07^{bcd}	0.81±0.04^d	61.8±0.05^{ab}
D5P10	82.8±0.09^f	87.6±0.04^{bcd}	0.9±0.04^e	62.8±0.03^{ab}
D5P15	88.9±0.01^f	87.8±0.06^{cd}	0.96±0.07^f	62.8±0.05^{ab}
D5P20	90.4±0.02^{ef}	88.2±0.04^d	1.11±0.02^g	65.4±0.03^b

Note: Different superscript letters in the same column of data represent significant differences in data between groups (P<.05).

3.5 *Effect of Dictyophora indusiata and purple rice addition on in vitro digestive characteristics of biscuits*

In Figure 3, the starch hydrolysis rate was the highest at all time points in the control group, indicating the fastest starch digestion in the control group. While the hydrolysis rate of starch gradually decreased with the increase of the substitution of purple rice and *Dictyophora indusiata*, especially in the D5P20 group at 180 min, the starch hydrolysis rate was the lowest and the slowest digested. The control group had the highest fast-digested starch content. With the increase of the substitution amount of the two raw materials, the content gradually decreased, and the fast-digested starch content decreased to the lowest when the addition amount reached the highest. The resistant starch, on the contrary, increased with the increase in the substitution of both ingredients, and the addition of purple rice and *Dictyophora indusiata* increased the content of resistant starch.

Regarding the glycaemic index (GI), usually high RDS leads to high GI, whereas high RS and SDS decrease GI.Therefore, the low RDS and high RS of the D5P20 group imply that it has a lower GI, and the fibres in purple rice and *Dictyophora indusiata* may encapsulate starch granules, slowing down enzyme action and thus reducing the digestion rate. Meanwhile, the presence of fibre may promote the release of antioxidants, creating a synergistic effect.

Combined with Tables 8 and 9, after digestion, the starch hydrolysis power of the biscuits in the control group was 99.3%, and the phenolic content of the digested biscuits was 1.11 mg GAE/100 g DM, while the starch hydrolysis of the control group was rapid and phenolics were released rapidly, but the total amount of the released substances was low, and the starch hydrolysis rate of the D5P20 group was 86.5%, with a decrease of 25% in the RDS, an increase

of 31% in the RS, and a GI Decreased, purple rice and *Dictyophora indusiata* significantly reduced the GI of the biscuits. The addition of purple rice and *Dictyophora indusiata* significantly reduced the rate of starch hydrolysis, elevated the content of resistant starch, and significantly reduced the glycaemic index of the biscuits.
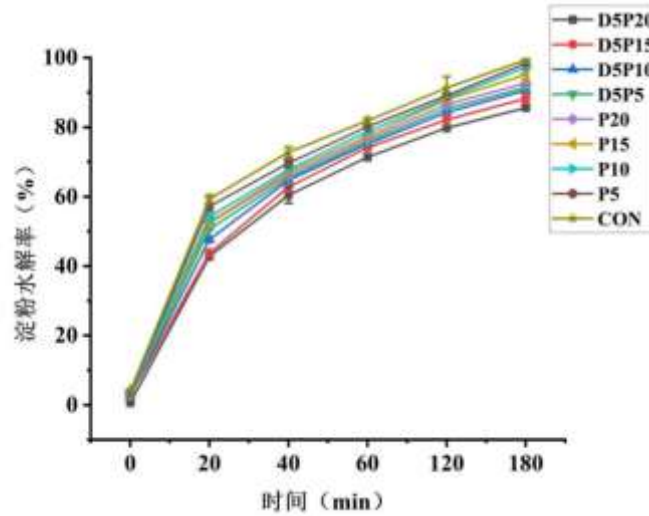

Figure 3 *In vitro* digestion characteristics of cookies with different addition amounts of purple rice and *Dictyophora indusiate*

Table 9 Starch content (g/100 g) of cookies with different amounts of purple rice and *Dictyophora indusiata*

Sample	Fast digestible starch	Slowly digestible starch	Resistant starch
CON	20.1±0.30[e]	11.7±0.20[a]	8.7±0.07[a]
P5	19.5±0.27[e]	11.7±0.25[a]	9.4±0.19[ab]
P10	18.4±0.11[d]	12.4±0.26[ab]	9.5±0.07[abc]
P15	17.9±0.27 [cd]	12.9±0.19[bc]	9.7±0.26[bcd]
P20	17.7±0.23[cd]	12.3±0.07[ab]	10.0±0.1[bcd]
D5P5	17.1±0.26[cd]	12.5±0.18[ab]	10.4±0.29[cd]
D5P10	16.0±0.13[b]	13.1±0.15[bc]	10.6±0.15[de]
D5P15	14.8±0.09[a]	13.8±0.18[c]	11.4±0.24[e]
D5P20	15.0±0.21[a]	13.2±0.10[bc]	11.4±0.18[e]

Note: Different superscript letters for data in the same column represent significant differences in data between groups (P<.05).

3.6 *Effects of dictyophora indusiata and purple rice addition on the flavour substances of biscuits*

The gradient substitution of purple rice and *Dictyophora indusiata* significantly altered the flavour profile of biscuits, and the changes in their content revealed a shift from traditional butter aroma to grain-wood composite aroma. Combined with Figure 5 and Table 10, the significant reduction of aldehydes, such as hexanal and nonanal, in the purple rice substitution group (P5-P20), and combined with Table 6, indicated that the antioxidant components (e.g., anthocyanins, flavonoids) in purple rice effectively inhibited lipid oxidation and alleviated the oxidative "hafting flavour"of the traditional biscuits due to the high fat content (Wang, Yang, and Liu, 2022); at the same time, the increase of terpenes d-limonene and elemene, which are unique to purple rice, relied on the increase of the addition of purple rice to give citrus aroma and woody undertones, respectively, and synergised with the caramel aroma of methyl heptenone and the creamy aroma of γ-nonanolactone to form a complex cereal aroma. The introduction of *Dictyophora indusiata* (D5P5-D5P20 group) further released pine aroma characteristic components such as β-cedrene and α-cedrene[13] , which formed a hierarchical overlay with the purple rice flavour, but the abnormal enrichment of 1-isocyanatobutane may have originated from the thermal degradation of nitrogenous polysaccharides of *Dictyophora indusiata*, and its pungent odour led to the reduction of the flavour scores of the D5P20 group in the organoleptic evaluation in Figure 7. Changes in the dynamic balance of key flavour presenting substances were particularly notable: the linear increase in vanillin and 2-acetylpyridine reinforced the baked char aroma, which corresponded to the rise in the surface a-value of the biscuits to 68.0 as a result of the enhanced Maillard reaction, but the content of ethyl caprate, the main aroma component of the esters, was significantly reduced, and the persistent loss of ethyl caprate weakened the fruity base of the traditional biscuits. This flavour reconstruction was manifested at the sensory level in the form of increased aroma complexity and enhanced feature recognition, such as a richer variety of volatiles in the D5P20 group compared with the control group, but the sensory clash triggered by the piney flavour of terpenes (e.g., τ-celestene) and the pungent odour of 1-isocyanatobutane, which may be the core causative factor leading to the overall acceptance of the D5P20 group being significantly lower than that of the ZiMi single-factor group.

By integrating the gas chromatography and electronic nose data, the remodelling of biscuit flavour characteristics by the gradient substitution of purple rice and *Dictyophora indusiata* showed a dual mechanism of changes in the content of major flavour substances and synergistic effects of special trace substances. Combined with Figures 4.4 and 4.6, at the level of the main flavour substances, ethyl decanoate, which dominates the fruity aroma of traditional biscuits, decreased linearly with the increase of the substitution ratio, and the loss of which was linked to

the weakening of the response of the e-nose aromatic hydrocarbon sensor S18, which weakened the fruity-sweet odour tone of the biscuits; whereas the increase of the terpenes introduced by zi mizanami, namely, d-limonene and elemi, echoed the responses of the gas and alkane sensors S7 and S11, respectively. response, which shifted the flavour tonality towards citrus woody notes, building a composite cereal aroma profile together with the caramel aroma of methylheptenone and the creamy aroma of γ-nonolactone. Combined with Table 10 and Figure 6, the dynamic changes of trace specific substances reveal the risks behind the increase of flavour complexity: the abnormal enrichment of 1-isocyanatobutane in the *Dictyophora indusiata* group is highly coincident with the response surge of the electronic nose amine sensor S15, and its irritating odour contrasts with the weak fluctuation of the sulphur sensor S4, suggesting that the off-flavour originates from nitrogen-containing pyrolysis products rather than sulphur compounds; whereas, the aldehydes (hexanal, hexanal, and γ-nonolactone) in the purple rice group are more important than the other aldehydes. Although the oxidative inhibitory effect of aldehydes (hexanal and nonanal contents were greatly reduced) was supported by the rise in response of the e-nose alkane sensor S11, the turpentine odour of trace terpenes such as τ-celestene and the fluctuation in response of the e-nose alicyclic hydrocarbon sensor S18 implied that the wood tones might have breached the sensory threshold. The effects of this change in flavour substance composition are manifested at the sensory level: the D5P10 group achieves an optimal blend of fruity and woody tones by balancing the ratio of ethyl decanoate to α-cedrene, which corresponds to the e-nose S18 response value of 1.51, whereas the D5P20 group's bad effects due to 1-isocyanatobutane are echoed by the e-nose S15 response value of 1.34, with 1-isocyanatobutane resulting in a decrease in flavour purity, confirming the bidirectional modulation of the overall flavour profile by specific trace substances.
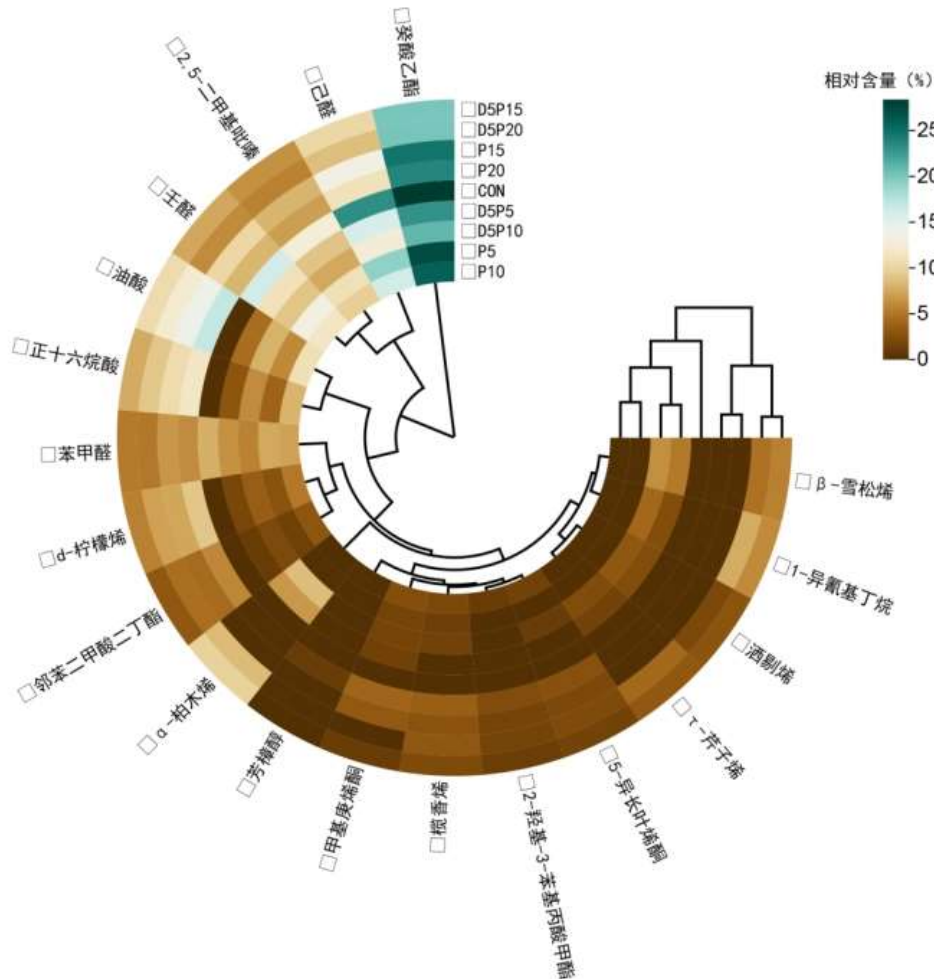
Figure 4 Heat map of relative content of total volatile compounds
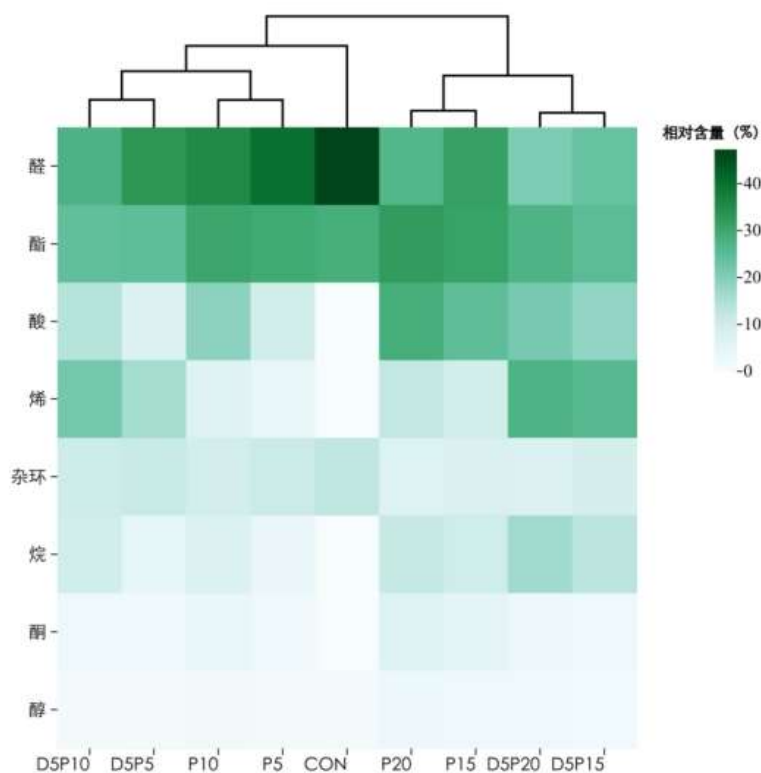
Figure 5 Heatmap of relative content of different kinds of volatile compounds
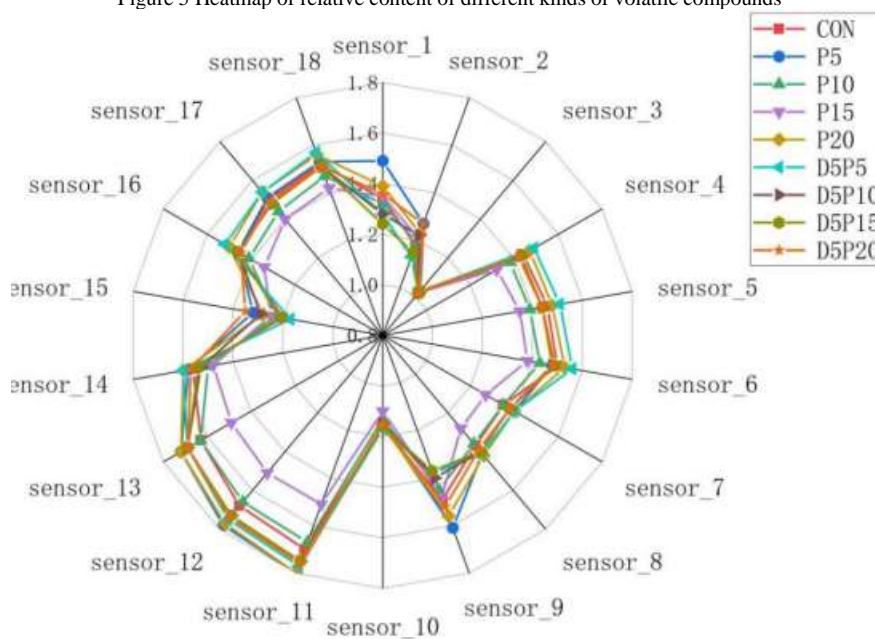
Figure 6 cookies electronic nose evaluation

Table 10 Flavour substances of cookies with different addition amount of purple rice and *Dictyophora indusiata*

Compound	Molecular formula	CSA number	CON	P5	P10	P15	P20	D5P5	D5P10	D5P15	D5P20
Methyl nonyl ketone	$C_{10}H_{20}O$	110-93-0	-	0.09	0.17	0.23	0.28	0.06	0.12	0.17	0.22
Methylheptenone	$C_8H_{14}O$	110-93-0	-	1.68	2.45	3.21	3.98	1.46	1.71	1.11	0.68
5-Isophyllenone	$C_{15}H_{24}O$	502-69-2	-	0.93	1.51	2.08	2.65	0.65	1.09	1.58	2.21
1-Isocyanobutane	C_5H_9N	111-35-5	-	-	-	-	-	2.43	4.19	6.01	7.62
2,5-Dimethylpyrazine	$C_6H_8N_2$	123-32-0	12.6	11.1	9.62	8.11	7.01	8.91	7.46	6.33	5.58
Vanillin	$C_8H_8O_3$	121-33-5	0.19	0.22	0.26	0.31	0.34	0.18	0.21	0.24	0.29
2-Acetylpyridine	C_7H_7NO	112-18-9	0.02	0.04	0.06	0.08	0.09	0.03	0.05	0.06	0.08
Sparteine	$C_{10}H_{16}$	5989-27-5	-	-	-	-	-	2.43	3.11	2.85	2.03

Compound	Molecular formula	CSA number	CON	P5	P10	P15	P20	D5P5	D5P10	D5P15	D5P20
d-Limonene	$C_{10}H_{16}$	5989-27-5	-	2.81	5.08	7.36	9.13	1.94	3.57	5.54	7.11
β-Cedrene	$C_{15}H_{24}$	502-69-2	-	-	-	-	-	5.18	6.21	5.54	4.74
α-Cedrene	$C_{15}H_{24}$	2830-06-7	-	-	-	-	-	6.64	8.54	9.82	8.46
Elemene	$C_{15}H_{24}$	515-13-9	-	1.31	2.07	2.83	3.61	0.97	1.55	2.21	3.05
τ-Celestene	$C_{15}H_{24}$	515-13-9	-	-	-	-	-	1.62	2.33	3.16	4.23
n-Hexadecanoic acid	$C_{16}H_{32}O_2$	47-10-3	-	3.92	8.09	10.5	11.7	2.92	6.06	7.59	9.14
Oleic acid	$C_{18}H_{34}O_2$	112-80-1	-	5.98	10.9	14.2	16.8	4.53	7.92	10.6	12.4
Caproic acid	$C_6H_{12}O_2$	142-62-1	0.15	0.19	0.23	0.26	0.31	0.15	0.17	0.21	0.25
Ethyl decanoate	$C_{12}H_{24}O_2$	110-38-3	28.4	27.2	25.9	24.7	23.7	23.1	20.9	20.1	20.1
Dibutyl phthalate	$C_{16}H_{22}O_4$	84-74-2	-	1.49	3.01	4.34	5.88	1.13	2.17	3.16	4.57
Methyl caprylate	$C_9H_{18}O_2$	111-11-5	-	-	-	-	-	0.13	0.23	0.36	0.51
Ethyl butyrate	$C_6H_{12}O_2$	105-54-4	0.28	0.34	0.43	0.45	0.51	0.26	0.31	0.35	0.42
γ-Nonanolactone	$C_9H_{16}O_2$	104-61-0	0.04	0.07	0.11	0.15	0.19	0.05	0.08	0.11	0.15
Methyl 2-hydroxy-3-phenylpropionate	$C_{10}H_{12}O_3$	121-33-5	-	0.56	1.13	1.72	2.28	0.32	0.78	1.27	1.69
Hexanal	$C_6H_{12}O$	66-25-1	23.2	19.2	16.1	13.5	11.1	15.8	12.5	10.2	8.63
Nonanal	$C_9H_{18}O$	124-19-6	16.1	13.2	11.6	10.2	8.15	11.1	9.01	7.43	6.09
Benzaldehyde	C_7H_6O	100-52-7	7.81	7.47	7.15	6.66	6.07	6.32	5.59	5.22	5.08

Table 10 Flavour substances of cookies with different addition amount of purple rice and *Dictyophora indusiata*

Compound	Molecular formula	CSA number	CON	P5	P10	P15	P20	D5P5	D5P10	D5P15	D5P20
2-Heptenal	$C_7H_{12}O$	111-71-7	-	0.22	0.47	0.72	0.93	0.16	0.34	0.55	0.73
trans-2,4-decadienal	$C_{10}H_{16}O$	25152-84-5	0.06	0.13	0.21	0.26	0.32	0.12	0.14	0.19	0.25
Valeraldehyde	$C_5H_{10}O$	110-62-3	-	0.09	0.13	0.17	0.21	0.25	0.13	0.12	0.16	0.23
Linalool	$C_{10}H_{18}O$	78-70-6	0.09	0.34	0.62	0.85	1.08	0.24	0.43	0.65	0.88
1-Octen-3-ol	$C_8H_{16}O$	3391-86-4	0.37	0.47	0.56	0.66	0.76	0.36	0.42	0.51	0.63
Phenylethanol	$C_8H_{10}O$	60-12-8	0.56	0.65	0.75	0.85	0.95	0.52	0.59	0.68	0.81
Erythritol	$C_4H_{10}O_4$	149-32-6	-	0.04	0.08	0.11	0.15	0.02	0.05	0.08	0.12
Cyclooctanediol	$C_8H_{16}O_2$	4430-24-6	-	0.06	0.11	0.17	0.23	0.03	0.08	0.13	0.17

3.7 Sensory evaluation Analysis of results

The sensory evaluation analysis showed that the substitution of wheat flour by purple rice and *Dictyophora indusiata* had a complex effect on the sensory characteristics of the biscuits, mainly in terms of contradictions in colour, taste, texture and consumer acceptability. In Figure 7, as the amount of purple rice substitution increased (especially up to 20%), the data in Table 6 showed that the biscuits became significantly darker in colour and the surface brightness (L-value) decreased from 43.9 to 29.1 in the control group, which originated from the anthocyanins in the bran of purple rice and the light-absorbing effect of cellulose in high-temperature baking. Although the light brown colour of the *Dictyophora indusiata* partially neutralised the purple colour of the purple rice (e.g. the surface L value of the D5P20 group rebounded to 38.9), its own Maillard reaction during baking led to an abnormally high reddish hue (a-value) on the surface of the biscuits (up to 68.0 in the D5P20 group), and instead strengthened the visual characteristics of the non-traditional biscuits, which may trigger consumers' concerns about "burnt" or "abnormal biscuits". This may trigger consumers' thoughts of "burnt" or "abnormal colour".

In terms of taste, the data in Table 9 showed that the increased substitution of purple rice significantly increased the hardness of the biscuits (3886 N in the P20 group, 77% higher than the control group), and the bran particles disrupted the gluten structure to form a hard and crispy texture, which, although considered "uniquely crispy" by some of the reviewers, exceeded the taste expectations of a conventional biscuit. On the other hand, the addition of *Dictyophora indusiata* made the biscuits hard but not crispy through β-glucan gelatinisation (hardness of 3544 N in the D5P20 group, a decrease of 8.8% compared to the P20 group), and the texture was closer to that of a tough biscuit, which led to a contrast between the highest crispy scores in the P20 group and the lowest in the D5P20 group, highlighting the differential effect of the type of fibre on the texture.

Flavour ratings were polarised, with the purple rice group receiving moderate ratings for the cereal aroma from the bran, but the possible introduction of fibre roughness by the *Dictyophora indusiata* led to a sudden drop in flavour ratings for the D5P20 group, which was the main limiting factor for sensory acceptability. Notably, despite the D5P20 group's optimal performance in terms of nutritional functions (3.25% fibre content and 7.5-fold improvement in antioxidant properties) and health attributes (reduced GI), it had the lowest overall acceptability score, significantly lower than the control group, reflecting that consumer acceptance of high-fibre health biscuits is still constrained by traditional sensory expectations. This contradiction was further exacerbated by the swelling characteristics: the insoluble fibre of *Dictyophora indusiata* almost completely inhibited vertical swelling (only 10.3% change in D5P20 thickness), whereas the elevated lateral ductility (45% change in diameter) resulted in a flattened biscuit morphology, which differed significantly from the fluffy appearance of the traditional biscuits.

Therefore, the core contradiction in sensory evaluation lies in the conflict between the abrupt changes in colour and texture brought about by nutritional fortification and consumers' inherent perception of golden, crispy and sweet biscuits.
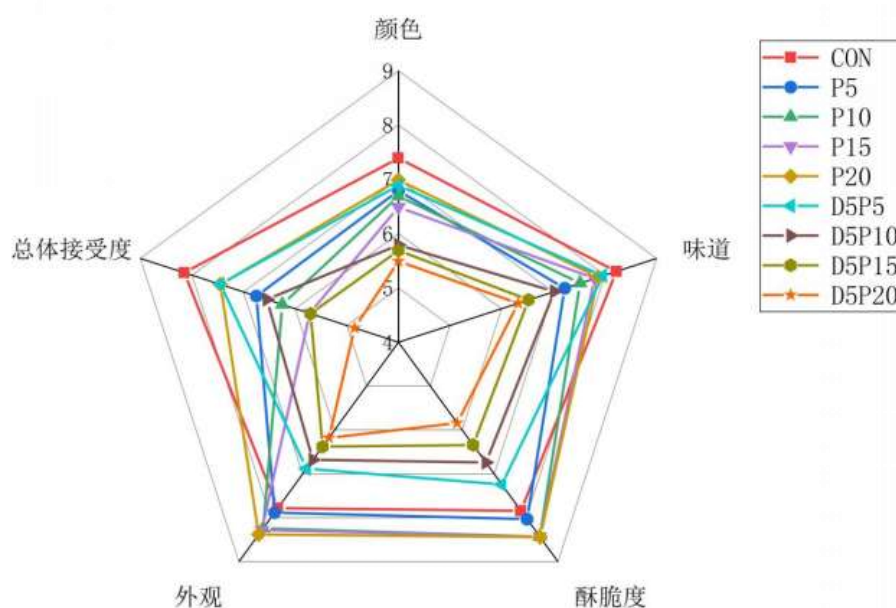
Figure 7 Sensory evaluation diagram of cookies with the same amount of purple rice and *Dictyophora indusiate*

4. Conclusions

The replacement of wheat flour by purple rice and *Dictyophora indusiata* provides a breakthrough direction for the nutritional upgrading of biscuits. The rich insoluble fibre and resistant starch in purple rice, together with the β-glucan and chitin of *Dictyophora indusiata*, formed a synergistic and synergistic dietary fibre network, which not only increased the total fibre content to more than twice that of the traditional biscuits, but also significantly enhanced the protein content and antioxidant activity, and at the same time, realised the potential of blood glucose regulation by inhibiting the rapid digestion of starch, which lays a scientific foundation for the development of functional low-GI bakery products. Although there were limitations in sensory evaluation, such as dark colour (the natural colour of purple rice anthocyanins) and high hardness, the purple rice group maintained acceptable crunchiness and cereal flavour with moderate substitution (e.g., P20), and the gel characteristics of *Dictyophora indusiata* gave the biscuits a unique and tough texture, which demonstrated the possibility of differentiating from traditional biscuits in terms of market positioning. The study confirms that by precisely controlling the substitution ratio (e.g. a medium ratio of 10% purple rice and 5% *Dictyophora indusiata*), the conflict between colour and texture can be effectively mitigated, which has a broad application prospect in the future in the fields of healthy snacks and special food. This exploration not only breaks through the nutritional defects of traditional biscuits, which are high in sugar and fat, but also provides an innovative example of the functional use of natural ingredients.

6. Acknowledgment

7. References

Herráiz-Gil,S, de Arriba M.C., Escámez M J. (2023). Multi-omic data integration in food science and analysis. Current Opinion in Food Science, 52: 101049.

Jayachandran M, Xiao J, Xu B. (2017). A critical review on health promoting benefits of edible mushrooms through gut microbiota. International journal of molecular sciences, 18(9): 1934.

Kowalski S, Mikulec A, Mickowska B. (2022). Nutritional properties and amino acid profile of buckwheat bread. Journal of Food Science and Technology, 59(8): 3020-3030.

Lai Y, Fang Q, Guo X. (2023). Effect of polysaccharides from *Dictyophora indusiata* on regulatinggut microbiota and short-chain fatty acids in mice. Journal of Food Measurement and Characterization, 17(1): 1-11.

Liu H, Xiang D, Cheng Z, 2024, Drying methods on fruit quality and antioxidant activity of two rare edible fungi (*Dictyophora rubrovolvata* and *Phallus impudicus L.*). LWT, 206: 116603.

Liu S.T., Liu Y.D., Zhang, H., (2021), Effect of Agaricus bisporus powder addition on bread quality and antioxidant properties[J]. Journal of Hainan Normal University (Natural Science Edition), 34(3): 300-307.

Qin Y.Y., Yu H.D., Chen K.J. (2025). Effects of adding purple rice powder and Morchella powder on dough and bread quality[J]. Science and Technology of Food Industry, 46(4): 42-49.

Shams R, Singh J, Dash K K. (2023). Utilization of button mushroom (*Agaricus bisporus*) powder to improve the physiochemical and functional properties of cookies. Sustainable Food Technology, 1(2): 306-318.

Wang L, Yang K, Liu L. (2022). Comparative flavor analysis of four kinds of sweet fermented grains by sensory analysis combined with GC-MS. International Journal of Food Engineering, 18(1): 75-85.

Wu L.G., Qu L.B., Wang A.N. (2018), Research progress on nutritional and functional characteristics of buckwheat and related food development. Science and Technology of Cereals, Oils and Foods, 26(3): 41-44. (148)

Wu, G., Hui, X., Wang, R. (2021). Sodium caseinate-blackcurrant concentrate powder obtained by spray-drying or freeze-drying for delivering structural and health benefits of cookies. Journal of Food Engineering, 299: 110466.

Yadav M.P., Hicks K.B. (2015). Isolation of barley hulls and straw constituents and study of emulsifying properties of their arabinoxylans. Carbohydrate polymers, 132: 529-536.

Zhou J, Feng T, Ye R., 2015, Differentiation of eight commercial mushrooms by electronic nose and gas chromatography-mass spectrometry[J]. Journal of Sensors, (1): 3740134.

Natural Colorant from *Chara corallina* and Application in Ma Muang Bao Gummy Jelly

Nopparat Mahae[a*], Donrudee Pichairat[a], Uraiwan Wattanakul[a] and Wanninee Chankaew[b]

[a] Department of Aquculture and fishery product, Faculty of Science and Fisheries Technology,
Rajamangala University of Technology Srivijaya, Trang, 92150 Thailand
[b] Department of Fisheries, Faculty of Agriculture, Rajamangala University of Technology Srivijaya, Nakhon Si Thammarat 80110 Thailand
* Corresponding author. Tel.: 08 1478 9381; E-mail address: nopparat.rmutsv@gmail.com

Abstract

This experiment investigated the application of natural colorant, which was stabilized chlorophyll from *Chara corallina*. Ma Muang Bao gummy jelly product was used for this application. The result showed that the basic recipe for Ma Muang Bao gummy jelly production consisted of 20 grams of mango, 20 grams of water, 10 grams of gelatin, 10 grams of glucose syrup, 39.2 grams of sugar and 0.8 grams of citric acid. Muang Bao gummy jelly supplemented with 0.5% colorant powder from *Chara coralline* was suitable. The obtained products had a preference score for each characteristic in the range of 7.94-8.46 (like moderately to like very much). For the analysis of physicochemical quality of Ma Muang Bao gummy jelly supplemented with colorant powder from *Chara corallina*, it was found that moisture, ash, protein, fat, fiber, carbohydrate and energy contents were 41.74%, 2.35%, 11.98%, 0.025%, 0.054%, 43.90% and 223.74%, respectively. The total acid content was 0.14% and the water activity (a_w) was 0.64. While the lightness (L*), greenness (-a*) and yellowness (b*) were 46.14, -0.82 and 22.71, respectively. Microbiological quality showed total viable counts less than 25 CFU/g, while yeast and mold counts were less than 10 CFU/g. Additionally, it can be concluded that the natural colorant (stabilized chlorophyll) from *Chara corallina* has the potential for application in food products.

Keywords: Natural Colorant, Chara Corallina, Gummy Jelly, Ma Muang Bao

1. Introduction

Natural colorants have recently gained increasing attention due to the increasing awareness for the safety of synthetic colors. Plants, including algae, are an important source of natural colorants. Large algae are generally divided into Chlorophyta (green algae), Phaeophyta (brown algae), and Rhodophyta (red algae) based on their production of pigments. The differences between algal pigments are environmental adaptations required to increase the efficiency of light capture for photosynthesis at different depths. The pigments of macroalgae can be divided into three types: chlorophyll, carotenoids, and phycobilins. Chlorophyll and carotenoids are water-insoluble pigments, while phycobilins are a group of water-soluble proteins (Dawes, 1998; Lee, 2008)

Food safety research is increasingly important and relevant today because of its impact on consumer health and government costs in treating patients caused by unsafe food intake. This research designed an experiment using *Chara corallina* as a source of natural colorant, as this algae has been consumed in some areas of the South of Thailand for a long time. These algae are eaten fresh like other local vegetables. Local people believe that this algae can cure diabetes and stomach diseases. However, there are no research reports showing the medicinal properties of this algae. Preliminary studies have shown that the amount of chlorophyll in the cells of *Chara corallina* is higher than that of other freshwater algae. The high amount of chlorophyll makes it interesting to use as a natural colorant. It is known that the use of chlorophyll as a natural pigment has been used for a long time. (Shahid et al., 2013) Many researchers have studied the benefits of pigments to develop them for human use, especially in food, pharmaceutical industries and other industries. Manufacturers have tried to produce natural pigments, such as chlorophyll and some carotenoids, to replace synthetic dyes that are known to be carcinogenic. Chlorophyll can stimulate the recovery of damaged tissue, boost immunity, improve blood circulation and digestion, and treat serious diseases. Furthermore, chlorophyll has been developed for the treatment of cancer using photodynamic therapy (PDT) because of its photosensitizing properties. (Park, et al., 1989; Agostinis et al. 2001; Lordan et al. 2011) Several natural colorants are commercially used and approved for use in the United States and the European Union, such as anthocyanin (from grape skin extract, grape pigment extract, berry or carrot and cabbage juice), carotenoids (from *Bixa orellana* L.), β-carotene (from carrots, carrot oil, corn endosperm and bell pepper), chlorophyll (from alfalfa (*Medicago sativa*)), curcuminoids (from turmeric), betalain (from beetroot powder), carminic acid (from cochineal extract) and caramel from heating of sugar (Sigurdson et al., 2017).

This research aimed to study the application of stabilized chlorophyll powder from *Chara corallina* as colorants in Ma Muang Bao (*(Mangifera indica L.*). gummy jelly. *Mangifera indica* L. was the local mango of the South of Thailand. The results of this study can be used in the food industry or other related industries. Additionally, the impact will generate income for communities in areas where *Chara corallina* is used, and the natural colorants will increase food safety for consumers.

2. Methodology

2.1 Preparation of colorant powder from Chara corallina

Chara corallina were washed thoroughly with tap water, then the algae were blanched in boiling water for 2 minutes, and ground the sample finely with a multi-purpose blender. 70 grams of blanched and ground algae were used and reacted with 0.3% $NaHCO_3$ salt solution. The reaction temperature was 90 °C and the reaction time was 10 minutes. Metal-chlorophyll complexes were extracted using a modified method of Rahayuningsih et al. (2018) and Salama & Moharram (2007). The obtained algae sample, 10 ml, were extracted with 25 ml of 96% ethanol in an erlenmeyer flask shaker. The flasks were closed with aluminum foil and placed in a shaker water bath at 60 °C and the samples were shaken at 135 rpm for 45 min. After that, the obtained solution was processed through encapsulation with a spray dryer using maltodextrin as wall material. The colorant powder was stored in a tightly closed container waiting to be used.

2.2 The application of colorant from Chara corallina in food

The application of colorants from *Chara corallina* was used in Ma Muang Bao gummy jelly product. Gummy jelly is the product that is popularly colored to make it more appetizing.

1) Physicochemical composition of Ma Muang Bao

The physicochemical compositions of Ma Muang Bao were studied as following:

- Proximate composition (moisture, ash, lipid, protein and carbohydrate content including crude fiber) according to the method of AOAC (2000)
  - Total titratable acids according to the method of AOAC (2000)
  - Water Activity (a_w) using Water Activity Meter (Aqulab series 3, Decagon Devices, Inc., USA)
  - Color value using Color Meter (HunterLab, model ColorFlex EZ, USA)

2) Ma Muang Bao gummy jelly basic recipe

Ma Muang Bao gummy jelly was produced by modifying the basic gummy jelly production formula of Garcia (2000). The appropriate basic recipe for Ma Muang Bao gummy jelly was studied, the formulas are shown in Table 1.

Table 1 Different formulas of Ma Muang Bao gummy jelly used in the basic formula study

Ingredient	Formula 1	Formula 2	Formula 3
Ma Muang Bao (g)	0.7	0.8	0.9
Water (g)	20.0	20.0	20.0
Gelatin (g)	10.0	10.0	10.0
Glucose Syrup (g)	10.0	10.0	10.0
Sugar (g)	39.3	39.2	39.1
Citric acid (g)	0.7	0.8	0.9

Mangifera indica L. preparation

Cold water was prepared for soaking the mango. 1 teaspoon of salt and 1 tablespoon of lime juice were added to 3 liters of water in the big bowl. 1 kilogram of ice was used to make cold water. Mixed everything well. Young mangoes were peeled and soaked in the prepared water. One young mango was cut into 4 pieces and soaked them back in the water. The mangoes were soaked for about 20 minutes and rinsed with clean water twice. After the mangoes were drained, they were ready for use.

Preparation of Ma Muang Bao gummy jelly

The prepared mangoes were soaked in 10% NaCl solution with a ratio of mango to brine (w/w) of 1:1 for 30 minutes. After the time was up, drained the water and blended until smooth. The water (in the formula) was divided into 2 parts: Part 1: The water was mixed with finely blended mango, sugar, glucose syrup and citric acid. Mixed ingredients were cooked over medium-low heat and simmered until the temperature reaches 120 °C. Part 2: The water was mixed with gelatin. After that, parts 1 and 2 were mixed together. The thick mixer was scooped out and dropped it into the mold. Then the samples were refrigerated at 4 °C for 24 hours before removing from the mold.

The experimental design consisted of 3 treatments according to the formula for preparing Ma Muang Bao gummy jelly. The appropriate formula was selected by sensory evaluation with 35 panellists using 9-point hedonic scale. Sensory characteristics such as appearance, color, odor, taste, texture and overall acceptance were considered. The RCBD experiment was designed and the means were compared using the Duncan's New Multiple Rang Test (DMRT).

3) The appropriate amount of colorant powder from Chara corallina use in gummy jelly

The appropriated amount of colorant powder from *Chara corallina* using in gummy jelly was studied with the appropriate formula from the previous study. Three levels of colorant powder were evaluated: 0.0, 0.5, 1.0 % of all ingredients. The appropriate treatment was selected by sensory evaluation with 35 panellists using 9-point hedonic scale. Sensory characteristics such as appearance, color, odor, taste, texture and overall acceptance were considered. The RCBD experiment was designed and the means were compared using the Duncan's New Multiple Rang Test (DMRT).

4) Quality of Ma Muang Bao gummy jelly supplemented with colorant powder from Chara corallina

Quality of Ma Muang Bao gummy jelly supplemented with colorant powder from *Chara coralline* was evaluated as following:

111

- Proximate composition (moisture, ash, lipid, protein and carbohydrate content including crude fibre) according to the method of AOAC (2000)
    - Total tritratable acids according to the method of AOAC (2000)
    - Water Activity (a_w) using Water Activity Meter (Aqulab series 3, Decagon Devices, Inc., USA)
    - Color value using Color Meter (HunterLab, model ColorFlex EZ, USA)
    - Total viable count according to the method of BAM (2001)
    - Yeast and mold according to the method of BAM (2001)

3. Results and Discussion

3.1 Physicochemical composition of Ma Muang Bao

Physicochemical compositions of Ma Muang Bao were evaluated, the results are shown in Table 2.

Table 2 Physicochemical compositions of Ma Muang Bao

Composition	Amount
Moisture (%)	90.58 ± 0.03
Ash (%)	0.28 ± 0.05
Protein (%)	0.31± 0.02
Fat (%)	0.08 ± 0.02
Fiber (%)	0.75 ± 0.17
Carbohydrate (%)	7.99 ± 0.15
Total titratable acids (%)	0.25 ± 0.00
Water Activity (a_w)	0.99 ± 0.00
Color value	
L*	71.88 ± 0.02
a*	-3.28 ± 0.01
b*	34.32 ± 0.02

Physicochemical compositions of Ma Muang Bao were evaluated, it was found that the moisture, ash, protein, fat, fiber, carbohydrate and total acid content were 90.58, 0.28, 0.31, 0.08, 0.75, 7.99 and 0.25%, respectively. The water activity (a_w) was 0.99, the lightness (L*) was 71.88, the redness (a*) was -3.28 and the yellowness (b*) was 34.32. Yuthachit (1998) studied physicochemical compositions of Ma Muang Bao, the result was as follows: 90.36% moisture content, 3.27% total acid in the form of citric acid, 6.51 % total soluble solids (°Brix), 4.34% total sugar, 2,96% reducing sugar, firmness was 7.08 Newton, density was 983.1 ± 0.02 kg/m3, L a b was 31.06, -1.48 and 9.27, respectively. Songwanphuak et al. (2012) studied the amount of active compounds and antioxidant activity in 13 species of Thai mango, the result showed that Ma Muang Bao was found to have the highest total phenol content. The antioxidant activity study by DPPH method found that it was in the group of mangoes with high antioxidant activity, while the analysis by FRAP method found that it was in the group of mangoes with moderate antioxidant activity.

3.2 Ma Muang Bao gummy jelly basic recipe

Ma Muang Bao gummy jelly basic recipe was examined with 3 different formulas, the results are shown in Table 3

Table 3 Sensory characteristics preference scores of Ma Muang Bao Gummy Jelly

Sensory characteristics	Mean of hedonic score		
	Formula 1	Formula 2	Formula 3
Color	7.83 ± 0.38[b]	8.11 ± 0.57[a]	7.80 ± 0.40[c]
Odor	6.71 ± 0.45[c]	7.43 ± 0.55[a]	6.86 ± 0.49[b]
Taste	7.20 ± 0.47[b]	8.57 ± 0.49[a]	7.17 ± 0.51[c]
Texture	7.31 ± 0.52[b]	8.20 ± 0.40[a]	7.29 ± 0.51[c]
Overall acceptance	7.14 ± 0.35[c]	8.26 ± 0.44[a]	7.20 ± 0.47[b]

Remark: -The different letters within the same column indicate significant differences between treatments (p<.05) according to Duncan's New Multiple Range Test (DMRT).

From Table 3, hedonic scores for color, odor, taste, texture and overall acceptance of Ma Muang Bao gummy jelly formula 2 were significantly higher than formulas 1 and 3 (p<.05). Therefore, the suitable formula for Ma Muang Bao gummy jelly production was Formula 2, which consisted of 20 grams of mango, 20 grams of water, 10 grams of gelatin, 10 grams of glucose syrup, 39.2 grams of sugar and 0.8 grams of citric acid. Takeungwongtrakul et al. (2020) developed gummy jelly products from strawberry syrup, it was found that the optimal formula consisted of 43% strawberry syrup, 40% sugar, 10% gelatin powder, 9% glucose syrup, and 1% ascorbic acid. The production process was as follows: Strawberry syrup was poured into a pot and heated at 45°C for 5 minutes. Glucose syrup, sugar, ascorbic acid and gelatin powder were mixed and stirred well, then boiled for 5 minutes to obtain a concentration of 78 ± 0.01°Brix. The mixed solution was poured into the mold and refrigerated for 24 hours. The formulas of three commercial gummy jelly, namely Jolly Bears, Zoo Gummy and Dole were observed for their ingredients. Jolly Bears contained 39% glucose, 35% sugar, 12% fruit juice, gelling agent (edible gelatin INS 428), acidity regulator INS 330, INS 331(iii), certified artificial colors INS 102, INS 110, INS 122, INS 124, INS 133, artificial flavoring agent and no preservatives. Zoo gummy contained 45% sucrose, 28% glucose syrup, 14% gelling agent (gelatin), 1.5% acidity

112

regulator (citric acid), artificial flavoring agent and artificial colors INS 102, INS 110, INS 122, INS 133. Dole's gummy jelly consisted of 60% mixed fruit puree, 18.16% water, 13.96% sugar, 1% malted rice syrup, natural orange flavor, 5% food additives, glycerin (INS 422), carrageenan (INS 407), locust bean gum (INS 410), citric acid (INS 330), natural orange flavor, potassium citrate (INS 332(ii)) and vitamin c (INS 300).

3.3 The appropriate amount of colorant powder from Chara corallina used in gummy jelly

The appropriate amount of colorant powder from *Chara corallina* used in Ma Muang Bao gummy jelly was examined with 3 different levels (0. 0.5 and 1.0), the results are shown in Table 4

Table 4 Sensory characteristics preference scores of Ma Muang Bao gummy jelly with different levels of colorant powder from *Chara corallina*

Sensory characteristics	Mean of hedonic score		
	0% colorant powder	0.5% colorant powder	1.0% colorant powder
Color	7.06 ± 0.48^c	8.37 ± 0.54^a	7.86 ± 0.32^b
Odor	7.09 ± 0.55^b	7.94 ± 0.71^a	7.20 ± 0.52^b
Taste	7.26 ± 0.44^b	8.46 ± 0.60^a	7.17 ± 0.51^b
Texture	7.31 ± 0.52^b	8.29 ± 0.45^a	7.23 ± 0.75^b
Overall acceptance	7.03 ± 0.17^c	8.46 ± 0.50^a	7.29 ± 0.51^b

Remark: -The different letters within the same column indicate significant differences between treatments
(p<.05) according to Duncan's New Multiple Range Test (DMRT).

Table 4 indicates that hedonic scores for color, odor, taste, texture and overall acceptance of Ma Muang Bao gummy jelly supplement with 0.5% colorant powder from *Chara corallina* were significantly higher than Ma Muang Bao gummy jelly supplement with 0 and 1% colorant powder from *Chara corallina* (p<.05). Therefore, the appropriate amount of colorant powder (or chlorophyll powder) from *Chara corallina* added to Ma Muang Bao gummy jelly product was 0.5%. For the application of chlorophyll in food, natural colorants from chlorophyll can be used as food additives and have potential health benefits (Minh et al., 2019). The study of Jayasinghe et al. (2016) investigated the extraction of chlorophyll and carotenoids from *Ulva lactuca*) and *Sargussum wighttiu* with acetone, methanol and water, while picobiliprotein was obtained from *Gracilaria verrucosa* ground with ice-cold potassium phosphate buffer. Then it was applied in jelly-type desserts and evaluated for its microbiological, sensory and stability qualities. The results of the study showed that yield of chlorophyll, carotenoids and crude phycoerythin were 45%, 31% and 33%, respectively. These pigments had a shelf life of more than six months in 5% citric acid at room temperature. While jelly candies retained their natural color for more than 30 days at room temperature, with a color loss of 30%, the same amount as with synthetic colors. Agar jelly prepared with natural food colorings provided significantly higher calcium (120 mg/L) and potassium (550 mg/L) concentrations compared to jellies prepared using synthetic colorings. In addition, jellies using natural colors also contain high amounts of protein (10.2-12.0%), carbohydrate (10.8-12.3%), and fat (1.16-1.93%). These natural colors are highly nutritious, indicating their potential as dietary supplements.

3.4 Quality of Ma Muang Bao gummy jelly supplemented with colorant powder from Chara corallina

The Quality of Ma Muang Bao gummy jelly supplemented with colorant powder from *Chara corallina* was evaluated, the results are shown in Table 5.

Table 5 Physicochemical quality and microbiological quality of Ma Muang Bao gummy jelly supplemented with colorant powder from *Chara corallina*

Quality	Amount
Physicochemical quality	
Moisture (%)	41.74 ± 0.33
Ash (%)	2.35 ± 0.17
Protein (%)	11.98 ± 0.47
Fat (%)	0.02 ± 0.00
Fibre (%)	0.05 ± 0.00
Carbohydrate (%)	43.90 ± 0.10
Energy (Kcal)	223.74 ± 2.29
Total tritratable acids (%)	0.14 ± 0.00
Water activity (a_w)	0.64 ± 0.02
Color value	
L*	46.14 ± 0.02
a*	-0.82 ± 0.01
b*	22.71 ± 0.02
Microbiological quality	
Total viable count (CFU/g)	< 25
Yeast and mold (CFU/g)	< 10

For the analysis of physicochemical quality of Ma Muang Bao gummy jelly supplemented with colorant powder from *Chara corallina*, it was found that moisture, ash, protein, fat, fiber, carbohydrate and energy contents were 41.74%, 2.35%, 11.98%, 0.025%, 0.054%, 43.90% and 223.74 Kcal, respectively. The total acid content was 0.14% and the water activity (a_w) was 0.64. While the lightness (L*), greenness (-a*) and yellowness (b*) were 46.14, -0.82 and 22.71, respectively. Microbiological quality showed total viable counts less than 25 CFU/g, while yeast and mold counts were less than 10 CFU/g. Karapairaw (2018) studied the physical, chemical and nutritional properties of

113

the developed formula of Torch ginger gummy jelly compared with the basic formula, it was found that basic formula of Torch ginger gummy jelly contains moisture, ash, protein, fat, fiber, carbohydrates and total sugars of 13.01, 7.36, 7.47, 0.02, not found, 75.56, and 74.96 percent, respectively. While total energy was 2934.33 cal/gram, water activity value (a_w) value was 0.76. Lightness (L*) value, redness (a*) value and yellowness (b*) value were 31.09, 11.59 and 9.39, respectively. The developed formula of Torch ginger gummy jelly contained 18.28% moisture, 1.62% ash, 9.26% protein, 0.02% fat, not found fiber, 65.87% carbohydrate and 65.78% total sugar, respectively.

4. Conclusions

Application of stabilized chlorophyll from *Chara corallina* as natural colorant in food product was investigated. Ma Muang Bao gummy jelly product was used for this application. The experimental results demonstrated the potential of natural colorant powder from *Chara corallina* for application in food products. Then this natural colorant will increase food safety for consumers.

5. Acknowledgements

6. References

Agostinis, P., Berg, k., Cengel, K. A., Foster, T. H. Girotti, A. W., Gollnick, S. O., Hahn, S. M., Hamblin, M. R., Juzeniene, A., Kessel, D., Korbelik, M., Moan, J., Mroz, P., Nowis, D., Piette, J., Wilson, B.C. and Jakub Golab, J. (2001). Photodynamic therapy of cancer: an update. *A Cancer Journal for Clinicians* 61(4), p. 250-281.

AOAC. (2000). *Official Methods of Analysis*, 17th Edition. Washington, DC: Association of Official Analytical Chemists.

BAM. (2001). *Bacteriological Analytical Manual Online.* Silver Spring, MD: Food and Drug Administration.

Dawes, C J. (1998). *Marine botany.* 2nd Edition. New York: John Wiley & Sons, Inc.

Garcia, T. (2000). Analysis of gelatin-based confections. *Manufacturing Confectioner* 80, p. 93-101.

Jayasinghe, P. S., Pahalawattaarachchi, V., Ranaweera, K. K. D. S. (2016). Seaweed extract as a natural food coloring agent in jelly desserts on chemical, microbial and sensory quality. *Academy of Agriculture Journal* 1(3), p. 65–69.

Karapairaw, K. (2018). Effect of sugar substitutes on the quality of Torch ginger gummy jelly. *Burapha Science Journal.* 23(2), p. 944-958. (in Thai)

Lee, R. E. (2008). *Phycology.* 4th Edition. New York: Cambridge University Press.

Lordan, S., Ross, R. P., Stanton, C. (2011). Marine bioactives as functional food ingredients: potential to reduce the incidence of chronic disease. *Marine Drugs* 9(6), p. 1056-1110.

Minh, N. P., Vo, T. T., Man, L. Van, Phong, T. D., Toan, N. Van, and Nam, V. H. (2019). Green pigment extraction from pandan (*Pandanus amaryllifolius*) and its application in food industry. *Journal of Pharmaceutical Sciences and Research* 11(3), p. 925–929.

Park, Y. J., Lee, W. Y., Hahn, B., Han, M. J., Yang, W. I. and Kim, B. S. (1989). Chlorophyll derivatives – a new photosensitizer for photodynamic therapy of cancer in mice. *Yonsei Medical Journal* 30(3), p. 212 – 218.

Rahayuningsih, E., Pamungkas, M. S., Olvianas, M. and Putera, A. D. P. (2018). Chlorophyll extraction from suji leaf (*Pleomele angustifolia* Roxb.) with $ZnCl_2$ stabilizer. *Journal of Food Science and Technology* 55(3), p. 1028-1036.

Salama, M. F. and Moharram, H. A. (2007). Relationship between colour improvement and metallo-chlorophyll complexes during blanching of peas and broccoli. *Alexandria Journal of Food Science and Technology* 4 (2), p. 11-18

Shahid, M., Shahid-Ul-Islam. and Mohammad, F. (2013). Recent advancements in natural dye applications: A review. *Journal of Cleaner Production* 53, p.310-331

Sigurdson, G. T., Tang, P., Giusti, M. M. (2017). Natural Colorants: Food Colorants from Natural Sources. *The Annual Review of Food Science and Technology* 8(1), p. 261-280.

Songwanphuak, K., Wongaree, C., Buanong, M., and Techawutthiphon, C. (2012). *The amount of active substances and antioxidant activity of raw mangoes in Thailand. Research report.* Thailand Research Fund Office.

Takeungwongtrakul, S., Thavarang, P. and Sai-Ut, S. (2020). Development of Strawberry gummy jelly with reduced sugar content from Strawberry syrup. *International Journal of Agricultural Technology* 16(5): 1267-1276.

Yuthachit, P. (1998). *Development of Dried Pickled Mango Production Process.* Master of Science Thesis. Food Technology Program, Prince of Songkla University, Hat Yai Campus, Songkhla. (in Thai)

Postharvest Preservation of Trimmed Coconuts: Evaluating Citric Acid, Sodium Chloride, and Peroxyacetic Acid Treatments

Jeeranan Wongwatanyu[a], Sansanee Thimthong[b], Nomjit Suteebut[c], Sansanee Tempiam[c], Supuksorn Masavang[c]*

[a]Division of Food Technology and Innovation, Faculty of Liberal Arts and Sciences, Sisaket Rajabhat University, Sisaket, Sisaket, 33000 Thailand
[b]Division of Food Service Industry, Faculty of Home Economics Technology, Rajamangala University of Technology Phra Nakhon, Bangkok, 10300 Thailand
[c]Division of Food Technology, Faculty of Home Economics Technology, Rajamangala University of Technology Phra Nakhon, Bangkok, 10300 Thailand
*Corresponding author. Tel.: (066) 0616353997; fax: 02-6653800; E-mail address: supuksorn.m@rmutp.ac.th

Abstract

The shelf life of trimmed coconuts can be extended through chemical treatments, such as the application of acids or chlorine-based compounds, which are commonly used to inhibit browning and microbial growth. However, the use of these substances is often restricted in fresh food applications due to regulatory limitations and consumer safety concerns. This study aimed to monitor the effects of pretreating trimmed coconuts with citric acid (CA), sodium chloride (NaCl), and peroxyacetic acid (PAA) solutions on their quality during 15 days of chilled storage. Trimmed coconuts were immersed for 5 minutes in solutions of CA at concentrations of 10% and 20%, NaCl at 10% and 20%, and PAA at 80 ppm before packaging. The treated samples were then compared to a control group that received no treatment. Throughout a 15-day storage period at 5°C, the treated coconuts were evaluated for visual quality, color values (L, a, b), total plate count, and yeast and mold count on their surfaces. Additionally, the chemical quality of the coconut water was assessed by measuring titratable acidity, pH, and total dissolved solids. The results indicated that coconuts treated with 20% CA and 20% NaCl solutions were most effective in preserving visual quality and color, and in controlling microbial growth (P<0.05). In contrast, coconuts soaked in PAA solution showed a reduction in bacterial count only for up to 6 days and exhibited yellowing immediately after treatment. Consequently, 20% CA and 20% NaCl solutions appear to be promising chemical treatments for controlling post-harvest deterioration of trimmed coconuts.

Keywords: Trimmed Coconut, Shelf–life Extension, Citric Acid, Sodium Chloride, Peroxyacetic Acid

1. Introduction

Aromatic coconuts are a key export crop for Thailand, contributing significantly to the national economy. Their distinctive aroma, present in both the coconut water and flesh, is similar to the volatile compounds found in pandan leaves (Jangchud et al., 2007). Trimmed aromatic coconuts are especially popular in international markets due to their convenience and reduced transportation costs (Mohpraman & Siriphanich, 2012). However, the removal of the outer exocarp significantly shortens the shelf life of coconuts, increasing their susceptibility to microbial spoilage and enzymatic browning. This degradation affects both the coconut water and flesh, leading to undesirable changes in sensory characteristics as a result of microbial contamination and oxidation. Therefore, effective postharvest processing methods are critical to ensure product stability while preserving its taste and nutritional value.

In recent years, sulfite-based compounds—including sodium metabisulfite, potassium metabisulfite, sulfur dioxide gas, sodium sulfite, and sodium bisulfite—as well as chlorine have been used to extend the shelf life of trimmed coconuts. However, these substances are associated with adverse health effects, including potential allergic reactions (Vally et al., 2009; Abadias et al., 2011). Due to these concerns, the use of sulfites has been banned, and chlorine residue in wash water in direct contact with food is now restricted to 4 ppm (CFR, 2011). This regulatory shift underscores the urgent need to identify safe and effective alternatives for maintaining the quality of trimmed aromatic coconuts.

Several alternative treatments have been evaluated for their potential to replace sulfites in fresh produce preservation, including ascorbic acid (Najjari & Bodaghi, 2024), calcium chloride ($CaCl_2$) (Capotorto et al., 2018), sodium chlorite (Ma et al., 2021), and combinations of sanitizers and inhibitors such as acidic electrolyzed water, peracetic acid (PAA), and chlorine (Wang et al., 2007). Among these, citric acid (CA) and sodium chloride (NaCl) are widely regarded as safe and effective agents for maintaining the quality of fresh-cut fruits and vegetables (Mohpraman & Siriphanich, 2012; Treesuwan et al., 2023; Plaza et al., 2003). Citric acid functions as a copper-chelating agent that inhibits polyphenol oxidase (PPO) activity by sequestering its metal cofactor (Treesuwan et al., 2023), while NaCl has been shown to inhibit PPO by altering the enzyme's active site through halide binding (Ma et al., 2021). The use of these agents can therefore prevent browning and extend the shelf life of fresh-cut produce.

However, the application of chemical treatments may be limited by factors such as reduced efficacy, undesirable odors, or surface damage to the product (Ma et al., 2021). Peracetic acid (PAA), a mixture of acetic acid (CH_3COOH) and hydrogen peroxide (H_2O_2), has emerged as a promising alternative disinfectant due to its strong antimicrobial properties and potential to replace chlorine in fresh produce sanitation (Fawell, 2000). Nonetheless, data remain limited regarding the comparative effects of different concentrations of citric acid, sodium chloride, and PAA

on both browning and microbiological quality in trimmed coconuts. This study aims to evaluate the effectiveness of these compounds in preserving the physical and microbial quality of trimmed aromatic coconuts during refrigerated storage under optimal conditions.

2. Methodology

2.1 Sample preparation

Aromatic coconuts at 6–8 months of maturity after inflorescence were sourced from a plantation in Ban Phaeo District, Samut Sakhon Province, Thailand (Paull and Ketsa, 2015). A total of 120 fruits, each weighing approximately 1,200–1,500 grams, were selected for the study. Initially, the basal end of each coconut was trimmed with a knife to create a flat, stable base. The coconuts were then inverted, and the pericarp was carefully carved at an angle to fully expose the endocarp, forming a conical top (Figure 1).

Figure 1: Trimmed coconut in a conical shape at the top of the fruit.

2.2 Pre-treatment with chemical soaking process

In this study, 10% (w/v) and 20% (w/v) citric acid solutions, 10% (w/v) and 20% (w/v) sodium chloride solutions, and an 80 ppm peroxyacetic acid solution were used as chemical pre-treatments. Following trimming, the coconuts were immediately immersed in the respective chemical solutions for 5 minutes at room temperature, as described by Nguyen et al. (2019) with slight modifications. After treatment, the coconuts were rinsed with tap water and gently blotted dry using paper towels. All treated samples were then wrapped in polyvinyl chloride (PVC) film and stored at 5 °C with 80–90% relative humidity under refrigerated conditions, simulating commercial storage. Quality assessments of the trimmed coconuts were conducted every 3 days over a 15-day storage period by randomly selecting three fruits from each treatment group. Trimmed coconuts without soaking were used as the control for comparison.

2.3 Study of changes in trimmed coconut during Storage

Trimmed coconuts were stored at approximately 5°C, with samples collected every three days over a 15-day period to assess changes in physical, chemical, and microbial qualities. The evaluated parameters included weight loss, total soluble solids, pH, color, and microbial count. The experiment followed a completely randomized design (CRD) with three replications, each consisting of a single coconut per replication.

1) Weight Loss Measurement of Trimmed Coconut

Collect samples of trimmed coconuts that have been soaked in chemical solutions for shelf-life extension and packaged in PVC plastic bags. Compare these samples with control coconuts that were not treated with chemicals. Measure and record the initial weight of each sample before storage, and then weigh them again after the storage period. Use the recorded weights to calculate changes according to Equation (1), and analyze the relationship between weight changes and time throughout the experiment. The weight loss percentage (%) can be calculated using the following formula:

$$\text{Weight Loss (\%)} = [\text{Initial Weight} - \text{Weight After Storage}] \times 100 \text{ / Initial Weight} \qquad (1)$$

This formula calculates the percentage of weight loss during storage by comparing the initial weight of the sample with its weight measured after storage.

2) Measurement of Total Soluble Solids (TSS) and pH of coconut meat and water

The coconuts were cut open, and the coconut meat and coconut water were collected and transferred into a clean stainless-steel bowl. The contents were homogenized using a handheld immersion blender. Total soluble solids (TSS) were measured using a hand-held refractometer (Atago, Model N-1E, Japan). Prior to measurement, the refractometer was calibrated to zero using distilled water. TSS values were recorded as a percentage (°Brix). The pH was subsequently determined using a pH meter (Mettler Toledo, Model FE20, USA). The relationships between TSS and storage time, as well as between pH and storage time, were analyzed throughout the storage period.

3) Determination of Total Acidity (TA)

The coconut meat and water were blended using a handheld immersion blender until a homogeneous mixture was obtained. Total titratable acidity was determined according to AOAC (2000) guidelines. A 10 g aliquot of the homogenized mixture was weighed and mixed with 25 mL of distilled water. The solution was titrated with 0.10 N sodium hydroxide (NaOH) using phenolphthalein as the pH indicator to determine the endpoint. The total acidity was calculated and expressed as malic acid equivalent per 100 g of fresh weight. The results were compared against standard reference values.

$$\text{Titratable Acidity (\%)} = (A \times B \times 0.067)/C \times 100 \tag{2}$$

Where   A = Concentration of the 0.10 N sodium hydroxide solution
                B = Volume of the sodium hydroxide solution (ml)
                C = Volume of the sample (ml)

4) Color Measurement of the Coconut Shell.

The color changes (L, a, b) of the mesocarp or shell of trimmed coconuts from each treatment condition are determined by assessing 10 points on each fruit using a colorimeter with the CIE Lab* system (Konica Minolta, model CR-400, Japan). Calculate the whiteness (W) and browning index (BI) of the mesocarp using the following equations:

$$W = 0.511L^* - 2.324a^* - 1.100b^* \tag{3}$$

$$BI = \left[\frac{X - 0.31}{0.172}\right] \times 100 \tag{4}$$

$$X = (a^* + 1.75L^*)/(5.646L^* + a^* - 3.012b^*) \tag{5}$$

5) Determination of Total Plate Count and Yeast and Mold Count in Coconut meat and water

Total plate count and yeast and mold count were conducted using the pour plate technique in accordance with the Bacteriological Analytical Manual (BAM, 1995). Coconut meat and water were blended in a sterile bag using a stomacher until a homogeneous mixture was achieved. For total microbial count, 1 mL of the sample was pipetted into a sterile Petri dish, followed by the addition of approximately 15–20 mL of plate count agar cooled to 40–45°C. The contents were gently swirled to mix. Plates were incubated at 37°C for 48 hours. For yeast and mold count, potato dextrose agar (PDA) was poured into sterile Petri dishes and allowed to solidify. A 0.1 mL aliquot of the sample, pre-diluted 1:100, was pipetted onto the surface of the agar and evenly spread. Tenfold serial dilutions were prepared using phosphate-buffered saline and distilled water to achieve the desired dilution range. The diluted samples were plated on PDA and incubated at 30°C for 48 hours. All microbiological analyses were performed in duplicate, using two coconuts per treatment.

2.4 Statistical Analysis

Analyze the experimental results using the SPSS program by conducting an Analysis of Variance (ANOVA) with a Completely Randomized Design (CRD). Compare differences among the experimental groups, which include various types and forms of packaging, using Duncan's Multiple Range Test (DMRT) at a 95% confidence level.

3. Results and Discussion

3.1 Effect of soaking solutions type and concentration on the physical and chemical qualities of trimmed coconuts during storage

The appearance of trimmed coconuts is summarized in Table 1. Soaking the coconuts in various chemical solutions significantly improved their visual quality compared to the untreated control samples over the 15-day storage period. On day 0, control samples exhibited a darker brownish-red mesocarp relative to those treated with chemical solutions. This discoloration is attributed to enzymatic browning that occurs once the outer green exocarp is removed, exposing the white mesocarp to oxygen. Enzymatic browning results from the oxidation of phenolic compounds catalyzed by two key oxidoreductases: polyphenol oxidase (PPO) and peroxidase (POD). PPO catalyzes two sequential reactions: a slower hydroxylation of monophenols to diphenols (colorless), followed by a rapid oxidation of diphenols to quinones, which polymerize into brown pigments (Tilley et al., 2023). This reaction requires oxygen as a co-substrate and is influenced by environmental factors such as temperature and humidity. Browning not only causes undesirable color changes but also diminishes nutritional quality, flavor, and overall sensory appeal, negatively impacting marketability. It is estimated that enzymatic browning contributes to the postharvest loss of over 50% of browning-prone foods (Hamdan et al., 2022). Postharvest treatments, including immersion in anti-browning agents, can mitigate these effects by preserving both physical appearance and chemical quality, thereby extending shelf life (Ayaz et al., 2008; Wessels et al., 2014).

In this study, untreated coconuts showed rapid browning of the trimmed shell, leading to a visibly undesirable appearance. In contrast, soaking coconuts in 10% and 20% sodium chloride (NaCl) solutions extended shelf life from 3 days to 6 days. Notably, coconuts treated with 10% and 20% citric acid solutions maintained a superior appearance

and achieved a shelf life of up to 15 days under refrigeration (approximately 5–8°C). Higher concentrations of citric acid and sodium chloride were more effective in maintaining appearance quality during cold storage than lower concentrations. The efficacy of citric acid and sodium chloride in reducing browning has previously been demonstrated in fresh-cut potato (Ma et al., 2021) and trimmed coconut (Nguyen et al., 2019; Pathomaim et al., 2023). However, peracetic acid (PAA) was not effective in preserving the visual quality of peeled, trimmed coconuts.

Table 1 Appearance of trimmed coconuts soaked in various browning inhibitors and stored for different periods

Sample	0 day	3 days	6 days	9 days	15 days
Control					
Citric acid 10% (w/w)					
Citric acid 20% (w/w)					
NaCl 10% (w/w)					
NaCl 20% (w/w)					
Peroxyacetic (PAA) 80 ppm					

Citric acid and sodium hydroxide inhibit browning through different mechanisms. Both citric acid and sodium chloride (NaCl) effectively preserve color, extend the shelf life of trimmed coconuts to a consumer-acceptable level. These findings are consistent with previous research that demonstrated the effectiveness of citric acid and NaCl in managing enzyme browning in tomato juice (Plaza et al., 2003). Acidulants, particularly those naturally occurring in plant tissues, are commonly used as anti-browning agents. These include ascorbic, malic, citric, and phosphoric acids. Typically, polyphenol oxidase (PPO) is active at a pH of 6–7, but becomes inactive below pH 3. Acidulants lower the pH, thus reducing PPO enzymatic activity. The enzymatic browning of sugarcane juice was effectively inhibited when treated with citric acid at pH levels below 4.1 (Hithamani et al., 2018), as was observed in the heads of litchi fruits (Ali et al., 2021). Citric acid act as PPO activity either by lowering the pH or chelating the copper at the active site of the PPO enzyme. This chelation, particularly at pH levels below 4, reduces PPO activity by disrupting copper binding at the enzyme's active site, thus inhibiting enzyme function (Xu et al., 2021). Manolopoulou & Varzakas (2011) demonstrated that treating fresh-cut cabbage with a 1% citric acid solution and storing it at low temperatures (0°C) extended its shelf life by 22 days. In the present study, the results demonstrated that immersing the trimmed coconuts in a 20% citric acid solution effectively preserved their color, overall acceptability, and quality for up to 15 days when stored at 5-8°C.

The inhibition of polyphenol oxidase (PPO) activity by sodium chloride has been documented in other studies. Zhang et al. (2005) found that NaCl concentrations above 20 mmol/L effectively inhibited PPO activity in two different potato cultivars. Lim et al. (2013) further explained that sodium chloride affects PPO by directly interacting with the enzyme's structure. Specifically, halides, including NaCl, inhibit PPO activity by binding to the enzyme's inhibitor site, which alters the active site's structure and impairs its functionality. For instance, Nguyen et al. (2019) found that a combination of 20% citric acid and 15% sodium chloride effectively inhibited browning reactions in coconut products, extending the shelf life of trimmed coconuts for up to 8 weeks at 2°C. This treatment

preserved the marketability of the coconuts without adversely affecting other quality attributes, such as color, pH, titratable acidity (TA), total soluble solids (TSS), and microbial counts. In this study, the results indicate that 20% citric acid and 20% NaCl solutions were the most effective in preventing browning and maintain the visual quality of trimmed coconut products.

Soaking trimmed coconuts in various solutions to inhibit browning over a 15-day storage period revealed that 10% and 20% citric acid solutions achieved the highest lightness (L*), followed by 10% and 20% sodium chloride (NaCl) solutions. The control samples, which were not soaked in any solution, exhibited the lowest lightness. Lightness values ranged from 68.66 to 72.90, while samples soaked in 80 ppm peracetic acid (PAA) solution had the lowest lightness values, ranging from 62.88 to 68.11 (Table 2), significantly lower than those of other treatments (P < .05). This indicates that PAA treatment resulted in notably reduced lightness compared to other solutions.

The study demonstrated that citric acid and NaCl were more effective in inhibiting browning reactions compared to PAA. This is due to their ability to inhibit polyphenol oxidase (PPO) enzyme activity, as discussed previously. Conversely, PAA not only failed to control browning but also caused additional browning, resulting in decreased L values, and increased Browning Index (BI). This effect is likely due to tissue damage caused by PAA, which releases enzymes from cells and promotes the oxidation of phenolic compounds. These findings are consistent with studies by Wang et al. (2007) and Ghidelli et al. (2013), which reported PAA's ineffectiveness in controlling browning in minimally processed persimmons and sliced apples.

The BI of coconuts not soaked in any browning inhibitors increased significantly (23.47–56.73) from day 0 to day 3. Coconuts soaked in 80 ppm PAA solution exhibited yellow or light brown colors, resulting in a higher BI compared to other treatments, with the BI remaining constant throughout the 15-day storage period. Among all treatments, 10% and 20% citric acid solutions were most effective in controlling browning, outperforming both sodium hydroxide and PAA.

Soaking trimmed coconuts in solutions designed to inhibit surface browning did not significantly affect the total acidity (TA), pH, or total soluble solids (TSS) of the coconut meat and water blend during storage (P>0.05). However, the results indicated that storage duration significantly impacted the quality of the coconut meat and water blend (P<.05), as shown in Table 2.

The TA of coconut water decreased rapidly during the first 3 days of storage at 5-8°C but remained relatively stable from days 3 to 15, with values ranging from 0.035% to 0.068%. The pH of the coconut water increased slightly as TA decreased (P>.05) (Table 2). Specifically, the pH of samples soaked in all browning-inhibiting solutions rose gradually during the first 3 days of storage (P≤0.05) before stabilizing, ranging from 6.38 to 7.58 for the remainder of the storage period. The TSS remained consistent, ranging from 5.43 to 6.62 °Brix throughout the storage period (P>.05).

The study demonstrated that coconut water quality changed gradually over storage at 5-8°C, with pH increasing and TA decreasing over time. Similar trends have been reported in studies on coconut water post-harvest (Haseena et al., 2010). After 8 weeks, the quality of coconut water in this study remained acceptable, as unacceptable coconut water typically has a pH and TA below 0.02% (Jangchud et al., 2007). Nguyen et al. (2019) found that after 8 weeks of storage at 2°C, the quality of coconut water remained acceptable, with pH ranging from 6.38 to 6.55, TA from 0.035% to 0.048%, and TSS from 7.35 to 7.84 °Brix. Generally, pH increased and TA decreased, while TSS slightly decreased over the storage period. Importantly, changes in TA, pH, and TSS were not statistically significant (P>.05) for coconuts soaked in browning-inhibiting solutions.

Table 2 Effects of different browning inhibitors and storage durations on the physical and chemical properties of trimmed coconut products

Treated solution	Storage time (day)	Lightness (L)	Browning index (BI, %)	TSS (°Brix)	TA (%)	pH
Control	0	84.65±1.20[a]	23.47±2.58[e]	8.50±0.08[a]	0.09±0.01[a]	5.43±0.10[c]
	3	72.90±2.91[d]	56.73±9.21[b]	8.45±0.05[a]	0.06±0.01[b]	5.58±0.08[c]
	6	72.74±2.58[d]	54.90±8.40[b]	7.42±0.09[ab]	0.04±0.00[bc]	5.81±0.05[c]
	9	68.66±4.77[de]	57.65±13.36[b]	7.01±0.05[ab]	0.03±0.00[c]	6.13±0.10[ab]
	15	69.79±.46d[de]	61.62±7.81[b]	6.75±0.10[bc]	0.03±0.00[c]	6.15±0.06[ab]
CA 10%	3	82.99±1.37[ab]	27.92±3.25[de]	8.85±0.05[a]	0.07±0.01[b]	5.64±0.10[c]
	6	83.47±1.41[a]	23.11±1.82[e]	7.46±0.10[ab]	0.04±0.00[bc]	5.95±0.07[c]
	9	80.29±1.77[b]	21.27±1.60[e]	7.24±0.05[ab]	0.03±0.01[c]	6.53±0.05[a]
	15	81.03±1.32[b]	20.95±1.60[e]	6.64±0.05[b]	0.03±0.00[c]	6.62±0.05[a]
CA 20%	3	83.64±0.94[a]	27.14±2.32[de]	8.45±0.05[a]	0.07±0.01[b]	5.54±0.05[c]
	6	83.69±1.24[a]	23.05±1.42[e]	7.42±0.09[ab]	0.04±0.00[bc]	5.67±0.05[c]
	9	83.72±1.30[a]	22.84±1.60[e]	7.01±0.05[ab]	0.03±0.00[c]	6.27±0.08[b]
	15	82.12±1.79[a]	21.34±1.78[e]	6.75±0.10[bc]	0.03±0.00[c]	6.43±0.10[a]
NaCl 10%	3	80.21±2.29[ab]	38.06±3.84[c]	8.62±0.05[a]	0.06±0.01[b]	5.48±0.05[c]
	6	79.09±2.75[b]	38.05±9.08[c]	7.58±0.10[ab]	0.04±0.00[bc]	5.64±0.05[c]
	9	77.03±2.41[b]	38.27±5.69[c]	7.24±0.06[ab]	0.03±0.00[c]	6.11±0.10[b]
	15	76.29±2.26[c]	42.13±4.72[bc]	6.92±0.05[bc]	0.03±0.00[c]	6.23±0.05[ab]
NaCl 20%	3	80.42±1.68[b]	34.95±4.08[d]	8.36±0.08[a]	0.06±0.01[b]	5.59±0.05[c]
	6	71.96±3.09[d]	33.72±7.77[d]	7.52±0.10[ab]	0.03±0.00[c]	5.62±0.05[c]
	9	74.54±3.76[d]	47.45±5.94[bc]	7.13±0.05[ab]	0.03±0.00[c]	6.16±0.10[b]
	15	73.20±2.06[d]	47.81±4.63[bc]	6.84±0.05[bc]	0.03±0.00[c]	6.27±0.05[b]
PAA	3	68.11±3.11[de]	89.71±11.61[a]	8.37±0.05[a]	0.06±0.01[b]	5.24±0.05[c]

Treated solution	Storage time (day)	Lightness (L)	Browning index (BI, %)	TSS (°Brix)	TA (%)	pH
80 ppm	6	63.42±4.19[e]	97.85±10.09[a]	7.35±0.05[ab]	0.03±0.00[c]	5.42±0.10[c]
	9	63.59±3.99[e]	98.86±8.16[a]	6.97±0.05[bc]	0.03±0.00[c]	6.15±0.05[b]
	15	62.88±3.32[e]	99.11±33.43[a]	6.52±0.08[c]	0.03±0.00[c]	6.27±0.05[ab]

Note: Values in the table are expressed as the mean ± standard deviation (S.D.). Means within each column followed by the same lowercase letter are not significantly different according to Duncan's multiple range test (P<.05).

3.2 Effect of soaking solutions type and concentration on the microbiological determinations of trimmed coconuts during storage

The effectiveness of browning inhibition solutions on microbial control in trimmed coconuts was significantly influenced by the concentration of citric acid and sodium chloride (NaCl) (Table 3). Soaking trimmed coconuts in a 20% citric acid solution proved to be the most effective for controlling microbial growth, including yeasts and molds. This treatment resulted in a total microbial count (TPC) of just 2.50×10^1 CFU and no detectable yeast or mold growth during the first 3 days of storage, in contrast to the control samples that were not treated with any chemical solutions. Throughout the storage period, TPC in the citric acid-soaked samples ranged from 2.50×10^1 to 1.58×10^3 CFU (P > .05). In general, the TPC increased with storage duration for all treated samples, but no yeast or mold growth was observed (P < .05). Control samples stored for 9-15 days, as well as samples soaked in NaCl and peracetic acid (PAA) solutions for 15 days, exhibited no microbial growth. However, these samples showed significant browning of the coconut shell, reducing their external quality below marketable standards, which precluded further microbiological analysis.

Soaking trimmed coconuts in 20% and 10% citric acid solutions effectively controlled microbial loads, including yeast and mold counts, up to day 15 of storage. This was followed in efficacy by treatments with 10% and 20% sodium chloride (NaCl) solutions, respectively. In contrast, peracetic acid (PAA) was initially effective in suppressing microbial growth during the first 6 days of storage but lost efficacy after day 9, resulting in increased microbial proliferation through the end of the storage period. Coconuts treated with PAA were ultimately rejected by consumers due to compromised microbiological and sensory quality, characterized by the development of a dark brown discoloration on the trimmed shell surface.

Trimmed coconuts treated with 20% citric acid exhibited only a slight increase in Total Plate Count (TPC) over the 15-day storage period at 5–8°C, in contrast to those treated with other solutions. This finding is consistent with previous studies demonstrating the strong antimicrobial activity of high-concentration citric acid, particularly in refrigerated leafy vegetables (Akbas & Olmez, 2007). The antimicrobial efficacy of citric acid is primarily due to its ability to lower pH, increase the concentration of undissociated acid molecules, and disrupt microbial cell physiology and metabolism. Owing to its multiple carboxyl groups (-COOH), citric acid has been reported to be more effective than lactic acid in reducing mesophilic bacterial populations (Poli et al., 1979).

Sodium chloride exerts its antimicrobial effect primarily through osmotic dehydration, removing water necessary for microbial growth. By reducing water activity (a_w), NaCl inhibits bacterial proliferation below a_w of 0.91 and can suppress yeast and mold growth when a_w falls below 0.60 (Potter & Hotchkiss, 1995). Furthermore, NaCl concentrations exceeding 8.5% have been shown to inhibit the growth of pathogenic microorganisms such as Escherichia coli O157:H7 (Casey & Condon, 2002).

Table 3 Total plate count (TPC) and yeast and mold count (YM) in coconut water and meat of trimmed coconuts soaked in various chemicals during storage at 5-8°C

Treated solution	Storage time (day)	Total plate count (CFU/g)	Yeasts and mold count (CFU/g)
Control	0	3.98×10^3	ND
	3	1.58×10^4	ND
	6	3.16×10^4	ND
	9	NA	ND
	15	NA	< 25
CA 10%	3	2.98×10^1	ND
	6	0.79×10^1	ND
	9	1.99×10^2	ND
	15	3.16×10^3	< 25
CA 20%	3	2.50×10^1	ND
	6	6.31×10^1	ND
	9	3.16×10^2	ND
	15	1.58×10^3	< 25
NaCl 10%	3	3.10×10^1	ND
	6	5.01×10^2	ND
	9	12.59×10^3	ND9
	15	NA	< 25
NaCl 20%	3	3.98×10^1	ND
	6	3.98×10^2	ND
	9	2.51×10^3	ND
	15	7.94×10^4	< 25

Treated solution	Storage time (day)	Total plate count (CFU/g)	Yeasts and mold count (CFU/g)
PAA 80 ppm	3	3.16×10^1	ND
	6	1.28×10^3	ND
	9	6.31×10^4	ND
	15	NA	< 25

Note: NA: Not analyzed due to external quality being below the marketability threshold. ND: not detected. The result fewer than 25 colonies were counted on the plate, the results were considered as < 25 CFU/g.

Peracetic acid (PAA) is an effective disinfectant that acts by oxidizing microbial cell membranes through an electron transfer mechanism. As a strong oxidizing agent, PAA rapidly disrupts microbial biochemical pathways by facilitating rapid electron transfer to microbial cells (Kitis, 2004). However, its efficacy in reducing native microflora varies depending on the type of fresh-cut produce. Microbial reduction tends to increase with higher PAA concentrations and shorter contact times, highlighting the importance of optimizing both concentration and exposure time for effective microbial control in fresh-cut fruit products (Vandekinderen et al., 2009). In this study, PAA was effective in suppressing total plate counts (TPC) for only 6 days, which may be attributed to insufficient contact time between the coconut samples and the PAA solution. This suggests that optimization of treatment parameters is essential for achieving desired outcomes in microbial reduction. Additionally, non-chemical approaches such as high-intensity ultrasound, blanching (Vandekinderen et al., 2009), and modified atmosphere packaging (Ali et al., 2021) show promise as alternative methods for extending shelf life and maintaining quality attributes in trimmed coconuts during cold storage. These techniques offer sustainable solutions for minimizing chemical usage while preserving product quality.

4. Conclusions

Pre-treatment of trimmed coconuts by soaking in 20% citric acid or 20% sodium chloride solutions was found to be the most effective method for extending shelf life and preserving the quality of aromatic coconuts, particularly those processed into green conical trimmed forms, over a 15-day storage period at 5–8°C. These findings present practical postharvest strategies for extending shelf life, inhibiting enzymatic browning, and controlling microbial growth—thereby effectively reducing postharvest deterioration. This study supports the development of value-added fresh coconut products with improved shelf stability and enhanced consumer acceptability, primarily through improved color retention and the suppression of enzymatic browning.

5.Acknowledgements

6. References

Abadias, M., Alegre, I., Usall, J., Torres, R., & Viñas, I. (2011). Evaluation of alternative sanitizers to chlorine disinfection for reducing foodborne pathogens in fresh-cut apple. *Postharvest Biology and Technology, 59*(3), 289–297.

Akbas, M. Y., & Olmez, H. (2007). Effectiveness of organic acid, ozonated water and chlorine dippings on microbial reduction and storage quality of fresh-cut iceberg lettuce. *Journal of the Science of Food and Agriculture, 87*(14), 2609–2616.

Ali, S., Khan, A. S., Malik, A. U., Anwar, R., Anjum, M. A., Nawaz, A., Shafique, M., & Naz, S. (2021). Combined application of ascorbic and oxalic acids delays postharvest browning of litchi fruits under controlled atmosphere conditions. *Food Chemistry, 350*, 129277.

AOAC. (2002). *Official methods of analysis* (17th ed.). Gaithersburg, MD: Association of Official Analytical Chemists.

Ayaz, F. A., Demir, O., Torun, H., Kolcuoglu, Y. A. K. U. P., & Colak, A. H. M. E. T. (2008). Characterization of polyphenoloxidase (PPO) and total phenolic contents in medlar (*Mespilus germanica* L.) fruit during ripening and over ripening. *Food Chemistry, 106*(1), 291–298.

BAM. (1995). *Bacteriological analytical manual* (8th ed.). Gaithersburg, MD: AOAC International.

Capotorto, I., Amodio, M., Diaz, M. T. B., de Chiara, M. L. V., & Colelli, G. (2018). Effect of anti-browning solutions on quality of fresh-cut fennel during storage. *Postharvest Biology and Technology, 137*, 21–30.

Casey, P. G., & Condon, S. (2002). Sodium chloride decreases the bacteriocidal effect of acid pH on *Escherichia coli* O157:H45. *International Journal of Food Microbiology, 76*(3), 199–206.

CFR. (2011). Title 21, Part 173.315. Secondary direct food additives permitted in food for human consumption: Chemicals used in washing or to assist in the peeling of fruits and vegetables. *Code of Federal Regulations of US Food and Drug Administration.*

Ghidelli, C., Rojas-Argudo, C., Mateos, M., & Pérez-Gago, M. B. (2013). Effect of antioxidants in controlling enzymatic browning of minimally processed persimmon 'Rojo Brillante'. *Postharvest Biology and Technology, 86*, 487–493.

Hamdan, N., Lee, C. H., Wong, S. L., Fauzi, C. E. N. C. A., Zamri, N. M. A., & Lee, T. H. (2022). Prevention of enzymatic browning by natural extracts and genome-editing: A review on recent progress. *Molecules, 27*(3), 1101.

Haseena, M., Bai, K. V. K., & Padmanabhan, S. (2010). Post-harvest quality and shelf-life of tender coconut. *Journal of Food Science and Technology, 47*(6), 686–689.

Hithamani, G., Medappa, H., Chakkaravarthi, A., Ramalakshmi, K., & Raghavarao, K. S. M. S. (2018). Effect of adsorbent and acidulants on enzymatic browning of sugarcane juice. *Journal of Food Science and Technology, 55*(10), 4356–4362.

Jangchud, K., Puchakawimol, P., & Jangchud, A. (2007). Quality changes of burnt aromatic coconut during 28-day storage in different packages. *LWT - Food Science and Technology, 40*(7), 1232–1239.

Kitis, M. (2004). Disinfection of wastewater with peracetic acid: A review. *Environment International, 30*(1), 47–55.

Lim, G. G. F., Imura, Y., & Yoshimura, E. (2012). Substrate inhibition competes with halide inhibition in polyphenol oxidase. *The Protein Journal, 31*, 609–614.

Ma, Y., Wang, H., Yan, H., Malik, A. U., Dong, T., & Wang, Q. (2021). Pre-cut NaCl solution treatment effectively inhibited the browning of fresh-cut potato by influencing polyphenol oxidase activity and several free amino acids contents. *Postharvest Biology and Technology, 178*, 111543.

Manolopoulou, E., & Varzakas, T. (2011). Effect of storage conditions on the sensory quality, colour and texture of fresh-cut minimally processed cabbage with the addition of ascorbic acid, citric acid and calcium chloride. *Food and Nutrition Sciences, 2*(9), 956–963.

Mohpraman, K., & Siriphanich, J. (2012). Safe use of sodium metabisulfite in young coconuts. *Postharvest Biology and Technology, 65*, 76–78.

Najjari, M., & Bodaghi, H. (2024). Inhibitory effect of ascorbic acid in enzymatic browning and preservation of quality in fresh pistachios (*Pistacia vera* L.). *Applied Fruit Science, 66*, 609–620.

Nguyen, D. T. N., Tongkhao, K., & Tongchitpakdee, S. (2019). Application of citric acid, sodium chloride and peroxyacetic acid as alternative chemical treatment for organic trimmed aromatic coconut. *Natural and Life Sciences Communications, 18*, 444–460.

Pathomaim, S., Jarussophon, S., Arikit, S., & Imsabai, W. (2023). Ozone-ultrafine bubbles for reducing concentration of citric acid and sodium chloride for trimmed young coconut preservation. *Horticulturae, 9*(2), 284.

Paull, R. E., & Ketsa, S. (2015). Coconut: Postharvest quality-maintenance guidelines. *Fruit, Nut, and Beverage Crops, FN-45*, 1–5.

Plaza, L., Muñoz, M., de Ancos, B., & Cano, M. P. (2003). Effect of combined treatments of high-pressure, citric acid and sodium chloride on quality parameters of tomato puree. *European Food Research and Technology, 216*, 514–519.

Poli, G., Biondi, A., Uberti, F., Ponti, W., Balsari, A., & Cantoni, C. (1979). Virucidal activity of organic acid. *Food Chemistry, 4*(4), 251–258.

Potter, N. N., & Hotchkiss, J. H. (1995). *Food science: Unit operations in food processing* (pp. 69–89). Heidelberg: Springer.

Tilley, A., McHenry, M. P., McHenry, J. A., Solah, V., & Bayliss, K. (2023). Enzymatic browning: The role of substrates in polyphenol oxidase mediated browning. *Current Research in Food Science, 7*, 100623. https://doi.org/10.1016/j.crfs.2023.100623

Treesuwan, K., Jirapakkul, W., Tongchitpakdee, S., Chonhenchob, V., Mahakarnchanakul, W., & Tongkhao, K. (2023). Antimicrobial mechanism of salt/acid solution on microorganisms isolated from trimmed young coconut. *Microorganisms, 11*(4), 873. https://doi.org/10.3390/microorganisms11040873

Vally, H., Misso, N. L., & Madan, V. (2009). Clinical effects of sulphite additives. *Clinical and Experimental Allergy, 39*(11), 1643–1651. https://doi.org/10.1111/j.1365-2222.2009.03362.x

Vandekinderen, I., Devlieghere, F., De Meulenaer, B., Ragaert, P., & Van Camp, J. (2009). Optimization and evaluation of a decontamination step with peroxyacetic acid for fresh-cut produce. *Food Microbiology, 26*(8), 882–888. https://doi.org/10.1016/j.fm.2009.06.004

Wang, H., Feng, H., & Luo, Y. (2007). Control of browning and microbial growth on fresh-cut apples by sequential treatment of sanitizers and calcium ascorbate. *Journal of Food Science, 72*(1), M001–M007.

Wessels, B., Schulze-Kaysers, N., Damm, S., & Kunz, B. (2014). Effect of selected plant extracts on the inhibition of enzymatic browning in fresh-cut apple. *Journal of Applied Botany and Food Quality, 87*, 16–23.

Xu, D., Gu, S., Zhou, F., Hu, W., Feng, K., Chen, C., & Jiang, A. (2021). Mechanism underlying sodium isoascorbate inhibition of browning of fresh-cut mushroom (*Agaricus bisporus*). *Postharvest Biology and Technology, 173*, 111357.

Zhang, Z., Mao, B., Li, H., Zhou, W., Takeuchi, Y., & Yoneyama, K. (2005). Effect of salinity on physiological characteristics, yield and quality of microtubers in vitro in potato. *Acta Physiologiae Plantarum, 27*, 481–489.

Effects of Protein- and Carbohydrate-Based Foaming Agents on Foam Stability and Microstructure in Freeze-Dried Coffee

Janyawat T Vuthijumnonk[a], Sureewan Rajchasom[a*], Penwarat Panpatarachai [a]
Maneerat Muangjai[a]

[a]*College of Integrated Science and Technology, Rajamangala University of Technology Lanna, Chiang Mai, 50300, Thailand*
Corresponding author. Tel:0909636248; E-mail address: vjanyawat@rmutl.ac.th

Abstract

The development of high-quality instant coffee products is essential for increasing market accessibility and economic value for local coffee producers. This study investigates the impact of various foaming agents—maltodextrin, whey protein isolate, and egg white powder—on the foam stability and microstructure of coffee extracts processed via foam-mat freeze drying. Coffee extract prepared from roasted Arabica beans sourced from Plang Yai community in Chiang Mai, Thailand, was combined with ten different formulations of foaming agents and evaluated through foam stability testing and scanning electron microscopy (SEM). Results showed that egg white powder was the most effective foaming agent, yielding stable foams and uniform pore structures, particularly when used in concentrations above 5%. While maltodextrin and whey isolate alone did not produce stable foams, they enhanced structural stability when used in combination with egg white powder. SEM imaging further confirmed that the optimal formulations exhibited well-developed porous networks, crucial for drying efficiency and product rehydration. The highest foam stability (96.1%) was achieved with a balanced formulation of all three agents. These findings confirm the synergistic interaction between proteins and carbohydrates in foam stabilization, offering a robust method for producing premium instant coffee. The integration of this approach enables smallholder enterprises to expand product lines while maintaining quality, enhancing the economic sustainability of coffee farming communities.

Keywords: Foam-mat Drying, Freeze-dried Coffee, Foaming Agents, Foam Stability, Coffee Microstructure

1. Introduction

Thailand's coffee industry has witnessed significant growth in recent years, particularly in the northern highlands, where the climate and elevation provide ideal conditions for Arabica coffee cultivation. Chiang Mai, one of Thailand's most well-known coffee-producing provinces, has a climate and elevation highly suitable for cultivating high-quality Arabica coffee. The province is home to over 8,000 hectares of coffee plantations, with annual production exceeding 6,000 tons (This Side Up, 2025). The majority of coffee farms in Chiang Mai are run by smallholder farmers, many of whom are part of local community enterprises aiming to create sustainable livelihoods through coffee production. The demand for Chiang Mai's specialty coffee has been growing steadily, both domestically and internationally, with exports increasing by approximately 15% annually (Bangkok Post, 2024). However, despite the high-quality beans produced in the region, Plang Yai community enterprises primarily sell roasted coffee beans, limiting their access to broader consumer markets.

While roasted coffee bean generally provide better aroma and flavor, the preparation requires grinding and brewing before consumption. This might not suitable to all potential customers. Many consumers, especially those seeking convenience, prefer instant coffee products that are ready to use. Freeze drying, also known as lyophilization, is a dehydration technique that involves freezing a material and then removing its moisture by sublimation under low pressure. This method is widely used in food processing due to its ability to preserve the structure, aroma, and nutrients of food products, making it particularly suitable for high-value commodities such as coffee (Bhatta et al., 2020). Compared to traditional drying methods, freeze drying minimizes heat exposure, which helps retain volatile compounds responsible for coffee's flavor and aroma (Rizzi, 2016). Additionally, freeze-dried coffee exhibits improved solubility and shelf life, making it a preferred choice for instant coffee production (Chen & Zhang, 2022).

Despite its benefits, freeze drying has limitations, including high operational costs and long processing times. To improve efficiency, foam-mat drying is often employed as a pre-treatment step. Foam-mat drying involves whipping the liquid coffee extract with a foaming agent to create a stable foam structure, which is then dried at a controlled temperature before undergoing freeze drying (Anandharamakrishnan, 2019). This technique reduces drying time, enhances rehydration properties, and helps maintain the microstructure of coffee particles (Liu & Kim, 2020). The foam structure allows for uniform drying, improving the overall quality of the final product (Kaya & He, 2018).

The stability and effectiveness of the foam-mat drying process largely depend on the choice of foaming agents, which help stabilize air bubbles and prevent foam collapse. Commonly used foaming agents include maltodextrin, whey protein isolate, and egg white powder. Maltodextrin acts as a carrier and stabilizer, reducing the stickiness of coffee powder and improving its solubility (Michael, 2023). Whey protein isolate contributes to foam formation by lowering surface tension, but on its own, it provides limited stability (Waghmare & Kumar, 2024). Egg white powder, on the other hand, is the most effective foaming agent due to its high protein content, which enhances foam stability by forming a strong protein network around air bubbles (Chatveera & Wongkamjan, 2001). Studies have shown that formulations containing a combination of these three agents, particularly with a higher proportion of egg white powder, result in the most stable foams, which is crucial for efficient freeze drying (Muthukumaran et al, 2021)

By integrating foam-mat drying and selecting appropriate foaming agents, freeze-dried coffee can be produced more efficiently while preserving its key sensory and functional properties. This approach provides a viable method for adding value to locally grown coffee, ensuring high-quality instant coffee production while supporting the local economy.

2. Methodology

2.1 Coffee extract preparation

The dark roasted coffee beans were received from the "Plang Yai" local community enterprise. The roasted coffee beans were ground to a particle size of 400–600 µm using a burr grinder (Mahlkönig EK43, Germany) to ensure uniform extraction. A ratio of 1:15 (coffee: water, w/v) was used for the extraction process. The ground coffee was brewed using a hot water extraction method at $92 \pm 2°C$ for 5 minutes. A coffee brewing system (Hario V60, Japan) was used to ensure uniform extraction. The brewed coffee was filtered using a 0.45 µm membrane filter (Millipore, USA) to remove any residual coffee grounds. The filtrate was immediately cooled to 4°C in an ice bath to prevent oxidation and degradation of volatile compounds. The cooled coffee extract was concentrated using a vacuum rotary evaporator (Büchi Rotavapor R-300, Switzerland) at 40°C under reduced pressure (100 mbar) until reaching a final total soluble solids (TSS) content of 20–25%. The TSS was measured using a hand refractometer.

2.2 Foam stability of foaming agents

Foam stability was evaluated by measuring the height of the foam over time. After preparing the foam using the optimized formulation, the generated foam was immediately transferred into a 50 mL beaker. The initial foam height (H_0) was recorded in millimeters (mm) using a ruler. Foam height was then measured at specific time intervals of 1, 5, 10, 15, and 30 minutes to assess the rate of foam collapse.

Foam stability was determined using the percentage of foam retained over time compared to the initial foam height (H_0). The foam stability percentage at a given time (H_t) was calculated using formula (1).

$$\text{Foam Stability}(\%)=(H_t/H_0) \times 100 \qquad (1)$$

where H_0 = Initial foam height, (mm)
            H_t = Foam height at a given time, (mm)

2.3 Freeze drying of coffee extract using foam-mat method

1) Optimization of Foam Formation in Coffee Extract Using Foaming Agents

A total of 10 treatments with various percentage of foaming agents were calculated as shown in table 1. The experiment began with weighing the required amount of egg white powder according to the specified formulation. Distilled water (175 mL) was then added to the egg white powder and mixed using a high-speed hand mixer for 2 minutes to initiate foam formation. After this initial foaming stage, the measured amounts of maltodextrin and whey isolate were incorporated into the foamed mixture, followed by an additional 2-minute mixing period to enhance foam stability. Once the foam was sufficiently developed, 30 mL of coffee extract was prepared separately and gently combined with the foamed mixture to ensure uniform dispersion without disrupting the foam structure. The final mixture was then transferred into a transparent storage container and placed in a freezer at a controlled temperature of -18°C to -20°C prior freeze-drying.

Table 1 Different percentages of foaming agents

Sample No.	Maltodextrin (%)	Whey Isolate (%)	Egg White Powder (%)
C1 (Blank)	0	0	0
C2	6.8	0	0
C3	0	6.8	0
C4	0	0	6.8
1	2	6	10
2	1.9	9.6	9.6
3	6.5	2.2	2.2
4	6	2	10
5	6	6	6
6	5.8	5.8	9.6
7	9.6	1.9	9.6
8	9.6	5.8	5.8
9	9.3	5.6	9.3
10	9.3	9.3	5.6

2) Freeze drying condition

The freeze-drying process was conducted using a vacuum freeze dryer (Food industry model, Kinetic Engineering Co., Ltd). The sample was initially frozen at -20.0°C for 60 minutes, with a ramp time of 20 minutes under atmospheric pressure (0.0 Pa vacuum). During the primary drying phase, the temperature was gradually increased to -20.0°C over 20 minutes, held for 60 minutes, then raised to -10.0°C over 20 minutes and maintained for

100 minutes, all under a vacuum of 20.0 Pa. In the secondary drying phase, the temperature was increased to +10.0°C over 20 minutes with a 100-minute hold time, then further increased to +40.0°C over 200 minutes, followed by a 1000-minute hold time, under 20.0 Pa vacuum. Finally, the temperature was maintained at +40.0°C for an additional 1000 minutes under the same vacuum conditions to ensure complete moisture removal. The dried coffee sample was then collected and stored in airtight containers at room temperature until further analysis.

2.4 SEM condition

The surface morphology of the samples was observed using a Scanning Electron Microscope (SEM, ThermoScientific: Prisma E). Imaging was performed at a high voltage (HV) of 10 kV with magnifications of 70× and 200× to examine the structural features of the samples.

3. Results and Discussion

3.1 Percentage of Foam stability with various foaming agents

The foam stability results reveal that the presence and composition of foaming agents significantly influence foam retention. The control samples (C1, C2, and C3) without egg white powder exhibited zero foam stability, indicating that maltodextrin and whey isolate alone do not contribute to foam formation. However, C4, which contained 6.8% egg white powder without other stabilizers, achieved a foam stability of 76.8%, demonstrating the critical role of egg white proteins in foam formation.

Among the tested formulations, sample 10 exhibited the highest foam stability at 96.1%, followed closely by sample 9 (94.3%) and sample 7 (92.3%). These samples contained a relatively high proportion of all three foaming agents, with maltodextrin and egg white powder concentrations ranging from 5.6% to 9.6%. This suggests that optimal foam stability is achieved when all three components are present in appropriate proportions, particularly when egg white powder is maintained above 5%.

Moderate stability was observed in samples with lower total foaming agent concentrations, such as sample 5 (70.2%) and sample 4 (67.3%), where maltodextrin and whey isolate were present in smaller amounts alongside egg white powder. Notably, sample 3, which contained a higher proportion of maltodextrin (6.5%) but minimal egg white powder (2.2%), resulted in the lowest stability (54%), indicating that excessive maltodextrin without sufficient protein-based stabilizers negatively affects foam retention.

Overall, these findings confirm that egg white powder plays a fundamental role in foam formation, while the combination of maltodextrin and whey isolate further enhances stability when used in balanced ratios. The highest foam stability (above 90%) was consistently observed in formulations with all three foaming agents present at relatively high levels, reinforcing the importance of ingredient synergy in optimizing foam retention.
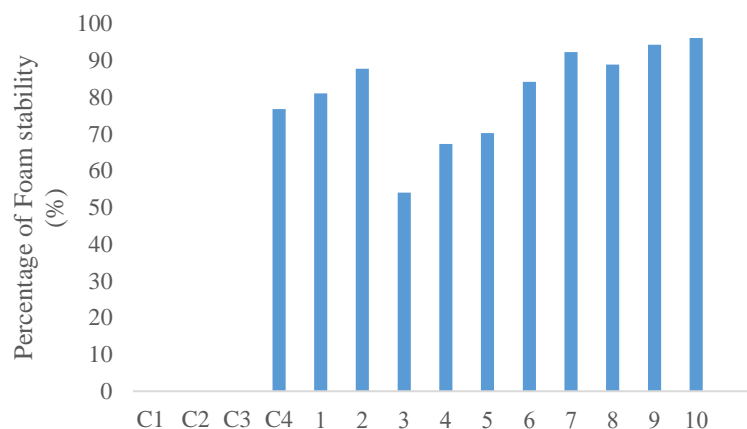
Figure 1 Percentage of foam stability

These results underscore a critical synergistic effect wherein maltodextrin and whey isolate act as structural and stabilizing agents rather than foaming initiators. The supporting evidence from Ganaie et al. (2021) illustrates that whey protein conjugated with maltodextrin via Maillard reactions enhances functional properties like emulsification and solubility—traits beneficial for foam stabilization under processing stress. Similarly, Xiang et al. (2021) showed that combining whey protein and maltodextrin through freeze-drying significantly improved the stability of encapsulated probiotics, a phenomenon that parallels the improved foam integrity observed in multi-agent systems. Moreover, the formulation containing 6.5% maltodextrin with only 2.2% egg white powder resulted in the lowest foam stability (54%), reinforcing the idea that an excessive carbohydrate component without adequate protein undermines the interfacial strength needed to retain air bubbles. This is supported by findings in Poopan et al. (2024), where maltodextrin beyond 5% did not enhance bioactive retention unless paired with protein-rich compounds. The synergistic effect between these components where protein unfolding at interfaces, viscosity increase from carbohydrates, and potential Maillard reaction contributions suggested a multi-level mechanism where protein content contributed to foam formation, and carbohydrate-protein interactions stabilize the formed structure.

3.2 Observation of Physical Appearance of Freeze-dried coffee samples using Scanning Electron Microscope (SEM)

SEM analysis revealed that foam morphology was significantly influenced by the relative concentrations of maltodextrin (MD), whey protein isolate (WPI), and egg white powder (EWP) (Figure 2). Among the control samples, C1 (without foaming agents) exhibited a compact, non-porous structure, serving as a reference for non-aerated material. C2, which contained only MD, produced a fine but shallow porous structure. While MD contributed to a more viscous medium, its ability to generate or maintain foam structures was limited, consistent with its role as a bulking and film-forming agent rather than a foaming agent (Ratti, 2001). In contrast, C3 (WPI only) showed larger, less uniform pores with some collapse, illustrating that while WPI facilitates foam formation due to its amphiphilic nature, its foams are generally less stable without the presence of a secondary stabilizing agent (Dickinson, 2003). The most stable and uniform foam among the controls was observed in C4 (EWP only), characterized by well-defined, rounded pores. This agrees with prior studies citing EWP's superior surface activity and strong network formation at the air–water interface (Mine, 1995).

The experimental formulations presented a range of foam structures, from highly porous and interconnected matrices to dense, minimally foamed textures. Samples with a high proportion of EWP, particularly when combined with moderate amounts of WPI and low to mid-levels of MD, exhibited the most desirable foam properties. Sample 1, which included EWP at its highest ratio with supportive levels of WPI and MD, demonstrated a highly stable and porous foam with well-distributed, spherical pores. This highlights a synergistic interaction where WPI promotes foam expansion and EWP provides stabilization, while MD acts as a rheological modifier without inhibiting structure formation (Campbell & Mougeot, 1999). Similar to Sample 4, where EWP remained dominant despite higher MD content, resulting in well-maintained pore architecture. On the other hand, samples where MD was the dominant component, such as Samples 3, 7, and 8, showed denser structures with reduced porosity or evident pore collapse. This supports the notion that excessive MD impairs foam expansion by excessively increasing the viscosity of the continuous phase, which restricts air incorporation and foam elasticity (Ozcelik & Kulozik, 2023).

Comparative trends also suggest that a balanced mixture of all three agents, such as in Sample 5, produced stable foam structures with moderate pore size and uniformity. This formulation avoided the extremes of either over-stiffening from MD or collapse due to excessive protein content, offering a structurally coherent foam. Interestingly, when WPI was increased disproportionately, as seen in Sample 2, the structure showed signs of pore deformation and partial collapse, implying that although WPI enhances foam volume, it does not necessarily improve foam stability unless complemented by EWP. Similarly, in high-MD systems where EWP was present in moderate quantities (e.g., Sample 10), the presence of WPI appeared to mitigate structural degradation to a degree, although not as effectively as in EWP-rich formulations. Collectively, the data confirm that EWP plays a dominant role in foam stability and integrity, while WPI contributes to foamability and MD must be carefully regulated to avoid over-thickening the matrix (Raikos et al., 2007).
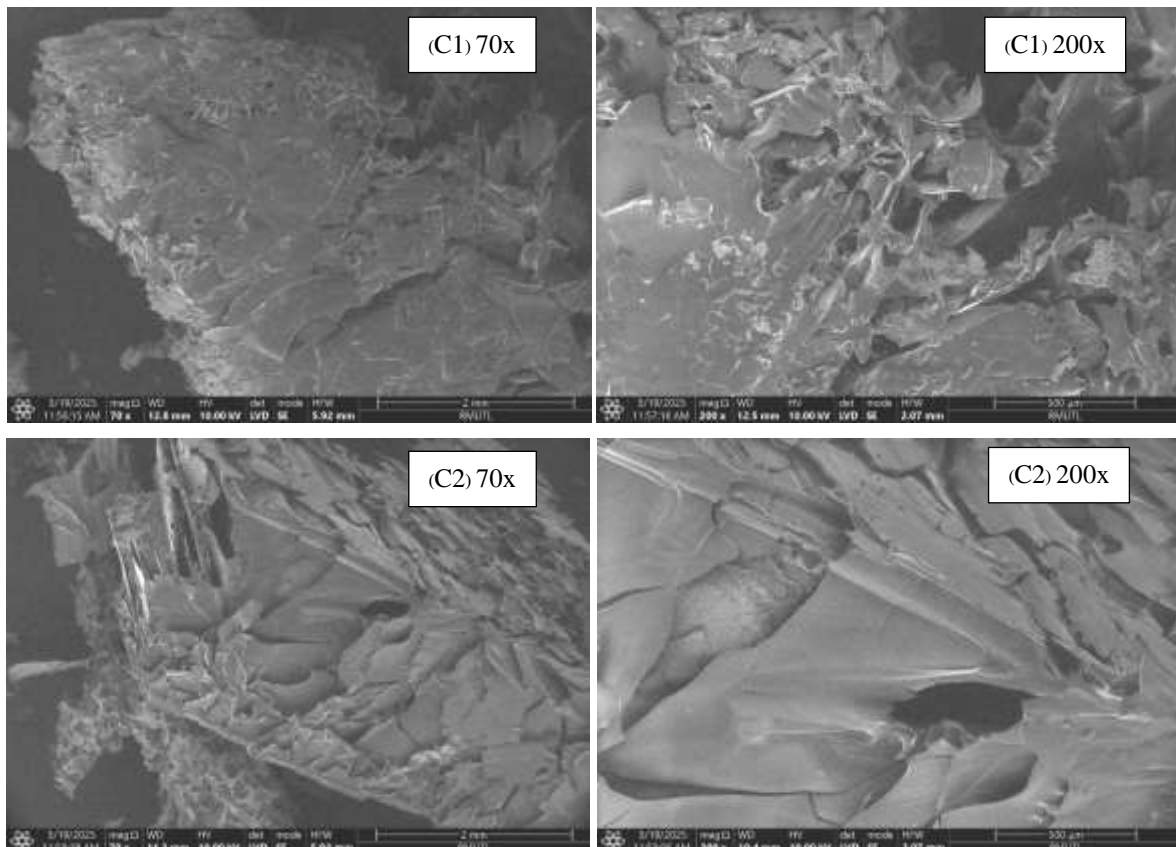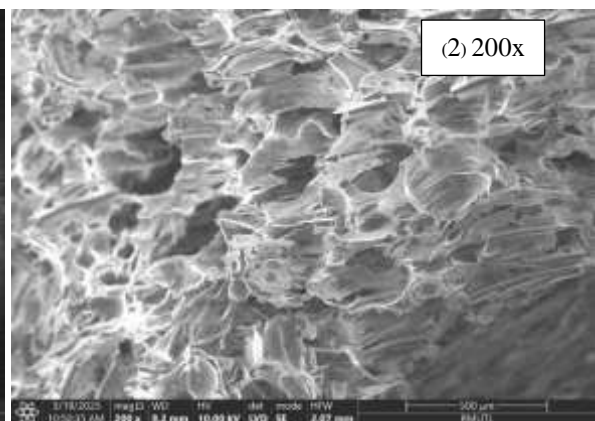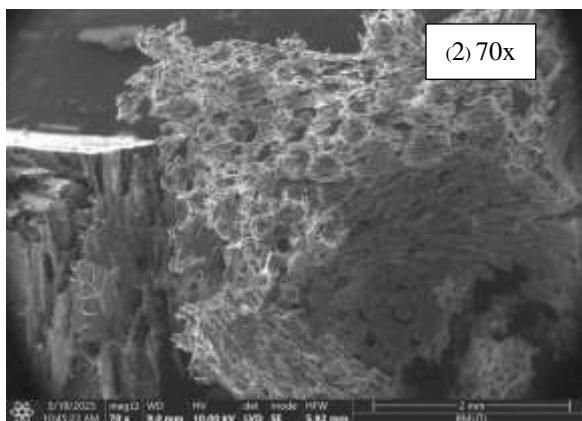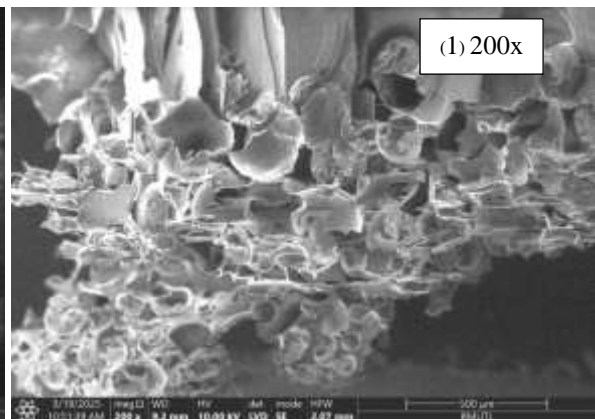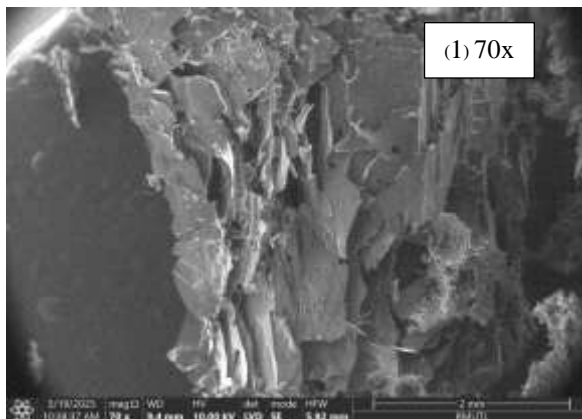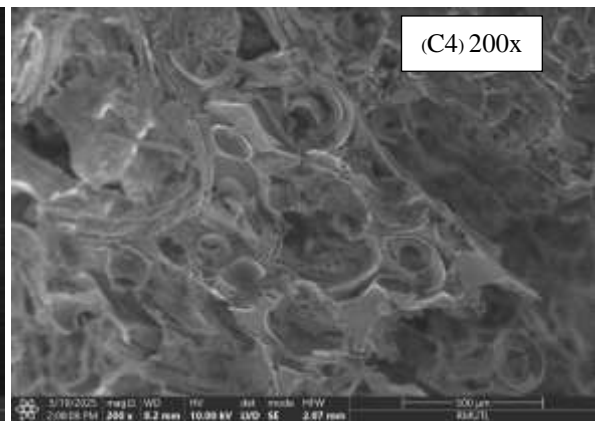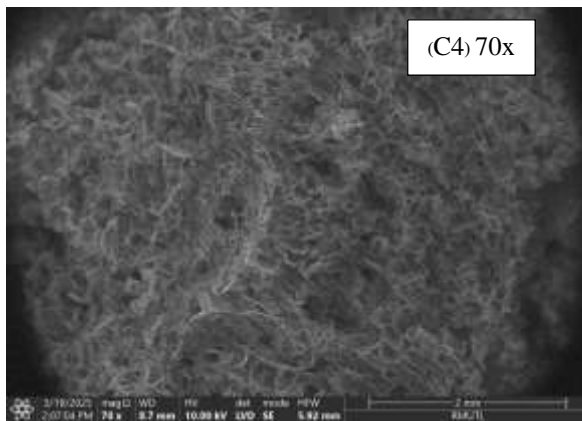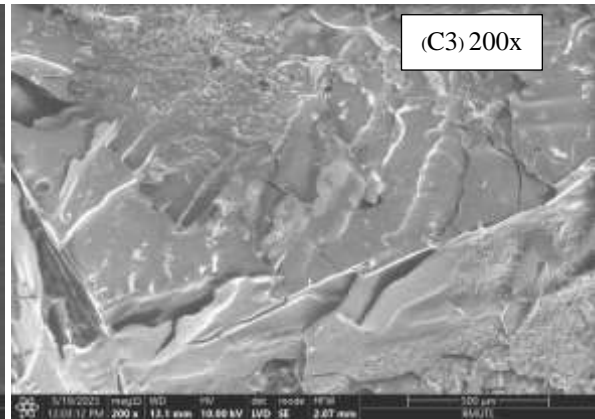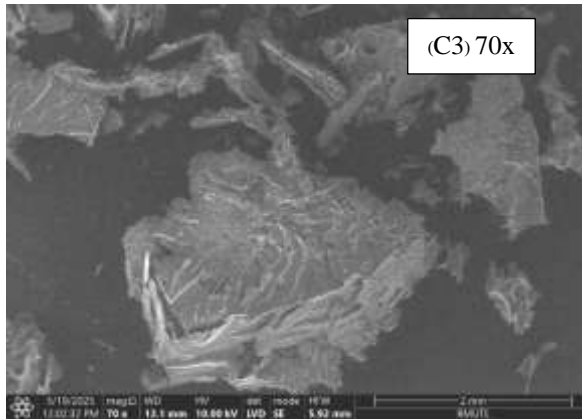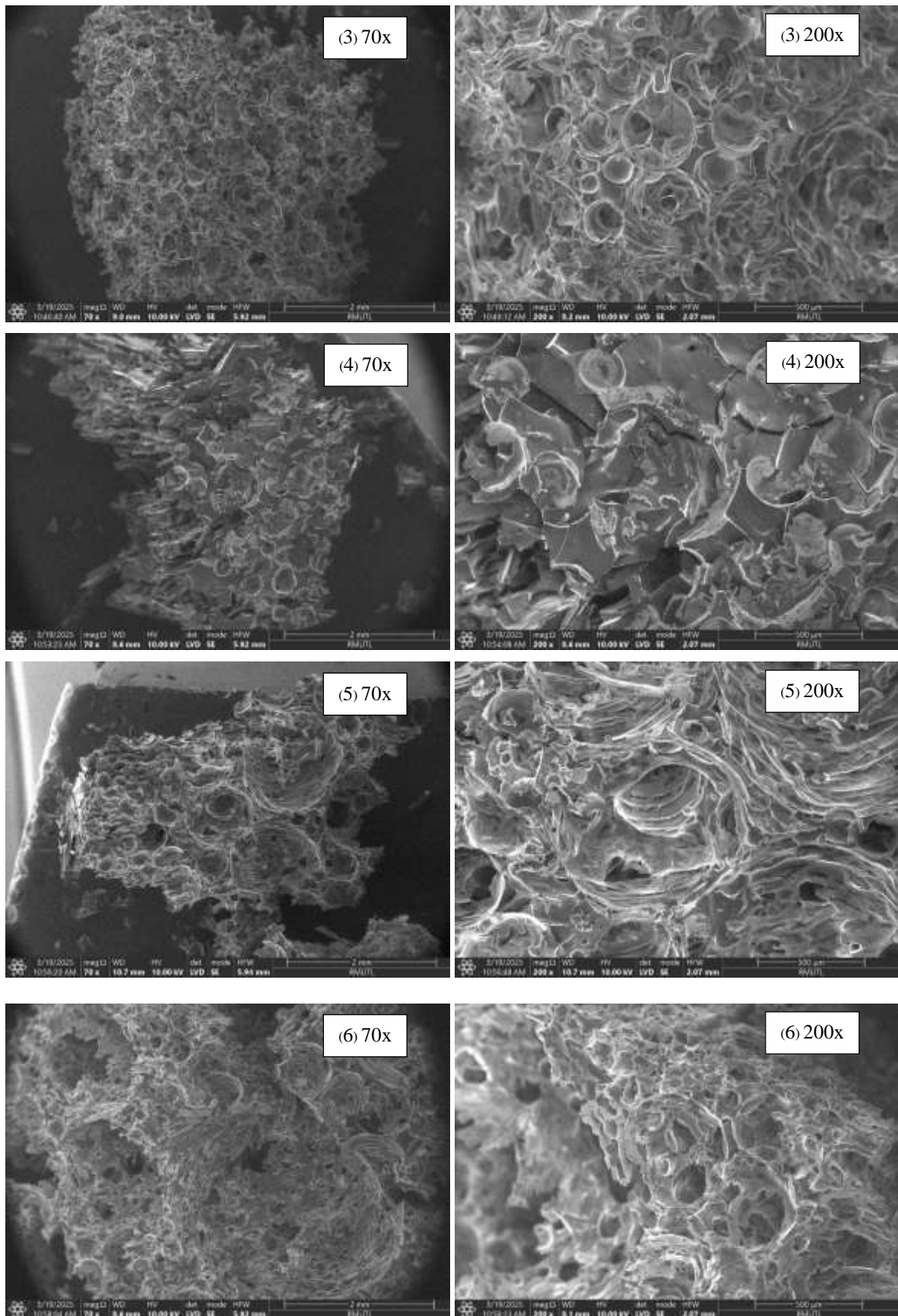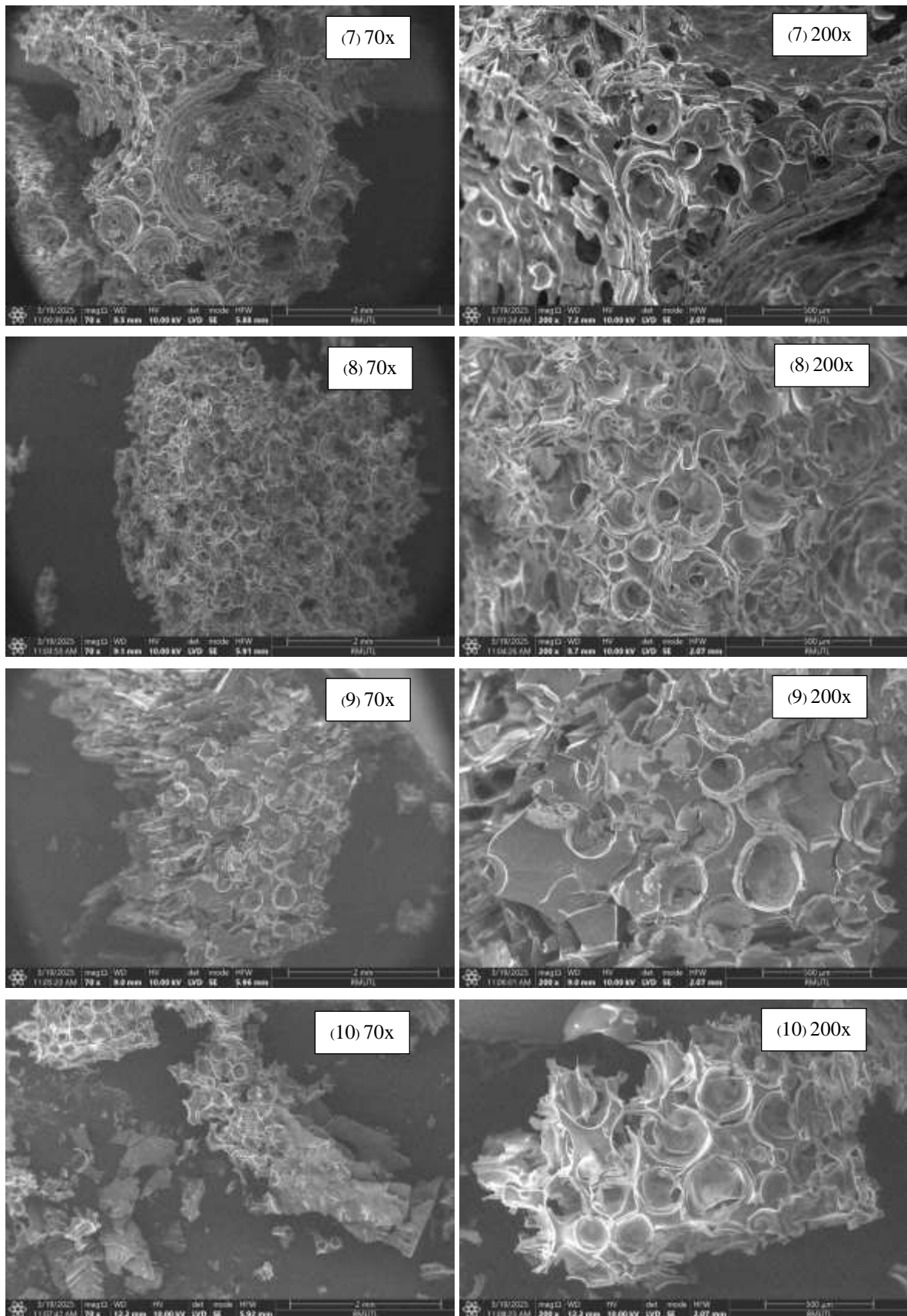
Figure 2 SEM images showing the surface structure and porosity of 14 samples with varying proportions of foaming agents at 70x and 200x magnification.

4. Conclusions

This study demonstrates that the selection and ratio of foaming agents significantly influence foam stability and microstructural integrity in freeze-dried coffee production using the foam-mat method. SEM analysis confirmed that formulations with higher concentrations of egg white powder yielded well-structured, stable foams with uniform pore distribution. Maltodextrin and whey protein isolate contributed to structural integrity and viscosity modulation but were ineffective as standalone foaming agents. The highest foam stability was achieved in samples containing balanced amounts of all three agents, particularly where egg white powder exceeded 5%. These findings underscore the synergistic role of protein-based foaming agents supported by carbohydrates in forming and stabilizing foam matrices during drying. The integration of foam-mat and freeze-drying techniques presents a viable approach to producing high-quality instant coffee while preserving aroma, solubility, and structure which will benefiting community enterprises like Plang Yai by enabling value-added processing of locally grown coffee.

5.Acknowledgements

6. References

Anandharamakrishnan, C. (2019). Spray-freeze-drying of coffee. *Caffeinated and Cocoa-Based Beverages, 1*(1), 1–10.

Bangkok Post. (2024). Coffee market posts healthy growth. *Bangkok Post, 1*(1), 1.

Bhatta, S., Stevanovic Janezic, T., & Ratti, C. (2020). Freeze-drying of plant-based foods. *Foods, 9*(1), 87.

Campbell, G. M., & Mougeot, E. (1999). Creation and characterisation of aerated food products. *Trends in Food Science & Technology, 10*(9), 283–296.

Chen, X., & Zhang, L. (2022). Comparison of freeze-dried and spray-dried coffee: Sensory and physicochemical properties. *Food Research International, 158*, 111577.

Dickinson, E. (2003). Interfacial, emulsifying and foaming properties of milk proteins. *Advanced Dairy Chemistry, 1*(3), 629–692.

Ganaie, T. A., Masoodi, F. A., Rather, S. A., & Gani, A. (2021). Exploiting maltodextrin and whey protein isolate as carriers for freeze-dried honey powder. *Carbohydrate Polymer Technologies and Applications, 2*(1), 100040.

Kaya, Z., & He, J. (2018). Optimization of freeze-drying conditions for coffee extract. *Journal of Food Engineering, 230*, 26–34.

Liu, Y., & Kim, J. (2020). Impact of freeze-drying on the microstructure of coffee particles. *Journal of Agricultural and Food Chemistry, 68*(12), 3409–3418.

Michael, M. (2023). Moisture optimization and heating process automation of freeze-dried coffee production (Master's thesis). *University of Twente, 1*(1), 1–60.

Mine, Y. (1995). Competitive adsorption of egg white proteins at the air–water interface. *Journal of Agricultural and Food Chemistry, 46*(3), 872–876.

Muthukumaran, A., Ratti, C., & Raghavan, V. G. S. (2021). Optimization of egg white foam stability in foam-mat freeze drying. *Journal of Food Engineering, 285*, 110092.

Poopan, B., Kasorn, A., Puttarat, N., Kasemwong, K., Pachekrepapol, U., & Taweechotipatr, M. (2024). Freeze drying microencapsulation using whey protein, maltodextrin and corn powder. *Korean Journal for Food Science of Animal Resources, 1*(1), 1–10.

Raikos, V., Dufresne, M., & McClements, D. J. (2007). Effect of protein type on the formation and stability of food foams. *Food Hydrocolloids, 21*(3), 345–354.

Ratti, C. (2001). Hot air and freeze-drying of high-value foods: A review. *Journal of Food Engineering, 49*(4), 311–319.

Rizzi, G. P. (2016). Volatile retention in freeze-dried coffee. *Food Chemistry, 210*, 585–591.

This Side Up. (2025). Thailand Beanspire. *This Side Up, 1*(1), 1.

Waghmare, R. B., & Kumar, M. (2024). Freeze-drying: Basic principles and processes. *Wiley Online Library, 1*(1), 1–20.

Xiang, J., Liu, F., Wang, B., Chen, L., Liu, W., & Tan, S. (2021). Maillard reaction based on milk proteins and carbohydrates in food and pharmaceuticals. *Foods, 10*(9), 1998.

Comparative Evaluation of Antioxidant Potential and Basic Chemical Properties of Thai Honeys from Four Floral Sources

Warawaran Shimbhanao[a*] Sureewan Rajchasom[b] Janyawat Tancharoenrat Vuttijamnong[a]
Veerin Peerathamrongrat[b] Maneerat Mueangjai[a] Phowpinyo Shimbhanao[b]

[a]*College of Integrated Science and Technology, Rajamangala University of Technology Lanna, Chiang Mai, Thailand 50300*
[b]*Faculty of Science and Agricultural Technology, Rajamangala University of Technology Lanna, Chiang Mai, Thailand 50300*
[c]*Faculty of Arts and Architecture, Rajamangala University of Technology Lanna, Chiang Mai, Thailand 50300*
Corresponding author email address: warawaran@rmutl.ac.th

Abstract

This study aimed to investigate the antioxidant activities and chemical compositions of honeys derived from four floral sources: coffee, lychee, longan, and Siam weed. Honey samples were collected from commercial honey producers in Chiangmai Thailand. The antioxidant activities were evaluated using FRAP and DPPH assays, while total phenolic content and chemical compositions, including total soluble solids (°Brix), total acidity, and pH, were also analyzed. The results showed that coffee flower honey exhibited the highest antioxidant capacity, with FRAP and DPPH inhibition values of 662.23 ± 0.42 µmol Fe^{2+}/100 g and $39.53\pm0.76\%$, respectively, along with a total phenolic content of 507.31 ± 1.69 mg GAE/kg. Lychee and longan honeys demonstrated similar moderate levels of antioxidant activity, whereas Siam weed honey showed the lowest values across all antioxidant parameters. In terms of chemical composition, coffee flower honey had the highest °Brix value (80.70 ± 0.26°Brix), while lychee honey exhibited the highest total acidity (21.25 ± 1.02 mEq/kg) and the lowest pH (3.40 ± 0.05). Siam weed honey presented the lowest total soluble solids and total phenolic content values, corresponding with its weak antioxidant properties. These findings indicate that coffee flower honey has the highest potential as a biologically valuable ingredient suitable for development into natural health supplements or beauty products. Lychee and longan honeys also demonstrated promising chemical and biological properties. This study provides essential baseline data for selecting high-value Thai honeys and for adding commercial value through product innovation.

Keywords: Honey, Floral Honey, Antioxidant Activity, Phenolic Compounds, Chemical Composition

1. Introduction

Honey is a natural product derived from the process in which bees collect nectar from flowers and store it in the honeycomb, where it undergoes both chemical and physical transformations. It ranges in color from light yellow to dark brown, has a viscous consistency, and possesses a sweet taste, which varies depending on the floral source specific to each region (Codex Alimentarius, 2001). Honey has long been popular as a health food in both nutritional and medicinal contexts. For example, honey consumption has been used to restore energy prior to athletic competitions (Eteraf-Oskouei and Najafi, 2013) and as a wound-healing agent due to its antibacterial properties (Nolan et al., 2019). Honey exhibits several notable natural properties, including antimicrobial activity, acidity, and the production of hydrogen peroxide, which contributes to pathogen inhibition (Albaridi et al., 2019). Moreover, honey contains beneficial nutrients such as natural sugars, vitamins, minerals, organic acids, and bioactive compounds like flavonoids and phenolic compounds, which play significant roles in antioxidant and anti-inflammatory activities (Al-Mamary et al., 2002; Samarghandian et al., 2017).

Due to these components, honey is recognized as one of the natural products possessing the properties of a functional food. It plays roles in promoting health, preventing diseases, and nourishing the body. It has been reported that consuming honey in appropriate amounts can help lower blood lipid levels, reduce blood pressure, and regulate blood sugar levels (Eteraf-Oskouei & Najafi, 2013). Additionally, honey exhibits immunomodulatory effects, supports gut microbiota balance, and reduces the risk of chronic diseases such as cardiovascular disease and cancer (Bogdanov et al., 2008).

Furthermore, honey possesses skincare properties due to its antioxidant activity, which helps protect cells from damage caused by ultraviolet radiation and slows down skin cell aging (Al-Mamary et al., 2002; Samarghandian et al., 2017). It also acts as a natural humectant that helps keep the skin soft and elastic (Samarghandian et al., 2017). These properties have contributed to the widespread popularity of honey as an ingredient in the development of health supplements, natural energy drinks, and personal care products for consumers who prioritize health and natural beauty.

Due to these special properties, honey has gained considerable attention in the health, beauty, and high-value product industries. In particular, honey produced from a single floral source (mono/unifloral honey) is highly popular and commands a higher market price than honey derived from multiple floral sources (multi/polyfloral honey), owing to its distinctive taste, aroma, and color characteristics that are widely accepted by consumers (Madras-Majewska et al., 2016). For example, Manuka honey, derived from the Manuka flower (Leptospermum Scoparium), a medicinal plant native to New Zealand, contains methylglyoxal, which exhibits significantly higher antimicrobial activity than

regular honey. This has resulted in Manuka honey being sold at a price many times higher than that of ordinary honey (Girma et al., 2019).

In Thailand, particularly in the northern region, honey is produced from various local plants, such as longan, lychee, coffee, and Siam weed flowers, which are key economic crops in the region. However, there is still a lack of systematic scientific studies on the chemical properties and biological activities of Thai honeys from different sources. This gap limits the ability to highlight the unique qualities of Thai honey and leverage them for commercial advantages, especially when compared to imported honeys that are supported by extensive research.

Honeys derived from different floral sources possess distinct chemical properties, including pH, total acidity, total soluble solids (°Brix), moisture content, reducing sugars, non-reducing sugars, as well as the quantity and type of phenolic compounds. These factors significantly influence the antioxidant activity and biological properties of honey (Truchado et al., 2010; Martos et al., 2000).

This study aims to investigate the antioxidant properties and chemical composition of honeys from four floral sources: coffee, lychee, longan, and Siam weed. The antioxidant activity was evaluated using the FRAP and DPPH inhibition assays, while the total phenolic content (TPC) was determined. Basic chemical parameters, including pH, total acidity, and °Brix, were also analyzed. The findings from this research will be valuable for selecting honeys with high potential for development into functional food supplements or natural products that meet the preferences of modern consumers who prioritize safety, health, and sustainability. Moreover, the results will contribute to promoting and enhancing the economic value and international trade competitiveness of Thai honey.

2. Methodology

Honey samples from four floral sources, including (1) longan flower honey, (2) lychee flower honey, (3) Siam weed flower honey, and (4) coffee flower honey, were obtained from producers in Chiang Mai Province, Thailand. Subsequently, the honey samples were analyzed for their antioxidant activities and chemical compositions as follows.

2.1 Determination of Antioxidant Activity by Ferric Reducing Antioxidant Power (FRAP)

The ferric reducing antioxidant power (FRAP) of the honey samples was determined following the method described by Benzie and Strain (1996) with slight modifications. The FRAP reagent was prepared by mixing acetate buffer (300 mM, pH 3.6), ferric chloride solution ($FeCl_3 \cdot 6H_2O$, 20 mM), and TPTZ solution (2,4,6-tripyridyl-s-triazine, 10 mM). A honey solution was prepared by dissolving 50 g of honey in distilled water and adjusting the volume to 100 mL to achieve a concentration of 0.5 g/mL (50% w/v). Subsequently, 0.2 mL of the honey solution was added to 1.5 mL of FRAP reagent, mixed thoroughly, and incubated at 37°C for 4 minutes. The absorbance was measured at 593 nm using a spectrophotometer (M509T, Spectronic Camspec Ltd, United Kingdom). All measurements were performed in triplicate using distilled water as a blank. The results were compared with a standard curve prepared from ferrous sulfate ($FeSO_4 \cdot 7H_2O$) solutions at concentrations of 300, 600, 900, 1500, and 2000 µg/mL in distilled water. The antioxidant capacity was expressed as micromoles of ferrous equivalents per 100 grams of honey (µmol Fe^{2+} equivalent/100 g honey).

2.2 Determination of Antioxidant Activity by DPPH Radical Scavenging Activity Assay

The antioxidant activity of the honey samples was evaluated using the DPPH radical scavenging assay, based on the method of Meda (2005) with slight modifications. A honey solution with a concentration of 0.3 g/mL (30% w/v) was prepared. The 2,2-diphenyl-1-picrylhydrazyl (DPPH) solution was prepared at a concentration of 0.1 mg/mL. Then, 0.75 mL of the honey solution was mixed with 1.5 mL of the DPPH solution using a vortex mixer. The mixture was left to stand for 15 minutes at room temperature. The absorbance was measured at 517 nm using a spectrophotometer. All measurements were performed in triplicate, using methanol as a blank. Ascorbic acid solutions at concentrations of 3, 5, 10, 20, and 50 µg/mL were used as positive controls. The percentage of DPPH inhibition (%inhibition) was calculated using the following equation:

$$\% \text{ inhibition } = ((\frac{A_{\text{control}} - A_{\text{sample}}}{A_{\text{control}}l}) \times 100$$

where A_{control} is the absorbance of the DPPH solution without the honey sample, and A_{sample} is the absorbance of the DPPH solution containing the honey sample.

2.3 Determination of Chemical Properties of Honey

The basic chemical properties of the honey samples were analyzed as follows. The total soluble solids (°Brix) were measured using a digital hand refractometer (ATAGO, Japan) (AOAC, 2010). The pH was determined using a pH meter (AOAC, 2010). The total acidity was assessed by dissolving 10 g of honey in distilled water and adjusting the volume to 100 mL. A 20 mL aliquot of the resulting honey solution at a concentration of 0.1 g/mL (10% w/v) was titrated with 0.05 N sodium hydroxide (NaOH) until a pH of 8.50 was reached (AOAC, 2010). The total acidity was expressed in milliequivalents per kilogram (mEq/kg). All measurements were performed in triplicate.

2.4 Statistical Analysis

A completely randomized design (CRD) was used for the experimental design. Analysis of variance (ANOVA) was performed to assess differences between mean values, followed by a least significant difference (LSD) test at a 95% confidence level. Statistical analysis was conducted using SPSS software version 23 (SPSS Inc., USA).

3. Results and Discussion

3.1 Antioxidant Activities of Honeys from Different Floral Sources

The antioxidant activities of honey samples from four floral sources—longan flower, lychee flower, Siam weed, and coffee flower—are presented in Table 1. All honey samples exhibited statistically significant differences ($P \leq 0.05$) in FRAP values, percentage of DPPH radical inhibition (% inhibition), and total phenolic content (TPC). Coffee flower honey demonstrated the highest antioxidant activity, with a FRAP value of 662.23 ± 0.42 µmol Fe^{2+}/100 g and a DPPH inhibition of $39.53 \pm 0.76\%$. These values were higher than those of longan flower honey (459.59 ± 1.30 µmol Fe^{2+}/100 g; $37.96 \pm 0.43\%$) and lychee flower honey (575.90 ± 1.52 µmol Fe^{2+}/100 g; $36.36 \pm 2.03\%$). Longan and lychee honeys exhibited comparable antioxidant activities. In contrast, Siam weed honey showed the lowest values across all parameters, with a FRAP value of 224.58 ± 0.49 µmol Fe^{2+}/100 g and a DPPH inhibition of $21.84 \pm 0.91\%$. These results corresponded with the lowest total phenolic content in the group, indicating that Siam weed honey possessed markedly lower antioxidant properties compared to the other honey types.

When comparing the total phenolic content of the four floral honeys, it was observed that lychee, longan, and coffee flower honeys had similar levels of bioactive compounds, measured at 538.57 ± 9.36, 535.82 ± 2.89, and 507.31 ± 1.69 mg GAE/kg, respectively. In contrast, Siam weed honey exhibited the lowest total phenolic content at 323.63 ± 2.78 mg GAE/kg, which corresponded with its lowest antioxidant activities across all evaluated parameters.

According to Table 1, coffee flower honey exhibited significantly higher antioxidant activities than longan and lychee flower honeys, demonstrating outstanding potential among the honeys produced under standard processing conditions. This finding aligns with the report by Chua *et al.* (2013), which indicated that honey derived from coffee flowers possesses high levels of antioxidant compounds, including various organic acids and flavonoids known for their effective free radical scavenging properties. Longan and lychee flower honeys showed lower FRAP and DPPH inhibition values than coffee flower honey but had similar total phenolic contents. In contrast, Siam weed honey displayed the lowest antioxidant activities, corresponding to its lowest total phenolic content among the samples.

These results were also consistent with the findings of Sudno *et al.* (2018), who investigated honeys from longan, lychee, and wildflowers and found that longan flower honey contained higher levels of ascorbic acid and phenolic compounds, along with significantly greater DPPH inhibition compared to other honey types. This reflects the direct influence of the floral source on the antioxidant activity of honey. When comparing the antioxidant properties of honeys derived from coffee, longan, lychee, and Siam weed flowers, coffee flower honey exhibited the highest antioxidant activity, which corresponded to its higher phenolic and flavonoid contents. These findings support the reports of Gül and Pehlivan (2018), which stated that polyphenols and flavonoids are the primary components enhancing the antioxidant potential of honey due to their electron-donating properties and their ability to inhibit oxidation reactions in biological systems. Similarly, Biluca *et al.* (2017) identified polyphenols as key contributors to the antioxidant capacity of honey.

The findings of this study demonstrated that honeys derived from the four floral sources—coffee, lychee, longan, and Siam weed—exhibited significantly different antioxidant activities. Coffee flower honey presented the highest antioxidant activity, surpassing those of longan and lychee honeys. Longan and lychee honeys displayed similar antioxidant capacities, while Siam weed honey showed the lowest antioxidant activity across all parameters. These results were consistent with the lower phenolic and flavonoid contents observed in Siam weed honey. This study provides fundamental information for selecting honey sources with high antioxidant potential for the development of health supplements or beauty products, which are increasingly popular among consumers seeking natural beauty solutions. Notably, coffee flower honey demonstrated superior potential and is domestically produced, making it a valuable raw material with promising commercial applications.

Table 1 Antioxidant activities of honeys from different floral sources.

Honey sample	Antioxidant Activity		
	FRAP value (µmol Fe^{2+} equivalent / 100 g honey)	DPPH inhibition (%)	Total Phenolic Content (mg GAE / kg honey)
Longan flower honey	459.59±1.30[c]	37.96±0.43[b]	535.82±2.89[a]
Siam weed honey	224.58±0.49[d]	21.84±0.91[c]	323.63±2.78[b]
Lychee flower honey	575.90±1.52[b]	36.36±2.03[b]	538.57±9.36[a]
Coffee flower honey	662.23±0.42[a]	39.53±0.76[a]	507.31±1.69[ab]

- Values are presented as mean ± standard deviation from triplicate determinations.
- Means with different superscript letters within each column indicate statistically significant differences at a 95% confidence level ($P \leq 05$).

3.2 *Chemical Properties of Honeys from Different Floral Sources*

From Table 2, honeys derived from longan, Siam weed, lychee, and coffee flowers exhibited significantly different chemical properties, including total soluble solids (°Brix), total acidity, and pH values ($P \leq 0.05$). The results showed that coffee flower honey had the highest total soluble solids at 80.70±0.16°Brix, followed by lychee flower honey and longan flower honey, which had values of 79.67±0.12 and 79.57±0.12°Brix, respectively. In contrast, Siam weed honey exhibited the lowest total soluble solids at 76.30±0.16°Brix.

The results also revealed that the four types of honey exhibited statistically significant differences ($P \leq 0.05$) in both total acidity and pH values. Lychee flower honey showed the highest total acidity at 21.25±1.02 mEq/kg, which corresponded to the lowest pH value of 3.40±0.05, indicating the most pronounced acidity. Following this, longan flower honey presented moderate acidity (20.17±0.47 mEq/kg) with a pH of 3.49±0.05. In contrast, Siam weed and coffee flower honeys demonstrated the lowest acidity levels at 16.92±0.51 and 16.75±0.54 mEq/kg, respectively, which corresponded to the highest pH values of 3.75±0.01 and 3.82±0.01. These findings reflect a consistent relationship between total acidity and pH among the honey samples.

The chemical properties of honey, such as total soluble solids, total acidity, and pH, are important indicators of quality, stability, and suitability for developing functional food and cosmetic products. The total soluble solids reflect the sugar content, which influences viscosity, taste, and storage potential. High-quality honey should have a total soluble solid content of no less than 80°Brix, according to the Codex Alimentarius Commission (2001) and the Thai Community Product Standard (TCPS 290/2547) (Thai Industrial Standards Institute, 2004). The results indicated that the three honey types—longan, lychee, and coffee flower honeys—had total soluble solid values close to 80°Brix. Although the Siam weed honey exhibited a slightly lower °Brix value, it still fell within an acceptable range.

Acidity is a key factor that correlates with taste, microbial inhibition, and chemical reactions in honey products. Generally, honey with higher acidity tends to exhibit better antimicrobial properties (Estevinho *et al*., 2008). The experimental results revealed that lychee and longan flower honeys had the highest total acidity levels, consistent with the antimicrobial properties of these honey types as reported in several previous studies (Molan, 1992).

Acidity is also an important parameter associated with taste, microbial inhibition, and chemical reactions in honey products. Typically, honey with higher acidity tends to have a stronger ability to inhibit microbial growth (Estevinho *et al*., 2008). The pH value plays a significant role in controlling microbial growth and chemical reactions, such as browning reactions and enzymatic changes. Lower pH levels generally help slow product spoilage (Bogdanov *et al*., 2008). The lychee and longan flower honeys, which exhibited the highest total acidity levels, reflected pronounced acidity and potentially enhanced antimicrobial activity and product stability. In contrast, coffee and Siam weed honeys, with the lowest acidity values, indicated milder acidity, which might correspond to lower antimicrobial potential and could affect chemical stability and storage properties. These differences may be related to the types of nectar from the source plants and the processing methods.

The findings of this study demonstrated that the four types of floral honeys exhibited significantly different chemical compositions. The total soluble solids (°Brix) of all honey samples ranged within acceptable international standards, especially longan, lychee, coffee, and Siam weed honeys, which showed values close to the 80 °Brix benchmark established by the Codex Alimentarius Commission (2001) and the Thai Community Product Standard (TCPS 290/2547) (Thai Industrial Standards Institute, 2004). Although the total soluble solid of Siam weed honey was slightly below 80 °Brix, it remained within an acceptable range. Lychee flower honey, which exhibited the highest total acidity and the lowest pH among the samples, indicated pronounced acidity, which may contribute to its antimicrobial activity and product stability. Longan flower honey showed moderately high acidity. Meanwhile, coffee and Siam weed honeys, which had the lowest acidity levels, reflected the mildest acidity, suggesting lower antimicrobial potential and potentially influencing chemical stability and storage properties. These results provide essential data for selecting honey types suitable for developing health supplement and cosmetic products, particularly lychee and longan flower honeys, which exhibited favorable chemical properties in several aspects.

Table 2 Chemical properties of honeys from different floral sources.

Honey Sample	Chemical properties		
	Total Soluble Solid (°Brix)	Total Acidity (mEq/kg)	pH Value
Longan flower honey	79.57±0.12[b]	20.17±0.47[ab]	3.49±0.05[c]
Siam weed honey	76.30±0.16[c]	16.92±0.51[b]	3.75±0.01[b]
Lychee flower honey	79.67±0.12[b]	21.25±1.02[a]	3.40±0.05[d]
Coffee flower honey	80.70±0.16[a]	16.75±0.54[b]	3.82±0.01[a]

- Values are presented as mean ± standard deviation from triplicate determinations.
- Means with different superscript letters within each column indicate statistically significant differences at a 95% confidence level ($P \leq 0.05$); ns means no significant difference ($P > .05$).

4. Conclusion

The study revealed that honeys derived from four floral sources—coffee flower, lychee flower, longan flower, and Siam weed—exhibited distinct antioxidant activities and chemical compositions. Coffee flower honey demonstrated the highest antioxidant activity, as indicated by both FRAP and DPPH inhibition values. In contrast, Siam weed honey showed the lowest values across all parameters, including the total phenolic content, which corresponded with its minimal antioxidant activity. Lychee and longan flower honeys exhibited moderate antioxidant activities at comparable levels. However, lychee flower honey presented the highest total acidity and the lowest pH value. The total soluble solids (°Brix) values for all honey types were within the acceptable standard range. The findings from this study provide essential baseline data for selecting honey from floral sources with high potential for the development of functional food supplements or natural beauty products. Notably, coffee flower honey, with its outstanding antioxidant properties and domestic availability, represents a valuable raw material with high market potential and opportunities for commercial advancement in the future.

5. Acknowledgements

6. References

Albaridi, N. A. (2019). Antibacterial potency of honey. *International Journal of Microbiology*, Article ID 2464507. https://doi.org/10.1155/2019/2464507

Al-Mamary, M., Al-Meeri, A., & Al-Habori, M. (2002). Antioxidant activities and total phenolics of different types of honey. *Nutrition Research, 22*(9), 1041–1047.

AOAC. (2010). *Official methods of analysis of AOAC International* (18th ed.). Gaithersburg, MD, USA: AOAC International.

Baltrusaityte, V., Venskutonis, P. R., & Ceksteryte, V. (2007). Radical scavenging activity of different floral origin honey and beebread phenolic extracts. *Food Chemistry, 101*(2), 502–514. https://doi.org/10.1016/j.foodchem.2006.02.049

Benzie, I. F., & Strain, J. J. (1996). The ferric reducing ability of plasma (FRAP) as a measure of antioxidant power: The FRAP assay. *Analytical Biochemistry, 239*(1), 70–76. https://doi.org/10.1006/abio.1996.0292

Bogdanov, S., Jurendic, T., Sieber, R., & Gallmann, P. (2008). Honey for nutrition and health: A review. *Journal of the American College of Nutrition, 27*(6), 677–689.

Cacu, M., Minda, D., Moldovan, R., Glevitzky, M., Cioca, G., & Bobis, O. (2021). Antioxidant capacity and phenolic profile of Romanian honey varieties. *Molecules, 26*(11), 3444. https://doi.org/10.3390/molecules26113444

Chua, L. S., Rahaman, N. L. A., Adnan, N. A., & Tan, T. T. E. (2013). Antioxidant activity of three honey samples in relation with their biochemical components. *Journal of Analytical Methods in Chemistry*, Article 313798. https://doi.org/10.1155/2013/313798

Codex Alimentarius Commission. (2001). *Revised codex standard for honey: CODEX STAN 12-1981 (Rev. 1)*. Rome, Italy: Food and Agriculture Organization of the United Nations/World Health Organization. Retrieved from http://www.fao.org

Estevinho, L. M., Pereira, A. P., Moreira, L., Dias, L. G., & Estevinho, A. (2008). Antioxidant and antimicrobial effects of phenolic compounds extracted from honey. *Food and Chemical Toxicology, 46*(12), 3774–3779.

Eteraf-Oskouei, T., & Najafi, M. (2013). Traditional and modern uses of natural honey in human diseases: A review. *Iranian Journal of Basic Medical Sciences, 16*(6), 731–742.

Girma, A., Seo, W., & She, R. C. (2019). Antibacterial properties of honey: A review. *BMC Complementary and Alternative Medicine, 19*(1), 57. https://doi.org/10.1186/s12906-019-2434-8

Gül, A., & Pehlivan, T. (2018). Antioxidant activities of some monofloral honey types produced across Turkey. *Saudi Journal of Biological Sciences, 25*(6), 1056–1065. https://doi.org/10.1016/j.sjbs.2018.02.011

Madras-Majewska, B., Rybak-Chmielewska, H., & Teper, D. (2016). Effect of storage on physicochemical properties and antioxidant activity of honeys of different floral origins. *Food Chemistry, 215*, 162–167.

Martos, I., Ferreres, F., & Tomás-Barberán, F. A. (2000). Identification of flavonoid markers for the botanical origin of Eucalyptus honey. *Journal of Agricultural and Food Chemistry, 48*(5), 1498–1502.

Meda, A., Lamien, C. E., Romito, M., Millogo, J., & Nacoulma, O. G. (2005). Determination of the total phenolic, flavonoid and proline contents in Burkina Fasan honey, as well as their radical scavenging activity. *Food Chemistry, 91*(3), 571–577. https://doi.org/10.1016/j.foodchem.2004.10.006

Molan, P. C. (1992). The antibacterial activity of honey. 1. The nature of the antibacterial activity. *Bee World, 73*(1), 5–28. https://doi.org/10.1080/0005772X.1992.11099109

Moniruzzaman, M., Khalil, M. I., Sulaiman, S. A., & Gan, S. H. (2014). Physicochemical and antioxidant properties of Malaysian honeys produced by *Apis cerana*, *Apis dorsata* and *Apis mellifera*. *BMC Complementary and Alternative Medicine, 14*, 43. https://doi.org/10.1186/1472-6882-14-43

Nolan, V. C., Harrison, J., & Cox, J. A. (2019). Dissecting the antimicrobial composition of honey. *Antibiotics, 8*(4), 251. https://doi.org/10.3390/antibiotics8040251

Peters, S. J., O'Connor, C. J., & Norris, J. E. (2013). Honey chemistry: Composition and properties. In D. M. Sabatini (Ed.), *Handbook of Honey Analysis* (pp. 1–27). London: Academic Press.

Rohman, A., Helmiyati, S., Hapsari, M., & Setyaningrum, D. L. (2009). Fourier transform infrared (FTIR) spectroscopy analysis of pure honey and adulterated honey. *International Food Research Journal, 18*(3), 867–875.

Samarghandian, S., Farkhondeh, T., & Samini, F. (2017). Honey and health: A review of recent clinical research. *Pharmacognosy Research, 9*(2), 121–127.

Sudno, P., Jaikam, P., & Suwan, P. (2018). Effects of honey from different floral sources on antioxidant properties. *Journal of Science and Technology, Udon Thani Rajabhat University, 6*(2), 29–42.

Thai Industrial Standards Institute. (2004). *Community Product Standard: Honey (TCPS 290/2004)*. Bangkok: Ministry of Industry.

Truchado, P., Ferreres, F., & Tomás-Barberán, F. A. (2010). Liquid chromatography-tandem mass spectrometry reveals the widespread occurrence of flavonoid glycosides in honey, and their potential as floral origin markers. *Journal of Chromatography A, 1216*(43), 7241–7248.

Wright, G. A., Baker, D. D., Palmer, M. J., Stabler, D., Mustard, J. A., Power, E. F., Borland, A. M., & Stevenson, P. C. (2013). Caffeine in floral nectar enhances a pollinator's memory of reward. *Science, 339*(6124), 1202–1204. https://doi.org/10.1126/science.1228806

Enhancing Protein and Functional Properties of Gluten-Free Black Rice Flour and Tapioca Starch Pasta Fortified with Chicken Meat

Supuksorn Masavang[a], Duangkamol Tungsatitporn[a*],
Kasarin Pedcharat[a], Chompoonuch Phuenpipob[a], Tinnapop Sompong[b]

[a] Department of Food Technology, Faculty of Home Economics Technology, Rajamangala University of Technology Phra Nakhon, Bangkok, 10300, Thailand
[b] Master of Home Economics, Faculty of Home Economics Technology, Rajamangala University of Technology Phra Nakhon, 10300, Thailand
*Corresponding author. Tel.: 0807704347; E-mail address: duangkamol.t@rmutp.ac.th

Abstract

This study investigated the effect of chicken meat fortification on the color, cooking quality, antioxidant properties, texture, proximate composition, and sensory characteristics of gluten-free pasta made with black glutinous rice flour and tapioca starch. Chicken meat incorporation significantly influenced the color values (L*, a*, and b*), with higher chicken meat content resulting in darker and more intense color due to the anthocyanins in black glutinous rice (p<.05). As chicken meat content increased, pasta exhibited longer cooking times, higher water absorption, and decreased cooking loss and volume expansion, indicating slower starch swelling and gelatinization (p<.05). Antioxidant activity, total phenolic compounds, and anthocyanin content were higher in chicken-fortified pasta compared to the control, but decreased as the chicken meat content increased. Textural analysis revealed that pasta containing higher levels of chicken meat exhibited reduced hardness, cohesiveness, springiness, gumminess, and chewiness. Proximate composition showed significant increases in protein, fat, and ash content, while crude fiber decreased with higher meat incorporation (p<.05). Sensory evaluation demonstrated that pasta with 20% chicken meat was the most acceptable in terms of appearance, odor, and taste. Overall, the study indicates that fortifying gluten-free pasta with chicken meat enhances nutritional properties but may affect sensory attributes, with 20% chicken meat being the most preferred variation.

Keywords: Gluten-free Pasta, Chicken Meat, Glutinous Black Rice Flour, Tapioca Starch

1. Introduction

Traditionally, pasta is made from wheat semolina flour, water, egg and optional ingredients which play a crucial role in determining its quality (Sissons, 2022). In recent years, significant efforts have been made to develop gluten-free alternatives by removing gluten from cereal-based products such as bread, biscuits, pasta, and cakes. This is achieved by substituting gluten-containing grains with other cereals and tubers. However, the absence of gluten presents a major challenge, particularly in retaining the desired texture of gluten-free products (Scarton et al., 2022). One approach is to use wheat substitutes, such as rice flour, sago starch, chickpea flour, and tapioca starch, to produce gluten-free pasta with improved nutritional profiles by diverse protein (egg, fish, shrimp, and legumes). In addition, the incorporation with specific ingredients, such as xanthan gum, hydroxypropyl methylcellulose, into the conventional formulation to enhance the functional properties, texture, and taste of gluten-free pasta (da Silva Ramos et al., 2023).

Black glutinous rice (Oryza sativa Linn. Var. glutinosa) is an indigenous Thai variety of glutinous rice, distinguished by the purple pigments found in its husk and pericarp. The bran hull of black rice is rich in bioactive compounds such as γ-oryzanol, phenolics, anthocyanins, and flavonoids, which contribute to improving lipid profiles, providing anti-inflammatory and anticancer properties, and reducing oxidative stress (Poonia and Pandey, 2021). As a result, black rice has attracted significant attention as a valuable raw material for the development of commercial health food products and supplements (Phonsakhan and Kong-Ngern, 2015). Previous research has explored the use of black rice flour as a gluten-free ingredient to enhance the nutritional value and bioactive properties of food products such as noodle (Kong et al., 2012) and pasta (Musika et al., 2024; Subanmanee et al., 2024). Gluten free rice noodles having resistant starch, inulin, and defatted rice bran (5%, w/w) significantly (p < 0.05) decreased the glycemic index and increased the cooking time and firmness (Raungrusmee et al., 2020). Sirichokworrakit et al. (2015) found that substitution of wheat flour with Riceberry flour decreased the stickiness, water absorption, cooking time and breaking length, while increasing the cooking loss and tensile strength of the cooked noodles. The replacement of Riceberry flour in wheat flour by up to 30% provided similar quality and a pleasant appearance as regular wheat noodle (Sirichokworrakit et al., 2015).

Tapioca starch, widely produced in Thailand, is a potential substitute for wheat flour but remains underutilized in the food industry. It is typically used in small proportions in gluten-free products, often blended with other flours for celiac diets (Yilmaz et al., 2015). Several studies have explored its application in gluten-free products, such as protein-enriched pasta with egg albumin (Milde et al., 2021), xanthan gum-enhanced gluten-free pasta (Milde et al., 2020), and pasta made from banana flour with added egg white and soy protein (Rachman et al., 2020). However, further research is needed to optimize tapioca starch formulations for better quality gluten-free products.

Many studies have reported that gluten-free products tend to be more brittle during cooking and exhibit undesirable texture, flavor, and color. These issues primarily stem from the absence of a gluten network, which plays a crucial role in dough elasticity and structure. Additionally, replacing wheat flour with alternative cereals or tubers does not necessarily improve the qualities of gluten-free products (Scarton et al., 2022). The lack of gluten results in

fragile, crumbly dough with poor processability, posing a significant challenge for the food industry (Cai et al., 2016). Therefore, various methods have been studied to improve the quality of gluten-free pasta. One effective approach is the incorporation of hydrocolloids with alternative starches in gluten-free pasta, such as xanthan gum (Milde et al., 2020), guar gum (Sanguinetti et al., 2015), and hydroxypropyl methylcellulose (Susanna & Prabhasankar, 2013; Norma et al., 2024), which help enhance dough structure and texture.

Food fortification is an essential element in nutrition strategies to alleviate micronutrient deficiencies. by adding essential nutrients, such as vitamins and minerals, to address dietary deficiencies (Olson et al., 2021). Chicken meat has long been a staple in human diets, and recent trends show a growing interest in incorporating meat into various food products. Poultry meat plays a crucial role in human nutrition due to its high nutritional value. Both its composition and organoleptic properties are essential to consumers and the meat industry alike. Chicken meat is a highly versatile, nutrient-dense, and affordable protein source, rich in essential vitamins and minerals while being lower in calories and cholesterol than red meat. According to Smithe et al. (2012), the nutritional composition of chicken breast meat includes 69.8 ± 0.3% moisture, 29.1 ± 0.3% protein, 0.9±0.1% lipid, and 2.9 ± 0.3% ash. Additionally, chicken is one of the most widely consumed meats globally, as it is free from religious and cultural restrictions. Various intrinsic and extrinsic factors can influence its nutritional composition and sensory characteristics Hailemariam et al., (2022). Previous studies have investigated the use of chicken meat as an alternative protein source in different food applications, including bread (Cakmak et al., 2013), crispy bread snacks (Cakmak et al., 2015), extruded chicken noodles with oat bran and konjac fibers (Liu et al., 2025), sago noodles (Verma et al., 2014), rice noodles (Lui et al., 2023). Among its potential applications, pasta stands out as a widely consumed, traditional cereal-based food. However, limited research has explored the fortification of rice-based pasta with minced chicken meat to enhance its protein content. While some studies have enriched pasta with alternative protein sources such as whey protein concentrate and fish powder (Gopalakrishnan et al., 2011), peas and soy isolate proteins, egg white, whey proteins, and Spirulina platensis (Messia et al., 2021), as well as cricket powder (Musika et al., 2024), further research is needed to assess the potential of chicken-fortified pasta.

To address nutritional deficiencies, pasta can be consumed with protein-rich foods or enriched with protein-rich ingredients. In this study, a new gluten-free pasta product was developed using black glutinous rice and tapioca starch as alternatives to wheat. The objective was to evaluate the impact of adding chicken meat, a rich source of nutrients, on the color, cooking qualities, chemical compositions (moisture, fat, protein, crude fiber, and ash), texture characteristics and sensory attributes (appearance, color, flavor, texture, and overall acceptability) of chicken-fortified pasta made from black glutinous rice flour and tapioca starch.

2. Methodology

2.1 Materials and pasta processing

All ingredients used for pasta elaboration were purchased in local markets, are national brands (Bangkok, Thailand). Doughs were elaborated using black glutinous rice flour (Fancy Carp Brand®, Charoenworakit Co., Ltd.) and tapioca starch (Red Cat Brand®, Kriangkrai Co., Ltd.) in 80:20 ratio, minced chicken breast (CP Fresh Mart), refined salt (Prung Thip®, Thai refined salt Co., Ltd.). Olive oil (Bertolli®, Deoleo)), and xanthan gum (Chemipan Corporation Co., Ltd.), were also used. To prepare the control pasta, all-purpose flour (KITE, United Flour Mill Public Co., Ltd.) and fresh whole eggs from the local market were hand-mixed with salt and olive oil. Water was gradually added until a smooth dough was formed. For chicken fortified pasta, black glutinous rice flour and tapioca starch, salt, xanthan gum and minced chicken meat were hand mixed. To this solid mixture, olive oil, and water were added until form homogeneous dough. Dough samples were processed using a pasta laminator machine (Pluselectric®, China), with the roller gap gradually reduced to approximately 1 mm. The dough sheet was then fed through the cutter attachment to produce 5 mm wide fettuccine strips. A Completely Randomized Design was used to incorporate minced chicken breast at three levels (10 g/100 g, 20 g/100 g, and 30 g/100 g) to create fortified pasta. The control pasta followed a conventional wheat flour formulation without chicken meat (0 g/100 g). Details of the chicken meat fortified pasta (CFP) formulation are provided in Table 1.

Table 1 Formulations of chicken meat fortified pasta (CFP) composed of black glutinous rice flour and tapioca starch in 80:20 ratio.

Ingredients (g/100 g)	Formulation			
	CFP 0	CFP 20	CFP 30	CFP 40
Black glutinous rice flour	-	58	50	42
Tapioca starch	-	15	13	11
Wheat starch	37	-	-	-
Whole egg fresh	20	-	-	-
Xanthan gum	-	3	3	3
Salt	1	1	1	1
Olive oil	3	3	3	3
Minced chicken breast	-	20	30	40
Water requirement (ml, approximately)	10	25.5	13.95	6.25

CFP 0: Control pasta, without chicken meat 0 g/100 g; CFP 20: pasta with 20 g/ 100 g chicken meat; CFP 30: pasta with 30 g/100 g chicken meat; CFP 40: pasta with 40 g/100 g chicken meat.

2.2 Color

The color values of the pasta were assessed using a portable colorimeter (Konica Minolta, Model CR-400, Japan) in reflectance mode, with standard D65 lighting and a 2-degree standard observer angle. The lightness (L*), redness-greenness (a*), and yellowness-blueness (b*) values of each sample were measured using the CIE-LAB color system. For each measurement, the sample was assessed at 10 random points on the surface of the cooked pasta. Three measurements were taken at each point, and the average of all measurements was reported.

2.3 Cooking quality evaluation

1) Optimum cooking time

A 10 g sample of dried pasta was boiled in 200 ml of boiling water in a beaker covered with a watch glass. The cooking time required for the pasta to be fully cooked was recorded by checking the sample every 30 seconds. The optimum cooking time was determined as the duration needed for starch gelatinization, indicated by the disappearance of the opaque white core inside the pasta when pressed between two glass slides.

2) Cooking Loss

The amount of solid loss during boiling was assessed by analyzing the cooking water used in the cooking yield measurement. The collected water was dried in a hot-air oven at 105°C until a constant weight was achieved. The remaining solids were then weighed, and cooking loss was calculated using the following equation:

$$\text{Cooking loss (\%)} = \left(\frac{\text{Weight of solids after drying}}{\text{Weight of pasta before cooking}}\right) \times 100 \qquad (1)$$

3) Volume Expansion

The volume expansion of pasta during cooking was measured using a graduated cylinder filled with toluene to a predetermined volume. A 10 g uncooked pasta sample was placed into the cylinder from the top, tapped gently to remove air bubbles, and the volume increase was recorded. The same process was repeated for the cooked pasta, and volume expansion was calculated using the following equation:

$$\text{Uncooked pasta volume (mL/100 g)} = \text{Increase in volume of uncooked pasta} \times 10$$
$$\text{Cooked pasta volume (mL/100 g)} = \text{Increase in volume of cooked pasta} \times 10$$
$$\text{Volume expansion due to cooking} = \left(\frac{\text{Volume of cooked pasta}}{\text{Volume of uncooked pasta}}\right) \times 100 \qquad (2)$$

4) Swelling index (%)

Swelling index and water absorption of cooked pasta were measured by using the method described by Sheti et al. (2020). Swelling index of cooked pasta was dried in hot air oven at 105 °C to obtain the constant weight and was calculated by the following equation:

$$\text{Water abortion index (\%)} = \left(\frac{\text{Weight of cooked pasta-Weight of pasta after drying}}{\text{Weight of pasta after drying}}\right) \qquad (3)$$

2.4 Antioxidant properties

The pasta samples were extracted using a method modified from Subanmanee et al. (2024). A 5 g sample of cooked pasta was extracted for 2 hours with 10 mL of 80% methanol at 150 rpm on an orbital agitator. The mixture was then centrifuged for 20 minutes at 1400 rpm, and the supernatant was decanted. The sediment was re-extracted under the same conditions. The supernatants were combined and used to determine antioxidant activities, including antioxidant activity, total phenolic compound and anthocyanin content.

1) Antioxidant activity

The antioxidant activity was determined using a DPPH radical scavenging assay, with slight modifications based on Subanmanee et al. (2024). A 1.0 mL aliquot of pasta extract was mixed with 1.0 mL of 95% ethanol containing 0.15 mM 2,2-diphenyl-1-picrylhydrazyl (DPPH). The mixture was stirred vigorously and allowed to react for 30 minutes at room temperature in the dark. The absorbance of the resulting solution was measured at 517 nm using a UV-spectrophotometer (Thermo Fisher Scientific, Genesys 180, Massachusetts, USA). The respective solvents were used as blanks in place of the DPPH solution. DPPH radical scavenging activity (%DPPH) was calculated using following equation.

$$\%\text{DPPH} = \left[\frac{\left(A_{517 \text{ of control}} - A_{517 \text{ of sample}}\right)}{A_{517 \text{ of control}}}\right] \times 100 \qquad (4)$$

2) Total phenolic compounds

The total phenolic content (TPC) of the samples was determined using the Folin–Ciocalteu spectrophotometric method, as described by Mohamad et al. (2014), with modifications. A 0.1 mL aliquot of pasta extract was added to 0.5 mL of 10% Folin–Ciocalteu reagent and allowed to react for 8 minutes. Then, 4.5 mL of 2% sodium carbonate (Na_2CO_3) was added, and the mixture was thoroughly mixed and incubated in the dark at 25 °C for 60 minutes. Absorbance was measured at 760 nm using a UV-spectrophotometer (Thermo Fisher Scientific, Genesys 180, Massachusetts, USA). TPC was quantified using a standard calibration curve of gallic acid (Sigma-Aldrich,

139

Steinheim, Germany) at concentrations ranging from 0 to 100 mg/g, and the results were expressed as gallic acid equivalents (GAE) per 100 g of sample.

3) Anthocyanin content

Approximately 2 g of pasta was added to a solvent mixture of 98% ethanol and 1.0 mol/L citric acid in an 80:20 ratio. The mixture was stirred for 3 hours, after which the extract was filtered using qualitative Whatman No. 1 filter paper. The residue was then rinsed with the extraction solvent until the final volume reached 50 mL. To determine anthocyanin content, each sample was diluted in two different buffers—potassium chloride buffer (pH 1.0) and sodium acetate buffer (pH 4.5)—to a final volume of 3 mL. Cyanidin-3-glucoside (Cy-3-GE) was used as the standard. The absorbance of the samples was measured at 520 nm and 700 nm using a UV–vis spectrophotometer (Thermo Fisher Scientific, Genesys, 180, Massachusetts, USA) with distilled water serving as the blank (Pang et al., 2018). The anthocyanin content, expressed as mg of Cy-3-GE per gram of dry-weight sample, was then calculated using the following formula:

$$\text{Anthocyanin content} = \frac{A \times MW \times DF \times 1000}{\varepsilon \times I} \quad (5)$$

A represents the absorbance difference, calculated as:

$$A = (A_{520nm} - A_{700nm})_{pH1.0} - (A_{520nm} - A_{700nm})_{pH4.5}$$

Where A is the absorbance, MW is the molecular weight for cyanidin-3-glucoside (449.2 g/mol), DF is the dilution factor, and ε is the molar absorbance of cyanidin-3-glucoside (26,900 L/(cm×mol)), L is cell path length (1 cm), and 1000 is the conversion factor from milliliter to liter.

2.5 Texture quality analysis

The Texture Profile Analysis (TPA) with two compression cycles test of the cooked pasta samples was conducted using a TA-XT2i Texture Analyzer (Stable Micro Systems, London, UK) equipped with a 25 kg load cell. For TPA analysis, 20 pasta strands were boiled in 1,000 mL of boiling water for 4 minutes. The texture of the pasta samples was measured 5 minutes after cooking to avoid rapid texture changes that occur immediately after boiling. The cooked pasta samples were cut to a length of 4 cm and subjected to a two-cycle compression test. A flat-ended cylindrical probe with a 50 mm diameter (P/50) was used, and the pre-test speed, test speed, and post-test speed were set at 5.0 mm/s. The compression strain was 75% of the original size with a trigger force of 5 grams. A 5-second resting period was applied between the first and second compression cycles. The test was conducted in triplicate for each sample, and the results were reported for hardness (N), adhesiveness (N·s), springiness, and chewiness.

2.6 Proximate composition

The chemical composition of control pasta and selected pasta was performed according to standard methods of AOAC (1995), ash (923.03), lipid (922.06), protein (984.13, nitrogen factors of 6.25); total fiber content (991.43, kit K-TDFR-200 A). Total carbohydrates were calculated by difference. Determinations were made in triplicate.

2.7 Sensory evaluation

The sensory panel consisted of sixty untrained consumers familiar with pasta products. The panel included 19 men and 41 women, aged between 20 and 51 years. Sensory evaluation of cooked pasta samples was conducted at the Faculty of Home Economics Technology, Rajamangala University of Technology Phra Nakhon, Bangkok, Thailand. The pasta samples were cooked under optimum cooking time (OCT) conditions in boiling water without salt, then drained and kept warm until testing. Each sample was coded and presented on white plastic plates. Panelists were provided with water to cleanse their palates between evaluations. Panelists assessed the pasta samples based on their degree of acceptance, including attributes such as color, flavor, taste, texture, and overall acceptability, using a 9-point hedonic scale. The study was approved by the Rajamangala University of Technology Phra Nakhon Research Ethics Committee (Approval number, IRB-COE-008-2024) on March 13, 2024.

2.8 Statistical analysis

The collected data were statistically analyzed using IBM SPSS software (version 23). Results were presented as means ± standard deviations (SD), and significant differences were determined using Duncan's multiple range test at a significance level of $p < 0.05$.

3. Results and Discussion

3.1 Color

Chicken meat fortification had a significant effect ($p < .05$) on the color values of L*, a*, and b* pasta (Figure 2) The L*, a*, and b* values of the chicken fortified pasta made by black glutinous rice flour and tapioca starch ranged from 35.09-38.82, 7.09–7.77, and 0.67-1.04, respectively, as shown in Table 2. The L* value of chicken fortified pasta made by black glutinous rice flour and tapioca starch produced ranged from 35.09 to 38.82. The L* value of pasta significantly ($p < .05$) decreased with fortification of 20-40% minced chicken meat, it could be seen from the decrease in the whiteness of the pasta. The color of black glutinous rice flour can be attributed to the presence of anthocyanins, which are responsible for the black, red, and purple pigments in the bran (Chen et al., 2024). These pigments contribute to the purple-black color of chicken-fortified pasta in this study. The natural anthocyanin pigments in glutinous black rice flour imparted the characteristic dark purple color, resulting in a darker and more intense red color in pasta formulations with a higher proportion of chicken meat. The anthocyanin content in black rice imparted a purple-red

color, while XG and tapioca starch likely maintained color stability during processing. In contrast, when minced chicken meat added in lower amounts, its impact on color was limited compared to black glutinous rice, resulting in the observed purple color characteristics. Pasta formulations with high chicken meat exhibited a darker color due to the pale-yellow of cooked chicken meat. Moreover, the complex interactions between these ingredients significantly affected the final color of the product. The increase in L* of partially substituting wheat flour with black glutinous rice flour have also been reported by Subanmanee et al., (2024) and pasta enriched with anthocyanin-rich black rice bran by Sheti et al. (2020).

The redness (a*) values of chicken fortified pasta made from black glutinous rice flour and tapioca starch showed significant increase with added chicken meat. The color a* value varied from 1,91 to 2,85. The a* value of redness in 40% minced chicken meat fortified pasta by 2,85 higher than 20-30% fortification and control pasta. Research results in accordance with Musika et al. (2024), indicated that redness a* value of gluten free pasta was higher with added 20% cricket powder supplementation. According to Chhikara et al. (2019), there was an increase in the value of redness and a decrease in the value of brightness with an increasing concentration of coloring pigment.

The yellowness (b*) value of control pastas was 10,39 and chicken fortified pasta made from black glutinous rice flour and tapioca starch decreased from 8,54 to 7,19 with an increase of chicken meat levels. The increase in chicken meat led to a reduction in the b* value, emphasizing the significant influence of black glutinous rice flour in providing purple color due to its anthocyanin content. Meanwhile, the pale-yellow color of chicken meat decreased at lower concentrations. The interaction of the protein with polysaccharides in the manufacture of black glutinous rice can cause decreased yellowish b* value. An increase in chicken meat from 20% to 40% had a significant effect on the color of cooked pasta, as seen from the changes in L*, a*, and b*. Brown and melanoid discoloration are caused by non-enzymatic browning reactions between reducing sugars and proteins during cooking (Chhikara et al., 2019). Sofi et al. (2020) explain that color values of protein enriched noodles have significant differences causes attributed to pigments associated with protein and the Maillard reaction.

Table 2 Color index of chicken fortified pasta made by black glutinous rice flour and tapioca starch

Color values	Lightness (L*)	Redness (a*)	Yellowness (b*)
CFP 0	78.46a ±0.37	-1.35c±0.13	18.03a±0.44
CFP 20	38.82b±0.55	7.09b±0.85	1.04b±0.12
CFP 30	37.13c±0.57	7.77a±0.50	0.67c±0.29
CFP 40	35.09d±0.43	7.68a±0.89	0.72c±0.13

CFP 0: Control pasta, without chicken meat 0 g/100 g; CFP 20: pasta with 20 g/100 g chicken meat; CFP 30: pasta with 30 g/100 g chicken meat; CFP 40: pasta with 40 g/100 g chicken meat.

a,b,c Different letters in same column show significant difference among the values (p< 0.05).

(a) CFP 0   (b) CFP 20   (c) CFP 30   (d) CFP 40
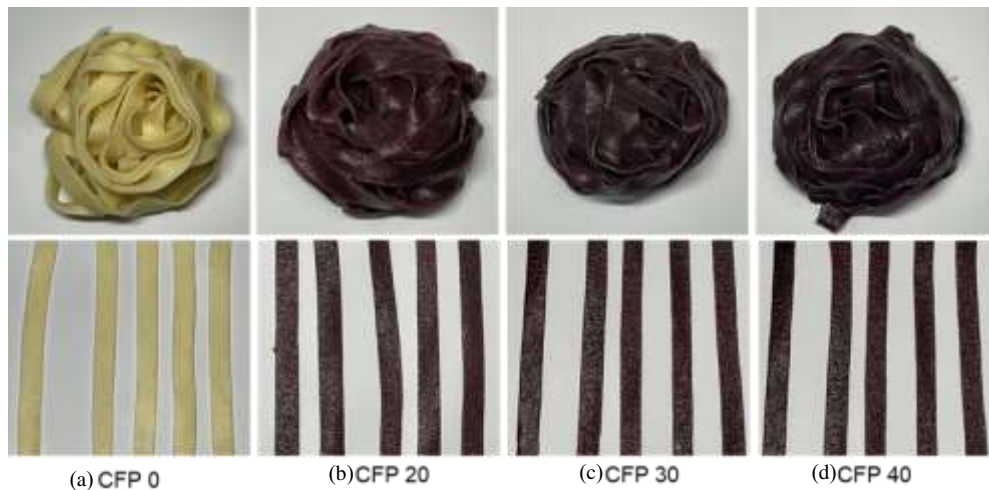
Figure 1. Image of cooked chicken fortified pasta (CFP) made by black glutinous rice flour and tapioca starch at different levels: (a) CFP 0: Control pasta, without chicken meat 0 g/100 g; (b) CFP 20: pasta with 20 g/100 g chicken meat; (c) CFP 30: pasta with 30 g/100 g chicken meat; (d) CFP 40: pasta with 40 g/100 g chicken meat.

3.2 Cooking quality of pasta

The substitution of a starch mixture (black glutinous rice flour and tapioca starch) with varying levels of chicken meat (0%, 20%, 30%, and 40%) had a significant effect (p<0.05) on the cooking qualities of chicken meat pasta. Table 3 presents the results for the cooking quality parameters of both gluten-free pasta fortified with chicken meat and the control pasta. As the chicken meat content increased, the optimum cooking time, water absorption index, and water solubility index increased. In contrast, cooking loss and volume expansion decreased with higher chicken meat incorporation.

The optimal cooking time report in Table 3 was 9.17-11.16 min for the various chicken fortified pastas, which was much more than the reported values of 7.65 min for the traditional wheat pasta. Enriched pasta required higher cooking times than control pasta. The prolonged optimum cooking time may be attributed to the competitive hydration between the proteins in the chicken meat, starch, and xanthan gum, which reduced starch swelling. The myofibrils in the meat likely inhibited starch gelatinization during cooking, especially when a high amount of protein surrounded the starch granules (Chang et al., 2011). These results indicate that pastas with higher chicken meat content lead to slower starch swelling, which subsequently requires a longer time for gelatinization. Similar findings have been reported for poultry-based noodles (Pal et al., 2017) and microwave-dried instant noodles enriched with chicken meat (Pongpichaiudom and Songsermpong, 2018).

Cooking loss values decreased compared to the control with the addition of chicken meat to the pasta (p < 0.05), with a more pronounced reduction at higher chicken meat levels (p < 0.05). This may be due to the structure being formed by chicken proteins, which are strengthen than those in traditional wheat flour pasta. The cooking loss of chicken-fortified pasta samples was primarily due to the solubilization of loosely bound gelatinized starch and strongly depended on the strength of the retrograded starch network. Starch gelatinization and adhesion may help reduce cooking loss, as starch that withstands boiling temperatures consists mainly of retrograded amylose. High-amylose starch gels are highly retrograded, resulting in more elastic and firm rice noodle strands with lower cooking loss (Tian et al., 2012). Tam et al. (2004) reported that bihon-type noodles made from normal maize starch, which contained 22% amylose, were able to withstand boiling temperatures primarily due to the formation of retrograded amylose. This sufficient retrogradation helped maintain the noodle structure. In contrast, noodles made from waxy maize starch broke into short pieces because the starch did not undergo sufficient retrogradation. A similar reduction in cooking loss has been observed in protein-fortified pasta made from sweet potato and three protein sources (whey protein, soy flour, and fish powder), attributed to gluten dilution and the weakening of the starch-protein network (Gopalakrishnan et al., 2011). Additionally, incorporating xanthan gum into the pasta formulation can enhance network formation, effectively trapping starch granules. However, when xanthan gum was added at concentrations lower than 0.5%, it failed to establish a sufficient network, resulting in high cooking loss in gluten-free pasta made with tapioca starch and xanthan gum (Milde et al., 2020).

As shown in Table 3, the control pasta exhibited the highest volume expansion, while the CFP 40 sample, which contained 40% chicken meat, had the lowest volume expansion. These results align with findings by Sethi et al. (2020), who reported a similar trend when incorporating black rice bran into pasta (0–25%), and Verma et al. (2014), who observed reduced volume expansion in chicken noodles where starch was partially replaced with chicken meat (0–50%). This decrease in volume expansion may be attributed to the higher proportion of protein fractions relative to the total starch content in the pasta formulation, as well as the formation of a protein network that restricts water availability for starch swelling and gelatinization (Liu et al., 2016).

The water solubility index exhibited a decreasing trend as the chicken meat content increased. Likewise, the overall mean values for volume expansion declined with higher chicken meat levels, possibly due to the increased moisture content in the pasta. In gluten-free pasta fortified with chicken meat, cooking loss showed a significant difference (p < 0.05) at meat levels ranging from 20% to 40%. Additionally, the volume expansion values of chicken meat pasta made from black rice and tapioca starch decreased as the chicken meat content increased (20%–40%). This reduction may be attributed to the higher protein and moisture content, along with a corresponding decrease in carbohydrate content (Verma et al., 2014).

The water absorption index is a crucial property of food products, as it reflects their ability to absorb water without dissolving proteins, resulting in viscous and thick textures (Li et al., 2010). In the present study, increasing the chicken meat content in pasta significantly enhanced the WAI from 1.47 to 1.79 g/g (p < 0.05) (Table 3). This increase may be attributed to the greater availability of polar amino acids, which serve as primary sites for hydrophilic interactions. The water absorption index is primarily influenced by the carbohydrate and protein content, as both contain hydrophilic components (Chinma et al., 2013). This suggests that higher water absorption capacity improves the textural properties and reconstitution ability of flour in cooked pasta.

Table 3 Cooking quality of chicken fortified pasta (CFP) made from black glutinous rice flour and tapioca starch

Sample	Cooking time (min)	Cooking losses (%)	Volume Expansion (%)	Water absorption index (g/g)	Water solubility index (%)
CFP 0	7.65d±0.03	7.29a±0.13	249.53a±2.87	1.47c±0.05	0.089a±0.002
CFP 20	9.17c±0.03	6.63b±0.10	213.47b±2.18	1.59b±0.08	0.076b±0.002
CFP 30	10.55b±0.05	5.51c±0.073	185.21c±1.55	1.63b±0.02	0.072b±0.003
CFP 40	11.16a±0.02	4.17d±0.04	159.44d±2.13	1.79a±0.02	0.062c±0.002

CFP 0: Control pasta, without chicken meat 0 g/100 g; CFP 20: pasta with 20 g/100 g chicken meat; CFP 30: pasta with 30 g/100 g chicken meat; CFP 40: pasta with 40 g/100 g chicken meat.
[a,b,c] Different letters in same column show significant difference among the values (p< .05).

3.3 Antioxidant properties

According to the results in Table 4, the antioxidant activity, total phenolic compound content, and anthocyanin content in pasta products vary depending on the proportion of chicken meat and black glutinous rice flour in the composition. The extract from control pasta had the lowest of %DPPH and total phenolic compound is consisted of wheat flour and fresh egg showed the lowest, while showed any anthocyanin content. The extracts from pasta

supplemented with chicken meat exhibited a higher anthocyanin content compared to the control ($p < 0.05$). However, a decreasing trend was observed as the level of chicken meat increased. This is because the control pasta contained fresh egg, a rich source of both nutritive and non-nutritive compounds essential for human health (Nimalaratne et al., 2011), whereas common wheat flour contains little to no anthocyanin pigments (Abdel-Aal et al., 2006). A decrease in the proportion of black glutinous rice flour, replaced by chicken meat, led to a reduction in antioxidant activity, total phenolic compounds, and anthocyanin content in the pasta. This trend likely resulted from the decline in anthocyanins and phenolic compounds intrinsic to black glutinous rice, leading to a corresponding decrease in antioxidant activity. Similarly, Subanmanee et al. (2024) reported that reducing the level of black glutinous rice flour in pasta by partially substituting wheat flour resulted in lower antioxidant activity, total phenolic compounds, and anthocyanin content in both uncooked and cooked pasta. Sethi et al. (2020) also reported a decrease in %DPPH, FRAP, and anthocyanin content as the amount of black rice bran decreased, consistent with the findings of this study. Additionally, chicken meat positively influences the bioactive compounds and antioxidant activity. According to Okarini et al. (2013), these researchers demonstrated the potential of indigenous chicken meat and broiler to provide a high total phenolic content (64.44-65.64 GAE mm/kg) and antioxidant activity (DPPH 19.04-20.77%). However, Msika et al. (2024) found that xanthan gum had no effect on antioxidant activity, total phenolic compounds, or anthocyanin content, as it functions solely as a thickening agent used to mimic gluten, without any significant bioactive properties. Therefore, the results indicate that gluten-free chicken-fortified pasta made from black glutinous rice and tapioca starch, which contains high levels of polyphenolic compounds and anthocyanins with significant antioxidant activity, is a potential food choice for bioactive compound intake.

Table 4 Antioxidant activities, total phenolic compounds and anthocyanin content of cooked chicken fortified pasta (CFP) made from black glutinous rice flour and tapioca starch at different percentages of meat.

Sample	Antioxidant activities (%DPPH)	Total phenolic compounds (mg GAE/100 g)	Anthocyanin content (Cyanidin-3-O-glucoside; mg/g)
CFP 0	38.93d±0.45	0.78d±0.12	ND
CFP 20	54.52a±0.82	1.56a±0.11	0.04a±2.18
CFP 30	48.06b±0.65	1.48b±0.07	0.02b±1.55
CFP 40	46.28c±0.63	1.42c±0.09	0.02b±2.13

CFP 0: Control pasta, without chicken meat 0 g/100 g; CFP 20: pasta with 20 g/100 g chicken meat; CFP 30: pasta with 30 g/100 g chicken meat; CFP 40: pasta with 40 g/100 g chicken meat. ND is not detected.
[a,b,c] Different letters in same column show significant difference among the values ($p < .05$).

3.4 Texture quality analysis

The texture of cooked pasta is one of the most critical factors in evaluating pasta qualities. Hardness values observed across all treatments ranged from 158.55 to 165.66 N (Table 5). CFP 40 exhibited the lowest hardness level; however, there was no significant difference among CFP 0, CFP 20, and CFP 30, all of which contained 3.0% xanthan gum to mimic gluten functionality. Hardness showed a decreasing trend with an increasing level of chicken meat (Table 2). Generally, gluten-free pasta products without wheat flour require additional ingredients to improve texture. Xanthan gum, a hydrocolloid with gelling properties, can form strong covalent bonds when combined with chicken meat, enhancing gel strength (Hua et al., 2003). However, increasing the amount of minced chicken meat led to a reduction in hardness. This may be attributed to the higher protein and moisture content associated with increased chicken meat levels, as well as a reduction in starch granules when the starch mixture is replaced with chicken meat. Furthermore, Ainsa et al. (2022) explained that the reduction in hardness of fish-enriched pasta is primarily due to the weakening of its three-dimensional structure. This occurs because the addition of fish introduces myofibrillar proteins, which disrupt the formation of the starch matrix. This suggests that while chicken meat enhances the nutritional composition by increasing protein content, it lacks the ability to interact effectively with other components of the pasta dough to improve firmness. Similar findings were reported by Verma et al. (2014). Additionally, black glutinous rice flour and tapioca starch lack the gluten proteins necessary to form the strong, elastic structure typical of traditional pasta, resulting in a less firm texture (Milde et al., 2020; Bouasla and Wójtowicz, 2021).

The adhesiveness of all chicken-fortified pasta samples was higher than that of the control, and a decreasing trend was observed as the amount of starch replaced by chicken meat increased. According to Milde et al. (2020), adhesiveness is related to the amount of starch granules that leach from the pasta matrix into the cooking water, forming a coating on the product's surface, resulting in the change of microstructure of pasta, loss of uniformity by the diffusion of water from the outside to the core, especially closer to the surface. The experimental results showed that CFP 20, which contains a higher proportion and less chicken meat than the other formulations, was chewier and more adhered better to the texture measuring probe than the other formulations ($p < 0.05$). According to Larrosa et al. (2016), cohesiveness can be an indicator parameter of how the matrix is held together during cooking. The results showed that the cohesiveness values of the pasta decreased when chicken meat was incorporated into the formulation. This may be due to weaker internal bonds between starch granules and other ingredients as chicken meat levels increased. Springiness refers to a pasta's ability to return to its original shape after compression, with higher springiness being desirable (Barak et al., 2014). Table 2 shows that the control pasta, made with wheat flour and egg, had the highest springiness compared to other samples. Significant differences ($p < 0.05$) were observed among the chicken-fortified samples, with springiness decreasing as the chicken meat content increased. Springiness is closely

related to the gluten network in pasta, which explains why the chicken-fortified samples exhibited lower springiness. The absence of a gluten network, as black glutinous rice flour and tapioca starch replaced wheat flour, likely contributed to the reduced elasticity and springy texture (Halim et al., 2023). Gumminess is expressed as the force used to shrink food ingredients so it can swallow (Szczesniak, 2002). The gumminess exhibited a decreasing trend with the increased incorporation of chicken meat (Table 5) (p<0.05). The decreased starch content with the increased incorporation of chicken meat could be positively correlated with the reduced protein-starch interactions, leading to diminished textural characteristics. Similarly, gumminess exhibited a decreasing trend, reaching its lowest level in pasta containing 40% chicken meat, likely due to the absence of gluten. Chewiness parameters is related to the elastic resistance of the structure and decreases with the leaching of starch into the cooking water (Sozer et al., 2007). The chewiness decreased with increase of chicken meat level in pastas, up to 40% chicken meat addition (p<0.05), This corresponds to the results obtained from higher solid loss, but it retains a firm structure (Table 5).

Table 5 Texture profile analysis of cooked free gluten pasta with black glutinous rice flour and tapioca starch

Texture attributes	Formulation (%Ratio of black glutinous rice flour and tapioca starch)			
	CFP 0	CFP 20	CFP 30	CFP 40
Hardness (N)	165.66a±12.74	164.70a±10.68	162.72a±14.21	158.55b±11.49
Adhesiveness (N.J)	0.49d±0.08	1.09a±0.09	0.79b±0.10	0.63c±0.08
Cohesiveness	0.92a±0.01	0.84b±0.01	0.84b±0.03	0.82c±0.03
Springiness (%)	93.48a±7.24	77.36b±8.16	70.58c±7.15	66.67c±6.37
Gumminess (g)	152.81a±11.13	141.19b±9.88	137.49b±6.09	130.45c±9.25
Chewiness (m.J)	142.70a±10.53	130.25b±7.13	96.81c±12.66	87.11d±10.65

CFP 0: Control pasta, without chicken meat 0 g/100 g; CFP 20: pasta with 20 g/100 g chicken meat; CFP 30: pasta with 30 g/100 g chicken meat; CFP 40: pasta with 40 g/100 g chicken meat.
a,b,c Different letters in same row show significant difference among the values (p<.05).

3.5 Proximate composition

The data obtained for chemical compositions were shown in the Table 6. The increase was significant (p<0.05) in moisture, ash, protein, fat values whereas decrease was significant (p<0.05) decrease for the values of crude fiber as the level of chicken meat replacement of flours increased. The increase in moisture content in treated noodles with increase in meat incorporation may be due to high moisture contents in chicken meat than flour. This finding was in favour of the reports given by Zayas (1997) on functionality of proteins in food. The highest protein (%) was observed in 40% chicken meat fortified enriched pasta (p<0.05). This was attributed to high protein content in minced chicken meat enriched pasta as compared to the control recipe which contain wheat flour and fresh egg. Similar trend was reported by Kumar et al. (2019) and Verma et al. (2015) on addition chicken meat in noodle and Litaay et al. (2022) in noodles fortified with anchovy flour. A significant (p<0.05) increase in fat and ash content on addition of chicken meat powder in noodles was recorded.

A significant (p < 0.05) increase in fat and ash content was observed with the addition of minced chicken meat to pasta. This increase can be attributed to the inherent differences in the proximate composition of raw materials. Kumar et al. (2019) reported a fat enhancement from 0.92% to 3.66% when 30% chicken powder was incorporated into refined wheat flour noodles. The overall mean fat content showed an increasing trend as the level of meat fortification in pasta rose. This is likely due to the higher fat content of chicken meat compared to the flours used. Verma et al. (2015) also reported a similar increase in fat content with higher meat replacement levels during the preparation of chicken meat noodles. The rise in ash content with increasing meat levels can be attributed to the higher mineral content of meat compared to refined wheat flour. A similar significant (p<0.05) effect on ash content was reported by Verma et al. (2015) in chicken meat-incorporated noodles and by Litaay et al. (2022) in noodles fortified with anchovy flour. Conversely, crude fiber content decreased significantly (p<0.05) as the amount of chicken meat in pasta increased, compared to the control. This reduction is likely due to the higher crude fiber content in grain-based flours than in animal-derived ingredients. A similar trend was reported by Verma et al. (2014) in the preparation of chicken meat noodles.

Table 6 Chemical composition of control pasta and chicken fortified pasta made from black glutinous rice flour and tapioca starch

Color values	Moisture content (%)	Ash (%)	Protein content (%)	Crude fat (%)	Crude fiber (%)
CFP 0	55.18c ± 1.34	2.447b±0.061	16.038ab±0.315	1.586d±0.082	0.26a±0.12
CFP 20	60.27b±0.21	2.025c±0.085	11.863c±0.487	2.539c±0.057	0.21b±0.06
CFP 30	68.37a±0.65	2.312b±0.055	14.705b±0.292	2.988b±0.085	0.18c±0.03
CFP 40	69.11a±0.66	2.857a±0.087	18.895a±0.54	3.427a±0.105	0.14d±0.08

CFP 0: Control pasta, without chicken meat 0 g/100 g; CFP 20: pasta with 20 g/100 g chicken meat; CFP 30: pasta with 30 g/100 g chicken meat; CFP 40: pasta with 40 g/100 g chicken meat.
a,b,c Different letters in same column show significant difference among the values (p< .05).

3.6 Sensory evaluation

According to the results shown in Table 7, the sensory evaluation scores were recorded for various attributes, including appearance, color, odor, taste, texture, and overall acceptability. All chicken meat pasta samples, along with the control, were well accepted by the sensory panelists. The control sample, made with wheat flour, received the

highest scores across all sensory attributes. Statistical analysis showed that the scores for appearance and color in pasta containing 20% chicken meat were not significantly different (p>0.05) from the control. This implied that the panelists still accepted pasta made with black rice flour and tapioca starch, even though these ingredients caused a significant change in color compared to traditional pasta. However, the scores for odor, taste, texture, and overall acceptability were significantly lower (p<0.05) than those of the control. Pasta samples with 30% (CFP 30) and 40% (CFP 40) chicken meat received significantly lower (p<0.05) scores compared to both the control and the 20% chicken meat sample (CFP 20). The decline in appearance and color scores may be attributed to enzymatic reactions, fat oxidation, and Maillard reactions occurring during pasta preparation and cooking. Similar findings were reported by Verma et al. (2015) in refined wheat flour-based noodles containing chicken meat and by Kumar et al. (2019) in noodles enriched with chicken meat powder. The scores for odor and taste in pasta containing 20–30% chicken meat was not significantly different from each other but were lower than those of the control. This may be due to the absence of a strong meat flavor. The overall acceptability scores of pastas containing 20%, 30%, and 40% meat were significantly lower (p<0.05) than those of the control, though they did not differ significantly from each other (p>0.05). Among the chicken meat pasta samples, the 20% meat formulation received scores closest to the control, making it the most acceptable variation. This may be attributed to improved binding between starch, xanthan gum, and chicken meat at this level, as well as enhanced emulsion properties. These findings align with Verma et al. (2014), who studied the incorporation of chicken meat in wheat-based noodles. The results suggest that the absence of wheat flour influenced consumer preferences, particularly regarding odor, taste, and texture. Musika et al. (2024) reported that gluten-free pasta containing Riceberry rice flour, cricket protein, and 1% xanthan gum received the highest overall acceptance scores. This was primarily due to xanthan gum's role in mimicking gluten's elastic texture and improving pasta firmness (Larrosa et al., 2013). Similarly, Cai et al. (2016) found that adding 5% xanthan gum to glutinous rice-based noodles increased overall acceptance by enhancing hardness and chewiness.

Table 7 Sensory attributes of cooked free gluten pasta with black glutinous rice flour and tapioca starch

Sensory attributes	Formulation (%Ratio of black glutinous rice flour and tapioca starch)			
	CFP 0	CFP 20	CFP 30	CFP 40
Appearance	6.64a±0.48	6.71a±0.46	6.42b±0.54	6.70a±0.46
Color	6.28ab±0.70	6.48a±0.50	6.22b±0.62	6.16b±0.62
Odor	6.66a±0.48	6.12b±0.48	5.94b±0.65	5.92b±0.49
Taste	6.50a±.0.51	6.26b±0.53	6.32ab±0.47	6.18b±0.39
Texture	6.86a±0.64	6.62b±0.53	6.22c±0.55	6.16c±0.55
Overall acceptability	7.16a±0.55	6.70b±0.46	6.64b±0.53	6.50b±0.74

CFP 0: Control pasta, without chicken meat 0 g/100 g; CFP 20: pasta with 20 g/100 g chicken meat; CFP 30: pasta with 30 g/100 g chicken meat; CFP 40: pasta with 40 g/100 g chicken meat.
a,b,c Different letters in same row show significant difference among the values (p< 0.05).

4. Conclusions

In conclusion, the fortification of gluten-free pasta with varying levels of chicken meat significantly influenced both the physical and sensory properties of the pasta. The addition of chicken meat resulted in darker pasta color due to the interaction of anthocyanins in black glutinous rice flour with the chicken meat. As the meat content increased, cooking time, water absorption, and solubility index rose, while volume expansion and cooking loss decreased. The higher protein content contributed to changes in texture, leading to reduced hardness, springiness, and chewiness in higher meat concentrations. The antioxidant properties, as indicated by decreased anthocyanin and phenolic content, were reduced as chicken meat replaced black rice flour. Sensory evaluations revealed that the 20% chicken meat fortification was the most acceptable to consumers, while higher meat levels led to decreased overall acceptability. Despite some declines in sensory attributes like taste and texture, chicken-fortified pasta demonstrated potential as a nutritious gluten-free alternative with enhanced protein and antioxidant content. Further optimization of formulation and cooking methods could improve consumer acceptance and texture quality.

5.Acknowledgements

6. References

Abdel-Aal, E. S. M., Young, J. C., & Rabalski, I. (2006). Anthocyanin composition in black, blue, pink, purple, and red cereal grains. *Journal of Agricultural and Food Chemistry, 54*(13), 4696–4704.

Ainsa, A., Roldan, S., Marquina, P. L., Roncalés, P., Beltrán, J. A., & Calanche Morales, J. B. (2022). Quality parameters and technological properties of pasta enriched with a fish by-product: A healthy novel food. *Journal of Food Processing and Preservation, 46*(2), e16261.

Barak, S., Mudgil, D., & Khatkar, B. S. (2014). Effect of compositional variation of gluten proteins and rheological characteristics of wheat flour on the textural quality of white salted noodles. *International Journal of Food Properties, 17*(4), 731–740.

Bouasla, A., & Wójtowicz, A. (2021). Gluten-free rice instant pasta: Effect of extrusion-cooking parameters on selected quality attributes and microstructure. *Processes, 9*(4), 693.

Cai, J., Chiang, J. H., Tan, M. Y. P., Saw, L. K., Xu, Y., & Ngan-Loong, M. N. (2016). Physicochemical properties of hydrothermally treated glutinous rice flour and xanthan gum mixture and its application in gluten-free noodles. *Journal of Food Engineering, 186*, 1–9.

Cakmak, H., Altinel, B., Kumcuoglu, S., & Tavman, S. (2013). Chicken meat added bread formulation for protein enrichment. *Food and Feed Research, 40*(1), 33–42.

Cakmak, H., Altinel, B., Kumcuoglu, S., Kisla, D., & Tavman, S. (2016). Production of crispy bread snacks containing chicken meat and chicken meat powder. *Anais da Academia Brasileira de Ciências, 88*(4), 2387–2399.

Chang, H. C., Chen, H. H., & Hu, H. H. (2011). Textural changes in fresh egg noodles formulated with seaweed powder and full or partial replacement of cuttlefish paste. *Journal of Texture Studies, 42*(1), 61–71.

Chen, T., Xie, L., Wang, G., Jiao, J., Zhao, J., Yu, Q., Chen, Y., Shen, M., Wen, H., Ou, X., & Xie, J. (2024). Anthocyanins–natural pigment of colored rice bran: Composition and biological activities. *Food Research International, 175*, 113722.

Chhikara, N., Kushwaha, K., Jaglan, S., Sharma, P., & Panghal, A. (2019). Nutritional, physicochemical, and functional quality of beetroot (Beta vulgaris L.) incorporated Asian noodles. *Cereal Chemistry, 96*(1), 154–161.

Chokchaithanawiwat, P., Rungsardthong, V., Thumthanaruk, B., Puttanlek, C., Uttapap, D., Boonraksa, S., & Wonngsa, J. (2019). Product development of dried noodle from wheat flour and Riceberry rice flour by extrusion. In *IOP Conference Series: Earth and Environmental Science, 346*(1), 012043. IOP Publishing.

da Silva Ramos, N. J., Rocha, E. B. M., Gusmão, T. A. S., Nascimento, A., Lisboa, H. M., & de Gusmão, R. P. (2023). Optimizing gluten-free pasta quality: The impacts of transglutaminase concentration and kneading time on cooking properties, nutritional value, and rheological characteristics. *LWT, 189*, 115485.

Gopalakrishnan, J., Menon, R., Padmaja, G., Sajeev, M. S., & Moorthy, S. N. (2011). Nutritional and functional characteristics of protein-fortified pasta from sweet potato. *Food and Nutrition Sciences, 2*(9), 944–955.

Hailemariam, A., Esatu, W., Abegaz, S., Urge, M., Assefa, G., & Dessie, T. (2022). Nutritional composition and sensory characteristics of breast meat from different chickens. *Applied Food Research, 2*(2), 100233.

Halim, Y., Angelina, B., Hardoko, H., & Handayani, R. (2023). Characteristics of dried noodle analogue made from sorghum flour and rice flour added with konac glucomannan. In *IOP Conference Series: Earth and Environmental Science, 1200*(1), 012032.

Hua, Y., Cui, S. W., & Wang, Q. (2003). Gelling property of soy protein–gum mixtures. *Food Hydrocolloids, 17*(6), 889–894.

Kong, S., Kim, D. J., Oh, S. K., Choi, I. S., Jeong, H. S., & Lee, J. (2012). Black rice bran as an ingredient in noodles: Chemical and functional evaluation. *Journal of Food Science, 77*(3), C303–C307.

Kumar, S., Khanna, N., Vaquil, R. D., & Yadav, S. (2019). Development and evaluation of quality of noodles enriched with chicken meat powder. *International Journal of Current Microbiology and Applied Sciences, 8*(8), 2282–2289.

Larrosa, V., Lorenzo, G., Zaritzky, N., & Califano, A. (2013). Optimization of rheological properties of gluten-free pasta dough using mixture design. *Journal of Cereal Science, 57*(3), 520–526.

Larrosa, V., Lorenzo, G., Zaritzky, N., & Califano, A. (2016). Improvement of the texture and quality of cooked gluten-free pasta. *LWT, 70*, 96–103.

Litaay, C., Indriati, A., Mayasti, N. K. I., Tribowo, R. I., Andriana, Y., & Andriansyah, R. C. E. (2022). Physical, chemical, and sensory quality of noodles fortification with anchovy (Stolephorus sp.) flour. *Journal of Food Science and Technology, 42*, 75421.

Liu, X. L., Mu, T. H., Sun, H. N., Zhang, M., & Chen, J. W. (2016). Influence of potato flour on dough rheological properties and quality of steamed bread. *Journal of Integrative Agriculture, 15*(11), 2666–2676.

Liu, Y., Chen, K., Zeng, Q., Wang, P., & Zhang, Y. (2025). The impact of dietary fibers on the construction and molecular network of extrusion-based 3D-printed chicken noodles: Unlocking the potential of specialized functional food. *Food Chemistry, 463*, 141065.

Maulani, R. R., Sumardi, D., & Pancoro, A. (2019). Total flavonoids and anthocyanins content of pigmented rice. *Drug Invention Today, 12*, 369–373.

Messia, M. C., Cuomo, F., Falasca, L., Trivisonno, M. C., De Arcangelis, E., & Marconi, E. (2021). Nutritional and technological quality of high protein pasta. *Foods, 10*(3), 589.

Milde, L. B., Chigal, P. S., Olivera, J. E., & González, K. G. (2020). Incorporation of xanthan gum to gluten-free pasta with cassava starch: Physical, textural and sensory attributes. *LWT, 131*, 109674.

Mohamad, A., Shah, N. N. A. K., Sulaiman, A., Adzahan, N. M., & Aadil, R. M. (2024). Characterization of rice noodles fortified with different levels of stabilized rice bran. *Food Research, 8*(7), 16–27.

Musika, J., Kapcum, C., Itthivadhanapong, P., Musika, T., Hanmontree, P., & Piayura, S. (2024). Enhancing nutritional and functional properties of gluten-free Riceberry rice pasta supplemented with cricket powder using D-optimal mixture design. *Frontiers in Sustainable Food Systems, 8*, 1417045.

Nimalaratne, C., Lopes-Lutz, D., Schieber, A., & Wu, J. (2011). Free aromatic amino acids in egg yolk show antioxidant properties. *Food Chemistry, 129*(1), 155–161.

Norma, V. M., García-Zepeda, R. A., Mitzy Belén, O. H., & Morales-Guerrero, J. C. (2024). Gluten-free pasta as an alternative in the diet of patients with celiac disease. *Journal of Food Science, 89*(6), 3384–3399. https://doi.org/10.1111/1750-3841.17035

Odabas, E., & Cakmak, H. (2022). Partial replacement of starch-based flours with quinoa or yellow lentil flour in the production of gluten-free noodles. *Journal of Food Processing and Preservation, 46*(8), 16776.

Okarini, I. A., Purnomo, H., Aulanni'am, A. A., & Radiati, L. E. (2013). Proximate, total phenolic, antioxidant activity and amino acids profile of Bali indigenous chicken, spent laying hen and broiler breast fillet.

Olson, R., Gavin-Smith, B., Ferraboschi, C., & Kraemer, K. (2021). Food fortification: The advantages, disadvantages and lessons from Sight and Life programs. *Nutrients, 13*(4), 1118. https://doi.org/10.3390/nu13041118

146

Ou, S., Yang, D., & Liu, M. H. (2021). Effects of black rice anthocyanin enrichment on bread digestibility and glycemic index. *Current Developments in Nutrition, 5*, 354.

Pal, G. K., Kumar, S. B., Prabhasankar, P., & Suresh, P. V. (2017). Inclusion of poultry based food ingredients in the formulation of noodles and their effects on noodle quality characteristics. *Journal of Food Measurement and Characterization, 11*, 939–947.

Pang, Y., Ahmed, S., Xu, Y., Beta, T., Zhu, Z., Shao, Y., & Bao, J. (2018). Bound phenolic compounds and antioxidant properties of whole grain and bran of white, red and black rice. *Food Chemistry, 240*, 212–221.

Phonsakhan, W., & Kong-Ngern, K. (2015). A comparative proteomic study of white and black glutinous rice leaves. *Electronic Journal of Biotechnology, 18*(1), 29–34.

Poonia, A., & Pandey, S. (2021). Bioactive compounds, nutritional benefits and food applications of black rice: A review. *Nutrition & Food Science, 52*(3), 466–482.

Rachman, A., Brennan, M. A., Morton, J., & Brennan, C. S. (2020). Gluten-free pasta production from banana and cassava flours with egg white protein and soy protein addition. *International Journal of Food Science & Technology, 55*(8), 3053–3060.

Raungrusmee, S., Shrestha, S., Sadiq, M. B., & Anal, A. K. (2020). Influence of resistant starch, xanthan gum, inulin and defatted rice bran on the physicochemical, functional and sensory properties of low glycemic gluten-free noodles. *LWT, 126*, 109279.

Sanguinetti, A. M., Secchi, N., Del Caro, A., Fadda, C., Fenu, P. A., Catzeddu, P., & Piga, A. (2015). Gluten-free fresh filled pasta: The effects of xanthan and guar gum on changes in quality parameters after pasteurisation and during storage. *LWT-Food Science and Technology, 64*(2), 678–684.

Scarton, M., & Clerici, M. T. P. S. (2022). Gluten-free pastas: Ingredients and processing for technological and nutritional quality improvement. *Food Science and Technology, 42*, 65622.

Sethi, S., Nanda, S. K., & Bala, M. (2020). Quality assessment of pasta enriched with anthocyanin-rich black rice bran. *Journal of Food Processing and Preservation, 44*(12), 14952.

Sirichokworrakit, S., Phetkhut, J., & Khommoon, A. (2015). Effect of partial substitution of wheat flour with Riceberry flour on quality of noodles. *Procedia - Social and Behavioral Sciences, 197*, 1006–1012.

Sissons, M. (2022). Development of novel pasta products with evidence based impacts on health—A review. *Journal of Foods, 11*(1), 123.

Smith, D. P., Northcutt, J. K., & Steinberg, E. L. (2012). Meat quality and sensory attributes of a conventional and a Label Rouge-type broiler strain obtained at retail. *Poultry Science, 91*(6), 1489–1495.

Sofi, S. A., Singh, J., Chhikara, N., Panghal, A., & Gat, Y. (2020). Quality characterization of gluten-free noodles enriched with chickpea protein isolate. *Food Bioscience, 36*, 100626.

Sozer, N., Dalgıç, A. C., & Kaya, A. (2007). Thermal, textural and cooking properties of spaghetti enriched with resistant starch. *Journal of Food Engineering, 81*(2), 476–484.

Subanmanee, N., Sarasuk, C., Wongtom, R., & Khampaen, W. (2024). Changes in the physical, chemical and sensory properties of pasta made by partially substituting wheat flour with black glutinous rice flour. *African Journal of Food, Agriculture, Nutrition and Development, 24*(8), 24138–24160.

Surasani, V. K. R., Singh, A., Gupta, A., & Sharma, S. (2019). Functionality and cooking characteristics of pasta supplemented with protein isolate from Pangas processing waste. *LWT, 111*, 443–448.

Szczesniak, A. S. (2002). Texture is a sensory property. *Food Quality and Preference, 13*(4), 215–225. http://dx.doi.org/10.1016/S0950-3293(01)00039-8

Tam, L. M., Corke, H., Tan, W. T., Li, J., & Collado, L. S. (2004). Production of Bihon-type noodles from maize starch differing in amylose content. *Cereal Chemistry, 81*(4), 475–480.

Tian, Y., Zhang, L., Xu, X., Xie, Z., Zhao, J., & Jin, Z. (2012). Effect of temperature-cycled retrogradation on slow digestibility of waxy rice starch. *International Journal of Biological Macromolecules, 51*(5), 1024–1027.

Verma, A. K., Pathak, V., & Singh, V. P. (2014). Quality characteristics of value added chicken meat noodles. *Journal of Nutrition & Food Sciences, 4*(1), 1.

Verma, A. K., Pathak, V., Umaraw, P., & Singh, V. P. (2015). Quality characteristics of refined wheat flour (maida) based noodles containing chicken meat stored at ambient temperature under aerobic conditions. *Nutrition & Food Science, 45*(5), 753–765.

Widodo, S., Hudiah, A., Qur'ani, B., & Nurramadhan, T. (2024). Acceptance of sweet bread with black rice flour as a substitute ingredient. In *BIO Web of Conferences, 98*, 04002. EDP Sciences.

Yilmaz, M. T., Yildiz, Ö., Yurt, B., Toker, O. S., Karaman, S., & Baştürk, A. (2015). A mixture design study to determine interaction effects of wheat, buckwheat, and rice flours in an aqueous model system. *LWT-Food Science and Technology, 61*(2), 583–589.

Characterization of a Commercial β-Mannanase: Activity and Molecular Weight Determination

Chompoonuch Phuenpipob[a*], Chaleeda Borompichaichartkul[b],
Kittipong Rattanaporn[c]

[a] *Division of Food Technology, Faculty of Home Economics Technology, Rajamangala University of Technology Phra Nakhon, Bangkok, 10330, Thailand*
[b] *Department of Food Technology, Faculty of Science, Chulalongkorn University, Bangkok, 10330, Thailand*
[c] *Department of Biotechnology, Faculty of Agro-Industry, Kasetsart University, Bangkok, 10900, Thailand*
* Corresponding author. Tel.: +666 1393 9863; fax:02-665-3800; E-mail address: chompoonuch.p@rmutp.ac.th

Abstract

β-Mannanase (endo-1,4-β-D-mannanase) is a glycoside hydrolase belonging to the GH5 family, with potential applications in producing manno-oligosaccharides (MOS), recognized for their prebiotic properties. This study aimed to characterize the activity and estimate the molecular weight of a commercially available β-mannanase (EC 3.2.1.78), Mannanase BGM "AMANO" 10. The enzyme activity was assayed using 2 mg mL^{-1} konjac glucomannan (KGM) in a 0.1 mL reaction mixture incubated at pH 5.0 and 70°C for 30 min. Reducing sugars were quantified by the 3,5-dinitrosalicylic acid (DNS) method (Miller, 1959), with mannose as standard (y = 0.3012x + 0.0103, R^2 > 0.99), and expressed as mannose equivalents (MW = 180.16 g mol^{-1}). One unit (U) was defined as the release of 1 µmol reducing sugar per minute, and 0.0003 mg of protein was used. The specific activity was approximately 96,790 U/g protein. SDS-PAGE revealed a molecular weight between 50-75 kDa. These findings support the enzyme's high catalytic efficiency, substrate specificity, and thermostability under acidic conditions, highlighting its potential for biotechnological applications in MOS production and functional food development.

Keywords: β-Mannanase, Enzymatic Activity, Specific Activity, Molecular Weight

1. Introduction

Konjac (*Amorphophallus muelleri*) is recognized as a significant source of konjac glucomannan (KGM), a non-ionic polysaccharide composed of β-1,4-linked D-mannose and D-glucose units in a molar ratio of approximately 1.6:1, with randomly distributed acetyl groups influencing its solubility and viscosity (Kaur and Dhawan, 2007). KGM is not only a rich source of fermentable glucomannan but also exhibits remarkable water-holding capacity, high viscosity, and biodegradability, which make it highly suitable for incorporation in food and pharmaceutical formulations (Zhang *et al*., 2021). Its physicochemical properties can influence the degree of enzymatic hydrolysis and the profile of resulting oligosaccharides. Enzymatic hydrolysis of KGM offers a controlled route to produce MOS, which are short-chain carbohydrates with a degree of polymerization (DP) typically ranging from 2 to 6.

β-Mannans constitute the second most abundant group of hemicellulosic polysaccharides in nature, exhibiting structural diversity as linear mannan, glucomannan, galactomannan, and galactoglucomannan (Singh *et al*., 2018). Glucomannan, characterized by its β-1,4-glycosidic linkages between D-mannose and D-glucose residues, is a key component of plant cell walls, particularly abundant in konjac tubers and hardwoods (Kaur *et al*., 2007). The selective hydrolysis of these linkages is crucial for generating functional oligosaccharides.

The enzymatic depolymerization of KGM necessitates the action of several glycoside hydrolases (GHs). According to the CAZy (Carbohydrate-Active Enzymes) database, mannanases are classified within the GH clan A, reflecting their conserved catalytic mechanism involving a double-displacement reaction with retention of anomeric configuration (Henrissat, 1991; Davies and Henrissat, 1995). Specifically, β-Mannanase facilitates the degradation of mannan-rich polysaccharides by targeting and hydrolyzing internal β-1,4-linkages, resulting in shorter oligosaccharide chains (Tamaru *et al*., 1995), yielding a mixture of MOS. Endo-mannanases share a conserved (β/α) barrel (TIM barrel) protein fold, a ubiquitous structure among glycoside hydrolases, and are further categorized into several GH families, including GH5, GH26, GH113, and GH134 (Kaur *et al*., 2007). These families exhibit variations in substrate specificity, catalytic efficiency, and optimal reaction conditions, reflecting the diverse roles of endo-mannanases in nature.

However, efficient enzymatic production of MOS continues to face several challenges, including the requirement for thermally stable and acid-tolerant β-mannanases, precise control over hydrolysis to yield specific DP, and scalable processing systems that retain enzymatic activity while maximizing yield (Murillo-Franco *et al*., 2024). Furthermore, the interaction of substrate structure, enzyme source, and reaction conditions can significantly affect the type and concentration of MOS produced.

MOS produced from the enzymatic hydrolysis of mannan are low molecular weight oligosaccharides (DP 2-6) that have garnered significant attention as potential prebiotics. Prebiotics are defined as non-digestible food ingredients that beneficially affect the host by selectively stimulating the growth and/or activity of one or a limited number of bacteria in the colon, thereby improving host health (Gibson *et al*., 2004; Roberfroid *et al*., 2010; Singh *et al*., 2019; Zhang *et al*., 2019). The prebiotic effects of MOS have been attributed to their selective fermentation by beneficial gut microbiota, such as Bifidobacteria and Lactobacilli, leading to the production of short-chain fatty acids (SCFAs) like acetate, propionate, and butyrate, which have various health-promoting effects (Gibson *et al*., 2004). In addition to their prebiotic function, MOS has been incorporated into functional foods and beverages, infant formula,

and synbiotic formulations, and has also been explored for its role in modulating the gut-brain axis and supporting immune function (Slavin, 2013; Hughes *et al.*, 2020).

Given the increasing interest in MOS as functional food ingredients, identifying and characterizing efficient and robust β-mannanase enzymes is crucial for optimizing their production from readily available sources like konjac. This study focused on the characterization of a commercially available β-mannanase by determining its activity using the DNS assay with KGM as a substrate and estimating its molecular weight via SDS-PAGE analysis.

2. Methodology

2.1 Enzyme activity assay

The enzymatic activity was determined spectrophotometrically using the 3,5-dinitrosalicylic acid (DNS) method by measuring absorbance at 540 nm, as Miller (1959) described.

1) Substrate, chemicals, and enzyme preparation

KGM was purchased from Thai Union (Thailand). KGM powder was commonly a commercial substrate that did not require pretreatment. Commercial β-mannanase (Mannanase BGM "AMANO" 10) was obtained from Amano Enzyme Inc. All other chemicals were of analytical grade.

2) Mannose standard curve preparation

A standard mannose curve was prepared using mannose solutions with concentrations ranging from 0 to 2 mg mL^{-1}. The absorbance of each standard solution was measured at 540 nm using a spectrophotometer.

3) Substrate preparation

The substrate solution was prepared by mixing 100 µL of 1% (w/v) KGM in 50 mM sodium acetate buffer, pH 5.0. The mixture was stirred using a magnetic stirrer until a homogeneous solution was obtained.

4) Enzyme preparation and treatment

The enzyme stock solution was prepared at a concentration of 2 mg mL^{-1} and subsequently diluted with distilled water. The diluted enzyme solutions were divided into two groups:

- Treatment Group: The enzyme dilutions in this group were heat-inactivated by boiling in a water bath for 10 minutes, followed by rapid cooling. This step served as a control for non-enzymatic reactions.
- Control Group: These enzyme dilutions were not subject to heat treatment.

5) Enzyme reaction and incubation

For each enzyme dilution (both treated and untreated), 100 µL was pipetted into separate test tubes in triplicate. Then, 100 µL of the prepared substrate solution was added to each test tube. The substrate and enzyme solutions were thoroughly mixed using a vortex mixer to ensure homogeneity. All reaction mixtures were incubated at 70°C for 30 minutes in a water bath.

6) Color development and measurement

Following the incubation period, 200 µL of DNS reagent was added to each test tube. The tubes were then heated in a boiling water bath for 10 minutes to develop the color. Subsequently, the reaction was stopped by rapidly cooling the tubes in an ice bath for 10 minutes. Next, 2 mL of distilled water was added to each test tube, and the solutions were mixed thoroughly using a vortex mixer. Finally, 200 µL from each test tube was transferred to a microplate, and the absorbance was measured at 540 nm using a spectrophotometer **(Fig. 1).**
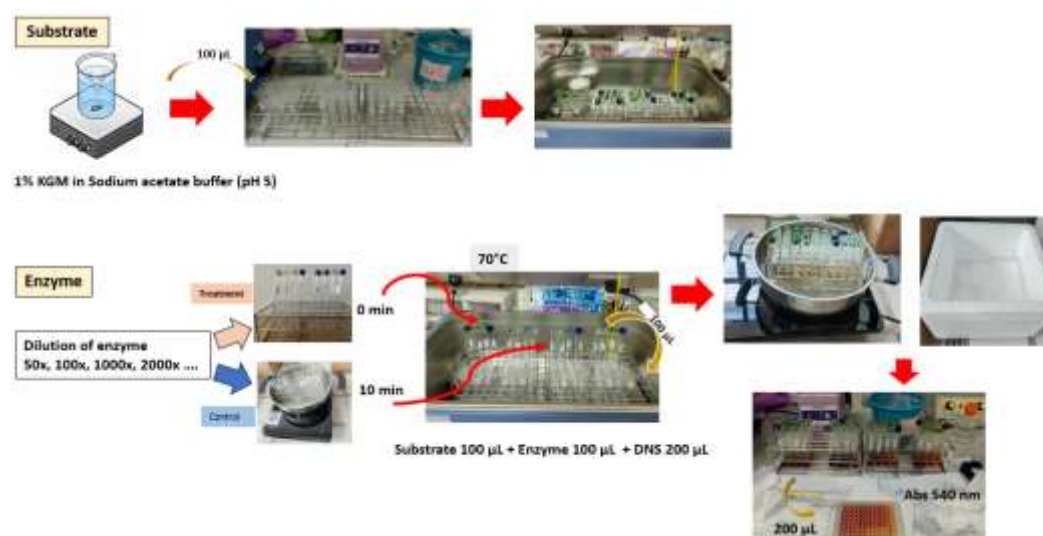
Figure 1. Schematic overview of the β-mannanase enzyme assay procedure. The assay involved incubation of the enzyme with 2 mg mL^{-1} KGM substrate at pH 5.0 and 70°C, followed by the quantification of reducing sugars using the DNS method. Absorbance was measured at 540 nm to calculate enzyme activity based on a mannose standard curve.

7) Calculation for enzyme activity (U mL^{-1})

The enzyme unit, or international unit for enzyme (symbol U, sometimes also IU), is a unit of enzyme's catalytic activity (IUPAC, 2018). 1 U (µmol min^{-1}) is defined as the amount of the enzyme that catalyzes the conversion of one micromole (µmol) of substrate per minute under the specified conditions of the assay method (NC-IUB, 1979). In this study, the enzyme activity was calculated according to **Equation 1**, which expresses one unit (U) as the quantity of enzyme required to convert 1 µmol of substrate per minute under the defined conditions.

The equation of enzyme activity (U mL^{-1})

$$\text{enzyme activity (U mL}^{-1}) = \frac{(OD\ sample - OD\ control) \times 1000 \times dilution\ factor}{slope \times MW \times time \times sample\ in\ reaction} \quad (1)$$

OD sample = absorbance of the enzyme solution
OD control = absorbance of control
Dilution factor = dilution (times)
Slope = m value of the standard curve
Mw = molecular weight of mannose
Time = reaction time (min)
Sample in reaction = the sample volume used for the reaction (mL)

8) Calculation for specific activity (U mg^{-1} protein)

The specific activity of β-mannanase was calculated by dividing the enzyme activity (U mL^{-1}) by the total protein concentration (mg mL^{-1}) of the enzyme solution, as shown in **Equation 2**. Protein concentration was determined using the Bradford assay, according to the method of Bradford (1976), with bovine serum albumin (BSA) as the standard. The specific activity was expressed as units of enzyme activity per milligram of protein (U mg^{-1}).

The equation of specific activity (U mg^{-1} protein)

$$\text{specific activity (U mg}^{-1}\ protein) = \frac{enzyme\ activity\ (U\ mL^{-1})}{protein\ concentration\ (mg\ mL^{-1})} \quad (2)$$

2.2 Determination of mannanase molecular mass by SDS-PAGE

The molecular mass of the mannanase was estimated using Sodium Dodecyl Sulfate-Polyacrylamide Gel Electrophoresis (SDS-PAGE) was performed according to the method of Laemmli (1970). The procedure involved gel preparation, sample preparation, electrophoresis, protein staining, and analysis of the resulting banding pattern. SDS-PAGE separates proteins based on their molecular weight by electrophoresing SDS-treated proteins through a polyacrylamide gel matrix.

1) Sample preparation

The mannanase sample was dissolved in sample buffer (0.125 M Tris-HCl, pH 8.0, containing 20% glycerol, 4% SDS, 0.004% bromophenol blue, and 10% β-mercaptoethanol). The protein sample was then denatured by heating at 100°C for 5 minutes.

2) Gel electrophoresis

SDS-PAGE was performed according to the Laemmli method using a vertical slab electrophoresis apparatus. A 12% resolving polyacrylamide gel was used. 25 µL of the prepared protein sample and appropriate molecular weight marker(s) were loaded into separate wells of the gel. Electrophoresis was carried out at a constant voltage of 100 V until the dye front reached the bottom of the gel (approximately 2 hours).

3) Gel staining and destaining

After electrophoresis, the gel was carefully removed from the apparatus and stained with Coomassie Brilliant Blue staining solution for a sufficient time to visualize the protein bands. Subsequently, the gel was destained using a destaining solution until the protein bands were visible against a clear background. The protein bands were then observed visually (Figure 2).
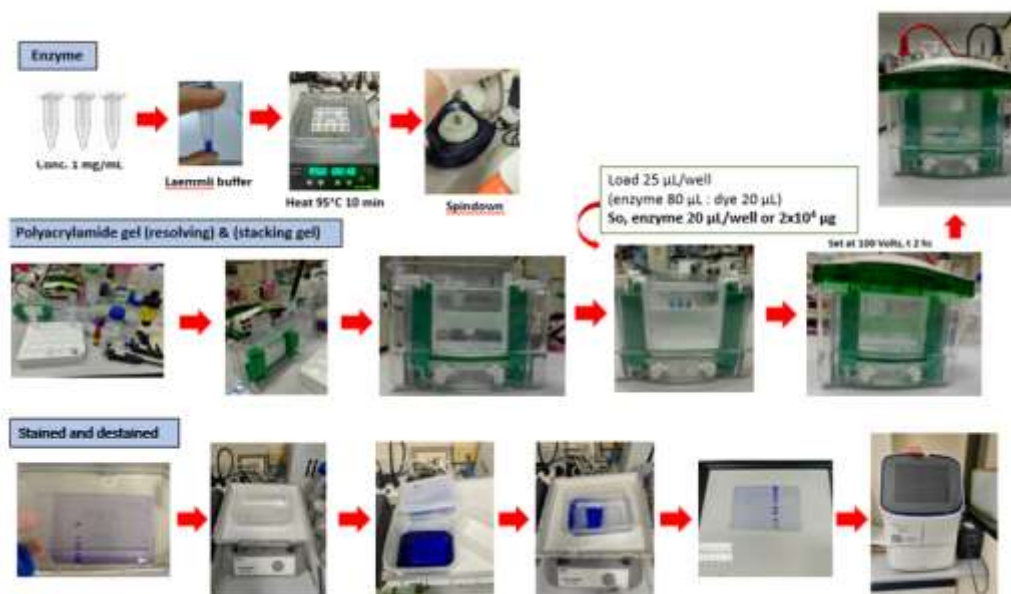
Figure 2. SDS-PAGE analysis for determining the purity of β-mannanase. The enzyme sample was subjected to electrophoresis on a 12% polyacrylamide gel under denaturing conditions. Protein bands were visualized by Coomassie Brilliant Blue staining. A distinct band observed between 50–75 kDa indicates the molecular weight range of the enzyme, confirming its purity and consistency across replicate lanes.

3. Results and Discussion

3.1 Enzyme assay of β-mannanase

The results presented in **Figure 3,** the D-mannose standard curve was constructed, yielding the linear regression equation $y = 0.3012x - 0.0103$ with an R^2 value of 0.9991. **Table 1** shows that to validate the enzyme performance under typical assay conditions, the absorbance value of 0.483, which lies near the center of the standard curve range, was selected as the representative reference point. At this point, the reducing sugar concentration was 1.569 mg mL^{-1}, yielding a total of 0.87 μmol of mannose equivalents being released. The calculated enzyme activity was 0.029 U, and the specific activity was 96.79 U mg^{-1} protein (~96,790 U g^{-1} protein).

(a) Increasing intensity of reddish-brown color in tubes indicates higher mannose concentrations after DNS reaction.
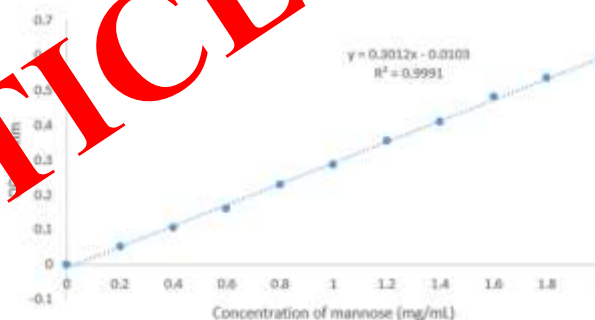
(b) Linear calibration curve (R^2 = 0.9991) between absorbance at 540 nm and mannose concentration (0–2.0 mg mL^{-1}).

Figure 3. **Figure 3.** A mannose-based standard system was developed for the determination of reducing sugars using the DNS method. (a) and (b) represent the visual color gradient and the corresponding standard calibration curve, respectively.

Comparing this to the standard curve trend confirms that the experimental results fall within the expected linear response zone of the DNS method ($R^2 > 0.9991$), thus confirming assay accuracy. The mid-range value serves as an internal control to validate experimental variation, ensuring that other absorbance readings in the series remain within scientifically acceptable limits (Bailey *et al*., 1992). Interestingly, values on either side of 0.483 (e.g., 0.547 and 0.651) demonstrated proportionally consistent increases in reducing sugar concentration and enzyme activity, reinforcing the reliability of the method. The highest specific activity (154.33 U mg^{-1}) was observed at an absorbance of 0.764, indicating enhanced catalytic efficiency under those conditions (Hu *et al*., 2020).   This approach of using a midpoint reference not only supports the validity of the assay but also provides a comparative baseline to highlight enzymatic efficiency at both lower and higher substrate conversion levels.

Table 1 Absorbance values at 540 nm, reducing sugar concentration, total reducing sugar, enzyme activity, and specific activity of β-mannanase as determined by the DNS assay. Mannose was used as the reducing sugar standard.

Absorbance (540 nm)	Reducing sugar conc. (mg mL^{-1})	Total reducing sugar (mg)	Reducing sugar (µmol)	Enzyme activity (U)	Protein Used (mg)	Specific activity (U mg^{-1})	Specific activity (U g^{-1})
0.764	2.502	0.25	1.39	0.046	0.0003	154.33	154,327.27
0.702	2.296	0.23	1.27	0.042	0.0003	141.63	141,632.18
0.651	2.127	0.213	1.18	0.039	0.0003	131.19	131,189.44
0.547	1.782	0.178	0.99	0.033	0.0003	109.89	109,894.45
0.514	1.672	0.167	0.93	0.031	0.0003	103.14	103,137.38
0.483	1.569	0.157	0.87	0.029	0.0003	96.79	96,789.84

Note: β-Mannanase activity was assayed using 2 mg mL^{-1} konjac glucomannan in a 0.1 mL reaction mixture incubated for 30 min. Reducing sugar was measured by the DNS method using mannose as the standard (y = 0.3012x + 0.0103, R² > 0.9991). Results were expressed as mannose equivalents (MW = 180.16 g/mol). One unit of activity (U) was defined as the release of 1 µmol reducing sugar/min; 0.0003 mg of protein was used.

The significantly higher specific activity observed in this study (96,789.84 U g^{-1}), compared to the manufacturer's specification of ≥10,000 U g^{-1} (approximately 10 U mg^{-1}), can be partially attributed to differences in substrate structure. The substrate used herein, KGM, is a glucomannan consisting of β-1,4-linked D-mannose and D-glucose units, whereas the manufacturer's assay typically utilizes galactomannan, characterized by a β-1,4-mannan backbone with galactose side chains. Glucose substitution in KGM, as opposed to galactose in galactomannan, might result in less spatial interference, potentially enhancing β-mannanase access and catalytic action on the substrate. Previous studies have demonstrated that side-chain substituents can significantly affect β-mannanase catalytic efficiency, influencing both binding affinity and turnover rates (Zhou *et al*., 2017).

The assay method used in this study also differs from that employed by the manufacturer. The DNS assay detects reducing ends of oligosaccharides through the reduction of 3,5-dinitrosalicylic acid, offering high sensitivity, particularly for small oligosaccharides generated during hydrolysis. In contrast, the Amano Somogyi method quantifies reducing sugars based on the reduction of copper (II) ions and may be less sensitive to certain oligosaccharide chain lengths. These methodological differences could lead to the apparent overestimation of enzyme activity when using the DNS method compared to the Somogyi-based assay, especially when using substrates like KGM that may produce a higher proportion of small oligosaccharides.

The extrapolated activity value obtained in this study (~96,790 U g^{-1}, assuming 100% protein purity) considerably exceeds the manufacturer's stated minimum of 10,000 U g^{-1}. This discrepancy is likely multifactorial, arising from differences in substrate specificity, assay sensitivity, and the assumption of complete protein purity in calculations. The commercial β-mannanase preparation may contain stabilizers or impurities that dilute the actual protein concentration, leading to an underestimation of specific activity in practical applications.

Although the present study emphasized enzyme activity and molecular weight estimation, these parameters were deliberately chosen to provide functionally relevant evidence for the enzyme's efficacy. Rather than merely characterizing the enzyme, this approach aimed to validate its suitability for downstream applications involving KGM. Based on the observed catalytic performance, these two parameters offer sufficient justification for the selection of this commercial β-mannanase in future experimental frameworks.

For a more comprehensive understanding of the enzyme's catalytic properties, future work should include comparative analyses using both KGM and galactomannan as substrates, evaluated under identical experimental conditions with both the DNS and Amano Somogyi assay methods. Additionally, determination of kinetic parameters (Km and Vmax) on both substrates would provide deeper insights into substrate affinity and catalytic efficiency, facilitating a clearer interpretation of the enzyme's industrial applicability.

3.2　Molecular mass of mannanase

SDS-PAGE analysis of the loaded enzyme sample showed consistent protein bands within the 50 and 75 kDa range across two replicate lanes (Figure 4) with both lanes displaying nearly identical banding patterns, confirming high reproducibility and uniformity in the protein profile. This molecular weight range corresponds closely with previously reported values for β-mannanases derived from *Aspergillus niger*, including those at approximately 56 kDa (Magengelele *et al*., 2021) and 66 kDa (Arunrattanamook *et al*., 2020; Alsarrani *et al*., 2011). The commercial enzyme BGM AMANO 10 used in this study is derived from a proprietary fermentation process involving a selected *A. niger* strain, and the observed banding pattern supports its fungal origin.

Variability in the apparent molecular mass of *A. niger* mannanases has been attributed to factors such as isoenzyme diversity and differential post-translational modifications, particularly N-linked glycosylation, which can shift electrophoretic mobility (Yang *et al*., 2015). In the present study, the presence of two distinct protein bands within the expected molecular weight range suggests the possibility of either post-translational modifications or the co-purification of isoenzymes. Further structural analyses, such as deglycosylation treatment or LC–MS, would aid in confirming the nature of these protein species.

The molecular mass of mannanases is a key determinant of their performance in industrial settings. Enzymes in the 50–75 kDa range have demonstrated favorable thermostability and catalytic efficiency when hydrolyzing mannose-rich polysaccharides, making them suitable for applications in food processing, animal feed, and biofuel

production (Zhou *et al.*, 2019). The molecular characteristics observed here reinforce the potential of AMANO-derived β-mannanase as an effective biocatalyst. Moreover, enzymes within this molecular weight range, especially those from *A. niger*, have been shown to efficiently release MOS from substrates such as galactomannan and glucomannan. These MOS serve as prebiotic compounds that selectively stimulate beneficial gut microbiota, particularly *Lactobacillus* and *Bifidobacterium* spp., and are widely incorporated in synbiotic product formulations (Zhou *et al.*, 2019). The enzyme profile observed in this study thus aligns well with the requirements for bioconversion processes, supporting its application in MOS production from agro-industrial residues like palm kernel cake or locust bean gum.
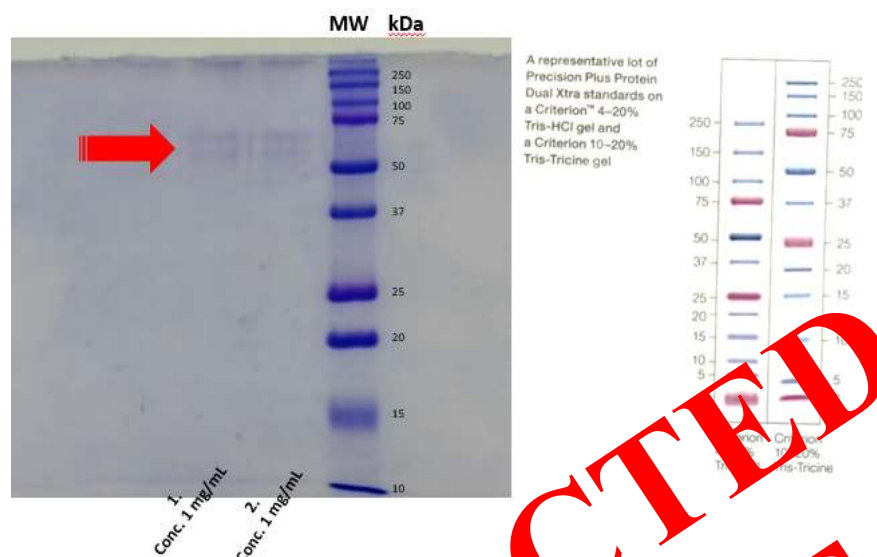
Figure 4. SDS-PAGE analysis of commercial β-mannanase BGM "AMANO"10; MW: molecular marker (BIO-RAD)
Noted: Lane 1-2: β-mannanase conc. 1 mg/ml; Lane M: Molecular weight mark

4. Conclusions

This study presents a detailed characterization of a β-mannanase enzyme derived from A. niger, with significant implications for industrial applications, particularly in the production of MOS. The enzyme demonstrated high specific activity of approximately 96,790 U g^{-1} under optimal conditions (2 mg mL^{-1} KGM, pH 5.0, and 70°C), indicating its robust catalytic efficiency under mildly acidic and thermophilic conditions. SDS-PAGE analysis revealed a molecular weight within the range 50–75 kDa, consistent with the reported profiles of fungal (A. niger) mannanases and supporting its biochemical identity.

Although the present study did not include quantitative or structural analysis of the hydrolysis products, the substantial enzymatic activity under the tested conditions suggests that the enzyme is capable of effectively cleaving β-1,4-mannosidic linkages in konjac glucomannan. These two core indicators, enzyme activity and molecular weight, were strategically selected to validate the enzyme's functional performance, providing a sufficient basis for its use in further MOS-related research. This property is a key prerequisite to produce MOS, with significant implications for the development of prebiotic-rich functional foods. Given its favourable operating parameters, the enzyme is well-suited for large-scale bioprocesses utilizing mannan- and glucomannan-rich agricultural residues. These findings position the AMANO-derived β-mannanase as a valuable tool for bioconversion processes in the food, feed, and bioethanol industries, particularly in synbiotic formulations designed to promote gut health.

5. Acknowledgements

6. References

Alsarrani, A., Q. 2011. Production of Mannan-degrading enzyme by *Aspergillus niger*. *Journal of Taibah University for Science*, Vol. 5, 1-6.

Arunrattanamook, N., Wansuksri, R., Uengwetwanit, T., and Champreda, V. 2020. Engineering of β-mannanase from *Aspergillus niger* to increase product selectivity towards medium chain length mannooligosaccharides. *Journal of Bioscience and Bioengineering*, 130:5, 443-449.

Bailey, M. J., Biely, P., and Poutanen, K. 1992. Interlaboratory testing methods for assay of xylanase activity. *Journal of Biotechnology*, 23(3), 257–270.

Bradford, M. M. 1976. A rapid and sensitive method for the quantitation of microgram quantities of protein utilizing the principle of protein-dye binding. *Analytical Biochemistry*, 72(1), 248–254. https://doi.org/10.1016/0003-2697(76)90527-3

Davies, G., and Henrissat, B. 1995. Structures of carbohydrate-active enzymes. *Current Opinion in Structural Biology*, 5(5), 637-644.

Gibson, G. R., Roberfroid, M. B., and Kolida, S. 2004. Dietary modulation of the human colonic microbiota: introducing the concept of prebiotics. *British Journal of Nutrition*, 91(S1), S1-S11.

Henrissat, B. 1991. A classification of glycosyl hydrolases based on amino acid sequence similarities. *Biochemical Journal*, 280(2), 309-316.

Hughes, R. L. 2020. A review of the role of the gut microbiome in personalized sports nutrition. *Frontiers in Nutrition*, 6, 191. https://doi.org/10.3389/fnut.2019.00191

Hu, X., Yu, J., Wang, X., & Wang, Y. 2020. High-level expression and characterization of a thermostable β-mannanase for mannooligosaccharide production. *International Journal of Biological Macromolecules*, 151, 1075–1083.

IUPAC. 2018. *Terminology of bioanalytical methods (IUPAC Recommendations 2018). Pure and Applied Chemistry*, 90(4), 641–684. https://doi.org/10.1515/pac-2017-0605

Kaur, G., Kumar, V., and Sharma, N. 2007. Microbial β-mannanases: production and applications. *Applied Microbiology and Biotechnology*, 75(2), 287-300.

Kaur, J., and Dhawan, S. 2007. Microbial mannanases: An overview of production and applications. *Critical Reviews in Biotechnology*, 27:4, 197-216.

Laemmli, U. K. 1970. Cleavage of structural proteins during the assembly of the head of bacteriophage T4. *Nature*, 227(5259), 680–685. https://doi.org/10.1038/227680a0

Magengelele, M., Hlalukana, N., Malgas, A., Rose, S. H., Zyl, W. H., and Pletschke, B. I. 2021. Production and *in vitro* evaluation of prebiotic manno-oligosaccharides prepared with a recombinant *Aspergillus niger* endo-mannanase, Man26A. *Enzyme and Microbial Technology*, 150, 109893.

Miller, G. L. 1959. Use of dinitrosalicylic acid reagent for the determination of reducing sugar. *Analytical Chemistry*, 31(3), 426–428. https://doi.org/10.1021/ac60147a030

Murillo-Franco, S. L., Galvis-Nieto, J. D., and Orrego, C. E. 2024. Mannooligosaccharide production from açaí seeds by enzymatic hydrolysis: Optimization through response surface methodology. *Environmental Science and Pollution Research*. https://doi.org/10.1007/s11356-024-33540-2

Nomenclature Committee of the International Union of Biochemistry. 1979. Units of enzyme activity. *European Journal of Biochemistry*, 97(2), 319–320.

Roberfroid, M. B., Gibson, G. R., Hoyles, L., McCartney, A. L., Rastall, R. A., Rowland, I. R., and Guarner, F. 2010. Prebiotic effects: metabolic and health benefits. *British Journal of Nutrition*, 104(S2), S1-S63.

Singh, R., Kaur, N., and Kennedy, J. F. 2018. Chemistry and applications of konjac glucomannan. *International Journal of Biological Macromolecules*, 112, 1030-1040.

Singh, S., Singh, G., and Arya, S. K. 2018. Mannans: an overview of properties and applications in food products, *International Journal of Biological Macromolecules*, 119: 79–95,

Singh, V., Patel, S., and Shah, N. 2019. Manno-oligosaccharides as prebiotics: Production, characterization and applications. *International Journal of Food Microbiology*, 301, 108197.

Slavin, J. 2013. Fiber and prebiotics: mechanisms and health benefits. *Nutrients*, 5(4), 1417–1435. https://doi.org/10.3390/nu5041417

Tamaru, Y., Araki, T., Amagoi, H., Mori, H., and Morishita, T. 1995. Purification and characterization of an extracellular beta-1,4-mannanase from a marine bacterium, *Vibrio* sp. strain MA-138. *Applied and Environmental Microbiology,* 61:4454–4458.

Yang, H., Shi, P., Lu, H., Wang, H., Luo, H., Huang, H., Yang, P., and Yao, B. 2015. A thermophilic β-mannanase from Neosartorya fischeri P1 with broad pH stability and significant hydrolysis ability of various mannan polymers. *Food Chemistry*, 173, 283-289. https://doi.org/https://doi.org/10.1016/j.foodchem.2014.10.022

Zhang, H., Liu, W., Zhang, J., and Chen, Y. 2019. Prebiotic potential of konjac glucomannan oligosaccharides and their effects on gut microbiota. *Food & Function*, 10(10), 6424-6433.

Zhang, W., Li, M., Wang, L., and Gong, Y. 2021. Structural properties and functional potential of konjac glucomannan: A review. *Food Hydrocolloids*, 120, 106987.

Zhao, D., Wang, Y., Na, J., Ping, W., and Ge, J. 2019. The response surface optimization of β-mannanase produced by *Lactobacillus casei HDS-01* and its potential in juice clarification. *Preparative Biochemistry and Biotechnology,* 49:202-207. https://doi.org/10.1080/10826068.2019 .1566151

Role of Calcium Silicate for Growth Enhancement and Possibility to Alternaria Leaf Spot Control in Chinese Cabbage

Santiti Bincader[a, b], Nutthawoot Premjit[a], Tanawan Promkhlibnil[a], Arunee Kongsorn[a], Sirorat Khienman[a], Chonlada Songnirundron[a], Thipwara Tiansawang[a], Pisut Keawmanee[c]*

[a]Division of Plant Science, Faculty of Agricultural Technology and Agro-Industry, Rajamangala University of Technology Suvarnabhumi Phra Nakhon Si Ayutthaya 13000, Thailand
[b]Agriculture and Food Research Unit, Center of Excellence in Agriculture and Food Safety, Rajamangala University of Technology Suvarnabhumi, Phra Nakhon Si Ayutthaya 13000, Thailand
[c] Department of Plant Pathology, Faculty of Agriculture at Kamphaeng Saen, Kasetsart University, Nakhon Pathom 73140, Thailand
*Corresponding author. Tel.: 034-351890; fax: 034-351890; E-mail address: fagrpske@ku.ac.th.

Abstract

Calcium silicate is an inorganic compound that plays a crucial role in strengthening plant cell walls, enhancing resistance to environmental stresses and pathogenic infections. It has also been reported to stimulate plant growth and induce defense mechanisms through physiological and biochemical pathways. This study aimed to evaluate the efficacy of calcium silicate in promoting seed germination, enhancing seedling physiological development, and possibility inhibiting the growth of the fungal pathogen responsible for leaf spot disease in Chinese cabbage (*Brassica rapa* subsp. *chinensis*). The fungus pathogen was isolated from diseased Chinese cabbage collected in Phra Nakhon Si Ayutthaya Province, Thailand. Based on morphological identification and molecular techniques using PCR amplification of the ITS1-5.8S-ITS2 region were identified the pathogen as *Alternaria brassicicola*, with identity level of 98.00–100.00%. The effect of calcium silicate on seed germination at three different concentrations (1%, 2%, and 3%) were investigated. The finding indicated that calcium silicate had no effect on seed germination within the first 72 hours, with all treatments showing a 100% germination rate. However, seedling development was significantly influenced by the treatment. The 3% of calcium silicate yielded the highest performance with seedlings at 28 days exhibiting an average height of 15.80 cm, an average of 7 roots per plant, and a mean root length of 5.43 cm with significantly greater than the control. For the possibility to fungal control using the poisoned food technique, calcium silicate at the highest concentration was able to inhibit *A. brassicicola* mycelial growth by 28.21%. Based on these findings, calcium silicate demonstrates potential as a growth-promoting agent for Chinese cabbage, particularly in enhancing root system development, while also providing partial suppression of fungal pathogens. Hence, calcium silicate could be considered as an effective seed coating or soil amendment to protect seeds during early germination and seedling establishment.

Keywords: Calcium Silicate, Chinese Cabbage, Fungal Pathogen, Seed Development

1. Introduction

Calcium silicate (Ca_2SiO_4) is an inorganic compound comprising calcium and silicon, which play significant roles in plant growth and defense. Calcium is essential for the structural integrity of plant cell walls, membrane stabilization, and intracellular signaling, while silicon, though not classified as essential, contributes to improved tolerance against abiotic and biotic stresses (Gupta et al., 2023). The combined application of these elements in the form of calcium silicate has shown beneficial effects in enhancing plant vigor, photosynthetic efficiency, and resistance to pathogens (Majláth et al., 2020). In agricultural practices, calcium silicate has been employed to amend soils deficient in silicon, leading to improved crop yields and quality. Its application has demonstrated benefits such as increased photosynthetic efficiency, enhanced root development, and strengthened plant defense mechanisms. Moreover, the incorporation of calcium silicate into soil management strategies has been associated with the suppression of certain plant pathogens, suggesting its potential as a component in integrated disease management programs (Prasad et al., 2017; Shelar et al., 2023). In parallel, climate change has become an increasingly significant factor influencing soil health and pathogen dynamics. Rising global temperatures, changes in precipitation patterns, and increased frequency of extreme weather events can alter soil microbial communities and promote the proliferation of soil-borne pathogens (Chakraborty et al., 2022). These changes may extend the geographic range and seasonal activity of pathogens, resulting in higher disease pressure on susceptible crops. Moreover, elevated soil moisture and temperature can create conducive conditions for fungal pathogens to thrive, complicating disease management in susceptible vegetable crops (Steinweg et al., 2013).

Chinese cabbage (*Brassica rapa* subsp. *chinensis*), commonly known as bok choy, is a leafy vegetable of significant economic importance, particularly in Asian countries. However, its cultivation faces challenges including abnormal seed germination, weak root systems, and susceptibility to diseases such as leaf spot caused by genus Alternaria (Kumar and Nowicki, 2018). This pathogen infects seeds and seedlings, leading to pre- and post-emergence damping-off, and significant yield reduction (Lee et al., 2018). Furthermore, inadequate early root growth exacerbates the plant's vulnerability to both biotic and abiotic stress, particularly under suboptimal field conditions. Early-stage infections and poor root development not only reduce plant establishment but also limit the crop's ability to absorb water and nutrients efficiently, especially under fluctuating environmental conditions (Hageman and Van Volkenburgh, 2021). These factors collectively diminish plant vigor and may increase reliance on chemical inputs, raising concerns about environmental safety and sustainable production. In addition, environmental stresses such as

fluctuating moisture levels and temperature extremes can enhance the virulence of soil-borne pathogens, further threatening seedling survival and crop productivity (Ahammed and Yang, 2021; Huang et al., 2023).

Current management strategies for disease primarily rely on synthetic fungicides, which are effective but raise concerns related to environmental contamination, human health, and the emergence of fungicide-resistant pathogen strains (Pongpisutta et al., 2023). Therefore, there is growing interest in sustainable alternatives that enhance plant immunity and reduce chemical uses. One such approach is the application of silicon- and calcium-based compounds, such as calcium silicate, which have demonstrated potential in improving germination, seedling vigor, and pathogen suppression (Lal et al., 2023). Recent developments in seed treatment technologies have explored the use of nanomaterials and mineral-based coatings to enhance seed performance under stress conditions (Shelar et al., 2023). Studies have shown that seed priming with calcium silicate can improve water uptake, accelerate enzymatic activation during germination, and promote early root elongation (Majláth et al., 2020). These physiological enhancements may contribute to more robust seedlings with increased resistance to early-season diseases, including those caused by *Alternaria* spp. (Gupta et al., 2023). Given these benefits, calcium silicate represents a promising candidate for sustainable crop management practices. This study aims to evaluate the efficacy of calcium silicate in enhancing seed germination, promoting physiological growth parameters, and inhibiting the growth of fungal pathogen in Chinese cabbage. This research will seek to develop a practical and environmentally safe strategy that enhances early-stage plant development while contributing to disease suppression.

2. Methodology

2.1 Fungal isolation

Chinese cabbage showing brown leaf spot symptoms with distinct concentric rings and dark brown margins were collected from private plantation in Phra Nakhon Si Ayutthaya Province, Thailand. Fungal isolation performed using the tissue transplanting method with symptomatic tissues (5×5 mm) were cut and surface-sterilized in 1.2% sodium hypochlorite solution for 3 minutes, then rinsing with sterile distilled water 2–3 times. The tissue was wiped and allowed to air dry, placed on the surface of potato dextrose agar (PDA) supplemented with streptomycin sulphate at a concentration of 200 ppm, and later incubated at 25°C under a 12-hr light/12 hr dark photoperiod for 5 days to induce mycelial and reproductive structure development. The fungus was purified using a single spore isolation technique on water agar (WA), and mycelia were transferred onto potato carrot agar (PCA) for further study.

2.2 Morphological, molecular identification and Phylogenetic tree

Petri dishes containing 15 mL of PDA mixed with 200 ppm streptomycin sulphate were inoculated with a 5-mm-diameter core taken from the edge of an actively growing 5-day old culture. The culture was incubated at 25°C under a photoperiod of 12 hr light/12 hr dark. Colony diameter of a five-replicate culture was recorded at day 5. Also, 30 conidia were randomly selected from each replicate to be measured their length and width at day 5 under Olympus CX31 binocular compound microscope at 400x magnification with Olympus CellSens standard software version 1.16.

The fungal genomic DNA was prepared and extracted following Rattanakreetakul et al. (2023) and using the kit "DNA Secure Plant Kit" (Tiangen Co., Ltd., Beijing, China) following the manufacturer's instructions. The internal transcribed spacer (ITS) region was amplified using the primer ITS1 (5′-TCCGTAGGTGAACCTGCGG-3′)/ITS4 (5′-TCCTC CGCTTATTGATATGC-3′) (White et al., 1990) following Bincader et al. (2025). PCR was carried out using the PCR thermal cycler (Sensoquest GmbH, Göttingen, Germany) under the following conditions: pre-denaturation at 94 °C for 5 min; 30 cycles of denaturation at 94 °C for 1 min, annealing at 56 °C or 1 min, and extension at 72 °C for 1 min; and a final extension step of 72 °C for 5 min. PCR products were rechecked and separated by 1.2% electrophoresis, then performed at ATGC Co., Ltd., in Pathum Thani, Thailand, for nucleotide sequencing analysis.

The nucleotide sequence was generated with Multiple alignments were performed using clustalW alignment routine (Thompson et al., 1994). The phylogenetic tree was created using the maximum parsimony (Kannan and Wheeler, 2012), and the confidence of the groupings was determined by bootstrap analysis (Felsenstein, 1985), with 1,000 replications to test the significance the trees. Analysis of the sequence data was performed by the MEGA version X software program (Kumar et al., 2018) to generate a phylogenetic tree.

2.3 Efficacy of calcium silicate on Seed Germination

The efficacy of calcium silicate in promoting seed germination of Chinese cabbage (hybrid cultivar Chan Jao F1 obtained from a commercial seed supplier) was evaluated using the blotter method. Seeds were soaked in calcium silicate solutions at 3 different concentrations (1%, 2%, and 3%) for 6 hr, while sterile distilled water was used as the control treatment. Germination rates were recorded at 24, 48, and 72 hr. described as below:

$$Seed\ germination\ (\%) = \left[\frac{Seed\ germinated}{Total\ seed}\right] \times 100$$

The experiment was arranged in a completely randomized design (CRD), with 7 replications per treatment. Statistical analysis was performed using R software (version 3.6.2). Mean comparisons were conducted using the Least Significant Difference (LSD) method at a significance level of P = 0.05.

2.4 Effect of Calcium Silicate to control fungal pathogen in vitro

Fungal pathogen was cultured on PDA and incubated at 25°C under a 12-hr light/12 hr dark photoperiod for 5 days. A 6-mm diameter mycelial plug was cut from the edge of colony margin using a cork borer and transferred onto PDA media amended with calcium silicate at 3 different concentrations, then incubated under the same conditions. Colony diameter was measured for 5 days. The experiment was arranged in a completely randomized design (CRD) with seven replications. Data were statistically analyzed using R software (version 3.6.2). Treatment means were compared using the Least Significant Difference (LSD) method at a significance level of P=0.05. The diameter of fungal colonies was calculated using the following formula:

$$Colony\ diameter\ (cm) = \left[\frac{\text{Diameter on axis X + Diameter on axis Y}}{2}\right]$$

$$Percent\ Inhibition\ (\%) = \left[\frac{\text{Control} - \text{treatment}}{Control}\right] \times 100$$

2.5 Calcium Silicate Efficacy on Growth Development

A field experiment was conducted in the greenhouse (28±2°C; RH=70-80%) at Division of Plant Science, Faculty of Agricultural Technology and Agro-Industry, Rajamangala University of Technology Suvarnabhumi, Phra Nakhon Si Ayutthaya, Thailand. The efficacy of calcium silicate was evaluated using seedlings obtained from the seed germination experiment above. The seedlings were transplanted into 6-inch nursery pots filled with peat moss previously sterilized by autoclaving at 121 °C and 15 psi for 20 minutes. The sterilization process was repeated after 24 hr to ensure complete disinfection. Experiments were treated with calcium silicate solutions at three concentrations and sterile distilled water used as the control treatment. The solutions were applied every 7 days (No other nutrients or fertilizers were added). Plant height, root length, and the number of roots were recorded weekly for 30 days (describe by Bejarano-Herrera et al., 2024). The experiment was arranged in a completely randomized design (CRD) with ten replications per treatment. Data were analyzed using R software (version 3.6.2). Mean comparisons were performed using the Least Significant Difference (LSD) method at a significance level of P=0.05.

3. Results and Discussion

3.1 Fungal isolation and morphological characteristics

The fungal isolate obtained from Chinese cabbage showing brown leaf spot symptoms, dark brown margins, and concentric ring patterns from private plantation in Phra Nakhon Si Ayutthaya Province. Morphological characteristics was consistent with *Alternaria* spp., as previously described by Pongpisutta et al. (2023). When cultured on PDA, the colony appeared olive green to gray with a smooth white margin and moderately raised mycelia on the surface of the medium. Microscopic examination at 400× magnification indicated that the isolate produced dictyospores (conidia) measuring approximately 6.15–9.51 × 16.98–48.64 μm. The conidia were light brown, with mostly smooth walls, although roughened walls were occasionally observed in older spores. The conidia were typically obclavate, 2–5 transverse septa, with an apical beak that was pale brown and short, and a rounded base. Conidia were observed in branched chains of approximately 7–15 spores, light brown conidiophores. Additionally, proliferation of spore cells into new conidiophores and the emergence of new conidia from the conidial apex were frequently observed (Figure 1).

Based on the morphological features described above and comparison with descriptions in Illustrated Genera of Imperfect Fungi (Barnett and Hunter, 1972), the isolate was identified as *Alternaria brassicicola*. This fungal pathogen has been reported to infect a wide range of host plants, particularly those in the Brassicaceae family such as cabbage, Chinese cabbage, and broccoli, as well as other economically important crops including lettuce and sunflower. Furthermore, *A. brassicicola* is known to occur in a saprophytic stage and may act as a secondary invader in some cases (Woudenberg et al., 2013; 2014; 2015).

3.2 Molecular analysis

The identification of fungal species using molecular techniques served as a reliable method to confirm the accuracy of the fungal strains obtained. The molecular data supported the morphological observations and ensured precise taxonomic placement of the isolates. The finding indicated that PCR amplification of the ITS1–5.8S–ITS2 region using ITS4/ITS5 primers showed a PCR product of approximately 550 bp. Nucleotide sequence analysis and comparison with the GenBank database revealed a high similarity to *Alternaria brassicicola*, with percent identity ranging from 98.41% to 98.61% and query coverage ranging from 98.00% to 100.00%.

Based on the phylogenetic analysis using the Neighbor-Joining method, the fungal isolate was clustered within the same clade as *A. brassicicola* isolates CBS118699 (accession no. JX499031) and PPRI:19555 (accession no. KT895944), with a bootstrap value of 98% (Figure 2). It was clearly separated from *A. brassicae* isolate CBS116528 (accession no. KC584185) and *A. alternata* isolate CBS916.96 (accession no. AF347031), a known pathogen of *Brassica* and lettuce plants, which formed a distinct clade with a bootstrap value of more than 90%. In addition, the fungal study was also clearly separated from *A. septorioides* isolate CBS106.41 (accession no.

KC584216), a morphologically similar species that causes comparable disease symptoms in plants (Woudenberg et al., 2013; 2015) (Figure 2).

Figure 1 Fungal isolation used in this study. Colony characteristics of fungal cultured on PDA and incubated at 25°C under a 12-hr light/12 hr dark photoperiod for 5 days (A); Leaf spot disease on Chinese cabbage (B); and conidia characteristics of the fungus observed under a light microscope at 20× magnification (C-D).

The internal transcribed spacer (ITS) region of ribosomal DNA has long been regarded as the universal DNA barcode for fungi due to its high variability and broad applicability across diverse fungal taxa. Recent advancements in molecular systematics have underscored the benefits of incorporating additional genetic markers to enhance phylogenetic resolution. Multi-gene phylogenetic analyses, which combine sequences from loci such as the large subunit (*LSU*) rRNA, RNA polymerase II subunit (*RPB2*), translation elongation factor 1-alpha (*TEF-1α*), and glyceraldehyde-3-phosphate dehydrogenase (*GAPDH*), have proven effective in delineating species boundaries and uncovering novel taxa. For instance, Zhu et al. (2024) employed a multi-gene approach to identify a new genus, Heteroxylaria, within the family Xylariaceae, highlighting the method's capacity to resolve complex taxonomic relationships. Moreover, the integration of deep learning techniques with molecular data has further refined fungal classification. The research of Liu et al. (2025) developed FungiLT, a deep learning model combining BiLSTM and Transformer architectures, which achieved a species-level classification accuracy of 98.77% using ITS sequences. This approach demonstrates the potential of combining computational tools with molecular data to improve identification accuracy, especially when dealing with large-scale sequencing datasets.

In our study, while ITS sequencing provided a foundational framework for fungal identification, the addition of multiple gene regions significantly enhanced the resolution and reliability of species delineation. This multi-locus strategy is particularly crucial when distinguishing among morphologically similar or closely related species, where single-locus analyses may fall short. Therefore, integrating multiple genetic markers not only corroborates morphological assessments but also ensures a more robust and accurate taxonomic classification.

Figure 2 Neighbor-Joining tree constructed based on ITS sequences of *Alternaria* species, including ex-type or epitype sequences. Bootstrap values greater than 10% are indicated above the nodes. Strains isolated in this study are highlighted in bold.

3.3 Efficacy of calcium silicate on Seed Germination

The effectiveness of calcium silicate in promoting seed germination of *Brassica rapa* subsp. *chinensis* was investigated under laboratory conditions using the blotter method. Seeds were soaked in calcium silicate solutions at three different concentrations: 1%, 2%, and 3%, and then incubated to monitor germination responses over a 72-hour period. Within the first 24 hours, germination rates ranged from 93.33% to 96.67%, with no statistically significant differences observed among the treatments. At 48 hours, all treatments demonstrated an equal germination rate of 96.67%, indicating a continued and uniform germination response across the concentration levels. By 72 hours post-treatment, complete germination (100%) was observed in all treatment groups, suggesting that calcium silicate at these concentrations did not inhibit germination and may support early seedling development. These findings suggest potential for calcium silicate application in enhancing seed performance (Table 1; Figure 3).

These results align with previous research demonstrating the beneficial role of silicon-based compounds in enhancing seed germination and seedling vigor. For instance, Attipoe et al. (2023) reported that calcium silicate application improved soybean growth and yield by enhancing shoot morphological and physiological traits, suggesting a positive impact on early plant development. Similarly, Jiang et al. (2022) indicated that silica-based nanomaterials promoted seed germination and seedling growth in rice (*Oryza sativa* L.), with low concentrations enhancing shoot and root lengths, as well as antioxidant enzyme activities. Moreover, the research of Kuzmanović et al. (2021) demonstrated that silicon seed priming mitigated cinnamic acid-induced autotoxicity in cucumber (*Cucumis sativus* L.) by improving sucrose mobilization and respiratory metabolism during germination.

The uniform germination observed across all calcium silicate concentrations in the current study suggests that Brassica rapa subsp. chinensis seeds possess a high tolerance to calcium silicate, and that the compound may play a supportive role in early seedling development. This is consistent with findings from previous studies indicating that silicon compounds can enhance seed germination and seedling growth by modulating physiological and biochemical processes, such as antioxidant enzyme activities and hormone metabolism (Meng et al., 2024; Jiang et al., 2022).

Table 1 Germination percentage of Chinese cabbage seeds soaked in calcium silicate solutions at three different concentrations (1%, 2%, and 3%) over a period of 24 to 72 hours.

Treatments	Seed germination (%)[1/]		
	Day 1	Day 2	Day 3
Control	93.33±11.54a	96.67±5.77a	100.00±0.00a
Calcium silicate 1%	93.33±11.54a	96.67±5.77a	100.00±0.00a
Calcium silicate 2%	96.67±5.77a	96.67±5.77a	100.00±0.00a
Calcium silicate 3%	93.33±5.77a	96.67±5.77a	100.00±0.00a
C.V. (%)	9.6942	5.9726	4.2633
F-test	NS	NS	NS
MSE	83.33	33.33	1.81

[1/] Column values followed by the same letter are not significantly different (P=.05)
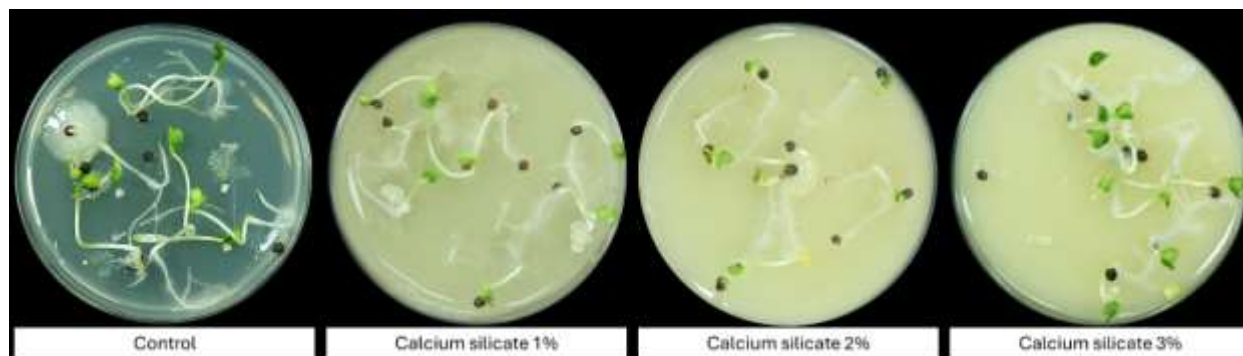
Figure 3 Efficacy of calcium silicate solutions at three different concentrations in promoting germination of *Brassica rapa* subsp. *chinensis* seeds after 72-hr incubation.

3.4 Effect of Calcium Silicate to control fungal pathogen in vitro

The efficacy of calcium silicate in inhibiting the mycelial growth of *Alternaria brassicicola*, the causal agent of leaf spot disease in Chinese cabbage, was evaluated using the poisoned food technique. The results indicated that at 1 day after inoculation, calcium silicate at concentrations of 2% and 3% exhibited the lowest fungal mycelial growth, with colony diameters of 2.25 cm. In comparison, the control and the 1% calcium silicate treatment resulted in colony diameters of 3.00 cm, respectively. However, statistical analysis indicated no significant differences among the treatments and the control at this time point. At 3 days after inoculation, calcium silicate at 3% and 2% concentrations significantly inhibited fungal growth, with colony diameters of 3.25 cm and 3.63 cm, respectively. In contrast, the 1% calcium silicate treatment and the control exhibited colony diameters of 4.75 cm and 4.88 cm, respectively. Similarly, at 5 days after inoculation, the results were consistent: the 3% calcium silicate treatment effectively reduced mycelial growth, showing a colony diameter of 7.00 cm. Treatments with 2% and 1% calcium silicate had colony diameters of 7.50 cm and 9.50 cm, respectively, whereas the control showed a colony diameter of 9.75 cm (Table 2; Figure 4).

The current study demonstrates the potential of calcium silicate as an effective agent to inhibit the growth of *Alternaria brassicicola* on Chinese cabbage, particularly at higher concentrations (2% and 3%). The observed dose-dependent inhibition aligns with findings from previous studies indicating the role of silicon-based compounds in enhancing plant resistance and suppressing fungal pathogens (Wang et al., 2017; Ahammed and Yang, 2021). Silicon amendments, such as calcium silicate, are known to fortify plant cell walls by promoting the deposition of silica, which acts as a physical barrier against fungal penetration and impairs pathogen colonization (Wang et al., 2017). Additionally, silicon may trigger systemic acquired resistance by activating defense-related enzymes and antioxidant pathways, thereby reducing pathogen virulence (Ahammed and Yang, 2021).

Comparable research on Alternaria species showed that silicon treatments significantly reduced mycelial growth and lesion development in various host plants (Ahammed and Yang, 2021; Denarié et al., 2025). These studies corroborate the inhibitory effects observed in our experiments, particularly the enhanced efficacy at 3% calcium silicate concentration.

Table 2 Efficacy of calcium silicate solutions at three different concentrations (1%, 2%, and 3%) in inhibiting the mycelial growth of *Alternaria brassicicola*, the causal agent of leaf spot disease in Chinese cabbage (*Brassica rapa* subsp. *chinensis*), measured at 1, 3, and 5 days of incubation.

Treatments	Colony Diameter (cm)[1/]		
	Day 1	Day 3	Day 5
Control	3.00±0.41a	4.88±0.64a	9.75±0.50a
Calcium silicate 1%	3.00±0.41a	4.75±0.48a	9.50±0.41a
Calcium silicate 2%	2.25±0.50a	3.63±0.63b	7.50±0.58b
Calcium silicate 3%	2.25±0.87a	3.25±0.29b	7.00±1.08c
C.V. (%)	2.1994	1.2856	4.2041
F-test	NS	**	***
MSE	0.33	0.28	0.47

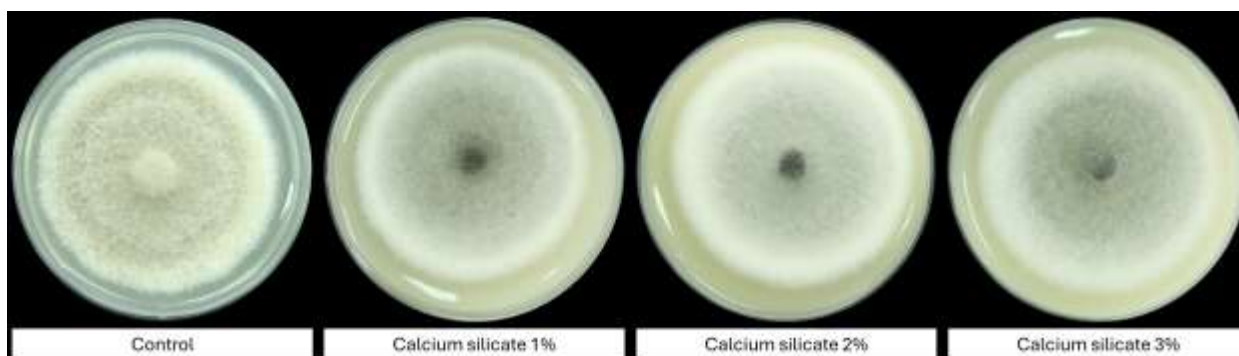[1/] Column values followed by the same letter are not significantly different (P=0.05)

Figure 4 Efficacy of calcium silicate solutions at three different concentrations in inhibiting the mycelial growth of *Alternaria brassicicola*, the causal agent of leaf spot disease in *Brassica rapa* subsp. *chinensis*. The antifungal activity was evaluated using the poisoned food technique incubated at 25°C under a 12-hr light/12 hr dark photoperiod for 5 days.

3.5. Calcium Silicate Efficacy on Growth Development

The efficacy of calcium silicate solutions on the physiological development of Chinese cabbage was investigated. The application of calcium silicate significantly influenced seedling growth. After 7 days of treatment, seedlings treated with the highest concentration of calcium silicate (3%) exhibited the greatest growth, with an average height of 2.23 cm. Seedlings treated with 2% and 1% calcium silicate showed average heights of 1.98 cm and 1.70 cm, respectively. At 14 days post-treatment, consistent results were observed: seedlings treated with 3% calcium silicate reached the highest average height of 7.68 cm, followed by those treated with 2% and 1% concentrations, which attained average heights of 6.53 cm and 5.58 cm, respectively. The control group seedlings exhibited an average height of 4.78 cm (Table 2; Figure 2). Similarly, at 21 and 28 days after treatment, seedlings exposed to 3% calcium silicate consistently showed the greatest height, with mean values of 12.70 cm and 15.80 cm, respectively. Those treated with 2% and 1% concentrations measured 11.30 cm and 10.30 cm at day 21, and 14.05 cm and 13.70 cm at day 28, respectively (Table 3; Figure 5).

Table 3 Efficacy of calcium silicate solutions at three different concentrations (1%, 2%, and 3%) in promoting the growth and development of Chinese cabbage seedlings.

Treatments	Length of seedling (cm) [1]			
	7 Day	14 Day	21 Day	28 Day
Control	1.70±0.53b	4.78±1.11c	8.48±0.78c	11.08±1.32b
Calcium silicate 1%	1.70±0.36b	5.58±0.45bc	10.30±0.80b	13.70±0.82a
Calcium silicate 2%	1.98±0.32a	6.53±0.98ab	11.30±0.91b	14.05±1.62a
Calcium silicate 3%	2.23±0.30a	7.68±0.85a	12.70±0.74a	15.80±1.44a
C.V. (%)	20.0356	14.3667	7.5621	9.7644
F-test	*	**	***	**
MSE	0.15	0.78	0.65	1.78

[1] Column values followed by the same letter are not significantly different (P=0.05)

Root development corresponded with the observed stem growth patterns. The highest calcium silicate concentration (3%) significantly enhanced root growth and root number, with seedlings developing up to 7 roots per plant and an average root length of approximately 5.43 cm. In comparison, seedlings treated with 2% and 1% calcium silicate had an average of 6 roots per plant. The control group showed an average root number of 5 roots per plant and average root lengths of 4.40 cm and 4.23 cm, respectively, compared to the control's average root length of 2.28 cm (Table 4; Figure 5).

These findings align with recent studies highlighting the role of silicon, particularly in the form of calcium silicate, as a beneficial element enhancing plant growth and stress tolerance. The research of Zargar et al. (2019) demonstrated that silicon application improved root architecture and biomass accumulation in leafy vegetables by modulating nutrient uptake and stress resistance mechanisms. Similarly, Li et al. (2021) reported enhanced growth and physiological performance in Brassica crops treated with silicon amendments, attributing the effects to improved cell wall rigidity and antioxidant capacity. Moreover, the observed root elongation and increased root numbers correspond with findings by Eichi et al. (2019), who noted silicon's role in stimulating root system development, which enhances water and nutrient absorption efficiency.

Moreover, silicon supplementation enhances photosynthetic efficiency and reduces reactive oxygen species in vegetable crops. Therefore, the increased seedling height and root system development observed in this study likely reflect the combined physiological benefits of calcium and silicon supplied by calcium silicate, supporting the plant's developmental processes (Wang et al., 2017).

Table 4 Efficacy of calcium silicate solutions at three different concentrations (1%, 2%, and 3%) on root development of 28-day-old Chinese cabbage seedlings.

Treatments	Number of Root (Root) [1/]	Length of Root (cm) [1/]
Control	5.00±1.26b	2.28±0.75C
Calcium silicate 1%	6.00±0.96ab	4.23±0.40b
Calcium silicate 2%	6.00±0.82ab	4.40±0.58b
Calcium silicate 3%	7.00±1.00a	5.43±0.68a
C.V. (%)	18.5567	15.1745
F-test	**	***
MSE	1.04	0.38

[1/] Column values followed by the same letter are not significantly different (P=0.05)
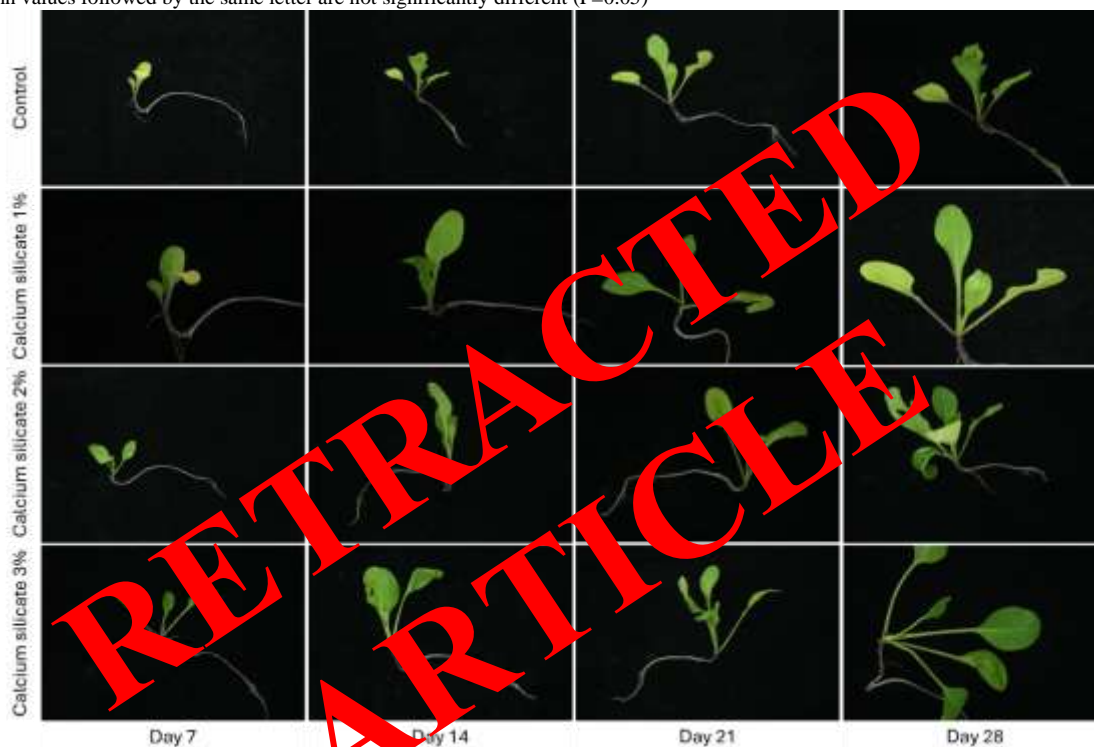
Figure 5 Efficacy of calcium silicate solutions at three different concentrations in promoting the growth of Chinese cabbage seedlings at 7, 14, 21, and 28 days after incubation.

4. Conclusions

The results of this study indicated that calcium silicate did not have a significant effect on the seed germination rate of Chinese cabbage. This suggests that calcium silicate is not directly involved in the seed germination process. Moreover, other factors such as moisture availability, seed quality, and environmental conditions may play a more critical role in influencing germination. However, calcium silicate was found to play a significant role in seedling growth, particularly at higher concentrations, by enhancing seedling height, root number, and root length. These findings are consistent with previous studies demonstrating that calcium silicate promotes plant cell development and strengthens the root system, resulting in longer and more extensively branched roots. In the case of fungal control, calcium silicate has shown potential in inhibiting the fungal pathogen Alternaria brassicicola, which causes leaf spot disease in Brassicaceae crops. The inhibitory mechanism may be associated with alterations in soil conditions that reduce spore dissemination, as well as the induction of systemic acquired resistance (SAR), a natural plant defence response. Therefore, the application of calcium silicate represents a promising strategy to improve plant growth performance, enhance crop quality, and contribute to environmentally friendly disease control. This approach aligns with the goals of sustainable agricultural practices for long-term productivity and ecosystem health.

5. Acknowledgements

6. References

Ahammed, G.J., and Yang, Y. 2021. Mechanisms of silicon-induced fungal disease resistance in plants. Plant Physiology and Biochemistry 165: 200-206. Doi: https://doi.org/10.1016/j.plaphy.2021.05.031.

Attipoe, J. Q., Khan, W., Tayade, R., Steven, S., Islam, M. S., Lay, L., Ghimire, A., Kim, H., Sereyvichea, M., Propey, T., Rana, Y. B., and Kim, Y. 2023. Evaluating the effectiveness of calcium silicate in enhancing soybean growth and yield. Plants 12(11): 2190. Doi: https://doi.org/10.3390/plants12112190.

Barnett, H.L. and Hunter, B.B. 1972. Illustrated Genera of Imperfect Fungi. Burgess Publishing Company, Minneapolis, Minnesota, USA.

Bejarano-Herrera, W.F., Marcillo-Paguay, C.A., Rojas-Tapias, D.F., and Estrada-Bonilla, G.A. 2024. Effect of mineral fertilization and microbial inoculation on cabbage yield and nutrition: A field experiment. Agronomy 14(1): 210. Doi: https://doi.org/10.3390/agronomy14010210.

Bincader, S., Pongpisutta, R., Tiansawang, T., Khienman, S., Boonyaritthongchai, P., Phuntumart, V., and Rattanakreetakul, C. 2025. *Brassica oleracea* var. *sabellica*: A New Host of *Agroathelia delphinii* in soilless cultivation systems in central Thailand. Horticulturae 11(4): 411. Doi: https://doi.org/10.3390/horticulturae11040411.

Chakraborty, S., Newton, A.C., Tubiello, F.N., Pathak, H., Thornton, P., and Campbell, B.M. 2022. Climate change effects on plant disease: Interactions between climate variables and pathogens. Annual Review of Phytopathology 60: 229–251. Doi: https://doi.org/10.1146/annurev-phyto-020620-095104.

Denarié, M-E., Nielsen, U.N., Hartley, S.E., and Johnson, S.N.2025. Silicon-mediated interactions between plant antagonists. Plants 14(8): 1204. Doi: https://doi.org/10.3390/plants14081204.

Eichi, V.R., Okamato, M., Haefele, S.M., Jewell, N., Brien, C., Garnett, T., and Langridge, P. 2019. Understanding the interactions between biomass, grain production and grain protein content in high and low protein wheat genotypes under controlled environments. Agronomy 9(11): 706. Doi: https://doi.org/10.3390/agronomy9110706.

Felsenstein, J. 1985. Confidence limit on phylogenies: An approach using the bootstrap. Evolution 39(4): 783-791.

Gupta, R., Jindal, S., and Sharma, P. 2023. Nano-calcium applications in modern agriculture: A review. Journal of Plant Nutrition, 46(2): 123–135. Doi: https://doi.org/10.1016/j.plana.2025.100147.

Hageman, A., and Van Volkenburgh, E. 2021. Sink strength maintenance underlies drought tolerance in common bean. Plants 10(3): 489. Doi: https://doi.org/10.3390/plants10030489.

Huang, X., Chen, J., Wang, Y., Liu, L., and Li, H. 2023. Climate change exacerbates the impact of soilborne pathogens on *Brassica* crops in East Asia. Frontiers in Plant Science 14: 1123498. Doi: https://doi.org/10.3389/fpls.2023.1123498

Jiang, Y., Yang, J., Li, M., Li, Y., Zhou, P., Wang, Q., Sun, Y., Zhu, G., Wang, Q., Zhang, P., and Rui, Y. 2022. Effect of silica-based nanomaterials on seed germination and seedling growth of rice (*Oryza sativa* L.). Nanomaterials 12(23): 4160. Doi: https://doi.org/10.3390/nano12234160.

Jindal, S., and Sharma, P. 2024. Role of calcium in plant development and stress tolerance. Plant Science Today 11(1): 45–58. Doi: https://doi.org/10.1016/j.pst.2024.01.005.

Kannan, L., and Wheeler, W.C. 2012. Maximum parsimony on phylogenetic networks. Algorithms Molecular Biology 7(1): 9. Doi: https://doi.org/10.1186/1748-7188-7-9.

Kumar, S., and Nowicki, M. 2018. *Alternaria brassicicola*–Brassicaceae pathosystem: Insights into the infection process and resistance mechanisms. European Journal of Plant Pathology 152(3): 1–15. Doi: https://doi.org/10.1007/s10658-018-1548-y.

Kumar, S., Stecher, G., Li, M., Knyaz, C., and Tamura, K. 2018. MEGA X: Molecular Evolutionary Genetics Analysis across computing platforms. Molecular Biology and Evolution 35(6): 1,547-1,549.

Kuzmanović, L., Giovenali, G., Ruggeri, R., Rossini, F., and Ceoloni, C. 2021. Small "Nested" introgressions from wild Thinopyrum species, conferring effective resistance to Fusarium diseases, positively impact durum wheat yield potential. Plants 10(3): 579. Doi: https://doi.org/10.3390/plants10030579

Lal, R., Nawaz, M., and de Medeiros, J. 2023. Nano primers in sustainable seed treatment: Molecular insights into seed germination and stress tolerance. Science of The Total Environment 789: 147–158. Doi: https://doi.org/10.1016/j.scitotenv. 2023.147158.

Lee, Y.H., Jang, S.J., Han, J.H., Bae, J.S., Shin, H., Park, H.J., Sang, M.K., Han, S.H., Kim, K.S., Han, S.W., and Hong, J.K. 2018. Enhanced tolerance of Chineese cabbage seedlings mediated by *Bacillus aryabhattai* H26-2 and *B. siamensis* H30-3 against high temperature stress and fungal infections. Plant Pathology Journal 34(6): 555-566. Doi: https://doi.org/10.5423/PPJ.OA.07.2018.0130.

Li, W., Ning, T., Chen, X. 2019. Postharvest storage quality of citrus fruit treated with a liquid ferment of Chinese herbs and probiotics. Scientia Horticulturae 255: 169-174. Doi: https://doi.org/10.1016/j.scienta.2019.03.030

Liu, K., Zhao, H., Ren, D., Ma, D., Liu, S., and Mao, J. 2025. FungiLT: A Deep learning approach for species-level taxonomic classification of fungal ITS sequences. Computers 14(3): 85. Doi: https://doi.org/10.3390/computers14030085.

Majláth, I., Éva, C., Tajti, J., Khalil, R., Elsayed, N., Darko, E., Szalai, G., Janda, T. 2020. Exogenous methylglyoxal enhances the reactive aldehyde detoxification capability and frost-hardiness of wheat. Plant Physiology and Biochemistry 149: 75-85. Doi: https://doi.org/10.1016/j.plaphy.2020.02.003.

Meng, X., Jin, N., Jin, L., Wang, S., Zhao, W., Xie, Y., Huang, S., Zhang, Z., Xu, Z., Liu, Z., Lyu J., and Yu, J. 2024. Silicon-seed priming promotes seed germination under CA-induced autotoxicity by improving sucrose and respiratory metabolism in cucumber (*Cucumis sativus* L.). BMC Plant Biology 24: 1164. Doi: https://doi.org/10.1186/s12870-024-05908-6.

Pongpisutta, R., Bincader, S., Rattanakreetakul, C., Khienman, S., Tiangsawang, T., Promkhlibnil, T., and Kongsorn, A. 2023. Leaf spot disease of cos lettuce (*Lactuca sativa* var. *longifolia*) and potential of fungicides for residual fungal protection in soilless cultivation. In The 6th National Academic Conference of Rajamangala University of Technology Suvarnabhumi: "Driving research and innovation to create an economic model for sustainable development" (pp. 360–369). Phra Nakhon Si Ayutthaya, Thailand: Rajamangala University of Technology Suvarnabhumi.

Prasad, R., Bhattacharyya, A., and Nguyen, Q.D. 2017. Nanotechnology in sustainable agriculture: Recent developments, challenges, and perspectives. Frontiers in Microbiology 8: 1014. Doi: https://doi.org/10.3389/fmicb.2017.01014.

163

Shelar, A., Nile, S.H., Singh, A.V. et al. 2023. Recent advances in nano-enabled seed treatment strategies for sustainable agriculture: Challenges, risk assessment, and future perspectives. Nano-Micro Letters 15: 54. Doi: https://doi.org/10.1007/s40820-023-01025-5.

Steinweg, J.M., Dukes, J.S., Paul, E.A., and Wallenstein, M.D. 2013. Microbial responses to multi-factor climate change: effects on soil enzymes. Frontiers in Microbiology 4:146. Doi: https://doi.org/10.3389/fmicb.2013.00146.

Thompson, J.D., Higgins, D.G., and Gibson, T.J. 1994. Clustal W: Improving the sensitivity of progressive multiple sequence alignment through sequence weighting, position-specific gap penalties and weight matrix choice. Nucleic Acids Research 22: 4673–4680.

Wang, M., Gao, L., Dong, S., Sun, Y., Shen, Q., Guo, S. 2017. Role of silicon on plant-pathogen interactions. Frontiers in Plant Science 5(8): 701. Doi: https://doi.org/10.3389/fpls.2017.00701.

White, T.J., Bruns, T., Lee, S.J.W.T., Taylor, J. 1990. Amplification and direct sequencing of fungal ribosomal RNA genes for phylogenetics. In PCR Protocols: A Guide to Methods and Applications; Innis, M.A., Gelfand, D.H., Sninsky, J.J., White, T.J., Eds.; Academic Press: Cambridge, MA, USA, pp. 315–322.

Woudenberg, J.H.C., Groenewald, J.Z., Binder, M., and Crous, P.W. 2013. *Alternaria* redefined. Studies in Mycology 75: 171–212. Doi: https://doi.org/10.3114/sim0015.

Woudenberg, J.H.C., Seidl, M.F., Groenewald, J.Z., de Vries, M., Stielow, J.B., Thomma, B.P.H.J., and Crous, P.W. 2015. *Alternaria* section *Alternaria*: species, formae speciales or pathotypes? Studies in Mycology 82: 1-21. Doi: http://dx.doi. org/10.1016/j.simyco.2015.07.001.

Woudenberg, J.H.C., Truter, M., Groenewald, J.Z., and Crous, P.W. 2014. Large-spored *Alternaria* pathogens in section *Porri* disentangled. Studies in Mycology 79: 1-47. Doi: http://dx.doi.org/10.1016/j.s imyco.2014.07.003.

Zargar, S.M., Mahajan, R., Bhat, J.A., Nazir, M., Deshmukh, R. 2019. Role of silicon in plant stress tolerance: opportunities to achieve a sustainable cropping system. 3 Biotech. 9(3): 73. Doi: https://doi.org/10.1007/s13205-019-1613-z.

Zhu, A.-H., Song, Z.-K., Wang, A.-F., Guan, H.-W., Qu, Z., and Ma, H.-X. 2024. Multi-gene phylogenetic analyses reveal Heteroxylaria Gen. Nov. and new contributions to Xylariaceae (Ascomycota) from China. Journal of Fungi 10(9): 645. Doi: https://doi.org/10.3390/jof10090645.

Efficacy of Probiotic Yeasts in Controlling Vibrio parahaemolyticus and Vibrio harveyi in Whiteleg Shrimp (Litopenaeus Vannamei)

Chakhriya Chalad[a*], Wikit Phinrub[b]

[a] Division of General Studies, Faculty of Science and Fisheries Technology, Rajamangala University of Technology Srivijaya, Trang 92150, Thailand
[b] Division of Aquaculture and Fishery Products, Faculty of Science and Fisheries Technology, Rajamangala University of Technology Srivijaya, Trang 92150, Thailand
* Corresponding author. Tel.: 0 7420 4070; 0 7520 4071; E-mail address: Chakhriya.c@rmutsv.ac.th

Abstract

Vibrio parahaemolyticus and *V. harveyi*, are the causative agent of disease are causative agents of disease in shrimp aquaculture. In this work, we isolated yeasts from intestine of wild shrimp possessing inhibitory activity against *V. parahaemolyticus* and *V. harveyi*. Sixteen of 48 yeast isolates inhibited *V. parahaemolyticus* and *V. harveyi*. YP8, YP12, YP15, YP16, YP18, YP20, YP24, YP26, YP30 and YP32 were ten yeast isolates with high inhibitory activity with inhibition zones ranging from 9.00 ± 0.07 to 21.80 ± 0.14 mm. The toxicity test of nine yeast isolates (excluding YP32) revealed no harmful effects on whiteleg shrimp (*Litopenaeus vannamei*) after 120 h. In addition, five isolates (YP26, YP24, YP20, Y18 and Y8) showed high survival rates in the shrimp intestine. Polymerase chain reaction targeting the internal transcribed spacer region was used to identify yeast species, which was validated by sequencing. *Saccharomyces cerevisiae*, *Candida tropicalis*, *Wickerhamomyces anomalus*, *Yarrowia lipolytica* and *Candida glabrata* were shown to have 99-100 % identity to GenBank sequences. These findings indicate that *Y. lipolytica*, *S. cerevisiae* and *W. anomalus* are suitable for use as probiotics to control *V. parahaemolyticus* and *V. harveyi* in shrimp aquaculture due to their strong inhibitory activity, safety to shrimp, and ability to survive in the shrimp intestine.

Keywords: Yeast, Inhibitory Activity, Vibrio Parahaemolyticus, Vibrio Harveyi, Whiteleg Shrimp

1. Introduction

Shrimp aquaculture requires the integration of biotechnology and microbiology into shrimp aquaculture requires integrating biotechnology and microbiology for improved quality and quantity of shrimp products is a crucial step toward obtaining improved quality and quantity of shrimp products, such as the inclusion of various substances to feed formulations to improve shrimp growth (Sarkar and Bhaskara Rao, 2016). In addition, shrimp diseases incidence can be reduced by managing water, soil, stock, nutrition, and the environment (Ringø et al., 2014). Bacterial infections are caused by a variety of parameters in shrimp aquaculture (Lazado et al., 2015). Both *Vibrio parahaemolyticus* and *Vibrio harveyi* are gram negative bacteria in the genus Vibrio, family Vibrionaceae and order Vibrionales. *V. parahaemolyticus* is indeed one of the significant pathogenic agents that pose a threat to the viability of the aquaculture industry, particularly shrimp farming (Pui et al., 2014). *V. harveyi* is a bacterium that has been associated with diseases in a wide range of warm water fish and invertebrates, with particular significance in shrimp culture (Zhang et al., 2020). The antimicrobial drugs and disinfectants have had limited success in preventing disease. Antibiotic overuse contributes greatly to the creation and spread of antibiotic-resistant bacteria (Seethalakshmi et al., 2021). Moreover, the accumulation of antibiotics in shrimp products is a significant concern, especially in the context of international markets (Kumar et al., 2016). The use of probiotics in shrimp culture has gained popularity for several reasons, including their environmental friendliness and contribution to sustainable aquaculture practices. Probiotics have the ability to improve water quality, host nutrition, reduce disease incidence, increase host survival, and enhance immune response in aquaculture (Bhassu et al., 2024). Many yeasts are capable of producing bioactive compounds like as glucans, nucleotides, polysaccharides, carotenoid pigments, lipids, proteins, vitamins (Ceseña et al., 2021), amino acids, polyamine, astaxanthin, protease and killer toxin (Mirzaei et al., 2021). The β-glucans and mannoproteins of yeast have potential role in the immunity of the host (Navarrete and Tovar-Ramírez, 2014). Their ability to bind to the intestinal mucosa. Additionally, the absence of demonstrated yeast mediated transmission of antibiotic resistance (Nayak, 2011).

This study focused on isolating yeasts from natural shrimp, evaluating their inhibitory effects against *Vibrio parahaemolyticus* and *Vibrio harveyi*, assessing their toxicity to shrimp, determining their survival in the shrimp intestine, and identifying the yeast strains.

2. Methodology

2.1 Sample collection and yeasts isolation

Whiteleg shrimp were collected from Sikao markets in Sikao district, Trang province, Thailand. The shrimp intestines were cultured in Sabouraud dextrose broth (SDB) containing antibiotic (gentamicin) and incubated at 30 ℃ for 48 h. The streaked Sabouraud dextrose agar (SDA) plates containing gentamicin were incubated at 30 ℃ for 48 h. After incubation, different yeast colonies were chosen from SDA. The selected yeast colonies were re-streaked on SDA to obtain pure yeast isolate.

2.2 Investigation of inhibitory activity of yeast against *V. parahaemolyticus* and *V. harveyi* using modified agar well diffusion technique

The selected yeasts were streaked on SDA and incubated at 30 ºC for 48 h. The agar pieces were made from SDA using a sterile pasteur pipette. The selected yeasts were pierced onto the agar piece and incubated at 30 ºC for 48 h. *V. parahaemolyticus* and *V. harveyi* were cultured in Mueller Hinton broth (MHB) with shaking at 150 rpm at 30 ºC for 3 h. After adjusting the bacterial suspension to 0.5×10^8 CFU/ml, it was distributed on Mueller Hinton agar (MHA). The pit agar of bacterial lawn was then taken out, yeast seeded agar pieces were put into the pits of the bacterial lawn and incubated at 30 ºC for 24 h. The diameter of the inhibition zones was measure. The experiment was carried out in triplicate.

2.3 Evaluation of yeast toxicity to shrimp

Whiteleg shrimp with an average weight of 5 g were collected from a shrimp farm in Sikao District, Trang Province, Thailand. The shrimp were transferred to experimental tanks and acclimated for five days. Each tank measured $30 \times 40 \times 30$ cm and contained 15 shrimp. The selected yeasts were cultured in SDB with shaking at 150 rpm at 30 ºC for 48 h. The cell pellet of yeast was collected by centrifugation at 8,000 rpm for 5 min and suspended in phosphate-buffered saline (PBS). The suspension was adjusted to amounts of 10^8 CFU/ml and then 20 µl of the suspension was injected into each shrimp (n=15/isolate). Shrimp mortality was recorded daily for five days to determine survival rates. The experiment was conducted in duplicate.

2.4 Investigation of the survival of yeast in the shrimp intestine

Whiteleg shrimp with an average weight of 5 g were transferred to shrimp tanks ($30 \times 60 \times 30$ cm) at a density of 30 shrimp/tank. Selected yeast isolates were cultured in SDB with shaking at 150 rpm at 30 °C for 48 h. After centrifugation at 8,000 rpm for 5 min, the yeast cell pellets were collected and suspended in PBS. The suspension was then mixed with shrimp feed and adjusted to 10^8 CFU/g of feed, followed by coating the mixture with fish oil.

All shrimp were fed three times a day (07:00, 14:00, and 19:00) with commercial shrimp feed at 8% of body weight/day. The water temperature in the shrimp tanks was maintained at 30 °C. Dissolved oxygen levels were controlled through continuous aeration. To maintain water quality, 50% of the water in each tank was replaced daily with fresh seawater. Remained feed and feces were removed daily through siphon. The feeding experiment was conducted in duplicate. The number of yeast cells in the shrimp intestine was determined every 24 h for 10 days using the spread plate technique on SDA.

2.5 Identification of yeast

Yeast genomic DNA was extracted to identify the selected yeasts. The species identification was performed by PCR targeting the internal transcribed spacer (ITS) region using primer ITS1F (5'TCCGTAGGTGAACCTGCGG3') and ITS4R (5'TCCTCCGCTTATTGATATGC3') (Cárdenas et al., 2012). The ITS region was amplified in 20 µl reaction volumes comprising 2 µl of extracted DNA, 4 µl of 5x buffer, 10.3 µl of milliQ water, 1.6 µl of 2.5 mM dNTP mixture, 1 µl of 10 µM of each primer and 0.1 µl of 5 U/µl *GoTaq* DNA polymerase. For the cycling conditions, the initial denaturation was done at 95 ºC for 5 min, followed by 35 cycles of 94 ºC for 1 min, 55 ºC for 2 min, 72 ºC for 2 min and a final extension at 72 ºC for 10 min. The PCR product was observed after 60 min of electrophoresis in 1% agarose gel. The PCR products were purified and sequenced. The obtained sequences were compared with the GenBank database using nucleotide blast.

2.6 Statistical analysis

Data were analyzed using one-way ANOVA, and results were reported as replicate means and standard deviations, with comparisons made using Duncan's multiple range test. A p-value of less than 0.05 was considered statistically significant

3. Results and Discussion

3.1 Yeast isolation by modified agar well diffusion technique

From the intestine of whiteleg shrimp, 48 yeast isolates were isolated. 16 of the 48 yeasts isolated showed inhibitory activity toward *V. parahaemolyticus* with inhibition zones ranging from 6.90 ± 0.35 and 13.80 ± 0.92 mm in diameter. While the inhibitory activity against *V. harveyi* with inhibition zones that ranged between 6.83 ± 0.21 and 21.80 ± 0.14 mm in diameter (Tables 1 and 2). Interestingly, ten out of 16 yeast isolates designated as YP8, YP12, YP15, YP16, YP18, YP20, YP24, YP26, YP30 and YP32 displayed high inhibitory activity against *V. parahaemolyticus* and *V. harveyi* with inhibition zones that ranged between 9.00 ± 0.07 and 21.80 ± 0.14 mm in diameter. In particular, YP26 and YP24 isolates exhibited high inhibitory activity against *V. harveyi* which was higher than *V. parahaemolyticus*. On SDA, most yeast isolates against *V. parahaemolyticus* and *V. harveyi* formed butyrous, cream-colored colonies (Figures 1a and 1b). Under the microscope, ellipsoidal and ovoid cells were observed. (Figures 1c and 1d).

Table 1 Isolation of yeasts against *V. parahaemolyticus* and *V. harveyi*.

Sources	No. yeast isolates	No. isolates active against *V. parahaemolyticus*	No. isolates active against *V. harveyi*
Sikao market 1	15	5	5
Sikao market 2	12	4	4
Sikao market 3	21	7	7
Total	48	16	16

Table 2 The inhibitory activity of 16 yeast isolates toward *V. parahaemolyticus* and *V. harveyi*.

Yeast isolates	Inhibitory activity of yeasts (mm)	
	V. parahaemolyticus	*V. harveyi*
YP4	7.23 ± 0.85[e]	7.30 ± 0.99[h]
YP7	6.90 ± 0.35[e]	7.10 ± 0.07[h]
YP8	10.20 ± 0.71[bc]	10.50 ± 0.71[de]
YP10	7.03 ± 0.14[e]	7.33 ± 0.49[h]
YP12	9.00 ± 0.07[cd]	10.10 ± 0.28[ef]
YP14	7.33 ± 0.21[e]	7.20 ± 0.07[h]
YP15	9.10 ± 0.28[cd]	9.53 ± 0.42[gh]
YP16	10.50 ± 0.35[b]	10.40 ± 0.35[e]
YP18	11.10 ± 0.71[b]	9.23 ± 0.14[g]
YP20	12.53 ± 0.64[a]	14.50 ± 0.49[c]
YP22	7.00 ± 0.14[e]	6.83 ± 0.21[h]
YP24	12.93 ± 0.14[a]	18.10 ± 0.35[b]
YP26	13.80 ± 0.92[a]	21.80 ± 0.14[a]
YP30	10.03 ± 0.78[bc]	11.23 ± 0.64[d]
YP32	11.01 ± 0.42[b]	14.60 ± 0.00[c]
YP34	7.80 ± 0.28[de]	7.10 ± 0.07[h]

Note: Values are presented as means ± SD, and different letters (a, b, c, d, e, f, g, h) indicate significant differences (p < .05).

Figure 1 Colonies of yeast on SDA plates (a, b) and yeast cells observed under the microscope at 100× magnification using light microscopy (c, d).

3.2 *Investigation of the toxicity of yeast on shrimp*

According to this study, isolates YP8, YP12, YP15, YP16, YP18, YP20, YP24, YP26, and YP30 did not affect shrimp after 120 h. However, shrimp treated with isolate YP32 showed a survival rate of 93.33% after 120 h (Table 3).

Table 3 The toxicity of 10 yeast isolates on shrimp.

Yeast isolates	Survival rate of shrimp (%) (n = 15)				
	24 h	48 h	72 h	96 h	120 h
YP8	100[a]	100[a]	100[a]	100	100[a]
YP12	100[a]	100[a]	100[a]	100	96.7 ± 4.7[a]
YP15	100[a]	100[a]	100[a]	96.7 ± 4.7[a]	96.7 ± 4.7[a]
YP16	100[a]	100[a]	100[a]	96.7 ± 4.7[a]	96.7 ± 4.7[a]
YP18	100[a]	100[a]	100[a]	100[a]	100[a]
YP20	100[a]	100[a]	100[a]	100[a]	100[a]
YP24	100[a]	100[a]	100[a]	100[a]	100[a]
YP26	100[a]	100[a]	100[a]	100[a]	100[a]
YP30	100[a]	100[a]	100[a]	100[a]	96.7±4.7[a]
YP32	100[a]	100[a]	100[a]	96.7 ± 4.7[ab]	93.3 ± 0[b]

Note: Values are presented as means ± SD, and different letters (a, b) indicate significant differences (p < .05).

3.3 *The survival of yeast in the shrimp intestine*

The numbers of yeast in shrimp intestine, yeast isolates YP26, YP24, YP20, YP18 and YP8 were 6.2×10, 4.9×10, 1.1×10, 0.6×10 and 0.3×10 CFU/ml after 1 day, respectively. After 10 days, the numbers increase to 2.9×10^4, 2.1×10^4, 1.8×10^4, 6.8×10^3 and 3.4×10^3 CFU/ml, respectively. In contrast, yeast isolates YP12, YP15 and YP30 were not detected after 1 days, while YP16 and YP32 were not detected after 3 days (Figure 2).
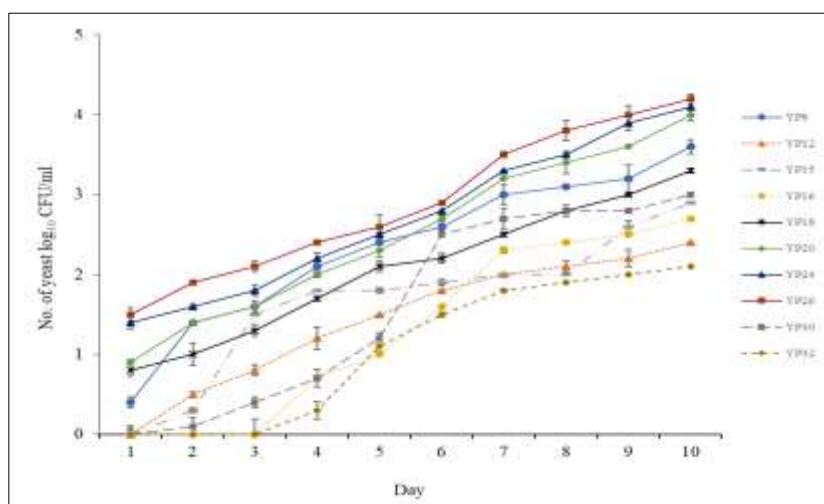
Figure 2 The survival of yeast in the shrimp intestine

3.4 Yeast identification

Saccharomyces cerevisiae, *Candida tropicalis*, *Wickerhamomyces anomalus*, *Yarrowia lipolytica*, and *Candida glabrata* were the four yeast genera and five species identified with 99-100 % identity to GenBank sequences using PCR targeting the ITS region (Table 4)

Table 4 Identification of 10 yeast isolates.

Yeast isolates	ITS region	% Identity
YP8	*Saccharomyces cerevisiae*	99
YP12	*Candida tropicalis*	99
YP15	*Candida tropicalis*	99
YP16	*Candida tropicalis*	99
YP18	*Wickerhamomyces anomalus*	99
YP20	*Saccharomyces cerevisiae*	99
YP24	*Saccharomyces cerevisiae*	100
YP26	*Yarrowia lipolytica*	99
YP30	*Wickerhamomyces anomalus*	100
YP32	*Candida glabrata*	100

The four yeast isolates identified, *Candida tropicalis* (YP12, YP15, YP16) and *Candida glabrata* (YP32) have been reported as human pathogens. They are the two most common pathogens responsible for candidemia (Yang et al., 2022). Hematological disease patients with *C. tropicalis* bloodstream infections had a high mortality rate. (Yang et al., 2023). It is rare for *C. glabrata* to cause significant illness in people. Nevertheless, *C. glabrata* is a pathogenic organism that colonizes epithelial surfaces including the mouth, gastrointestinal system, vagina, skin, and present in stool (Hassan et al., 2021).

The five identified yeast isolates, *Y. lipolytica* (YP26), *S. cerevisiae* (YP8, YP20, YP24) and *W. anomalus* (YP18) are of particular interest because they exhibited high inhibitory activity against *V. parahaemolyticus* and *V. harveyi*, caused no harm to shrimp, and were able to survive in the shrimp intestine. *Y. lipolytica* has a high protein content and an entire amino acid profile. It has been demonstrated to have a probiotic effect in addition to containing a high-quality single cell protein (Worland et al., 2020). *Y. lipolytica* naturally secretes a number of extracellular metabolites, such as lipases and esterases (Fabiszewska et al., 2024). This yeast can activate non-specific immunological parameters as well as the antioxidant immune mechanism in Pacific red snapper leukocytes from the head, kidney, and spleen, making it a potential immunostimulant (Alamillo et al., 2017).-*Y. lipolytica* has been use to enhance the survival and growth of the pearl oyster (*Pinctada mazatlanica*) (Aguilar et al., 2010), as well as to stimulates non-specific immunity in Pacific red snapper (*Lutjanus peru*) (Alamillo et al., 2017). Likewise, the cell wall of *S. cerevisiae* can synthesize the essential substance β-glucan, which stimulates non-specific immunity (Lei et al., 2021). Ayiku et al. (2020) reported the potential of probiotic feed derived from *S. cerevisiae* as an immunostimulant for shrimp infected with *V. harveyi*. Moreover, the use of *W. anomalus* in the diets of Atlantic salmon (*Salmo salar*) and rainbow trout (*Oncorhynchus mykiss*) has been shown to improve growth performance (Agboola et al., 2021). Many yeasts can produce bioactive substances (Mirzaei et al., 2021), including β-glucans and mannoproteins (Navarrete and Tovar-Ramírez, 2014). Yeasts are used as alternative feed ingredients in aquaculture because of their nutritional value (Ceseña et al., 2021). They can be incorporated into aquaculture diets and are generally obtained through biotechnological processes or as by-products of the agri-food industry (Aguirre-Guzman et al., 2023).

4. Conclusions

In this work, *Yarrowia lipolytica*, *Saccharomyces cerevisiae* and *Wickerhamomyces anomalus* exhibited high inhibitory activity against *Vibrio parahaemolyticus* and *V. harveyi*. Additionally, these yeasts were non-toxic and able to survive in the shrimp intestine, demonstrating their potential effectiveness in shrimp aquaculture.

5. Acknowledgements

6. References

Agboola, J.O., Øverland, M., Skred, A. and Hansen, J.Ø., 2021, Yeast as Major Protein-Rich Ingredient in Aquafeeds: A Review of The Implications for Aquaculture Production, Reviews in Aquaculture, Vol 13(2), p.1-22.

Aguilar-Macias, O.L., Ojeda-Ramirez, J.J., Campa-Cordova, A.I. and Saucedo, P.E., 2010, Evaluation of Natural and Commercial Probiotics for Improving Growth and Survival of The Pearl Oyster, *Pinctada mazatlanica*, During Late Hatchery and Early Field Culturing, Journal of the World Aquaculture Society, Vol 41, p.447-454.

Aguirre-Guzman, G., Campa-Cordova, Á. and Salinas-Chavira, J., 2023, Use of Active Yeasts in Shrimp Nutrition, Journal MVZ Cordoba, Vol 28(2), p.e2929.

Alamillo, E., Reyes-Becerril, M., Cuesta, A. and Angulo, C., 2017, Marine Yeast *Yarrowia lipolytica* Improves The Immune Responses in Pacific Red Snapper (*Lutjanus peru*) Leukocytes, Fish and Shellfish Immunology, Vol 70, p.48-56.

Ayiku, S., Shen, J.F., Tan, B.P., Dong, X.H. and Liu, H.Y., 2020, Effects of Dietary Yeast Culture on Shrimp Growth, Immune Response, Intestinal Health and Disease Resistance Against *V. harveyi,* Fish and Shellfish Immunology, Vol 102, p.286-295.

Bhassu, S., Shama, M., Tiruvayipati, S., Soo, T.C.C., Ahmed, N. and Yusoff, K., 2024, Microbes and Pathogens Associated with Shrimps - Implications and Review of Possible Control Strategies, Frontiers in Marine Science, Vol 11, p.397708.

Cárdenas, G.M., Galván, M., Barrera, V. and Carmona, M., 2012, First Report of Target Spot of Tobacco Caused by *Rhizoctonia solani*, Plant Disease, Vol 96(3), p.456.

Ceseña, C.E., Vega-Villasante, F., Aguirre-Guzman, G., Luna-González, A. and Campa-Córdova, Á.I., 2021, Update on The Use of Yeast in Shrimp Aquaculture: A minireview, International Aquatic Research, Vol 13, p.1-16.

Fabiszewska, A., Zieniuk, B., Jasińska, K., Nowak, D., Sasal, K., Kobus, J. and Jankiewicz, U., 2024, Extracellular Lipases of *Yarrowia lipolytica* Yeast in Media Containing Plant Oils Studies Supported by the Design of Experiment Methodology, Applied Sciences, Vol 14(23), p.11449.

Hassan, Y., Chew, S.Y. and Than, L.T.L., 2021, *Candida glabrata*: Pathogenicity and Resistance Mechanisms for Adaptation and Survival, Journal of fungi, Vol 8, p.667.

Kumar, V., Roy, S., Meena, D.K. and Sarkar, U.K., 2016, Application of Probiotics in Shrimp Aquaculture: Importance, Mechanisms of Action, and Methods of Administration, Reviews in Fisheries Science and aquaculture, Vol 24(4), p.342-368.

Lazado, C.C., Lacsamana, J.I. and Caipang, C.M.A., 2015, Mechanisms of Probiotic Actions in Shrimp: Implications to Tropical Aquaculture, Biotechnological Advances in shrimp Health Management in the Philippines, Vol p.89-114.

Lei, H., Li, S., Lu, X. and Ren, Y., 2021, Oral Administration of *Saccharomyces cerevisiae* Displaying VP28-VP24 Confers Protection Against White Spot Syndrome Virus in Shrimp, Virus Research, Vol 302, p.198467.

Mirzaei, M., Shavandi, A., Mirdamadi, S., Soleymanzadeh, N., Motahari, P., Mirdamadi, N., Moser, M., Subra, G., Alimoradi, H. and Goriely, S., 2021, Bioactive Peptides from Yeast: A Comparative Review on Production Methods, Bioactivity, Structure-Function Relationship, and Stability Trends in Food Science and Technology, Vol 118, p.297-315.

Navarrete, P. and Tovar-Ramírez, D., 2014, Use of Yeasts as Probiotics in Fish Aquaculture. In: Sustainable Aquaculture Techniques (eds. M. HernandezVergara. and C. Pérez-Rostro), INTECH Open Science, p.135-172.

Nayak, S.K., 2011, Biology of Eukaryotic Probiotics, Springer Verlag Berlin Heidelberg, New York, USA.

Pui, C.F., Bilung, L.M., Zin, N.B.M. Abidin, N.N.B.Z., Vincent, M. and Apun, K., 2014, Risk of Acquiring *Vibrio parahaemolyticus* in Water and Shrimp from an Aquaculture Farm, Kuroshio Science, Vol 8, p.59-62.

Ringø, E., Olsen, R.E., Jensen, I., Romero, J. and Lauzon, H.L., 2014, Application of Vaccines and Dietary Supplements in Aquaculture: Possibilities and Challenges, Reviews in Fish Biology and Fisheries, Vol 24, p.1005-1032.

Sarkar, A. and Bhaskara Rao, D K.V., 2016, Marine Yeast: A Potential Candidate for Biotechnological Applications - A Review, Asian Journal of Microbiology, Biotechnology and Environmental Sciences, Vol 18(3), p. 627-634.

Seethalakshmi, P.S., Rajeev, R., Kiran, G.S., and Selvin, J., 2021, Shrimp Disease Management for Sustainable Aquaculture: Innovations from Nanotechnology and Biotechnology, Aquaculture International, Vol 29, p.1591-1620.

Worland, A.M., Czajka, J.J., Xing, Y., Harper Jr, W.F., Moore, A., Xiao, Z., Han, Z., Wang, Y., Su, W.W. and Tang Y.J., 2020, Analysis of *Yarrowia lipolytica* Growth, Catabolism, and Terpenoid Biosynthesis During Utilization of Lipid-Derived Feedstock, Metabolic Engineering Communications, Vol 11, p.e00130.

Yang, B., Wei, Z., Wu, M., Lai, Y. and Zhao, W., 2023, A Clinical Analysis of *Candida tropicalis* Bloodstream Infections Associated With Hematological Diseases, and Antifungal Susceptibility: A Retrospective Survey, Frontiers in Microbiology, Vol 14, p.01-09.

Yang, X., Liu, M., Yu, X., Wang, Z. and Xu, Y., 2022, Time to Positivity Facilitates an Early Differential Diagnosis of *Candida tropicalis* from Other *Candida* Species, Infection and Drug Resistance, Vol 15, p.5879-5886.

Zhang, X-H., He, X.X. and Austin, B., 2020, *Vibrio harveyi*: A Serious Pathogen of Fish and Invertebrates in Mariculture, Marine Life Science and Technology, Vol 2(3), p.231-245.

SESSION
Science and Engineering Technology

The Cytotoxicity and Alkaline Phosphatase Activity of Water-Soluble Extract from the Abalone Nacre on the Preosteoblast

Nijjareeya Sirisriro[a*], Ruethairat Boonsombat[b]

[a] Faculty of Veterinary Sciences, Rajamangala University of Technology Srivijaya, Nakhon Si Thammarat, 80240 Thailand
[b] Department of Biology, Faculty of Science, Ramkhamhaeng University, Bangkok 10240, Thailand.
* Corresponding author. E-mail address: nsirisriro@outlook.com

Abstract

Nacre, a calcium carbonate-based biomaterial, has traditional pharmaceutical applications in bone regeneration. This study explored the osteoinductive potential of nacre from abalone Haliotis diversicolor, specifically its water-soluble extract (HD-WSM), on MC3T3-E1 mouse osteoblasts. HD-WSM was extracted and tested for cytotoxicity using the AlamarBlue Assay. Results indicated HD-WSM was non-cytotoxic within a 50-250 µg/ml concentration range, with cell viability remaining consistent with controls after 48 hours. A slight increase in cell proliferation was observed at 150-250 µg/ml after six days, leading to the selection of 100 and 200 µg/ml for further analysis. Alkaline phosphatase (ALP) activity, a marker of osteoblast differentiation, was measured using an ALP Assay Kit. HD-WSM significantly enhanced ALP activity in a dose-dependent manner across 50-250 µg/ml concentrations, starting from day three. The untreated cells also showed increasing ALP levels, reflecting natural osteoblast proliferation. The results demonstrate that HD-WSM promotes both cell proliferation and ALP activity in MC3T3-E1 cells, suggesting its potential as an osteoinductive material.

Keywords: Cytotoxicity, Alkaline Phosphatase, Nacre, Preosteoblast

1. Introduction

Nacre, or mother of pearl, is a biological ceramic. It consists of calcium carbonate platelets embedded in an organic matrix with a highly controlled structural organization. Mollusk nacre is a biocompatible, biodegradable, and osteoinductive biomaterial. Chips, powder, and extracts from oyster and mussel nacre demonstrate strong evidence of osteoblast stimulation and bone mineralization both in vitro and in vivo (Green et al., 2014). Studies have demonstrated that nacre attracts and activates bone marrow stem cells and osteoblasts (Green et al., 2014, 2015). In vivo studies show that mollusk nacre from oysters and mussels induces osteogenesis and bone mineralization in ectopic bone environments. In bone graft tests, nacre fragments or powder can be grafted into the bones of sheep (Rousseau et al., 2012), guinea pigs (Asvanund and Chunhabundit, 2012), rats (Liao et al., 2002), and rabbits (Lamghari et al., 2001). In patients with bone defects, fresh woven bone fused with the nacre implant, facilitated by osteoclasts and osteoblasts (Green et al., 2014, 2015). Nacre implantations stimulated osteogenesis and integration of the nacre into the host bone without fibrous tissue interposition or a significant inflammatory reaction (Asvanund and Chunhabundit, 2012; Lamghari et al., 2001; Liao et al., 2002; Rousseau et al., 2012). While nacre is tolerated in vivo, its slow degradation and resorption may hinder its use in calcified tissues requiring rapid self-renewal (Lamghari et al., 2001). Although the nacre organic matrix constitutes only 1-5% w/w of the mollusk shell, it plays a critical role in shell formation. This includes the synthesis of transient amorphous minerals, their crystallization, the selection of calcium carbonate polymorphs (calcite or aragonite), and the organization of crystallites into complex shell textures (Marin et al., 2008). The nacre organic matrix can be separated into water-soluble (WSM) and water-insoluble (WISM) fractions. WISM biopolymers determine the framework structure of the shell layer, while WSM modulates calcium ion deposition at nucleation sites (Marin et al., 2008; Espinosa et al., 2011). The nacre biogenic composite, particularly the WSM, has been considered a promising biomaterial for bone repair due to its osteogenic potential. Researchers suggest that WSM contains signaling molecules that can be released in a physiological medium and activate osteoblasts. Therefore, these signaling molecules may serve as homologous components between nacre and bone tissue (Lao et al., 2007; Rousseau et al., 2008). This project aimed to determine whether the water-soluble matrix of abalone *Haliotis diversicolor nacre* (HD-WSM) contains signal proteins that promote the stimulation and differentiation of MC3T3-E1 osteoblasts. Cytotoxicity and alkaline phosphatase activity were investigated.

2. Methodology

2.1 Extraction and purification of nacre water-soluble matrix

The HD-WSM was extracted from powdered nacre, by a non-decalcifying process. One hundred grams of the nacre powder was suspended in 200 ml of autoclaved deionized water for 24 hours at room temperature, with continuous stirring. The suspension was then centrifuged for 30 min at 4000 rpm. The supernatant was called the HD-WSM (Mouriès et al., 2002). The HD-WSM was purified and concentrated by Vivaspin sample concentrators (Amersham Pharmacia Biotech) prior to being run onto SDS-PAGE.

2.2 Cell culture

To maintain and propagate the cells, MC3T3-E1 Subclone 4 ATCC ® CRL-2593, was cultured in MEM-alpha supplemented with 10% heat-inactivated fetal calf serum, 2 mM glutamine, and 1% penicillin/streptomycin (Hyclone) in a humidified incubator at 37°C and 5% CO_2. The cells were subcultured every three days in the presence of 0.25% trypsin. MC3T3-E1 cells were plated out at 10^3 cells/well of 96 well plates, or 10^5 cells/well of 6 well plates

and after reaching the 70% confluency level, cells were treated with HD-WSM in various concentrations for 28 days. The medium was changed every third day.

2.3 Cell proliferation and viability assay

To estimate the effect of HD-WSM on proliferation and viability of MC3T3-E1 cell, the assay of Alamarblue® cell viability reagent (Thermo Scientific) was performed. Resazurin, the active ingredient of AlamarBlue® reagent, is a non-toxic, cell-permeable compound that is blue in color and virtually non-fluorescent. Upon entering cells, resazurin is reduced to resorufin, a compound that is red in color and highly fluorescent. Viable cells continuously convert resazurin to resorufin, increasing the overall fluorescence and color of the media surrounding cells.

After completing the incubation, alamarBlue® reagent was added 10 μL to 100 μL sample, followed by 2 hours of incubation at 37°C. The resulting fluorescence is read on a plate reader or spectrophotometer (Model 680 Microplate Reader; Bio-Rad, Hercules, CA, USA). The proliferation rate of the cells was calculated according to the following formula: (ODsample - ODblank) / (ODcontrol - ODblank).

2.4 Alkaline phosphatase activity

At the end of the treatment period, the cells were washed with PBS and lysed. Alkaline phosphatase (ALP) activity in the cell lysates was measured in 0.2 M bicarbonate buffer pH 10, 0.05% Triton X-100, 4 mM $MgCl_2$ and 2 mM p-nitrophenolphosphate by incubating the lysates for 60 min at 25 °C, protected from light. The reactions were stopped by adding 1 M NaOH. The absorbance at 405 nm was measured. Activities were normalized to the cell protein content, as measured by the Bradford method (BioRad), using standard protein provided in the Alkaline Phosphatase Assay Kit (ab83369, Abcam).

$$ALP \ activity \ (U/mL) = (AV)/T$$

where
- A = amount of pNP generated in samples calculated from a standard curve (μmol)
- V = volume of sample added in the assay well (mL)
- T = reaction time (in minutes)

3. Results and Discussion

3.1 HD-WSM is non-cytotoxic to preosteoblasts MC3T3-E1

To determine the experimental doses of HD-WSM for evaluation of bone differentiation in MC3T3-E1, the cytotoxicity of HD-WSM was determined by AlamarBlue Assay (Thermo Fisher Scientific). The HD-WSM was added to culture media at the concentration of 0, 50, 100, 150 and 200 ug/ml for 24 and 48 hours. Initial findings indicated that HD-WSM, across the concentration range of 50 to 250 μg/ml, did not exhibit cytotoxic effects on MC3T3-E1 cells after 24 and 48 hours of treatment. Cell viability and proliferation rates remained comparable to those of untreated control cells, confirming its non-cytotoxic nature during acute exposure.
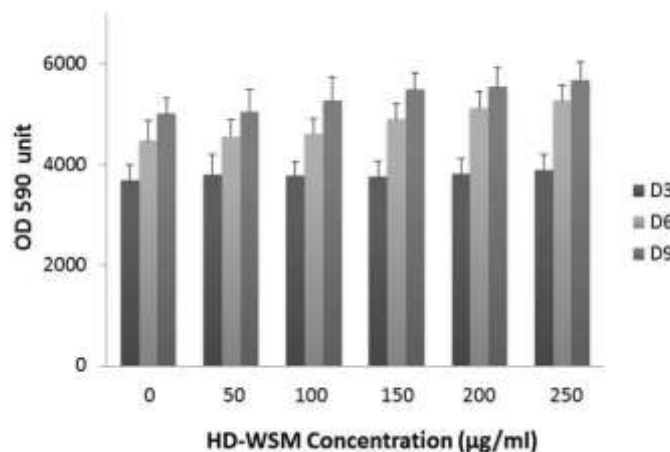
Figure 1 Cell viability assays of MC3T3-E1 cells. Effect of HD-WSM on cell viability percentage as measured by AlamarBlue® Cell Viability Reagent (Thermo Fisher Scientific) indicating non-toxic nature of WSM for MC3T3-E1 cells. The experiment was performed at concentration of 0, 50, 100, 150, 200 and 250 ug/ml for 3, 6 and 9 days.

Extending the observation period to 3, 6, and 9 days (Figure 1) further supported the sustained non-cytotoxic profile of HD-WSM. At Day 3 (D3), OD 590 unit values across all concentrations were largely similar, reinforcing the initial lack of cytotoxicity. By Day 6 (D6), concentrations of HD-WSM between 150 and 250 μg/ml demonstrated a weak, yet discernible, enhancement in cell proliferation compared to the control and lower concentrations. This

subtle pro-proliferative effect appeared to persist and slightly strengthen at Day 9 (D9) for these higher concentrations, suggesting a potential long-term benefit on cell growth.

Based on these results, HD-WSM was confirmed to be non-cytotoxic to MC3T3-E1 preosteoblasts within the tested range. The observed weak enhancement in cell proliferation at higher concentrations (150-250 µg/ml) after extended exposure presents a promising indication for its potential osteogenic properties. Consequently, concentrations of 100 µg/ml and 200 µg/ml were judiciously selected for further bioactivity studies. This selection ensures that subsequent experiments are conducted within a safe, non-toxic range while encompassing concentrations that demonstrated a potential positive effect on cell proliferation, allowing for the exploration of dose-dependent responses on bone differentiation markers.

3.2 HD-WSM enhances alkaline phosphatase activity (ALP) in MC3T3-E1 cells.

To investigate the potential of HD-WSM to enhance early osteoblast differentiation, alkaline phosphatase (ALP) activity was evaluated in MC3T3-E1 preosteoblasts over 3, 6, and 9 days of treatment. ALP activity, an established early marker of osteoblast differentiation and in vitro bone formation, was quantified using an Alkaline Phosphatase Assay Kit (ab83369, Abcam).At the commencement of the experiment (D0), ALP activity was minimal across all groups. In the untreated control group (0 µg/ml), a natural increase in ALP activity was observed over time, rising from approximately 0.1 U/ml at D0 to 0.8 U/ml at D6, and further to 1.7 U/ml by D9, consistent with the intrinsic differentiation potential of proliferating MC3T3-E1 cells. Treatment with HD-WSM significantly enhanced ALP activity in a dose- and time-dependent manner (Figure 1). By Day 3 (D3), concentrations of HD-WSM as low as 50 µg/ml initiated a noticeable increase in ALP activity compared to the untreated control. This enhancement became markedly stronger at higher concentrations and longer incubation periods. For instance, at 200 µg/ml, ALP activity reached approximately 2.3 U/ml by D3, increasing substantially to 5.2 U/ml at D6, and peaking at over 7.3 U/ml by D9. Comparatively, at D9, ALP activity in the 200 µg/ml HD-WSM group was nearly 4.3 times higher than that of the untreated control. A similar dose-dependent trend was observed, with 150 µg/ml and 100 µg/ml also showing substantial increases in ALP activity compared to lower concentrations and the control group at each time point. Data are presented as average ± SD.
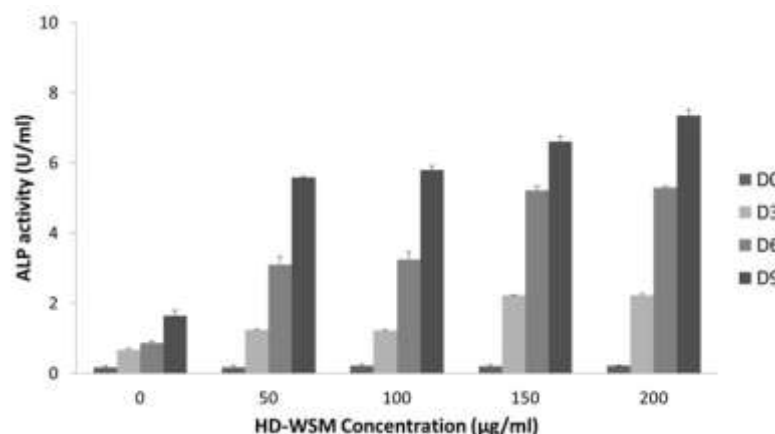
Figure 2 Alkaline phosphatase activity (ALP) of MC3T3-E1 cells. The experiment was performed at concentration of 0, 50, 100, 150, and 200 µg/ml for 3, 6 and 9 days. ALP activity was measured by Alkaline Phosphatase Assay Kit (Abcam) indicating HD-WSM enhances ALP in MC3T3-E1 cells.

This experiment aimed to assess the effect of HD-WSM on the early osteoblast differentiation marker, ALP activity, in MC3T3-E1 preosteoblasts. ALP activity is widely recognized as a crucial indicator of early osteoblast maturation, with its upregulation preceding matrix mineralization during in vitro bone formation. The observed dose- and time-dependent increase in ALP activity upon HD-WSM treatment strongly suggests that this extract positively influences early osteoblast differentiation. While the untreated control group exhibited an expected baseline increase in ALP activity due to the inherent proliferative and differentiative capacity of MC3T3-E1 cells, the dramatic elevations seen with HD-WSM treatment signify a distinct inductive effect. From as early as Day 3, HD-WSM concentrations starting from 50 µg/ml demonstrated a strong enhancing effect on ALP, which was amplified with increasing concentrations, reaching its highest level at 200 µg/ml by Day 9.

These findings are particularly significant when considered in conjunction with the preceding cytotoxicity study, which confirmed the non-cytotoxic nature of HD-WSM across the tested concentration range. This ensures that the observed increase in ALP activity is a genuine pro-osteogenic effect, rather than a consequence of cellular stress or altered cell viability. The sustained increase in ALP activity over 9 days further indicates that HD-WSM promotes not only the initiation but also the progression of early osteoblast differentiation.

4. Conclusions

Based on the comprehensive findings from both the cytotoxicity and alkaline phosphatase (ALP) activity experiments, a clear conclusion can be drawn regarding the initial characterization of Haliotis divericolor-water soluble extract (HD-WSM) on MC3T3-E1 preosteoblasts.

Firstly, the cytotoxicity assessment unequivocally demonstrated that HD-WSM is non-cytotoxic to MC3T3-E1 cells across the entire concentration range tested (50-250 µg/ml) and over an extended period of up to 9 days. Cell viability and proliferation rates remained comparable to untreated controls, ensuring that any subsequent biological effects observed are genuine and not confounded by cellular distress or death.

Secondly, the investigation into ALP activity, a pivotal early marker of osteoblast differentiation, revealed that HD-WSM significantly enhances this enzymatic activity in a dose- and time-dependent manner. This strong upregulation of ALP, observed as early as Day 3 and escalating with increased concentration and duration of treatment, provides compelling evidence of HD-WSM's osteoinductive properties. The observed effects were substantial, exceeding the natural increase in ALP activity seen in proliferating osteoblasts.

In conclusion, the combined results from these two foundational experiments indicate that HD-WSM is a safe and promising agent that actively promotes early osteoblast differentiation. Its non-cytotoxic nature, coupled with its robust ability to enhance ALP activity, strongly positions HD-WSM as a compelling candidate for further research into its potential applications in bone regeneration and tissue engineering.

5. Acknowledgements

6. References

Asvanund, P., & Chunhabundit, P. (2012). Alveolar bone regeneration by implantation of nacre and β-tricalcium phosphate in guinea pig. *Implant Dentistry, 21*(3), 248–253.

Espinosa, H. D., Juster, A. L., Latourte, F. J., Loh, O. Y., Gregoire, D., & Zavattieri, P. D. (2011). Tablet-level origin of toughening in abalone shells and translation to synthetic composite materials. *Nature Communications, 2*, 173.

Green, D. W., Kwon, H. J., & Jung, H. S. (2015). Osteogenic potency of nacre on human mesenchymal stem cells. *Molecular Cell, 38*(3), 267–272.

Green, D. W., Lai, W. F., & Jung, H. S. (2014). Evolving marine biomimetics for regenerative dentistry. *Marine Drugs, 12*(5), 2877–2912.

Lamghari, M., Antonietti, P., Berland, S., Laurent, A., & Lopez, E. (2001). Arthrodesis of lumbar spine transverse processes using nacre in rabbit. *Journal of Bone and Mineral Research, 16*(12), 2232–2237.

Lao, Y., Zhang, X., Zhou, J., Su, W., Chen, R., Wang, Y., Zhou, W., & Xu, Z. F. (2007). Characterization and in vitro mineralization function of a soluble protein complex P60 from the nacre of *Pinctada fucata. Comparative Biochemistry and Physiology Part B, 148*(2), 201–208.

Liao, H., Mutvei, H., Hammarström, L., Wurtz, T., & Li, J. (2002). Tissue responses to nacreous implants in rat femur: An in situ hybridization and histochemical study. *Biomaterials, 23*(13), 2693–2701.

Marin, F., Luquet, G., Marie, B., & Medakovic, D. (2008). Molluscan shell proteins: Primary structure, origin, and evolution. *Current Topics in Developmental Biology, 80*, 209–276.

Rousseau, M., Boulzaguet, H., Biagianti, J., Duplat, D., Milet, C., Lopez, E., & Bédouet, L. (2008). Low molecular weight molecules of oyster nacre induce mineralization of the MC3T3-E1 cells. *Journal of Biomedical Materials Research Part A, 85*(2), 487–497.

Rousseau, M., Delattre, O., Gillet, P., & Lopez, E. (2012). Subchondral nacre implant in the articular zone of the sheep's knee: A pilot study. *Bio-Medical Materials and Engineering, 22*(4), 227–234.

Vannate, P., Ruth, S., & Saowaluck, Y. (2014). Maize planting in the North of Thailand and air pollution from haze. *Thai Journal of Animal Science, 1*(2), 20–36.

Sitting Posture Detection and Prevention of Office Syndrome Using MediaPipe Technology

Panadda Solod[a*] Napaphat Kongrit[a] Thapanic Teerapan[a] Wasu Suksuwan[b] and Wannadear Nawae[a]

[a] *Faculty of Industrial and Education and Technology, Rajamangala University of Technology Srivijaya, Thailand*
[b] *Faculty of Engineering, Rajamangala University of Technology Srivijaya, Thailand*
* Corresponding author, E-mail address: panadda.s@rmutsv.ac.th

Abstract

With the increasing prevalence of office syndrome caused by prolonged sitting and poor posture, this paper proposes a real-time posture detection system aimed at improving ergonomic practices in the workplace. The system leverages the MediaPipe Framework, an advanced deep learning-based tool for human pose estimation, to monitor and assess upper body posture. This study aims to assess the accuracy and responsiveness of a MediaPipe-based system in detecting incorrect sitting postures associated with office syndrome. The proposed system continuously tracks posture throughout work hours, thereby reducing the likelihood of developing musculoskeletal pain. The research process began with the development of a posture detection algorithm that utilized MediaPipe's pose estimation model to calculate angular deviations based on landmarks for the shoulder and head. This was followed by the implementation of the system, real-time testing, and performance evaluation under simulated office conditions. Through an experiment with 10 volunteers, selected to represent a manageable and diverse group for initial validation. The system's accuracy was evaluated by comparing the calculated angles with the actual angles in three key positions: neutral, left-side tilt, and right-side tilt. The results showed that the system performed with high accuracy in the neutral position, with a Mean Absolute Error (MAE) close to 0%, but had a higher MAE of approximately 20% in the tilted positions. The system demonstrated an average processing time of 0.20 seconds per frame, which corresponds to approximately 5 frames per second, indicating its potential for real-time posture monitoring. This study contributes to the development of efficient workplace health technologies that promote better posture and reduce the risk of office syndrome.

Keywords: Posture Detection, Human Pose Estimation, MediaPipe Framework, Office Syndrome

1. Introduction

The rapid advancement of digital technologies in the workplace has greatly transformed the nature of office-based work. Tools for data storage, accounting, procurement, and other essential business functions are now predominantly computer-based, offering significant convenience and efficiency to office employees. However, this technological shift has also introduced unintended health consequences, particularly as employees increasingly spend over seven hours a day interacting with computers and other digital devices. While technology has enhanced productivity, it has inadvertently contributed to a rising concern: musculoskeletal pain among office workers.
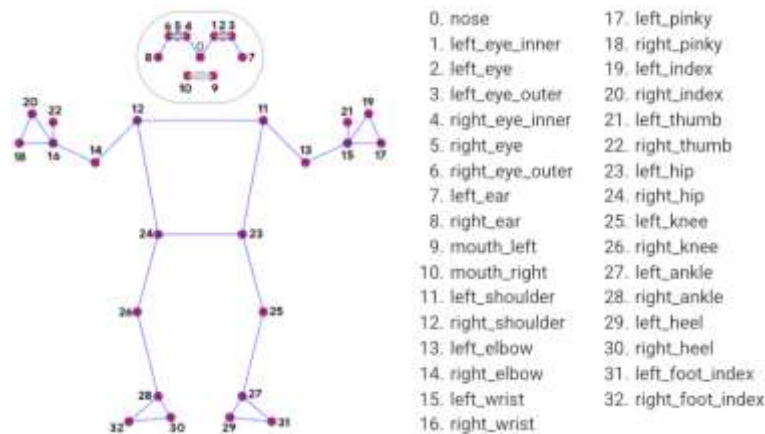
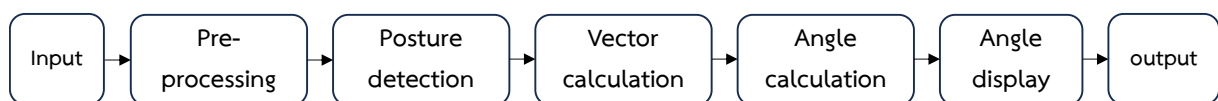Figure 1 MediaPipe Pose Landmarks (Kim et al., 2023)

Figure 2 Posture Detection Process Flow

Recent studies have highlighted the widespread occurrence of musculoskeletal disorders among office employees, especially those engaged in sedentary work. Research by (Lazko et al., 2021) indicates that 44.2% of female office employees report experiencing wrist pain (radiocarpal), 40.4% suffer from neck pain, and 38.5% do not

report pain, suggesting a significant issue with workplace ergonomics. This pain is often attributed to factors such as prolonged sitting, incorrect posture, and insufficient physical activity throughout the workday. Musculoskeletal pain, resulting from poor ergonomic practices, is a key contributor to what is increasingly recognized as "office syndrome" a collection of conditions that affect the musculoskeletal and nervous systems due to long periods of poor posture and sedentary behavior.

The rise in the office syndrome has led to significant concerns not only about the well-being of employees but also about the long-term impact on productivity. The root causes of these disorders include prolonged sitting, lack of movement, poor ergonomics, and inadequate posture. A lack of proper ergonomic practices, such as sitting with poor posture or without appropriate breaks, can lead to pain in the wrist, neck, shoulders, and back, which, in turn, can escalate into more severe conditions like chronic pain or repetitive strain injuries (RSI). As such, addressing these issues has become a key challenge in improving workplace health and preventing long-term physical harm to employees.

Several technological solutions have been proposed to address this growing problem. (Paliyawan et al., 2014). introduced a novel approach for preventing office syndrome by detecting prolonged sitting using a model that utilizes Kinect cameras and data mining classification. The Kinect camera can monitor body posture and movements, alerting employees to the need to adjust their positions or take breaks. Similarly, (Srahongthong, et al.,2023) developed an application that uses augmented reality (AR) to provide personalized treatment programs for office syndrome. The AR system uses a user questionnaire to propose therapy programs tailored to individual needs, such as specific exercises or stretches to alleviate pain and prevent further injury.

In another approach, (Amin et al., 2024) examined the effectiveness of an app-based neck exercise program grounded in the McKenzie protocol, which was shown to reduce pain intensity by 46%. This program offers six neck movements designed to help relieve tension and reduce discomfort. Likewise, (Lee et al., 2017) proposed a series of stretching exercises aimed at reducing neck and shoulder pain, demonstrating the positive impact of such routines when practiced consistently over four weeks.

Additionally, (Kim et al., 2023) leveraged deep learning models such as MediaPipe to optimize human pose detection for applications that monitor the movements of individuals, providing real-time alerts in cases of falls or injuries at home. MediaPipe, a tool developed for accurate pose tracking, uses pre-trained deep-learning models to monitor and analyze human movements, providing valuable insights for both injury detection and prevention.

Despite these promising advancements, most solutions still focus on postural correction in specific instances, rather than providing a comprehensive, real-time solution that proactively helps employees avoid developing musculoskeletal pain in the first place. There is a growing need for an integrated system that combines the principles of ergonomics with real-time feedback to detect and correct sitting posture before it leads to discomfort or injury.

This research aims to fill that gap by developing and testing a real-time sitting posture detection system based on MediaPipe, an advanced deep learning-based tool that specializes in human pose detection. The proposed system will provide continuous feedback to office workers, allowing them to adjust their posture during work hours and reduce the likelihood of developing office syndrome. By incorporating ergonomic principles into the detection and analysis of sitting posture, this system will help promote healthier work habits and minimize the risk of musculoskeletal pain. In doing so, this research contributes to the growing body of work in workplace health technology, offering a proactive approach to managing and preventing office syndrome.
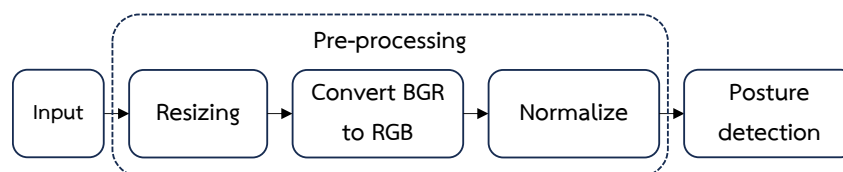

Figure 3 Pre-processing Flow

Furthermore, this paper will explore the theoretical underpinnings of ergonomic design in office work, the specific role of posture in preventing musculoskeletal disorders, and the potential benefits of integrating deep learning technologies like MediaPipe into real-time posture detection systems. The study will also evaluate the effectiveness of such a system in a workplace setting, examining both the technological feasibility and the potential for widespread adoption to improve employee health and productivity.

2. Methodology

2.1 System Design

The proposed system utilizes the MediaPipe Framework, an open-source solution developed by Google, to detect and analyze upper-body posture in real time. MediaPipe supports detection of 33 key landmarks across the human body, which are used for posture classification as illustrated in Figure 1. The system is designed to operate efficiently on standard computing devices, ensuring responsive performance during prolonged work sessions. The overall process follows four key stages: Pre-processing, Posture Detection, Vector Calculation, and Angle Calculation, as shown in Figure 2.
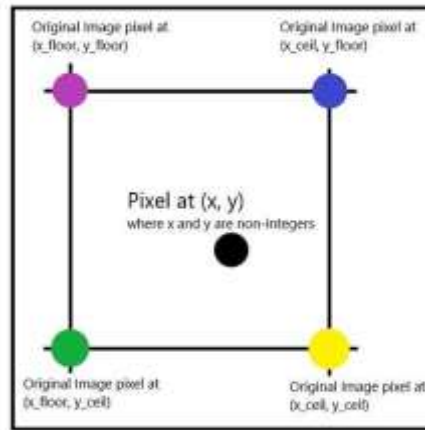
Figure 4 Linear Interpolation [7]

2.2　Pre-processing

The input image is first resized to 640x480 pixels to optimize processing speed without significant loss in quality. The resizing is achieved using the Bilinear interpolation method, which balances the preservation of image quality with the need for improved processing efficiency. Bilinear interpolation works by considering four neighboring pixels surrounding the target point. These four pixels, typically arranged in a rectangle, are selected based on their proximity to the target point. The algorithm then performs linear interpolation first along one axis (typically the x-axis) and then along the second axis (typically the y-axis). This approach ensures that the resizing process is computationally efficient while maintaining an acceptable level of image detail, thereby allowing for smooth and timely ergonomic tracking according to Figure 3 and 4. Then, the color format is converted from BGR (default in OpenCV) to RGB, which is compatible with MediaPipe. Lastly, pixel values are normalized to the [0, 1] range by dividing each by 255. This standardization ensures consistent input for pose estimation.

2.3　Posture Detection

At this stage, the MediaPipe framework is utilized to identify specific anatomical landmarks crucial for upper-body posture analysis, including the nose (landmark 0), left shoulder (landmark 11), and right shoulder (landmark 12). These landmarks are tracked in three-dimensional space (x, y, z), enabling the system to monitor head and shoulder alignment in real-time and provide reliable spatial data for subsequent angle and vector calculations.

Figure 5 Pose Estimation and Angle Calculation
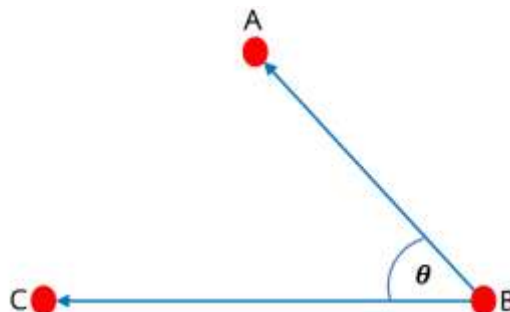
Figure 6 Corresponding Vector

MediaPipe's pose detection process operates through two key stages: person detection and landmark estimation. Initially, a lightweight bounding box detector identifies the presence and position of a person within the image frame. Once the individual is localized, a pose landmark model estimates the 3D coordinates of 33 key points across the body, including the head, shoulders, elbows, wrists, hips, knees, and ankles. These coordinates are continuously updated for each frame and normalized for image dimensions to ensure consistency.

Figure 7 Actual Angle Measurement

Figure 8 Angle Tracking Result

2.4 Vector and Angle Calculation

To determine head posture, vectors are computed between key landmarks as illustrated in Figure 5 and 6. Specifically, point A represents the nose (landmark 0), while points B and C represent the left shoulder (landmark 11) and right shoulder (landmark 12), respectively. Two vectors are constructed: vector AB from the left shoulder to the nose, and vector BC from the left shoulder to the right shoulder. The angle between these vectors is calculated using the dot product formula, which provides a geometric measure of the orientation between the two vectors following to equation (1) to (5) respectively.

$$Dot\ product = AB_x \cdot BC_x + AB_y \cdot BC_y + AB_z \cdot BC_z \qquad (1)$$

$$|AB| = \sqrt{AB_x^2 + AB_y^2 + AB_z^2} \qquad (2)$$

$$|BC| = \sqrt{BC_x^2 + BC_y^2 + BC_z^2} \qquad (3)$$

$$\cos \theta = \frac{dot\ product}{|AB| \cdot |BC|} \qquad (4)$$

$$\theta = \cos^{-1}(\cos \theta) \qquad (5)$$

To ensure that the calculated angles are consistent and independent of the image size or resolution, normalization is applied. Each coordinate (x, y) from the pose landmarks is divided by the corresponding width and height of the input image, respectively. This results in dimensionless values in the range [0, 1], which allows the angle computation to be invariant to scale. This is particularly important for real-time posture detection across different camera setups and environments.

2.5 Posture Classification Thresholds

Head posture classification is based on the angular deviation between the vector from the left shoulder to the nose (vector AB) and the vector from the left shoulder to the right shoulder (vector BC), as computed in the previous section. The resulting angle serves as a geometric indicator of head tilt direction.

To interpret these angles, thresholds were empirically defined through experimental calibration. A neutral posture is identified when the measured angle remains within ±10° of a reference baseline, typically centered around

178

90° in the vector configuration. If the angle decreases significantly (less than 70°), the posture is classified as a left-side tilt, indicating the nose is closer to the left shoulder. Conversely, an angle greater than 110° indicates a right-side tilt, where the nose is positioned closer to the right shoulder. These threshold values were validated using manual protractor measurements during the experiment and aligned with ergonomic literature, which identifies 15°–20° of lateral tilt as a common boundary for detecting non-neutral posture (Chapman et al., 2021; Mingels et al., 2016). This classification system allows the posture detection algorithm to reliably differentiate between normal and incorrect sitting positions associated with office syndrome risk.

3. Results and Discussion

$$\text{MAE} = \frac{1}{n}\sum_{i=1}^{n}|\theta_i^{measured} - \theta_i^{actual}| \qquad (6)$$

Where $\theta_i^{measured}$ = the angle detected by the system
θ_i^{actual} = the manually measured angle
n = the number of observations

For the evaluation of the proposed system, an experimental setup was established in a controlled environment with a lighting level of approximately 300 LUX to simulate typical office conditions. The experiment involved 10 volunteers, comprising 6 females and 4 males, to assess the system's effectiveness in real-world scenarios. The volunteers were asked to perform standard office tasks while their posture was continuously monitored by the system. The data collected from these tests were used to evaluate the accuracy, responsiveness, and usability of the posture detection system, as well as its impact on promoting ergonomic practices.
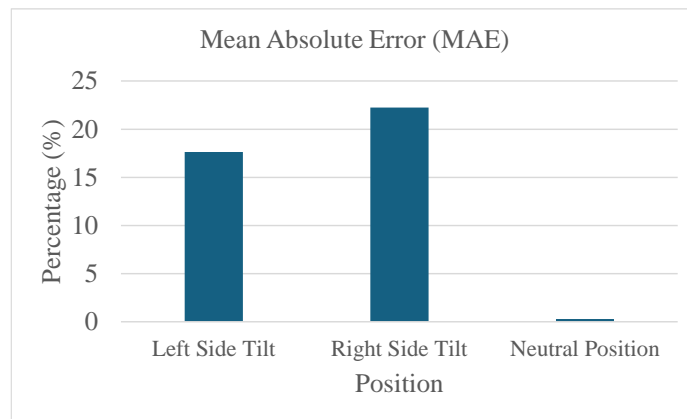
Figure 9 Mean Absolute Error (MAE) for Different Head Positions

To evaluate the accuracy of the proposed system, an experiment was conducted by comparing the actual angles (Figure 7) with the calculated angles (Figure 8) derived by the system. The experiment was divided into three parts: the first part involved measuring the angle in the neutral position, where the volunteer maintained a neutral head posture facing directly forward. The second part assessed the system's performance in detecting the angle during a left side tilt, where the volunteer tilted their head to the left. The final part measured the angle with the right-side tilt, where the volunteer tilted their head to the right. Each part of the experiment was conducted 20 times by 10 volunteers (6 females and 4 males) to ensure robust data collection. The calculated angles for each tilt position were compared with the actual angles to determine the system's accuracy and its ability to detect head movements in different directions. To validate the accuracy of the system, the actual angles were measured using a standard manual protractor application, which was placed and aligned along the participant's head and shoulder axis during each posture. These measurements served as reference angles for comparing against the automated detection angles calculated by the MediaPipe's pose estimation model according to Figure 8. The results were analyzed to assess the precision of the system in accurately detecting and calculating head posture.

To quantify the accuracy of the system, the Mean Absolute Error (MAE) was used as the primary metric for evaluating posture angle detection. For each trial, the angle calculated by the system using MediaPipe landmarks was compared to the corresponding actual angle, which was measured manually using a standard protractor aligned with the participant's head and shoulder axis. The absolute error for each instance was computed as the absolute difference between the measured angle and the actual reference angle. These individual errors were then averaged across all repetitions for each posture type—neutral, left tilt, and right tilt—to determine the final MAE, according to the equation (6).

The results of the Mean Absolute Error (MAE) analysis are presented in Figure 9, which shows the error percentages for three different head positions: Neutral Position, Left Side Tilt, and Right-Side Tilt. In the Neutral Position, the system demonstrated a very low MAE, close to 0%, indicating that the calculated angles closely match

the actual angles when the head is in a neutral, straight-forward posture. This suggests that the system is highly accurate in detecting the posture in this position. However, as the head tilts to the left or right, the MAE increases, with both the Left Side Tilt and Right-Side Tilt showing an error of approximately 20%. These higher error values suggest that the system's accuracy decreases as the head tilts away from the neutral position. The increased MAE in tilted positions may be attributed to challenges in detecting and differentiating smaller changes in posture, or potential variations in individual head movements during tilting. Overall, while the system performs optimally in the neutral position, further refinement may be needed to improve accuracy in detecting head tilts.

Additionally, the processing time for the proposed system, executed on an **11**th Gen Intel® Core™ i**7**-1165G7 processor at 2.80 GHz, was evaluated. The system processed each frame with an average time of 0.20 seconds per frame, corresponding to approximately **5** frames per second (fps). This processing time demonstrates the system's capability to perform real-time posture detection efficiently, providing timely feedback for posture correction during typical office tasks.

4. Conclusions

This study presented the development of a real-time posture detection system utilizing the MediaPipe Framework to address the growing issue of office syndrome associated with prolonged sitting and poor ergonomic habits. The system was evaluated for its ability to detect head posture across various positions, demonstrating high accuracy in identifying neutral postures, with moderate deviations observed during head tilts.

Despite these limitations, the system's consistent performance in neutral alignment and its low-latency operation underscores its potential for practical use in workplace environments. The findings also highlight the importance of further refinement, particularly in improving sensitivity to subtle postural deviations.

In addition, the analysis revealed that factors such as individual body structure, user height, camera angle, and involuntary movements can affect detection accuracy. These insights support the need for adaptive calibration strategies and personalized posture baselines to enhance system robustness across diverse users.

Overall, the proposed system offers an efficient and scalable approach for promoting ergonomic awareness and reducing musculoskeletal risks in office settings. Future work will aim to improve detection reliability, extend posture analysis to full-body tracking, and incorporate intelligent feedback mechanisms for real-time posture correction and user engagement.

5. Acknowledgements

6. References

Lazko, O., Byshevets, N., Kashuba, V., Lazakovych, Y., Grygus, I., Andreieva, N., & Skalski, D. (2021). Prerequisites for the development of preventive measures against office syndrome among women of working age. *Teorìâ ta Metodika Fìzìčnogo Vihovannâ*, 21(3), 227–234. https://doi.org/10.17309/tmfv.2021.3.06

Paliyawan, P., Nukoolkit, C., & Mongkolnam, P. (2014). Prolonged sitting detection for office workers syndrome prevention using Kinect. In *Proceedings of the 2014 IEEE International Conference on Biomedical Engineering and Technology (BME)* (pp. 1–6). https://doi.org/10.1109/BME.2014.6762480

Srahongthong, P., & Nimkoompai, A. (2023). Office syndrome treatment using augmented reality technology on mobile applications. In *Proceedings of the 20th International Joint Conference on Computer Science and Software Engineering (JCSSE 2023)* (pp. 443–447).

Amin, D. I., Mohamed, G. I., & ElMeligie, M. M. (2024). Effectiveness of McKenzie exercises plus stabilization exercises versus McKenzie exercises alone on disability, pain, and range of motion in patients with nonspecific chronic neck pain: A randomized clinical trial. *Journal of Back and Musculoskeletal Rehabilitation*, 37(6), 1507–1517. https://doi.org/10.3233/BMR-230352

Lee, J., Lee, Y., Kim, J., & Park, S. (2017). Effectiveness of an application-based neck exercise as a pain management tool for office workers with chronic neck pain and functional disability: A pilot randomized trial. *European Journal of Integrative Medicine*, 12, 87–92. https://doi.org/10.1016/j.eujim.2017.04.012

Kim, J.-W., Choi, J.-Y., Ha, E.-J., & Choi, J.-H. (2023). Human pose estimation using MediaPipe Pose and optimization method based on a humanoid model. *Applied Sciences*, 13(4), 2700. https://doi.org/10.3390/app13042700

Gonzalez, R. C., & Woods, R. E. (2018). *Digital image processing* (4th ed.). Upper Saddle River, NJ: Pearson.

Chapman, S., Bridge, M., and Parry, R., 2021, Postural Variability in Comfortable Sitting Among Office Workers, *Journal of Occupational Health Studies*, Vol.18(1), p. 55–63.

Mingels, S., Horsch, A., and Klussmann, A., 2016, Head-Tilt Patterns in Laptop Users with and without Posture-Induced Pain, *Ergonomics Research Journal*, Vol.9(3), p. 211–223.

Real-Time pH Monitoring and Automated Control System for Sustainable Aquaculture

Wannadear Nawae[a] Wasu Suksuwan[b] and Panadda Solod[a]

[a] Faculty of Industrial and Education and Technology, Rajamangala University of Technology Srivijaya, Thailand
[b] Faculty of Engineering, Rajamangala University of Technology Srivijaya, Thailand
* Corresponding author, E-mail address: wannadear.n@rmutsv.ac.th

Abstract

Fluctuations in pH levels can have a detrimental impact on the health, productivity, and ecosystem balance of aquatic organisms. Maintaining a stable pH within the optimal range is essential to ensure water quality and fish well-being. This study presents the design and validation of a real-time automated pH monitoring and control system to support sustainable aquaculture practices by regulating water pH using 0.2% (W/V) vinegar solution and 5% (W/V) dolomite solution. The system features real-time pH monitoring via a pH sensor and utilizes the ESP32 microcontroller to automate pH adjustments, with data logged to Google Sheets for remote tracking. The research process was conducted in two phases: The first phase involved determining the appropriate quantities of each solution for safe and effective pH regulation through incremental dosage trials, ensuring that the pH change did not exceed 2 units per day. The second phase evaluated the system's performance in actual control scenarios by adjusting the pH in a 1500 ml water container from acidic and basic conditions toward neutral, and by measuring the required time and solution saturation dynamics. The results show that the system can efficiently adjust the pH from acidic to neutral or from basic to neutral, with the required application of 4 ml of dolomite solution and 2 ml of vinegar solution per cycle. The time required for pH adjustment was approximately 1 day for changing pH from 4 to 7 and 1.5 days for adjusting pH from 8.5 to 7. These findings validate the effectiveness of the proposed system in controlling pH levels in aquaculture and demonstrate its potential for large-scale applications in water quality management.

Keywords: pH Control System, Aquaculture, Real-Time Monitoring, IoT-based Monitoring, Vinegar Solution, Dolomite Solution

1. Introduction

Fish farming has quickly become one of Thailand's most important agricultural industries, driven by the rising demand for domestic and international fish. As the global population grows and the need for sustainable seafood increases, the fish farming sector continues to expand, with various farming systems being employed to meet these needs. These systems include monoculture, extensive, and semi-intensive farming methods, each offering unique benefits and challenges based on the objectives of the operation (Soltan, 2016). Among these, monoculture has gained popularity due to its efficiency in managing feeding schedules and monitoring fish growth and health. The highly controlled environment of monoculture allows for higher production in a shorter time, making it an appealing choice for both small and large-scale operations.

However, while monoculture offers significant advantages in terms of productivity, it also comes with a range of challenges that must be addressed to ensure sustainability over the long term. One of the most pressing issues associated with monoculture farming is water quality degradation. The high density of fish in these systems puts considerable strain on the water, leading to the accumulation of waste products like ammonia and organic matter. This can create a harmful environment for the fish, with poor water quality often causing stress, diseases, and slower growth rates. Additionally, the buildup of nutrients in the water can disrupt the balance of the ecosystem, diminish biodiversity and interfere with natural biological processes. Furthermore, monoculture farming tends to rely heavily on large quantities of feed and chemicals, which not only leads to inefficient use of natural resources but also contributes to environmental pollution. Therefore, while monoculture is a highly productive and profitable method of fish farming, it is crucial to address these challenges to ensure that the system remains ecologically balanced and sustainable in the long run.

One of the most important factors influencing the success of fish farming is water quality, specifically the pH level. The pH of water affects the health and growth of fish, and maintaining a stable pH within an optimal range is crucial for maximizing productivity. Various factors, including ammonia levels, water temperature, and dissolved oxygen, interact to determine the overall water quality. Among these, pH levels play a critical role in fish health, and it has been widely recognized that water pH should remain between 6.5 and 8.5 for optimal fish growth (Craig et al., 2008). However, pH levels in natural waters tend to fluctuate, with pH typically around 5.6 due to dissolved carbon dioxide, which forms carbonic acid. During daylight hours, photosynthesis by aquatic plants removes carbon dioxide from the water, causing a rise in pH. Conversely, in the evening when photosynthesis decreases, carbon dioxide accumulates, leading to a decrease in pH. This diurnal variation can be problematic in fish farming, where maintaining a stable pH is critical for fish well-being.

To address this challenge, various strategies have been proposed for controlling and balancing the pH of water in aquaculture systems. One such method involves the use of vinegar solutions to lower the pH. Studies have shown that apple cider vinegar (ACV) and coconut sap vinegar (CSV) can significantly improve shrimp growth performance by maintaining a stable pH of approximately 7.9 in the water (Jamis et al., 2018). In situations where the water becomes too acidic, limestone has been used successfully to raise the pH to a more favorable level (Queiroz et

al., 2004), with improvements observed within two weeks of application. These solutions, combined with technological advancements such as the Internet of Things (IoT), offer an integrated approach for real-time monitoring and management of water quality.

The integration of IoT-based systems in aquaculture has revolutionized the ability to monitor water quality in real time. IoT sensors can continuously track parameters such as pH, temperature, and dissolved oxygen, and send this data to a central control system. This allows for precise adjustments to be made automatically to maintain optimal water quality. Sodium carbonate and calcium carbonate are commonly used to buffer the water and prevent drastic fluctuations in pH levels (Abinaya et al., 2019). In addition to these methods, acidic liquids can be applied to neutralize high pH levels, particularly when the pH exceeds 7.5 (Budiman et al., 2019).

Despite the availability of these methods, there is still a need for more efficient and automated systems that can effectively balance the pH levels in fish farming environments. This work aims to develop a comprehensive pH monitoring and control system for fish farming, utilizing vinegar and dolomite solutions to adjust pH levels. The proposed system will automatically dispense vinegar solutions when the pH exceeds 8 and use dolomite solutions to raise the pH when the water becomes too acidic. By integrating real-time monitoring and automated control, this system will help maintain water quality within the optimal range for fish farming, thereby improving fish health, growth, and overall productivity.
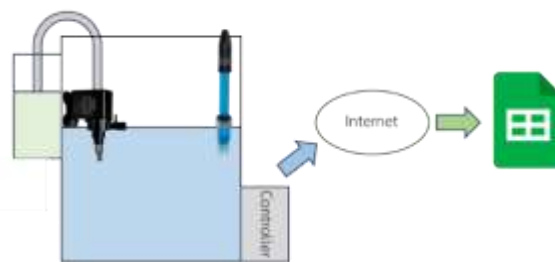
Figure 1 Proposed system installation
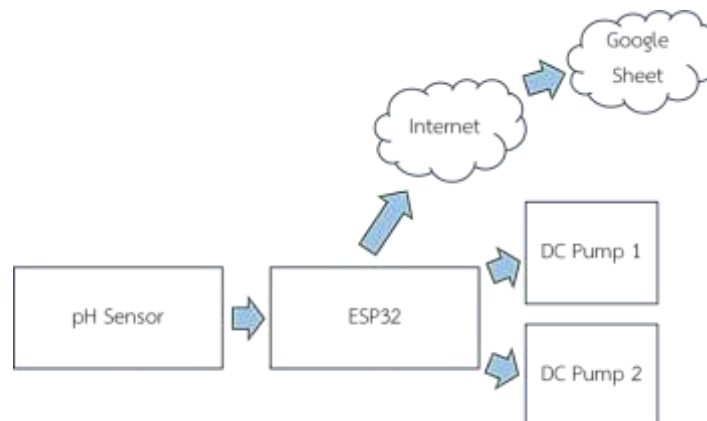
Figure 2 Proposed system block diagram

2. Methodology

In the proposed system, water pH is regulated using a 0.2% (W/V) vinegar solution as an acidifying agent and a 5% (W/V) dolomite solution as an alkalizing agent, with real-time monitoring and data logging performed via Google Sheebts through the ESP32 microcontroller. The 0.2% (W/V) vinegar solution was prepared by dissolving 2 grams of vinegar in 1 liter of water. Given that commercial vinegar typically contains 5% acetic acid, this results in an approximate acetic acid concentration of 0.01% (100 mg/L) in the working solution. During system operation, 2 ml of this vinegar solution was added to a 1,500 ml water tank, resulting in an acetic acid concentration of approximately 0.133 mg/L in the tank. This value is significantly lower than reported LC_{50} values for acetic acid (typically ranging from 45 to 1,000 mg/L), indicating the solution's safe application in aquatic environments. The 5% (W/V) dolomite solution was prepared by dissolving 5 grams of dolomite powder in 100 ml of water, yielding a mineral concentration of 50 g/L. For each alkalizing cycle, 4 ml of this solution was dispensed into the 1,500 ml water tank, resulting in an added mineral content of approximately 133 mg/L. This dosage is also well below known toxicity thresholds and was selected to gradually buffer the pH toward neutral without adversely affecting aquatic organisms.
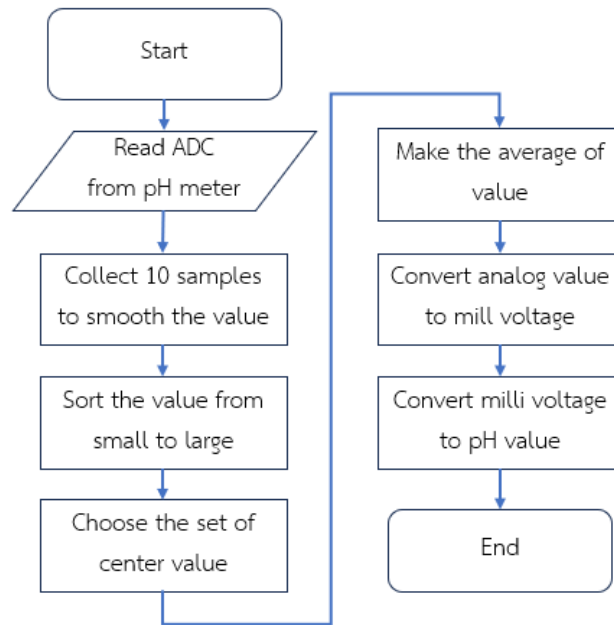
Figure 3. Data Acquisition

Figure 1 illustrates the setup of the proposed system. The system includes a pH sensor, and an oxygen pump installed inside the tank. The pH sensor continuously measures the water's pH level, while the oxygen pump ensures adequate water circulation. The dispensers for the acid and base solutions, along with their controllers, are positioned on the side of the tank.
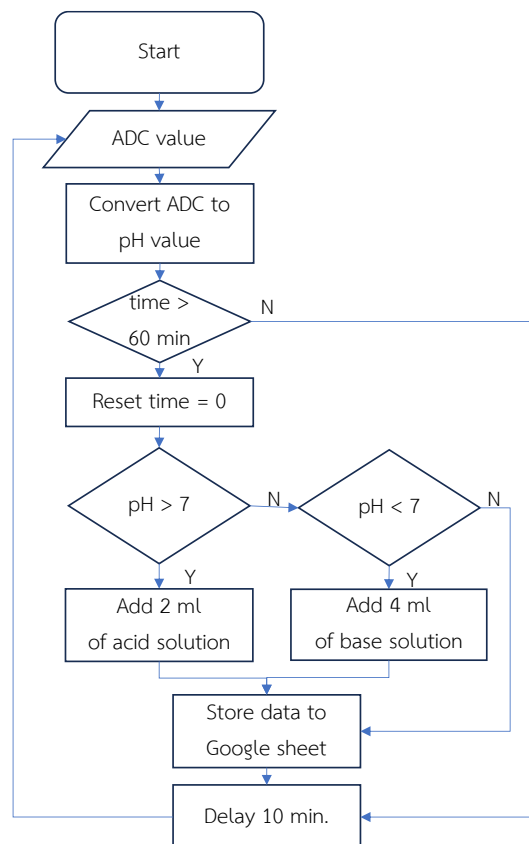

Figure 4 Control System Design

Figure 2 presents the block diagram of the proposed system, outlining the interactions between the pH sensor, controller, pumps, and the Google Sheets interface. The pH sensor serves as the input device to capture the water's pH readings, which are then transmitted to the ESP32 controller. Based on these readings, the controller determines when

183

to activate the DC pumps (DC pump 1 and DC pump 2) to correct any pH imbalances. The system is designed to adjust the pH by dispensing either vinegar or dolomite solution, depending on whether the water is too acidic or basic. Additionally, the pH values are logged in real-time to Google Sheets via the controller's internet connection, providing remote monitoring and tracking of the pH levels.

2.1 Data Acquisition

The pH measurement and control system begin according to Figure 3 by acquiring the analog signal from the pH sensor, which is then converted into a digital value by the ESP32 microcontroller's ADC using the equation (1). To enhance accuracy and reduce noise, 10 samples are collected, sorted from smallest to largest, and the center values are averaged. The digital value is subsequently converted back to the analog voltage using equation (2). Finally, the analog voltage is mapped to a pH value using the linear calibration formula in equation (3) where m is the slope and b is the intercept derived from sensor calibration. This method ensures accurate real-time pH monitoring, allowing for precise control over water quality in aquaculture environments.

2.2 Control Design

The control system of the proposed design is illustrated in Figure 4. The proposed pH control system utilizes real-time monitoring and automated pH adjustments to maintain optimal water quality in aquaculture. The system is equipped with a pH sensor that continuously measures the water's pH, which is then processed by an ESP32 microcontroller. Based on the measured pH, the system activates either a 0.2% (W/V) vinegar solution or a 5% (W/V) dolomite solution to adjust the pH levels, ensuring they stay within the desired range. The pH values and adjustment data are logged in Google Sheets, enabling remote tracking and real-time monitoring. The system employs a controlled dispensing mechanism that ensures pH changes do not exceed 2 units per day, and each solution is applied in precise amounts based on the pH level. A critical feature of the system is that after each adjustment, a minimum of 60 minutes is allowed to pass before the process continues, ensuring that the pH has stabilized before further changes are made. This automated approach, coupled with data logging and time checking, ensures efficient and accurate pH regulation, contributing to better water quality management in aquaculture.

$$\text{Digital value} = (\frac{\text{Analog input voltage}}{5.0}) \times 4095 \quad (1)$$

$$pH = m \times V_{analog} + b \quad (2)$$

Table 1 pH Difference of Dolomite Solution at Various Quantities

Quantity of solution	pH value (before adding solution)	pH value (after adding solution)	pH difference
8 ml	6.83	7.11	0.28
6 ml	6.82	7.07	0.25
4 ml	6.71	6.82	0.11
3 ml	6.32	6.39	0.07
2 ml	6.69	6.73	0.04

Table 2 pH Difference of Vinegar Solution at Various Quantities

Quantity of solution	pH value (before adding solution)	pH value (after adding solution)	pH difference
8 ml	6.87	6.43	0.44
6 ml	6.82	6.53	0.29
4 ml	6.84	6.63	0.21
2 ml	6.84	6.72	0.12

3. Result

The pH control system was developed and tested through a two-part experiment. The first part involved solution analysis, where vinegar and dolomite solutions were selected as the pH control agents. The goal of this phase was to determine the appropriate quantities of each solution required for effective pH regulation.

The mock container, holding 1500 ml of water, was used for the experiment. The quantity of solution added was adjusted based on the principle of pH adjustment in aquaculture, where the pH change should not exceed 2 units per day. As shown in Table 1, it was determined that the maximum allowable quantity of 5% (W/V) dolomite solution to be added to the container at any given time is 4 ml. Similarly, as indicated in Table 2, the maximum allowable quantity of 0.2% (W/V) vinegar solution is 2 ml per application.

In the second part of the experiment, we investigated the saturation time of pH changes when each solution was applied. The results revealed that the 5% (W/V) dolomite solution reached its saturation point in approximately 10 minutes, as illustrated in Figure 1. Similarly, the 0.2% (W/V) vinegar solution also reached its saturation point within the same timeframe of 10 minutes, as shown in Figure 5.
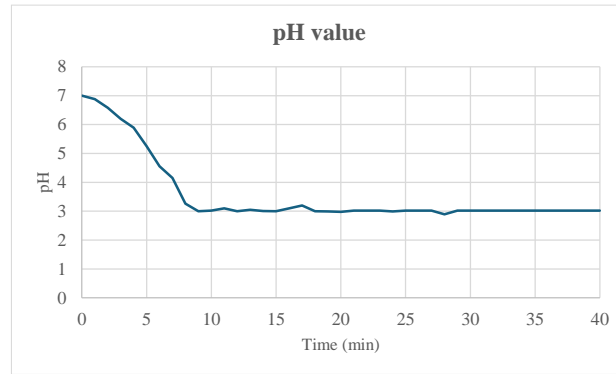
Figure 5 saturation time of pH value of vinegar solution

These findings provide valuable data for optimizing the pH control system and ensuring that both dolomite and vinegar solutions are used effectively without exceeding the maximum allowable pH changes for aquaculture environments.
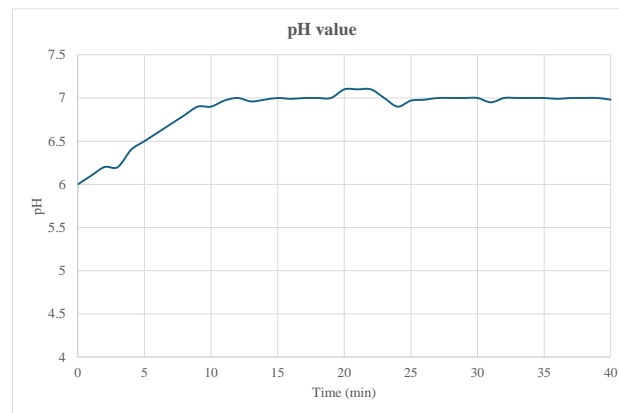

Figure 6 saturation time of pH value of dolomite solution

The second phase of the experiment aimed to evaluate the effectiveness of the pH-controlling system. A test container, holding 1500 ml of water, was equipped with an oxygen pump to facilitate water circulation. To adjust the pH from acidic to neutral, a 5% (W/V) dolomite solution was used, while a 0.2% (W/V) vinegar solution was employed to adjust the pH from basic to neutral. Each experiment was repeated three times for consistency.
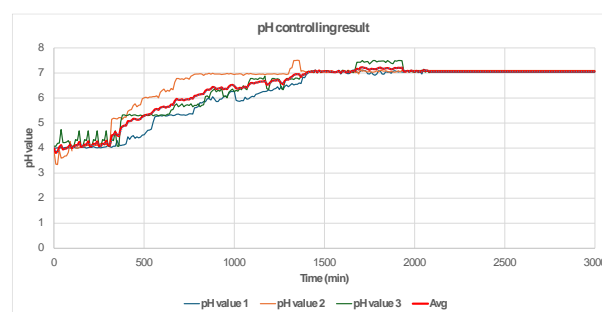
Figure 7 effectiveness of the pH-controlling system

As shown in Figure 6, the average time required to adjust the pH from 4 to 7 was approximately 1500 minutes, or about 1 day. Similarly, Figure 7 illustrates that the average time required to adjust the pH from 8.5 to 7 was approximately 2000 minutes, or 1 day and a half.

These results demonstrate the efficiency of the pH-controlling system in restoring water to a neutral pH within a reasonable time frame for both acidic and basic conditions.

4. Conclusion

The proposed pH control system demonstrated effective and efficient regulation of pH levels in aquaculture environments. By utilizing a combination of 0.2% (W/V) vinegar solution and 5% (W/V) dolomite solution, the

system successfully adjusted the pH from both acidic and basic conditions to neutral, within the optimal range. The experiment confirmed that the maximum allowable quantities of each solution (4 ml of dolomite and 2 ml of vinegar) did not exceed the recommended pH change of 2 units per day, ensuring water quality stability.

The system's performance was further validated by testing its saturation time for pH changes. Results showed that both the vinegar and dolomite solutions reached their saturation points in approximately 10 minutes, highlighting the system's quick response. Additionally, the time required to adjust pH from 4 to 7 and from 8.5 to 7 was approximately 1 day and 1.5 days, respectively, indicating the system's efficiency in maintaining stable pH levels over a reasonable period.

These findings suggest that the integration of real-time pH monitoring with automated pH adjustment can significantly improve control over water conditions in aquaculture. Future developments will focus on enhancing the system's scalability and efficiency for broader applications in various water quality management scenarios.

Although the experiments were conducted in a fixed volume of 1500 ml, the system design is inherently modular and suitable for scale-up. Adapting the system to larger tanks or ponds would require proportional calibration of dosing volumes, optimization of sensor positioning, and enhancements in water circulation and mixing. However, in larger-scale deployments, additional factors such as buffering capacity, non-uniform pH gradients, and slower reaction kinetics must be considered. Future work will focus on evaluating the system's performance in larger aquaculture environments and under variable field conditions. Investigations will include scalability assessment, adaptive control strategies, and integration with multi-parameter water quality monitoring to support broader applications in sustainable aquaculture and environmental management.

5. Acknowledgment

6. References

Soltan, M. (2016). Aquaculture systems. Faculty of Agriculture, Benha University, Egypt.

Tumwesigye, Z., Tumwesigye, W., Opio, F., Kemigabo, C., & Mujuni, B. (2022). The effect of water quality on aquaculture productivity in Ibanda District, Uganda. *Aquaculture Journal*, 2, 23–26.

Craig, S. T., & Louis, R. D. (2008). Managing high pH in freshwater ponds (SRAC Publication No. 4604).

Jhumar Jamis, J. O., Tumbokon, B. L., Caigoy, M. J. C., Bunda, C. M. G., & Serrano, E. A. (2018). Effect of vinegars and sodium acetate on the growth performance of Pacific white shrimp (Penaeus vannamei). *The Israeli Journal of Aquaculture – Bamidgeh*, IJA_70.2018.1506, 1–8.

Jamis, J. O., Tumbokon, B. L., Caigoy, M. J. C., Bunda, C. M. G., and Serrano, E. A., 2018, Effect of vinegars and sodium acetate on the growth performance of Pacific white shrimp (Penaeus vannamei), *The Israeli Journal of Aquaculture – Bamidgeh*, IJA_70.2018.1506, p. 1–8.

Queiroz, J. F. D., Nicolella, G., Wood, C. W., & Boyd, C. E. (2004). Lime application methods, water and bottom soil acidity in freshwater fish ponds. *Scientia Agricola (Piracicaba, Brazil)*, 61(5), 469–475.

Abinaya, T., Ishwarya, J., & Maheswari, M. (2019). A novel methodology for monitoring and controlling of water quality in aquaculture using Internet of Things (IoT). In *Proceedings of the 2019 International Conference on Computer Communication and Informatics (ICCCI-2019)* (pp. 1–4).

Budiman, F., Rivai, M., & Nugroho, M. A. (2019). Monitoring and control system for ammonia and pH levels for fish cultivation implemented on Raspberry Pi 3B. In *Proceedings of the 2019 International Seminar on Intelligent Technology and Its Applications (ISITIA)* (pp. 68–73).

IoT-Based Remote Monitoring and Alert System for Bedridden Patient Care in Thailand

Teerayut Luengsrisakul[a], Natthawich Nilsakoo[a], Wutthikrai Buakaew[a], Vorakamol Bookyayothin[b], and Nattasit Dancholvichit [a*]

[a] *Department of Mechatronics Engineering, Faculty of Engineering, Rajamangala University of Technology Rattanakosin, Nakhon Pathom, 73170, Thailand*
[b] *Department of Occupational Health and Safety, Faculty of Public Health, Mahidol University, Nakhon Pathom, 73170, Thailand*
* Corresponding author. Tel.: +66-(2)441-6000 ext 2640-1; E-mail address: nattasit.dan@rmutr.ac.th

Abstract

An increasing aging population in Thailand has placed a growing burden on healthcare resources. By 2030, the number of bedridden elderly is expected to reach 153,000, nearly three times the current figure. To address this, we have developed an IoT-based remote monitoring and alert system designed to assist caregivers in patient management. This system integrates smart sensors and cloud connectivity to provide real-time monitoring and alerts. A mobile application prototype, built using Google Sheets and AppSheet, offers real-time data visualization and allows caregivers and doctors to remotely track patient conditions. The app provides two access levels: caregivers or doctors can monitor multiple patients, while patients can view their own records. Instant alerts notify caregivers of critical changes ensuring timely intervention. Two IoT medical devices are implemented within this framework. The first device is an automatic hospital bed equipped with an inertial measurement unit and radar sensors to track patient activities, and head of bed elevation. The second device is a blood pressure and heart rate monitoring device that measures vital signs in intervals. Enabling IoT functionality increases the power consumption of both tested devices compared to their non-IoT versions. This power increase is observed in idle states and is also evident during active operational modes of the second device due to the demands of active components.

Keywords: IoT-based healthcare integration, caregiver alert system, real-time health monitoring

1. Introduction

Thailand is experiencing a significant demographic shift characterized by a rapidly aging population. This trend is projected to result in a substantial increase in the number of bedridden elderly, reaching an estimated 153,000 by 2030, nearly triple the current figures (Tantirat, Suphanchaimat, Rattanathumsakul, & Noree, 2020) [1]. This escalating need places a growing strain on the nation's healthcare resources. Remote patient monitoring (RPM) is increasingly recognized as a valuable tool for managing chronic conditions, facilitating the early detection of health deterioration, and improving patient outcomes (Malasinghe, Ramzan, & Dahal, 2019) [2]. However, while a growing number of medical devices are equipped with integrated IoT capabilities, a significant portion of existing equipment lacks direct network connectivity. Replacing all non-IoT devices with their smart counterparts can be financially prohibitive for many healthcare providers and individuals (Chakravarty, 2022) [3]. Adding another layer of complexity is the reality that while IoT-enabled medical devices are increasing, a substantial amount of existing equipment lacks direct network connectivity Kane, Bakker, & Balkenende, (2018) [4]. The prohibitive cost of replacing all these legacy devices underscores the critical need for innovative solutions that can bridge the gap between this existing infrastructure and modern cloud-based platforms.

This paper presents a case study focused on the development of an innovative IoT-based remote monitoring and alert system designed to empower caregivers in managing their patients more effectively. This system combines smart sensors and cloud connectivity to deliver real-time patient monitoring and timely alerts. A mobile app prototype, created with Google Sheets and AppSheet (Ferreira, 2014) [5], offers real-time data visualization and allows caregivers and doctors to remotely monitor patient conditions with different access levels for comprehensive and individual views. The system currently integrates two key IoT medical devices: an automatic hospital bed equipped with movement and elevation sensors, and a continuous blood pressure and heart rate monitoring device, laying a foundation for future integration of additional medical IoT technologies.

2. Methodology

2.1 Remote Monitoring Framework

The depicted system architecture represents a layered approach to IoT-based remote patient monitoring, aligning with established principles in distributed systems as shown in Figure 1. The perception layer, comprising sensor-equipped IoT medical devices, facilitates real-time data acquisition. This data is subsequently relayed via an Application Programming Interface (API) to the network layer, where Google Cloud is employed as a cloud-based server performing critical functions including data ingestion, processing, and persistent storage within a database. Google Cloud is utilized alongside AppScripts, a cloud-based scripting language by Google designed for automating tasks (Hassan, Mohd Rusli, & Mohd Salleh, 2023; Kurniawan, Wardani, & Zaki Hamidi, 2023). [6], [7]. The application layer provides a user-centric mobile interface, enabling remote visualization of patient data and the dissemination of timely alerts to caregivers. AppSheet is used to develop this mobile application as a no-code platform that provides an

interface for caregivers, doctors, and patients to monitor and interact with system data hosted on Google Cloud. It also allows the use of AppScripts for custom functionalities and integrations.

The provision of differentiated access levels within the mobile application is a critical design consideration that addresses the diverse needs and roles of stakeholders in the healthcare ecosystem. Caregivers and doctors can monitor multiple patients, improving oversight and resource management through real-time data. The cloud server offers scalable data storage, real-time visualization, historical trend analysis, and integration with systems like Electronics Health Records (EHRs) or nurse alerting systems. Conversely, granting patients access only to their own records promotes transparency and empowers them to actively participate in their health management. This patient-centric approach can enhance understanding of their condition, encourage adherence to treatment protocols, and foster a greater sense of control over their well-being [8]. Furthermore, these distinct access levels are crucial for maintaining data privacy and security, ensuring that sensitive patient information is appropriately restricted and accessible only to authorized individuals.
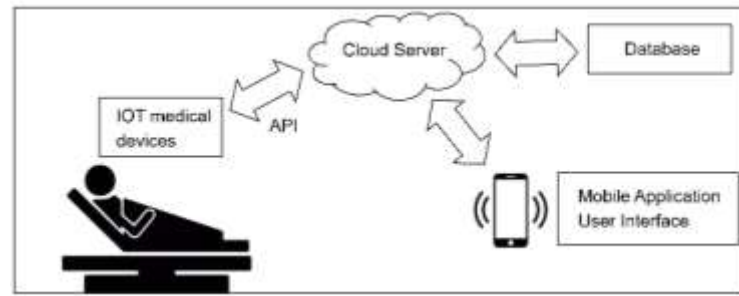
Figure 1 A framework for remote monitoring

2.2 IOT enablement and retrofitting

A significant aspect of this research involves the digitalization and IoT enablement of conventional medical devices through targeted hardware and software integration and retrofitting. The strategy of retrofitting existing infrastructure with IoT capabilities is a recognized and cost-effective approach for upgrading systems in various sectors (Pietrangeli, Mazzuto, Ciarapica, & Bevilacqua, 2023). [8]. In this study, we focus on enhancing two devices to improve the efficiency of caregivers and doctors. The first device is a motor-driven bed modified to provide adjustable head of bed elevation (HOBE) and track patient activity, discerning if they are sitting, lying, or off the bed. Adjustable HOBE is recommended for patients receiving enteral feeding to reduce aspiration pneumonia risk and for individuals with certain respiratory conditions to improve oxygenation and ventilation in Positional Obstructive Sleep Apnea (POSA) (Iannella, G., et al., 2022). [9]. This integrated activity tracking facilitates more efficient remote monitoring of the patient's status. The modification process is performed by retrofitting existing standard motor-driven bedframes with an external IoT-based sensor module. The head of bed elevation (HOBE) monitoring is achieved by retrofitting the existing mechanical structure of the motor-driven bedframe with an Inertial Measurement Unit (IMU) to capture angular orientation and acceleration data to monitor head of bed elevation and activity of the patient, respectively as shown in Figure 2. The sensor module is designed to be attached to the existing mechanical structure of a motor-driven bed frame as shown on the right of This section of the frame can elevate the patient up and down. In this study, MPU6050, a 6-axis sensor that integrates a 3-axis accelerometer and a 3-axis gyroscope on a single chip, is chosen. This combination allows it to measure both linear acceleration and angular velocity, providing comprehensive data about a device's movement Figure 3. and orientation in three dimensions. A key feature is its onboard Digital Motion Processor (DMP), which can handle complex sensor fusion algorithms, offloading processing tasks from the main microcontroller and providing more accurate orientation data, especially the calculation of the HOBE. This module uses a DC 24V from external power supply and the IMU communicates with an ESP8266 via an Inter-Integrated Circuit (I^2C) interface with a sampling time of 10 seconds.
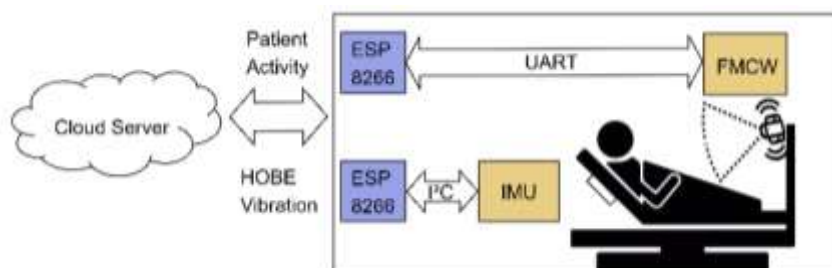

Figure 2 A framework of IoT-enabled hospital bed

Another module that tracks patient activity incorporates non-contact sensing technology to monitor patient discreetly without requiring wearables or direct contact. A non-contact monitoring system is less constrained by

monitoring conditions and accommodates long-term signal detection needs while minimizing discomfort from the detection process (Lv, He, Lin, & Miao, (2021) [10]. Here, A Frequency-Modulated Continuous-Wave (FMCW) radar sensor is chosen. The sensor transmits a continuous chirp signal of slope m during the signal's round trip to the target and back (τ), the received signal's frequency is offset from the frequency being transmitted at the moment of reception. This frequency difference is called the Doppler shift or beat frequency (f_b), and it is directly proportional to both the chirp slope and the time delay as $f_b = m \cdot \tau$. Since the time delay is also directly proportional to the target's range (R) and the speed of light (c), specifically $\tau = \frac{2R}{c}$, substituting this into the beat frequency equation reveals a direct relationship between the beat frequency and the target's range as $R = \frac{c \cdot f_b}{2m}$. Therefore, by measuring f_b, the sensor can detect the presence, position (such as sitting or lying, which affects range and angular position), and micro-movements of a patient on the bed. In this application the LD2420, which communicates via a Universal Asynchronous Receiver-Transmitter (UART) interface is chosen. The LD2420 is a 24GHz millimeter wave (mmWave) radar sensor module specifically designed for intelligent human body detection. Operating at 3.3V, this compact module offers a configurable detection range up to 8 meters, and 60° field of view. The sensor is integrated into ESP8266 with UART with a sampling time of 10 seconds. As shown on the left of Figure 3, the module is mounted on the bottom panel of the bed frame and operated with 24 V from external power supply.
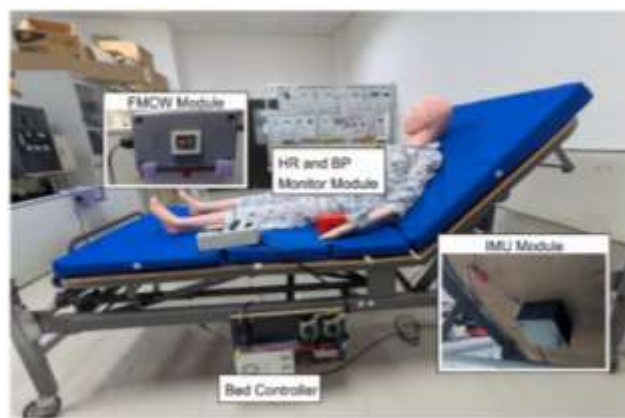

Figure3 A hospital motor-driven bed frame with IOT-enabled features

The second device focuses on enabling capabilities for a standard heart rate and blood pressure (HR and BP) monitor for IOT connectivity. This was achieved through the development of a custom embedded system prototype board (See Figure 4). The non-IoT HR and BP monitor underwent modification to interface with this newly designed board, allowing for the decoding of its communication protocol and data format. The board was specifically designed to communicate with the monitor's internal Inter Integrate Circuit (I²C) bus. By reverse engineering the monitor's hardware, the specific data fields representing HR, systolic BP, and diastolic BP readings were successfully identified. Operating in an I²C master configuration, the custom board initiates data requests and receives the raw physiological data from the monitor's internal controller, which is then transmitted to an ESP8266. Data handling and processing are executed after the successful acquisition of the HR and BP measurements. The original user interface of the monitor, including its physical buttons, remains operational. The combination of the custom-designed board and the ESP8266 thus forms a system that imbues the monitor with IoT functionality.
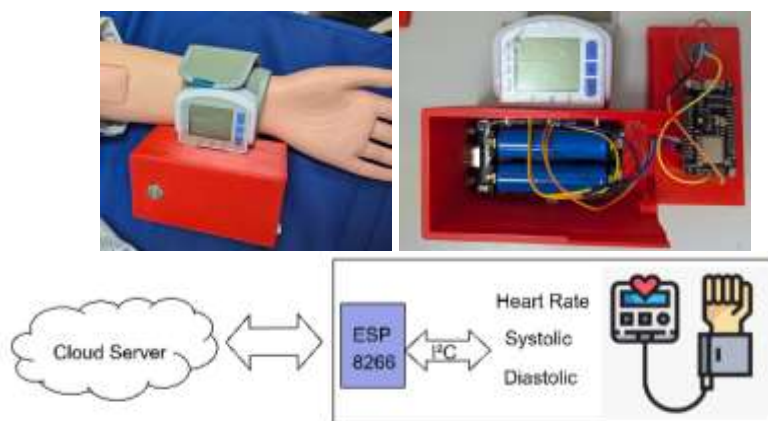

Figure 4 IoT-enabled blood pressure and heart rate monitor

3. Results and Discussion

3.1 Application Interface

The application interface shown in Figure 5 initiates with a secure login (top-left), requiring username and password, with a status indicator and a logout option. Upon successful login, the application presents a concise list of individuals currently being monitored. Each entry provides essential identification through Name and a unique ID. The accompanying Edit icon allows the authorized users to manage the profiles of these individuals, including updating assigned monitoring devices, or other relevant administrative details. This screen acts as a central hub for selecting a specific patient to access their real-time and historical health data transmitted from the connected IoT devices.

Selecting a patient from the list navigates the user to their dedicated profile screen, where Name and ID can be edited. The modifiable field represents monitored conditions such as "heart diseases," "kidney complications," or "stroke", can be checked or unchecked for each field for individual patients. Patient profiles can be appended with extra medical details and monitoring instructions via the "Add" button. Photos can be edited using icons. The lower section of Figure 5 presents specific connected IoT devices connected to specific patients. These tiles provide a direct interface for monitoring device status. The first icon (1) provides a more detailed view of the blood pressure and heart rate data. The second icon (2) indicates the status of the HOBE of the adjustable bed. The last icon (3) indicates whether the patient is detected in bed within the vicinity of a microwave motion sensor. Each of the data is labeled with date and timestamps. In addition, the data is stored in Google Sheets for a comprehensive record of each patient.
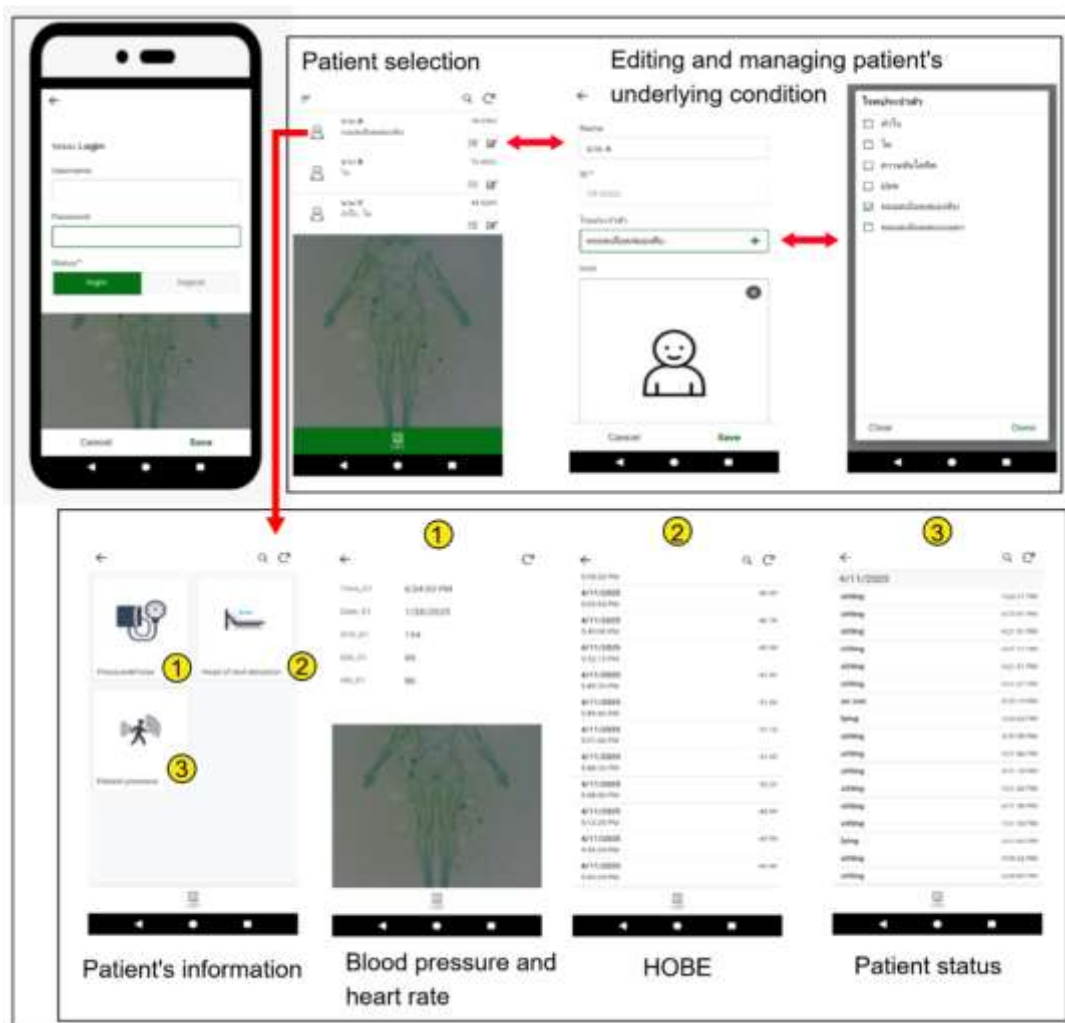

Figure 5 Application User Interface

3.2 Power Consumption Comparison

To assess the power consumption of both devices, the IOT is enabled and disabled to compare the current consumption Here Fluke 117 multimeter is used to measure the power consumption in each scenario. The IOT Bed device exhibits an idle power consumption of 1.09 W, which decreases to 0.86 W when its IOT functionality is disabled, indicating a power contribution from these smart features; notably, the FMCW component is the most significant power consumer, accounting for 63.6% of the total energy usage. Table 1 summarizes the electrical current

consumption of the second device, comparing both its non-IoT version and our modified IoT-enabled variant across different operational modes: *Idle*, *Pump*, *Measure*, and *Upload*. The data reveals a more nuanced picture. While the idle current is slightly higher for the IoT version, the active states (*Pump* and *Measure*) also show increased power consumption, suggesting that the integration of sensing, processing, and network connectivity concurrently demands more power.

Table 1 Current consumption of blood pressure and heart rate monitor

	Idle (A)	Pump (A)	Measure (A)	Upload (A)
Non-IOT	0	0.27	0.11	N/A
IOT	0.06	0.35	0.18	0.07

4. Conclusions

This paper details the development of an innovative IoT-based remote monitoring and alert system aimed at enhancing caregiver effectiveness through smart sensors, Google Cloud connectivity, and a user-friendly mobile application prototype providing real-time data visualization and differentiated access. The system integrates a retrofitted smart bed that includes monitoring movement, head of bed elevation, and status of the patient. The system also enables the IoT capabilities of a digitized blood pressure and heart rate monitor. Both devices can transmit the data wirelessly to the cloud database and ultimately the application. The power consumption analysis reveals an energy overhead associated with IoT enablement in both devices during data transmission and active operation compared to their traditional counterparts, offering foundational insights into the power implications of IoT integration for remote patient monitoring. Power consumption analysis revealed that enabling IoT features increases the power usage of both tested devices. The bed's idle power consumption rose from 0.86 W to 1.09 W, with the FMCW component accounting for a significant 63.6% of its energy usage. For the second device, integrating IoT resulted in higher current consumption not only in idle but also during active Pump and Measure states, indicating that concurrent sensing, processing, and network connectivity demand more power. These two devices are integrated into the system, enabling compatibility with additional IoT medical devices in the future.

5. Acknowledgements

6. References

Tantirat, P., Suphanchaimat, R., Rattanathumsakul, T., & Noree, T. (2020). Projection of the number of elderly in different health states in Thailand in the next ten years, 2020–2030. *International Journal of Environmental Research and Public Health, 17*(22), 8703.

Malasinghe, L. P., Ramzan, N., & Dahal, K. (2019). Remote patient monitoring: A comprehensive study. *Journal of Ambient Intelligence and Humanized Computing, 10*(1), 57–76. https://doi.org/10.1007/s12652-017-0598-x

Chakravarty, S. (2022). Resource constrained innovation in a technology intensive sector: Frugal medical devices from manufacturing firms in South Africa. *Technovation, 112*, 102397. https://doi.org/10.1016/j.technovation.2021.102397

Kane, G. M., Bakker, C. A., & Balkenende, A. R. (2018). Towards design strategies for circular medical products. *Resources, Conservation and Recycling, 135*, 38–47. https://doi.org/10.1016/j.resconrec.2017.07.030

Ferreira, J. (2014). *Google Apps Script: Web application development essentials*. O'Reilly Media, Inc.

Hassan, M. K., Mohd Rusli, M. H., & Mohd Salleh, N. A. (2023). Development of an order processing system using Google Sheets and Appsheet for a Malaysian automotive SME factory warehouse. *Journal of Mechanical Engineering (JMechE), 20*(3), 63–81.

Kurniawan, A., Wardani, K., & Zaki Hamidi, E. A. (2023, July). Cloud based daily periodic inspection Dozer Komatsu D31P using Google Appsheet development platform. In *2023 9th International Conference on Wireless and Telematics (ICWT)* (pp. 1–5). https://doi.org/10.1109/ICWT58823.2023.10335457

Pietrangeli, I., Mazzuto, G., Ciarapica, F. E., & Bevilacqua, M. (2023). Smart retrofit: An innovative and sustainable solution. *Machines, 11*(5), 523. https://doi.org/10.3390/machines11050523

Iannella, G., et al. (2022). Head-of-bed elevation (HOBE) for improving positional obstructive sleep apnea (POSA): An experimental study. *Journal of Clinical Medicine, 11*(19), 5620. https://doi.org/10.3390/jcm11195620

Lv, W., He, W., Lin, X., & Miao, J. (2021). Non-contact monitoring of human vital signs using FMCW millimeter wave radar in the 120 GHz band. *Sensors, 21*(8), 2732. https://doi.org/10.3390/s21082732

Herbal Sheet-Free Peel-off Facial Mask Development from Cissampelos spp. Leaf Powder

Wiphada   Temram[a], Araya Ranok[a], Chanida Kupradit[a],
Chompoonuch Khongla[a], Sumalee Musika[a], Seksan Mangkalanan[a,*]

*[a] Department of Applied Biology, Faculty of Science and Liberal Arts, Rajamangala University of Technology Isan,
Nakhon Ratchasima, 30000 Thailand*
*Corresponding author. Tel.: 044233000 ext. 4340; E-mail address: sek.mangkalanan@gmail.com

Abstract

This study aimed to determine the optimal formulation ratio of a herbal facial mask powder derived from *Cissampelos* spp. leaves, eliminating the necessity for a sheet mask. The formulation incorporated turmeric (*Curcuma longa*), mulberry twigs (*Morus alba*), and silk cocoon extracts as active ingredients, with an additional objective of evaluating the cosmeceutical properties of the mask. The findings indicated that the most suitable ratio for mask formation was 1:15 (powder to water). Antioxidant activity was assessed using the ABTS and FRAP assays. Turmeric extract at concentrations of 50 and 100 mg/mL exhibited the highest antioxidant capacity, yielding values of $2{,}733.79 \pm 10.97$ and $2{,}764.09 \pm 16.97$ Trolox mM eq./g extract for ABTS, while FRAP activity was recorded at 331.65 ± 0.02 and 386.50 ± 0.01 Trolox mM eq./g extract, respectively. Regarding tyrosinase inhibition, crude mulberry twig extract at 25 mg/mL demonstrated the highest inhibitory effect, with $51.96 \pm 0.01\%$ inhibition. A comparative evaluation of four mask formulations, based on moisture content analysis, revealed that the F4 (control) exhibited the highest moisture percentage at $26.67 \pm 0.05\%$. Additionally, the F1 (turmeric extract) demonstrated the strongest antioxidant properties, yielding ABTS and FRAP values of $4{,}777.12 \pm 0.03$ and $3{,}633.75 \pm 0.22$ Trolox mM eq./g extract, respectively. Conversely, the F2 (mulberry twig extract) exhibited the highest tyrosinase inhibition at $58.87 \pm 0.45\%$ inhibition. Sensory evaluation of cosmeceutical attributes indicated no significant differences among the herbal mask formulations. Clinical testing further revealed that the F1 (turmeric extract) effectively reduced the number of fine lines by 11.00 ± 0.20 lines.

Keywords: Cissampelos spp, Facial Mask, Gelling agent, Pectin

1. Introduction

Facial masks represent an integral component of skincare formulations, designed to address hydration, exfoliation, and a range of dermatological concerns. These masks exist in various forms, including clay masks, sheet masks, gel-based masks, and peel-off masks, each offering distinct functional advantages. This study aimed to develop a novel non-fabric facial mask formulation that integrated multiple mask types into a single product, utilizing *Cissampelos spp.* leaf powder as the primary gelling agent to optimize texture and stability.

Cissampelos spp., a member of the Menispermaceae family, is a climbing plant characterized by simple, heart-shaped leaves with an acuminate apex and closed-base structure. The leaf margins are smooth, featuring stiff trichomes, and the plant produces flowers in clustered formations. This species is predominantly found in northeastern Thailand, where it has been traditionally utilized for medicinal purposes. Ethnobotanical surveys indicate that various parts of *Cissampelos spp.* have been employed in traditional healing practices. Specifically, the leaves are used as a topical treatment for dermatological conditions, whereas the stems are applied to alleviate fever toxicity and enhance female blood circulation (Peng-ngummuang, Jansuta, Sangdech, & Somkhow, 2019). Thai ethnobotanical knowledge classifies *Cissampelos spp.* into two primary domains: food and medicinal uses. In northeastern Thai cuisine, the plant is incorporated into traditional dishes such as *Lap Krung Khamoa* (spiced minced meat salad). Beyond its culinary applications, *Cissampelos spp.* has been explored for industrial and agricultural purposes, functioning as a gelling agent in *Cissampelos spp.* derived jelly formulations and various processed food products. Additionally, its cosmeceutical potential has facilitated its integration into herbal facial mask formulations that leverage natural botanical ingredients.

Due to its high pectin content, particularly low-methoxyl pectin with thermoirreversible properties, *Cissampelos spp.* enables gel formation without requiring thermal activation. This study proposes a non-sheet facial mask formulation incorporating *Cissampelos pareira* leaf powder in conjunction with Thai herbal ingredients recognized for their dermatological benefits, including turmeric (*Curcuma longa*), mulberry twigs (*Morus alba*), and silk cocoons. The cosmeceutical efficacy of this formulation is evaluated based on its functional properties in skincare applications. Prior investigations have explored the use of *Cissampelos spp.* in jelly production. Chunthanom et al. (2013) (Chunthanom, Somboon, Sakulkoo, & Sihamala, 2013) reported that aqueous extracts derived from its leaves contributed to traditional Thai desserts such as *Wun Khreu Manoi*, a soft gelatinous confection. The yield and quality of pectin extracted from *Cissampelos spp.* are significantly influenced by the employed extraction methods, which in turn affect the jelly's textural attributes. Further studies by Boonvoraphat (2017) (Boonvoraphat, 2017) identified nutritional and medicinal properties associated with this species, including detoxification, fever reduction, gastrointestinal relief, and the absorption of toxins resulting from microbial digestion or residual contaminants. Tebumroong (2003) (Tebumroong, 2003) quantified pectin content in *Cissampelos spp.* leaves, estimating a yield of approximately 30% by weight. Given its extensive ethnobotanical applications, research continues to explore its value-added processing within food and cosmeceutical sectors. The commercial fruit jam industry has experienced significant expansion, attracting consumers across multiple demographic groups. Most fruit jams consist of puréed or

processed fruits blended with sugar or alternative sweeteners, producing a semi-solid gel suitable for consumption. Concurrently, the herbal-based product industry—including functional foods, dietary supplements, and cosmeceuticals—has witnessed substantial growth.

Cissampelos spp. leaves contain approximately 30% pectin, predominantly of the low-methoxyl variety, which exhibits the ability to form gels in cold water without requiring acid or sugar. This characteristic has contributed to its application in food product development as well as cosmeceutical formulations. Beyond its culinary significance, *Cissampelos spp.* has been integrated into skincare products due to its high pectin content, which facilitates enhanced skin hydration, improved texture, and a cooling effect that soothes the skin (Pranakhon, Sombun, Saithi, Phueakchroey, & Pongnarathorn, 2005). These properties substantiate its inclusion in herbal facial mask formulations and broader cosmeceutical preparations. This study proposed the development of a non-sheet peel-off facial mask formulation incorporating *Cissampelos spp.* leaf powder. The formulation integrates Thai herbal ingredients recognized for their dermatological benefits, including turmeric (*Curcuma longa*), mulberry twigs (*Morus alba*), and silk cocoons extracts. The cosmeceutical efficacy of the *Cissampelos spp.*-based mask was further assessed to determine its functional properties in skincare applications.

2. Methodology

2.1 Crude Extract Preparation and Drying Process for Herbal Ingredients

The extraction procedure began with the cleaning of turmeric (*Curcuma longa*), and mulberry twigs (*Morus alba*) to remove contaminants and residual debris. Following the cleaning process, the plant materials were subjected to hot-air oven drying at 50°C for 3 days until complete dehydration was achieved. Once dried, the samples were finely ground using a pulverizer to enhance extractability and increase surface area exposure during the extraction process. For bioactive compound extraction, 95% ethanol was utilized as the extraction medium. Each sample—turmeric and mulberry—was weighed at 5 g per 100 mL ethanol and subjected to overnight maceration in a shaking incubator at ambient temperature. This process facilitated the diffusion of bioactive compounds into the solvent. The resulting extracts were subsequently filtered through Whatman No.1 filter paper using vacuum filtration to remove insoluble residues, followed by solvent evaporation using a rotary evaporator at 45°C under a pressure range of 350–500 Pa. This concentration step ensured maximum yield of the bioactive constituents. The final concentrated extracts were reconstituted in 95% ethanol for bioactivity evaluation, while a portion of the dried extract powder was integrated into the development of herbal facial mask formulations. For silk cocoon extraction, cleaned silk cocoons were boiled for 1 hour to release silk proteins into the aqueous medium. The extraction liquid (boiling water) was then collected and subjected to oven drying at 50°C for 3 days to remove excess moisture. Once fully dehydrated, the dried silk protein extract was finely powdered and combined with pulverized *Cissampelos* spp. leaf powder for final incorporation into the herbal facial mask formulation. This methodological approach ensured optimal retention of bioactive compounds, preserving their functional properties for cosmeceutical applications. Additionally, the drying and extraction conditions were carefully controlled to maintain extract stability, facilitating their use in advanced skincare formulations.

2.2 Mask Formation Period and Peel-off Ability Rate Assessment of Cissampelos spp. Leaf Mask Powder

The experiment commenced with the cleaning of *Cissampelos* spp. leaves, followed by hot-air oven drying at 50°C for 3 days until complete dehydration was achieved. The dried leaves were then finely ground into powder using a pulverizer and subsequently blended with silk extract powder at a 1% concentration (by weight) to develop the herbal mask powder. To investigate the mask formation period and peel-off ability, the mask powder was mixed with water at varying ratios (1:5, 1:10, 1:15, 1:20, and 1:25). The mixtures were observed for gelation and sheet formation, with the time required for the development of a gel-like consistency and its ability to be peeled off as a mask sheet recorded for comparative analysis.

2.3 Antioxidant Activity Evaluation

ABTS Radical Scavenging Activity Assay

Antioxidant activity was assessed using a modified method by Re et al. (1999) (Re et al., 1999). The ABTS radical solution was prepared by mixing 7 mM ABTS with 2.5 mM potassium persulfate (KPS) at a 2:1 ratio. The mixture was then incubated for 12 hours to allow radical generation, ensuring the stability of the ABTS radical solution for subsequent analysis. Turmeric (*Curcuma longa*) extract was diluted and adjusted to an absorbance of 0.700 ± 0.020 at 734 nm. The extract was prepared at concentrations of 0.19, 0.39, 0.78, 1.56, 3.12, 6.25, 12.5, 25, 50, and 100 mg/mL, ensuring a broad concentration range for effective antioxidant assessment. A 20 µL sample of the turmeric extract solution was mixed with 1,980 µL of ABTS working solution and incubated for 5 minutes in the dark to prevent photodegradation of radical species. The absorbance of the mixture was then measured using a spectrophotometer at 734 nm. The absorbance (OD values) obtained from the spectrophotometric analysis was used to calculate the Trolox equivalent antioxidant capacity (mM Trolox eq.), based on a standard calibration curve. This quantitative assessment provided insights into the scavenging potential of turmeric extract against ABTS radicals, supporting its efficacy in antioxidant applications.

2.4 Ferric Reducing Antioxidant Power (FRAP) Assay

The FRAP assay, adapted from Kubola and Siriamornpun (2008) (Kubola & Siriamornpun, 2008), was performed to evaluate the ferric-reducing antioxidant capacity of turmeric (*Curcuma longa*) extract. The assay measures the ability of antioxidants to reduce ferric ions (Fe^{3+}) to ferrous ions (Fe^{2+}), correlating with the antioxidant

potential of the sample. Turmeric extract samples were prepared at concentrations of 0.19, 0.39, 0.78, 1.56, 3.12, 6.25, 12.5, 25, 50, and 100 mg/mL to establish a comprehensive concentration range for assessment. A 100 µL aliquot of each turmeric extract solution was transferred into a test tube, ensuring precise quantification for comparative analysis. Following sample preparation, 1,000 µL of FRAP working solution was added to each test tube containing the turmeric extract. The reaction mixture was incubated at 37°C for 15 minutes, allowing sufficient time for the reduction of ferric-TPTZ (tripyridyltriazine) complexes and the subsequent development of a measurable color change. After incubation, absorbance was recorded at 595 nm using a spectrophotometer to quantify the reduction of ferric ions. The absorbance values obtained were compared against a Trolox standard curve, with results expressed in millimolar Trolox equivalents (mM Trolox eq.), indicating the antioxidant strength of turmeric extract relative to the standard antioxidant compound.

2.5 Tyrosinase Inhibition Assay for Mulberry Twig Extract

The tyrosinase inhibition activity was assessed using a modified method based on Saewan et al. (2011) (Saewan, Koysomboon, & Chantrapromma, 2011). The assay evaluates the inhibitory effects of *mulberry* twig extract on tyrosinase enzyme activity, which plays a critical role in melanin synthesis. The reaction mixture was prepared by adding 180 µL of 0.1 M sodium phosphate buffer (pH 6.8) to a test tube, followed by the addition of 10 µL of 2.5 mol/L L-DOPA, a substrate for tyrosinase enzyme-catalyzed oxidation reactions. Mulberry twig (*Morus alba*) extract was prepared at varying concentrations (0.19, 0.39, 0.78, 1.56, 3.12, 6.25, 12.5, 25, 50, and 100 mg/mL). A 10 µL aliquot of each extract concentration was introduced into the reaction system. Subsequently, 10 µL of tyrosinase enzyme (138 units) was added, and the mixture was incubated for 15 minutes, allowing enzymatic conversion of L-DOPA into dopachrome. The formation of dopachrome, the oxidation product, was measured using a spectrophotometer at 475 nm. The percentage inhibition of tyrosinase activity was calculated using the following equation:

$$\%\text{Tyrosinase inhibition} = \frac{[A-(B-C)]}{A} \times 100$$

Where:

- **A** = Absorbance of the control sample (without test extract)
- **B** = Absorbance of the test sample (with tyrosinase enzyme)
- **C** = Absorbance of the test sample (without tyrosinase enzyme)

The percentage of tyrosinase inhibition values obtained from the spectrophotometric analysis was used to construct a standard inhibition curve. This curve facilitated the determination of IC_{50}, which represents the extract concentration required to achieve 50% inhibition of tyrosinase activity. To ensure accurate comparative analysis, standard compounds (kojic acid) were included as reference controls. These controls provided a benchmark for evaluating the tyrosinase inhibition efficacy of *Morus alba* extract relative to known inhibitors. The calculated IC_{50} value served as a quantitative indicator of the extract's potency in suppressing tyrosinase activity, supporting its potential application in cosmeceutical formulations targeting melanin regulation and skin brightening.

2.6 Development of a Herbal Facial Mask Formulation Based on Cissampelos spp.

The formulation process involved the integration of herbal extracts into the mask powder, specifically turmeric (*Curcuma longa*) and mulberry twig (*Morus alba*) extracts at optimized concentrations. These extracts had previously undergone antioxidant activity and tyrosinase inhibition testing to confirm their efficacy in skincare applications. The selected herbal components were blended in precise ratios to achieve the desired functional and cosmetic properties in the facial mask formulation. Careful adjustment of extract concentrations ensured optimal bioactivity while maintaining stability and usability into four formulations including:

- **F1:** Herbal mask powder blended with turmeric (*Curcuma longa*) extract (5.88% by weight)
- **F2:** Herbal mask powder blended with mulberry twig (*Morus alba*) extract (3.03% by weight)
- **F3:** Herbal mask powder blended with a combination of turmeric (5.88% by weight) and mulberry twig (3.03% by weight) extracts
- **F4 (Control):** Base herbal mask powder without additional extracts

Following initial formulation, the mask underwent further antioxidant and tyrosinase inhibition assays utilizing established methodologies to validate its cosmeceutical potential. These assessments provided critical insights into the formulation's effectiveness, supporting its application in skincare product development.

2.7 Moisture Release assessment of Herbal Facial Mask Formulation Based on Cissampelos spp.

The hydrated mask formulation (mask: water = 1: 15) was poured onto circular filter paper (1-inch diameter) and allowed to solidify into a gel. Upon complete setting, the mask was peeled off, and the filter paper was weighed to quantify the moisture released from the mask formulation. This assessment provided insights into the hydration retention capacity of the mask gels, contributing to the optimization of formulation stability and efficacy.

2.8 Sensory Evaluation of Cosmeceutical Properties

The sensory evaluation of herbal facial mask formulations was conducted to assess key attributes, including gel formation time, color, fragrance, hydration levels, and overall user preference from 30 untrained panelists. A structured approach was employed to ensure consistency and accuracy in data collection. The assessment was performed using the 9-point hedonic scale, which provided a quantitative measure of user satisfaction across multiple

sensory attributes. The evaluations facilitated a comparative analysis of four distinct mask formulations. Each formulation was systematically evaluated to determine variations in sensory attributes and consumer preference. The results provided insights into formulation effectiveness, supporting further optimization of cosmeceutical applications.

2.9 Clinical Testing Procedure

A skin compatibility and wrinkle reduction study were conducted using five human test participants with Certificate of Exemption from Human Research Ethics Committee, Rajamangala University of Technology Isan Project Code: HEC-01-67-061. Each subject applied all four mask formulations to the forearm for a duration of 30 minutes. To assess cosmetic efficacy and potential adverse reactions, daily photographs were taken to monitor skin conditions over an 18-day evaluation period under stereomicroscope SMZ745 (Nikon).

2.10 Statistical Analysis

Experimental results were analyzed using one-way ANOVA to determine significant differences between formulations, followed by Duncan's Multiple Range Test (DMRT) for post-hoc comparisons. Statistical computations were performed using statistical analysis software, with data expressed as mean ± standard deviation (SD) at a significance level of $p < 0.05$. Each experimental trial was replicated at least three times to ensure the reliability and validity of the findings.

3. Results and Discussion

3.1 Mask Formation Period and Peel-off Ability of Cissampelos spp. Leaf Powder Mask

The optimal powder-to-water ratio for mask formation was determined to achieve desirable gelation and peeling properties. The findings indicated that a ratio of 1:15 was the most suitable, yielding a gelation time of 9.67 ± 0.58 seconds and a peel-off duration of 30.33 ± 6.79 minutes. The second-most effective ratio, 1:10, resulted in gelation within 10.00 ± 1.00 seconds and peel-off within 36.33 ± 5.43 minutes. At a ratio of 1:20, gelation was observed at 26.00 ± 1.00 seconds, with a peel-off time of 42.00 ± 3.61 minutes. The gel-like consistency of the formed mask sheets was attributed to the presence of low-methoxyl pectin in Cissampelos spp. leaves, which exhibited thermoirreversible gelation properties (Ratri Pranakorn & Parinda Kaengkhan, 2005). A summary of these results was provided in Table 1 and Figure 1. Conversely, the powder-to-water ratios of 1:5 and 1:25 did not yield viable masks. The 1:5 ratio resulted in excessive clumping due to inadequate water volume, preventing successful gelation. In contrast, the 1:25 ratio produced an excessively liquid consistency, inhibiting the formation of a cohesive gel sheet. These findings highlighted the critical role of precise formulation ratios in optimizing the textural and functional properties of cosmeceutical applications.

Table 1 Mask Formation and Peeling Properties

Mask-to-Water Ratio (g/mL)	Gelation Time (s)	Peel-Off Duration (min)	Mask Formation Ability	Formation Characteristics
1:5	14.67 ± 0.58	-	Not formable	Mask powder clumped together
1:10	10.00 ± 1.00	36.33 ± 5.43	Formable	Mask formed successfully and could be peeled off
1:15	9.67 ± 0.58	30.33 ± 6.79	Rapid formation	Mask formed quickly and could be peeled off effectively
1:20	26.00 ± 1.00	42.00 ± 3.61	Formable	Mask formed successfully and could be peeled off
1:25	43.33 ± 1.53	-	Not formable	Mask powder remained liquid and could not form a cohesive sheet

Note: (-) Indicates that the mask could not be peeled off as a cohesive sheet.

Figure 1 Mask formation ability of *Cissampelos* spp. Leaf Powder Mask
A=1:5; B =1:10; C=1:15; D=1:20; E=1:25.

3.2 Antioxidant Activity Analysis of Turmeric Extract Using ABTS Assay

The antioxidant properties of turmeric (*Curcuma longa*) extract were evaluated using the ABTS assay. The results demonstrated that the 50 mg/ml and 100 mg/mL concentration exhibited the highest antioxidant capacity, quantified at 2,733.79 ± 10.97 and 2,764.09 ± 16.97 mM Trolox eq./g extract, respectively. This strong radical-scavenging activity was attributed to the high extract concentration. However, statistical analysis indicated no significant difference between the 100 mg/mL and 50 mg/mL concentrations, as presented in Table 3. The ABTS radical scavenging activity was assessed using Trolox as the reference standard, with turmeric extract tested at concentrations ranging from 0.19–100 mg/mL. The findings revealed a positive correlation between extract concentration and antioxidant capacity, as illustrated in Figure 4.3. The 100 mg/mL crude turmeric extract exhibited the highest ABTS radical scavenging activity, quantified at 2764.09 ± 16.97 mM Trolox eq./g extract. The second-

highest antioxidant activity was observed at 50 mg/mL, yielding 2733.79 ± 10.97 mM Trolox eq./g extract. The antioxidant capacity progressively declined at lower concentrations, with recorded values for 25.00, 12.50, 6.25, 3.12, 1.56, 0.78, 0.39, and 0.19 mg/mL, respectively. These findings highlighted the dose-dependent antioxidant potential of turmeric extract, reinforcing its applicability in functional food and cosmeceutical formulations.

Table 2 Antioxidant Properties Assessed by the ABTS Assay

No.	Crude Extract Concentration (mg/mL)	Trolox Equivalent Concentration (mM)
1	0.19	26.90 ± 0.16[a]
2	0.39	27.08 ± 0.18[a]
3	0.78	27.46 ± 0.38[a]
4	1.56	27.86 ± 0.21[a]
5	3.12	28.49 ± 0.34[a]
6	6.25	272.94 ± 0.24[b]
7	12.50	275.69 ± 1.65[b]
8	25.00	282.15 ± 2.36[b]
9	50.00	2,733.79 ± 10.97[c]
10	100.00	2,764.09 ± 16.97[c]

Note: Different lowercase letters in the same column indicate statistically significant differences.
Ferric Reducing Antioxidant Power (FRAP) Assay for Turmeric Extract

The FRAP assay was conducted to evaluate the ferric-reducing antioxidant potential of crude turmeric (*Curcuma longa*) extract at various concentrations. The results indicated that the highest ferric-reducing capacity was observed at 100 mg/mL, yielding 336.50±0.01 mM Trolox eq./g extract. The effectiveness of FRAP activity was directly correlated with extract concentration, where higher turmeric extract concentrations resulted in greater ferric-reducing capability, as presented in Table 3. The findings confirmed that the 100 mg/mL extract exhibited the strongest FRAP activity, followed by the 50 mg/mL extract, which yielded 331.65 ± 0.02 mM Trolox eq./g extract. The antioxidant potential progressively declined at lower concentrations, with recorded values for 25.00, 12.50, 6.25, 3.12, 1.56, 0.78, 0.39, and 0.19 mg/mL, respectively. These findings reinforced the dose-dependent ferric-reducing potential of turmeric extract, supporting its relevance in antioxidant-enriched formulations for cosmeceutical and nutraceutical applications.

Table 3 Ferric Reducing Antioxidant Power (FRAP)

No.	Crude Extract Concentration (mg/mL)	Trolox Equivalent Concentration (mM)
1	0.19	8.65 ± 0.03a
2	0.39	11.05 ± 0.02ab
3	0.78	12.58 ± 0.01bc
4	1.56	53.00 ± 0.05c
5	3.12	64.81 ± 0.06c
6	6.25	163.92 ± 0.02d
7	12.50	239.87 ± 0.06e
8	25.00	321.10 ± 0.11f
9	50.00	331.65 ± 0.02g
10	100.00	336.50 ± 0.01g

Note: Different lowercase letters in the same column indicate statistically significant differences.

3.3 Tyrosinase Inhibition Assay for Mulberry Twig Extract
The tyrosinase inhibition activity of mulberry twig (*Morus alba*) extract was evaluated at concentrations ranging from 0.19–100 mg/mL. The results indicated that the highest tyrosinase inhibition was observed at 25 mg/mL, yielding an inhibition rate of 51.96 ± 0.01%. The effectiveness of tyrosinase inhibition at higher concentrations (50 mg/mL and 100 mg/mL) was reduced. Consequently, the optimal inhibition was achieved at 25 mg/mL, followed by decreasing inhibitory effects at 50, 100, 12.5, 6.25, 3.12, 1.56, 0.78, 0.39, and 0.19 mg/mL, respectively. These findings, as presented in Table 4 highlighted the concentration-dependent inhibitory effects of mulberry twig extract, with potential implications for cosmeceutical applications in skin brightening formulations.

Table 4 Tyrosinase Inhibition Properties of Mulberry Twig Extract

No.	Crude Extract Concentration (mg/mL)	% Tyrosinase Inhibition
1	0.19	11.31 ± 0.02a
2	0.39	15.94 ± 0.02b
3	0.78	18.33 ± 0.02c
4	1.56	22.36 ± 0.01d
5	3.12	28.17 ± 0.02e
6	6.25	31.20 ± 0.01f
7	12.50	40.39 ± 0.02g
8	25.00	51.96 ± 0.01i
9	50.00	43.52 ± 0.02h
10	100.00	40.41 ± 0.01g

Note: Different lowercase letters in the same column indicate statistically significant differences.

3.4 Development of a Herbal Facial Mask Formulation Based on Cissampelos *spp.*

Moisture Release Rate Assessment in Cissampelos spp. Facial Mask

The study examined the moisture release rate of *Cissampelos* spp. based facial mask formulations using an initial mask powder quantity of 0.3 g and a water volume of 4.5 g. The results indicated that the F4 (control) mask formulation exhibited the highest moisture content at $26.67 \pm 0.06\%$, followed by F1 (Turmeric) mask: $22.92 \pm 0.05\%$, F3 (Turmeric and mulberry twig) mask: $20.83 \pm 0.02\%$ and F2 (Mulberry twig) mask: $20.00 \pm 0.04\%$. These findings, as presented in Table 5, demonstrated variations in moisture retention properties across different formulations, which influenced their potential hydrating effects in cosmeceutical applications. The mean moisture content values differ significantly among the formulations, demonstrating a statistically meaningful variation in hydration retention across different mask compositions.

Table 5 Moisture Release Rate of Cissampelos spp. Facial Masks

Formulation	Herbal Extract	Moisture Content (%)
F1	Turmeric	22.92 ± 0.06^b
F2	Mulberry Twig	20.00 ± 0.04^a
F3	Turmeric + Mulberry Twig	20.83 ± 0.02^a
F4	Control	26.67 ± 0.05^c

Note: Different lowercase letters in the same column indicate statistically significant differences.

3.5 Antioxidant Properties (ABTS and FRAP Assays)

The antioxidant activity of the four herbal facial mask formulations was evaluated using the ABTS and FRAP methods. The results indicated that the turmeric-based mask formulation (F1) exhibited the highest antioxidant activity, yielding $4,777.12 \pm 0.03$ mM Trolox eq./g extract (ABTS assay) and $3,633.75 \pm 0.22$ mM Trolox eq./g extract (FRAP assay). This strong antioxidant capacity was likely attributed to the presence of curcumin, the primary bioactive polyphenol in turmeric (*Curcuma longa*), which exhibited lipophilic antioxidant properties. These findings aligned with the research conducted by (Jurenka, 2009), which demonstrated curcumin's efficacy in wound healing and oxidative stress reduction. The second-highest antioxidant activity was observed in the turmeric–mulberry twig (F3) blend, followed by the control formulation (F4), while the mulberry twig-based mask (F2) exhibited the lowest antioxidant activity. These results were presented in Table 6.

3.6 Tyrosinase Inhibition Activity

The ability of each formulation to inhibit tyrosinase enzyme activity, which is associated with skin pigmentation regulation, was assessed. The results indicated that the mulberry twig-based mask (F2) exhibited the highest tyrosinase inhibition, with an inhibition rate of $58.87 \pm 0.45\%$. The second-best formulation was the turmeric–mulberry twig blend (F3), followed by the turmeric-based mask (F1), while the control formulation (F1) exhibited the lowest inhibitory activity. These findings were presented in Table 6. These results highlighted the potential of turmeric and mulberry extracts in antioxidant-rich and skin-brightening cosmeceutical applications.

Table 6 Biological Activity of Cissampelos *spp.* Based Herbal Facial Mask Formulations

Formulation	Herbal Extract	ABTS Trolox (mM/g Extract)	FRAP Trolox (mM/g Extract)	Tyrosinase Inhibition (%)
F1	Turmeric	$4777.12 \pm 0.03c$	$3633.75 \pm 0.22d$	$37.47 \pm 0.03b$
F2	Mulberry Twig	$1160.31 \pm 0.04a$	$3115.25 \pm 0.61a$	$58.87 \pm 0.45d$
F3	Turmeric + Mulberry Twig	$2361.83 \pm 0.16b$	$3508.69 \pm 0.06c$	$45.60 \pm 0.60c$
F4	Control	$1162.78 \pm 0.03a$	$3272.33 \pm 0.14b$	$18.60 \pm 0.06a$

Note: Different lowercase letters in the same column indicate statistically significant differences.

3.7 Sensory Evaluation of Cosmeceutical Properties

The sensory evaluation of the four herbal facial mask formulations was conducted using the 9-point hedonic scale, where 1 represented the lowest preference ("disliked the most") and 9 represented the highest preference ("liked the most"). The study involved 30 participants, who assessed the formulations based on appearance, color, fragrance, hydration, and overall preference. The results indicated that no statistically significant differences ($p \geq 0.05$) were observed among the four formulations in terms of sensory attributes, with participants generally rating their preference at approximately level 7, indicating a moderate liking for all formulations. These findings suggested that the inclusion of turmeric (F1, F3)) and mulberry twig (F2, F3) extracts in the mask formulation did not significantly alter sensory perception compared to the base mask formulation (F4) without additional herbal extracts. The data supporting this conclusion was presented in Table 7.

Table 7 Sensory Evaluation of Cosmeceutical Properties

Attribute	Formulation			
	F1: Turmeric	F2: Mulberry Twig	F3: Turmeric + Mulberry Twig	F4: Control
Appearance [NS]	7.23 ± 1.30	6.73 ± 1.86	7.53 ± 1.33	7.23 ± 1.22
Color [NS]	7.23 ± 1.22	6.87 ± 1.43	7.60 ± 1.33	7.27 ± 1.39
Fragrance [NS]	6.80 ± 1.86	6.87 ± 1.76	6.70 ± 1.92	6.97 ± 1.52
Hydration [NS]	7.43 ± 1.25	7.43 ± 1.25	7.30 ± 1.18	7.60 ± 1.25
Overall Preference [NS]	7.33 ± 1.09	7.40 ± 1.33	7.43 ± 1.25	7.57 ± 0.97

Note: NS = non-significant, indicating no statistically significant differences among formulations

3.8 Clinical Testing of Facial Mask Formulations

The clinical evaluation was conducted on five individuals selected for direct application tests. Each participant underwent facial mask application on the forearm for 30 minutes, with trials performed every three days over six sessions, totaling 18 days of observation. After each application, photographs of wrinkle patterns were taken 30 minutes post-mask removal, allowing for comparative analysis across treatment sessions. According to the findings presented in Table 8, the turmeric-based mask (F1) formulation demonstrated the most significant wrinkle reduction by day 18, with wrinkles reduced by 11.00 ± 0.20 lines. The second-best formulation, the turmeric–mulberry twig blend (F2), resulted in a wrinkle reduction of 9.80 ± 0.82 lines. The mulberry twig-based mask (F3) exhibited a moderate reduction of 3.60 ± 0.65 lines, whereas the control formulation displayed the least effect, reducing wrinkles by 1.80 ± 0.37 lines. These results suggested that turmeric extract contributed substantially to skin rejuvenation and wrinkle reduction, reinforcing its potential application in cosmeceutical formulations.

Following the third application, two test participants reported noticeable skin lightening effects in areas where the mulberry twig-based mask had been applied. After washing off the mask, the pigment intensity appeared to have diminished, resulting in visibly brighter skin, as documented in Figure 2. This finding aligned with the research conducted by Wang et al. (2013) (Wang, Xiang, Wang, Tang, & He, 2013), which examined the bioactive properties of mulberry twigs and leaves. Their study demonstrated that mulberry extracts exhibited tyrosinase inhibition activity, effectively blocking melanin synthesis and contributing to skin brightening effects. These results suggested that the mulberry-based facial mask formulation could serve as a potential cosmeceutical product for pigmentation regulation and skin tone enhancement.

Table 8: Reduction in Wrinkle Count During Clinical Testing

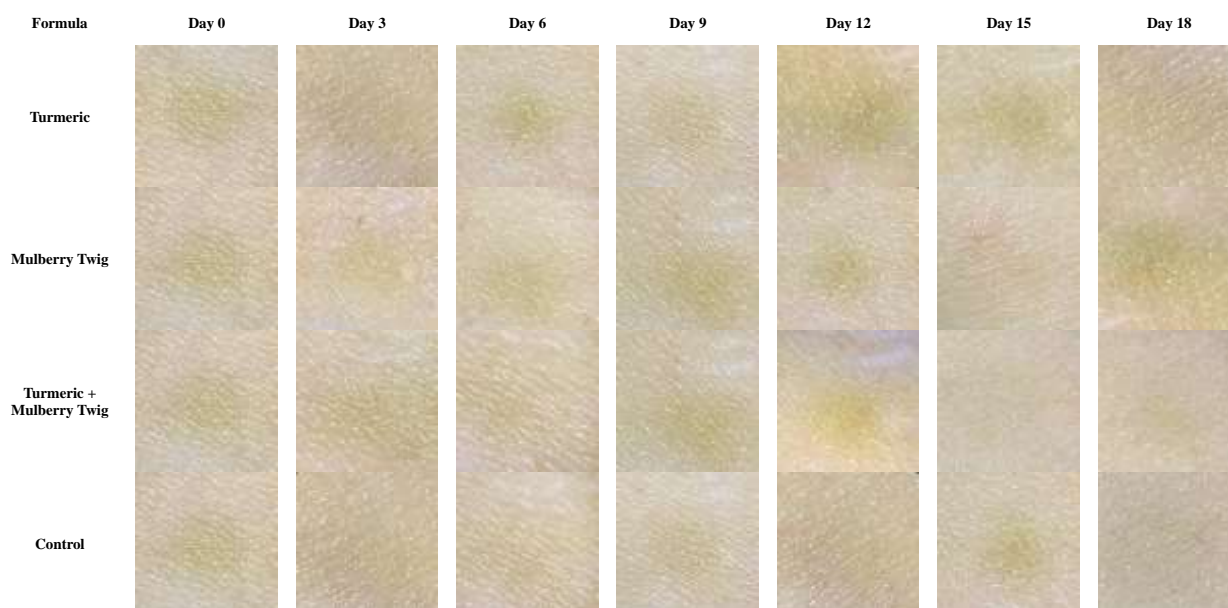| Day	Formulation			
	Turmeric	Mulberry Twig	Turmeric + Mulberry Twig	Control
0	0.00 ± 0.00	0.00 ± 0.00	0.00 ± 0.00	0.00 ± 0.00
3	2.60 ± 0.01	1.40 ± 0.91	1.60 ± 0.53	1.00 ± 0.90
6	3.00 ± 0.02	2.40 ± 0.39	1.60 ± 0.68	1.00 ± 0.41
9	3.20 ± 0.74	2.60 ± 0.03	2.40 ± 0.50	1.40 ± 0.34
12	3.60 ± 0.29	2.80 ± 0.26	4.00 ± 0.86	1.20 ± 0.47
15	6.80 ± 0.34	3.40 ± 0.73	6.40 ± 0.69	2.80 ± 0.49
18	11.00 ± 0.20	3.60 ± 0.65	9.80 ± 0.82	1.80 ± 0.37

Figure 2 Clinical test of herbal face mask

An additional participant in the clinical study exhibited noticeable wrinkle reduction after applying the turmeric–mulberry twig mask formulation. Beginning with the fifth application, the participant reported that fine lines had become less pronounced, suggesting potential skin rejuvenation effects. Furthermore, feedback from all five test participants indicated positive dermatological responses following mask use, including: enhanced skin smoothness, improved hydration and a cooling sensation during application. These results highlighted the moisturizing and soothing properties of the herbal mask formulations, reinforcing their cosmeceutical potential for skin care treatments.

4. Conclusions

This study established a systematic approach for evaluating gelling efficiency and moisture retention in mask formulations incorporating *Cissampelos spp.* leaf powder. The findings supported its potential applications in

cosmeceutical product development. The results provided essential insights into the antioxidant potential of turmeric extract, reinforcing its applicability in cosmeceutical and pharmaceutical formulations. The ability of turmeric extract to effectively reduce ferric ions highlighted its functional role in skincare and therapeutic applications, demonstrating its suitability for incorporation into antioxidant-rich products. Additionally, this analysis quantified the inhibitory effects of *mulberry twig* extract on tyrosinase activity, providing insights into its potential application in cosmeceutical formulations targeting melanin regulation and skin brightening. The findings indicated that the herbal facial mask formulations derived from *Cissampelos spp.* exhibited considerable potential for cosmeceutical applications, with demonstrated antioxidant, anti-aging, and skin-brightening properties. The results supported further development of these formulations for use in functional skincare products. This methodological approach ensured a comprehensive evaluation of sensory attributes, clinical effectiveness, and statistical significance, supporting the formulation development and cosmeceutical applicability of the herbal facial mask.

5. Acknowledgements

6. References

Boonvoraphat, W. (2017). *40 properties and benefits of Krung Khema (Mhanoi vine)*. Retrieved from https://www.medthai.com

Chunthanom, P., Somboon, K., Sakulkoo, S., & Sihamala, O. (2013). *Effect of extraction method on quality of pectin from Ma Noy (Cissampelos pareira) leaves in Phupan Valley. Khon Kaen Agriculture Journal, 41*(1), 556–562.

Jurenka, J. S. (2009). Anti-inflammatory properties of curcumin, a major constituent of *Curcuma longa*: A review of preclinical and clinical research. *Alternative Medicine Review, 14*(2), 141–153.

Kubola, J., & Siriamornpun, S. (2008). Phenolic contents and antioxidant activities of bitter gourd (*Momordica charantia* L.) leaf, stem and fruit fraction extracts in vitro. *Food Chemistry, 110*(4), 881–890. https://doi.org/10.1016/j.foodchem.2008.02.076

Peng-ngummuang, K., Jansuta, T., Sangdech, S., & Somkhow, P. (2019). Study of medicinal plants utilization in the community of Tambon Kho-ae, Amphoe Khueang Nai, Ubon Ratchathani. *UBRU Journal for Public Health Research, 8*(2), 150–165. Retrieved from https://he02.tci-thaijo.org/index.php/ubruphjou/article/view/240321

Pranakhon, R., Sombun, K., Saithi, S., Phueakchroey, G., & Pongnarathorn, P. (2005). *Khruea ma noi "Cyclea brabata Miers." Miracle wild plant*. [Online article – URL or publisher information needed]

Re, R., Pellegrini, N., Proteggente, A., Pannala, A., Yang, M., & Rice-Evans, C. (1999). Antioxidant activity applying an improved ABTS radical cation decolorization assay. *Free Radical Biology and Medicine, 26*(9–10), 1231–1237. https://doi.org/10.1016/s0891-5849(98)00315-3

Saewan, N., Koysomboon, S., & Chantrapromma, K. (2011). Anti-tyrosinase and anti-cancer activities of flavonoids from *Blumea balsamifera* DC. *Journal of Medicinal Plants Research, 5*(6), 1018–1025.

Tebumroong, P. (2003). *Quantitative and qualitative determination of pectin from Cissampelos pareira Linn. leaves*. [Unpublished thesis/report – specify institution if known]

Wang, Y., Xiang, L., Wang, C., Tang, C., & He, X. (2013). Antidiabetic and antioxidant effects and phytochemicals of mulberry fruit (*Morus alba* L.) polyphenol enhanced extract. *PLOS ONE, 8*(7), e71144. https://doi.org/10.1371/journal.pone.0071144

Analysis of the Advancement Technologies and Development Trends of Photovoltaic Module

Pasist Suwanapingkarl[a*], Surachet Dechphung[a], Manat Boonthienthonga[a], Nati Sukyam[a]
Thanaporn Buakarn[a], Aphichat Saisud[a], Kwanchanok Srivallop[b]

[a]*Department of Electrical Engineering, Faculty of Engineering, Rajamangala University of Technology Phra Nakhon, Bangkok, 10800, Thailand.*
[b]*3 Green KP Co., Ltd., Bangkok, 10900, Thailand.*
Pasist Suwanapingkarl. Tel.: 080-044-1915; E-mail address: pasist.s@rmutp.ac.th

Abstract

Photovoltaic (PV) systems are continually growing and increasingly recognised as one of the crucial keys to clean and resilient energy infrastructures. Therefore, the technology of PV has undergone significant advancements that aim to improve energy conversion efficiency, reduce production costs, and develop system integration into residential and industrial areas. This research provides a comprehensive analysis of the evolution of solar cell technologies from traditional conventional, such as silicon-based cells, to emerging innovations, such as perovskite. The research also explores future trends, including developing highly flexible modules capable of operating under low-light conditions and integrating with modern technologies such as the Internet of Things (IoT) and advanced electric vehicle charging station systems. In addition to practical applications, mathematical models play essential parts in this research and analysis, where they are used to evaluate new materials, cell architectures, and emerging technologies. The typical mathematical modelling approaches include the single-diode and double-diode models, which offer varying degrees of accuracy and complexity, as well as empirical models derived from experimental data, as these models are indispensable tools for understanding, predicting, and optimising the electrical behaviour of PV devices under varying environmental and operational conditions. This paper explains the critical role of mathematical modelling in designing, analysing, and evaluating PV systems before physical deployment to minimise financial risk and accelerate innovation in PV technology.

Keywords: Photovoltaic (PV) Systems, Mathematical Modelling, Solar Cell Technologies, Technological Innovation

1. Introduction

1.1 Economic drivers of cost reduction in PV module manufacturing

PV technologies and industries have experienced significant economic transformation driven by technological and industrial scaling advancements. Therefore, the average market price of PV modules declined. The three main factors, automation in manufacturing, economies of scale, and material innovations, play an essential role in decreasing the market price. The manufacturer that installs an automation system, such as integrating a robotics arm or artificial intelligence (AI) robotics, through streamlined production processes has significantly lowered labour costs, improved product consistency, and reduced waste. Consequently, economies of scale have enabled large-scale manufacturers to minimise per-unit costs through bulk procurement, optimised logistics, and reduced overhead costs.

Furthermore, advancements in material science, including the development of thin-film technologies, perovskite-based cells, and bifacial modules, have contributed to cost efficiency and performance enhancement. The decline in the market price has encouraged both residential and commercial consumers to install PV modules as this affordable price has improved the Return on Investment (ROI) for solar energy projects and accelerated the global adoption of solar technologies (Diab, Sultan, Do, Kamel, and Mossa, 2020).

1.2 The Necessity of mathematical modelling in PV Research

Mathematical modelling plays an important role in PV research because it is a foundational tool for analysing, predicting, and optimising the performance of solar energy systems. These models arise from several technical imperatives from both theoretical investigations and practical applications. It can be noted that PV cells are inherently nonlinear semiconductor devices whose behaviour is governed by the typical characteristic of the Shockley diode equation. To accurately represent their electrical characteristics and performance, most researchers employ models such as the single-diode model conFigureuration, which represents the essential behaviour of a solar cell. In contrast, the double-diode model conFigureuration enhances accuracy by incorporating recombination loss conFigureurations.

Moreover, the PV model is also affected by environmental dependency as well. Because the output of PV cells is susceptible to environmental variables such as solar irradiance, ambient temperature, shading, and the angle of incidence. Hence, the mathematical models enable the simulation of these dependencies by using temperature coefficients and irradiance scaling functions. These capabilities are essential for analysing the performance of PV in diverse climatic conditions. Most mathematical models are embedded in widely adopted simulation platforms such as MATLAB/Simulink, PVsyst, LTspice, HOMER Pro, Google Sheets and Microsoft Excel. These models allow researchers to conduct dynamic simulations and analyse PV performance without the physical prototypes. As such, they significantly reduce development costs and accelerate innovation (Diab, Sultan, Do, Kamel, and Mossa, 2020; Abdelminaam, Alluhaidan, Ismail, and El-Rahman, 2024; Yadav et al., 2023; Batzelis, and Papathanassiou, 2016; Batzelis, Kampitsis, Papathanassiou, and Manias, 2015; Toledo, Herranz, Blanes, and Galiano, 2022; Horiba, n.d.; Ridha, Hizam, Mirjalili, Othman, Ya'acob, and Abualigah, 2022; Hejri, Mokhtari, Azizian, Ghandhari and Söder, 2014; Kumar, Gupta, Safaraliev, Zeinoddini-Meymand, and Ghanizadeh, 2024; Shongwe, and Hanif, 2015; Wang, Chen, Guo, Hu, Chang, Wu, Han, and Li, 2021).
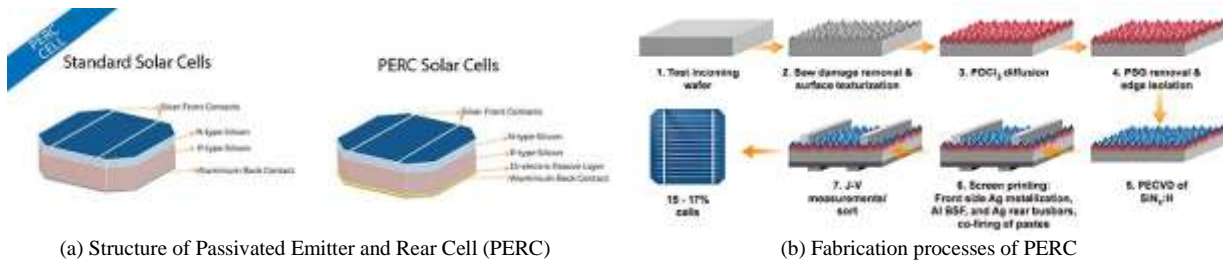
2. Methodology

2.1 Crystalline Silicon (c-Si) technologies

In general, the continued advancement of monocrystalline and polycrystalline PV technologies features the importance of tailored manufacturing strategies that balance performance, cost, and scalability, as this technology has potentially increased performance through hybrid materials and fabrication techniques. The fabrication of monocrystalline and polycrystalline photovoltaic (PV) cells reflects the convergence of materials science, semiconductor physics, and advanced engineering practices. Each technology presents distinct advantages and trade-offs that influence its suitability for various applications within the solar energy sector, as shown in Figure 1.

(a) Structure and fabrication processes of Monocrystalline Silicon (Mono-Si)

(b) Structure and fabrication processes of Polycrystalline Silicon (Poly-Si)
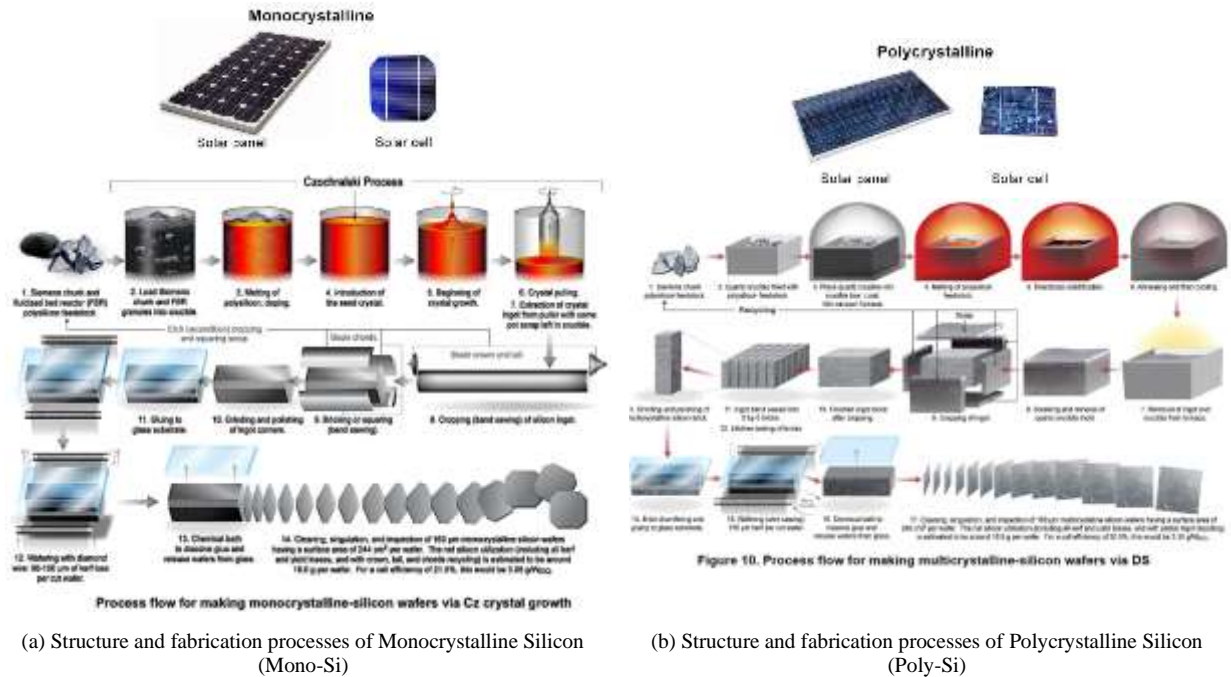
Figure 1 Crystalline Silicon (c-Si) Technology for PV module

Figure 1 also shows the comparative structure between monocrystalline silicon and polycrystalline silicon due to the cell fabrication. The production of monocrystalline silicon is a highly refined and technologically intensive process that involves the extraction of silicon from quartz sand (SiO_2), which is first reduced to metallurgical-grade silicon through carbothermic reduction in an electric arc furnace. To achieve the ultra-pure silicon required for photovoltaic applications, this silicon undergoes further refinement via the Siemens process, producing electronic-grade silicon with impurity levels below one part per billion to ensure minimal recombination losses and high carrier mobility in the final device. On the other hand, polycrystalline silicon production begins with silicon extraction from quartz (SiO_2), similar to monocrystalline silicon. However, to meet the purity requirements for photovoltaic applications, this silicon is further refined using the Siemens process, which involves the chemical vapour deposition of trichlorosilane ($SiHCl_3$) onto heated rods to produce solar-grade silicon with impurity levels below one ppm .

Figure 2 The Passivated Emitter and Rear Cell (PERC) architecture represents a significant advancement in enhancing the performance of conventional crystalline silicon solar cells. The primary keys are improving light absorption and minimising electron recombination losses. Hence, the PERC cells introduce two critical enhancements to this structure. The first is the addition of a dielectric passivation layer on the rear surface, commonly made from materials such as aluminium oxide or silicon nitride. This layer serves a dual purpose: it passivates surface defects that would otherwise act as recombination sites for electrons and holes, and it reflects unabsorbed photons into the silicon wafer, thereby increasing the probability of photon absorption and subsequent charge generation. The second innovation involves the use of localised rear contacts. PERC cells feature small, strategically placed openings in the passivation layer through which metal contacts are formed. This design reduces the contact area, further limiting recombination and enhancing cell efficiency (Diab, Sultan, Do, Kamel, and Mossa, 2020; Abdelminaam, Alluhaidan, Ismail, and El-Rahman, 2024; Yadav et al., 2023; Batzelis, and Papathanassiou, 2016; Batzelis, Kampitsis, Papathanassiou, and Manias, 2015; Toledo, Herranz, Blanes, and Galiano, 2022; Horiba, n.d.; Ridha, Hizam, Mirjalili, Othman, Ya'acob, and Abualigah, 2022; Hejri, Mokhtari, Azizian, Ghandhari and Söder, 2014; Kumar, Gupta, Safaraliev, Zeinoddini-Meymand, and Ghanizadeh, 2024; Shongwe, and Hanif, 2015; Wang, Chen, Guo, Hu, Chang, Wu, Han, and Li, 2021).
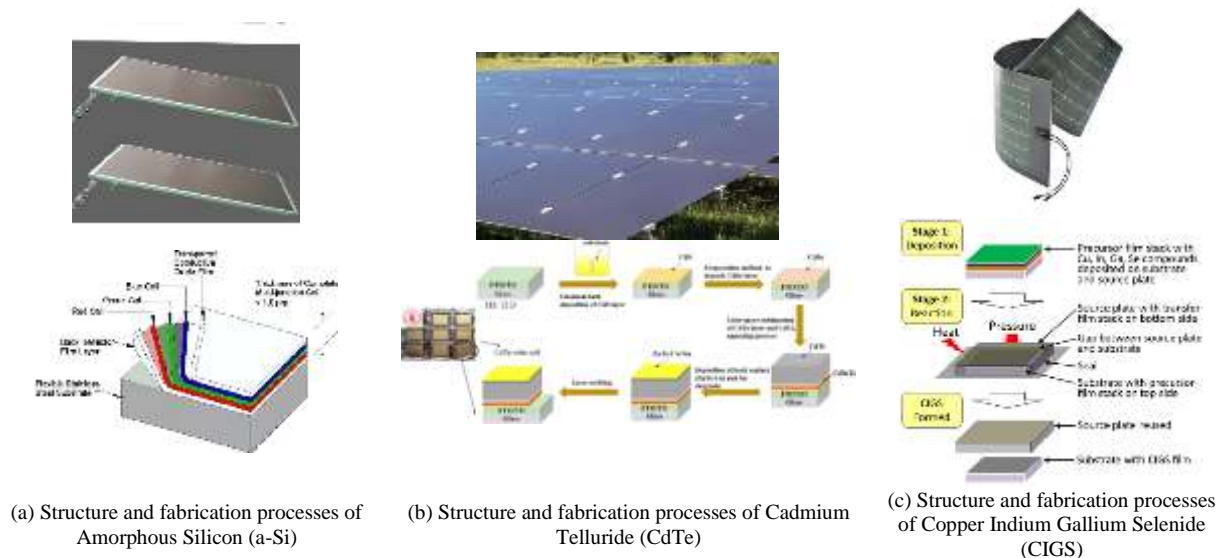
(a) Structure of Passivated Emitter and Rear Cell (PERC)   (b) Fabrication processes of PERC

Figure 2 Comparative between the Crystalline Silicon (c-Si) and the Passivated Emitter and Rear Cell (PERC) Technology for PV module

2.2 Thin-Film Solar Cells (TFSC) technologies

The production processes of Amorphous Silicon (a-Si), Cadmium Telluride (CdTe), and Copper Indium Gallium Selenide (CIGS) PV cells reflect distinct technological approaches, each with unique advantages, limitations, and implications for scalability and efficiency. Because these cells are characterized by the deposition of one or more thin layers of photovoltaic material onto a substrate such as glass, plastic, or metal. The total thickness of the active layers is typically in the range of a few micrometers, making them lightweight, flexible, and suitable for a wide range of applications as shown in Figure 3 (Diab, Sultan, Do, Kamel, and Mossa, 2020; Abdelminaam, Alluhaidan, Ismail, and El-Rahman, 2024; Yadav et al., 2023; Batzelis, and Papathanassiou, 2016; Batzelis, Kampitsis, Papathanassiou, and Manias, 2015; Toledo, Herranz, Blanes, and Galiano, 2022; Horiba, n.d.; Ridha, Hizam, Mirjalili, Othman, Ya'acob, and Abualigah, 2022; Hejri, Mokhtari, Azizian, Ghandhari and Söder, 2014; Kumar, Gupta, Safaraliev, Zeinoddini-Meymand, and Ghanizadeh, 2024; Shongwe, and Hanif, 2015; Wang, Chen, Guo, Hu, Chang, Wu, Han, and Li, 2021).

(a) Structure and fabrication processes of Amorphous Silicon (a-Si)   (b) Structure and fabrication processes of Cadmium Telluride (CdTe)   (c) Structure and fabrication processes of Copper Indium Gallium Selenide (CIGS)

Figure 3 Crystalline Silicon (c-Si) Technology for PV module

Amorphous Silicon (a-Si) PV cells are manufactured using low-temperature deposition techniques such as Plasma-Enhanced Chemical Vapor Deposition (PECVD). This process allows for deposition on flexible substrates and supports large-area manufacturing. However, a-Si suffers from relatively low conversion efficiency and light-induced degradation (Staebler-Wronski effect), which limits its long-term performance. It uses low material usage and compatibility with roll-to-roll processing, making it attractive for low-cost, lightweight applications.

Cadmium Telluride (CdTe) cells are produced using high-throughput methods such as Close-Spaced Sublimation (CSS) or Vapor Transport Deposition (VTD). CdTe technology benefits from a near-optimal bandgap and high absorption coefficient, enabling thin absorber layers and efficient material utilization. The production process is relatively simple and cost-effective, contributing to CdTe's dominance in utility-scale installations. However, concerns over cadmium toxicity and tellurium scarcity pose environmental and supply chain challenges.

CIGS cells involve more complex fabrication techniques, including co-evaporation or sputtering followed by selenization. These processes require precise control over composition and temperature to achieve optimal stoichiometry and crystal quality. While CIGS offers high efficiency and flexibility in substrate choice, its production is less mature and more capital-intensive compared to CdTe and a-Si.

2.3 Emerging technologies

The production processes of Gallium Arsenide (GaAs), Perovskite, and Transparent Luminescent Solar Concentrator (TLSC) photovoltaic cells reflect the diversity and innovation within next-generation solar technologies. Each technology offers unique advantages and faces distinct challenges in terms of fabrication complexity, material

stability, scalability of manufacturer, efficiency, cost, and application potential, as shown in Figure 4 (Diab, Sultan, Do, Kamel, and Mossa, 2020; Abdelminaam, Alluhaidan, Ismail, and El-Rahman, 2024; Yadav et al., 2023; Batzelis, and Papathanassiou, 2016; Batzelis, Kampitsis, Papathanassiou, and Manias, 2015; Toledo, Herranz, Blanes, and Galiano, 2022; Horiba, n.d.; Ridha, Hizam, Mirjalili, Othman, Ya'acob, and Abualigah, 2022; Hejri, Mokhtari, Azizian, Ghandhari and Söder, 2014; Kumar, Gupta, Safaraliev, Zeinoddini-Meymand, and Ghanizadeh, 2024; Shongwe, and Hanif, 2015; Wang, Chen, Guo, Hu, Chang, Wu, Han, and Li, 2021).

Gallium Arsenide (GaAs) solar cells are fabricated using epitaxial growth techniques such as Metal-Organic Chemical Vapor Deposition (MOCVD), which allow for precise control over crystal quality and layer composition. This results in exceptionally high efficiency and radiation resistance, making GaAs ideal for aerospace and concentrated photovoltaic (CPV) applications. However, the production process is highly capital-intensive, requires ultra-clean environments, and is limited by the high cost and scarcity of gallium and arsenic materials.

Perovskite solar cells are manufactured using solution-based processes such as spin coating, slot-die coating, or inkjet printing. These methods are low-cost, compatible with flexible substrates, and suitable for roll-to-roll manufacturing. The simplicity and tunability of perovskite fabrication have led to rapid efficiency gains in laboratory settings. Nevertheless, challenges remain in terms of long-term stability, lead toxicity, and scalability for commercial deployment.

Transparent Luminescent Solar Concentrators (TLSCs) represent a novel approach, utilizing organic or quantum dot-based luminescent materials embedded in transparent substrates. These devices are fabricated through techniques like layer-by-layer deposition or printing, allowing integration into windows and building facades. While TLSCs offer aesthetic and architectural advantages, their power conversion efficiencies are currently lower than those of conventional PV technologies, and their production processes are still in the early stages of industrial development.
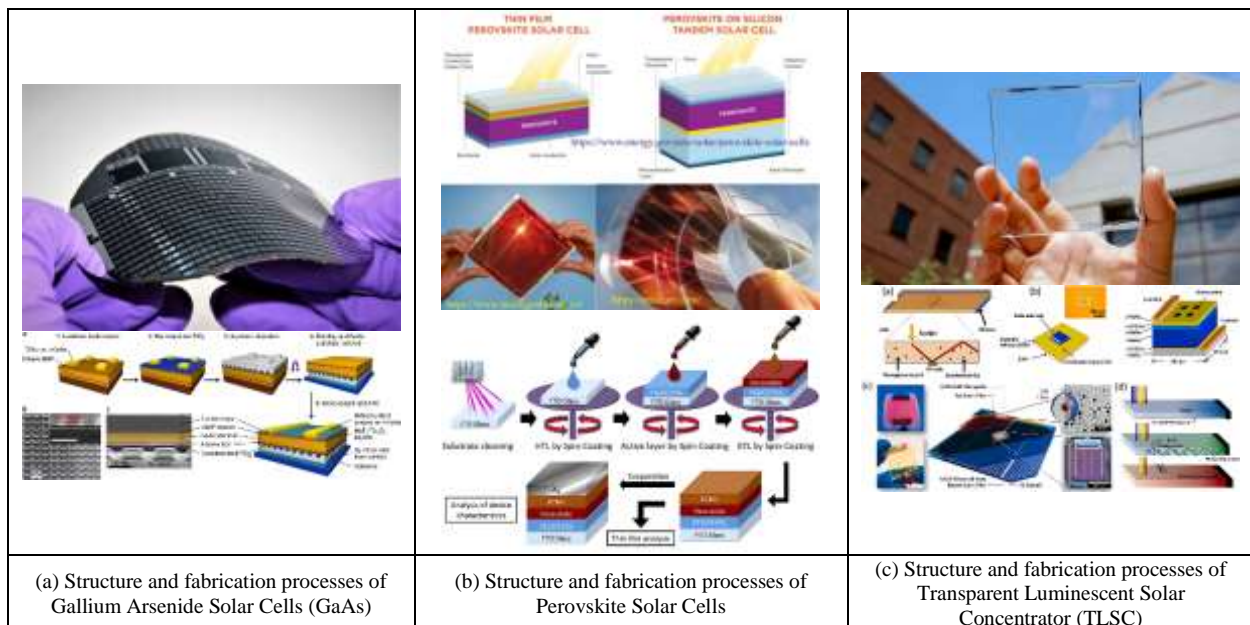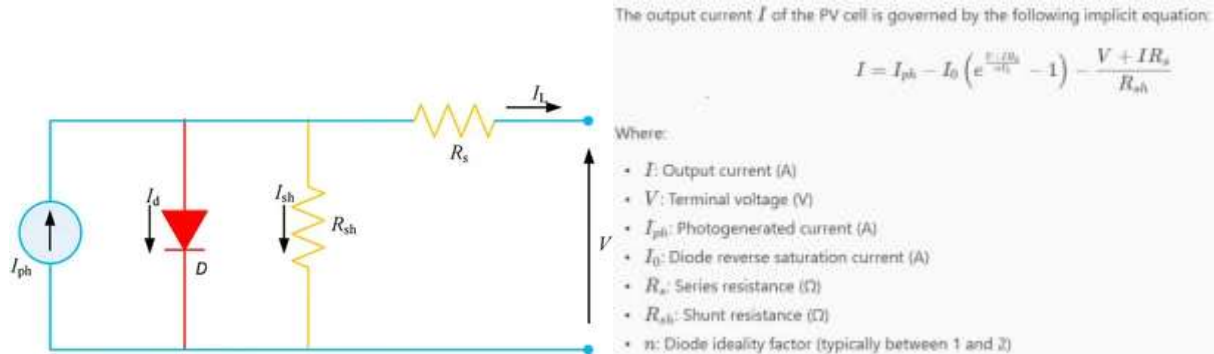

| (a) Structure and fabrication processes of Gallium Arsenide Solar Cells (GaAs) | (b) Structure and fabrication processes of Perovskite Solar Cells | (c) Structure and fabrication processes of Transparent Luminescent Solar Concentrator (TLSC) |

Figure 4 Emerging Technologies Technology for PV module

3. Results and Discussion

3.1 Single Diode model

The single-diode model is a foundational tool in analysing and simulating photovoltaic (PV) cells. While it offers a practical balance between simplicity and accuracy, it has limitations. Because the model assumes a single ideal diode to represent the p-n junction, which oversimplifies the recombination dynamics, particularly in the depletion region and bulk material, this can lead to significant deviations in predicted current-voltage (I-V) characteristics, especially under low irradiance or high-temperature conditions. Understanding these limitations is essential for researchers and engineers aiming to enhance PV system performance and reliability. The single-diode model is primarily designed for crystalline silicon solar cells. It does not adequately represent the behaviour of emerging PV technologies such as thin-film, organic, or multi-junction cells, which exhibit more complex electrical characteristics. For these technologies, more sophisticated models are required to capture the nuances of their operation.

The model typically treats parameters such as series resistance (R_s), shunt resistance (R_{sh}), and the diode ideality factor (n) as constants and static parameter assumptions. In reality, these parameters are dynamic and vary with temperature, irradiance, and ageing of the PV cell. The assumption of static parameters can lead to errors in long-term performance prediction and real-time control applications. Therefore, this is inherently static and does not account for capacitive effects or transient behaviours. As a result, it is unsuitable for high-frequency or time-dependent

analyses, such as those required in power electronics interfacing or fault diagnostics. This limits its applicability in advanced PV system simulations that require dynamic modelling, as shown in Figure 5 (Batzelis, Kampitsis, Papathanassiou, and Manias, 2015; Toledo, Herranz, Blanes, and Galiano, 2022; Horiba, n.d.; Ridha, Hizam, Mirjalili, Othman, Ya'acob, and Abualigah, 2022; Hejri, Mokhtari, Azizian, Ghandhari and Söder, 2014; Kumar, Gupta, Safaraliev, Zeinoddini-Meymand, and Ghanizadeh, 2024; Shongwe, and Hanif, 2015; Wang, Chen, Guo, Hu, Chang, Wu, Han, and Li, 2021).

The output current I of the PV cell is governed by the following implicit equation:

$$I = I_{ph} - I_0 \left(e^{\frac{V+IR_s}{nV_t}} - 1 \right) - \frac{V + IR_s}{R_{sh}}$$

Where:

- I: Output current (A)
- V: Terminal voltage (V)
- I_{ph}: Photogenerated current (A)
- I_0: Diode reverse saturation current (A)
- R_s: Series resistance (Ω)
- R_{sh}: Shunt resistance (Ω)
- n: Diode ideality factor (typically between 1 and 2)

Figure 5 Single Diode model

Accurate parameter extraction is essential for the effective use of the single-diode model. However, the implicit nature of the model's governing equation makes parameter estimation computationally intensive and sensitive to measurement noise. This poses challenges in practical applications, particularly when real-time or large-scale modelling is required. Thus, the model performs poorly under low-light conditions, where the assumptions of linearity and ideal diode behaviour break down. It often fails to accurately predict the open-circuit voltage and fill factor, which are critical parameters for evaluating PV performance. This limitation is particularly problematic for applications involving partial shading or diffuse light environments.

3.2 Double Diode model

The double diode model is an advanced equivalent circuit representation of a photovoltaic (PV) cell that improves upon the single diode model by incorporating additional physical phenomena, particularly recombination losses in the depletion region. This model is beneficial for high-accuracy simulations and for modelling modern solar cell technologies under a wide range of operating conditions. Because the second diode allows for more accurate modelling of recombination losses, especially under low-light and high-temperature conditions. Hence, the model matches measured I-V characteristics, particularly in the knee region of the curve. Therefore, it is more suitable for modelling thin-film, organic, and multi-junction solar cells, as shown in Figure 6 (Ridha, Hizam, Mirjalili, Othman, Ya'acob, and Abualigah, 2022; Hejri, Mokhtari, Azizian, Ghandhari and Söder, 2014; Kumar, Gupta, Safaraliev, Zeinoddini-Meymand, and Ghanizadeh, 2024; Shongwe, and Hanif, 2015; Wang, Chen, Guo, Hu, Chang, Wu, Han, and Li, 2021).

The output current I of the PV cell in the double diode model is given by:

$$I = I_{ph} - I_{01} \left(e^{\frac{V+IR_s}{n_1 V_t}} - 1 \right) - I_{02} \left(e^{\frac{V+IR_s}{n_2 V_t}} - 1 \right) - \frac{V + IR_s}{R_{sh}}$$

Where:

- I: Output current (A)
- V: Terminal voltage (V)
- I_{ph}: Photogenerated current (A)
- I_{01}, I_{02}: Saturation currents of the first and second diodes (A)
- n_1, n_2: Ideality factors of the diodes (dimensionless)
- R_s: Series resistance (Ω)
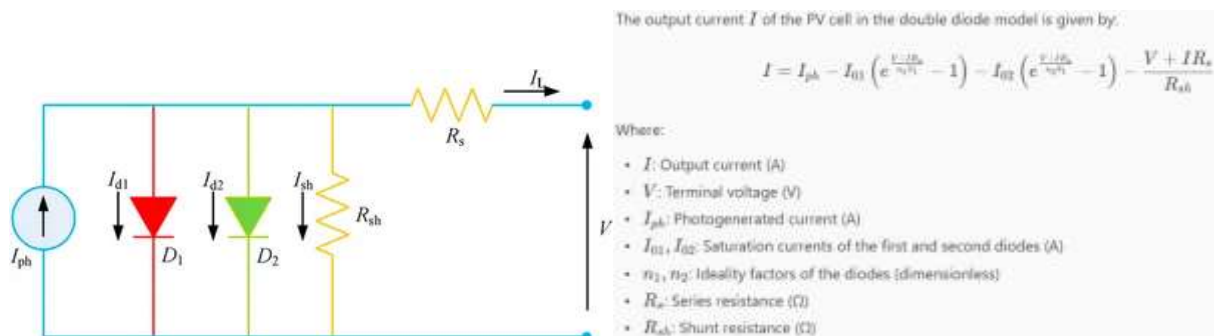- R_{sh}: Shunt resistance (Ω)

Figure 6 Double Diode model

The implicit nature of the model's governing equation makes parameter estimation computationally intensive and sensitive. It requires sophisticated numerical techniques and high-quality experimental data. The model performs poorly under dynamic or capacitive effects as it cannot be used in transient simulations. This limitation is particularly problematic for partial shading applications or real-time or large-scale modelling.

3.3 Five-parameter model

The five-parameter model is a widely used equivalent circuit model for simulating the electrical behaviour of photovoltaic (PV) cells. It extends the single-diode model by incorporating more accurate representations of the physical processes within the cell, particularly under varying environmental conditions. The five-parameter model is closely related to the single-diode model but is not precisely the same. Their models are differences in system-level simulations, performance prediction, and maximum power point tracking (MPPT) algorithm development. Thus, this

model provides a more accurate fit for experimental I-V data. It allows for modelling the effects of irradiance and temperature on cell performance. It is suitable for large-scale simulations because it balances computational simplicity and physical realism. However, the I-V relationship is implicit and requires iterative numerical methods for a solution and higher fidelity or dynamic behaviour, as shown in Figure 7 (Ridha, Hizam, Mirjalili, Othman, Ya'acob, and Abualigah, 2022; Hejri, Mokhtari, Azizian, Ghandhari and Söder, 2014; Kumar, Gupta, Safaraliev, Zeinoddini-Meymand, and Ghanizadeh, 2024; Shongwe, and Hanif, 2015; Wang, Chen, Guo, Hu, Chang, Wu, Han, and Li, 2021)

Feature	Single Diode Model	Five-Parameter Model
Parameterization	General or empirical	Explicitly defines 5 physical parameters
Accuracy	Moderate	Higher, especially under varying conditions
Use Case	Conceptual understanding, basic simulation	Detailed simulation, performance prediction
Parameter Extraction	Often simplified or assumed	Requires calibration from experimental data
Environmental Sensitivity	Limited	Explicitly models irradiance and temperature effects

Figure 7 Five-parameter model

3.4 Seven-parameter model

The seven-parameter model is an advanced equivalent circuit model used to simulate the electrical behaviour of photovoltaic (PV) cells. It extends the five-parameter model by incorporating additional parameters that account for more complex physical phenomena within the cell. This model is beneficial for high-accuracy simulations and modelling of modern solar cell technologies under various operating conditions. Compared to simpler models, it can provide a more accurate fit to experimental I-V data. It also supports the sensitivity of the environment, such as the effects of irradiance and temperature on cell performance. Therefore, this model is suitable for modelling thin-film, organic, and multi-junction solar cells. However, the model also introduces additional parameters, making it more computationally intensive and challenging to fit, especially since it requires sophisticated numerical techniques and high-quality experimental data, as shown in Figure 8 (Shongwe, and Hanif, 2015; Wang, Chen, Guo, Hu, Chang, Wu, Han, and Li, 2021).

Feature	Double Diode Model	Seven-Parameter Model
Diodes	2 (D_1 for diffusion, D_2 for recombination)	2 (same as double diode)
Photocurrent Source	Yes	Yes
Series Resistance (R_s)	Yes	Yes
Shunt Resistance (R_{sh})	Yes	Yes
Diode Ideality Factors (n_1, n_2)	Yes	Yes
Temperature Coefficients	Not explicitly included	Yes: α_{Isc} and β_{Voc}
Total Parameters	Typically 5–6	7 (hence the name)

Figure 8 Seven-parameter model

4. Conclusions

The theoretical structure, critical components, and mathematical modelling of PV are necessary to analyse and support the development of advanced technologies between laboratory research and physical prototype deployment.

4.1 Comparative evaluation of research and commercial software

This research has demonstrated the critical role of understanding PV cells' internal structure and operational behaviour, which is fundamental to advancing solar energy technologies. PV cells are inherently nonlinear semiconductor devices, and the Shockley diode equation governs their electrical behaviour. Hence, the internal structure and mathematical modelling in the analysis and optimisation of PV modules, particularly the single-diode

and double-diode models. The single-diode model effectively captures the essential electrical characteristics of a solar cell. In contrast, the double-diode model provides enhanced accuracy by incorporating recombination losses, particularly relevant under low-light or high-temperature conditions. These models enable accurate simulation of electrical behaviour under varying environmental conditions, which is essential for theoretical studies and practical implementations. The single-diode and double-diode models (on Google Sheets and Microsoft Excel) are usually compared to commercial software platforms such as PVsyst, MATLAB/Simulink, and HOMER Pro, which provide user-friendly interfaces, integrated databases, and robust validation, making them more suitable for large-scale deployment and industry use.

4.2 Limitations and challenges in this research

Despite the simplicity and strengths of mathematical modelling, several limitations persist. One of the primary limitations of mathematical modelling is the certain assumptions of material properties. Because the mathematical modelling is limited by certain assumptions used in standard models, such as idealised environmental conditions and uniform material properties, these simplifications can lead to discrepancies between simulated and physical prototype performance. It can be noted that the complexity of accurately modelling emerging technologies such as perovskite poses significant challenges due to their unique material behaviours and degradation mechanisms

4.3 Future research

Future work related to this research should focus on integrating advanced modelling techniques with real-time data analytics and machine learning algorithms to enhance the economic scalability of this research. Moreover, developing and aligning technical innovation with economic feasibility could democratise access to high-fidelity modelling tools, supporting broader adoption in academia and industry with the widespread deployment of PV systems as a cornerstone of sustainable energy infrastructure.

5. Acknowledgements

6. References

Diab,A. A. Z., Sultan,H. M., Do, T. D., Kamel, O. M., and Mossa, M. A. (2020). Coyote Optimization Algorithm for Parameters Estimation of Various Models of Solar Cells and PV Modules," in *IEEE Access*, 8, 111102-111140, 2020 doi: 10.1109/ACCESS.2020.3000770

Abdelminaam, D. S., Alluhaidan, A. S., Ismail, F. H., and El-Rahman, S. A. (2024). Parameters Extraction of the Three-Diode Photovoltaic Model Using Crayfish Optimization Algorithm. in *IEEE Access*, 12, 109342-109354, 2024, doi: 10.1109/ACCESS.2024.3421286.

Yadav, D. et al., "Analysis of the Factors Influencing the Performance of Single- and Multi-Diode PV Solar Modules," in *IEEE Access*, 11, 95507-95525, 2023, doi: 10.1109/ACCESS.2023.3306473.

Batzelis, E. I. and Papathanassiou, S. A. (2016). A Method for the Analytical Extraction of the Single-Diode PV Model Parameters, in *IEEE Transactions on Sustainable Energy*, 7(2), 504-512, April 2016, doi: 10.1109/TSTE.2015.2503435.

Batzelis, E. I., Kampitsis, G. E., Papathanassiou, S. A. and Manias, S. N. (2015) Direct MPP Calculation in Terms of the Single-Diode PV Model Parameters. in *IEEE Transactions on Energy Conversion*, 30(1), 226-236, March 2015, doi: 10.1109/TEC.2014.2356017

Toledo, F. J., Herranz, M. V., Blanes, J. M. and Galiano, V. (2022). Quick and Accurate Strategy for Calculating the Solutions of the Photovoltaic Single-Diode Model Equation. in *IEEE Journal of Photovoltaics*, 12(2), 493-500, March 2022, doi: 10.1109/JPHOTOV.2021.3132900.

Horiba. (n.d.). *Photovoltaic Manufacturing Process.* Retrieved May 15, 2025, from https://www.horiba.com/gbr/semiconductor/markets/advanced-materials/photovoltaic-manufacturing-process/

Ridha, H. M., Hizam, H., Mirjalili, S. M., Othman, L., Ya'acob, M. E., and Abualigah, L. (2022). A Novel Theoretical and Practical Methodology for Extracting the Parameters of the Single and Double Diode Photovoltaic Models. in *IEEE Access*, 10, 11110-11137, 2022, doi: 10.1109/ACCESS.2022.3142779.

Hejri, M., Mokhtari, H., Azizian, M. R., Ghandhari M., and Söder, L. (2014). On the Parameter Extraction of a Five-Parameter Double-Diode Model of Photovoltaic Cells and Modules. in *IEEE Journal of Photovoltaics*, 4(3), 915-923, May 2014, doi: 10.1109/JPHOTOV.2014.2307161.

Kumar Singla, M., Gupta, J., Safaraliev, M., Zeinoddini-Meymand, H. and Ghanizadeh, A. J. (2024). Mathematical Modeling for Solar Cell Optimization: Evaluating Sustainability With Different Diode ConFigureurations. in IEEE Access, 12, 93802-93822, 2024, doi: 10.1109/ACCESS.2024.3424416.

Shongwe, S. and Hanif, M. (2015). Comparative Analysis of Different Single-Diode PV Modeling Methods. in IEEE Journal of Photovoltaics, 5(3), 938-946, May 2015, doi: 10.1109/JPHOTOV.2015.2395137

Wang, L., Chen, Z., Guo, Y., Hu, W., Chang, X., Wu, P., Han, C., & Li, J. (2021). Accurate Solar Cell Modeling via Genetic Neural Network-Based Meta-Heuristic Algorithms. Frontiers in Energy Research, 9, 696204. https://doi.org/10.3389/fenrg.2021.696204

Uncovering the Role of Fe in Geopolymers via Synchrotron XANES and EXAFS: Insights from Fly Ash, Bagasse Ash, and Calcium Carbide Residue Systems

Teerapon Saowapan[a], Rattapon Somna[b], Wanwisa Limphirat[c], and Kiatsuda Somna[d*]

[a]Ph.D. Candidate, [b] Assistant Professor, [d*]Associate Professor, Department of Civil Engineering, Faculty of Engineering and Technology, Rajamangala University of Technology Isan, Nakhon Ratchasima, Thailand
[c]Researcher, Synchrotron Light Research Institute (Public Organization), Synchrotron Research and Applications Division, Nakhon Ratchasima, Thailand
* Corresponding author E-mail address: kiatsuda.so@rmuti.ac.th

Abstract

Geopolymers made from industrial waste like fly ash (FA), bagasse ash (BA), and calcium carbide residue (CR) are being explored as sustainable alternatives to Portland cement. This study focuses on how adding 5 wt% of iron oxide (Fe_2O_3) affects the internal structure of these geopolymers. We used advanced synchrotron techniques—X-ray absorption near-edge structure (XANES) and extended X-ray absorption fine structure (EXAFS)—to understand how iron behaves inside the material. All samples with added iron showed an absorption edge around 7120 eV, confirming that iron mainly exists in the +3 oxidation state (Fe^{3+}). It can be noticed that the way iron atoms were arranged depended on the type of raw materials. In samples with high fly ash, iron seemed to bond more neatly inside the structure. In contrast, samples with more calcium carbide residue had more disorder and signs of separate iron oxide phases. These changes were supported by XRD and compressive strength results, which showed that better iron incorporation led to better structure and performance. Our findings suggest that the raw material composition strongly affects how iron fits into the geopolymer and influences the material's strength. This study highlights the value of synchrotron techniques in designing better geopolymers and deepens our understanding of how iron interacts in different systems.

Keywords: Geopolymer, Iron Incorporation, XANES, EXAFS

1. Introduction

Geopolymers are **a** type of inorganic binder formed through the alkali activation of aluminosilicate materials, offering a more sustainable option compared to ordinary Portland cement (OPC). These materials not only show high strength and chemical resistance, but also help lower CO_2 emissions thanks to their low-temperature processing and the use of industrial by-products (Davidovits, J, (1991); Provis, J L and van Deventer, J S J, (2009)). Common raw materials used as geopolymer precursors include fly ash (FA), a residue from coal combustion; bagasse ash (BA), produced from sugarcane waste; and calcium carbide residue (CR), a by-product rich in calcium hydroxide from acetylene gas production. When combined, these materials can produce blended geopolymer systems that balance silica, alumina, and calcium, forming hybrid gel structures like N–A–S–H and C–A–S–H (Wang, Q et al., 2022; Amin, M N et al., 2022).

Although the roles of silica- and calcium-rich precursors in geopolymer chemistry are well documented, the effect of transition metals—especially iron (Fe)—is still not fully understood. Iron is commonly found in waste materials and can also be added intentionally as Fe_2O_3. Depending on the chemical environment, iron may either bond with the aluminosilicate structure or stay as a separate crystalline phase. This behavior can influence the type of gel that forms and affect the final strength and durability of the geopolymer matrix (Lemougna, P N et al., 2013; Tchakouté, H K et al., 2017).

To explore how Fe behaves inside the geopolymer structure, this study uses synchrotron-based X-ray absorption techniques—X-ray absorption near edge structure (XANES) and extended X-ray absorption fine structure (EXAFS). These methods are very sensitive to oxidation states and local atomic bonding and are ideal for studying Fe distribution in disordered geopolymer matrices (Parsons, J G et al., 2002; Newville, M, 2004). Samples with various FA–BA–CR proportions, both with and without 5 wt% Fe_2O_3, were examined to see how different raw material combinations influence Fe bonding.

This study provides new understanding of how iron interacts with geopolymer gels, and shows the potential of advanced synchrotron techniques to help develop stronger and more sustainable construction materials.

2. Methodology

2.1 Raw Materials

Fly Ash (FA): From Mae Moh power plant, rich in Si and Al
Bagasse Ash (BA): From Surin Sugar Co., moderate reactivity
Calcium Carbide Residue (CR): From Thai Acetylene Co., high in $Ca(OH)_2$
Fe Source: Commercial Fe_2O_3, added at 5 wt%

2.2 Mix Design

Seven geopolymer paste formulations were prepared using different ratios of fly ash (FA), bagasse ash (BA), and calcium carbide residue (CR) as aluminosilicate precursors. Each mixture was prepared in both a control version (without Fe) and a modified version with 5 wt% Fe_2O_3 added as an iron source. The 5 wt% Fe_2O_3 dosage was selected

based on preliminary studies and literature indicating that this level of iron oxide can influence structural incorporation without causing excessive crystallization or segregation. Previous studies such as Tchakouté et al. (2017) and Lemougna et al. (2013) used similar or slightly lower amounts for investigating Fe coordination in geopolymer systems. The alkaline activator consisted of 5 molar sodium hydroxide (NaOH) and sodium silicate (Na_2SiO_3), mixed in a ratio of 1:0.5 by volume. The binder-to-solution ratio was maintained at 1:0.75 for all mixtures to ensure consistency in workability. After thorough mixing, the pastes were cast into molds and cured at ambient temperature. These formulations were designed to evaluate the influence of precursor composition and Fe addition on the structure and properties of the resulting geopolymers. The mix proportions of the geopolymer samples are presented in Table 1, while Table 2 displays the XRF-derived oxide compositions (wt%) of the FA–BA–CR-based mixes with 5 wt% Fe_2O_3 addition.

Table 1 The mix proportions of the geopolymer samples

Samples	Ratio of starting materials			Fe_2O_3 (%)	5 M NaOH	Na_2SiO_3
	FA	BA	CR			
0.16FA0.16BA0.67CR	0.16	0.16	0.67	5	0.5	0.25
0FA0BA1CR	0.00	0.00	1.00	5	0.5	0.25
0.67FA0.16BA0.16CR	0.67	0.16	0.16	5	0.5	0.25
0.33FA0.33BA0.33CR	0.33	0.33	0.33	5	0.5	0.25
0.16FA0.67BA0.16CR	0.16	0.67	0.16	5	0.5	0.25
0FA1BA0CR	0.00	1.00	0.00	5	0.5	0.25
1FA0BA0CR	1.00	0.00	0.00	5	0.5	0.25

Table 2 XRF-derived oxide composition (wt%) of FA–BA–CR-based geopolymer mixes with 5 wt% Fe_2O_3 addition

Samples	SiO_2	Al_2O_3	Fe_2O_3	CaO	MgO	SO_3	K_2O
0.16FA0.16BA0.67CR	20.61	3.56	7.76	65.03	0.54	1.70	0.80
0FA0BA1CR	4.10	1.58	5.07	88.94	0.00	0.30	0.00
0.67FA0.16BA0.16CR	33.56	9.24	14.93	35.02	0.54	5.25	1.46
0.33FA0.33BA0.33CR	37.12	5.53	10.45	41.10	1.09	3.10	1.60
0.16FA0.67BA0.16CR	57.19	3.82	8.66	23.28	2.17	2.35	2.54
0FA1BA0CR	77.26	2.10	6.87	4.92	3.26	1.60	3.49
1FA0BA0CR	30.01	12.94	19.42	28.92	0.00	7.39	1.31

2.3 Characterization Techniques

A combination of laboratory and synchrotron-based techniques was employed to analyze the phase composition, iron coordination, and mechanical properties of the geopolymer samples.

1) X-ray Diffraction (XRD)

XRD was used to identify crystalline phases in the geopolymer matrix. The patterns were recorded in the 2θ range of 10°–70°, using Cu Kα radiation. Phases such as quartz, calcite, portlandite, and hematite were identified to evaluate reaction products and residual precursors.

2) X-ray Absorption Spectroscopy (XAS)

XAS experiments, including X-ray Absorption Near-Edge Structure (XANES) and Extended X-ray Absorption Fine Structure (EXAFS), were conducted at the Fe K-edge to investigate the oxidation state and local coordination of iron in the geopolymer matrix. Measurements were performed in fluorescence mode at the Synchrotron Light Research Institute (Thailand). Data analysis was carried out using the Demeter software package (Athena and Artemis).

3) Compressive Strength Testing

Compressive strength was measured on cubic geopolymer specimens ($50 \times 50 \times 50$ mm) at 28 days. A universal testing machine was used with a loading rate of 1 mm/min. Strength values were compared between Fe-modified and control samples to assess the effect of iron incorporation.

3. Results and Discussion

3.1 Fe Oxidation State and Local Coordination (XANES)

X-ray absorption near-edge structure (XANES) analysis was conducted to investigate the oxidation state of Fe and its coordination behavior in geopolymer samples containing 5 wt% Fe_2O_3. All samples exhibited a distinct Fe K-edge absorption feature at approximately 7120 eV, which is characteristic of iron in the +3 oxidation state (Fe^{3+}). This confirms that the added Fe_2O_3 remained predominantly in its trivalent form throughout the alkali activation process.

Although the edge position remained consistent across all compositions, significant differences were observed in the intensity of the white line—the peak immediately following the absorption edge. Samples with higher fly ash content, such as 1FA0BA0CR-Fe and 0.67FA0.16BA0.16CR-Fe, exhibited lower white line intensities, suggesting a more ordered Fe coordination environment. In contrast, CR-rich compositions such as 0.16FA0.16BA0.67CR-Fe and 0FA0BA1CR-Fe showed higher white line intensities, which may indicate a more distorted or disordered local structure around the Fe atoms.

These variations reflect the influence of precursor composition on Fe incorporation. High FA systems, rich in reactive silica and alumina, likely promote the integration of Fe into the aluminosilicate framework. Meanwhile,

calcium-rich systems (CR-dominant) tend to hinder polymerization and may result in Fe existing as isolated species or secondary phases (Zhang, G and Provis, J L (2020), Ngnintedem, D L V et.al(2002).
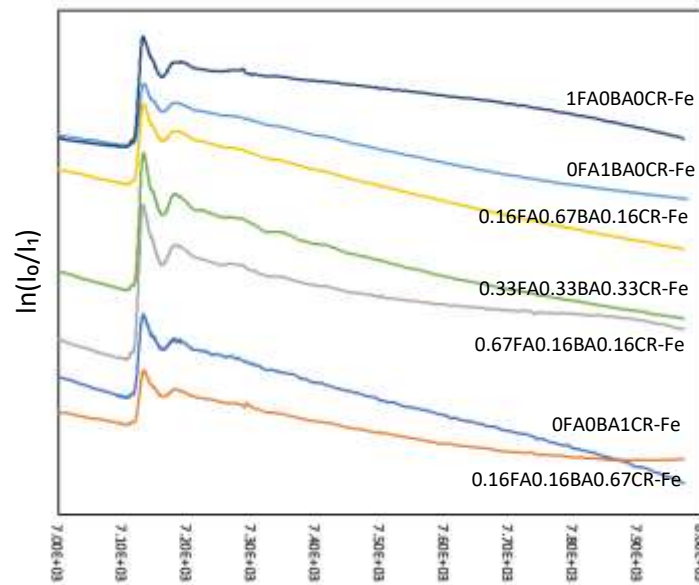

Figure 1 The Fe K-edge XANES spectra of geopolymer samples made with different amounts of fly ash (FA), bagasse ash (BA), and calcium carbide residue (CR), all containing 5 wt% Fe_2O

3.2 Fe Coordination Environment (EXAFS)

Extended X-ray absorption fine structure (EXAFS) analysis was performed to evaluate the local atomic arrangement around Fe atoms in the geopolymer matrix. The Fourier-transformed EXAFS (FT-EXAFS) spectra in R-space revealed clear differences in Fe–O coordination among the various precursor combinations.

All samples exhibited a primary FT peak in the range of 1.5–2.2 Å, corresponding to the first coordination shell of Fe–O bonds. The amplitude and sharpness of this peak varied depending on the mix composition. In fly ash-rich systems such as 1FA0BA0CR-Fe and 0.67FA0.16BA0.16CR-Fe, the Fe–O peaks were sharper and more intense, indicating a more ordered and symmetric local coordination environment. This suggests that Fe was better incorporated into the aluminosilicate gel framework, potentially by substituting for Al in the tetrahedral structure.

In contrast, samples with high calcium carbide residue, such as 0.16FA0.16BA0.67CR-Fe and 0FA0BA1CR-Fe, showed broader and less intense Fe–O peaks. These features point to a more disordered coordination environment, which may result from Fe existing outside the gel network, either as amorphous species or as segregated iron oxide phases. The reduced second-shell features in these samples further support the lack of long-range order, consistent with weak Fe integration.

These EXAFS observations align with the XANES results, reinforcing the conclusion that the degree of Fe incorporation is strongly influenced by the precursor composition. High FA content facilitates more stable Fe–O coordination, while high CR content leads to increased disorder and potential phase separation.
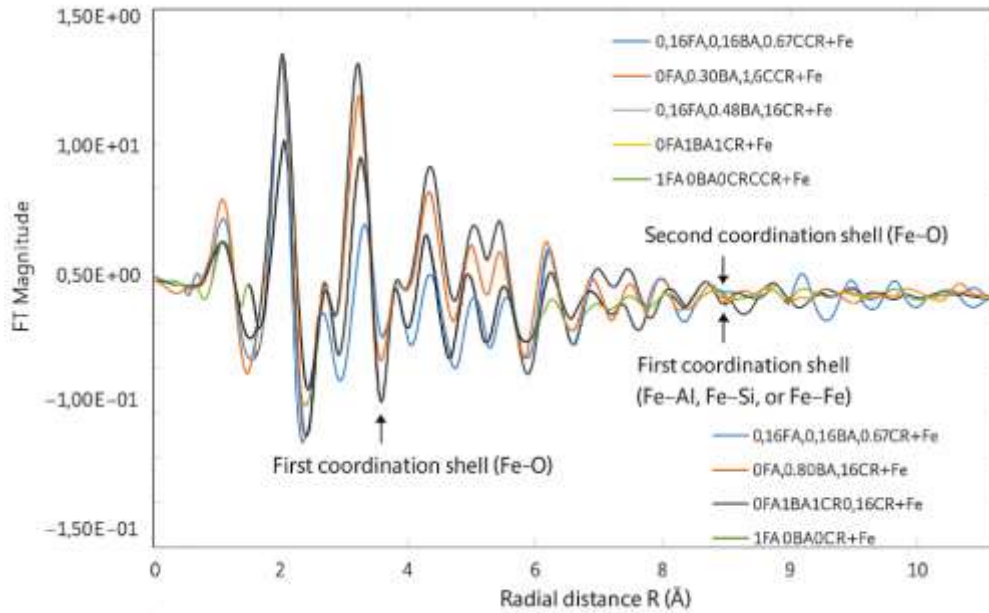
Figure 2 The Fourier-transformed EXAFS (FT-EXAFS) spectra at the Fe K-edge for geopolymer samples with 5 wt% Fe_2O_3, made using different amounts of fly ash (FA), bagasse ash (BA), and calcium carbide residue (CR)

3.3 Phase Composition (XRD)

X-ray diffraction (XRD) analysis was conducted to identify the crystalline phases present in the geopolymer samples with and without Fe_2O_3 addition. All diffractograms exhibited a broad hump between 25° and 35° 2θ, indicative of the amorphous aluminosilicate gel typically formed in geopolymer systems. Superimposed on this amorphous background, several crystalline phases were identified, including quartz (Q), calcite (C), portlandite (H), and dolomitic calcite (M), primarily originating from unreacted raw materials.

In CR-rich samples such as 0.16FA0.16BA0.67CR and 0FA0BA1CR, strong diffraction peaks of portlandite ($Ca(OH)_2$) and gaylussite ($Na_2Ca(CO_3)_2$) were observed. These phases indicate incomplete reaction of calcium hydroxide from CR, which may hinder the formation of a continuous gel network. Upon addition of Fe_2O_3, new peaks appeared at ~33.2° 2θ, corresponding to hematite (Fe_2O_3). These peaks were most pronounced in Fe-modified CR-rich systems (e.g., 0.16FA0.16BA0.67CR-Fe and 0FA1BA0CR-Fe), suggesting limited Fe incorporation and a tendency toward phase segregation.

In contrast, samples with higher FA content, such as 1FA0BA0CR-Fe and 0.67FA0.16BA0.16CR-Fe, showed broader and weaker hematite reflections. This implies that Fe was more successfully incorporated into the amorphous geopolymer matrix rather than forming distinct crystalline phases. These trends are consistent with the EXAFS findings, which revealed more ordered Fe coordination environments in FA-rich systems [11].

The absence of additional crystalline aluminosilicate phases (e.g., zeolites or feldspathoids) suggests that the majority of geopolymerization products remained in an amorphous state. This was further supported by the prominence of the amorphous hump in all XRD patterns.
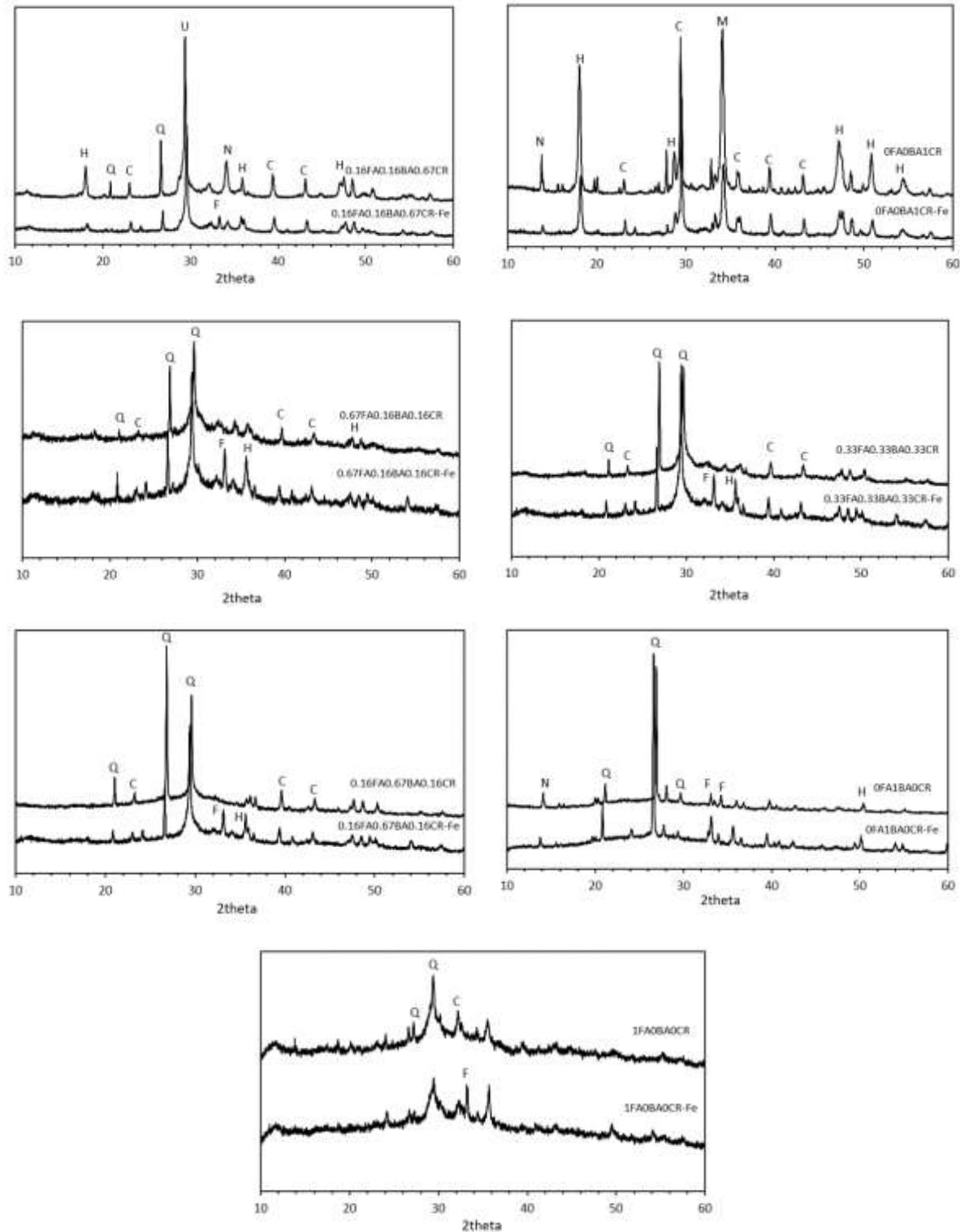
Figure 3 presents the XRD patterns of geopolymer samples synthesized from various proportions of fly ash (FA), bagasse ash (BA), and calcium carbide residue (CR), with and without 5 wt% Fe_2O_3 addition

H: $Ca(OH)_2$ Portlandite C: $CaCO_3$ Calcite N: $Na_2Ca(CO_3)_2$ Gaylussite Q: SiO_2 Quartz U: SiO_2 Quartz

M: $(Mg_{0.03}Ca_{0.97})(CO_3)$ Calcite S: Ca_3SiO_5 Hatruite F: Fe_2O_3 Hematite

3.4 Mechanical Performance (Compressive Strength)

The compressive strength at 28 days showed clear differences based on both the raw material mix and whether Fe_2O_3 was added. Fly ash–rich samples gave the best strength results. For example, the mix with 100% fly ash (1FA0BA0CR) reached about 43 MPa without Fe. But when Fe_2O_3 was added, the strength dropped to around 25 MPa. This might be because iron, while well integrated into the structure, slightly disrupted the gel network that holds the material together.

211

On the other hand, samples with high calcium carbide residue (like 0FA0BA1CR) had very low strength, below 10 MPa. Adding Fe to these mixes made the strength even worse. XRD results showed leftover portlandite and clear peaks of hematite, meaning that Fe did not enter the gel but instead formed separate crystals, which weakened the material.

Blends with balanced amounts of FA, BA, and CR (like 0.33FA0.33BA0.33CR and 0.67FA0.16BA0.16CR) gave medium to good strengths (around 25–35 MPa). Adding Fe to these balanced mixes didn't hurt the strength much and sometimes slightly improved it. EXAFS and XANES results showed that Fe was only partly included in the structure in these cases, and the gel stayed stable.

In summary, Fe helps or hurts depending on the mix. It works better when there's enough silica and alumina (from FA), but not when there's too much calcium (from CR).
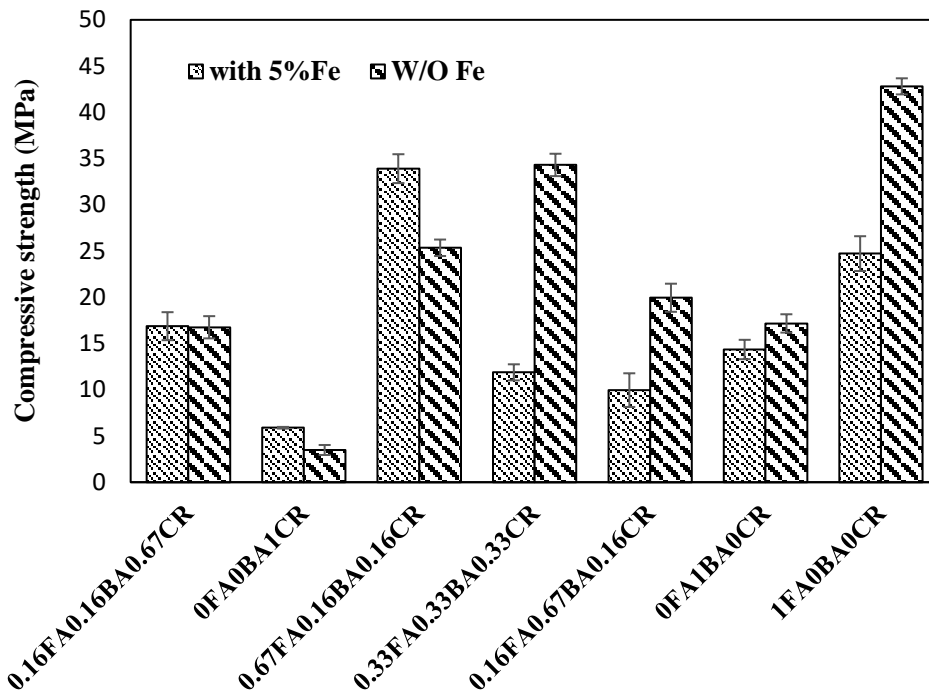
Figure 4 the 28-day compressive strength of geopolymer samples made from different amounts of fly ash (FA), bagasse ash (BA), and calcium carbide residue (CR), with and without 5% Fe_2O_3

3.5 Cross-Technique Correlation

The results from all techniques—XANES, EXAFS, XRD, and compressive strength—show a clear link between the local structure of iron and how strong the geopolymer becomes.

In fly ash–rich samples, Fe was better incorporated into the gel network. XANES showed low white line intensity (meaning less disorder), and EXAFS showed sharp Fe–O coordination peaks (meaning more order). These samples also had weak or no hematite peaks in XRD and gave high compressive strength. This suggests that when Fe is well integrated into the aluminosilicate structure, it does not harm strength—and may even help slightly.

In contrast, CR-rich mixes showed the opposite. XANES white lines were strong, EXAFS peaks were broad, and XRD showed clear hematite crystals. These samples had the lowest strength. The data suggest that Fe was not part of the gel but formed separate phases that disrupted the structure.

Balanced mixes (with moderate FA, BA, and CR) gave medium strength. Fe was only partly incorporated, and the structure stayed stable. The XRD, XANES, and EXAFS results for these mixes showed intermediate behavior—some Fe coordination, mild hematite peaks, and moderate disorder.

Overall, Fe can support or weaken the geopolymer depending on the composition. It works best when FA is high and CR is limited, which allows Fe to become part of the amorphous gel. When calcium is too high, Fe tends to separate out and reduce performance (Tchakouté, H K et.al, 2016).
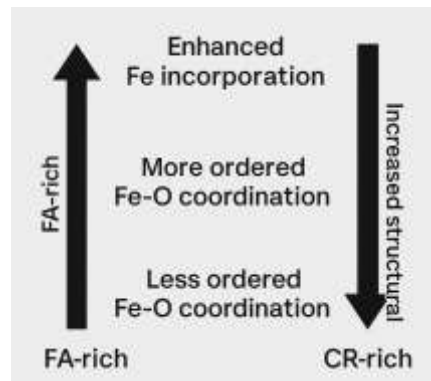
Figure 5 Cross-Technique Correlation

4. Conclusions

This study explored how iron (Fe) affects the structure and strength of geopolymers made from fly ash (FA), bagasse ash (BA), and calcium carbide residue (CR). Using synchrotron-based XANES and EXAFS techniques, we found that Fe remained in the +3 oxidation state in all samples, but its local coordination environment varied depending on the mix design.

In FA-rich systems, Fe was better integrated into the amorphous aluminosilicate gel, as shown by lower white line intensities and more ordered Fe–O environments. These systems maintained higher compressive strength. In contrast, CR-rich compositions showed more crystalline hematite phases and disordered Fe coordination, leading to weaker strength due to poor gel formation and incomplete polymerization.

Overall, the results demonstrate that the role of Fe in geopolymer systems is highly dependent on the precursor blend. Fly ash helps stabilize Fe in the gel network, while excessive calcium from CR can hinder Fe incorporation and reduce performance. These insights support the potential of using Fe as a structural modifier in geopolymer systems, provided that precursor balance is carefully optimized.

5. Acknowledgements

6. References

Amin, M. N., Ahmad, A., Shahzada, K., Khan, K., & Qadir, M. G. (2022). Mechanical and microstructural performance of concrete containing high-volume of bagasse ash and silica fume. *Scientific Reports, 12*, 5719.

Davidovits, J. (1991). Geopolymers: Inorganic polymeric new materials. *Journal of Thermal Analysis, 37*(8), 1633–1656.

Lemougna, P. N., MacKenzie, K. J. D., Jameson, G. N. L., Rahier, H., & Chinje Melo, U. F. (2013). The role of iron in the formation of inorganic polymers (geopolymers) from volcanic ash: A ^{57}Fe Mössbauer spectroscopy study. *Journal of Materials Science, 48*(15), 5280–5286.

Newville, M. (2004). *Fundamentals of XAFS*. Consortium for Advanced Radiation Sources, University of Chicago.

Ngnintedem, D. L. V., Lampe, M., Tchakouté, H. K., & Rüscher, C. H. (2022). Effects of iron minerals on the compressive strengths and microstructural properties of metakaolin-based geopolymer materials. *Gels, 8*(8), 525.

Parsons, J. G., Aldrich, M. V., & Gardea-Torresdey, J. L. (2002). Environmental and biological applications of extended X-ray absorption fine structure (EXAFS) and X-ray absorption near edge structure (XANES) spectroscopies. *Applied Spectroscopy Reviews, 37*(2), 187–222.

Provis, J. L., & van Deventer, J. S. J. (2009). *Geopolymers: Structure, processing, properties and industrial applications*. Woodhead Publishing.

Tchakouté, H. K., Rüscher, C. H., Elimbi, A., & Djobo, J. N. Y. (2016). Influence of iron content on the structure and mechanical properties of metakaolin-based geopolymer cements. *Applied Clay Science, 119*, 258–265.

Wang, Q., Guo, H., Yu, T., Yuan, P., Deng, L., & Zhang, B. (2022). Utilization of calcium carbide residue as solid alkali for preparing fly ash-based geopolymers: Dependence of compressive strength and microstructure on calcium carbide residue, water content and curing temperature. *Materials, 15*(3), 973.

Zhang, G., & Provis, J. L. (2020). Effect of calcium additions on N–A–S–H cementitious gels. *Cement and Concrete Research, 135*, 106141.

Influence of Pozzolanic Materials in Ternary Blend Systems on Strength and Chloride Resistance of Concrete

Chakkarphan Sangsuwan[a], Gritsada Sua-Iam[a], Nutchapongpol Kongchasing[a*], Kwanchanok Oonta-on[a], Buchit Maho[a], Tanapat Namjan[a], Phattharachai Pongsopha[a] Darrakorn Intarabut[a]

[a] Department of civil engineering, Faculty of engineering, Rajamangala University of Technology Phra Nakhon (RMUTP), Bangkok,10800, Thailand.
* Corresponding author, E-mail address: Nutchapongpol.k@rmutp.ac.th

Abstract

Pozzolanic materials (fly ash, meta kaolin, and silica powder) were investigated to partially replace cement based on their impact on the strength and chloride resistance of the concrete. The compressive strength was investigated in the range 240–350 kg/cm^2 with a water-to-binder ratio (w/b) of 0.40 for the best performance, while varying the amount of cement replaced by ternary blended systems using cement with the main quantities by weight of cement being fly ash (65%), kaolin (10–15%), and silica powder (2.5 or 5%) compared to the controlled sample and cementitious mixtures. The concrete mix included high volume water-reducing agent (superplasticizer Type F) of a special water-reducing type. Along with tests of the mechanical properties of compressive strength, splitting tensile strength, flexural strength, and also chloride ion movement test electrolysis using the chloride migration test. The test results showed that the ternary blended systems of the concrete containing the pozzolanic materials at w/b equal to 0.40 had the best mechanical properties. The concrete mixture with replacement of cement with fly ash and metakaolin with alumina oxide had a greater effect on compressive strength than adding silica. The tensile strength and flexural strength were better in the mixture of fly ash and silica powder, as was the electrophoretic movement of chloride ions in the concrete, with better binding of chlorine. However, the physical properties of the metakaolin and silica powder, such as their particle distribution and high specific surface area, resulted in a more rapid pozzolanic reaction that increased the CSH and CAH, and increased the opacity of the concrete, resulting in overall improved mechanical properties of the concrete.

Keywords: Pozzolans, Compressive Strength, Flexural Strength, splitting Tensile Strength, Chloride Migration

1. Introduction

Traditionally, most general structures use reinforced concrete based on the expectation that the structure should be durable under normal conditions. In fact, most designs do not consider resistance. However, reinforced concrete structures containing steel that comes into contact with seawater or brackish water or is used for construction in coastal areas, including underground structures, can be damaged by environmental factors that affect the mechanical properties of the concrete. This results in the structural strength being continuously reduced, making this a problem that must be addressed as a high priority. Maintenance and repair can help to extend the life of the structure so that it can be used for a long time. In the past, many researchers have studied the development and improvement of the properties of concrete to make it stronger and denser [Cheng et al., 2017; Mindess et al., 2003, Neville A.M, 1996] by modifying the materials used. Concrete improvement has commonly used pozzolanic materials, such as fly ash and kaolin (meta kaolin), which when mixed in the concrete in appropriate amounts will cause a pozzolanic reaction, resulting in more CSH and CAH compounds in the concrete and producing concrete having a denser internal structure and higher strength [Gopalan M.K., 1993 and Sangsuwan C., Sujjavanich S, 2020]. However, such studies focused mainly on improving the compressive strength and density of the concrete [Ichikawa T., 2009]. In addition, there have been reports on the properties associated with resistance to chloride penetration to prevent corrosion of the steel reinforcement in concrete, especially in a marine environment involving contact of concrete with sea or brackish water, where the life span is reduced and may include resistance to alkaline silica reaction (ASR) [Arya C et al., 1996; Sangsuwan C., Sujjavanich S, 2012; Prince W., Gagné R., 2001]. The current research studied resistance to chloride permeation in concrete mixed with pozzolanic materials (fly ash and silica powder) with the aim of identifying the most appropriate concrete mixture based on testing compressive strength, splitting tensile strength, flexural strength, and the permeability of chloride solution in the concrete.

2. Materials and Methods

2.1 Materials

Pozzolanic material, a waste material from industrial plants, and natural materials were used as a partial replacement for cement. The ternary blended systems used Ordinary Portland cement type 1 (OPC) and fly ash (FA) as the main contents (65%), with metakaolin (MK) varying between 10% and 15% and silica powder (SP) at 2.5 or 5%, as well using control samples. The tested mechanical properties consisted of: compressive strength, split tensile strength, flexural strength, and a chloride migration test of the concrete.

1) Cement

The OPC had a specific gravity of 3.13, with details provided in Table 1.

2) Pozzolans

FA, MK, and SP were used, with the FA from power plants in Lampang province Thailand, the MK from Metamax Co., Ltd, imported from the United States, and the SP from the Herosign Marketing Co., Ltd, imported from China, as shown in Table 1.

3) Aggregate

Fine aggregate was obtained from river sand that had passed through sieve number 4 with mixed sizes according to the ASTM C 33 standards and a fineness modulus (F.M.) of 2.58, absorption 2.15 (%), surface moisture of 3.95% and specific gravity of 2.65. The coarse aggregate consisted of crushed limestone in the size range 10–19 mm, with mixed sizes according to ASTM C 33 standards, and an F.M. value of 2.85, water absorption equal to 1.00, 0.65% surface moisture, 2.85 specific gravity, and a density of 1,680 kg/m^3.

4) Admixture

Special water reducer type HRWR Admixture (Superplasticizer) of Sika (THAILAND) Limited.

Table 1 Chemical compositions of raw materials.

Oxide	Chemical Composition, %										
	SiO_2	Al_2O_3	Fe_2O_3	CaO	MgO	Na_2O	K_2O	MnO_2	SO_3	$Na2O_{eq}$	LOI
Cement	17.2	4.95	3.89	61.23	0.73	0.057	0.48	0.047	2.14	0.373	2.01
Fly ash	35.21	18.54	12.25	16.24	2.14	1.158	1.98	-	2.98	2.461	0.475
Metakaolin	49.58	41.22	0.287	0.018	<0.00	0.24	0.12	-	0.057	0.319	-
Silica powder	99.72	0.074	0.010	0.0094	0.0033	0.004	0.005	-	-	0.007	-

2.2 Mixture Proportions

The influence was studied of using pozzolanic materials (FA, MK and SP) in partial replacement of cement. The manufactured concrete was designed to have a compressive strength in the range 350–400 kg/cm^2. Different concrete samples were investigated using three levels or cement replacement (0.40, 0.45 and 0.50). The main component was the OPC and FA (65%), with MK levels of 15% or 10% and SP levels of 5% or 2.5% by weight of cement. The following terms were used to define the respective samples: OPC/FA20/MK15, OPC/FA25/MK10, OPC/FA20/SP5, and OPC/FA25/SP2.5.

2.3 Sample Preparation and Test Methods

Test samples were prepared for the concrete mix proportions used in the design test according to the recommendations of ACI 211.1-1, with water-to-binder (w/b) ratios of 0.40, 0.45, or 0.50 and a cement- to-sand-to-coarse aggregate ratio equal to 1:2:4 by volume. The materials used to produce 1 m^3 of concrete are provided in Table 2.

Table 2 Mix proportions of ternary blended concrete (kg/m^3).

Mix	w/b	HRWR (%)	OPC (kg/m^3)	FA (kg/m^3)	MK (kg/m^3)	SP (kg/m^3)	Coarse Aggre. (kg/m^3)	Fine Aggre. (kg/m^3)	Water
OPC	0.40	-	440	-	-	-	721	1,066	176
OPC/FA20/MK15		0.5	286	88	66	-			
OPC/FA25/MK10		0.5	286	110	44	-			
OPC/FA20/SLP5		0.75	330	88	-	22			
OPC/FA25/SLP2.5		0.75	319	110	-	11			
OPC	0.45	-	440	-	-	-	721	1,066	198
OPC/FA20/MK15		0.5	286	88	66	-			
OPC/FA25/MK10		0.5	286	110	44	-			
OPC/FA20/SLP5		0.75	330	88	-	22			
OPC/FA25/SLP2.5		0.75	319	110	-	11			
OPC	0.50	-	440	-	-	-	721	1,066	220
OPC/FA20/MK15		0.5	286	88	66	-			
OPC/FA25/MK10		0.5	286	110	44	-			
OPC/FA20/SLP5		0.75	330	88	-	22			
OPC/FA25/SLP2.5		0.75	319	110	-	11			

Sample preparation and curing of concrete were performed according to ASTM C192. After mixing the concrete samples were tested for collapse, according to ASTM C143. After the concrete had hardened for 24 hours, it was removed from the mold and immersed in water for 28 days. The compressive strength of the hardened concrete was measured, using the procedures in ASTM C39. Cube-shaped samples of (10x10x10 cm) were prepared and cured for 28 days before testing. The splitting tensile strength test was measured, using the standard test method (ASTM C494). Cylindrical-shaped samples (20 cm height and 10 cm diameter) were produced and immersed in water for 28 days before testing. The flexural strength test was in accordance with the standard test method (ASTM C78-94) using a small simple beam (10×10×60 cm) with third-point loading. UTM (1500 kN) equipment was used for the test. The chloride migration test method was in accordance with the standard test (JSCE-G571-2003).

The chloride migration test by cylindrical concrete samples (4 inches diameter) were made using the ternary blended mixtures and the control mixture, as shown in Table 2. Each concrete sample was soaked in water for 28 days. Then, the concrete was cut into slices (2 inches thick) and installed in the testing device. The movement of chloride ions was determined based on electrolysis using the chloride migration test and Nernst Planck's equation (modified Fick's second law) [Polder R.B, 1996] from the JSCE -G571-2003 standard. The sample was soaked in distilled water for 24 hours and then an electric potential difference of 12 V was applied and the amount of chloride ions in the solution was measured every 5 days using a chloride analyzer.

Other studies have investigated the coefficient of chloride diffusion in concrete for a steady state (steady state diffusion) [Goto S, and Roy, D.M., 1981], which may be quite slow and time consuming, especially for high performance concrete. For this reason, an effective method is applied to accelerate the movement of chloride ions in hardened concrete by means of "electrical conduction" or "migration" [El-Belbol S.M, and Buenfeld, N.R., 1988 and McGrath P.F and Hooton R.D., 1996]. The test uses a direct current electric potential difference to apply power to the positive and negative terminals on either side of the test specimen. Chloride ions penetrate the concrete sample and are deposited in the solution at the anode. Chloride permeability can be determined based on the steady-state chloride flux, the conduction current, or the steady-state chloride permeability.

With non-steady state diffusion and conduction, Nernst Planck's second law or Fick's second law is used to describe the transport of chloride ions in the accelerated chloride test, as shown in Equation 1:

$$\frac{dC}{dt} = -\frac{dj}{dx} = D\left[\frac{d^2C}{dx^2} - \frac{zF\Delta V}{RTl} * \frac{dC}{dx}\right] \tag{1}$$

The exact analytical solution for Equation 2 is:

$$C = \frac{C_o}{2}\left[e^{\alpha x} * erfc\left(\frac{x+\alpha Dt}{2\sqrt{Dt}}\right) + erfc\left(\frac{x-\alpha Dt}{2\sqrt{Dt}}\right)\right] \tag{2}$$

where:
$$\alpha = \frac{zF\Delta V}{RTl}$$

and Z = the ion valence, F = Faraday's constant, ΔV= the potential drop across the sample, R = the gas constant, T = the temperature in Kelvin, l = the sample length, C = the pore solution concentration at any depth and time t , and C is the pore solution concentration at the surface [McGrath P.F, and Hooton R.D., 1996].

For the case of a steady state conduction flux, where the diffusion component is small, Equation 3 simplifies to:

$$J_{cl} = D_e\frac{z_{cl}FC_{cl}(\Delta E - \Delta E_c)}{RTl} \tag{3}$$

Where J_{Cl} = the flux of chloride ions in a steady state (mol/(cm^2 /year) , D_e = effective diffusion coefficient (cm^2 /year), R = the gas constant (8.31 J/(mol K)), Z_{Cl} = charge of chloride ion (-1), L = the length (mm), F = Faraday's constant (96,500 C/mol), C_{Cl} = the chloride ion concentration (mol/l), ΔE - ΔE$_C$= the potential gradient (V), and T = time

For the test, a cylindrical concrete sample was prepared with a diameter of 4 inches and incubated for 28 days. After that, the concrete was cut to measure the movement of chloride ions based on electrolysis using the chloride migration test using Nernst Planck's (Modified Fick's second law) [14] from the JSCE–G571-2003 standard. Each sample was immersed in distilled water for 24 hours, then an electric potential difference of 15 V was applied, as shown in Figure 4 (c), and the chloride content was measured in the solution every 5 days using a chloride analyzer, as shown in Figure 1 (a) and (b).
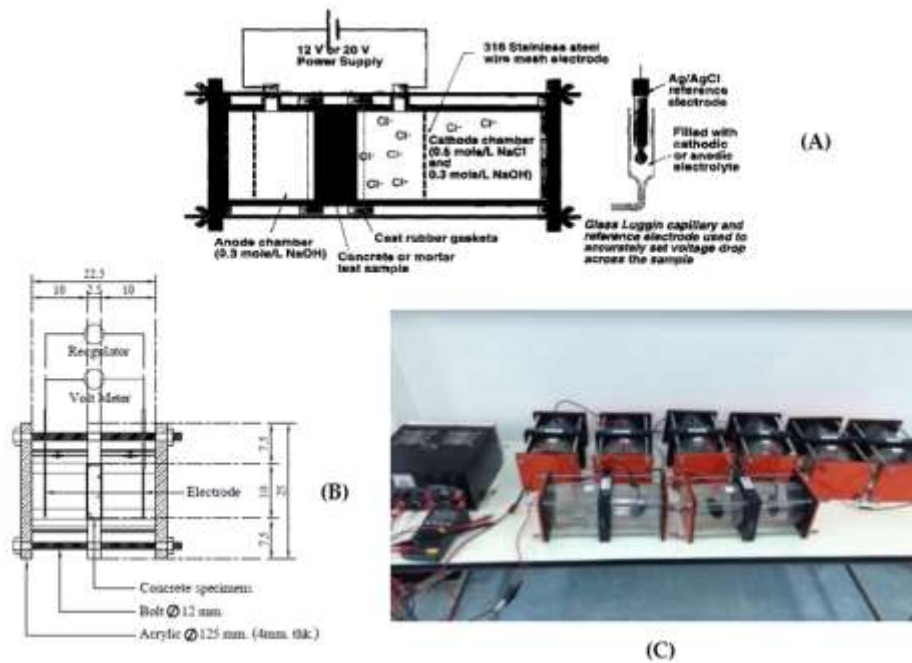
Figure 1 (a) shows amount of chloride released from the concrete to accumulate in solution based on chloride migration test, (b) [McGrath P.F, and Hooton R.D., 1996] and (c) Equipment and specimens for testing chloride ion mobility based on electrolysis.

3. Results and Discussion
3.1 Compressive Strength

Figure 2 shows the results of the compressive strength of concrete after 28 days that was equal to 450 kg/cm². Using the lowest ratio (w/b = 0.40) produced better results than from 0.45 or 0.50, with the cement with the highest compressive strength being for M/PFA20/MK15 (580 kg/cm²) that was 26% more than for the control, 16% more than for M/PFA25/MK10, and more than M/PFA20/SP5 and M/PFA25/SP2.5 by 10% and 18%, respectively. Thus, the mixtures including meta kaolin (10–15%) had 5–9% higher compressive strength than from using an increased amount of silica powder (2.5–5%), which were considered to little different in practice, similar to the mixtures with increased fly ash content (20–25%) not being very different in compressive strength. According to the research reported [10], it affects the improvement of concrete properties in terms of reaction sensitivity and the characteristics of increasing the amount of cementitious CSH and CAH from the pozzolanic reaction, resulting in a micro filler effect decreasing the number of gaps. and slowing the movement of the solution making the concrete more dense, with increased mechanical properties and durability [Li G., 2004 and Shafiq N et al., 2015].
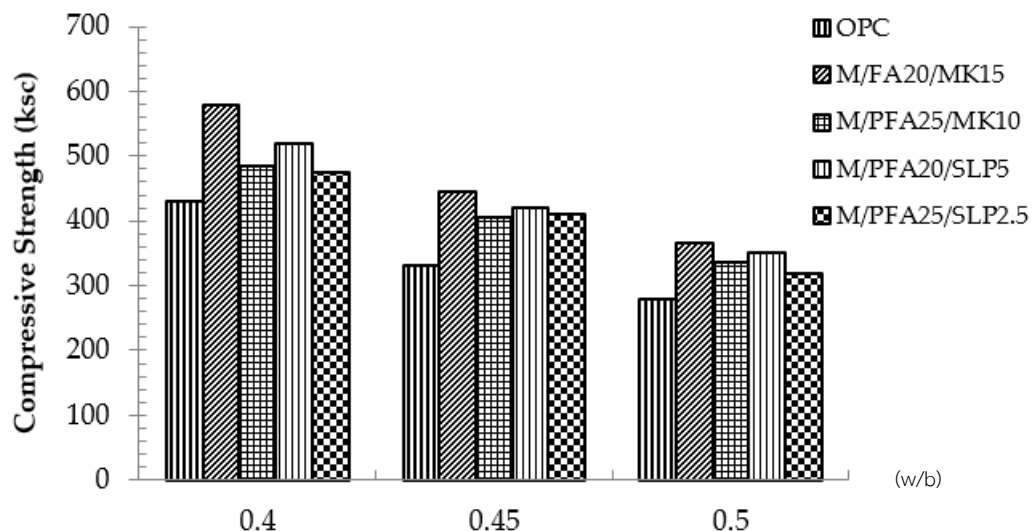
Figure 2. The relationship between compressive strength of control concrete and concrete mixed with tri-interlocking pozzolanic materials (w/b =0.40, 0.45, and 0.50).

3.2 Splitting Tensile Strength and Flexural Strength

From Figure 3, the split tensile strength of concrete after 28 days in the control concrete mix was 24 kg/cm^2 using the lowest water-to-binder ratio (w/b = 0.40), which was a better result than from using either 0.45 or 0.50. The hemispherical tensile strength of the M/PFA20/MK15 mix was 35 kg/cm^2, being 31% higher than the control concrete mix. It was observed that the control mixture had a lower tensile strength than every mixture involving the pozzolanic materials, with values in the range 14–31%. From Figure 4, the results of the flexural strength of concrete after 28 days showed that the control concrete mix had a flexural strength of 60 kg/cm^2, using a low water-to-binder ratio. The highest flexural strength was with w/b = 0.40. The results for the flexural strength of the control mixture showed a similar trend to the compressive and tensile strengths of the hemi section. The M/PFA20/MK15 tri-admixture had the highest flexural strength of 69 kg/cm^2 that was 13% higher than for the control concrete mix, with every tri-adhesive mixture producing the same results with the flexural strength being greater than that of the control mixture, with similar values in the range 10–13%.

However, the mixture containing 10–15% MK developed higher compressive strength than from using 2.5–5% SP. The compressive strength of MK is 5–9% greater than that of silica powder which is not considered to much different in practice. The mixtures with 20–25% fly ash content and ternary blended had very different compressive strength values. Various researchers have reported the improved properties of concrete in terms of reactivity and other characteristics due to the increased amount of cementitious C-S-H and C-A-H from the pozzolanic reaction, resulting in a micro filler effect, filling in voids and slowing the movement of the solution as the concrete is denser, with increased mechanical properties and durability. In addition, SP contains a relatively high amount of SiO_2 and a high specific surface area, which are beneficial to the pozzolanic reaction, causing increased CSH with a low Ca/Si ratio and greater compression power [Shafiq N et al., 2015 and Qureshi L.A et al., 2020].
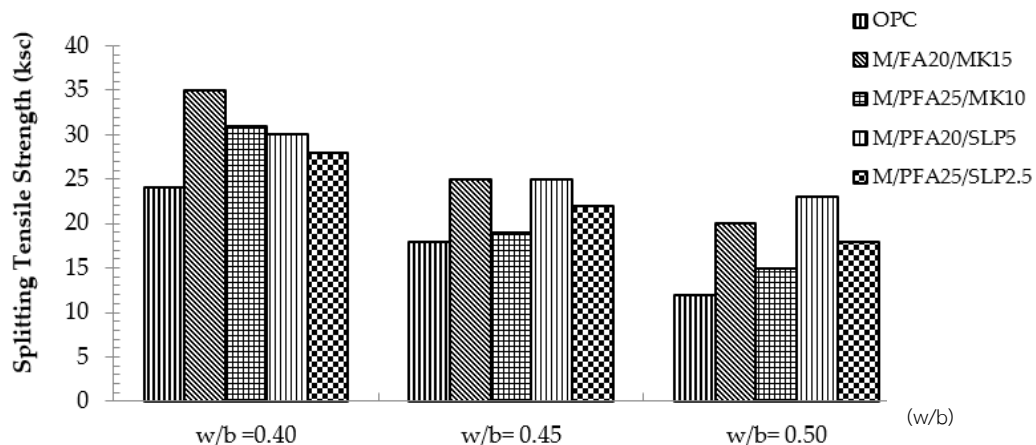

Figure 3 The relationship between tensile strength of control concrete and concrete mixed with pozzolanic materials (w/b =0.40, 0.45, or 0.50).
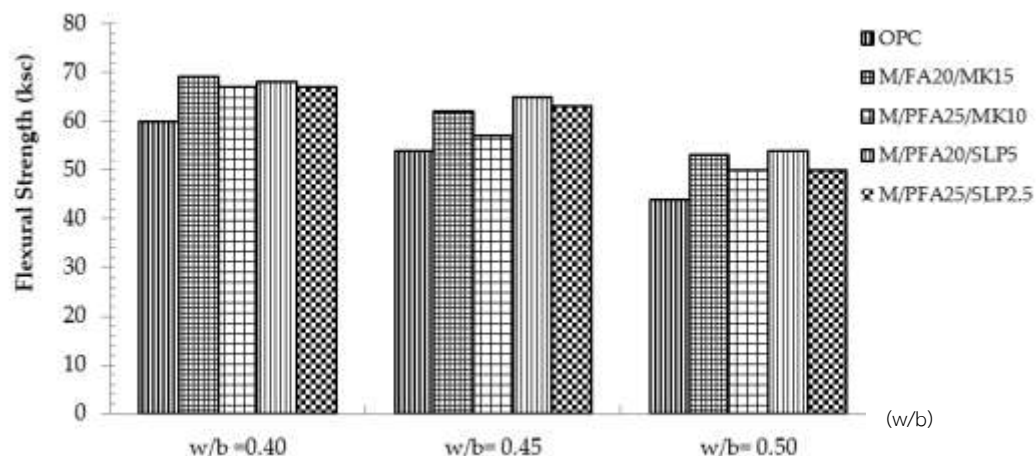

Figure 4 The relationship between flexural strength of control concrete and concrete mixed with pozzolanic materials (w/b =0.40, 0.45, or 0.50).

3.3 Chloride Migration Test

The results of the chloride migration test in terms of the flow rate (Flux, J_{Cl}) of chloride ions and the diffusion coefficient of the concrete in the test were used as data to predict the reduction of chloride content based on electrochemical methods to compare with the laboratory experimental results.

From Figure 1, considering the movement of chloride ions based on electrolysis in concrete aged 28 days, the w/b ratio of 0.40 produced the best cumulative movement of chloride content compared to w/b =0.45 and 0.50. The mixture of control concrete at an initial age of 5 days had an accumulated chloride amount of 200 mg/l, which continued to increase until 35 days of age, with an accumulated chloride amount of 1,300 mg/l. In contrast, at age 5 days, of the three cementitious mixtures, the lowest decrease in permeability by chloride ion content was for the mixture M/PFA25/SLP2.5 (50 mg/l), reduced by 25% compared to the control mixture, while the other mixtures tended to decrease similarly. The greatest decrease in chloride permeability was for the 35-day-old mixture of M/PFA25/SLP2.5 with reductions of 12, 14, 18, and 27% compared to the control mixture: M/PFA20/SLP5, M/PFA25/MK10, and M/PFA20/MK15, respectively.

These results suggested that the ternary blended mixtures M/PFA25/SLP2.5 and M/PFA20/SLP5 were more effective in reducing the amount of chloride permeability in ternary blended concrete than the other tested material mixes. The SiO_2 content in the SP from the pozzolanic reaction changed some calcium hydroxide in the concrete to cementitious materials (C-S-H, C-A-H), helping to improve various properties of the concrete, such as water permeability and durability [Ustabaş İ, and Kaya, A., 2018] In addition, the small kaolin particles helped to improve the quality of the concrete by filling small spaces (the microfiller effect), reducing porosity, and making the concrete more opaque, resulting in higher concrete strength and durability [Malhotra V et al., 2000 and Hasan Z.A et al., 2021]. The optimal amounts of fly ash, metakaolin, and silica powder to replace cement to improve concrete properties were approximately 2.5–5% by weight.
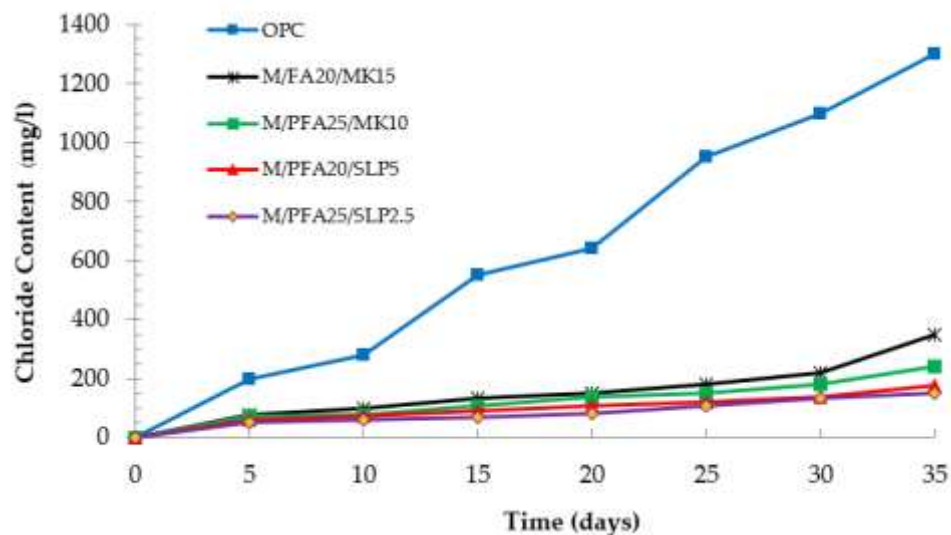
Figure 5. Amount of chloride accumulated in (NaOH) solution of ternary blended concrete and control samples based on chloride migration test (w/b =0.40).

4. Conclusions

The waste materials were investigated from an electric plant for use in natural concrete works by incorporating fly ash, metakaolin and silica powder as SCM use mixes with concrete. In addition, the effects were investigated of the SCM ternary blended systems on the freshness and hardness properties of concrete and mortar cement. The main conclusions drawn are provided below.

In addition, every ingredient of the ternary blended system used a different amount of HRWR (superplasticizer), especially the mixture containing silica powder that contained 0.75% more HRWR water-reducing agent than the mixture containing kaolin that contained 0.50% because the silica powder had a higher specific surface area, resulting in more water absorption than the mixtures containing metakaolin.

The mechanical properties (Compression strength, Flexural strength and split tensile strength) were all positively affected when the cement was partially replaced with 20% FA, 15% MK and 5% SP. The addition of 2.5-5% SP slightly increased the mechanical strength of the concrete in contrast with the partial replacement of cement with FA and MK that had greater silica and alumina oxide contents than silica, which improves the mechanical properties of concrete, resulting in higher strength.

Using the three coordinated ingredients of M/PFA25/SP2.5 and M/PFA20/SP5 was more effective in reducing the amount of chloride permeability in the three-cement concrete system than any of the other mixtures. Due to the amount of SiO_2 in the silica powder from the pozzolanic reaction, some calcium hydroxide in the concrete was changed to cementitious materials (CSH, CAH), helping to improve various properties of the concrete such as water permeability and durability. In addition, metakaolin clay improved the quality of the concrete by inserting kaolin particles into small voids (micro filler effect), reducing porosity and making the concrete more opaque, resulting in the concrete having greater power and durability.

The studied binary blended systems produce very similar pozzolanic reaction results, especially metakaolin yields more alumina than silica and produces more C-S-H and C-A-H products in the mortar. The CaO/SiO$_2$ ratio was low, resulting in an increased number of nuclei and higher opacity. This C-S-H gel partially fills the pores of the voids, causing the cement paste to have an increased density in the Interfacial Transition Zone (ITZ).

5. Acknowledgments

6. References

Arya, C. Sa'id-Shawqi, Vassie, P.R.W. 1996. 6AU (Refereed) (Received November 7. in Final Form April 9, 1996). Cem. Concr. Res. 26, 851–860.

Cheng, S. Shui, Z. Sun, T. Yu, R. Zhang, G. Ding, S. 2017. Effects of Fly Ash, Blast Furnace Slag and Metakaolin on Mechanical Properties and Durability of Coral Sand Concrete. Appl. Clay Sci. 141, 111–117. doi:10.1016/j.clay.2017.02.026.

El-Belbol, S.M. Buenfeld, N.R. 1988. Accelerated Chloride Ion Diffusion Test. MRS Online Proc. Libr. 137, 203–208. doi:10.1557/PROC-137-203.

Gopalan, M.K. 1993. Nucleation and Pozzolanic Factors in Strength Development of Class Fly Ash Concrete. ACI Mater. J. 90. doi:10.14359/4005.

Goto, S. Roy, D.M. 1981. Diffusion of Ions through Hardened Cement Pastes. Cem. Concr. Res. 11, 751–757. doi:10.1016/0008-8846(81)90033-8.

Hasan, Z.A. Nasr, M.S. 2021. Abed, M.K. Properties of Reactive Powder Concrete Containing Different Combinations of Fly Ash and Metakaolin. Mater. Today Proc. 42. 2436–2440. doi:10.1016/j.matpr.2020.12.556.

Ichikawa, T. 2009. Alkali-Silica Reaction, Pessimum Effects and Pozzolanic Effect. Cem. Concr. Res. 39, 716–726. doi:10.1016/j.cemconres.2009.06.004.

Li, G. 2004. Properties of High-Volume Fly Ash Concrete Incorporating Nano-SiO 2. Cem. Concr. Res. 34. 1043–1049. doi:10.1016/j.cemconres.2003.11.013.

Malhotra, V. Zhang, M.-H. 2000. Read, P.; Ryell, J. Long-Term Mechanical Properties and Durability Characteristics of High-Strength/High-Performance Concrete Incorporating Supplementary Cementing Materials under Outdoor Exposure Conditions. Aci Struct. J. 97. 518–525.

McGrath, P.F. Hooton, R.D. 1996. Influence of Voltage on Chloride Diffusion Coefficients from Chloride Migration Tests. Cem. Concr. Res. 26, 1239–1244. doi:10.1016/0008-8846(96)00094-4.

Mindess, S. Young, J.F. Darwin, D. 2003. Concrete; Prentice-Hall civil engineering and engineering mechanics series; Prentice Hall. ISBN 9780130646323.

Neville, A.M. 1996. Properties of Concrete: Fourth and Final Edition. Wiley. ISBN 9780582230705.

Polder, R.B. 1996. Electrochemical Chloride Removal from Concrete Prisms Containing Chloride Penetrated from Sea Water. Constr. Build. Mater. 1996. 10. 83–88. doi:10.1016/0950-0618(95)00062-3.

Prince, W. Gagné, R. 2001. The Effects of Types of Solutions Used in Accelerated Chloride Migration Tests for Concrete. Cem. Concr. Res.- CEM CONCR RES. 31. 775–780. doi:10.1016/S0008-8846(01)00473-2.

Qureshi, L.A. Ali, B. Ali, A. 2020. Combined Effects of Supplementary Cementitious Materials (Silica Fume, GGBS, Fly Ash and Rice Husk Ash) and Steel Fiber on the Hardened Properties of Recycled Aggregate Concrete. Constr. Build. Mater. 263. 120636. doi:10.1016/j.conbuildmat.2020.120636.

Sangsuwan, C. Sujjavanich, S. 2012. Effects of Moderate Calcium Oxide Fly Ash on Expansion of Mortar Bar Due to Thai Reactive Aggregates. Eng. J. 16. doi:10.4186/ej.2012.16.3.101.

Sangsuwan, C. Sujjavanich, S. 2020. Influence of Type and Compositions of SCMs on Expansion of Mortar Bars from Alkali Silica Reaction. Eng. J. 24. 1–10. doi:10.4186/ej.2020.24.1.1.

Shafiq, N. Nuruddin, M.F, Khan, S.U, Ayub, T. 2015. Calcined Kaolin as Cement Replacing Material and Its Use in High Strength Concrete. Constr. Build. Mater. 81. 313–323. doi:10.1016/j.conbuildmat.2015.02.050.

Thomas, M. 2011. The Effect of Supplementary Cementing Materials on Alkali-Silica Reaction: A Review. Cem. Concr. Res. 41. 1224–1231 doi:10.1016/j.cemconres.2010.11.003.

Ustabaş, İ. Kaya, A. 2018. Comparing the Pozzolanic Activity Properties of Obsidian to Those of Fly Ash and Blast Furnace Slag. Constr. Build. Mater.164. 297–307. doi:10.1016/j.conbuildmat.2017.12.185.

Gamma Shielding Efficiency of Sedimentary Rock-Based Bricks for Low-Energy Applications

Pitchpilai Khoonphunnarai[a], Sutthisa Konruang[b], Phayao Yongsiriwit[a],

[a] Division of Physics, Faculty of Science and Technology, Songkhla Rajabhat University City Songkhla, ZipCode 90000 Country Thailand
[b] Division of Physics, Faculty of Science, Thaksin University City Phatthalung, ZipCode 93210.Country Thailand
* Corresponding author. Tel.098-3966415; *E-mail address:* pitchpilai.kh@skru.ac.th

Abstract

Ensuring human safety requires understanding the radiation shielding capabilities of building materials alongside their strength and durability. This study investigates the potential of concrete made from two types of sedimentary rocks, shale and calcareous, for shielding against Co-60 gamma rays at energy levels of 960 keV and 1180 keV. The sedimentary rocks were sourced from the Global Geopark region in Satun Province, Thailand. The shielding performance of sedimentary rock-based concrete is compared with standard construction concrete, with both having identical dimensions of 15 cm × 15 cm × 15 cm and a cement-to-sand-to-stone ratio of 1:2:4. Engineering properties such as density and compressive strength are analyzed. Gamma shielding efficiency is assessed using the linear attenuation coefficient (μ_l), mass attenuation coefficient (μ_m), mean free path (MFP), half-value layer (HVL), and tenth-value layer (TVL). The results indicate that standard concrete exhibits the highest compressive strength, while shale-based concrete provides superior attenuation of gamma rays at the studied energy levels. The effectiveness of gamma radiation shielding in construction materials is influenced by the internal composition of the stone or concrete mixture.

Keywords: Gamma Radiation Shielding, Sedimentary Rocks, Concrete Against Radiation

1. Introduction

Gamma radiation, a form of ionizing radiation, poses significant risks to human health and the environment due to its high energy and strong penetrating ability. Effective shielding against gamma radiation is therefore essential in a wide range of sectors, including medical facilities, nuclear power plants, and radiation-related construction applications. Traditionally, radiation shielding has relied heavily on materials such as lead and concrete, which are known for their high attenuation capacity. However, these conventional materials present notable drawbacks, including high costs, substantial weight, and environmental concerns related to their production, handling, and disposal.

In recent years, there has been a growing interest in the development of alternative shielding materials that are more sustainable, lightweight, cost-effective, and environmentally friendly. Among these alternatives, sedimentary rocks have garnered attention due to their natural abundance, compositional diversity, and potential radiation attenuation properties. Sedimentary rocks are formed through the long-term accumulation, compaction, and lithification of mineral and organic particles. Their distinct physical and chemical characteristics—such as density, mineral composition, and porosity—may make them viable candidates for radiation shielding applications.

Rocks are fundamental materials commonly used in construction, both for coating and flooring. The scientific definition of rocks encompasses a solid aggregate naturally formed from one or more minerals, volcanic glass, or organic materials (Kadir Günoğlu et al., 2024). Concrete, a widely used composite material, consists of a mixture of cement paste and aggregates. The mechanical and gamma radiation attenuation properties of concrete can be altered by varying the types of aggregate used. Concrete composites are well-recognized for their adaptability and effectiveness in shielding applications in sectors such as nuclear power plants, radioactive waste disposal, and nuclear medicine (R.S. Aita et al., 2024).

Incorporating cement into a composite material with sedimentary rocks presents a promising approach to enhance radiation shielding efficiency. Cement-based composites have been extensively studied for their mechanical strength, durability, and cost-effectiveness in construction. When combined with sedimentary rocks such as sandstone and shale, these composites may further improve gamma radiation attenuation while maintaining the desired structural integrity. The versatility of composite materials allows them to be molded into various forms, which makes them applicable for radiation shielding in medical and nuclear settings as well as in construction.

The addition of cement to sedimentary rocks also optimizes the porosity and density of the composite, which directly influences its ability to reduce gamma radiation penetration. Moreover, these composite materials are relatively cost-effective and can be locally produced, making them an attractive option for countries where traditional shielding materials are either prohibitively expensive or difficult to obtain. In particular, composite materials align with the growing demand for eco-friendly and sustainable building materials, as they can be designed to minimize environmental impact during production and disposal.

This study investigates the feasibility of utilizing bricks made from sedimentary rocks—specifically shale and calcareous—as effective shielding materials against gamma radiation. The goal is to evaluate the shielding efficiency of these sedimentary rock-based bricks by analyzing key parameters, such as their density, composition, and compressive strength, and comparing them to traditional shielding materials. This research aims to contribute to the development of practical, sustainable alternatives for gamma radiation shielding, particularly in contexts where accessibility, cost, and environmental impact are key considerations.

2. Methodology

2.1 Samples preparation

This study investigates the effectiveness of solid concrete, derived from sedimentary rocks, in shielding low-energy gamma radiation. The research evaluates key physical properties, including density, compressive strength, and gamma-ray shielding performance. Two types of sedimentary rocks, shale and calcareous, were selected for the study. These rocks were sourced from the UNESCO Global Geopark in Satun Province, Thailand. The rocks were then mixed with cement in a proportion of 1:2:4 by weight (cement: sand: rock), which is an optimal concrete mix ratio for construction in Thailand as shown in Figure 1.

The mixture was thoroughly blended in a concrete mixer to ensure uniformity. Subsequently, the mixture was poured into a 15 cm × 15 cm × 15 cm concrete mold and compacted to ensure density. The concrete was then cured in water for a minimum of 28–30 days, following standard curing procedures for construction-grade concrete. After curing, the physical and mechanical properties, including density, compressive strength, and gamma-ray shielding performance, were assessed. The gamma-ray shielding efficacy was tested using a NaI(Tl) detector and a Geiger-Muller counter, with a standard Co-60 gamma radiation source at energy levels of 960 keV and 1180 keV. Measurements were recorded over a period of 300 seconds.

Figure 1 Preparation of sedimentary rock blocks of size 15 cm x15 cm x15 cm

2.2 Rock-Based Bricks Characteristics

1) Chemical Composition

To analyse the elemental composition and compounds of the shale and calcareous samples, X-ray fluorescence (XRF) analysis was performed to quantify the concentration of individual elements present in the samples. This analysis was conducted using the Zetium X-ray fluorescence spectrometer (PANalytical, Netherlands). In addition, X-ray diffraction (XRD) analysis was employed to examine the crystallographic structure of the samples, utilizing the Empyrean X-ray diffractometer (PANalytical, Netherlands). The results, including the elemental composition and identified compounds, are provided.

2) Physical and Mechanical properties

The density of the prepared concrete samples was evaluated by dividing the dry weight (M) of each specimen by its calculated volume (V). The mass measurements were obtained using a digital precision balance, while the sample volumes were derived from dimensional measurements of the concrete cubes. The density was then computed in accordance with equation (1). Compressive strength refers to the maximum axial load that concrete can endure before structural failure occurs, such as cracking or crushing as shown figure 2. It serves as a critical parameter in evaluating the material's mechanical performance under compressive stress. For the testing procedure, two steel bearing platens with hardened surfaces were mounted on the testing machine to ensure uniform load distribution during compression testing and determined in equation (2) (Aita et al., 2024).

$$\rho = \frac{M}{V} \tag{1}$$

$$F_c = \frac{P}{A} \tag{2}$$

3) Gamma Ray Attenuation Coefficient

The intensity of gamma radiation (I_0) decreases when it passes through a shielding material of thickness x. The reduction in radiation intensity (I) is directly proportional to the intensity of the incident radiation as it travels through the medium. The attenuation coefficient (μ) can be determined using the following equations 3 and 4 (Wisarut Rungcharoenkit and Withit Pansuk, 2021 and Kadir Günoğlu et al., 2024):

$$I = I_0 e^{-\mu x} \tag{3}$$

Figure 2 Assessment of Compressive Strength

Alternatively, the equation can be expressed in terms of the mass attenuation coefficient as:

$$I = I_0 e^{-(\frac{\mu}{\rho})(\rho x)} \qquad (4)$$

where:

I = intensity of gamma radiation after transmission through the material (in counts per second or other suitable units),

I_o = initial intensity of gamma radiation before interaction with the material,

x = thickness of the shielding material (cm),

ρ = density of the material (kg/m³),

μ = linear attenuation coefficient $(cm^2)^{-1}$,

$\frac{\mu}{\rho}$ = mass attenuation coefficient (cm²/g).

Several factors influence the attenuation coefficient (μ), which measures the amount of radiation absorbed by a material:

The characteristics of radiation or particles: Various forms of radiation interact with matter in unique ways. Alpha particles have a significant attenuation coefficient owing to their considerable mass and strong electric charge, resulting in a higher propensity for absorption by materials. On the other hand, gamma rays can penetrate much better and have no charge, so they usually have lower μ values and require denser or thicker materials to reduce their strength.

The atomic number of a substance primarily determines its efficacy in attenuating radiation. Elements with high atomic numbers, such as lead, are better at blocking radiation because their tightly packed atoms make it more likely for radiation to hit them. Materials with lower atomic numbers are often less efficient in absorbing energetic particles and light.

The energy level of incoming radiation correlates positively with its penetrating capability. High-energy gamma rays may traverse several materials with minimum contact, leading to less attenuation. Conversely, under identical circumstances, lower-energy radiation absorbs more efficiently, leading to an elevated value.

Once the attenuation coefficient is determined, it can be used to calculate the Mean Free Path (MFP), Half Value Layer (HVL), and Tenth Value Layer (TVL) as follows:

MFP (Mean Free Path) refers to the average distance that radiation travels before interacting with the shielding material.

$$MFP = \frac{1}{\mu} \qquad (5)$$

HVL (Half Value Layer) is the thickness of the shielding material required to reduce the intensity of radiation to 50% of its initial value from the source.

$$HVL = \frac{ln\,(2)}{\mu} \qquad (6)$$

TVL (Tenth Value Layer) is the thickness of the shielding material required to reduce the intensity of radiation to 10% of its initial value from the source.

$$TVL = \frac{\ln{(10)}}{\mu} \qquad (7)$$

Figure 3 Examination of the radiation shielding characteristics of sedimentary rock block bricks

3. Results and Discussion
3.1 Chemical Composition

Table 1 Elemental and Compound Composition Analysis of Sedimentary Rocks (XRF)

Calcareous		Shale	
compound	Concentration (%)	compound	Concentration (%)
Al_2O_3	11.418	Al_2O_3	10.823
SiO_2	30.756	SiO_2	28.461
K_2O	4.370	K_2O	3.892
CaO	22.826	CaO	24.965
Fe_2O_3	3.081	Fe_2O_3	3.472

Table 2 Types of Compounds and Chemical Formula of Sedimentary Rocks (XRD)

Calcareous		Shale	
Mineral/compound name	Chemical Formular	Mineral/compound name	Chemical Formular
Quartz	SiO_2	Calcite	$Ca(CO_3)$
Calcite	$Ca(CO_3)$	Quartz	SiO_2
Pyrite	FeS_2	Dolomite	$CaMg(CO_3)_2$
Orthoclase	$K(AlSi_3O_8)$	Pyrite	FeS_2
Muscovite	$KAl_2Si_3AlO_{10}(OH)_2$	Orthoclase	$K(AlSi_3O_8)$
Dolomite	$CaMg(CO_3)_2$	Muscovite	$KAl_2Si_3AlO_{10}(OH)_2$

Tables 1 and 2 present the analysis results regarding the elements, compounds, and structure of shale and calcareous. The research indicates that both rock types include identical elements and chemicals, although they vary in their concentrations. The researcher identified the five most common elements and compounds present in both categories of rocks as follows: SiO_2 CaO Al_2O_3 K_2O and Fe_2O_3

3.2 Physical and Mechanical properties

An investigation of the physical and mechanical properties of concrete made from shale and calcareous. This study examines the physical and mechanical characteristics of concrete produced using sedimentary rocks, specifically shale and calcareous. Two key properties were assessed:

1) The density of solid concrete samples made from each rock type, and
2) Their respective compressive strengths.

According to the data presented in Table 3, the density and compressive strength of concrete blocks made from both types of sedimentary rocks were compared to those of standard construction concrete. The highest values were observed in typical construction concrete, with a density of 2,194.66 kg/m^3 and a compressive strength of 259.69 Ksc. Shale-based concrete blocks followed, with a density of 1,993.72 kg/m^3 and a compressive strength of 138.72 Ksc. The lowest values were recorded for concrete made from calcareous, at 1,883.37 kg/m^3 and 53.20 Ksc, respectively.

Table 3 Physical and Mechanical properties of Sedimentary Rock-Based Bricks

Type concrete	m (kg)	Volume (m³)	Density (kg/ m³)	Compressive strength (Ksc)
Calcareous	6.375	0.0034	1,883.37	53.20
Shale	6.789	0.0034	1,993.72	138.72
concrete	7.526	0.0034	2,194.66	259.69

3.3 Radiation shielding properties

This research examines the efficacy of solid concrete as a gamma radiation shield by incorporating sedimentary rock samples with cement. The analysed sedimentary rocks consist of two varieties: shale and calcareous, combined with cement in a ratio of 1:2:4 for cement, sand, and stone, respectively. The sedimentary rock samples included in the study were sourced from the La-Ngu District in Satun Province, which is included in the Satun Geopark. Next, the effectiveness of the dense concrete in blocking radiation was tested by using it to measure how well it reduced gamma radiation with a Geiger-Muller counter and a standard gamma radiation source, Co-60, which has an intensity of 74 kBq and a half-life of 5.3 years. The measurement duration was 300 seconds to ascertain the attenuation coefficient of thick concrete from both varieties of sedimentary rock samples and to compare it with standard building concrete. The experimental findings are shown in Table 4.

Table 4 Radiation Shielding properties

Energy (keV)	Type concrete	μ_l (cm²)⁻¹	μ_m (cm²/g)	MFP (cm)	HVL (cm)	TVL (cm)
960	Calcareous	0.15	0.08	6.90	4.78	15.90
	Shale	0.18	0.09	5.59	3.87	12.86
	Concrete	0.17	0.08	5.88	4.08	13.54
1180	Calcareous	0.07	0.04	13.51	9.37	31.12
	Shale	0.08	0.04	12.05	8.35	27.74
	Concrete	0.04	0.02	27.78	19.25	69.79
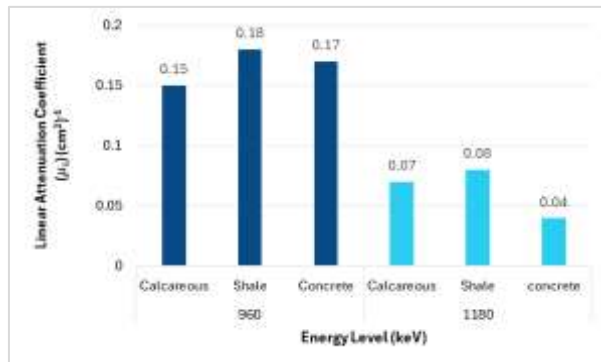
Figure 4 A graph shows the relationship between the linear attenuation coefficient and the energy levels of each kind of
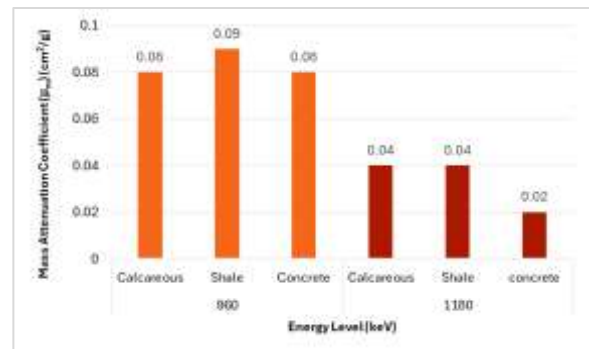
brick block.

Figure 5 A graph shows the relationship between the mass attenuation coefficient and the energy levels of of each kind

brick block.

From Figures 4 and 5, the graphs illustrate the relationships between the linear attenuation coefficient and the gamma-ray energy levels, and between the mass attenuation coefficient and the gamma-ray energy levels, respectively. The values of both the linear (μ_l) and mass (μ_m) attenuation coefficients presented in these graphs were calculated using Equation (4).

The results indicate that shale brick blocks exhibited the highest linear attenuation coefficients for gamma rays at energy levels of 960 keV and 1180 keV, with values of 0.18 (cm²)⁻¹ and 0.08 (cm²)⁻¹, respectively. Standard concrete showed a slightly lower linear attenuation coefficient at 960 keV, measured at 0.17 (cm²)⁻¹ while the calcareous brick blocks had the lowest value of 0.15 (cm²)⁻¹. At 1180 keV, the calcareous brick blocks outperformed standard concrete, with linear attenuation coefficients of 0.07 (cm²)⁻¹ and 0.04 (cm²)⁻¹, respectively.

Regarding mass attenuation coefficients (μ_m) at 960 keV, shale brick blocks again demonstrated the highest value at 0.09 cm²/g. Both the calcareous bricks and standard concrete had equal mass attenuation coefficients of 0.08 cm²/g. At 1180 keV, shale and calcareous brick blocks had the same mass attenuation coefficient of 0.04 cm²/g, while standard concrete showed the lowest value of 0.02 cm²/g.

The radiation attenuation coefficient of shielding materials serves as an indicator of their ability to absorb or reduce radiation intensity. Higher attenuation coefficients signify greater shielding effectiveness, making the material more suitable for radiation protection applications.
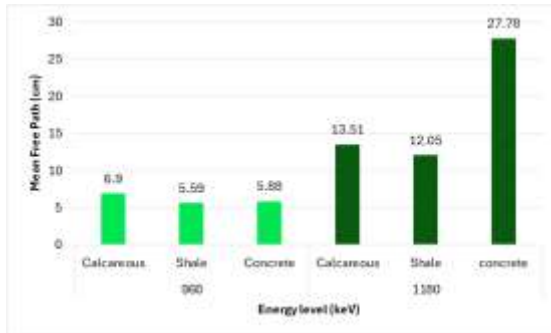
Figure 6 A graph showing the relationship between the mean free path and energy levels of each kind of brick block.
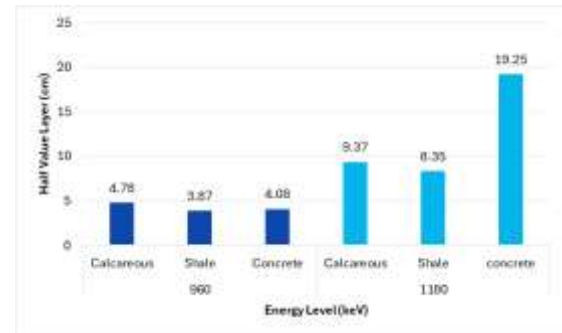

Figure 7 A graph showing the relationship between the half value layer and energy levels of each kind of brick block.
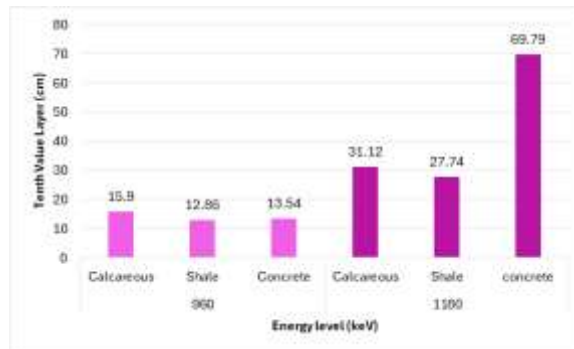

Figure 8 A graph showing the relationship between the tenth value layer and energy levels of each kind of brick block.

Analysis of radiation shielding parameters in concrete blocks made from shale and calcareous under Co-60 gamma ray energies.

Figures 6 through 8 present the graphs of three key thickness parameters—Mean Free Path (MFP), Half Value Layer (HVL), and Tenth Value Layer (TVL)—plotted against gamma-ray energy levels from Co-60 at 960 keV and 1180 keV, respectively. At 960 keV, the MFP, HVL, and TVL values for shale-based concrete blocks were 5.59 cm, 3.87 cm, and 12.86 cm. For blocks made from calcareous, the corresponding values were 6.90 cm, 4.78 cm, and 15.90 cm. Conventional standard concrete showed slightly higher values of 5.88 cm, 4.08 cm, and 13.54 cm. When the energy increased to 1180 keV, shale blocks showed values of 12.05 cm (MFP), 8.35 cm (HVL), and 27.74 cm (TVL). The calcareous blocks recorded 13.51 cm, 9.37 cm, and 31.12 cm, respectively. In contrast, standard concrete demonstrated significantly larger values of 27.78 cm, 19.25 cm, and 69.79 cm for the same parameters.

All three parameters were calculated according to the formulas provided in equations (5) through (7). The results clearly indicate that shale blocks had the lowest values across both energy levels, suggesting their superior ability to attenuate gamma radiation. Calcareous blocks performed moderately well, while standard concrete showed the least effectiveness in radiation shielding.

In practical terms, lower values of MFP, HVL, and TVL imply that a thinner material layer is needed to reduce radiation intensity. Hence, materials with lower values in these parameters are more efficient in shielding against gamma rays, particularly in applications where compactness and material economy are important.

3.4 Discussion

1) Physical and mechanical properties from density and compressive strength. This study focuses on concrete made from two types of sedimentary rocks: shale and calcareous. The mix ratio used was a fixed 1:2:4 ratio by weight of cement, sand, and aggregate. This ratio was chosen based on Surapong Daram's (2019) research, which recommends this standard mix for public construction and small-scale buildings. The highest density was found in standard concrete, at 2,194.66 kg/m^3. Concrete made with shale had a density of 1,993.72 kg/m^3, while the lowest density was observed in calcareous blocks, at 1,883.37 kg/m^3. These density values correlate closely with compressive strength, which generally increases with higher density. The compressive strengths measured were 259.69 Ksc for standard concrete, 138.72 Ksc for shale blocks, and 53.20 Ksc for calcareous blocks. While standard concrete met standard expectations, the sedimentary rock-based blocks showed lower results. This decrease may be due to the uneven nature of the aggregate mix. As noted in Surapong Daram's (2019) work, sedimentary rocks like shale and calcareous tend to have higher porosity compared to granite, which is typically used in standard concrete mixes. This porosity likely weakens the overall concrete structure, reducing both density and strength.

2) Radiation shielding properties in relation to the chemical composition of sedimentary rocks in this study, the radiation shielding performance of concrete blocks made from shale and calcareous was examined in connection with the chemical makeup of these rocks. Based on Table 1, both rock types share several chemical components. Importantly, both contain metallic compounds such as Al_2O_3 and Fe_2O_3. These compounds may play a part in improving the radiation attenuation capability of the blocks compared to those made from ordinary concrete. Previous research by Shamsan S. Obaid et al. (2017) investigated gamma-ray shielding in rocks at energy levels from 122 to 1330 keV. Rocks tested included feldspathic basalt, volcanic rock, granite, and sandstone. Among them, sandstone—also a sedimentary rock—had attenuation coefficients that are comparable to the results found here. For example, at 960 keV, the values for calcareous, and shale in this study were 0.15 $(cm^2)^{-1}$ and 0.18 $(cm^2)^{-1}$. At 1180 keV, the values were 0.07 $(cm^2)^{-1}$ and 0.08 $(cm^2)^{-1}$. These are in the same range as sandstone from the earlier study, which had a coefficient of 0.056 $(cm^2)^{-1}$ at 1170 keV. The difference in this study lies in the chemical composition. The calcareous used here contains 11.419% Al_2O_3 and 10.823% Fe_2O_3, while the shale contains 3.081% and 3.472%, respectively. This characteristic may help explain why these blocks perform better at radiation shielding. Although lead is well-known for its radiation shielding effectiveness, its toxicity makes it less desirable. This study explores safer alternatives. The presence of metallic oxides and the density of the resulting concrete appear to significantly affect shielding performance. According to R.S. Aita et al. (2024), both factors—chemical makeup and density—play a role in how well a material can block radiation. In conclusion, the findings suggest that blocks made from these sedimentary rocks, especially due to their chemical content, can offer better shielding than conventional concrete blocks.

In the study conducted by R.S. Aita et al. (2024), the team explored how concrete mixed with siltstone—a type of sedimentary rock—could block gamma radiation. Tests were done at three energy levels: 0.662 MeV (662 keV), 1.173 MeV (1173 keV), and 1.332 MeV (1332 keV). Siltstone was added to the concrete in different amounts, ranging from 0% to 40% by weight. The results showed that when the amount of siltstone increased, the concrete became better at absorbing radiation. This enhancement was seen in the higher values of the linear attenuation coefficient (μ_l). The improvement was mainly due to two factors: the concrete's electron density increased, and the cross-sectional area for interaction between the radiation and the material became larger. Them used cylindrical concrete blocks for this part of the experiment. Another significant finding was that adding more siltstone increased the MnO content. This made the concrete denser. As a result, the effective atomic number of the concrete also increased. These factors together suggest that siltstone can improve the radiation shielding ability of concrete, especially when used in higher amounts.

In both the findings of this study and the review of related literature, it can be seen that the effectiveness of gamma radiation shielding, particularly at low energy levels, in materials made from cement and sedimentary rocks depends on a few key factors. First, the density and compressive strength of the material are directly related to how well it can block radiation. Materials with higher density and compressive strength tend to perform better in terms of shielding low-energy gamma rays. Second, the chemical makeup of the material is important. If the material contains compounds with heavy metals or elements with relatively high atomic numbers, it tends to show improved shielding capabilities at lower energies. Based on this study, there are several directions for future research. For instance, varying the proportion of sedimentary rock by weight in the mix could help better understand how the composition affects shielding. It would also be valuable to compare different types of sedimentary rock to other types of stone used in construction materials. Finally, exploring additional parameters that relate to shielding across different energy levels—beyond those examined here—could further improve the development of radiation-resistant materials.

4. Conclusions

This study aimed to investigate how well concrete blocks made from sedimentary rocks in La-ngu District, within the Satun UNESCO Global Geopark, can shield against gamma radiation. The research focused on examining the physical and mechanical properties, as well as the radiation attenuation parameters, of the concrete blocks. These blocks, measuring 15 cm × 15 cm × 15 cm, were mixed using a fixed ratio of cement, sand, and rock at 1:2:4 by weight. The study compared the radiation levels before and after shielding using blocks made from shale and calcareous. Next, the effectiveness of shielding against gamma rays from a Co-60 source was contrasted with that of regular concrete used in construction. The results from the study are as follows: The concrete used in general construction showed the highest density and compressive strength, followed by the shale-based blocks and then the calcareous blocks. The study looked at how well different materials block gamma radiation at energy levels of 960 keV and 1180 keV by measuring the linear attenuation coefficient (μ_l), mass attenuation coefficient (μ_m), mean free path (MFP), half-value layer (HVL), and tenth-value layer (TVL). At 960 keV, the shale blocks provided the best radiation shielding, followed by standard concrete and calcareous blocks. At 1180 keV, the shale blocks again offered the most effective shielding, followed by calcareous, with standard concrete providing the least.

5. Acknowledgements

6. References

Günoğlu, K., Akkurt, I., & Sayyed, M. I. (2024). Radiation shielding properties of some igneous rocks in Isparta province at different gamma energies: Experimental and theoretical study. *Journal of Radiation Research and Applied Sciences, 17*, 1–9.

Aita, R. S., Mahmoud, K. A., Abdel Ghany, H. A., Ibrahim, E. M., El-Feky, M. G., & El Aassy, I. E. (2024). Impacts of siltstone rocks on the ordinary concrete's physical, mechanical and gamma-ray shielding properties: An experimental examination. *Journal of Nuclear Engineering and Technology, 56*, 2063–2070.

Rungcharoenkit, W., & Pansuk, W. (2021). Gamma and neutron attenuation coefficients of heavyweight concrete using domestic aggregates. In *Proceedings of the 26th National Convention on Civil Engineering: Civil Engineering and Beyond the Limit Development* (pp. 1–7), 23–25 June 2021.

Daram, S. (2019). Concrete mix proportioning by nominal mix method. In *Proceedings of the 4th National RMUTR Conference and the 1st International RMUTR Conference: Increasing Research to Sustainable Economic and Society* (pp. 1–10), 26–28 June 2019.

Obaid, S. S., Gaikwad, D. K., & Pawar, P. P. (2017). Determination of gamma ray shielding parameters of rocks and concrete. *Radiation Physics and Chemistry*, 1–5.

Electrochemical Behavior and Characterization of Nanochitosan-2, 4-dihydroxybenzaldehyde as a Sensor for the determination of Copper(II) ion

Rattiya Saradit[a] and Pijittra Saknarong[a]

[a] Department of Science, Faculty of Science and Technology, Rajamangala University of Technology Srivijaya, Thailand
* Corresponding author E-mail address: rattiya.s@rmutsv.ac.th

Abstract

Chitosan nanoparticle-2,4-dihydroxybenzaldehyde was synthesized via the reaction between the 2-amino groups of nanochitosan and 2,4-dihydroxybenzaldehyde, yielding 75%. Chemically modified rotating gold disk electrodes incorporating chitosan nanoparticle-2,4-dihydroxybenzaldehyde were prepared and employed as sensors for the detection of copper(II) ions. The electrochemical characterization of copper (II) at the modified electrodes was investigated using cyclic voltammetry. Optimal performance was achieved with a paste composition of 74% (w/w) graphite powder, 5% (w/w) chitosan, and 21% (w/w) paraffin oil in a 0.2 M sodium acetate solution at pH 7, using a scan rate of 0.8 V/s, a deposition time of 40 s, and an equilibration time of 25 s. A linear response was observed in the range of 1 to 10 mg/L, with a correlation coefficient of 0.98 and a detection limit of 0.176 mg/L.

Keywords: Copper, Sensor, Nanochitosan, Modified Electrode

1. Introduction

Copper is an important element in biological systems. It is an essential micronutrient involved in at least thirty enzymatic processes. However, it becomes toxic above a certain concentration. The World Health Organization (WHO) and the European Water Quality Directive recommend that the concentration in drinking water should not exceed 2 mg/L (Dalibor et al., 2011).

In recent years, the application of electrochemical methods using chemically modified electrodes has attracted significant interest in various areas of research and development, particularly for biosensors and electroanalytical techniques (Martínez-Huitle et al., 2010). Modified electrodes are those that incorporate chemically active species, achieved through the immobilization of a modifying agent on the surface of a base electrode. This process allows for the control and customization of the physicochemical properties at the electrode–solution interface, thereby enhancing the reactivity and selectivity of the base sensor. Electrode modification can be performed in various ways using different materials (Souza et al., 1997), such as carbon paste electrodes modified with DTPT (3,4-dihydro-4,4,6-trimethyl-2(1H)-pyrimidine thione) (Abbaspour and Moosavi, 2002), and nanocomposites based on polyaniline (PANI) and single-walled carbon nanotubes (SWCNTs) modified with ethylenediaminetetraacetic acid (EDTA) chelating ligands (Megha et al., 2018) for the potentiometric determination of Cu(II).

Chitosan has been identified as an effective reactant for the chemical extraction and determination of metals. The amino groups ($-NH_2$) of chitosan can react with aldehydes or ketones to form imines, commonly known as Schiff bases (Nuriye et al., 2012). It has been reported that chitosan-based Schiff bases exhibit excellent chelation ability with heavy metal ions. Multidentate Schiff bases have been widely used as ligands because they readily bind to metal ions through the formation of highly stable coordination compounds. Additionally, these compounds have recently been utilized as ionophores in metal ion sensors (Kucukkolbasi et al., 2013).

Modified carbon paste electrodes have gained increasing attention in recent years due to their desirable properties, such as ease of preparation and suitability for electrochemical detection

In this study, a chitosan-modified rotating gold disk electrode was developed and applied for the determination of trace levels of copper ions (Cu^{2+}).

2. Methodology

2.1 Apparatus and Electrochemical Measurements

The electrochemical performance of the prepared electrode for the detection of copper(II) ions was evaluated using cyclic voltammetry (CV). All measurements were conducted at room temperature using a VA 797 Computrace Electrochemical Analyzer (Metrohm). A conventional three-electrode system was employed, consisting of a rotating gold disk electrode modified with the sensing material as the working electrode, an Ag/AgCl (3 M KCl) electrode as the reference electrode, and a platinum wire as the auxiliary electrode.

2.2 Preparation of Chitosan Nanoparticles (CN)

Sodium tripolyphosphate (TPP) was dissolved in deionized water, while chitosan was dissolved in 1% (v/v) acetic acid. Chitosan nanoparticles (CN) were produced by the dropwise addition of 2 mL of TPP solution into 10 mL of chitosan solution. The gelation process was carried out under constant magnetic stirring, followed by ultrasonication at room temperature. The resulting nanoparticles were separated by centrifugation at 15,000 rpm and 4 °C for 30

minutes. The supernatant was removed, and the CN were rinsed with deionized water and subsequently freeze-dried (Nuriye et al., 2012).

2.3 Preparation of Chitosan Nanoparticles – 2,4-dihydroxybenzaldehyde

One gram of chitosan nanoparticles (CN) was added to 100 mL of methanol, and the mixture was continuously stirred to obtain a homogeneous solution. Subsequently, an equimolar amount of 2,4-dihydroxybenzaldehyde—relative to the nitrogen content in CN—was added to the mixture. The reaction mixture was refluxed for 48 hours. The resulting chitosan Schiff base (CNSB) was separated by centrifugation at 15,000 rpm and washed several times with ethanol. After drying in a vacuum oven at 50 °C for 24 hours, a yellow powder of CNSB was obtained (Nuriye et al., 2012).

2.4 Preparation of Chitosan Nanoparticle-2,4-dihydroxybenzaldehyde modified electrode

The modified electrode was prepared by manually mixing 73.7% graphite powder with 5.3% chitosan nanoparticle–2,4-dihydroxybenzaldehyde, followed by the addition of 21% paraffin oil in a mortar. The mixture was thoroughly blended for approximately 10 minutes to obtain a homogeneous paste. After homogenization, the paste was packed into the cavity of the working electrode body. The electrode surface was polished with weighing paper until a shiny appearance was observed. It was then used directly for voltammetric measurements without any preconditioning. When not in use, the electrodes were rinsed with distilled water and stored in a refrigerator at +4 °C (Kucukkolbasi et al., 2013).

2.5 Analytical Procedure

A volume of 25 mL of sodium acetate solution (0.2 mol/L) and 3 mL of copper standard solution (1×10^{-3} mol/L) were added to the measuring vessel. A three-electrode system was used, consisting of the modified electrode as the working electrode, a platinum wire as the counter electrode, and an Ag/AgCl electrode as the reference electrode. Nitrogen gas was purged through the solution for 3 minutes to eliminate dissolved oxygen. The electrochemical behavior of the modified electrode was investigated using cyclic voltammetry (CV). A series of Cu (II) standard solutions were measured under the optimized working conditions described above.

3. Results and Discussion

3.1 Particle Size of Chitosan Nanoparticle (CN)

The particle size of chitosan nanoparticles (CN) was measured using a zeta potential analyzer. The average particle size was determined to be 28.4 nm (Fig. 1), which is smaller than that reported in previous research (33 nm) (Kucukkolbasi et al., 2013).
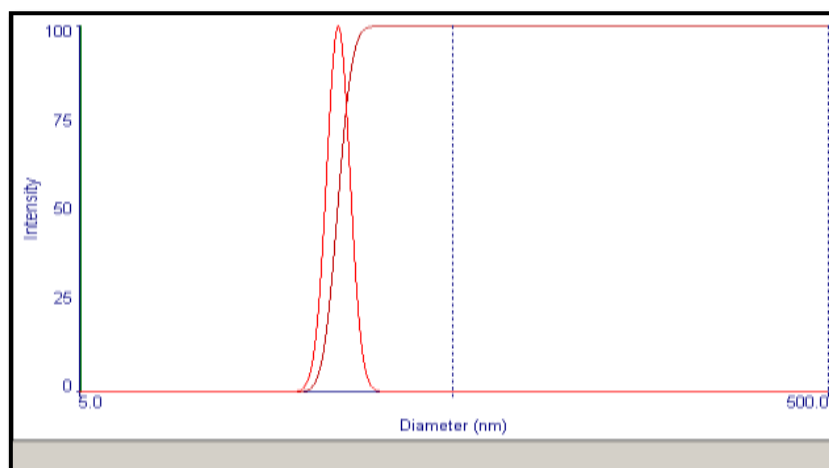

Figure 1 The size distribution by intensity of Chitosan Nanoparticle (CN)

3.2 Electrochemical behaviors of copper (II)

The electrochemical behavior of copper (II) ions on the nanochitosan–2,4-dihydroxybenzaldehyde modified rotating gold disk electrode was investigated using cyclic voltammetry.
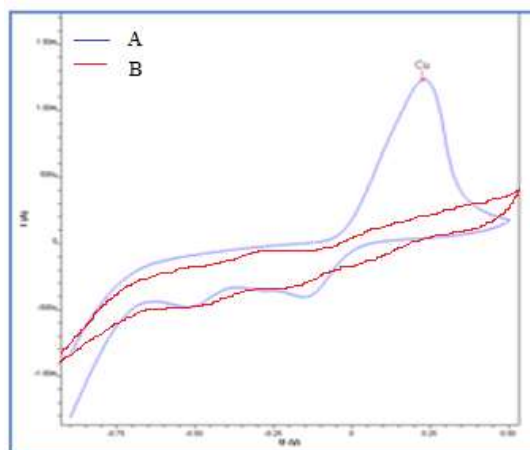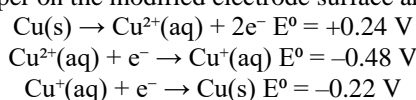
Figure 2 Cyclic voltammograms of copper (II) at (A) nanochitosan–2,4-dihydroxybenzaldehyde modified rotating
gold disk electrode and (B) unmodified (bare) rotating gold disk electrode, versus Ag/AgCl in sodium acetate buffer (pH 7.0)

Redox Reactions of Cu(II) on the Nanochitosan–2,4-Dihydroxybenzaldehyde Modified Rotating Gold Disk Electrode. The redox processes of copper on the modified electrode surface are as follows:

$$Cu(s) \rightarrow Cu^{2+}(aq) + 2e^- \quad E^0 = +0.24 \text{ V}$$
$$Cu^{2+}(aq) + e^- \rightarrow Cu^+(aq) \quad E^0 = -0.48 \text{ V}$$
$$Cu^+(aq) + e^- \rightarrow Cu(s) \quad E^0 = -0.22 \text{ V}$$

The electrochemical behavior of the prepared electrode was examined over a potential range from –1.50 to +0.50 V (vs. Ag/AgCl) using a scan rate of 0.8 V s^{-1}. Measurements were conducted in a copper (II) standard solution using sodium acetate (NaAc) buffer at pH 7.0. The oxidation peak of Cu (II) at the modified electrode was significantly higher than the reduction peaks. These results indicate that the modified electrode facilitates the preconcentration of Cu (II) and substantially enhances the sensitivity for Cu (II) detection. The peak current obtained using the modified electrode was markedly higher than that observed with a bare electrode. This enhanced performance can be attributed to the strong interaction between the Cu (II) ions and the nanochitosan–2,4-dihydroxybenzaldehyde, forming stable coordination complexes. Overall, the nanochitosan–2,4-dihydroxybenzaldehyde modified rotating gold disk electrode demonstrates high efficiency and sensitivity for the determination of Cu (II) ions.

3.3 Optimization of analytical conditions

1) pH and Supporting Electrolyte

The effect of pH on the Cu(II) signal was investigated in the range of 3.0 to 10.0 in the presence of 1000 mg/L Cu(II). The peak current increased as the pH increased from 3 to 7, then decreased beyond pH 8 (Figure 3). At lower pH (pH < 5) and higher pH (pH > 8), the modifier lost its ability to complex with Cu(II), resulting in a decrease in peak current. This behavior is attributed to the degradation of the nanochitosan–2,4-dihydroxybenzaldehyde structure, which compromises its ability to immobilize Cu(II) ions. The optimal pH was found to be 7.0, and this condition was used in all subsequent experiments.

The choice of supporting electrolyte significantly affects the voltammetric response of the sensor. The effect of various supporting electrolytes—namely HCl, NaNO$_3$, KNO$_3$, and sodium acetate (NaAc)—on the stripping peak currents of Cu(II) was evaluated at pH 7.0. Among these, the best voltammetric response was observed when using NaAc as the supporting electrolyte.
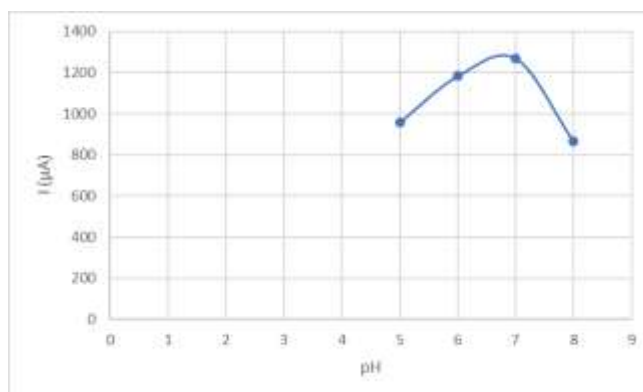

Figure 3 Relationship between peak current and pH for the copper (II) solution

231

2) Deposition time and Equilibration time

Deposition time significantly influences the determination of Cu (II). The peak currents were investigated over a range of 0–70 s in the presence of 1000 mg/L Cu (II). As expected, the peak current increased with longer deposition times. However, beyond 40 s (Figure 4), the signal began to decrease. This phenomenon is likely due to an initial increase in surface area caused by modified electrode dispersion, followed by a reduction in conductivity as the surface becomes blocked. At higher Cu (II) concentrations, the metal ion uptake rate increases, leading to the rapid saturation of the binding sites on the modified electrode (Dalibor et al., 2011). An optimal deposition time of 40 s was selected for use in the experimental procedures.

Equilibration time was evaluated in the range of 5–30 s, also in the presence of 1000 mg/L Cu (II). The peak current increased as equilibration time was extended, reaching a maximum at 25 s (Figure 5). This equilibration time was used in all subsequent experiments.
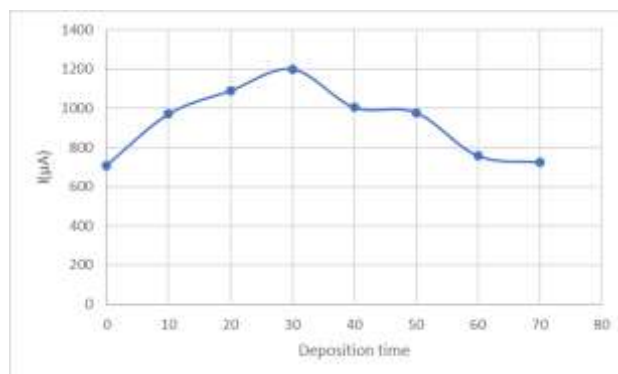

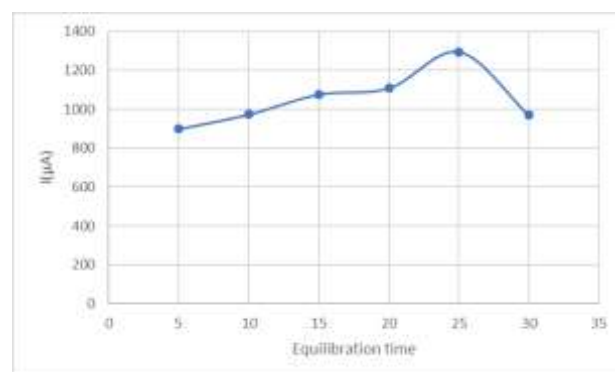Figure 4 Relationship between peak current and deposition time for the copper (II) solution

Figure 5 Relationship between peak current and equilibration time for the copper(II) solution

3) Scan rate

The influence of scan rate on the Cu (II) signal was investigated in the range of 0.1–1.0 V/s in the presence of 1000 mg/L Cu (II). The peak current increased with the scan rate, reaching a maximum at 0.8 V/s (Figure 6). Therefore, a scan rate of 0.8 V/s was used in all subsequent experiments.
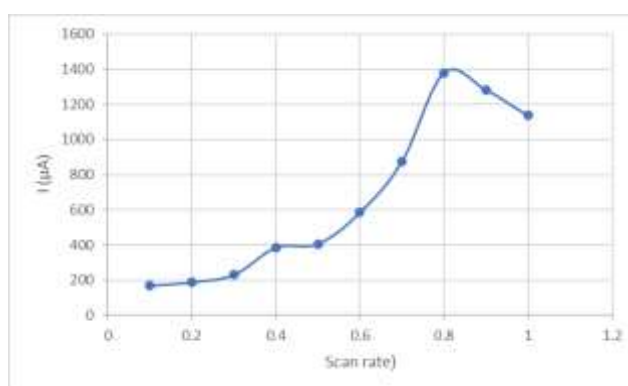

Figure 6 Relationship between peak current and scan rate for the copper(II) solution

4) Ion Interference

Experimental results showed that cadmium and lead ions interfered with copper determination. The copper current decreased as the concentration of interfering metal ions increased, indicating an inverse relationship. In other words, higher concentrations of heavy metal ions led to a significant reduction in the measurable copper signal, as shown in Table 1.

Copper could still be accurately analyzed in the presence of cadmium and lead ions when their concentrations were below 0.01 mg/L. However, at concentrations above 0.01 mg/L, the measured signal values were lower than the actual copper concentrations, resulting in inaccurate analysis.

Table 1 Relative Signal of Copper Standard Solution in the Presence of Different Concentrations of Interfering Ions

Ion interfering	Concentration (ppm)	Relative signal (%)
Cd^{2+}	0.01	97.10
	0.10	90.96
	1.00	58.29
	10.00	10.29
Pb^{2+}	0.01	98.02
	0.10	86.68
	1.00	65.36
	10.00	14.22

5) Linear Range and Detection Limit

The peak current exhibited a linear relationship with Cu (II) concentration in the range of 1 to 10 mg/L, with a correlation coefficient of 0.98. The detection limit (3σ) of Cu (II) using the developed method under optimized conditions was determined to be 0.176 mg/L.

4. Conclusion

In this study, an optimal paste composition was identified, consisting of 74% (w/w) graphite powder, 5% (w/w) nanochitosan, and 21% (w/w) paraffin oil. Nanochitosan was successfully synthesized via ionotropic gelation of chitosan and tripolyphosphate, and subsequently functionalized with 2,4-dihydroxybenzaldehyde to form Schiff base-modified nanoparticles. The synthesized compound was effectively used as a modifier for the rotating gold disk electrode. The major achievement of this work lies in the development of a simple and selective electrochemical sensor for trace-level determination of copper (II) ions using nanochitosan–2,4-dihydroxybenzaldehyde-modified electrodes.

5. Acknowledgements

6. References

Abbaspour, A., & Moosavi, S. M. M. (2002). Chemically modified carbon paste electrode for determination of copper (II) by potentiometric method. *Talanta, 56*(1), 91–96.

Amir, D., Ebrahim, V. F., & Mohammad, I. (2008). Preparation of chitosan nanoparticles loaded by dexamethasone sodium phosphate. *Iranian Journal of Pharmaceutical Sciences, 4*(2), 111–114.

Boutron, C. F. (2002). Direct determination of lead in Vostok Antarctic ancient ice by laser excited atomic fluorescence spectrometry. *Atmospheric Environment, 24*(7), 1797–1800.

Dalibor, S., Goran, R., Jelena, M., Ivan, A., Marijana, M., & Dragan, M. (2011). Determination of copper in water by anodic stripping voltammetry using Cu-DPABA–NA/GCE modified electrode. *International Journal of Electrochemical Science, 6*, 5617–5625.

Deng, P., Xu, Z., Feng, Y., & Li, J. (2012). Electrocatalytic reduction and determination of p-nitrophenol on acetylene black paste electrode coated with salicylaldehyde-modified chitosan. *Sensors and Actuators*, 381–389.

Hiroshi, I., Maiko, M., Boonma, L., & Tomoyo, I. (1994). Synthesis of chitosan-amino acid conjugates and their use in heavy metal uptake. *International Journal of Biological Macromolecules, 17*, 21–23.

Kucukkolbasi, S., Özden Erdogan, Z., Sahin, B. M., & Kocak, N. (2013). A novel chitosan nanoparticle–Schiff base modified carbon paste electrode as a sensor for the determination of Pb(II) in wastewater. *International Journal of Electrochemical Science, 8*, 2164–2181.

Martínez-Huitle, C. A., Suely, F. N., Cerro-Lopez, M., & Quiroz, M. A. (2010). Determination of trace metals by differential pulse voltammetry at chitosan modified electrodes. *Portugaliae Electrochimica Acta*, 39–49.

Megha, A. D., Raimonda, C., Almira, R., Mahendra, D. S., & Arunas, R. (2018). EDTA–PANI/SWCNTs nanocomposite modified electrode for electrochemical determination of copper (II), lead (II), and mercury (II) ions. *Electrochimica Acta, 259*, 930–938.

Ng, J. C. Y., Cheung, W. H., & McKay, G. (2002). Equilibrium studies of the sorption of Cu(II) ions onto chitosan. *Journal of Colloid and Interface Science, 255*, 64–74.

Nuriye, K., Mustafa, S., Semahat, K., & Zehra, O. E. (2012). Synthesis and characterization of novel nano-chitosan Schiff base and use of lead (II) sensor. *International Journal of Biological Macromolecules, 51*, 1159–1166.

Pipat, C. (2017). Modified electrodes for determining trace metal ions. In R. Z. (Ed.), *Applications of voltammetry* (pp. 129–152). InTech Open.

Rong, M. W., Nai, P. H., Peng, F. S., Yu, F. H., Lan, D., & Zi, Q. L. (2009). Preparation of nano-chitosan Schiff-base copper complexes and their anticancer activity. *Polymers for Advanced Technologies, 20*(12), 959–964.

Souza, M. F. B. (1997). Eletrodos quimicamente modificados aplicados à eletroanálise: Uma breve abordagem. *Química Nova, 20*, 191–195.

Ye, X., Yang, Q., Wang, Y., & Li, N. (1998). Electrochemical behavior of gold, silver, platinum and palladium on the glassy carbon electrode modified by chitosan and its application. *Talanta, 47*, 1099–1106.

Zheng, M., Gao, F., Wang, Q., Cai, X., Jiang, S., Huang, L., & Gao, F. (2013). Electrocatalytic oxidation and sensitive determination of acetaminophen on glassy carbon electrode modified with graphene–chitosan composite. *Materials Science and Engineering: C, 33*, 1514–1520.

Enhancement of Electrical Energy Generation using Banana-Based Electrolytes for Science Education

Chompunooch Saengpheng[a], Yingkhun Praha[a], Thanitkarn Yurungrueang[a], Chajchawin Masom[a], Pannavat Rasuso[a], Natthawath Umpavanont[a], Jakkrit Saengpeng[a*]

[a] *Faculty of Technical Education, Innovation Demonstration School of Rajamangala University of Technology Thanyaburi, Pathumtani, 12110, Thailand*
* Corresponding author. Tel.: +6683-0775149; E-mail address: jakkrit_s@rmutt.ac.th

Abstract

Renewable energy represents a viable alternative in response to the global decline in fossil fuel resources. Batteries function by storing chemical energy and converting it into electrical energy through electrochemical reactions. In this study, a microbial fuel cell kit was designed and developed as an educational tool aligned with STEAM-based learning for upper secondary school students. Banana pseudostem sap (BPS) was investigated as a potential natural electrolyte for constructing a simple biobattery using zinc and copper electrodes. The primary objective of the experiment was to enhance electrical output by optimizing the fermentation time of the BPS electrolyte. The acidity of the fermented electrolyte, indicated by pH levels, was found to play a critical role in electrical performance. Experimental results demonstrated that a seven-day fermentation period produced the highest output, with a maximum voltage of 0.99 V, electric current of 2.74 mA, and power output of 2.71 mW, corresponding to the lowest pH value of approximately 4.86. These findings suggest that banana-based biobatteries can generate measurable electrical energy, offering a cost-effective and environmentally sustainable approach to green energy storage, particularly in educational and low-resource settings.

Keywords: STEAM Learning, Electrical Energy, Banana Pseudostem Sap (BPS), Electrochemical and Renewable Energy

1. Introduction

The combustion of fossil fuels has been shown to exert profound and far-reaching impacts on both the environment and human health (Cao et al., 2006; Perera et al., 2019). In contrast, renewable energy—derived from naturally replenishing sources—plays a critical role in achieving a sustainable future by reducing environmental degradation, fostering economic development, and enhancing energy security (International Energy Agency, 2007; Patel, 2021). Batteries, in general, are electrochemical devices that convert stored chemical energy into electrical energy through redox reactions. Among various types, biobatteries represent a promising green technology that utilizes plant-based fluids or organic waste to generate environmentally friendly electricity (Golberg et al., 2010; Muske et al., 2007). These systems typically involve copper and zinc electrodes serving as the cathode and anode, respectively. Organic acids function as electrolytes, facilitating the flow of electrons from zinc to copper and thereby producing an electric current (Purnima et al., 2024; Sorey et al., 2012). In the present study, a microbial fuel cell kit was employed as an instructional tool to demonstrate the generation of electrical energy from banana pseudostem sap (BPS). The experiment investigated the influence of fermentation time on the electrical output, with the aim of enhancing students' understanding of renewable bioelectrochemical energy through hands-on learning experiences.

2. Methodology

2.1 Microbial Fuel Cell Kit Assembly

A cost-effective microbial fuel cell (MFC) educational kit was constructed for the experiment. Zinc (Zn) and copper (Cu) electrodes were selected as the anode and cathode, respectively. Each electrode measured 20 mm in width, 2 mm in thickness, and 150 mm in length (W × T × L).

2.2 Electrolyte Preparation

The electrolyte was derived from post-harvest banana pseudostems (BPS), considered agricultural waste. Samples were collected from local farms in Thanyaburi, Pathum Thani Province, Thailand. To ensure cleanliness, the banana trunks were washed three times with distilled water to remove residual dirt. The pseudostem sap was then extracted and prepared in 500 mL volumes, which were stored in sealed glass containers for subsequent fermentation.

2.3 Experimental Procedure

For each trial, 500 mL of the prepared BPS was transferred into the electrolyte compartment of the microbial fuel cell kit. Measurements of temperature, pH, voltage, and electric current were recorded daily at 9:00 AM over a seven-day fermentation period (as illustrated in Figure 1). Each experiment was conducted in triplicate under identical conditions to ensure reproducibility. The power output was calculated using the following equation:

$$P = IV \qquad (1)$$

Where P = power (W)
V = voltage (Voltage)
I = current (Ampere)

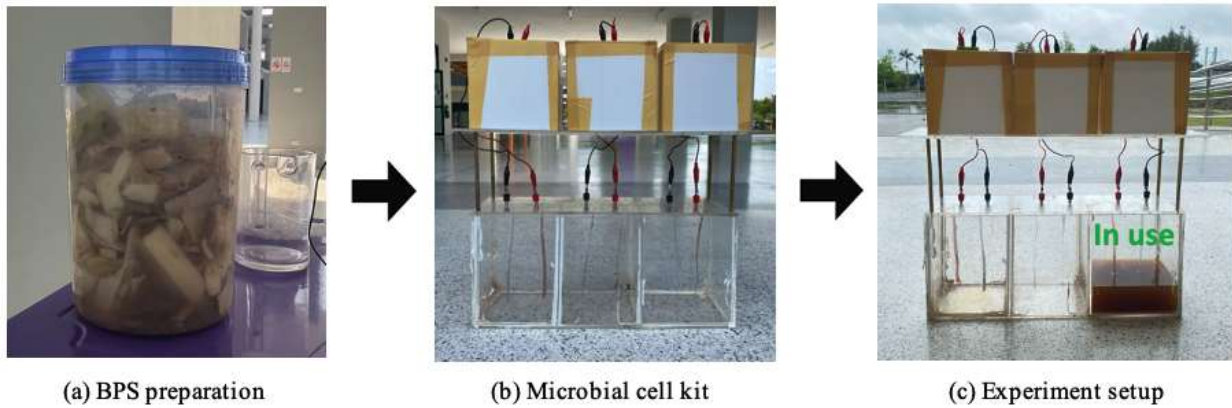(a) BPS preparation   (b) Microbial cell kit   (c) Experiment setup

Figure 1 (a) BPS preparation (b) Microbial cell kit (c) Experiment setup

3. Results and Discussion

3.1 Temperature and pH level at fermentation time

The average ambient temperature during the experimental period was approximately 28°C, which lies within the optimal range for yeast fermentation. Temperature is a critical factor influencing microbial activity, particularly that of yeast, which typically thrives between 20°C and 30°C. Maintaining an appropriate temperature range enhances the metabolic efficiency of probiotic microorganisms, thereby facilitating a more effective fermentation process (Walker, 1998; Lee, 2008). The pH values observed throughout the fermentation process exhibited a gradual decline over time, indicating an increase in acidity. The lowest pH value recorded was 5.02 on the seventh day of fermentation, corresponding to the highest level of acidity. This acidification trend is consistent with microbial fermentation activity, as the proliferation of yeast and other microorganisms often contributes to acid production through metabolic byproducts (Vatansever et al., 2017), as summarized in Table 1.

The biobattery system employed in this study operates based on fundamental redox reactions occurring between two dissimilar metal electrodes immersed in an organic electrolyte. Zinc (Zn) and copper (Cu) electrodes were utilized as the anode and cathode, respectively. The electrolyte medium, derived from fermented banana pseudostem sap (BPS), contains organic acids that facilitate ion transport and contribute to the overall conductivity of the system. During operation, the zinc electrode undergoes oxidation by releasing electrons and dissolving into the electrolyte as zinc ions:

Anode (oxidation): $Zn\,(s) \rightarrow Zn^{2+}\,(aq) + 2e^-$

These electrons then flow through an external circuit to the copper electrode, where a reduction reaction takes place. Hydrogen ions (H^+), derived from organic acids present in the BPS, accept the electrons and form molecular hydrogen:

Cathode (reduction): $2H^+\,(aq) + 2e^- \rightarrow H_2\,(g)$

This electron flow from the zinc to the copper electrode constitutes the electric current observed in the circuit. The overall cell reaction can be summarized as:

$$Zn\,(s) + 2H^+\,(aq) \rightarrow Zn^{2+}\,(aq) + H_2\,(g)$$
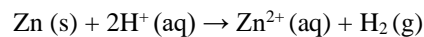
The efficiency of the electrochemical cell is influenced by factors such as the acidity (pH) of the electrolyte, electrode surface area, and fermentation duration of the banana sap, which alters the concentration of organic acids (Lee, 2008; Vatansever et al., 2017).

Table 1 Temperature and pH data of electrolyte fermentation time

Fermentation Day	pH	Temperature
1	5.82	29
2	5.75	28
3	5.64	27
4	5.45	27
5	5.24	28
6	5.18	29
7	5.02	29

3.2 Electrical energy

In this experiment, a pair of dissimilar metal electrodes—zinc (Zn) and copper (Cu)—were employed, functioning as the anode and cathode, respectively. During the electrochemical reaction, the zinc electrode undergoes oxidation, releasing electrons and dissolving into the electrolyte as zinc ions (Zn^{2+}). Simultaneously, the copper electrode serves as the site of reduction, where it receives electrons through an external circuit, thereby facilitating the generation of an electric current.

Table 2 Electrical energy measurement of voltage, current and power from Banana pseudostem sap (BPS)

Fermentation Day	Electrical energy		
	Voltage (V)	Current (mA)	Power (mW)
1	0.55	1.25	0.69
2	0.68	1.28	0.87
3	0.75	1.65	1.24
4	0.84	1.95	1.64
5	0.92	2.35	2.16
6	0.95	2.65	2.52
7	0.99	2.74	2.71

Table 2 presents the electrical energy output generated from banana pseudostem sap (BPS) over a seven-day fermentation period. The results indicate a progressive increase in electrical performance correlating with the fermentation duration. This trend is attributed to the rising acidity of the electrolyte, which plays a pivotal role in enhancing the electrochemical activity and facilitating effective energy generation within the system.

Table 2 summarizes the electrical performance metrics—voltage (V), current (mA), and power output (mW)—obtained from the biobattery system using banana pseudostem sap (BPS) as the electrolyte over a fermentation period of seven days. The results reveal a progressive increase in both current and power output from Day 1 through Day 7. The current increased from 1.25 mA on Day 1 to a peak of 2.74 mA on Day 7. Correspondingly, the power output rose from 0.69 mW to 2.71 ± 0.05 mW, demonstrating a consistent enhancement in energy generation efficiency with prolonged fermentation time. This increase in electrical performance correlates strongly with the declining pH of the BPS, indicating increased acidity due to microbial fermentation. The lowest pH value recorded was 5.02 on Day 7, supporting the hypothesis that increased proton availability enhances ionic conductivity and facilitates redox reactions at the electrodes.

1) Electric Voltage value of Banana pseudostem sap (BPS)

The voltage generated from the fermented banana pseudostem sap was measured daily over a seven-day period. The results revealed a consistent upward trend in voltage output as the fermentation progressed. The lowest recorded voltage was approximately 0.55 V on Day 1, while the highest voltage, reaching approximately 0.99 V, was observed on Day 7. This increase in voltage corresponds with the extended fermentation time, suggesting a positive correlation between microbial activity and electrochemical potential. The detailed voltage progression is illustrated in Figure 2.
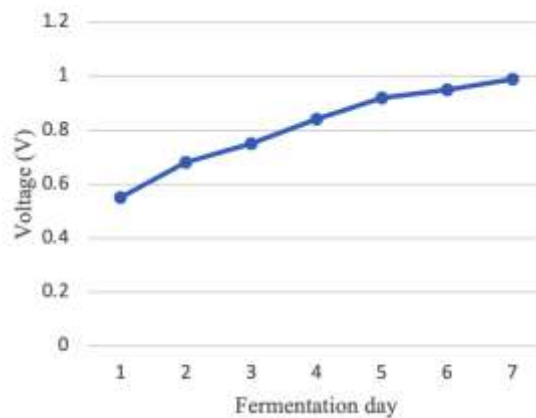

Figure 2 Value of electric voltage of Banana pseudostem sap (BPS)

The voltage output recorded throughout the seven-day fermentation process exhibited a distinct upward trajectory, as depicted in Figure 2. The measured voltage increased progressively from 0.55 V on Day 1 to a peak of 0.99 V on Day 7, reflecting a continuous enhancement in the electrochemical potential of the system over time. This trend can be primarily attributed to the gradual accumulation of organic acids—most notably lactic and acetic acids—resulting from microbial metabolic activity within the banana pseudostem sap (BPS). As the fermentation progressed, the concentration of hydrogen ions (H^+) within the electrolyte increased, leading to a marked decrease in pH. This heightened proton availability significantly improved the ionic conductivity of the medium, which in turn facilitated more efficient electron transfer between the zinc (anode) and copper (cathode) electrodes. This phenomenon is consistent with the Nernst equation, which describes how variations in ionic concentration influence the electrochemical cell potential. Furthermore, the acidic environment enhanced the kinetics of the redox reactions occurring at the electrodes. At the anode, zinc underwent oxidation to produce Zn^{2+} ions and electrons, while at the cathode, hydrogen ions were reduced to molecular hydrogen (H_2). These reactions were more effectively sustained in low-pH conditions, thereby maximizing the electrical output. Overall, the observed correlation between fermentation duration, electrolyte acidification, and voltage generation underscores the pivotal role of biochemical conditions in optimizing the performance of BPS-based biobatteries.

237

2) Electric current value of Banana pseudostem sap (BPS)

The electric current generated from the banana pseudostem sap (BPS) was measured over a seven-day fermentation period. The results revealed a steady increase in current output corresponding with fermentation duration. The lowest current, approximately 1.25 mA, was recorded on Day 1, while the highest value, reaching 2.74 mA, was observed on Day 7. This trend indicates a direct correlation between microbial activity and current generation, as illustrated in Figure 3.
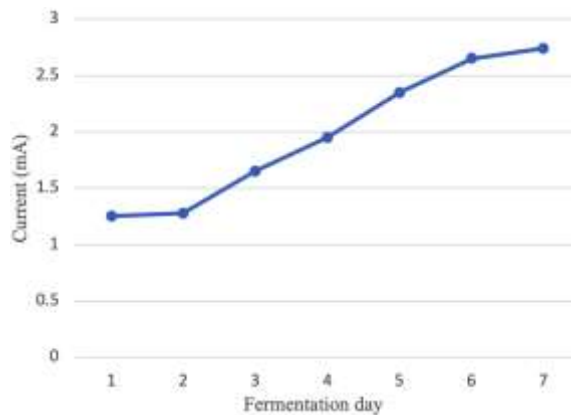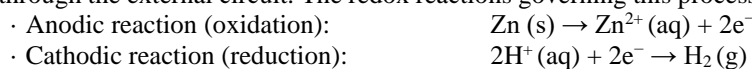

Figure 3 Value of electric current of Banana pseudostem sap (BPS).

The electric current generated from banana pseudostem sap (BPS) exhibited a progressive increase over the seven-day fermentation period. The current rose from an initial value of 1.25 mA on Day 1 to a peak of 2.74 mA on Day 7, indicating a continual enhancement in electrochemical activity in conjunction with microbial development. This increasing trend in current output is primarily attributed to the metabolic activity of indigenous microorganisms present within the BPS. Throughout fermentation, microbial species such as *Lactobacillus* spp. and *Acetobacter* spp. metabolize complex polysaccharides and organic substrates into simpler metabolites, predominantly short-chain organic acids, including lactic and acetic acid. These fermentation-derived acids incrementally elevate the concentration of hydrogen ions (H^+) in the electrolyte, leading to a corresponding reduction in pH. The accumulation of H^+ ions enhances the ionic conductivity of the electrolyte, thereby improving the mobility of charge carriers between electrodes. This improvement reduces internal resistance within the electrochemical cell, facilitating more efficient electron transfer through the external circuit. The redox reactions governing this process can be described as follows:

· Anodic reaction (oxidation): $\quad\quad\quad\quad$ $Zn\,(s) \rightarrow Zn^{2+}\,(aq) + 2e^-$
· Cathodic reaction (reduction): $\quad\quad\quad\quad$ $2H^+\,(aq) + 2e^- \rightarrow H_2\,(g)$

Within this redox system, the zinc electrode functions as the electron donor, while hydrogen ions serve as the electron acceptors at the copper electrode. As fermentation progresses and acidity intensifies, the availability of protons at the cathode interface increases, subsequently accelerating the reduction kinetics and enhancing overall current output. This synergistic interplay between microbial acidogenesis and electrochemical processes underscores the pivotal role of fermentation in optimizing biobattery performance. The sustained increase in current not only reflects the dynamic maturation of microbial populations but also highlights the direct influence of biochemical transformations on the electrochemical efficiency of the system.

3) Power value of Banana pseudostem sap (BPS)

The power output generated from the fermented banana pseudostem sap substrate over a seven-day period exhibited a notable upward trend. The lowest power value, approximately 0.69 mW, was recorded on Day 1, while the highest value, reaching 2.71 mW, was observed on Day 7. This increase in power output corresponds closely with the concurrent rise in both voltage and current as fermentation progressed. These findings highlight the direct influence of extended fermentation time on electrochemical performance, as illustrated in Figure 4.
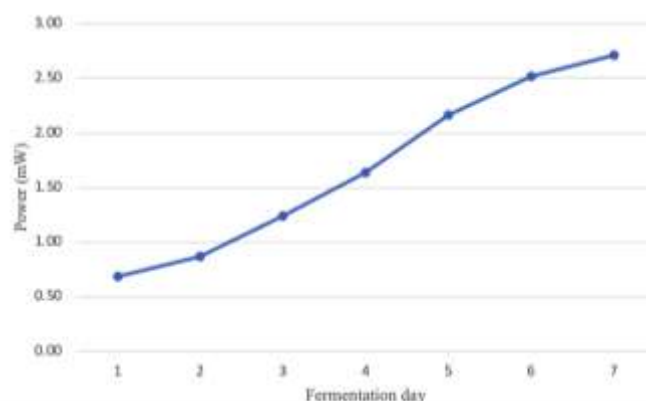

Figure 4 Value of power of Banana pseudostem sap (BPS)

The experimental results indicate that fermentation duration plays a crucial role in determining the electrical performance of the biobattery system. An extended fermentation period was positively correlated with increased values of both voltage and current, reflecting enhanced electrochemical activity over time. This improvement is primarily attributed to microbial metabolism, wherein naturally occurring microorganisms decompose fermentable sugars into organic acids. These biological transformations release free electrons and ions, which are key contributors to electrical energy generation (Sigalingging et al., 2022).

Among the critical physicochemical factors, electrolyte acidity exerts a substantial influence on the efficiency of electricity generation. Increased acidity results in a higher concentration of free hydrogen ions (H^+), which significantly enhances the ionic conductivity of the electrolyte. A more conductive medium facilitates faster ion migration and more efficient charge transfer between electrodes, thereby reducing internal resistance and increasing current output. Furthermore, elevated H^+ availability at the cathode accelerates reduction reactions, contributing to a greater overall energy yield (Sigalingging et al., 2022; Supratomo, 2019). Consequently, the progressive acidification of the medium during fermentation emerges as a key determinant in optimizing biobattery performance.

4. Conclusion

A hands-on science experiment was conducted to demonstrate the generation of electrical energy from banana waste through electrochemical reactions, specifically designed for senior high school students. The results confirmed that banana pseudostem sap (BPS), derived from agricultural waste, can be effectively converted into electrical energy. The system achieved a maximum voltage of approximately 0.99 V and an electric current of 2.74 mA, with both parameters exhibiting a consistent increase over the seven-day fermentation period. The observed enhancement in electrical performance is closely linked to fermentation-induced acidification, which increases the concentration of hydrogen ions (H^+) in the electrolyte. This rise in acidity improves ionic conductivity and facilitates redox reactions at the electrodes, thereby increasing current and voltage outputs. These findings underscore the feasibility of utilizing BPS as a sustainable and environmentally friendly energy source for low-power applications. Moreover, the experiment highlights the educational and technological potential of agricultural waste in advancing renewable energy innovations.

5. Acknowledgments

6. References

Cao, Y., Wang, Y., Riley, J. T., & Pan, W. P. (2006). A novel biomass air gasification process for producing tar-free, higher heating value fuel gas. *Fuel Processing Technology, 87*(4), 343–353.

Golberg, A., Rabinowitch, H. D., & Rubinsky, B. (2010). Zn/Cu vegetative batteries: Bioelectrical characterizations and primary cost analyses. *Journal of Renewable and Sustainable Energy, 2*(3), 033103.

International Energy Agency. (2007). *World energy outlook*. OECD/IEA.

Lee, Y. K., & Salminen, S. (Eds.). (2008). *Handbook of probiotics and prebiotics* (pp. 177–200). Wiley.

Muske, K. R., Nigh, C. W., & Weinstein, R. (2007). Lemon cell battery for high power applications. *Journal of Chemical Education, 84*(4), 635–638.

Patel, P., Modi, A., Minipara, D., & Kumar, A. (2021). Microbial biosurfactants in management of organic waste. In V. K.

Mishra & A. Kumar (Eds.), *Sustainable environmental clean-up* (pp. 211–230). Elsevier.

Perera, F., Ashrafi, A., Kinney, P., & Mills, D. (2019). Towards a fuller assessment of benefits to children's health of reducing air pollution and mitigating climate change due to fossil fuel combustion. *Environmental Research, 172*, 55–72.

Purnima, K. S., Rao, T. J. V. S., Aswini, T. V. N. L., & Sharma, D. (2024). Living plant or tree as a renewable energy source of long lasting battery. *Tuijin Jishu / Journal of Propulsion Technology, 45*(1).

Sigalingging, R., Panjaitan, V. C. S., & Sigalingging, C. (2022). The effect of fermentation time on fruits as a producer of electrical energy. *IOP Conference Series: Earth and Environmental Science, 1065*, 012038.

Sorey, T., Hunt, V., Balandova, E., & Palmquist, B. (2012). A new twist on the old lemon battery. *In NSTA Press: Exemplary Science in Informal Education Settings* (pp. 91–98). National Science Teaching Association.

Supratomo, S., Laga, A., Tahir, M., Mochtar, A., & Salengke, S. (2019). The effect of fermentation on fruit battery performance. *Journal of Engineering and Applied Sciences, 14*, 1515–1520.

Vatansever, S., Vegi, A., Garden-Robinson, J., & Hall, C. A. (2017). The effect of fermentation on the physicochemical characteristics of dry-salted vegetables. *Journal of Food Research, 6*(5).

Walker, G. M. (1998). *Yeast physiology and biotechnology*. John Wiley & Sons.

Probiotic-Driven Hair Care Using Combining Herbal Dyes with a Microbiome-Modulating Conditioner

Yanapat Sukhontaman[a], Duongruitai Nicomrat[a]*, Patarika Soongsombat[a], Kansinee Kantip[a], Nipaporn Panay[b], Nitipat Aewsakul[c], Padipan Tinprabath[d], Gritsada Sua-iam[e]

[a] Department of Environmental Science and Technology, Faculty of Science and Technology, Rajamangala University of Technology Phra Nakhon, 1381 Pracharat 1 Road, Wongsawang, Bang Sue, Bangkok 10800.
[b] Department of Computer Science, Faculty of Science and Technology, Rajamangala University of Technology Phra Nakhon, 1381 Pracharat 1 Road, Wongsawang, Bang Sue, Bangkok 10800.
[c] Faculty of Industrial Education, Rajamangala University of Technology Phra Nakhon, 399 Samsen Rd., Wachira Phayaban, Dusit, Bangkok 10300.
[d] Department of Mechanical Engineering, Faculty of Engineering, Rajamangala University of Technology Phra Nakhon, 1381 Pracharat 1 Road, Wongsawang, Bang Sue, Bangkok 10800.
[e] Department of Civil Engineering, Faculty of Engineering, Rajamangala University of Technology Phra Nakhon, 1381 Pracharat 1 Road, Wongsawang, Bang Sue, Bangkok 10800.
* Corresponding author, E-mail address: duongruitai.n@rmutp.ac.th

Abstract

Conventional chemical hair dyes frequently cause adverse effects, including hair damage and scalp irritation, driving consumer interest towards safer, natural alternatives. This study successfully developed an eco-friendly hair care system combining natural herbal dyes (*Clitoria ternatea*, *Curcuma longa*, *Lawsonia inermis*) with a restorative probiotic-enriched conditioner (*Zingiber officinale* prebiotic, *Lactobacillus* spp. probiotics) as a safer alternative to conventional chemical treatments, which often cause hair damage and scalp irritation. Optimized bleaching as the first step prepared and then hair dyeing with butterfly pea achieved the highest initial color intensity (72%), though colorfastness was limited. The ginger-based conditioner supported probiotic viability and improved hair softness and smoothness without observed toxicity. While the green hair care system was refrigerated, its stability was better promising than room temperature, though its long-term preservation (more than 3 months) requires further improvement.

Keywords: Eco-friendly Hair Probiotics, Herbal Hair Dye, Herbal Hair Conditioner Formulation, Scalp health improvement.

1. Introduction

Hair dyeing with conventional chemical formulations presents significant drawbacks, notably causing damage to the hair structure, leading to issues like brittleness, dryness, and breakage (He et al., 2023). Furthermore, these chemical agents, such as ammonia and hydrogen peroxide, can induce scalp irritation and allergic reactions, manifesting as inflammation or rashes (Handa et al., 2012; He et al., 2023; Palaniappan et al., 2024). These adverse effects extend beyond physical discomfort, impacting overall well-being and self-esteem (Smith et al., 2018). Recognizing these issues, a growing segment of health-conscious consumers is actively seeking safer, herbal-based alternatives for hair coloring (Park et al., 2012; Brandwein et al, 2016; Jhamb et al., 2023). While natural hair dyes derived from botanical sources typically offer less vibrant and long-lasting color compared to their synthetic counterparts, they possess a crucial advantage: the absence of known carcinogenic and allergenic substances commonly found in chemical dyes (Brandwein et al., 2016). Regular applications of these natural colorants can contribute to improved color uniformity and potentially enhance user confidence (Kumari et al., 2024). Moreover, many of the botanicals utilized in these formulations offer additional therapeutic benefits for hair health (Siu-Yin et al., 2019). These include mitigating hair loss, managing thinning or prematurely graying hair, and promoting healthy hair growth (Xu et al., 2016; Choi et al., 2024; Patel et al., 2015). As recently concerned to the users, the development of safer hair care practices also necessitates attention to post-dyeing treatments as complementary to the dyeing process, functioning in maintaining and restoring hair health. Conditioners typically contain ingredients like proteins, silicones, vitamins, and plant oils that help smooth the cuticle, retain moisture, and improve strength and resilience (Fernandes et al., 2023; Leite &Campos, 2018).

Recently works have expanded to include probiotics—beneficial live microorganisms such as *Lactobacillus* spp.—within cosmetic and scalp care formulations (Yin et al, 2024; Siu et al., 2019; Clayaud et al., 2013; Park et al., 2012; Pagac et al., 2024). These microorganisms, naturally topically present on the skin and scalp, can help maintain a healthy microbial balance, potentially preventing infections and improving overall hair and scalp condition (Theodorou et lk et al., 2024; Sash et al, 2024). To further enhance the efficacy of probiotics, prebiotics—non-digestible compounds that foster the growth of beneficial microbes—can be incorporated (Bermudez-Brito et al., 2012). Certain herbal extracts, such as *Zingiber officinale* (ginger), can serve as natural prebiotics, providing nourishment for probiotics and contributing additional anti-inflammatory and antimicrobial properties beneficial to scalp health (Tan et al., 2020; Habeebuddin et al., 2022). the dyeing properties of aqueous extracts from *Clitoria ternatea* (butterfly pea) (Hariadi et al., 2018), *Curcuma longa* (turmeric) (Suryawanshi et al., 2017), and *Lawsonia inermis* (henna) (Singam et al., 2020) have been long used for natural herbal dyes for hair dyeing as ecofriendly and non-toxic approach compared to common chemical hair dyes ((Cui et al, 2020; Packianathan et al., 2010; Adeel et al., 2018)

Therefore, from overall, this research objective was to develop and evaluate an innovative, natural hair care system composed of two synergistic components: a herbal hair dye and a probiotic-enriched conditioner. Specifically, the study investigated the dyeing properties of aqueous extracts from *Clitoria ternatea* (butterfly pea), *Curcuma longa* (turmeric), and *Lawsonia inermis* (henna). Simultaneously, a restorative conditioner was formulated, incorporating probiotics derived from yogurt (*Lactobacillus* spp.) and a prebiotic-rich *Zingiber officinale* (ginger) extract. The overarching aim was to determine the feasibility of this dual system as a safer, efficacious, and sustainable alternative to conventional chemical hair treatments, addressing consumer demand for non-toxic personal care products. Key evaluation parameters included dye performance, conditioning effects, toxicity on biological models, and preliminary stability under various storage conditions.

2. Methodology

An integrated approach to improving hair and scalp health through hair dyeing and conditioning involves the following steps, presented in sequential order below.

2.1 Preparation and Determination of Herbal Extract Concentration for Dyeing

This step outlines the process of obtaining and preparing the herbal extracts intended for hair dyeing and determining the appropriate concentrations for effective coloration to obtain and evaluate the bioactive compounds from selected Thai herbal plants—butterfly pea (Clitoria ternatea), turmeric (Curcuma longa), and henna (Lawsonia inermis)—these herbs were utilized as natural hair dyes due to their pigment and antioxidant properties. The herbs were individually weighed (butterfly pea: 0.15 g; turmeric and henna: 4 g each), boiled with 50 ml of distilled water for 1 hour, and filtered to obtain clear aqueous extracts. Each filtrate was further diluted with 10 ml of distilled water. Photographic documentation was made for extraction, filtration, and dilution steps. The concentration of each extract was calculated using a standard formula using the following formula:

$$\text{Concentration (mg/ml)} = \frac{\text{Weight of dry herbal material (mg)}}{\text{Final volume of extract (ml)}}$$

2.2 Hair Preparation and Bleaching Process

Hair bleaching is the essential preliminary step undertaken to ensure a controlled and accurate evaluation of the herbal dyes' efficacy. This crucial preliminary step details the preparation of hair samples to ensure uniform dye uptake and evaluation. To achieve this, the natural melanin pigment within the hair samples must first be removed. This decolorization creates a uniform, light canvas, enabling optimal absorption of the herbal colorants and allowing for a clear assessment of their dyeing properties, uninfluenced by the hair's original shade. Hair samples were standardized for size, cleanliness, and condition. Each bundle (2 g) was divided into two groups: Group A (treated with perchloric acid ($HClO_4$) at concentrations of 2%, 5%, and 12%) and Group B (treated with hydrogen peroxide and ammonia (H_2O_2, 6–12%) and ammonia (NH_3, 6M). These bleaching procedures includes two distinct bleaching methods:

1) Bleaching with Perchloric Acid

This specific procedure using perchloric acid was to remove natural hair pigment. Hair samples were treated with varying concentrations of perchloric acid ($HClO_4$) to investigate the effect of a strong acid on melanin bleaching in hair fibers, providing a comparison with conventional bleaching methods. Three treatment groups were prepared: (1) 2% $HClO_4$ diluted in 250 mL of distilled water, (2) 5% $HClO_4$ diluted in 240 mL of distilled water, and (3) 12% $HClO_4$ used without dilution. The hair samples were fully immersed in each solution and left at room temperature (approximately 25°C) for 30 minutes. After treatment, the samples were rinsed with distilled water and air-dried before further analysis.

2) Bleaching with Hydrogen Peroxide and Ammonia

In the alternative, more conventional bleaching method, hair samples were treated with a combination of ammonia (NH_3) and varying concentrations of hydrogen peroxide (H_2O_2). This method aimed to replicate a standard commercial bleaching procedure, allowing for a direct comparison with the bleaching effects of strong acid. According to most referred by commercialized hair dyeing usage, four treatment groups were selectively prepared using H_2O_2 at concentrations of 6%, 9%, or 12%, each mixed with 6 M NH_3. The hair samples were fully immersed in each mixture and treated for four different durations: 5, 15, 30, and 45 minutes at room temperature (approximately 25°C). After treatment, the samples were rinsed thoroughly with distilled water and air-dried before further analysis.

2.3 Hair Dyeing with Herbal Extracts

This section details the application of the prepared herbal extracts onto the bleached hair samples to achieve coloration. The extracted dyes were applied to both bleached and unbleached samples to assess their dyeing effectiveness. Hair samples were immersed in herbal extracts for 5, 10, 30, and 45 minutes, then rinsed, shampooed, and dried. The optimized method involved bleaching with H_2O_2 + NH_3 for 15 minutes and dyeing for 30 minutes, repeated three times for enhanced retention.

2.4 Development of Post-Dyeing Herbal Hair Conditioner with Probiotics

The formulation of a conditioner designed to be used after the herbal dyeing process, incorporating both herbal extracts and probiotics for hair and scalp health. With a natural conditioner developed to restore hair health after dyeing, the herbal and probiotic elements to nourish and protect the hair and scalp involve several sub-steps:

241

1) Preparation of Probiotic Culture

Details the cultivation and preparation of the probiotic microorganisms to be included in the conditioner. Probiotic bacteria were isolated from 0.5 ml of concentrated yogurt ($\sim 10^6$–10^7 CFU/ml) via centrifugation at 4,000 rpm. The pellet was re-suspended in distilled water. Nutrient broth (NB) was prepared with: peptone 10 g, meat extract 8 g, yeast extract 4 g, glucose 4 g, sodium acetate 5 g, Tween 80 1 g, K_2HPO_4 2 g, $MgSO_4$ 0.04 g. NB (5 ml) was dispensed into 10 test tubes, to which 1 ml of each herbal extract and 0.5 ml of probiotic culture were added and serially diluted. Tubes were incubated at 37°C for 24 hours, and bacterial growth was confirmed microscopically.

2) Preparation of Herbal Extract for Use in Conditioning Solution

The process of extraction and preparation was carried out to yield specific herbal extracts possessing beneficial properties suitable for the conditioning formulation. To prepare the ginger extract for a conditioning cream, 100 g of thinly sliced ginger (Zingiber officinale) was soaked in 70% ethanol for 72 hours, filtered, and subsequently dried by evaporation at 55°C, yielding 2.13 g of dry extract per 50 ml of processed liquid. This extract was then incorporated into a hair conditioning cream designed for use after herbal hair dyeing, which was formulated by melting and combining coconut oil and beeswax with pre-warmed aloe vera and the ginger extract. A water phase was gradually added to this oil phase under stirring to create an emulsion. After cooling to 40°C, probiotic biomass (obtained from centrifuged yogurt), vitamin E, and essential oil were added. The final conditioner was stored in sterile, dark containers at 4°C and is intended for application to damp hair and scalp after shampooing, where 2–5 ml is gently massaged in, left for 3–5 minutes, and then rinsed with warm water.

3) Developing Hair Conditioner Formulation

The process of combining the probiotic culture, herbal extracts, and other ingredients was to create the final hair conditioner product. According to previous data used in our lab (data not shown), the formulation consisted of the following ingredients:

Ingredient	Function	Amount
Coconut oil (cold-pressed)	Base oil; moisturizes and conditions hair	20 ml
Ginger extract (Zingiber officinale)	Stimulates scalp, adds shine, antifungal	10 ml
Aloe vera gel (100% pure)	Soothes scalp, hydrates hair	10 ml
Probiotic biomass (Lactobacillus spp.)	Scalp microbiome balance, hair strength	5 ml
Beeswax	Emulsifying agent, added texture	3 g
Vitamin E oil	Antioxidation, prevents oxidative damage	5 drops
Distilled water	Solvent	50 ml

3. Results and Discussion

To establish a hair dyeing and conditioning system that effectively combines aesthetic appeal with the maintenance of optimal hair and scalp health, this research prioritized the development of a novel formulation and centered on the integration of pro-prebiotic principles derived from carefully selected herbal extracts. Recognizing the increasing consumer preference for natural and safer alternatives in personal care, the initial phase of the study focused on identifying and rigorously evaluating specific botanical types.

The inherent color-imparting properties suitable for hair and subsequent details in the findings in formulating the optimal conditions for this natural hair care system was developed as a post-dyeing hair conditioning product enriched with prebiotics and natural herbal extracts. The restoration and maintain hair health following coloration was the key of this innovative protocol together with the involved integrating probiotic and prebiotic components of bioactive plant-based extracts were from these processes are presented as follows:

3.1 Herbal Extracts for Hair Dyeing and Conditioning

The formulation of a natural hair dyeing and conditioning system prioritized the incorporation of carefully selected herbal extracts, specifically ginger (*Zingiber officinale*), turmeric (*Curcuma longa*), and butterfly pea flower (*Clitoria ternatea*). These botanicals were chosen for their established antioxidant, antimicrobial, and hair-conditioning properties. For dyeing and conditioning applications, aqueous extracts of butterfly pea (*Clitoria ternatea*), turmeric (*Curcuma longa*), and henna (*Lawsonia inermis*) were prepared. The extraction process involved individually boiling each herb (1 g/100 ml distilled water), followed by drying the resulting liquid extracts at 55°C. The yields from 50 ml of extract were: butterfly pea – 0.15 g, turmeric – 4.0 g, and henna – 4.0 g. As illustrated in Fig 1, the redissolved herbal extracts demonstrated effective dyeing capabilities upon application to hair. Butterfly pea imparted a dark brown to black hue, turmeric produced a brown tint, and henna yielded a deep brown coloration. The visual characteristics of the initial aqueous extracts are shown in Figure 4.1: (a) butterfly pea – deep indigo, (b) turmeric – bright yellow-orange, and (c) henna – brown.

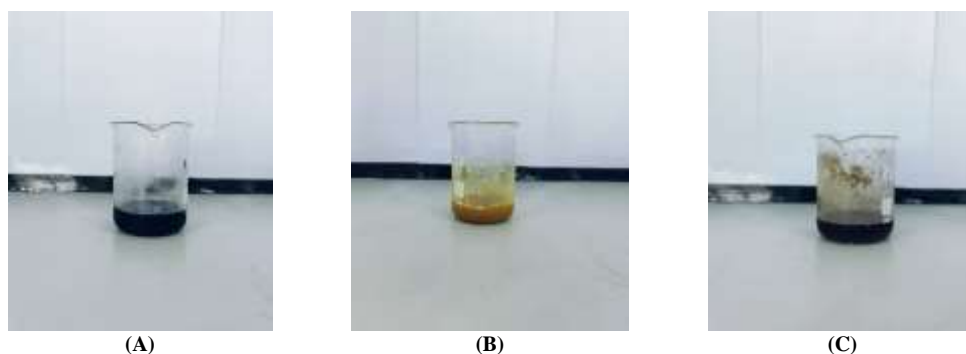| (A) | (B) | (C) |

Figure 1 The appearance and color of three herbal extracts at the concentration of 1 g/100 mL after boiling in water. (A) Butterfly Pea (*Clitoria ternatea*) (B) Turmeric (*Curcuma longa*), and (C) Henna (*Lawsonia inermis*).

3.2 Hair Bleaching and Dyeing with Herbal Extracts

Before dyeing hair with herbal extracts, a crucial initial step is bleaching, which removes the natural melanin pigment to create a uniform, light base for accurate color absorption and evaluation. The study evaluated two chemical agents for their bleaching efficacy: perchloric acid ($HClO_4$) at 2–12% concentrations and a mixture of hydrogen peroxide (H_2O_2, 6–12% (v.v)) with 12% (v/v) of 6 M ammonia (NH_3) were chosen to remove the natural melanin pigment present in the hair by eliminating the inherent color. As visually demonstrated in Figure 2, perchloric acid failed to significantly lighten the hair and induced undesirable dryness, brittleness, and a rough texture, rendering it unsuitable for cosmetic application. In contrast, the hydrogen peroxide and ammonia mixture effectively lightened hair color, particularly at concentrations between 6% and 12%. A 15-minute exposure time was determined to be optimal, providing a balance between noticeable lightening and minimizing hair damage, making it the preferred method for preparing hair for subsequent herbal dyeing. The necessity of a bleaching step prior to herbal dyeing raises an important consideration when comparing it to conventional chemical dyeing processes. Chemical dyes often utilize ammonia to swell the hair cuticle, allowing smaller synthetic dye molecules to penetrate the hair cortex and react with the hair structure to create a permanent color change. The bleaching step in this study, using hydrogen peroxide and ammonia, similarly opens the hair cuticle and removes the natural melanin. This pre-treatment theoretically enhances the hair surface's receptivity, improving the adhesion of larger natural pigment molecules from herbal extracts. However, unlike the chemical reactions of synthetic dyes within the hair cortex, the herbal dyes primarily coat the outer layers of the hair shaft. This difference in mechanism likely contributes to the observed poorer colorfastness of the herbal dyes. The bleaching process, while aiding initial color uptake of the herbal extracts by providing a clean, light base and a slightly opened cuticle, does not facilitate the same level of chemical bonding or deep penetration achieved by synthetic dyes.

Following the successful bleaching process using hydrogen peroxide and ammonia, three herbal extracts – Butterfly Pea (*Clitoria ternatea*), Turmeric (*Curcuma longa*), and Henna (*Lawsonia inermis*) – were applied to the lightened hair samples. All three extracts effectively imparted brown tones, with Butterfly Pea exhibiting the most intense coloration (72%), followed by Turmeric (68%) and Henna (65%). These color changes were visually apparent and corroborated by color measurements taken from photographs of the treated hair (as shown in Figure 2), confirming the dyeing capabilities of these natural extracts on bleached hair. However, a significant limitation was observed: the colorfastness of these herbal dyes was notably lower compared to conventional commercial dyes. After repeated washing, the colors faded considerably, indicating a weaker binding affinity to the hair shaft. Consequently, for individuals opting for these herbal coloring methods, regular reapplication, potentially on a weekly basis, is recommended to maintain color vibrancy. This reduced long-term durability presents a key challenge in the sustained use of these natural dyes for hair coloring.

A. Hair before bleaching

B. Hair bleached with 2% (v/v) HClO₄

C. Hair bleached with 5% (v/v) HClO₄

D. Hair bleached with 12% (v/v) HClO₄

Figure 2 Appearance of hair bleached with HClO₄ at concentrations of 2%, 5%, and 12% (v/v)

| A. Hair sample unbleached (control) | B. Hair bleached with H_2O_2 and NH_3 for 5 minutes | C. Hair bleached with H_2O_2 and NH_3 for 15 minutes | D. Hair bleached with H_2O_2 and NH_3 for 30 minutes | E. Hair bleached with H_2O_2 and NH_3 for 45 minutes |

Figure 3 Appearance of hair bleached with H_2O_2 and NH_3 at different times: 5, 15, 30, and 45 minutes.

3.3 Hair Dyeing with Herbal Extracts

Having established the optimal hair preparation method using X% hydrogen peroxide and Y% ammonia bleaching, the subsequent phase of this study involved assessing the dyeing capability of three herbal extracts: *Clitoria ternatea* (butterfly pea), *Curcuma longa* (turmeric), and *Lawsonia inermis* (henna). As visually documented in Figure 4, the application of each extract to the pre-lightened hair samples resulted in noticeable color transformations, yielding various shades of dark brown. Colorimetric analysis, alongside visual comparisons through photographic documentation (Figure 4.5), further corroborated these findings. Notably, the turmeric extract imparted the most intense coloration (registering 72% relative to untreated black hair), closely followed by henna (at 68%) and butterfly pea (at 65%).

While these herbal dyes clearly demonstrated their capacity to impart visible color to the bleached hair substrate, a significant drawback was the observed colorfastness, which proved to be considerably lower than that exhibited by conventional commercial dyes. The treated hair displayed rapid fading after only a few washing cycles, suggesting a less robust interaction and binding of the natural pigment molecules to the hair shaft in comparison to their synthetic counterparts. Consequently, to maintain color vibrancy and ensure consistent coverage, frequent reapplication, estimated at approximately weekly intervals, would be a practical necessity for individuals opting for these herbal coloring methods. Although these herbal extracts represent a promising direction for the development of natural and potentially safer alternatives to chemical hair dyes, their current performance appears to lack the long-lasting durability that characterizes synthetic formulations. This underscores the need for further investigation into strategies aimed at enhancing the color retention properties of these natural dyes.

| a. Hair dyed with *Clitoria ternatea* extract | b. Hair dyed with *Curcuma longa* extract | c. Hair dyed with *Lawsonia inermis* extract |

Figure 4 Appearance of hair color after dyeing with herbal extracts.

3.4 Development of Hair Conditioning Cream Formulation with Probiotics and Herbal Extracts

This part of the study focused on developing a hair conditioning cream enriched with probiotic microorganisms, with the goal of promoting both hair and scalp health through a more natural and biologically supportive approach. In the initial stage, suitable probiotic strains were selected based on their ability to survive within the cream formulation and remain active during use—an essential requirement that was successfully met (data not shown). Probiotic survival in cosmetic formulations is crucial as it ensures the delivery of live and functional microorganisms to the scalp. Factors like water activity, pH, and the presence of preservatives can significantly impact their viability.

To evaluate their suitability in more detail, the selected probiotics were incorporated into the cream base and monitored for their survivability. The results revealed that the microorganisms maintained a high survival rate—ranging from 70% to 90%—under the formulation conditions (though specific data are not presented here). These findings suggest that the cream's environment, including its ingredients and pH level, was well-suited to support the viability and function of the beneficial bacteria. Common probiotic strains used in cosmetics often belong to the *Lactobacillus* and *Bifidobacterium* genera, known for their skin and scalp benefits. Furthermore, the findings confirmed that the chosen probiotic strains were highly compatible with the hair conditioner. Their presence in the formulation was not merely passive; they remained active at an efficacy rate of approximately 70–80%, indicating that they could meaningfully contribute to the overall conditioning and scalp-care benefits of the product. Probiotic efficacy in hair and scalp care can manifest through various mechanisms, including balancing the scalp microbiome, reducing inflammation, and potentially improving hair follicle health. This demonstrates that it is indeed possible to integrate living, health-promoting microorganisms into a topical cosmetic formulation without compromising their viability or beneficial effects.

3.5 Probiotics and Prebiotic Herbal Extracts in Hair Conditioner

To develop a bioactive hair conditioning cream aimed at promoting scalp and hair health through a balanced scalp microbiome, probiotics derived from yogurt were incorporated. Recognizing that probiotic survival is crucial for their beneficial effects, the formulation was enriched with ginger (*Zingiber officinale*) extract as a natural prebiotic. Prebiotics, non-digestible compounds typically found on the hair and scalp, selectively stimulate the growth and/or activity of beneficial microorganisms, providing a nutrient source for a healthy microbial ecosystem. Probiotic cultures of the *Lactobacillus* genus, known for their beneficial effects on the scalp, were prepared from freshly re-inoculated yogurt and diluted 1:10 in PBS containing 0.1–0.5% ginger extract. These cultures, intended to function in this way, demonstrated strong microbial growth (7–8 log units at OD600) and high cell viability under microscopic observation (Figures 5) after 24 hours of incubation at 37°C. This confirms that ginger extract effectively supports *Lactobacillus* survival, highlighting its potential as a prebiotic in this formulation. Beyond its prebiotic function, ginger extract also offers inherent antioxidant and antimicrobial properties that can further contribute to a healthy scalp environment. Additional tests showed that diluted herbal dye extracts (*Clitoria ternatea* (butterfly pea), *Curcuma longa* (turmeric), and *Lawsonia inermis* (henna)) at a 1:1000 dilution did not negatively impact probiotic activity, indicating their compatibility with the microbial growth. Overall, these results confirm the viability and activity of probiotics within the ginger-based formulation, supporting the development of a natural conditioner designed to nurture the hair and scalp ecosystem.
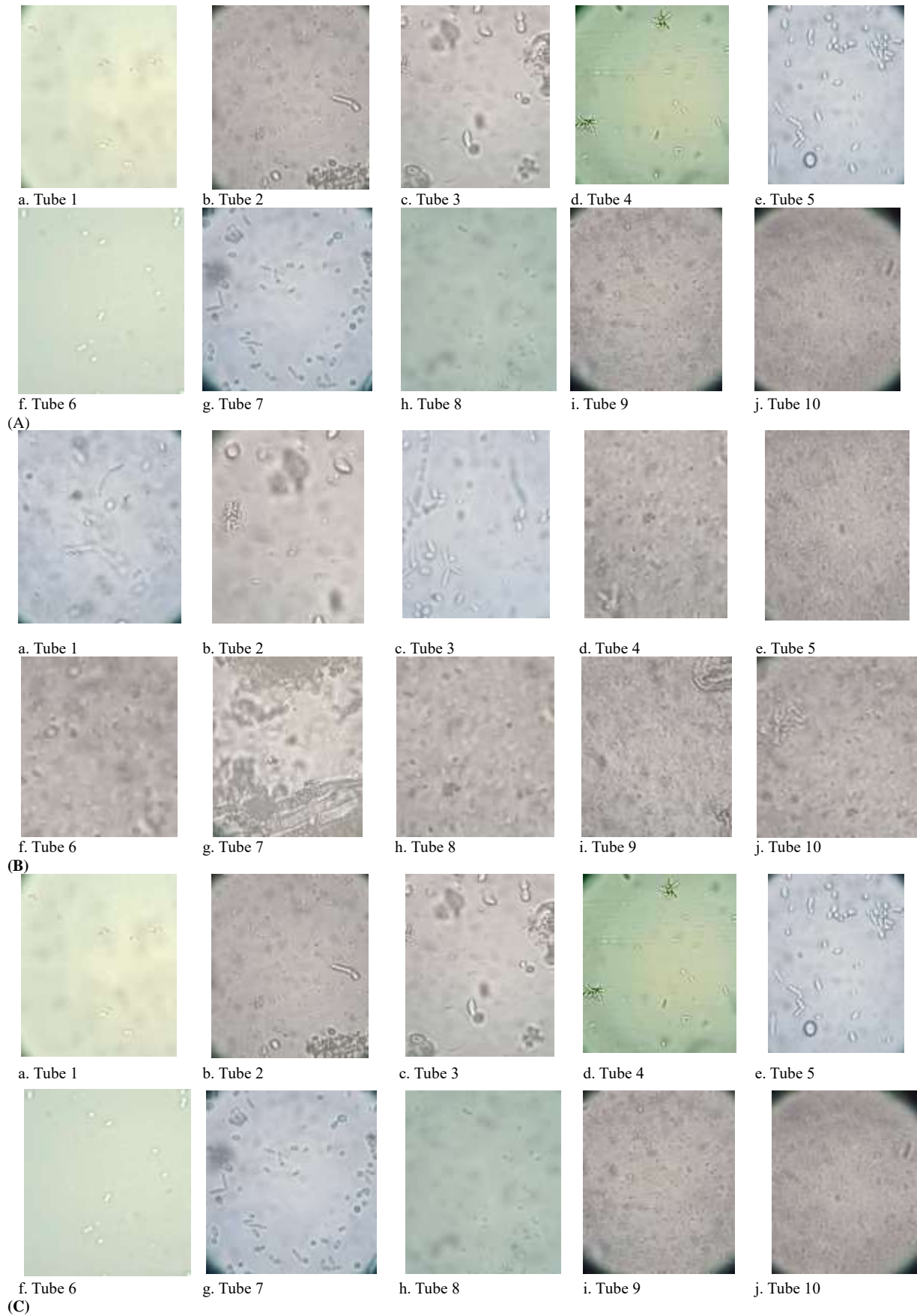.

a. Tube 1   b. Tube 2   c. Tube 3   d. Tube 4   e. Tube 5

f. Tube 6   g. Tube 7   h. Tube 8   i. Tube 9   j. Tube 10

(A)

a. Tube 1   b. Tube 2   c. Tube 3   d. Tube 4   e. Tube 5

f. Tube 6   g. Tube 7   h. Tube 8   i. Tube 9   j. Tube 10

(B)

a. Tube 1   b. Tube 2   c. Tube 3   d. Tube 4   e. Tube 5

f. Tube 6   g. Tube 7   h. Tube 8   i. Tube 9   j. Tube 10

(C)

Figure 5 Microorganisms under a microscope in the hair conditioning cream formula combined with (A) *Clitoria ternatea* extract (1 mg/mL), (B) *Curcuma longa* extract (1 mg/mL), or (C) *Lawsonia inermis* extract (1 mg/mL). Tubes a-j represent samples from tubes 1 to 10, with dilutions ranging from 1:10 to $1:10^{10}$.

3.6 Evaluating Probiotic Conditioner for Herbally-Dyed Hair

A natural and effective post-treatment conditioner, composed of herbal extracts, oils, and probiotics, was developed with the goals of reducing hair damage, enhancing softness, and maintaining scalp balance after the dyeing process. This formulation was specifically designed to restore and nourish hair following the application of herbal dyes. After applying the probiotic-enriched hair conditioning cream to hair previously dyed with herbal extracts, the treated hair exhibited noticeably improved softness and smoothness. Both visual and tactile assessments indicated that its texture was comparable to that of hair treated with commercially available conditioners (Figure 6).

While these initial results are promising, the probiotic-based formulation currently lacks the diversity of functional ingredients commonly found in commercial products, which often include a wide range of additives for targeted hair benefits. To broaden its appeal and efficacy, further research is needed to explore alternative formulations and additional bioactive components. This would help improve product performance and better address the varying needs of consumers.
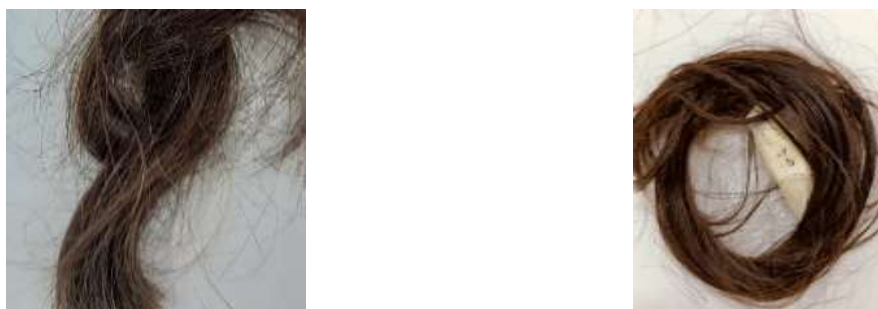
a. Hair dyed with herbal extracts and treated with commercial conditioner

b. Hair dyed with herbal extracts and treated with probiotic-enriched conditioner

Figure 6 Comparison of hair dyed with herbal extracts and treated with either a probiotic-enriched conditioner or a commercial conditioner

Overall, these findings indicate the potential of a hair care system integrating natural herbal dyes and a probiotic-enriched conditioner. The herbal dyes, while effective in imparting color, demonstrated limitations in long-term color retention. Conversely, the probiotic-based conditioner showed promising results in improving hair softness and smoothness post-dyeing, suggesting its potential to mitigate some of the adverse effects associated with hair treatments. However, further optimization of both the dyeing and conditioning formulations is warranted to enhance longevity, broaden efficacy, and ultimately provide a comprehensive and appealing natural alternative to conventional chemical hair treatments.

4. Conclusion

The findings from this study provide valuable insights into the potential of eco-friendly hair care formulations that combine natural herbal dyes and probiotics. To fully realize the commercial and functional potential of this formulation, further research is needed to enhance key aspects such as the stability of probiotic activity through techniques like encapsulation (Habeebuddin et al., 2022; Natarajan et al., 2025). Additionally, improving texture consistency and storage stability under various conditions will be crucial for product optimization (Maurya et al., 2021). Long-term studies on the formulation's effectiveness across different hair types (Yin et al., 2024) and consumer satisfaction surveys will help ensure its broad market appeal. Moreover, integrating biodegradable or recyclable packaging can improve the formulation's environmental sustainability, aligning it with the growing consumer demand for green, eco-conscious cosmetics (Nipurte et al., 2022).

5. Acknowledgement

6. References

Adeel, S., Abrar, S., Kiran, S., Farooq, T., Gulzar, T., & Jamal, M. (2018). Sustainable application of natural dyes in cosmetic industry. In *Handbook of renewable materials for coloration and finishing* (pp. 189-214). Scrivener Publishing.

Brandwein, M., Steinberg, D., & Meshner, S. (2016). Microbial biofilms and the human skin microbiome. *NPJ Biofilms and Microbiomes, 2*(1), 3. https://doi.org/10.1038/s41522-016-0004-z

Choi, J. Y., Boo, M. Y., & Boo, Y. C. (2024). Can plant extracts help prevent hair loss or promote hair growth? A review comparing their therapeutic efficacies, phytochemical components, and modulatory targets. *Molecules, 29*(10), 2288. https://doi.org/10.3390/molecules29102288

Clavaud, C., Jourdain, R., Bar-Hen, A., Tichit, M., Bouchier, C., & Pouradier, F. (2013). Dandruff is associated with disequilibrium in the proportion of the major bacterial and fungal populations colonizing the scalp. *PLoS One, 8*(3), e58203. https://doi.org/10.1371/annotation/bcff4a59-10b7-442a-8181-12fa69209e57

Cui, H., Xie, W., Hua, Z., Cao, L., Xiong, Z., Tang, Y., & Yuan, Z. (2022). Recent advancements in natural plant colorants used for hair dye applications: a review. *Molecules, 27*(22), 8062. https://doi.org/10.3390/molecules27228062

Fernandes, C., Medronho, B., Alves, L., & Rasteiro, M. G. (2023). On hair care physicochemistry: from structure and degradation to novel biobased conditioning agents. *Polymers, 15*(3), 608. https://doi.org/10.3390/polym15030608

Habeebuddin, M., Karnati, R. K., Shiroorkar, P. N., Nagaraja, S., Asdaq, S. M. B., Anwer, M. K., & Fattepur, S. (2022). Topical probiotics: more than a skin deep. *Pharmaceutics, 14*(3), 557. https://doi.org/10.3390/pharmaceutics14030557

Handa, S., Mahajan, R., & De, D. (2012). Contact dermatitis to hair dye: an update. *Indian Journal of Dermatology, Venereology and Leprology, 78*(5), 583-590. https://doi.org/10.4103/0378-6323.100307

Hariadi, H., Sunyoto, M., Nurhadi, B., & Karuniawan, A. (2018). Comparison of phytochemical characteristics pigment extract (Antosianin) sweet purple potatoes powder (*Ipomoea batatas* L) and *Clitoria ternatea* flower as natural dye powder. *Journal of Pharmacognosy and Phytochemistry, 7*(4), 3420-3429.

He, Y., Cao, Y., Nie, B., & Wang, J. (2023). Mechanisms of impairment in hair and scalp induced by hair dyeing and perming and potential interventions. *Frontiers in Medicine, 10*, 1139607. https://doi.org/10.3389/fmed.2023.1139607

Jhamb, D., Chandel, A., Mittal, A., & Tandon, U. (2023). Does the use of organic personal care products persuade sustainable consumption behaviour? Understanding the moderating role of health consciousness. *Young Consumers, 24*(6), 807-830. https://doi.org/10.1108/YC-08-2022-1563

Kumari, S., Singh, P. A., Hazra, S., Sindhwani, R., & Singh, S. (2024). *Ocimum sanctum*: the journey from sacred herb to functional food. *Recent Advances in Food Nutrition & Agriculture, 15*(2), 83-102.

Leite, M. G. A., & Campos, P. M. B. G. M. (2018). Development and efficacy evaluation of hair care formulations containing vegetable oils and silicone. *International Journal of Phytocosmetics and Natural Ingredients, 5*(1), 9-9.

Maiti, S., Sasmal, K., Sinha, S. S., & Singh, M. (2016). Analysis of cytotoxicity and genotoxicity on *E. coli*, human blood cells and *Allium cepa* suggests a greater toxic potential of hair dye. *Ecotoxicology and Environmental Safety, 124*, 248-254. https://doi.org/10.1016/j.ecoenv.2015.11.017

Maurya, P., Maury, S., Yadav, P., Yadav, M. K., Maurya, S., & Jaysawal, S. (2021). A Review Article on Herbal Shampoo. *Journal of Emerging Technologies and Innovative Research, 8*(5), g366-g375.

Natarajan, V., Jaishankar, D., Sugumar, L., Suresh, N., & Thiruvengadam, R. (2025). Comprehensive Review on Formulation and Evaluation of Herbal Shampoo. *Journal of Neonatal Surgery, 14*(19s).

Nipurte, D. S., Datir, M. B., & Fulsundar, A. S. (2022). A review on formulation and evaluation of herbal shampoo. *World Journal of Pharmaceutical Research, 11*(3), 412-418.

Pagac, M. P., Gempeler, M., & Campiche, R. (2024). A new generation of postbiotics for skin and scalp: *in situ* production of lipid metabolites by *Malassezia*. *Microorganisms, 12*(8), 1711. https://doi.org/10.3390/microorganisms12081711

Packianathan, N., & Karumbayaram, S. (2010). Formulation and evaluation of herbal hair dye: an ecofriendly process. *Journal of Pharmaceutical Sciences and Research, 2*(10), 648-654.

Palaniappan, V., Karthikeyan, K., & Anusuya, S. (2024). Dermatological adverse effects of hair dye use: A narrative review. *Indian Journal of Dermatology, Venereology and Leprology, 90*(4), 458-470. https://doi.org/10.4103/ijdvl.ijdvl_520_23

Park, H. K., Ha, M. H., Park, S. G., Kim, M. N., Kim, B. J., Kim, W., & Lee, J. Y. (2012). Characterization of the fungal microbiota (mycobiome) in healthy and dandruff-afflicted human scalps. *PLoS One, 7*(3), e32847. https://doi.org/10.1371/journal.pone.0032847

Patel, S., Sharma, V., Chauhan, N. S., Thakur, M., & Dixit, V. K. (2015). Hair growth: focus on herbal therapeutic agent. *Current Drug Discovery Technologies, 12*(1), 21-42. https://doi.org/10.2174/1873528112666150521120447

Preethi, P. J., Padmini, K., Srikanth, J., Lohita, M., Swetha, K. P. V. R., & Rao, P. V. (2013). A review on herbal shampoo and its evaluation. *Asian Journal of Pharmaceutical Analysis, 3*(4), 153-156.

Siu-Yin Ho, B., Xin Pei Ho, E., Wenhan Chu, C., Ramasamy, S., Bigliardi-Qi, M., Florez de Sessions, P., & Bigliardi, P. L. (2019). Microbiome in the hair follicle of androgenetic alopecia patients. *PLoS One, 14*(5), e0216330. https://doi.org/10.1371/journal.pone.0216330

Singam, T., Marsi, N. B., Abdul Rashid, A. H. B., Nasir, S. H. B., Ibrahim, S. A. B., Roslan, M. N. B., ... & Mohd Fodzi, M. H. B. (2020). A review on characteristics and potential applications of henna leaves (*Lawsonia inermis*). *Journal of Computational and Theoretical Nanoscience, 17*(2-3), 603-612. https://doi.org/10.1166/jctn.2020.8747

Suryawanshi, H., Naik, R., Kumar, P., & Gupta, R. (2017). *Curcuma longa* extract–Haldi: A safe, eco-friendly natural cytoplasmic stain. *Journal of Oral and Maxillofacial Pathology, 21*(3), 340-344. https://doi.org/10.4103/jomfp.JOMFP_161_17

Xu, Z., Wang, Z., Yuan, C., Liu, X., Yang, F., Wang, T., & Zhang, X. (2016). Dandruff is associated with the conjoined interactions between host and microorganisms. *Scientific Reports, 6*(1), 24877. https://doi.org/10.1038/srep24877

Yin, C. S., Nguyen, T. T. M., Yi, E. J., Zheng, S., Bellere, A. D., Zheng, Q., ... & Yi, T. H. (2024). Efficacy of probiotics in hair growth and dandruff control: A systematic review and meta-analysis. *Heliyon, 10*(9), e30160. https://doi.org/10.1016/j.heliyon.2024.e30160

From Waste to Worth Eco-Friendly Antimicrobial Postbiotics from Fermented Garlic Peels as a New Frontier in Natural Fruit Preservation and Shelf-Life Extension

Duongruitai Nicomrat[1]*, Patarika Soongsombat[1], Nipaporn Panay[2], Gritsada Sua-iam[3]

[1]Department of Environmental Science and Technology, Faculty of Science and Technology, Rajamangala University of Technology Phra Nakhon, 1381 Pracharat 1 Road, Wongsawang, Bang Sue, Bangkok 10800.
[2]Department of Computer Science, Faculty of Science and Technology, Rajamangala University of Technology Phra Nakhon, 1381 Pracharat 1 Road, Wongsawang, Bang Sue, Bangkok 10800.
[3]Department of Civil Engineering, Faculty of Engineering, Rajamangala University of Technology Phra Nakhon, 1381 Pracharat 1 Road, Wongsawang, Bang Sue, Bangkok 10800.
* Corresponding Author E-mail address: duongruitai.n@rmutp.ac.th

Abstract

Postbiotics, bioactive compounds produced during microbial fermentation, offer promising health and food preservation benefits. This study presents a novel postbiotic product developed by fermenting Chinese garlic peel extracts with *Lactobacillus* probiotics, aiming to reduce postharvest spoilage in tomatoes. The fermented garlic peel kombucha solution demonstrated antimicrobial activity against common spoilage and pathogenic bacteria, including *Pseudomonas* sp. and *Escherichia coli*. Safety assessment showed low hemolytic activity at concentrations below 200 mg/mL, with no alteration in red blood cell morphology. Antioxidant properties were significantly enhanced compared to regular kombucha, with total phenolic content (TPC) reaching 90.55 ± 10.1 mg GAE/100 mL and total flavonoid content (TFC) at 55.97 ± 8.5 mg RE/100 mL. Application of the fermented solution via surface spraying effectively reduced tomato weight loss, delayed ripening by lowering titratable acidity (TA), and maintained quality by modulating total soluble solids (TSS). These results suggest that fermented garlic peel postbiotics represent an innovative, safe, and environmentally friendly approach for extending the shelf life of fruits, with potential for broader agricultural applications.

Keywords: Kombucha, Garlic Peel Extract, Shelf-life Extension, Antioxidant Activity, Eco-Friendly

1. Introduction

At present, more focus on health and environmental sustainability has catalyzed substantial innovation within the food sector, notably in the realms of probiotics and functional foods. Probiotics, defined as beneficial live microorganisms, particularly lactic acid bacteria (LAB) such as *Lactobacillus* and *Bifidobacterium* species, have garnered considerable scientific and public interest due to their established capacity to enhance gut microbiota balance and bolster immune function (Kozyrovska et al., 2012; Liu, Pang, Zhang, & Cai, 2014; Afiati, et al., 2020). These microorganisms are increasingly incorporated into a diverse range of food products, including yogurt, kefir, and various fermented foods, and their application has expanded into dietary supplements, microencapsulated formulations designed for targeted delivery (Krasaekoopt, Bhandari, & Deeth, 2003; Drywien et al., 2015; Hardinsyah et al., 2023), and even pharmaceutical preparations aimed at specific health outcomes (Bogdan et al., & Gabriela, 2018; Maguire, & Maguire, 2019; Jakubczyk et al., 2020). Ongoing research continues to identify novel probiotic strains with enhanced resilience to the gastrointestinal environment, improved adhesion properties for sustained colonization, and the ability to produce a wider spectrum of beneficial metabolites (da Silva Júnior et al., 2022; Onsun, Toprak, & Sanlier, 2025; Pawlos, Szajnar, Kowalczyk, & Znamirowska-Piotrowska, 2024; Delzenne et al., 2011; Giovannucci et al., 2002).

Complementary to the well-established field of probiotics, significant attention is now directed towards postbiotics—bioactive compounds synthesized during the fermentation processes carried out by probiotic bacteria (Khubber et al., 2022; Calvanese et al., 2025; Cunha et al., 2025; Smolinska, Popescu, & Zemelka-Wiacek, 2025). Unlike their live counterparts, postbiotics exert their beneficial effects without requiring microbial viability, offering functional attributes such as demonstrable antimicrobial activity against spoilage organisms and pathogens, significant anti-inflammatory effects, and the potential to enhance the preservation of food products (Afiati et al., Abrol, & Kumar, 2019; D'Amore et al., 2025). Notably, recent research has highlighted the capacity of specific postbiotics to extend the shelf life of perishable food items and to serve as natural alternatives to synthetic preservatives, addressing consumer preferences for cleaner food labels and more sustainable preservation methods (Khubber et al., 2022; Abrol, & Kumar, 2019; D'Amore et al., 2025; Rameez et al., 2024; Ivanišová et al., 2020; Yeganeh et al., 2020). Advances in understanding the specific bioactive molecules within postbiotic mixtures and their mechanisms of action are paving the way for targeted applications in food science and technology (Leal et al., 2018; Martyniak et al., 2021; Moradi, Molaei, & Guimarães, 2021; Nataraj et al., 2020; Rajam, & Subramanian, 2022). Despite the growing recognition of postbiotics' potential in food preservation, a notable gap persists in the comprehensive exploration of agricultural waste streams as sustainable and cost-effective resources for their production (Afiati, Setyoningrum, Priadi, & Handoyo, 2020; Borek, 2001). Garlic peels, a substantial byproduct of garlic processing often discarded as waste, are

known to be rich in a diverse array of bioactive compounds with inherent antimicrobial and antioxidant properties (Vinderola, Sanders, & Salminen, 2022; Borek, 2001; Ifesan, Fadipe, & Ifesan, 2014; Matto et al., 1975; Queiroz et al., 2009; Sharma, Sharma, & Sharma, 2021). This research endeavors to bridge this gap by investigating the production of environmentally friendly antimicrobial postbiotics derived from the controlled fermentation of garlic peels. This approach aligns with the increasing global emphasis on circular economic principles, aiming to transform waste materials into value-added solutions that are both ecologically sound and beneficial for human health (Kim et al., 2012; Kim, Park, & Jang, 2011; Queiroz et al., 2009; Simon, 1995; Wang, Zhu, Chen, & Zhang, 2019). By harnessing the inherent potential of fermented garlic peels, this study seeks to contribute to the development of innovative and natural strategies for food preservation, offering a sustainable alternative to conventional chemical preservatives and opening new avenues in the creation of functional foods with enhanced shelf life and consumer appeal.

Tomatoes (*Solanum lycopersicum* L.) are of significant global economic importance as a widely consumed horticultural commodity. They are rich in lycopene, a potent antioxidant, which has been associated with a reduced risk of various diseases, including prostate cancer (Giovannucci et al., 2002; Sesso et al., (2003). The substantial postharvest losses incurred due to their rapid spoilage present considerable challenges to food security and economic sustainability, underscoring the critical need for effective preservation strategies (D'Amore et al., 2025; Matto et al., (1975). As a classic climacteric fruit, tomatoes exhibit a pronounced and continuous ripening process even after harvest, characterized by a surge in ethylene production and altered respiration rates. This leads to a cascade of readily observable and quantifiable changes, including rapid softening, distinct color transitions from green to red, and significant alterations in key physicochemical properties such as total soluble solids (TSS), titratable acidity (TA), sugar content, and ascorbic acid levels, all measurable through standard laboratory techniques (Sadasivam, & Manickam, 1991). Their inherent sensitivity to both microbial spoilage by bacteria and fungi, as well as physiological deterioration, further positions tomatoes as an ideal model system for evaluating the efficacy of novel preservation treatments. Consequently, demonstrating a natural and effective method for extending the shelf life and maintaining the quality of tomatoes, as explored in this study using kombucha fermented with garlic peel extract, holds considerable relevance for broader applications in food preservation, potentially reducing the reliance on synthetic chemical additives (Nataraj et al., 2020; Morales, 2020). The measurable and visually apparent changes during tomato ripening and senescence provide robust and objective data to assess the potential of this fermented extract in delaying these natural processes and thus proving its efficacy as a natural food preservation agent.

The escalating consumer demand for natural and sustainable food preservation methods, coupled with the well-established health benefits of probiotics and the emerging potential of postbiotics, is a significant driver of innovation in the food industry (Păcularu-Burada, & Bahrim, 2021; Thorakkattu et al., 2022; Quigley, 2010; Rangana, 1986). Postbiotics, the bioactive compounds generated during microbial fermentation, have demonstrated promising antimicrobial and antioxidant properties that can effectively extend the shelf life of perishable foods while reducing the need for synthetic preservatives (Onsun, Toprak, & Sanlier, 2025; Yeganeh et al.,2020; Sesso, Liu, Gaziano, & Buring, 2003). Simultaneously, the growing consumer awareness of health and environmental sustainability has significantly propelled research into probiotics, beneficial live microorganisms like lactic acid bacteria (LAB), recognized across numerous studies for their capacity to enhance gut health and modulate the immune system (Maguire, & Maguire, 2019; Delzenne et al., 2011; Cunha et al., 2025; Smolinska, Popescu, & Zemelka-Wiacek, 2025; Păcularu-Burada, & Bahrim, 2021; Hussein, Hameed, & Hadi, 2017; Ryu, & Kang, 2017). Building upon these established benefits, a substantial body of research now focuses on postbiotics, highlighting their significant functional properties, including demonstrable antimicrobial activity and the potential to enhance food preservation without requiring microbial viability (Cunha, Santos-Sodré, Teixeira-Costa, & Santos, 2025; Smolinska, Popescu, & Zemelka-Wiacek, 2025; Martyniak et al., 2021; Moradi, Molaei, & Guimarães, 2021; Matto et al., 1975). Furthermore, research increasingly explores the utilization of agricultural waste streams, rich in various bioactive compounds, as cost-effective substrates for producing these valuable postbiotics, contributing to waste valorization and the development of environmentally friendly food preservation strategies (Cunha, Santos-Sodré, Teixeira-Costa, & Santos, 2025; Smolinska, Popescu, & Zemelka-Wiacek, 2025; Rameez, Santhoshkumar, Yoha, & Moses, 2024).

Therefore, from this comprehensive background, this research aims to innovate the production of postbiotics and leverage the benefits of probiotics derived from natural food ferments, enhanced by the incorporation of garlic peels. This research aims to innovate the production of postbiotics derived from probiotic fermentation of garlic peel extract, particularly when incorporated into kombucha, and to evaluate their efficacy in enhancing food quality and extending the shelf life of tomatoes. The specific objectives include: (1) assessing the antioxidant activity of the fermented extract, (2) determining its antimicrobial activity against food-related microorganisms, (3) evaluating its ability to preserve the physicochemical quality of postharvest tomatoes, (4) assessing its potential to mitigate physical deterioration and extend the shelf life of tomatoes, and (5) conducting a preliminary safety evaluation through hemolytic toxicity assessment. Ultimately, this work contributes to sustainable food preservation strategies by valorizing agricultural waste and offering a natural alternative to synthetic chemicals.

2. Methodology

2.1 Preparation of Fermented Kombucha and Garlic Peel Extract

Garlic Peel Preparation:

Fresh garlic bulbs were rinsed with sterile distilled water and allowed to air dry at room temperature. The outer peels were separated and washed again with sterile distilled water to remove any surface contaminants. The cleaned peels were then dried in an oven at 40°C. Sixty grams of the dried garlic peels were subjected to high-temperature and high-pressure steam treatment at 100°C for 15 minutes, followed by further drying at 70°C for 10 minutes. The dried peels were then ground and sieved through a 2 mm mesh. The resulting garlic peel powder was stored in a dark glass container until further use.

Extraction of Bioactive Compounds from Garlic Peel:

Garlic peel powder (20 g) was soaked in 100 mL of 80% (w/v) ethanol. The mixture was agitated at 120 rpm at 50°C for 18 hours. The resulting solution was filtered through multiple layers of sterile gauze and then concentrated by heating in a water bath at 60°C followed by centrifugation at 5000 rpm. The supernatant was filtered through Whatman No. 4 filter paper. The garlic peel extract was then dried using a rotary evaporator and resuspended in 0.2% Tween 80 in sterile distilled water to achieve a final concentration of 10 mg/mL. This garlic peel extract was subsequently used for antimicrobial and antioxidant activity studies.

Preparation of Kombucha Fermented with Garlic Peel Extract:

A black tea-based kombucha SCOBY (Symbiotic Community of Bacteria and Yeast) was used as the starter culture. For the fermentation, 10-20 grams of steam-treated, sliced, and blended garlic peels were added to 100 mL of a 20% (w/v) sucrose solution. The fermentation was initiated by adding 0.5-1.0% (v/v) of the prepared garlic peel and SCOBY solution. The fermentation was carried out in bottles covered with sterile cheesecloth for 7 days at 35±2°C. The total phenolic content (TPC) and total flavonoid content (TFC) of the resulting fermented kombucha with garlic peel extract were measured. All experiments were performed in triplicate.

Preparation of Kombucha Starter

A symbiotic community of Bacteria and Yeast (SCOBY) culture, previously grown in a standard black tea kombucha fermentation, was used as the starter for subsequent experiments. The SCOBY was maintained in a liquid medium consisting of sterile distilled water, 10% (w/v) sucrose, and 1% (w/v) brewed black tea infusion. The culture was incubated statically at room temperature (approximately 25-30°C) and allowed to form a new cellulose pellicle. For use as a starter, a portion of the liquid medium containing a piece of the cellulose pellicle was transferred to initiate the fermentation processes described in section 1.3. The starter culture was routinely subcultured to maintain its viability and activity.

2.2 Determination of bioactivity

Total Phenolic Content (TPC) Measurement: A modified spectrophotometric method at 740 nm was used to determine TPC in fermented garlic peel extracts. Results were expressed as mg gallic acid equivalent (GAE)/g dry weight, calculated against a gallic acid standard curve. For comparison, fresh garlic underwent maceration in distilled water, followed by extraction via boiling at 90°C for 2 hours.

DPPH Radical Scavenging Activity Assay:

The antioxidant activity was assessed using the DPPH radical scavenging assay. The assay measures the ability of extracts to scavenge the stable radical 2,2-diphenyl-1-picrylhydrazyl (DPPH). In the study, the antioxidant compounds present in the garlic peel, including inherent natural antioxidants, vitamins, and microbial metabolites produced during fermentation, contribute to this activity. The potential for fermentation to enhance or preserve these antioxidant compounds was also considered. The anti-free radical scavenging activity of kombucha fermented with garlic peel extract was determined using the DPPH assay. Serial dilutions of the extract and ascorbic acid (Vitamin C, as a positive control) were prepared in ethanol. One mL of each dilution was mixed with 2 mL of 0.1 mM DPPH solution, incubated in the dark for 30 minutes, and the absorbance was measured at 517 nm. The percentage inhibition of the DPPH radical was calculated using the formula:

% Inhibition = [(A_control - A_sample) * 100 / A_control]

The IC50 values for the extract and ascorbic acid were determined from the inhibition curves.

Antimicrobial activity Based on Agar Well Diffusion Assay: Antimicrobial activity was assessed Cultures of *Staphylococcus* sp., *Bacillus* sp., *E. coli*, *Streptococcus* sp., *Pseudomonas* sp., and *S. cerevisiae* were prepared and spread onto agar plates. Wells were created, and equal volumes of a control solution, standard kombucha, and kombucha fermented with garlic peel extract (Kb+Garlic Peels) were introduced into separate wells. Following incubation under appropriate conditions, the diameters of the zones of inhibition surrounding each well were measured in millimeters using a calibrated caliper.

Hemolytic Toxicity Assessment

The hemolytic toxicity of kombucha fermented with garlic peel extract was evaluated using porcine erythrocytes. Fresh porcine blood was collected and erythrocytes were isolated. The erythrocytes were then washed and resuspended in phosphate-buffered saline (PBS). The kombucha fermented with garlic peel extract, prepared as previously described, was tested at concentrations of 50 mg/mL and 200 mg/mL. Erythrocyte suspensions were incubated with each concentration of the extract at room temperature. Aliquots were taken at 5, 10, and 30 minutes and observed under a light compound microscope at 100X and 400X magnification to assess changes in cell

morphology, including swelling and lysis, compared to an untreated control erythrocyte suspension incubated with PBS alone. Hemolysis was determined by visual observation of erythrocyte integrity and the presence of released hemoglobin in the surrounding medium.

Physicochemical Properties of Stored Tomatoes

Mature green tomatoes were harvested and divided into two groups: a control group sprayed with distilled water and a treatment group sprayed with kombucha fermented with garlic peel extract (Kb+Garlic Peels). Both groups were stored at ambient temperature (approximately 28-32 °C and 70-80% relative humidity) for 21 days. Samples were analyzed every 3 days for TSS (using a refractometer), TA (by titration with NaOH and expressed as % citric acid), total sugars (by the phenol-sulfuric acid method and expressed as %), and ascorbic acid content (by titration with 2,6-dichloroindophenol and expressed as mg/100 g).

3. Results and Discussion

The results of the production of postbiotics from Chinese garlic peel fermented with *Lactobacillus* probiotics for the purpose of inhibiting microbial contamination in food In developing the potential of the fermentation process of lactic acid-producing probiotic strains to break down garlic peel raw materials (controlling suitable conditions such as temperature, pH, and time to create a suitable environment, such as the addition of nutrients to create a suitable environment for growth), followed by fermentation to produce postbiotics and separation of postbiotics under suitable conditions to obtain a large quantity of postbiotics, this research work fermented garlic extract in kombucha using a process developed in the laboratory (results not shown in this study). The physical and chemical properties obtained from the kombucha water did not differ from the control kombucha fermented with tea, but the biological properties were different. The study results are as follows: 3.1 To study the selection and development of efficient probiotic microorganisms. 3.2 To study and develop the fermentation process of garlic peel with probiotics. 3.3 To study the biological properties of microbial inhibition and food spoilage prevention.

3.1 Study on the Selection and Development of Efficient Probiotic Microorganisms

The selection and development of probiotic microorganisms to be efficient in producing postbiotics and able to inhibit pathogenic microorganisms was carried out by preparing lactic acid bacteria from kimchi, *Khao Mak* (fermented sweet glutinous rice), and commercially available probiotic-supplemented beverages that were suitable for indicating probiotic properties and the ability to grow in microbial culture media containing garlic peel as a raw material. The experimental results showed that a group of rod-shaped and spherical microorganisms could be cultured, as shown in Figures 1-3, indicating the growth of probiotics obtained from the presence of garlic and garlic peel in MRS culture medium, which required the addition of 0.5% glucose to promote growth well. Within 10-12 hours at 32-35°C, the results are shown in the figures and growth curve.

From the study of the growth of 3 probiotic strains in MRS culture medium with and without 0.5% glucose (Figures 4-5), it was found that strain 2 (orange) had the highest growth under conditions with MRS and 0.5% glucose, with the optical density peaking at approximately 2 at the 5th hour. Strain 3 (light blue) and strain 1 (dark blue) showed relatively stable growth at an OD of approximately 0.5, regardless of the presence or absence of glucose. The result of treatment with MRS without glucose (green) showed slower growth in all strains. This result indicates that strain 2 is sensitive to the increase in glucose and can grow rapidly in the presence of this supplement, while strains 1 and 3 did not show much growth in either the presence or absence of glucose, which may indicate limitations in utilizing glucose for growth. The condition of MRS without glucose clearly reduced the growth of all strains due to the lack of a crucial energy source. From Figures 4-5, it can be seen that bacterial strains 1 and 2 have growth responses to different environments. Strain 1 grows well in the presence of 1.5% glucose, while strain 2 responds well in MRS with 0.5% glucose. However, strain 3 seems to have minimal response in all conditions.

3.2 Developing Efficient Probiotic Microorganisms: Towards Postbiotic Production from Garlic Peel for Antimicrobial Applications

The crucial step of developing efficient probiotic microorganisms for the production of postbiotics derived from Chinese garlic peel. The ultimate goal is to utilize these postbiotics to combat microbial contamination in food. The initial phase involved the selection and development of lactic acid bacteria (LAB) from diverse sources, including kimchi, *Khao Mak*, and probiotic supplements. From preliminary findings highlight the successful cultivation of specific microorganisms (rod-shaped and spherical) that thrive in MRS culture medium containing garlic peel. Notably, the addition of 0.5% glucose and optimal incubation conditions (32-35°C for 10-12 hours) significantly enhanced microbial growth.

A comparative growth study of three probiotic strains in MRS medium with and without glucose revealed that *Lactobacillus* sp. strain 2 exhibited the highest growth rate in the presence of 0.5% glucose. In contrast, Strains 1 and 3 showed less significant growth responses across varying glucose concentrations, indicating differing nutritional requirements and metabolic capabilities. The absence of glucose in the culture medium demonstrably hindered the growth of all strains, underscoring the importance of an energy source.

Overall, this initial phase research showed success based on the developing efficient probiotic microorganisms, which is central to the successful production of garlic peel-derived postbiotics for effective antimicrobial applications in food preservation.
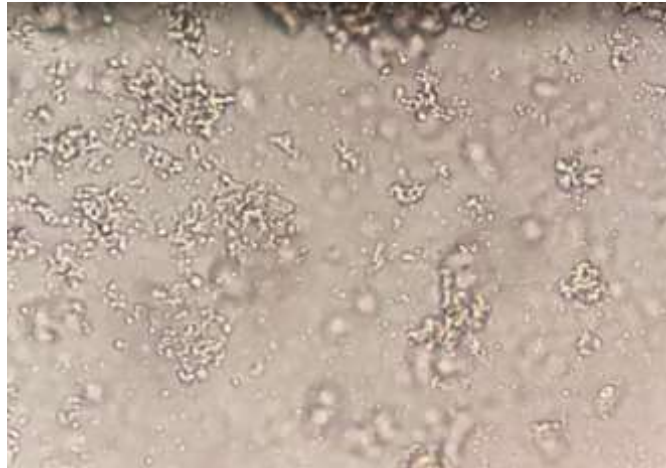
Figure 1 An example of *Bacilli* group bacteria obtained from probiotics from a dietary supplement source isolated from kimchi (strain 1, KM-43)
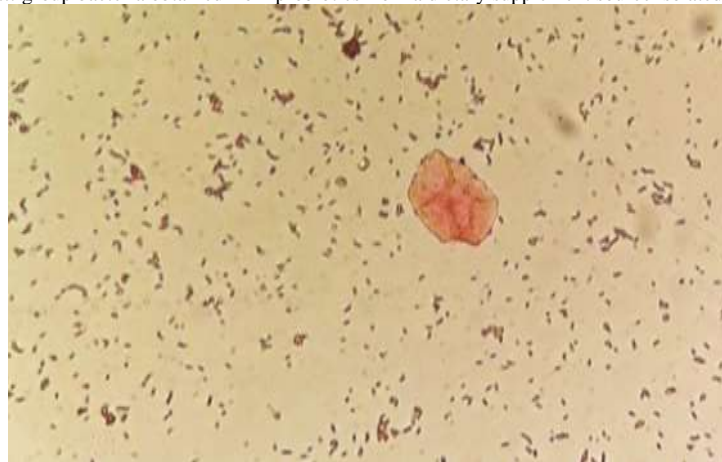

Figure 2 Example of *Bifidobacteria* group bacteria obtained from a probiotic dietary supplement source for gut health (strain 3, Gt-37)
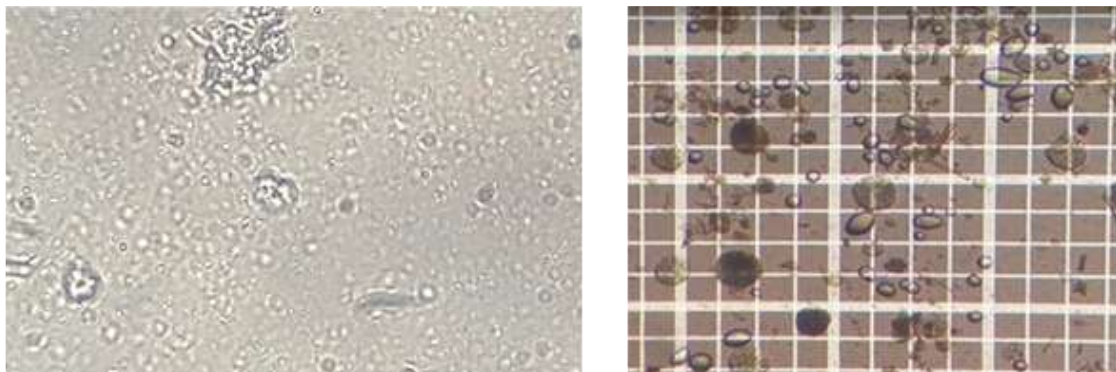

Figure 3 Examples of bacteria (strain 3) (a) and yeast (b) in the *Probiotics* group from a *Khao Mak* (fermented sweet glutinous rice) source (RF-18)

3.3 *Probiotic Growth Kinetics in MRS Medium with and without Glucose*

The studies demonstrated the growth dynamics of selected three probiotic Lactobacilli strains (strain 1, strain 2, and strain 3) under this evaluated in MRS medium with and without 0.5% glucose over a 48-hour incubation period (Figure 4). There are variations in the probiotic growth according to the variation in Microorganism activities. These findings underscore the diverse nutritional preferences and growth efficiencies among the tested probiotic strains, providing critical insights for the selection and optimization of strains for potential postbiotic production processes. Strain 2, in particular, demonstrates a high growth potential in glucose-rich conditions, suggesting its suitability for applications where rapid and high biomass production is desired. Strain 2 exhibited the most robust growth, characterized by a rapid increase in optical density and a high final biomass yield in the presence of glucose, indicating a strong preference for this carbon source and confirming that the observed growth attributable to the inoculated probiotic strains.
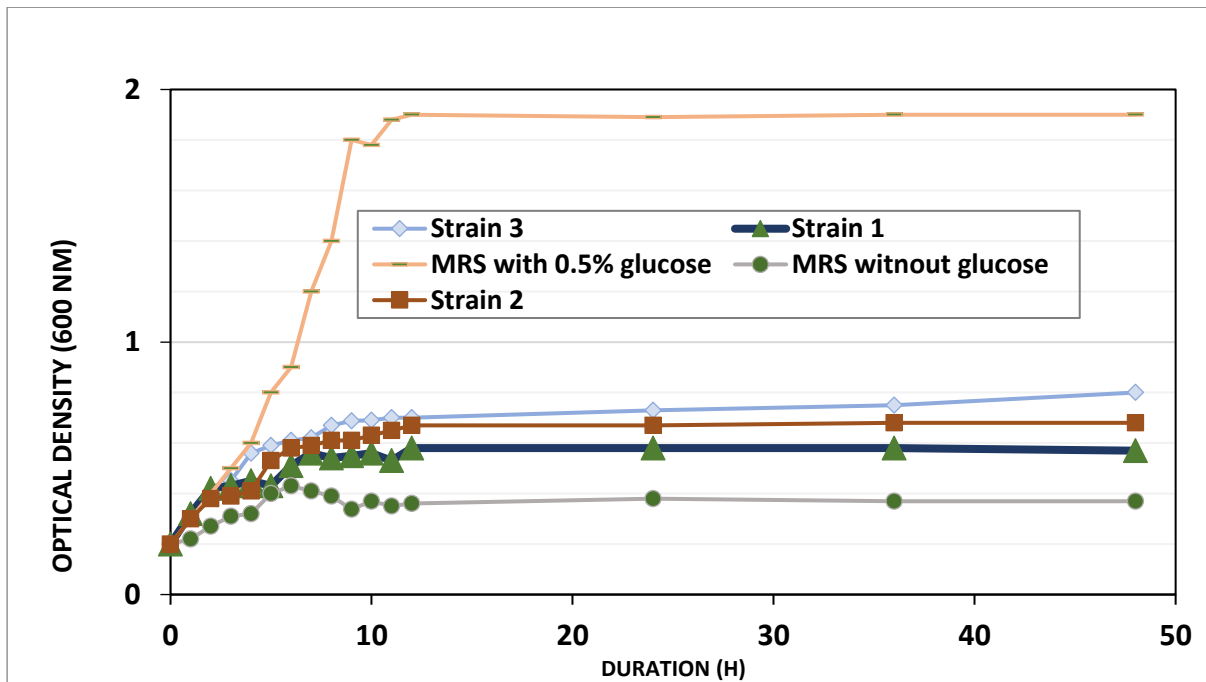
Figure 4 Growth of probiotics in MRS culture medium with and without Glucose supplementation.

3.4 Probiotic Isolates in MRS Medium Containing Garlic Peel and 1.5% Glucose

The growth curves indicate distinct responses of the probiotic isolates to the MRS medium supplemented with 1.5% glucose and containing garlic peel and garlic extract. Strain 2 demonstrated the most promising growth among the three isolates in this specific environment, exhibiting both a relatively rapid initial growth and the highest final optical density. This suggests that Strain 2 may be better adapted to utilize the available nutrients, including glucose and potentially compounds derived from the garlic peel and extract. Strain 1 showed a more consistent but slower growth rate, reaching a moderate final cell density. This isolate may have a different metabolic strategy or a lower affinity for the available substrates compared to Strain 2. Strain 3 exhibited poor growth under these conditions, suggesting that this specific environment might not be optimal for its proliferation. This could be due to an inability to effectively utilize the carbon source, potential inhibitory effects from the garlic compounds at the tested concentration, or other factors not investigated in this study.
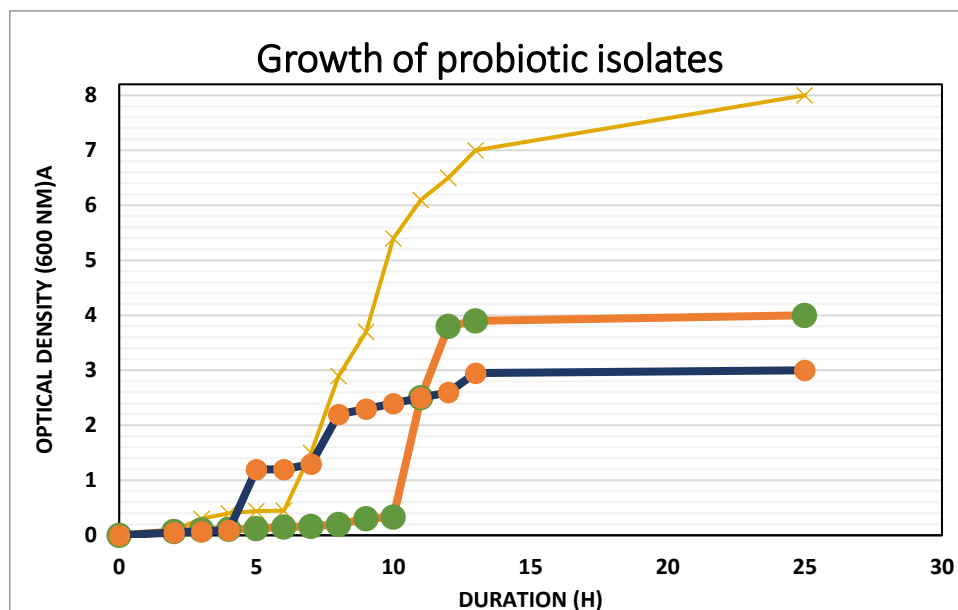

Figure 5 Growth curves of probiotic isolates in MRS broth supplemented with garlic peel, garlic extract, and 1.5% glucose (blue, orange, and green lines represent strain 1, 3, and 2 respectively) and lactic acid bacteria isolated from a specific source in MRS with 1.5% glucose (yellow line with crosses).

The significantly higher growth observed in the yellow line likely represents a different condition or a highly adapted isolate not directly comparable to the three main isolates under the garlic peel/extract condition. The

description suggests it might be a control or a separate experiment focusing on a specific lactic acid bacterium. These findings highlight the importance of screening and selecting probiotic strains that exhibit robust growth in the presence of the specific substrate (garlic peel and extract in this case) intended for postbiotic production. Further investigation into the metabolic pathways and tolerance mechanisms of the more successful strains (particularly Strain 2) could provide valuable insights for optimizing fermentation strategies utilizing garlic byproducts.

Since Garlic and its peel, which are known sources of antioxidant phenolic compounds, it can enhance their more effectiveness through probiotic fermentation, leading to the application in production of postbiotics with combined beneficial properties [11, 19, 32, 37-38, 49]. The ability to generate phenolic substances from garlic peel is crucial as it indicates a significant antioxidant potential. This potential can be enhanced through probiotic fermentation, leading to the production of postbiotics with combined beneficial properties. The total phenolic content (TPC) and antioxidant activity of fermented garlic peel, comparing it to unfermented garlic, and exploits the antioxidant properties of kombucha fermented with garlic peel extract.

3.5 Efficient Postbiotics from Fermented Garlic Peel with Probiotics: Investigation of Antioxidant Properties

A gallic acid standard solution was prepared, and its absorbance values were measured to generate a standard curve (Figure 6), The antioxidant capacity was also assessed against an ascorbic acid standard curve could reveal the antioxidation properties of both kombucha Fermented with Garlic Peel Extract in Table 1. It demonstrated that the antioxidant properties of standard kombucha and kombucha fermented with garlic peel extract. The TPC of kombucha with garlic (90.55 ± 10.1 mg GAE/100 mL) was slightly higher than that of standard kombucha (89.43 ± 12.0 mg GAE/100 mL), indicating no significant difference due to garlic addition. However, the total flavonoid content (TFC) of kombucha with garlic (55.97 ± 8.5 mg RE/100 mL) was significantly higher than that of standard kombucha (48.80 ± 7.8 mg RE/100 mL), suggesting that garlic peel extract significantly increased the flavonoid content of the kombucha.

Table 1 Antioxidant Properties of Kombucha and Kombucha with Garlic Peel Extract (Total Phenolic Content and Total Flavonoid Content)

Sample	Total Phenolic Content (mg GAE/100 mL)	Total Flavonoid Content (mg RE/100 mL)
Standard Kombucha	89.43 ± 12.0	48.80 ± 7.8
Kombucha with Garlic Extract	90.55 ± 10.1	55.97 ± 8.5

Overall, although the initial levels might not drastically differ from garlic flesh, the antioxidant capacity of garlic peel can be enhanced through fermentation and processing techniques. Notably, the fermented garlic peel extract exhibited antioxidant properties and antioxidative efficacy comparable to ascorbic acid, suggesting its potential as a beneficial antimicrobial agent. Preliminary results from the fermentation of garlic peel to obtain postbiotics demonstrate promising antioxidant properties. Garlic peels, often considered as one type of biological waste, are significant source of antioxidants and phenolic compounds. Anaerobic fermentation with lactic acid bacteria (probiotics) resulted in increased antioxidant production, particularly postbiotics with antioxidative properties. The fermented garlic peel extract exhibited high polyphenol content, including compounds like gallic acid, catechin, epicatechin, and quercetin, known for their potent antioxidant activity. The DPPH assay showed that fermented garlic peel extract had higher antioxidant efficacy than garlic flesh. While ABTS assay was not used in this study, existing research supports the ability of garlic peel polyphenols to effectively inhibit lipid peroxidation, reducing cell damage and preventing various diseases. Future steps involve large-scale kombucha fermentation with the selected probiotic strains and garlic peel extract to study protein and sugar changes during fermentation, aiming to develop a potent antimicrobial agent for food products.

3.6 Biological Properties of Postbiotics from Probiotic-Fermented Garlic: Microbial Inhibition and Food Spoilage Prevention

Antimicrobial Properties Against Pathogens

The antimicrobial activity of kombucha fermented with garlic peel extract (Kb+Garlic Peels) was evaluated against a panel of microorganisms, and the resulting inhibition zone diameters are graphically presented in Figure 6. As visually depicted in the graph, Kb+Garlic Peels consistently yielded the largest inhibition zones for most of the tested microorganisms, indicating a superior antimicrobial activity compared to the other treatments. Notably, the inhibitory effect of Kb+Garlic Peels was substantially greater against *Bacillus* sp. (approximately 3.5 mm), *E. coli* (approximately 4.6 mm), *Streptococcus* sp. (approximately 4.0 mm), and *Pseudomonas* sp. (approximately 4.8 mm). This enhanced activity is likely attributable to the synergistic interaction between the organic acids and other antimicrobial metabolites produced during kombucha fermentation and the diverse array of bioactive compounds, including sulfur-containing compounds and phenolic acids, extracted from garlic peel and integrated into the fermented matrix. These compounds are known to disrupt microbial cell membranes and interfere with essential metabolic processes.

While standard kombucha also exhibited some inhibitory activity, its effect was generally less pronounced than that of Kb+Garlic Peels. For *Staphylococcus* sp., both kombucha formulations showed relatively modest inhibition (approximately 1.5 mm for standard kombucha and 2.0 mm for Kb+Garlic Peels). The yeast, *S. cerevisiae*, displayed the least susceptibility to all treatments, with Kb+Garlic Peels exhibiting a small inhibition zone (approximately 2.2 mm). The control treatment consistently resulted in minimal or no inhibition zones, confirming

that the observed antimicrobial activity was a direct consequence of the compounds present in the fermented kombucha, particularly those augmented by the inclusion of garlic peel extract.

The enhanced antimicrobial activity of Kb+Garlic Peels suggests its potential as a natural biopreservative in food systems. The broad-spectrum inhibition observed against both Gram-positive and Gram-negative bacteria, including potential foodborne pathogens like E. coli and spoilage organisms like Pseudomonas sp., highlights its versatility. The incorporation of garlic peel, a readily available agricultural byproduct, into the kombucha fermentation not only enhances its antimicrobial properties but also adds value to this waste stream. Further research should focus on identifying the specific bioactive compounds responsible for the observed inhibition and optimizing the fermentation process to maximize their production for targeted applications in food preservation and safety [17, 24].
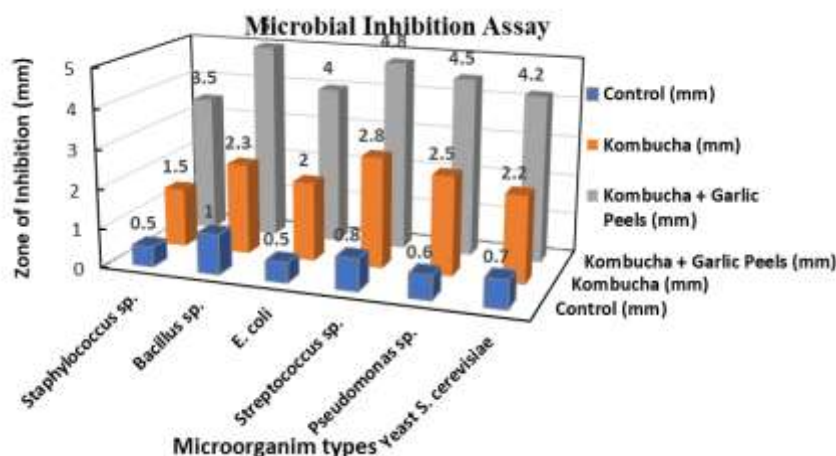

Figure 6 The ability of kombucha fermented with garlic peel extract to inhibit pathogenic microorganisms

3.7 Effect of Kombucha Fermented with Garlic Peel Extract on the Physicochemical Properties of Stored Tomatoes

To understand the efficient potential of kombucha fermented with garlic peel extract as natural preservation method, leveraging the antimicrobial and antioxidant properties of garlic-derived compounds and the acidic environment of kombucha. It showed the effective treatment on key physicochemical attributes associated with tomato ripening and senescence as in table 2. Since tomato (*Solanum lycopersicum* L.) which is a climacteric fruit susceptible to rapid postharvest deterioration. Therefore, maintaining its quality during storage is crucial to minimizing losses

Table 2. Physical and Chemical Properties of Kombucha Fermented with Garlic Peel

	TSS (°Bric)		Titrable actidity (%)		Total sugars (%)		Ascorbic acid (mg/100 g)	
Storage day	Control	Kb+Garlic Peele	Control	Kb_Garlic Peels	Control	Kb+Garlic Peels	Control	Kb+Garlic Peels
0	4.1	3.8	0.604	0.763	1.70	1.76	14.44	14.40
3	4.3	3.2	0.764	0.734	1.86	1.79	13.28	14.62
6	3.9	3.2	0.651	0.754	1.99	1.88	11.76	12.78
9	4.2	3.9	0.607	0.634	2.11	1.92	12.04	13.41
12	4.9	4.5	0.432	0.592	2.25	2.07	9.88	10.74
15	4.8	4.0	0.372	0.406	2.32	2.09	8.64	10.61
18	5.7	5.0	0.346	0.444	2.52	2.16	8.42	9.02
21	4.5	4.3	0.300	0.402	2.58	2.28	7.65	8.76

The application of kombucha fermented with garlic peel extract (Kb+Garlic Peels) as a postharvest treatment demonstrated a significant impact on the physicochemical properties of stored tomatoes, effectively slowing down changes associated with ripening and senescence. Over the 21-day storage period, tomatoes treated with Kb+Garlic Peels consistently maintained higher titratable acidity (TA) and ascorbic acid content while exhibiting a slower increase in total soluble solids (TSS) and total sugars compared to the control group. For instance, on day 21, the control tomatoes showed a TA of 0.300%, whereas the treated tomatoes retained a significantly higher TA of 0.402%, indicating a delayed breakdown of organic acids. Similarly, the ascorbic acid content in the treated group at day 21 was 8.76 mg/100 g, demonstrably higher than the 7.65 mg/100 g observed in the control, suggesting a protective effect against vitamin C degradation.

These findings strongly suggest that natural treatment has the potential to extend the shelf life and preserve the quality of tomatoes. The slower decline in TA and ascorbic acid, coupled with the moderated changes in TSS and total sugars, points towards a retardation of the metabolic processes associated with ripening. These physicochemical property results are consistent with the findings of Rathore et al. (2007), where similar natural treatments with the observed effects could extend the shelf life of mangoes. The preservation of these vital compounds also implies that

natural treatments with postbiotics could offer a sustainable alternative to other chemical and physical preservation methods, without compromising the nutritional value and taste of tomatoes. In terms of observation details, the acidic environment of kombucha, along with the bioactive compounds present in garlic peel extract, contributes to this preservation effect. The antimicrobial properties of garlic-derived substances may inhibit microbial spoilage, while their antioxidant capacity could mitigate oxidative stress, both factors contributing to the delayed deterioration of the treated tomatoes [47, 50]. The observed maintenance of higher TA in the treated tomatoes, as exemplified by the 0.402% compared to 0.300% on day 21, implies a slower metabolic rate and a potentially delayed conversion of acids into sugars, a key aspect of fruit ripening.

The results align with existing research highlight the efficacy of natural extracts and fermentation products in extending the postharvest life of fruits and vegetables. The kombucha fermented with garlic peel extract appears to be a promising, sustainable alternative to synthetic preservatives for maintaining the physicochemical quality of tomatoes during storage. The observed trend of a slower increase in TSS in the treated group, although subtle, could be attributed to a delayed enzymatic breakdown of complex carbohydrates into simpler sugars. Further research is warranted to optimize the application methods, such as concentration and frequency of spraying, and to delve deeper into the specific underlying mechanisms through which this treatment exerts its protective effects on tomato quality.

3.8 Hemolytic Toxicity Assessment

The hemolytic potential of kombucha fermented with garlic peel extract was assessed against porcine erythrocytes at concentrations of 50 and 200 mg/mL using light microscopy (Figure 7). Untreated erythrocytes displayed their characteristic biconcave disc morphology with a clear surrounding medium (Figure7a). Upon exposure to 200 mg/mL of the extract, a time-dependent hemolytic effect was observed. After 5 minutes (Figure 7b), subtle swelling and a slight alteration in the biconcave shape of some erythrocytes were noted. This effect became more pronounced after 10 minutes (Figure 7c), with a significant number of cells exhibiting spherical morphology and the surrounding medium appearing more granular, indicative of initial membrane damage and release of cellular contents. Prolonged exposure for 30 minutes at 200 mg/mL (Figure 7d) resulted in evident hemolysis, characterized by numerous swollen and lysed erythrocytes, with a distinctly opaque and reddish background due to the release of hemoglobin.

In contrast, when erythrocytes were exposed to a lower concentration of 50 mg/mL of the kombucha extract for 30 minutes (Figure 7e), no significant changes in cellular morphology or integrity were observed compared to the untreated control. The erythrocytes retained their normal biconcave shape, and no evidence of swelling or lysis was apparent, with the surrounding medium remaining clear. These findings demonstrate a clear concentration-dependent hemolytic toxicity of the kombucha fermented with garlic peel extract. While a high concentration (200 mg/mL) induced rapid erythrocyte lysis, lower concentrations ($\leq$ 50 mg/mL) appeared to be non-hemolytic under the tested conditions. This suggests that the potential application of this fermented extract would necessitate careful consideration of its concentration to mitigate potential cytotoxic effects on blood components.
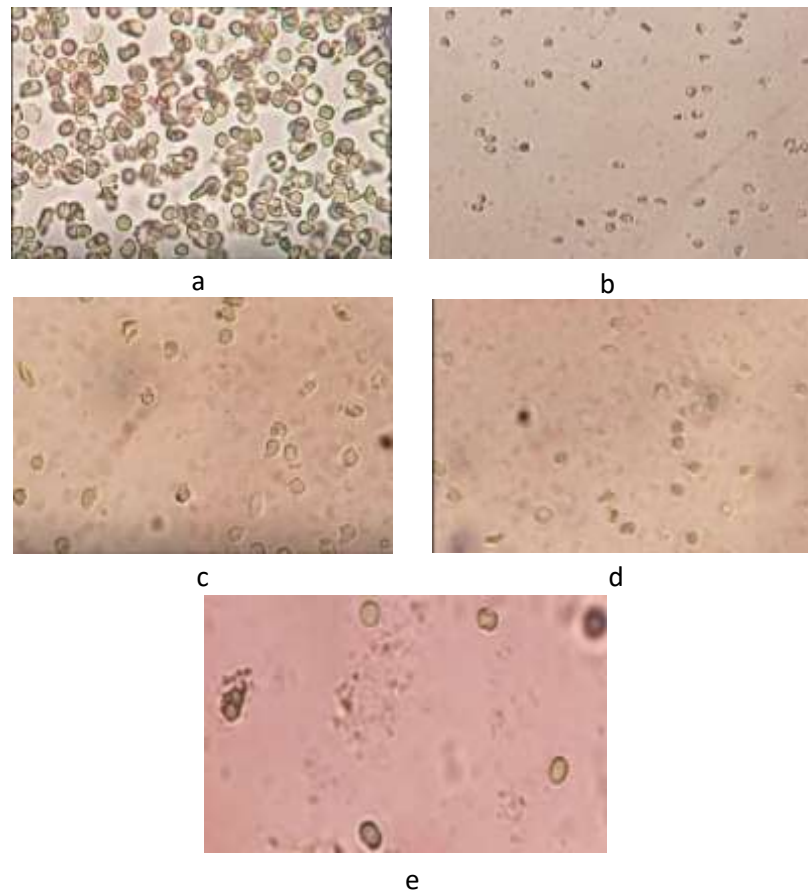
Figure 9 Toxicity of kombucha to pig red blood cells at a concentration of 200 mg/mL: (a) untreated red blood cell control, (b) treated for 5 min at 100X magnification, (c) treated for 10 min at 400X magnification, (d) treated for 30 min at 400X magnification, and (e) treated at 50 mg/mL for 30 min.

4. Conclusion

From overall, kombucha fermented with garlic peel extract (Kb+Garlic Peels) demonstrated the ability to enhance antioxidant properties, particularly flavonoid content, and exhibited significant potential for extending the shelf life and maintaining the long-term quality of tomatoes. This finding could open up new opportunities for applying natural treatments to a wider range of horticultural products. The observed antimicrobial properties of the fermented extract likely contributed to reducing microbial contamination, a primary cause of spoilage, thereby preserving the overall physical and chemical quality of the tomatoes. Furthermore, the application of Kb mixed with extracts of Garlic Peels as a spray effectively slowed down the physiological loss in weight (PLW) of tomatoes compared to the control group, particularly after 10 days of storage indicating a delayed physical deterioration and water loss, further supporting the potential of this treatment to extend the marketable lifespan and maintain the quality of tomatoes during postharvest storage. The combined effects of enhanced antioxidant activity, antimicrobial properties, and the ability to mitigate physical deterioration underscore the promising application of kombucha fermented with garlic peel extract as a natural and effective postharvest treatment for tomatoes.

5. Acknowledgement

6. References

Abrol, G. S., & Kumar, S. (2019). Effect of garlic extract coating on storage behaviour of tomato fruit. Journal of Postharvest Technology, 7(4), 1-5.

Afiati, F., Setyoningrum, F., Priadi, G., & Handoyo, C. H. (2020). Characteristics of solo black garlic fermented in kombucha black tea. IOP Conf. Series: Earth and Environmental Science, 439, Article 012053. https://doi.org/10.1088/1755-1315/439/1/012053

Bogdan, M., Justine, S., Filofteia, D. C., Petruta, C. C., Gabriela, L. U. Ț. Ă., Roxana, U. E., ... & Gabriela, L. (2018). Lactic acid bacteria strains isolated from Kombucha with potential probiotic effect. Romanian Biotechnological Letters, 23(3), 13592-13598.

Borek, C. (2001). Antioxidant health effects of aged garlic extract. The Journal of Nutrition, 131(3), 1010S–1015S.

Calvanese, C. M., Villani, F., Ercolini, D., & De Filippis, F. (2025). Postbiotics versus probiotics: Possible new allies for human health. Food Research International, 116869.

Cunha, N., Santos-Sodré, S. D. J. L., Teixeira-Costa, B. E., & Santos, O. V. D. (2025). New Trends in the Development of Products with Probiotics, Prebiotics, Symbiotics, Paraprobiotics and Postbiotics. Brazilian Archives of Biology and Technology, 68, e25240323.

D'Amore, T., Zolfanelli, C., Lauciello, V., Di Ciancia, A., Vagliasindi, A., Smaoui, S., & Varzakas, T. (2025). Using Postbiotics from Functional Foods for Managing Colorectal Cancer: Mechanisms, Sources, Therapeutic Potential, and Clinical Perspectives. Microorganisms, 13(6), 1335.

da Silva Júnior, J. C., Mafaldo, T. M., de Lima Brito, I., & de Magalhães Cordeiro, A. M. T. (2022). Kombucha: Formulation, chemical composition, and therapeutic potentialities. Current Research in Food Science, 5, 360–365. https://doi.org/10.1016/j.crfs.2022.01.023

Delzenne, N. M., Neyrinck, A. M., Bäckhed, F., & Cani, P. D. (2011). Targeting gut microbiota in obesity: effects of prebiotics and probiotics. Nature Reviews Endocrinology, 7(11), 639-646.

Drywien, M., Frackiewicz, J., Górnicka, M., Gadek, J., & Jalosinska, M. (2015). Effect of probiotic and storage time of thiamine and riboflavin content in the milk drinks fermented by Lactobacillus casei KNE-1. Roczniki Państwowego Zakładu Higieny, 66(4).

Giovannucci, E., Rimm, E. B., Liu, Y., Stampfer, M. J., & Willett, W. C. (2002). A prospective study of tomato products, lycopene, and prostate cancer risk. Journal of the National Cancer Institute, 94(5), 391–398.

Hardinsyah, H., Gunawan, W. B., Nurkolis, F., Alisaputra, D., Kurniawan, R., Mayulu, N., Taslim, N. A., & Tallei, T. E. (2023). Antiobesity potential of major metabolites from Clitoria ternatea kombucha: Untargeted metabolomic profiling and molecular docking simulations. Current Research in Food Science, 6(100464), 1–9. https://doi.org/10.1016/j.crfs.2023.100464

Hussein, H. J., Hameed, I. H., & Hadi, M. Y. (2017). A review: Anti-microbial, anti-inflammatory effect and cardiovascular effects of garlic: Allium sativum. Research Journal of Pharmacy and Technology, 10(11), 4069-4078.

Ifesan, B. O. T., Fadipe, E. A., & Ifesan, B. T. (2014). Investigation of antioxidant and antimicrobial properties of garlic peel extract (Allium sativum) and its use as a natural food additive in cooked beef. Journal of Scientific Research and Reports, 3(5), 711-721.

Ivanišová, E., Měnhartová, K., Terentjeva, M., Harangozo, L., Kántor, A., & Kačániová, M. (2020). The evaluation of chemical, antioxidant, antimicrobial and sensory properties of kombucha tea beverage. Journal of Food Science and Technology, 57(5), 1840-1846. https://doi.org/10.1007/s13197-019-04217-3

Jakubczyk, K., Kalduńska, J., Kochman, J., & Janda, K. (2020). Chemical profile and antioxidant activity of the kombucha beverage derived from white, green, black and red tea. Antioxidants, 9(5), 447-462. https://doi.org/10.3390/antiox9050447

Khubber, S., Marti-Quijal, F. J., Tomasevic, I., Remize, F., & Barba, F. J. (2022). Lactic acid fermentation as a useful strategy to recover antimicrobial and antioxidant compounds from food and by-products. Current Opinion in Food Science, 43, 189-198. https://doi.org/10.1016/j.cofs.2021.11.013

Kim, J. H., Nam, S. H., Rico, C. W., & Mi Young Kang, M. Y. (2012). A comparative study on the antioxidative and anti-allergic activities of fresh and aged black garlic extracts. International Journal of Food Science and Technology, 47(6), 1176–1182. https://doi.org/10.1111/j.1365-2621.2012.02957

Kim, N. Y., Park, M. H., & Jang, E. Y. (2011). Volatile distribution in garlic (Allium sativum L.) by solid phase microextraction (SPME) with different processing conditions. Food Science and Biotechnology, 20, 775–782. https://doi.org/10.1007/s10068-011-0108-4.

Kozyrovska, N. O., Reva, O. M., Goginyan, V. B., & De Vera, J. P. (2012). Kombucha microbiome as a probiotic: a view from the perspective of post-genomics and synthetic ecology. Biopolymers and Cell. 28(2), 103-113.

Krasaekoopt, W., Bhandari, B., & Deeth, H. (2003). Evaluation of encapsulation techniques of probiotics for yoghurt. International dairy journal, 13(1), 3-13.

Leal, J. M., Suárez, L. V., Jayabalan, R., Oros, J. H., & Escalante-Aburto, A. (2018). A review on health benefits of kombucha nutritional compounds and metabolites. CYTA–Journal of Food, 16, 390-399. https://doi.org/10.1080/19476337.2017.1410499

Liu, W., Pang, H., Zhang, H., & Cai, Y. (2014). Biodiversity of lactic acid bacteria. Lactic acid bacteria: Fundamentals and practice, 103-203.

Maguire, M., & Maguire, G. (2019). Gut dysbiosis, leaky gut, and intestinal epithelial proliferation in neurological disorders: towards the development of a new therapeutic using amino acids, prebiotics, probiotics, and postbiotics. Reviews in the Neurosciences, 30(2), 179-201.

Martyniak, A., Medyńska-Przęczek, A., Wędrychowicz, A., Skoczeń, S., & Tomasik, P. J. (2021). Prebiotics, probiotics, synbiotics, paraprobiotics and postbiotic compounds in IBD. Biomolecules, 11(12), 1903.

Matto, A. K., Murata, T., Pantastico, E. B., Chachin, K., Ogata, K., & Phan, C. T. (1975). Chemical changes during ripening and senescence, in postharvest physiology, handling and utilization of tropical and subtropical fruit and vegetables. AVI Publishing, Westport, CT, pp. 13-15.

Moradi, M., Molaei, R., & Guimarães, J. T. (2021). A review on preparation and chemical analysis of postbiotics from lactic acid bacteria. Enzyme and Microbial Technology, 143, 109722.

Morales, D. (2020). Biological activities of kombucha beverages: The need of clinical evidence. Trends in Food Science and Technology, 105, 323–333. https://doi.org/10.1016/j.tifs.2020.09.025 305 0940191832

Nataraj, B. H., Ali, S. A., Behare, P. V., & Yadav, H. (2020). Postbiotics-parabiotics: The new horizons in microbial biotherapy and functional foods. Microbial cell factories, 19(1), 1-22.

Olukemi, O., Fadaka, A., Adewale, O., Oluloye, O., Ojo, O., Ajiboye, B., Adewumi, D., & Kuku, A. (2019). In vitro anthelmintic and antioxidant activities of the leaf extracts of Theobroma cacao L. AIMS Agriculture and Food, 4(3), 568-577. https://doi.org/10.3934/agrfood.2019.3.568.

Onsun, B., Toprak, K., & Sanlier, N. (2025). Kombucha Tea: A Functional Beverage and All its Aspects. Current Nutrition Reports, 14(1), 69.

Pǎcularu-Burada, B., & Bahrim, G. E. (2021). Extraction and antioxidant activity assessment of postbiotic exopolysaccharides produced by selected lactic acid bacteria. Innovative Romanian Food Biotechnology, (20), 1-16.

Pawlos, M., Szajnar, K., Kowalczyk, M., & Znamirowska-Piotrowska, A. (2024). Probiotic Milk Enriched with Protein Isolates: Physicochemical, Organoleptic, and Microbiological Properties. Foods, 13(19), 3160.

Queiroz, Y. S., Ishimoto, E. Y., Bastos, D. H., Sampaio, G. R., & Torres, E. A. (2009). Garlic (Allium sativum L.) and ready-to-eat garlic products: In vitro antioxidant activity. Food Chemistry, 115(1), 371–374. https://doi.org/10.1016/j.foodchem.2008.12.041

Quigley, E. M. (2010). Prebiotics and probiotics; modifying and mining the microbiota. Pharmacological research, 61(3), 213-218.

Rajam, R., & Subramanian, P. (2022). Encapsulation of probiotics: Past, present and future. Beni-Suef University Journal of Basic and Applied Sciences, 11(1), 1-18.

Rameez, K. M., Santhoshkumar, P., Yoha, K. S., & Moses, J. A. (2024). Biopreservation of food using probiotics: Approaches and challenges. Current Research in Nutrition and Food Science Journal, 12(2), 539-560.

Rangana, S. (1986). Handbook of analysis and quality control for fruit and vegetable products. McGraw Hill, New Delhi

Rathore, H. A., Masud, T., Sammi, S., & Soomro, A. H. (2007). Effect of storage on physico-chemical composition and sensory properties of mango (Mangifera indica L.) variety Daeshari. Pakistan Journal of Nutrition, 6(2), 143-148.

Reyes-Flores, S., Pereira, T. S. S., & Ramírez-Rodrigues, M. M. (2023). Optimization of hempseed-added kombucha for increasing the antioxidant capacity, protein concentration, and total phenolic content. Beverages, 9(2), 50. https://doi.org/10.3390/beverages9020050

Ryu, J. H., & Kang, D. (2017). Physicochemical properties, biological activity, health benefits, and general limitations of aged black garlic: A review. Molecules, 22(6), 1–14. https://doi.org/10.3390/molecules22060919

Sadasivam, S., & Manickam, A. (1991). Biochemical methods. New Age International Ltd., New Delhi.

Sesso, H. D., Liu, S. M., Gaziano, J. M., & Buring, J. E. (2003). Dietary lycopene, tomato-based food products, and cardiovascular disease in women. The Journal of Nutrition , 133(2), 399-404.

Sharma, S., Sharma, R. K., & Sharma, A. (2021). Pharmacological effects of garlic: A review. European Journal of Medicinal Plants, 32(6), 25-37. https://doi.org/10.9734/ejmp/2021/v32i630416.

Simon, P. W. (1995). Breeding vegetables without genetic engineering. Horticultural Reviews, 17, 1-40.

Smolinska, S., Popescu, F. D., & Zemelka-Wiacek, M. (2025). A Review of the Influence of Prebiotics, Probiotics, Synbiotics, and Postbiotics on the Human Gut Microbiome and Intestinal Integrity. Journal of Clinical Medicine, 14(11), 3673. https://doi.org/10.3390/jcm14113673

Thorakkattu, P., Khanashyam, A. C., Shah, K., Babu, K. S., Mundanat, A. S., Deliephan, A., ... & Nirmal, N. P. (2022). Postbiotics: Current trends in food and Pharmaceutical industry. Foods, 11(19), 3094.

Vinderola, G., Sanders, M. E., & Salminen, S. (2022). The concept of postbiotics. Foods, 11(8), 1077.

Wang, H., Zhu, C., Chen, W., & Zhang, Y. (2019). Anti-inflammatory effects of fermented garlic extract. Journal of Ethnopharmacology, 241, Article 111898. https://doi.org/10.1016/j.jep.2019.111898

Yeganeh, F., Khodabakhsh, M. M., Dehnavi, A., & Moosavi-Movahedi, A. A. (2020). Effect of fermentation on bioactive compounds of kombucha: A comprehensive review. Trends in Food Science & Technology, 105, 319–322. https://doi.org/10.1016/j.tifs.2020.08.016

SESSION
4
Architecture and Creative Works

Knowledge Set about Online Media, Gingerbread House Architecture to Promote Tourism

Patravadee Siriwan[a], Weerawan Sathonghoi[b]

[a] Division of Engineering and Architecture, Faculty of Architecture, Institution Rajamangala University of Technology Suvarnabhumi City Nonthaburi, ZipCode 11000 Country Thailand
[b] Division of Engineering and Architecture, Faculty of Architecture, Institution Rajamangala University of Technology Suvarnabhumi City Nonthaburi, ZipCode 11000 Country Thailand
* Corresponding author. Tel.: 0 93609 9657; Fax: 0 2526 6423; E-mail address: pla012@windowslive.com

Abstract

This research aims to study the architecture of Gingerbread houses, Case Study: Bangkok Metropolitan Region and prepare a knowledge set of the media of the architecture of the Gingerbread houses in order to promote tourism among young generation and Thai tourists. The research starts from 1) the collection of data obtained from related documents and research, 2) the surveys of actual locations, 3) the interviews and observations by using questionnaires as a tool for surveying data. The sample group includes 40 second-year students of the Faculty of Engineering and Architecture, Rajamangala University of Technology Suvarnabhumi Nonthaburi Campus and young Thai tourists aged 15-30 years, 4) the photography and video recording of the architecture of the Gingerbread houses, 5) the preparation of the knowledge set of online media of the Gingerbread houses, 6) the collection of data, 7) the analyses of data applying SPSS for qualitative analysis, and 8) the conclusion, discussion and suggestions. The Gingerbread houses in this study are as follows: 1) Gingerbread House Monk Cells, 2) Golden Teak Museum, Thewarat Kunchorn Temple, Bangkok Metropolis, 3) Ekanak Museum, Bangkok Metropolis, 4) Diamond Residence, Bowon Niwet Temple, Bangkok Metropolis, 5) Moon Residence, Bowon Niwet Temple, Bangkok Metropolis, and 6) Ruean Phra Thanesuan. The research result shows that the knowledge set of the architectural media of Gingerbread houses for promoting tourism has a link to the website. https://www.gingerbreadhouseonline.com. Links to YouTube: 1) Gingerbread Houses – Abbot Cell, Monk Cells and Panthawakarn School Building, Suan Phlu Temple, Bangkok Metropolisouses, https://youtu.be/R-_hP4c7RK4, 2) Gingerbread Houses – Moon Residence, Diamond Residence and Boonyarattawet Monk Cell, Bowon Niwet Temple, Bangkok Metropolis, https://youtu.be/T1OshjjB9gs, 3) Gingerbread Houses – Golden Teak Museum, Thewarat Kunchorn Temple, Bangkok Metropolis, https://youtu.be/rS01EcVfFMk, 4) Gingerbread Houses – Ekanak Museum, Bansomdejchaopraya Rajabhat University, https://youtu.be/Ua0BxT2ToJU, 5) Gingerbread Houses - Ruean Phra Thanesuan, Sanam Chan Palace, Nakhon Pathom Province, https://youtu.be/epircwkK_nw. Link to E-Book of Gingerbread Houses: 1) Knowledge Set of Gingerbread Houses, https://my.eboox.cc/JOT/L1/, 2) Abbot Cell, Monk Cells and Panthawakarn School Building, Suan Phlu Temple, Bangkok Metropolis, https://my.eboox.cc/JOT/L2/, 3) Chandra Residence, Diamond Residence and Boonyarattawet Monk Cell, Bowon Niwet Temple, Bangkok Metropolis, https://my.eboox.cc/JOT/L3/, 4) Ekanak Museum, Bansomdejchaopraya Rajabhat University, Bangkok Metropolis, https://my.eboox.cc/JOT/L4/, 5) Golden Teak Museum, Thewarat Kunchorn Temple, Bangkok Metropolis, https://my.eboox.cc/JOT/L5/, and 6) Ruean Phra Thanesuan, Sanam Chan Palace, Nakhon Pathom Province, https://my.eboox.cc/JOT/L6/. The Evaluation of E-Book and Knowledge Set of Gingerbread House Architecture Online Media for Promoting Tourism. For media, the overall quality is at a very good level, the mean of which equals 3.74. Upon considering each area, the qualities of all areas (image, sound, techniques and methods) have been found to be at a very good level. The area with the highest mean is the techniques and methods, equaling 3.93. The second area is the image with the mean of 3.71, and the mean of the sound is 3.56 respectively. When reckoning each area, the results are as follows: Image: The qualities of each area are at a very good level, the mean of which is 3.71. Upon considering the mean of each area, the highest mean has been found to be the interesting still image with the mean of 3.98, and the quality is at a very good level. The second area is the quality of the still image with the mean of 3.89, and the quality is at the very good level. The next area is the appropriateness of the illustration with the mean of 3.69, and the quality is at a very good level. The next area is the clarity of the meaning of the still image with the mean of 3.62, and the quality is at a very good level. In addition, the mean of the appropriateness of the still image is 3.38, and the quality is at a good level respectively. Sound: The overall quality is at a very good level with the mean of 3.56. Upon reckoning the mean of each area, the area with the highest mean has been found to be the clarity of the audio description with the mean of 3.78, and the quality is at a very good level. The second area is the appropriateness of the music with the means of 3.33, and the quality is at a good level respectively. Techniques and Methods: The qualities of the overall areas are at a very good level with the mean of 3.93. Upon considering the mean of each area, the qualities of all areas have been found to be at a very good level, and the highest mean is the creation of knowledge and direct experience with the mean of 3.93. The next area is the appropriateness of visual and audio sequences with the mean of 3.89 respectively. According to students' responses, more students are interested in visiting the Gingerbread houses. The students have seen the splendid and magnifience of the Gingerbread houses, as the Gingerbread houses are the heritage of Thailand.

Keywords: Knowledge Set, Online Media, Gingerbread House, Promote Tourism

1. Introduction

The Gingerbread pattern was an architectural pattern that flourished during the two reigns mentioned above. Now the pattern and some ancient buildings disappeared. Therefore, data were collected, studied and explained to provide a clearer perspective. Appropriate illustrations were arranged to help readers for better understanding.

The Gingerbread pattern is assumed to be a pattern influenced by the Western nations, which were most prosperous during the era of Queen Victoria. Countries all over Europe and Asia were under the rule of the British Empire. During the colonial era, Siam had to improve and change the entire system, resulting in politics, economy, society, traditions and culture that the Siamese people were accustomed to having to adjust their minds in order to maintain it. Outside of sovereignty, King Chulalongkorn inherited the royal policy of his father in developing the country to be prosperous in every aspect to be equal to the Western nations. What indicates how much Siam has developed according to the Westerners is the beauty of architecture, constructions, buildings, houses, public utilities, and conveniences in life that imitate the Western way of life. The beauty of the Gingerbread fretwork was in the old days of the capital city, decorated in Dusit Palace since King Chulalongkorn, Rama V, traveling to Europe and neighboring countries, including to Malay. The popularity began to spread to royal palaces, religious sites, government officials' houses, wealthy houses and shophouses. Evidence of buildings and houses decorated with this type of pattern was very limited because the fretwork of the Gingerbread pattern was created from wood materials decorated with old architectural buildings. Some ancient buildings were not less than 100 years old.

Patravadee Siriwan's research is as follows:

1) Study the pattern of the architecture of the Gingerbread houses. Case Study: Bangkok Metropolitan Region in 2016.

2) Study the pattern of the Gingerbread fretwork. Case Study: Bangkok Metropolitan Region.

3) Study the physical characteristics of the architecture of Gingerbread houses in Bangkok Metropolis in 2021.

The researcher has had the following conclusions. The architecture of the Gingerbread houses and the Gingerbread fretwork is splendid, exquisite, magnificent and impressive, being attractive to spectators. It is the uniqueness of the Thai craftsmen needing conservation and promotion to young generation. The research team has been aware of the importance of the Gingerbread houses; therefore, the online knowledge set on the architecture of the Gingerbread houses has been produced, aiming to promote tourism among young generation aged 15-30 years. In addition, the Gingerbread houses are the Thai heritage admired by young generation and tourists, and they are splendidly, exquisitely and magnificently built by the Thai craftsmen.

2. Methodology

1) Collection of Data from Relevant Research Documents

2) Survey of the Actual Location (Field Study): The Gingerbread houses studied are as follows:
   2.1) Gingerbread Monk Cells, Suan Phlu Temple, Bangkok Metropolis
   2.2) Golden Teak Museum, Thewarat Kunchorn Temple, Bangkok Metropolis
   2.3) Ekanak Museum, Bangkok Metropolis
   2.4) Diamond Residence, Bowon Niwet Temple, Bangkok Metropolis
   2.5) Moon Residence, Bowon Niwet Temple, Bangkok Metropolis
   2.6) Boonyarattawet Monk Cell, Bowon Niwet Temple, Bangkok Metropolis
   2.7) Ruean Phra Thanesuan, Sanam Chan Palace, Nakhon Pathom Province

3) Interviews and observations Using Questionnaires as a Tool for Data Collection

The sample group for this study comprises the 40 second-year students of the Faculty of Engineering and Architecture, Rajamangala University of Technology Suvarnabhumi, Nonthaburi Campus. Additionally, questionnaires and observation forms have been utilized.

4) Photography and Video Recording of the Architecture of Gingerbread Houses for Field Survey

5) Create a knowledge set about online media on the architecture of the Gingerbread houses.

6) Collect data.

7) Analyze data. SPSS has been used for analyzing qualitative data and evaluating the online knowledge set on the architecture of the Gingerbread houses in order to promote tourism, and the observation forms have been used to evaluate the architecture of the Gingerbread for promoting tourism.

8) Summary of Results, Discussion and Suggestions

3. Results and Discussion

Research Result and Knowledge Set of Gingerbread House Architecture for Promotion of Tourism

Link to the Website

https://www.gingerbreadhouseonline.com

Links to YouTube

1) Gingerbread Houses – Abbot Cell, Monk Cells and Panthawakarn School Building, Suan Phlu Temple, Bangkok Metropolis, https://youtu.be/R-_hP4c7RK4

2) Gingerbread Houses – Moon Residence, Diamond Residence and Boonyarattawet Monk Cell, Bowon Niwet Temple, Bangkok Metropolis, https://youtu.be/T1OshjjB9gs

3) Gingerbread Houses - Gold Teak Museum, Thewarat Kunchorn Temple, Bangkok Metropolis, https://youtu.be/rS01EcVfFMk

4) Gingerbread House - Ekanak House Museum, Rajabhat Bansomdejchaopraya University, Bangkok, https://youtu.be/Ua0BxT2ToJU

5) Bread House - Phra Thanesuan House, Sanam Chandra Palace, Nakhon Pathom Province, https://youtu.be/epircwkK_nw

Links to E-Book of Gingerbread Houses

1) Knowledge Set of Gingerbread Houses, https://my.eboox.cc/JOT/L1/

2) Abbot Cell, Monk Cells and Panthawakarn School building, Suan Phlu Temple, Bangkok Metropolis, https://my.eboox.cc/JOT/L2/

3) Moon Residence, Diamond Residence and Boonyarattawet Monk Cell, Bowon Niwet Temple, Bangkok Metropolis, https://my.eboox.cc/JOT/L3/

4) Ekanak Museum, Bansomdejchaopraya Rajabhat University, Bangkok Metropolis, https://my.eboox.cc/JOT/L4/

5) Golden Teak Museum, Thewarat Kunchorn Temple, Bangkok Metropolis, https://my.eboox.cc/JOT/L5/ Ruean Phra Thanesuan, Sanam Chan Palace, Nakhon Pathom Province, https://my.eboox.cc/JOT/L6/

Evaluation Results of E-Book for Tourism Promotion: Knowledge Set on Online Media of Gingerbread House Architecture for Tourism Promotion

The evaluation results of the E-Book are to promote tourism and the knowledge set of online media of Gingerbread architecture, promoting tourism. For media, the overall quality is at a very good level with the mean of 3.74. Upon considering each area, the overall areas have been found to be at a very good level (image, sound and techniques and methods), and the quality is at a very good level, and the highest mean is the technique and method with the mean of 3.93. The second area is the image with the mean of 3.71 and sound with the mean of 3.56 respectively. When considering each area, the results are as follows:

In terms of image, the overall quality of each area is at a very good level with the mean of 3.71. Upon considering mean of each area, the area with the highest mean is the size of the still interesting image with the mean of 3.98, and the quality is at a very good level. The second area is the quality of the still image with the mean of 3.89, and the quality is at a very good level. The next area is the appropriateness of the illustration with the mean of 3.69, and the quality is at a very good level. The next area is the clarity of the meaning of the still image with the mean of 3.62, and the quality is at a very good level. In addition, the appropriateness of the still image has the mean of 3.38, and the quality is at a good level respectively.

In terms of sound, the overall quality of each area is at a very good level with the mean of 3.56. Upon considering the mean of each area, the area with the highest mean is the clarity of the audio description with the mean of 3.78, and the quality is at a very good level, followed by the appropriateness of the music with the mean of 3.33, and the quality is at a good level respectively.

In terms of techniques and methods, the overall quality of each area is at a very good level with the mean of 3.93. Upon considering the mean each area, the qualities of all areas are found to be at a very good level, creating knowledge and direct experience with the mean of 3.96, followed by appropriateness of the presentation format with the mean of 3.93, and the appropriateness of the image and sound with the mean of 3.89 respectively.

For the results of the evaluation of the knowledge set of the Gingerbread house architecture to promote tourism, students are able to understand correctly and completely with the mean of 2.85. Upon considering the mean of each area, the students are able to understand correctly and completely in every area. The area with the highest mean is the meaning and location of Gingerbread fretwork with the mean of 2.98, followed by the Gingerbread fretwork with the mean of 2.91, followed by the type of the buildings in Bangkok Metropolis decorated with the Gingerbread fretwork, and the location of the buildings that are popularly decorated with the Gingerbread fretwork with the mean of 2.76 respectively.

Suggestions: QR codes for the 6 Gingerbread houses should be created to promote tourist attractions and provide the knowledge of the Gingerbread houses, as the Gingerbread houses are the heritage of Thailand, and the Gingerbread houses and the Thai craftsmen's skills should be conserved, and the narration on YouTube should be improved.
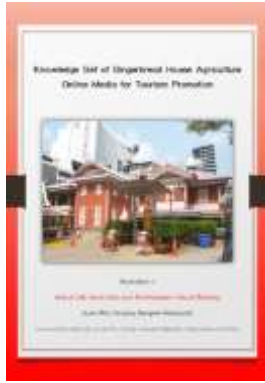
Figure 1: Abbot Cell, Monk Cells
and Panthawakarn School Building,
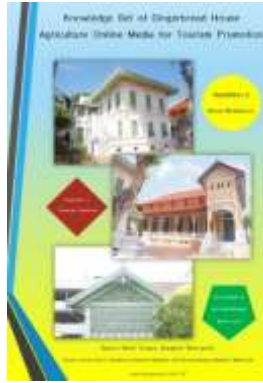Suan Phlu Temple, Bangkok Metropolis

Figure 2: Moon Residence, Diamond Residence,
Boonyarattawet Monk Cell, Bangkok Metropolis

Figure 3: Ekanak Museum,
Bansomdejchaopraya Rajabhat University,
Bangkok Metropolis

https://my.eboox.cc/JOT/L2/
https://youtu.be/R-_hP4c7RK4
https://www.gingerbreadhouseonline.com

https://my.eboox.cc/JOT/L3/
https://youtu.be/T1OshjjB9gs
https://www.gingerbreadhouseonline.com

https://my.eboox.cc/JOT/L4/
https://youtu.be/Ua0BxT2ToJU
https://www.gingerbreadhouseonline.com

Figure 4: Golden Teak Museum,
Thewarat Kunchorn Temple,
Bangkok Metropolis

Figure 5: Ruean Phra Thanesuan,
Sanam Chandra Palace,
Nakhon Pathom Province

Figure 6: Ruean Phra Thanesuan,
Sanam Chandra Palace,
Nakhon Pathom Province

https://my.eboox.cc/JOT/L5/
https://youtu.be/rS01EcVfFMk
https://www.gingerbreadhouseonline.com

https://my.eboox.cc/JOT/L6/
https://youtu.be/epircwkK_nw
https://www.gingerbreadhouseonline.com

https://my.eboox.cc/JOT/L6/
https://youtu.be/epircwkK_nw
https://www.gingerbreadhouseonline.com

4. Conclusions

4.1 Summary of Results

The architecture of the Gingerbread pattern in Bangkok Metropolitan Region can be classified into the following issues:

1) Buildings with Gingerbread Pattern

    1.1) Traditional Thai style buildings include:

        1. Gingerbread Monk Cells, Suan Phlu Temple
        2. Golden Teak Museum, Thewarat Kunchorn Temple
        3. Ekanak Museum
        4. Diamond Residence, Bowon Niwet Temple
        5. Moon Residence, Bowon Niwet Temple
        6. Boonyarattawet Monk Cell, Bowon Niwet Temple
        7. Ruean Phra Thanesuan, Sanam Chan Palace, Nakhon Pathom Province

2) Three groups of materials have been used for building Gingerbread houses as follows:
    2.1) Buildings Made Entirely of Wood
        1. Gingerbread Monk Cells, Suan Phlu Temple
        2. Ruean Thanesuan, Sanam Chan Palace, Nakhon Pathom Province
        3. Boonyarattawet Monk Cell, Bowon Niwet Temple
    2.2) Half Concrete Half Wood Buildings
        1. Ekanak Museum
    2.3) Brick and Mortar Buildings
        1. Golden Teak Museum, Thewarat Kunchorn Temple
        2. Diamond Residence, Bowon Niwet Temple
        3. Moon Residence, Bowon Niwet Temple
3) Three Drawing Plans Used for Building Gingerbread Houses
    3.1) Rectangular Drawing Plan includes Gingerbread monk cells, Suan Phlu Temple, Ruean Thanesuan, Diamond Residence, Moon Residence, Boonyarattawet Monk Cell, Bowon Niwet Temple.
    3.2) Square Drawing Plan connected with octagonal room in the end consists of Ekanak Museum.
    3.3) Independent Drawing Plan comprises Golden Teak Museum, Thewarat Kunchorn Temple.
4) Three Types of Gingerbread Roof
    4.1) Manila roof includes Gingerbread monk cells, Suan Phlu Temple
    4.2) Mixed hipped gable roof consists of Golden Teak Museum in Thewarat Kunchorn Temple, Ekanak Museum, Ruean Phra Thanesuan, Moon Residence in Bowon Niwet Temple.
    4.3) Gable roof comprises Gingerbread monk cells in Suan Phlu Temple, Diamond Residence in Bowon Niwet Temple and Boonyarattawet Monk Cell in Bowon Niwet Temple.
5) The total number of floors is as follows:
    5.1) Two-story buildings include Gingerbread monk cells in Suan Phlu Temple, Golden Teak Museum Building, Ekanak Museum, Diamond Residence in Bowon Niwet Temple, Moon Residence in Bowon Niwet Temple and Boonyarattawet Monk Cell in Bowon Niwet Temple.
    5.2) One-story building comprises Ruean Phra Thanesuan, Nakhon Pathom Province
6) The Popular Colors of Gingerbread Houses
    6.1) Yellow buildings with red roofs include Golden Teak Museum, Thewarat Kunchorn Temple and Ekanak Museum.
    6.2) Repainted buildings consist of red, white, red roof, such as Gingerbread monk cells in Suan Phlu Temple.
    6.3) Green and white buildings comprise Ruean Phra Thanesuan and Moon Residence in Bowon Niwet Temple in Bowon Niwet Temple.
    6.4) Orange building with orange roof includes Diamond Residence in Bowon Niwet Temple.
7) Decorative elements found in every building are as follows:
    Fretwork Grille, Stair Balustrade, Stair Railing, Sun Fin, Balcony Railing, Eave above Doors, Stairs, Gable, Door Frame, Window Panel, Awning
8) Six Gingerbread Patterns
    8.1) Artificial Flower Pattern Found in Ekanak Museum, Golden Teak Museum in Thewarat Kunchorn Temple, Chan Residence in Bowon Niwet Temple, Diamond Residence in Bowon Niwet Temple, Boonyarattawet Monk Cell in Bowon Niwet Temple, Ruean Thanesuan
    8.2) Club Pattern Found in Golden Teak Museum in Thewarat Kunchorn Temple
    8.3) Cross Pattern Found in Golden Teak Museum in Thewarat Kunchorn Temple
9) The Current Uses of Gingerbread Houses
    9.1) Adjusted to Be a Museum Opened to the Public: Golden Teak Museum in Thewarat Kunchorn Temple and Ruean Thanesuan
    9.2) Applied as Office Buildings and Government Offices (Not Museum): Gingerbread Monk Cells in Suan Phlu Temple, Ekanak Museum, Diamond Residence in Bowon Niwet Temple, Moon Residence in Bowon Niwet Temple and Boonyarattawet Monk Cell in Bowon Niwet Temple
10) Awarded Gingerbread Houses
    10.1) Award for Outstanding Conservation from the Association of Siamese Architects under Royal Patronage: Gingerbread Monk Cells in Suan Phlu Temple
    10.2) Award for Outstanding Architectural Conservation 2012 in the Category of Institutional and Public Buildings from the Association of Siamese Architects under Royal Patronage: Ekanak Museum

Recommendations

1) Policy: The curriculum of tourism by conserving the architecture of the Gingerbread houses should be supported in order to promote tourism for the architecture of the Gingerbread houses among young generation aged 15-30 years, admiring the Thai craftsmen. Schools and universities should visit the Gingerbread houses, so that young generation can admire the splendid of the architecture of the Gingerbread houses.

2) The Gingerbread houses should be promoted in order to provide young generation with the information of the Gingerbread houses and tourists for benefits in the future.

5. References

Department of Archaeology, Fine Arts Department, Ministry of Culture. (2017). Gingerbread Fretwork: The Aesthetics of Rattanakosin, *Bangkok Metropolis*, pp. 31-44, pp. 101-108.

Pensupa Sukkata, Visiting the Past, Bangkok, Join Together 2000.

Pharadee Panthuphakorn and Seksan Tanyaphirom. (2002). *A Study of Rattanakosin Architecture in Chanthaburi Province, Research on the Conservation of Arts and Culture,* Faculty of Fine Arts, Burapha University, pp. 8-20, pp. 27-38.

Pharadee Panthuphakorn. (2004). *A Study of the Collection of Gingerbread Fretwork of Chanthaburi Craftsmen, Research on the Preservation of Arts and Culture*, Faculty of Fine Arts, Burapha University.

Patravadee Siriwan. (2016) *A study of the Architectural Style of the Gingerbread Houses in Thailand: Case Study: Bangkok Metropolitan Region and Phrae Province, Complete Research,* Faculty of Engineering and Architecture, Rajamangala University of Technology Suvarnabhumi, Nonthaburi, 2016, pp. 41-45, pp. 54-55, pp 76-77

Patravadee Siriwan. (2018). *The Study of the Gingerbread Fretwork. Case Study: Bangkok Metropolitan Region and Phrae Province*. Rajamangala University of Technology Suvarnabhumi, Nonthaburi.

Patravadee Siriwan. (2022). *The Study of the Physical Characteristics of Gingerbread Architecture*. Bangkok Metropolis Rajamangala University of Technology Suvarnabhumi, Nonthaburi.

Patravadee Siriwan. (2024). *Online Knowledge Set on the Architecture of the Gingerbread Houses for Promoting Tourism*. Rajamangala University of Technology Suvarnabhumi, Nonthaburi.

Sponsors

บริษัท ออโตไดแด็กติก จำกัด
Auto-Didactic Co., Ltd.

บริษัท เรฟโวลูชั่น ไดแดคติค จำกัด
Revolution Didactic Co., Ltd.

บริษัท ทางยกระดับดอนเมือง จำกัด (มหาชน)
Don Muang Tollway Public Company Limited

บริษัท เอ สยาม อินฟรา จำกัด
A Siam Infra Co., Ltd.

บริษัท แอลฟา ดี เอ็ม เทค จำกัด
Alpha DM Tech Co., Ltd.

บริษัท ยิบอินซอย จำกัด
Yip In-Tsoi Co., Ltd.

บริษัท ยิบอินซอย คอนซัลติ้ง จำกัด

Yip In-Tsoi Consulting Co., Ltd.

บริษัท ยูโร เบสท์ เทคโนโลยี จำกัด

Euro Best Technology Co., Ltd.

บริษัท เคมิท กรุ๊ป จำกัด

Kemit Group Co., Ltd.

บริษัท เทิร์นออนโซลูชั่น จำกัด

Turn-On Solution Co., Ltd.

บริษัท พีอาร์ที สยามเอ็นจิเนียร์ จำกัด

PRT Siam Engineer Co., Ltd.

บริษัท วีเอสพีเอ็ม เอ็นจิเนียริ่ง จำกัด

VSPM Engineering Co., Ltd.